EXTRACELLULAR ENZYMES IN AQUATIC ENVIRONMENTS: EXPLORING THE LINK BETWEEN GENOMIC POTENTIAL AND BIOGEOCHEMICAL CONSEQUENCES

EDITED BY: Maria Montserrat Sala, Judith Piontek, Sonja Endres, Anna Maria Romani, Sonya Dyhrman and Andrew Decker Steen

PUBLISHED IN: Frontiers in Microbiology and Frontiers in Marine Science

frontiers Research Topics

frontiers

ISSN 1664-8714
ISBN 978-2-88963-004-2
DOI 10.3389/978-2-88963-004-2

About Frontiers

Frontiers is more than just an open-access publisher of scholarly articles: it is a pioneering approach to the world of academia, radically improving the way scholarly research is managed. The grand vision of Frontiers is a world where all people have an equal opportunity to seek, share and generate knowledge. Frontiers provides immediate and permanent online open access to all its publications, but this alone is not enough to realize our grand goals.

Frontiers Journal Series

The Frontiers Journal Series is a multi-tier and interdisciplinary set of open-access, online journals, promising a paradigm shift from the current review, selection and dissemination processes in academic publishing. All Frontiers journals are driven by researchers for researchers; therefore, they constitute a service to the scholarly community. At the same time, the Frontiers Journal Series operates on a revolutionary invention, the tiered publishing system, initially addressing specific communities of scholars, and gradually climbing up to broader public understanding, thus serving the interests of the lay society, too.

Dedication to Quality

Each Frontiers article is a landmark of the highest quality, thanks to genuinely collaborative interactions between authors and review editors, who include some of the world's best academicians. Research must be certified by peers before entering a stream of knowledge that may eventually reach the public - and shape society; therefore, Frontiers only applies the most rigorous and unbiased reviews.
Frontiers revolutionizes research publishing by freely delivering the most outstanding research, evaluated with no bias from both the academic and social point of view. By applying the most advanced information technologies, Frontiers is catapulting scholarly publishing into a new generation.

What are Frontiers Research Topics?

Frontiers Research Topics are very popular trademarks of the Frontiers Journals Series: they are collections of at least ten articles, all centered on a particular subject. With their unique mix of varied contributions from Original Research to Review Articles, Frontiers Research Topics unify the most influential researchers, the latest key findings and historical advances in a hot research area! Find out more on how to host your own Frontiers Research Topic or contribute to one as an author by contacting the Frontiers Editorial Office: researchtopics@frontiersin.org

EXTRACELLULAR ENZYMES IN AQUATIC ENVIRONMENTS: EXPLORING THE LINK BETWEEN GENOMIC POTENTIAL AND BIOGEOCHEMICAL CONSEQUENCES

Topic Editors:
Maria Montserrat Sala, Institut de Ciències del Mar (ICM-CSIC), Spain
Judith Piontek, Leibniz Institute for Baltic Sea Research Warnemünde, Germany
Sonja Endres, Business Development and Technology Transfer Corporation of Schleswig-Holstein (WTSH), Germany
Anna Maria Romani, University of Girona, Spain
Sonya Dyhrman, Columbia University, United States; Lamont-Doherty Earth Observatory, United States
Andrew Decker Steen, University of Tennessee, United States

Image: Maria Montserrat Sala

Microbial extracellular enzymes are fundamental to the cycling of elements in aquatic systems. The regulation of these enzymatic reactions in oceans, lakes and streams is under complex multiple control by environmental factors and the metabolic capacities of different taxa and communities. While the environmental control of enzyme-mediated processes has been investigated for over 100 years, in recent years tremendous progress in techniques to characterize the metabolic potential of microbial communities ("omics" techniques) has been made, such as high-throughput sequencing and new analytical algorithms.

This book explores the controls, activities, and biogeochemical consequences of enzymes in aquatic environments. It brings together experimental studies and fieldwork conducted with natural microbial communities in marine and freshwater ecosystems as well as physiological, biochemical and molecular studies on microbial

communities in these environments, or species isolated from them. Additionally, the book contributes to the ongoing debate on the impact of anthropogenic climate change and pollution on microbes, extracellular enzymes and substrate turnover.

Citation: Sala, M. M., Piontek, J., Endres, S., Romani, A. M., Dyhrman, S., Steen, A. D., eds. (2019). Extracellular Enzymes in Aquatic Environments: Exploring the Link Between Genomic Potential and Biogeochemical Consequences. Lausanne: Frontiers Media. doi: 10.3389/978-2-88963-004-2

Table of Contents

frontiers in Microbiology

EDITORIAL
published: 26 June 2019
doi: 10.3389/fmicb.2019.01463

Editorial: Extracellular Enzymes in Aquatic Environments: Exploring the Link Between Genomic Potential and Biogeochemical Consequences

Maria M. Sala[1], Judith Piontek[2], Sonja Endres[3], Anna M. Romani[4], Sonya Dyhrman[5,6] and Andrew D. Steen[7]*

[1] Department of Marine Biology and Oceanography, Institut de Ciències del Mar (ICM-CSIC), Barcelona, Spain, [2] Biological Oceanography, Leibniz Institute for Baltic Sea Research Warnemünde, Rostock, Germany, [3] Business Development and Technology Transfer Corporation of Schleswig-Holstein (WTSH), Kiel, Germany, [4] Department of Environmental Sciences, Institute of Aquatic Ecology, University of Girona, Girona, Spain, [5] Department of Earth and Environmental Sciences, Columbia University, New York, NY, United States, [6] Lamont-Doherty Earth Observatory, Palisades, NY, United States, [7] Departments of Microbiology and Earth and Planetary Sciences, University of Tennessee, Knoxville, TN, United States

Keywords: enzymes, microorganisms, aquatic environment, degradation, bacterial activity

OPEN ACCESS

Edited by:
Hongyue Dang,
Xiamen University, China

Reviewed by:
George S. Bullerjahn,
Bowling Green State University, United States

****Correspondence:***
Maria M. Sala
msala@icm.csic.es

Specialty section:
This article was submitted to Aquatic Microbiology, a section of the journal Frontiers in Microbiology

Received: *15 April 2019*
Accepted: *11 June 2019*
Published: *26 June 2019*

Citation:
Sala MM, Piontek J, Endres S, Romani AM, Dyhrman S and Steen AD (2019) Editorial: Extracellular Enzymes in Aquatic Environments: Exploring the Link Between Genomic Potential and Biogeochemical Consequences. Front. Microbiol. 10:1463. doi: 10.3389/fmicb.2019.01463

Editorial on the Research Topic

Extracellular Enzymes in Aquatic Environments: Exploring the Link Between Genomic Potential and Biogeochemical Consequences

Microbes drive the Earth's biogeochemical cycles, exerting profound control over the global cycling of carbon and other elements (Falkowski et al., 2008). In aquatic systems, the importance of microbial extracellular enzymes to the mobilization, transformation, and turnover of organic and inorganic compounds in aquatic environments has been proved since the 80's (Hoppe, 1983; Chróst, 1989) and was summarized in the book "Microbial enzymes in aquatic environments" (Chróst, 1991). Since then, the field has advanced considerably, with new observations, assay methods, and molecular-level studies (Arnosti et al., 2014) and the measurement of extracellular enzyme activities has become standard in many labs. We now have rates of enzymatic activities in a wide variety of freshwater and marine environments, from polar to tropical and from surface to deep ocean, and from isolates obtained even from extreme environments. Additionally, in recent years measurement of enzyme activities has become an important tool to assess the impact of anthropogenic changes on microbial communities and biogeochemical cycles, such as in the events of oil spills, acidification, or global warming (e.g., Piontek et al., 2010; Sala et al., 2016; Ziervogel et al., 2016; Freixa et al., 2017).

In this special issue, twelve articles highlight new findings on extracellular enzyme activities in aquatic environments, bringing together experimental and field studies conducted in marine and freshwater ecosystems as well as physiological, biochemical, and molecular studies on microbial communities or species isolated from those environments.

The first part of the volume is devoted to field studies, both in marine and freshwater ecosystems. To begin, the perspective article by Baltar advocates the need to go "beyond the living things" and study cell-free enzymatic activities to fully constrain the future and evolution of marine biogeochemical cycles. In marine environments, Hoarfrost and Arnosti show that the spectrum of substrates hydrolyzed in mesopelagic and deep waters of the Atlantic Ocean is positively related to the strength of stratification depth patterns, which may influence the efficiency of the biological carbon pump. Apart from their enzyme activities, knowing the types of bacteria that metabolize polymers can help make the critical connection between the taxonomic composition of microbial communities and their biogeochemical function. Liu et al. show, by using stable isotope probing, that a more diverse group of bacteria is involved in metabolizing peptides in normoxic surface water than in hypoxic bottom seawater from the Gulf of Mexico. In freshwaters, kinetic measurements of 5 substrates for exo- and endo-acting extracellular peptidases in 28 freshwater bodies in the Pocono Mountains (Mullen et al.) show variable ratios between aminopeptidases (APs) and trypsin, highlighting that measuring only Leu- AP activity may underestimate the total peptidolytic capacity in an environment. Spatial, but not seasonal, variability is also observed in a multi-season investigation in two North Carolina rivers examining the activities of extracellular enzymes used to hydrolyze polysaccharides and peptides (Bullock et al). Collectively, these studies expand our understanding of the role of microbial enzymes in the biogeochemistry of aquatic ecosystems.

Experimental approaches are increasingly used to tease apart the complex role aquatic microbial enzymes have on the biogeochemistry and functioning of ecosystems. Traving et al. in a mesocosm experiment observed the effect of increased loads of dissolved organic matter (DOM) in bacterioplankton community composition and a stimulation of protease activity. This suggests that parts of future elevated riverine DOM supply to the Baltic Sea will be efficiently mineralized by microbes and will have consequences in bacterioplankton and phytoplankton community composition and function. Indeed, organic matter released by phytoplankton fuels bacterial growth and the transformation of this DOM plays a role in the formation of chromophoric DOM which is ubiquitous in the ocean. Kinsey et al. investigated CDOM formation mediated by microbial processing of phytoplankton-derived aggregates. Measurements of hydrolytic enzyme rates along with the fluorescent properties of organic matter suggest that bacterial degradation activity changes the composition of chromophoric dissolved organic matter to more humic-like compounds. Another experimental study by Kamalanathan et al. reports on the role of bacterial extracellular enzymes during exposure to hydrocarbons and dispersant in mesocosm tanks and observed enhanced EPS (extracellular polymeric substances) production and extracellular enzyme activities in the oil amended treatment. These studies, which span both the field and laboratory, highlight the role of microbial enzymes in processing organic matter and the ramifications for diversity, resource remineralization, and community responses to anthropogenic perturbations.

Two of the papers in this issue address methodological concerns or improvements on enzyme activity measurements. Obayashi et al. use kinetic experiments to suggest improvements in material and methods for measurements of extracellular protease activities, and specifically highlight the relevance of using low protein binding materials. Also, Vrba et al. propose the fluorescence-labeled enzyme activity (FLEA) assay based in a novel substrate, ELF97 phosphate, that allows tagging extracellular phosphatase activity on single cells in an epifluorescence microscope and has shown to be useful in green algae cultures. This assay is shown being a strong tool for exploring plankton P metabolism.

The last part of the issue is focused on the characterization of new enzymes: a novel salt-tolerant esterase from deep-sea sediment of the South China Sea (Zhang et al.) and a new S8 serine protease from marine sedimentary *Photobacterium* sp. A5-7 (Li et al.).

The broad-range of articles presented in this topic deepens our understanding on the controls, activities, and biogeochemical consequences of microbial enzymes in aquatic environments. This body of work has, not only increased our knowledge, but also identified challenges and questions that remain open and should be addressed in the future.

AUTHOR CONTRIBUTIONS

All authors listed have made a substantial, direct and intellectual contribution to the work, and approved it for publication.

FUNDING

This study was supported by grant ANIMA (CTM2015-65720-R) funded by the Spanish Government to MS and by the NSF grant OCE-1464392 to AS.

REFERENCES

Arnosti, C., Bell, C., Moorhead, D. L., Sinsabaugh,. R. L., Steen, A. D., Stromberger, M., et al. (2014). Extracellular enzymes in terrestrial, freshwater, and marine environments: perspectives on system variability and common research needs. *Biogeochemistry* 117, 5–21. doi: 10.1007/s10533-013-9906-5

Chróst, R. J. (1989). Characterization and significance of beta-glucosidase activity in lake water. *Limnol.Oceanogr*. 34, 660–672. doi: 10.4319/lo.1989.34.4.0660

Chróst, R. J. (1991). *Microbial Enzymes in Aquatic Environments*. New York, NY: Springer Verlag, 317.

Falkowski, P. G., Fenchel, T., and Delong, E. F. (2008). The microbial engines that drive earth's biogeochemical cycles. *Science* 320, 1034–1039. doi: 10.1126/science.1153213

Freixa, A., Acuña, V., Casellas, M., Pecheva, S., and Romaní, A. M. (2017). Warmer night-time temperature promotes microbial heterotrophic activity and modifies stream sediment community. *Global Change Biol.* 23, 3825–3837. doi: 10.1111/gcb.13664

Hoppe, H. G. (1983). Significance of exoenzymatic activities in the ecology of brackish water: measurements by means of methylumbelliferyl substrates. *Mar- Ecol. Prog. Ser.* 11, 299–308. doi: 10.3354/meps011299

Piontek, J., Lunau, M., Handel, N., Borchard, C., Wurst, M., and Engel, A. (2010). Acidification increases microbial polysaccharide degradation in the ocean. *Biogeosciences* 7, 1615–1624. doi: 10.5194/bg-7-1615-2010

Sala, M. M., Aparicio, F., Balagué V., Boras, J. A., Borrull, E., Cardelús, C., et al. (2016). Contrasting effects of ocean acidification on the microbial food web under different trophic conditions. *ICES J. Mar. Sci.* 73, 670–679. doi: 10.1093/icesjms/fsv130

Ziervogel, K., Joye, S. B., and Arnosti, C. (2016). Microbial enzymatic activity and secondsary production in sediments affected by the sedimentation pulse following the Deepwater Horizon oil spill. *Deep Sea Res. II* 129, 241–248. doi: 10.1016/j.dsr2.2014.04.003

Conflict of Interest Statement: The authors declare that the research was conducted in the absence of any commercial or financial relationships that could be construed as a potential conflict of interest.

frontiers in Microbiology

PERSPECTIVE
published: 04 January 2018
doi: 10.3389/fmicb.2017.02438

Watch Out for the "Living Dead": Cell-Free Enzymes and Their Fate

Federico Baltar[1,2]*

[1] Department of Marine Science, University of Otago, Dunedin, New Zealand, [2] NIWA/University of Otago Research Centre for Oceanography, Dunedin, New Zealand

Microbes are the engines driving biogeochemical cycles. Microbial extracellular enzymatic activities (EEAs) are the "gatekeepers" of the carbon cycle. The total EEA is the sum of cell-bound (i.e., cell-attached), and dissolved (i.e., cell-free) enzyme activities. Cell-free enzymes make up a substantial proportion (up to 100%) of the total marine EEA. Although we are learning more about how microbial diversity and function (including total EEA) will be affected by environmental changes, little is known about what factors control the importance of the abundant cell-free enzymes. Since cell-attached EEAs are linked to the cell, their fate will likely be linked to the factors controlling the cell's fate. In contrast, cell-free enzymes belong to a kind of "living dead" realm because they are not attached to a living cell but still are able to perform their function away from the cell; and as such, the factors controlling their activity and fate might differ from those affecting cell-attached enzymes. This article aims to place cell-free EEA into the wider context of hydrolysis of organic matter, deal with recent studies assessing what controls the production, activity and lifetime of cell-free EEA, and what their fate might be in response to environmental stressors. This perspective article advocates the need to go "beyond the living things," studying the response of cells/organisms to different stressors, but also to study cell-free enzymes, in order to fully constrain the future and evolution of marine biogeochemical cycles.

Keywords: marine biogeochemical cycling, carbon cycle, organic matter hydrolysis, extracellular enzymatic activity, cell-free enzymes, climate change, warming

OPEN ACCESS

Edited by:
Maria Montserrat Sala, Institute of Marine Sciences (CSIC), Spain

Reviewed by:
Sachia Jo Traving, University of Copenhagen, Denmark
Carol Arnosti, University of North Carolina at Chapel Hill, United States

***Correspondence:**
Federico Baltar
federico.baltar@otago.ac.nz

Specialty section:
This article was submitted to Aquatic Microbiology, a section of the journal Frontiers in Microbiology

Received: *26 September 2017*
Accepted: *24 November 2017*
Published: *04 January 2018*

Citation:
Baltar F (2018) Watch Out for the "Living Dead": Cell-Free Enzymes and Their Fate. Front. Microbiol. 8:2438. doi: 10.3389/fmicb.2017.02438

IMPORTANCE OF MICROBES AND THEIR EXTRACELLULAR ENZYMATIC ACTIVITIES (EEA)

The marine environment plays a critical role in global biogeochemical cycles (Daily, 2003; Harley et al., 2006; Hutchins and Fu, 2017). Microbes are the engines driving Earth's biogeochemical cycles (Falkowski et al., 2008). These tiny organisms have the set of core genes coding for the enzymes of the major reactions responsible for transforming energy and matter into (usable) substrates essential for life (Falkowski et al., 2008). We live in a time of change, and anthropogenic impacts can alter the structure and functioning of marine microbial communities, and consequentially, the role of the ocean in the global biogeochemical cycles. Thus, if we aim to understand what the future of marine biogeochemical cycling is going to be, we need to understand what the fate of microbes, and their enzymes, will be.

When it comes to the consumption of organic matter for transformation and recycling, microbes seem to have a preference for specific types of organic matter. According to the

"size-reactivity" model, heterotrophic microbes preferentially degrade high molecular weight dissolved organic matter (DOM) because it tends to be more bioavailable than the low molecular weight DOM (Benner and Amon, 2015). But, that food selectivity comes at a price: heterotrophic prokaryotes will need to hydrolyze most of those molecules into subunits small enough to be incorporated, because most molecules need to be smaller than 600 Da to pass through the prokaryotic cell wall (Weiss et al., 1991). For that purpose they use extracellular enzymes; so due to the central role of those enzymes they are referred to as the 'gatekeepers' of the C cycle (Arnosti, 2011). However, an alternative polysaccharide uptake mechanism of bacteria was recently revealed, which allows them to directly incorporate large molecular weight DOM compounds (Cuskin et al., 2015; Reintjes et al., 2017). Yet, not all high molecular weight DOM can be transported by this mechanism (i.e., biochemical and microbiological studies suggest that the binding/hydrolysis/transport is very selective for specific polysaccharides), and that mechanism still involve extracellular hydrolysis – but the binding proteins hang onto the pieces, such that they are transported into the cell with no loss to the external environment (Cuskin et al., 2015). Nevertheless, extracellular enzymatic activities (EEAs) are found from epipelagic to bathypelagic waters, commonly observing an increasing ratio of EEA to cell abundance with depth (Hoppe and Ullrich, 1999; Hoppe et al., 2002; Baltar et al., 2009).

THE LIVING AND THE 'LIVING DEAD': CELL-ATTACHED VERSUS CELL-FREE EEA

Extracellular enzymes exist in two forms; cell-bound (i.e., cell-attached), and dissolved (i.e., cell-free, operationally defined as passing through a 0.22 μm filter). The total EEA is the result of the combination of cell-associated and cell-free enzymes (**Figure 1**). Using the Internet as an analogy, we could say that cell-bound EEA would be the equivalent of a "wired" Internet connection, whereas cell-free EEA would be a "wireless" connection (i.e., would still provide the end product – data transfer/hydrolysate – even if not physically connected to the hardware/cell). Different sources of cell-free enzymes have been suggested, including the active release by bacteria in response to an appropriate substrate (Alderkamp et al., 2007) and bacterial starvation (Albertson et al., 1990), and changes in cell permeability (Chrost, 1990). These studies indicate that marine bacteria can release enzymes into the environment not only to facilitate the hydrolysis of specific substrates during exponential growth on specific substrates, but also that starved cells during stationary phase showed a greater release of extracellular enzymes than at the onset of starvation. In fact, even during this starvation period, *de novo* protein synthesis occurs for the production and/or release of the cell-free enzymes into the surrounding environment, highlighting the importance of this process for some marine bacteria (Albertson et al., 1990). Besides direct release, there are other indirect sources of cell-free enzymes, including grazing on bacterial communities (Bochdansky et al., 1995), and viral lysis (Karner and Rassoulzadegan, 1995).

The question then is whether the strategy of releasing enzymes into the aquatic environment is energetically and ecologically efficient. Extracellular enzymes released by bacteria have been shown to produce sufficient products from particulate organic carbon to support the growth of the bacteria in the absence of any other significant source of organic carbon and without direct contact between the cell and particulate substrate (Vetter and Deming, 1999). These empirical results obtained by Vetter and Deming (1999) support the predictions they formulated in a model (Vetter et al., 1998), suggesting that dissolved extracellular enzymes are advantageous when bacteria are attached to particles and when the substrate is within a well-defined distance from the enzyme source. Furthermore, other model simulations later revealed that when enzyme-producing microbes competed with non-producers: (1) non-producers were favored by higher enzyme costs, (2) producers were favored by lower rates of enzyme diffusion, and (3) non-producers and producers coexisted in highly organized spatial patterns at intermediate enzyme costs and diffusion rates (Allison, 2005). These studies are also in agreement with the recently proposed solutions to the 'public good dilemma' in bacterial biofilms (Drescher et al., 2014). In that study, the secretion of public goods (i.e., chitinases) that potentially could be exploited by non-producing cells was explained by two mechanisms: cells can produce thick biofilms that confine the goods to producers, or fluid flow can remove soluble products of chitin digestion, denying access to non-producers. More recently, another model suggested that not only might cell-free enzymes be a profitable strategy to microbes live near or attached to particles, but went further to indicate that cell-free enzymes might be a viable strategy even for free-living cells, if substrate utilization is viewed as a cooperative effort (Traving et al., 2015). These authors also suggested that even small amounts of long-lived cell-free enzymes released by cell-free microbes could contribute significantly to the dissolved enzyme activity pool.

Once these enzymes are free, they can retain activity (i.e., are able to carry out their function) until they reach a specific substrate and then hydrolyze it. There are not many studies looking at the lifetime of these cell-free enzymes in seawater, but the ones available suggest that they can have half-life times of up to 20 days (Ziervogel et al., 2010; Steen and Arnosti, 2011; Baltar et al., 2013), and that deep water enzymes seem to have longer lifetimes than surface ones (Baltar et al., 2013). These observations are especially interesting because although it was originally thought that only cell-bound activity would be relevant in the marine environment (Rego et al., 1985; Chrost and Rai, 1993), evidence have been accumulating clearly indicating that the fraction of dissolved EEA is comparable to the bound fraction (Karner and Rassoulzadegan, 1995; Li et al., 1998; Baltar et al., 2010, 2013, 2016; Duhamel et al., 2010; Allison et al., 2012). In fact, in many cases, it has been observed that the proportion of dissolved EEA can reach a value of 100%, meaning that all the enzymatic activity, in those waters at the time of sampling, was being performed

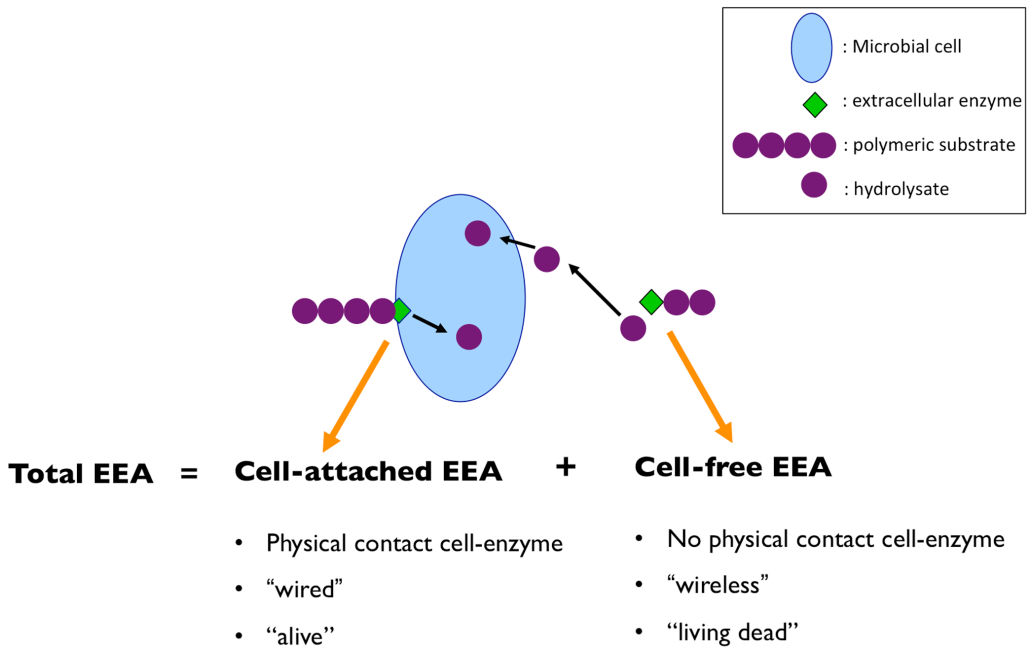

FIGURE 1 | Total extracellular enzymatic activity (EEA) is the result of the combination of cell-associated and cell-free enzymes. Using the analogy of internet connection; cell-bound EEA would be the equivalent of a "wired" connection, whereas cell-free EEA would be a "wireless" connection. Moreover, the cell-bound EEA will be closely linked to the living cell's behavior, whereas the cell-free enzymes will not necessarily be related to the factors affecting the microbial cells that originally produced them, and will remain active for a prolonged period of time, away from the cell. Thus, using another analogy, we could say that the cell-attached EEA would be more closely related to an "alive" activity, whereas cell-free EEA would be in the "living dead" realm.

by cell-free enzymes (e.g., Karner and Rassoulzadegan, 1995; Baltar et al., 2010, 2016). Thus, a disconnect between rates of EEA and community composition is not surprising (D'ambrosio et al., 2014). When cell-free enzymes are responsible for a high proportion of the total EEA, a disconnection is produced between the microbes and the enzymatic activities; that is, a decoupling of *in situ* hydrolysis rates from actual microbial dynamics. Thus, a high proportion of dissolved EEA could indicate a greater importance of the history of the water mass than of the actual processes occurring at the time of sampling (Karner and Rassoulzadegan, 1995; Baltar et al., 2010, 2016; Arnosti, 2011).

Potential differences in temporal scales of activity for cell-attached and cell-free enzymes raises the question about controls on these pools of enzymes. The cell-bound EEA will be closely linked to the living cell's behavior (i.e., be affected by the same factors controlling the growth, activity and diversity of living cells). In contrast, the cell-free enzymes will not necessarily be affected by the same factors influencing the cells, but will remain active for a prolonged period of time, and probably be affected by different factors (or in a different way in response to the same factors) than the cell-bound EEA. Bearing this in mind, using another analogy, we could say that the cell-bound EEA is an activity of the "living," since that activity is performed attached to a cell which is alive, and thereby that activity will change in response to the cell's needs and in response to the cells/community dynamics (**Figure 1**). Whereas the cell-free EEA is closer to an activity of the "living dead," in the sense that it is not "alive" anymore because it is separated from the living cell, but still remains in some way "alive" in the sense that it can still perform its function when it encounters the right substrate.

However, it is important to realize that particle encounter is not necessarily the end of the line for an enzyme, and a large fraction of the cell-free enzymes may be trapped by particles including colloids or liposomes. In fact, the lifetime of cell-free enzymes can be extended if they are associated with particles (Gianfreda and Scarfi, 1991; Ziervogel et al., 2007), since surface associations can offer an improved resistance to physicochemical degradation (Lähdesmäki and Piispanen, 1992), and protection from remineralization (Lozzi et al., 2001). Evidence of bacterial cell-free enzymes embedded in an exopolymeric matrix have been reported (Decho, 1990), where cell-free EE attached to this matrix can form a complex similar to the enzyme–humic complexes in soils (Chrost, 1990). Also, some enzymes might be associated with particles due to trapping of digestive enzymes within partially degraded bacterial membranes which act as micelles (liposomes) (Nagata and Kirchman, 1992).

FATE OF THE 'LIVING DEAD' CELL-FREE EEA

The activities of extracellular enzymes control the rate at which organic matter is processed in the ocean. Given the evidence of

high activities of cell-free enzymes, understanding the controls on the lifetimes and activities of these cell-free enzymes is essential.

There are very few studies on this topic but they are already starting to reveal some of the key factors controlling the relative importance of cell-free EEA, and temperature seems to be a major one. In a Baltic Sea seasonal (1.5 y-long) study, a significant inverse relation was found between the proportion of dissolved relative to total EEA (Baltar et al., 2016). In a lab experiment, incubating microbial communities from the Great Barrier Reef waters (Australia) at three different temperatures (i.e., *in situ*, +3 and −3°C), a significant inverse relation was found again between temperature and the relative proportion of dissolved to total EEA (Baltar et al., 2017). These results are consistent with the increased observed in the proportion of dissolved relative to total EEA with depth as the temperature drops along the whole water column in a (sub) tropical Atlantic Ocean transect (Baltar et al., 2010). These studies signpost, from different angles (i.e., seasonal, climate change lab, and transect cruise studies), temperature as the main factor affecting the relative importance and activity of cell-free EEA. All those studies seem to indicate that the warmer the temperature the lower the proportion of dissolved EEA. This is also consistent with the longer lifetime of cell-free enzymes found for deep relative to the surface waters (Baltar et al., 2013).

Another factor that seems to be significantly contributing to controlling the lifetimes of cell-free enzymes is ultraviolet radiation (UVR). Very few studies are available on this topic too. The effect of UVR on cell-free enzymes directly was tested in Arctic seawater, finding that although natural illumination did not produce significant effects of photodegradation, a reduction in cell-free enzyme activity was found at artificially high UVR doses (i.e., UV-B intensity 5–10 times higher than *in situ*) (Steen and Arnosti, 2011). Interestingly, these authors found a significant effect of UVR on leucine aminopeptidase and alkaline phosphatase but not on beta-glucosidase at any treatment level. A recent study with cell-free enzymes from New Zealand waters revealed that environmentally relevant UVR irradiances reduced cell-free enzyme activities up to 87% in 36 h when compared to dark controls, likely a consequence of photodegradation (Thomson et al., 2017). This study also revealed that the magnitude of the effect of UVR on cell-free enzymes varied depending on the UVR fraction. Interestingly, consistent with the findings from Steen and Arnosti (2011), the effect of UVR differed depending on the enzyme; significantly decreasing the activity of cell-free leucine aminopeptidase and alkaline phosphatase, but not affecting β-glucosidase. This indicates that UVR (at ambient levels of radiation) can be a key factor reducing the activity (and lifetime) of cell-free enzymes (Thomson et al., 2017). Also, the fact that UVR effects vary among different enzymes indicates that UVR might change the spectrum of the EEA and thereby the composition of the resulting organic matter pool. Moreover, this effect of UVR on the cell-free EEA might help explain why the proportion of dissolved EEA tends to be lower in surface waters, and why the proportion of cell-free EEA is higher in winter and lower in summer.

More research is needed to fully constrain the factors and the mechanisms controlling the activity and lifetime of cell-free EEA as other factors, like pH, might be relevant. Moreover, the activities measured using externally-added substrates such as Leucine-MCA (7-amido-4-methylcoumarin) or MUF (4-Methylumbelliferyl)-β-glucose as substrates, reflect the activity of an unknown number/type of different enzymes that cleave the same substrate (Steen et al., 2015). Furthermore, enzymes of different primary and tertiary structure may hydrolyze the same substrate, but these enzymes would likely be susceptible to different degrees to UV radiation, heat inactivation, etc. Nevertheless, based on the evidence available thus far, and bearing in mind the projected warming ocean environment and the variable UVR light regime, it seems like there could be major changes in the activity of cell-free EEA and their contribution to organic matter remineralization in the near future.

CONCLUSION AND FUTURE OUTLOOK

It is clear now that, in any given marine location at any given time, cell-free EEA can be at least as important as cell-attached EEA. This has some strong implications on how we look and interpret many of the microbial parameters we measure since it can imply a decoupling between the community composition/function and the actual hydrolysis rates we measure. For instance, this complicates the study of functional redundancy in the marine environment if based on these extracellular enzymes, since changes in the microbial community composition might happen at a different temporal scale to the changes in EEA. Thus, it is important to consider the need to determine the cell-free fraction of EEAs (and not only the total fraction), if our aim is to link EEA to other microbial parameters.

In the near future, the advance in technology (e.g., gene- and protein-based techniques as well as organic matter characterization tools, etc.) will allow for a deeper understanding of the function and fate of cell-free EEA. For example, abundant periplasmic proteins were recently discovered using metaproteomics on seawater concentrates of the cell-free fraction (Xie et al., 2017). Based on that, these authors suggested that free proteins released from microbes could be important to ecosystem function (Xie et al., 2017). They admitted not having a clear explanation for the high presence of periplasmic proteins in the "non-bacterial" world. But, having in mind what has been discussed in this article, it is possible that many of those so-called "non-bacterial world" proteins by Xie et al. (2017) could indeed be cell-free (here described as "living dead") extracellular enzymes. This is an example of how the use of novel technologies can help to make new discoveries in this field. However, we should not only focus on the development of new technologies but also complement those with the use of classical rate measurements. A more refined characterization of the DOM pool (e.g., LC–MS/MS) coupled with a combined determination of hydrolysis rates and gene/protein expression might open new avenues and discoveries in this field of research. Furthermore, these kinds of experiments, performed under

different anthropogenic stressors, might also help elucidate how the role of these enzymes might change in response to different climatic scenarios. These studies will probably confirm that the 'engines' of the marine biogeochemical cycles are not only the microbial cells but that there are other processes taking place away from cells which are also an important part of that engine.

To conclude, the findings discussed in this article advocate for the need to go beyond the "living things," – and study not only how the living cells/organisms will respond to anthropogenic perturbations, but also how the "living dead" cell-free active molecules will, if we really aim to fully constrain the future of marine biogeochemical cycles.

AUTHOR CONTRIBUTIONS

The author confirms being the sole contributor of this work and approved it for publication.

ACKNOWLEDGMENTS

FB was supported by a Rutherford Discovery Fellowship (Royal Society of New Zealand). The author would like to acknowledge the support and insightful comments of the reviewers, which clearly helped improve the overall merit of the manuscript.

REFERENCES

Albertson, N. H., Nyström, T., and Kjelleberg, S. (1990). Exoprotease activity of two marine bacteria during starvation. *Appl. Environ. Microbiol.* 56, 218–223.

Alderkamp, A. C., Rijssel, M. V., and Bolhuis, H. (2007). Characterization of marine bacteria and the activity of their enzyme systems involved in degradation of the algal storage glucan laminarin. *FEMS Microbiol. Ecol.* 59, 108–117. doi: 10.1111/j.1574-6941.2006.00219.x

Allison, S. D. (2005). Cheaters, diffusion and nutrients constrain decomposition by microbial enzymes in spatially structured environments. *Ecol. Lett.* 8, 626–635. doi: 10.1111/j.1461-0248.2005.00756.x

Allison, S. D., Chao, Y., Farrara, J. D., Hatosy, S., and Martiny, A. (2012). Fine-scale temporal variation in marine extracellular enzymes of coastal southern California. *Front. Microbiol.* 3:301. doi: 10.3389/fmicb.2012.00301

Arnosti, C. (2011). Microbial extracellular enzymes and the marine carbon cycle. *Annu. Rev. Mar. Sci.* 3, 401–425. doi: 10.1146/annurev-marine-120709-142731

Baltar, F., Arístegui, J., Gasol, J. M., Sintes, E., Aken, H. M. V., and Herndl, G. J. (2010). High dissolved extracellular enzymatic activity in the deep central Atlantic Ocean. *Aquat. Microb. Ecol.* 58, 287–302. doi: 10.3354/ame01377

Baltar, F., Arístegui, J., Gasol, J. M., Yokokawa, T., and Herndl, G. J. (2013). Bacterial versus archaeal origin of extracellular enzymatic activity in the Northeast Atlantic Deep Waters. *Microb. Ecol.* 65, 277–288. doi: 10.1007/s00248-012-0126-7

Baltar, F., Arístegui, J., Sintes, E., van Aken, H. M., Gasol, J. M., and Herndl, G. J. (2009). Prokaryotic extracellular enzymatic activity in relation to biomass production and respiration in the meso- and bathypelagic waters of the (sub)tropical Atlantic. *Environ. Microbiol.* 11, 1998–2014. doi: 10.1111/j.1462-2920.2009.01922.x

Baltar, F., Legrand, C., and Pinhassi, J. (2016). Cell-free extracellular enzymatic activity is linked to seasonal temperature changes: a case study in the Baltic Sea. *Biogeosciences* 13, 2815–2821. doi: 10.5194/bg-13-2815-2016

Baltar, F., Morán, X. A. G., and Lønborg, C. (2017). Warming and organic matter sources impact the proportion of dissolved to total activities in marine extracellular enzymatic rates. *Biogeochemistry* 133, 307–316. doi: 10.1007/s10533-017-0334-9

Benner, R., and Amon, R. M. (2015). The size-reactivity continuum of major bioelements in the ocean. *Annu. Rev. Mar. Sci.* 7, 185–205. doi: 10.1146/annurev-marine-010213-135126

Bochdansky, A. B., Puskaric, S., and Herndl, G. J. (1995). Influence of zooplankton grazing on free dissolved enzymes in the sea. *Mar. Ecol. Prog. Ser.* 121, 53–63. doi: 10.3354/meps121053

Chrost, R. J. (1990). "Microbial ectoenzymes in aquatic environments," in *Aquatic Microbial Ecology. Biochemical and Molecular Approaches*, eds J. Overbeck and R. J. Chróst (New York, NY: Springer), 47–78.

Chrost, R. J., and Rai, H. (1993). Ectoenzyme activity and bacterial secondary production in nutrient-improverished and nutrient-enriched mesocosms. *Microb. Ecol.* 25, 131–150. doi: 10.1007/BF00177191

Cuskin, F., Lowe, E. C., Temple, M. J., Zhu, Y., Cameron, E. A., Pudlo, N. A., et al. (2015). Human gut bacteroidetes can utilize yeast mannan through a selfish mechanism. *Nature* 517, 165–169. doi: 10.1038/nature13995

Daily, G. (2003). "What are ecosystem services," in *Global Environmental Challenges for the Twenty-First Century: Resources, Consumption and Sustainable Solutions*, ed. D. E. Lorey (Lanham, MD: Rowman & Littlefield), 227–231.

D'ambrosio, L., Ziervogel, K., Macgregor, B., Teske, A., and Arnosti, C. (2014). Composition and enzymatic function of particle-associated and free-living bacteria: a coastal/offshore comparison. *ISME J.* 8, 2167–2179. doi: 10.1038/ismej.2014.67

Decho, A. W. (1990). Microbial exopolymers secretions in ocean environments: their role(s) in food webs and marine processes. *Oceanogr. Mar. Biol. Ann. Rev.* 28, 73–153.

Drescher, K., Nadell, C. D., Stone, H. A., Wingreen, N. S., and Bassler, B. L. (2014). Solutions to the public goods dilemma in bacterial biofilms. *Curr. Biol.* 24, 50–55. doi: 10.1016/j.cub.2013.10.030

Duhamel, S., Dyhrman, S. T., and Karl, D. M. (2010). Alkaline phosphatase activity and regulation in the North Pacific Subtropical Gyre. *Limnol. Oceanogr.* 55, 1414–1425. doi: 10.4319/lo.2010.55.3.1414

Falkowski, P. G., Fenchel, T., and Delong, E. F. (2008). The microbial engines that drive Earth's biogeochemical cycles. *Science* 320, 1034–1039. doi: 10.1126/science.1153213

Gianfreda, L., and Scarfi, M. R. (1991). Enzyme stabilization: state of the art. *Mol. Cell. Biochem.* 100, 97–108. doi: 10.1007/BF00234161

Harley, C. D., Randall Hughes, A., Hultgren, K. M., Miner, B. G., Sorte, C. J., Thornber, C. S., et al. (2006). The impacts of climate change in coastal marine systems. *Ecol. Lett.* 9, 228–241. doi: 10.1111/j.1461-0248.2005.00871.x

Hoppe, H.-G., Arnosti, C., and Herndl, G. J. (2002). "Ecological significance of bacterial enzymes in the marine environment," in *Enzymes in the Environment: Activity, Ecology, and Applications*, eds R. G. Burns and R. P. Dick (New York. NY: Marcel Dekker, Inc), 73–108.

Hoppe, H.-G., and Ullrich, S. (1999). Profiles of ectoenzymes in the Indian Ocean: phenomena of phosphatase activity in the mesopelagic zone. *Aquat. Microb. Ecol.* 19, 139–148. doi: 10.3354/ame019139

Hutchins, D. A., and Fu, F. (2017). Microorganisms and ocean global change. *Nat. Microbiol.* 2:17058. doi: 10.1038/nmicrobiol.2017.58

Karner, M., and Rassoulzadegan, F. (1995). Extracellular enzyme activity: indications for high short-term variability in a coastal marine ecosystem. *Microb. Ecol.* 30, 143–156. doi: 10.1007/BF00172570

Lähdesmäki, P., and Piispanen, R. (1992). Soil enzymology: role of protective colloid systems in the preservation of exoenzyme activities in soil. *Soil Biol. Biochem.* 24, 1173–1177. doi: 10.1016/0038-0717(92)90068-9

Li, H., Veldhuis, M. J. W., and Post, A. F. (1998). Alkaline phosphatase activities among planktonic communities in the northern Red Sea. *Mar. Ecol. Prog. Ser.* 173, 107–115. doi: 10.3354/meps173107

Lozzi, I., Calami, L., Fusi, P., Bosetto, M., and Stotzky, G. (2001). Interaction of horseradish peroxidase with montmorillonite homoionic to Na+ and Ca2+: effects on enzymatic activity and microbial degradation. *Soil Biol. Biochem.* 33, 1021–1028. doi: 10.1016/S0038-0717(01)00005-0

Nagata, T., and Kirchman, D. L. (1992). Release of macromolecular organic complexes by heterotrophic marine flagellates. *Mar. Ecol. Progr. Ser.* 83, 233–240. doi: 10.3354/meps083233

Rego, J. V., Billen, G., Fontigny, A., and Someville, M. (1985). Free and attached proteolytic activity in water environments. *Mar. Ecol. Progr. Ser.* 21, 245–249. doi: 10.3354/meps021245

Reintjes, G., Arnosti, C., Fuchs, B. M., and Amann, R. (2017). An alternative polysaccharide uptake mechanism of marine bacteria. *ISME J.* 11, 1640–1650. doi: 10.1038/ismej.2017.26

Steen, A. D., and Arnosti, C. (2011). Long lifetimes of beta-glucosidase, leucine aminopeptidase, and phosphatase in Arctic seawater. *Mar. Chem.* 123, 127–132. doi: 10.1016/j.marchem.2010.10.006

Steen, A. D., Vazin, J. P., Hagen, S. M., Mulligan, K. H., and Wilhelm, S. W. (2015). Substrate specificity of aquatic extracellular peptidases assessed by competitive inhibition assays using synthetic substrates. *Aquat. Microb. Ecol.* 75, 271–281. doi: 10.3354/ame01755

Thomson, B., Hepburn, C. D., Lamare, M., and Baltar, F. (2017). Temperature and UV light affect the activity of marine cell-free enzymes. *Biogeosciences* 14, 3971–3977. doi: 10.5194/bg-14-3971-2017

Traving, S. J., Thygesen, U. H., Riemann, L., and Stedmon, C. A. (2015). A model of extracellular enzymes in free-living microbes: which strategy pays off? *Appl. Environ. Microbiol.* 81, 7385–7393. doi: 10.1128/AEM.02070-15

Vetter, Y. A., and Deming, J. W. (1999). Growth rates of marine bacterial isolates on particulate organic substrates solubilized by freely released extracellular enzymes. *Microb. Ecol.* 37, 86–94. doi: 10.1007/s002489900133

Vetter, Y. A., Deming, J. W., Jumars, P. A., and Krieger-Brockett, B. B. (1998). A predictive model of bacterial foraging by means of freely released extracellular enzymes. *Microb. Ecol.* 36, 75–92. doi: 10.1007/s002489900095

Weiss, M., Abele, U., Weckesser, J., Welte, W., Schiltz, E., and Schulz, G. E. (1991). Molecular architecture and electrostatic properties of bacterial porin. *Science* 254, 1627–1630. doi: 10.1126/science.1721242

Xie, Z.-X., Chen, F., Zhang, S.-F., Wang, M.-H., Zhang, H., Kong, L.-F., et al. (2017). Metaproteomics of marine viral concentrates reveals key viral populations and abundant periplasmic proteins in the oligotrophic deep chlorophyll maximum of the South China Sea. *Environ. Microbiol.* doi: 10.1111/1462-2920.13937 [Epub ahead of print].

Ziervogel, K., Karlsson, E., and Arnosti, C. (2007). Surface associations of enzymes and of organic matter: consequences for hydrolytic activity and organic matter remineralization in marine systems. *Mar. Chem.* 104, 241–252. doi: 10.1016/j.marchem.2006.12.001

Ziervogel, K., Steen, A. D., and Arnosti, C. (2010). Changes in the spectrum and rates of extracellular enzyme activities in seawater following aggregate formation. *Biogeosciences* 7, 1007–1015. doi: 10.5194/bg-7-1007-2010

Conflict of Interest Statement: The author declares that the research was conducted in the absence of any commercial or financial relationships that could be construed as a potential conflict of interest.

frontiers in Marine Science

ORIGINAL RESEARCH
published: 23 June 2017
doi: 10.3389/fmars.2017.00200

Heterotrophic Extracellular Enzymatic Activities in the Atlantic Ocean Follow Patterns Across Spatial and Depth Regimes

Adrienne Hoarfrost and Carol Arnosti*

Department of Marine Sciences, University of North Carolina at Chapel Hill, Chapel Hill, NC, United States

Heterotrophic microbial communities use extracellular enzymes to initialize degradation of high molecular weight organic matter in the ocean. The potential of microbial communities to access organic matter, and the resultant rates of hydrolysis, affect the efficiency of the biological pump as well as the rate and location of organic carbon cycling in surface and deep waters. In order to investigate spatial- and depth-related patterns in microbial enzymatic capacities in the ocean, we measured hydrolysis rates of six high-molecular-weight polysaccharides and two low-molecular-weight substrate proxies at sites spanning 38°S to 10°N in the Atlantic Ocean, and at six depths ranging from surface to bottom water. In surface to upper mesopelagic waters, the spectrum of substrates hydrolyzed followed distinct patterns, with hydrolytic assemblages more similar vertically within a single station than at similar depths across multiple stations. Additionally, the proportion of total hydrolysis occurring above the pycnocline, and the spectrum of substrates hydrolyzed in mesopelagic and deep waters, was positively related to the strength of stratification at a site, while other physichochemical parameters were generally poor predictors of the measured hydrolysis rates. Spatial as well as depth-driven constraints on heterotrophic hydrolytic capacities result in broad variations in potential carbon-degrading activity in the ocean. The spectrum of enzymatic capabilities and rates of hydrolysis in the ocean, and the proportion of organic carbon hydrolyzed above the permanent thermocline, may influence the efficiency of the biological pump and net carbon export across distinct latitudinal and depth regions.

Keywords: carbon cycling, extracellular enzymes, heterotrophy, functional biogeography, deep ocean, microbial activity, biogeochemistry

OPEN ACCESS

Edited by:
Maria Montserrat Sala, Consejo Superior de Investigaciones Científicas(CSIC),Spain

Reviewed by:
Hila Elifantz, Bar-Ilan University, Israel
Zhanfei Liu, University of Texas at Austin, United States

****Correspondence:***
Adrienne Hoarfrost
adrienne.l.hoarfrost@unc.edu

Specialty section:
This article was submitted to Aquatic Microbiology, a section of the journal Frontiers in Marine Science

Received: *12 April 2017*
Accepted: *12 June 2017*
Published: *23 June 2017*

Citation:
Hoarfrost A and Arnosti C (2017) Heterotrophic Extracellular Enzymatic Activities in the Atlantic Ocean Follow Patterns Across Spatial and Depth Regimes. Front. Mar. Sci. 4:200. doi: 10.3389/fmars.2017.00200

INTRODUCTION

Microbial communities are major drivers of organic carbon cycling in the ocean. The carbon cycling capacities of these communities ultimately affect the inventories of oxygen and CO_2 in the atmosphere, the magnitude and composition of organic carbon export from the surface to the deep ocean, and resource availability to higher trophic levels (Azam and Malfatti, 2007; Jiao et al., 2010). Although 99.9% of autochthonous organic carbon is remineralized before it reaches sediments, a large standing pool of dissolved organic carbon (DOC) persists in the water column (Hedges, 1992),

demonstrating that some fraction of marine organic carbon is not readily amenable to microbial degradation. The microbial enzymatic capacities to access organic carbon is a potentially important driver shaping the ocean carbon reservoir, but the factors that determine whether and how much organic matter is remineralized are poorly understood (Arnosti, 2011). Biogeographical patterns in microbial communities and their enzymatic capacities (Arnosti et al., 2012; Gomez-Pereira et al., 2012; Sunagawa et al., 2015), and their net effect on organic carbon transformations in the ocean, may in turn be shaped by a poorly constrained set of factors (Hanson et al., 2012).

The enzymatic capacity of a microbial community is a critical determinant of the breadth of organic compounds which may be recycled. Most organic carbon is biosynthesized as high molecular weight compounds, which are typically hydrolyzed by both endo-acting (mid-chain cleaving) and exo-acting enzymes (Warren, 1996). In order for heterotrophs to access natural organic matter, they must produce the appropriate enzymes to hydrolyze a particular substrate into sizes small enough to be transported into the cell. These enzymes have highly targeted structural specificities and are very diverse (Aspeborg et al., 2012; Teeling et al., 2012), reflecting both the complexity of natural organic matter and of the microbial communities that access it.

Differences in microbial enzymatic capacities thus may result in functional biogeographical patterns in carbon export and recycling. Field studies measuring activities of extracellular enzymes that degrade organic carbon have demonstrated that the types of substrates hydrolyzed and their rates of hydrolysis vary along latitudinal gradients (Arnosti et al., 2011, 2012), a pattern that parallels biogeographical patterns in microbial community composition (Fuhrman et al., 2008). Beyond community composition, the genetic capacity to hydrolyze individual substrates may also follow biogeographical patterns. Although, most of the enzymes involved in the extracellular breakdown of organic carbon have not yet been annotated, a targeted study of the biogeography of enzymes in glycosyl hydrolase family 5 revealed wide diversity and variation in relative abundance across the North Atlantic (Elifantz et al., 2008). Genetic distributions of polysaccharide-degrading enzymes in common heterotrophic marine microbial clades also vary considerably across oceanic provinces (Gomez-Pereira et al., 2012), as do the activities of polysaccharide hydrolyzing enzymes (Arnosti et al., 2012).

Organic carbon cycling capabilities are thus heterogeneously distributed across both microbial phylogenies (Zimmerman et al., 2013) and the natural environment. In order to examine latitudinal and depth-related patterns in hydrolytic capabilities of heterotrophic microbial communities, we measured extracellular enzyme activities across a broad range of latitude and depth, identified geospatial patterns in those activities, and investigated potential environmental factors affecting heterotrophic enzymatic activity. The hydrolysis of six high-molecular-weight and two low-molecular-weight organic substrates was measured across 48 degrees of latitude and from surface to bottom waters in the South and Equatorial Atlantic Ocean. These data enable us to explore the connectivity of hydrolytic capacities between stations and depths, and the relationship of hydrolysis rates to stratification and physicochemical parameters. These factors may shape biogeographical patterns in heterotrophy, and ultimately affect the location and magnitude of organic carbon remineralization, and thus carbon sequestration, by the biological pump.

METHODS

Seawater Sampling

Seawater was collected via Niskin rosette equipped with a conductivity-temperature-depth sensor (CTD) at nine stations spanning 38°S to 10°N in the subtropical to equatorial Atlantic Ocean (**Figure 1**). Hydrolysis rates of polysaccharides and of monomeric substrates were measured at 6 stations, ranging from 38°S to 3.5°N; only activities of monomeric substrates could be measured at the northernmost three stations due to lack of time for extended substrate incubations.

At each station (stations 2, 4, 7, 10, 15, 18, 21, 22, and 23; part of the DeepDOM cruise, Kujawinski, 2013), seawater was collected from six depths: surface (SuW, 5 m), deep chlorophyll maximum (DCM, ∼50–100 m), mesopelagic (meso, 250 m), Antarctic Intermediate Water (AAIW, ∼750–850 m), North Atlantic Deep Water (NADW, 2,500 m), and bottom water (bot, ∼3,700–4,600 m). Specific depths of DCM, AAIW, and bottom water were chosen according to a maximum in fluorescence (DCM), a minimum in salinity and peak in oxygen (AAIW), and a few meters above bottom (bot), respectively (Supplementary Figure 1), and thus varied by station.

At each depth, 1 L glass Duran bottles were rinsed three times with seawater from the corresponding depth, then filled without using tubing from a single Niskin bottle. 200 mL of seawater from each depth was autoclaved in a separate glass Duran bottle for use in killed control incubations.

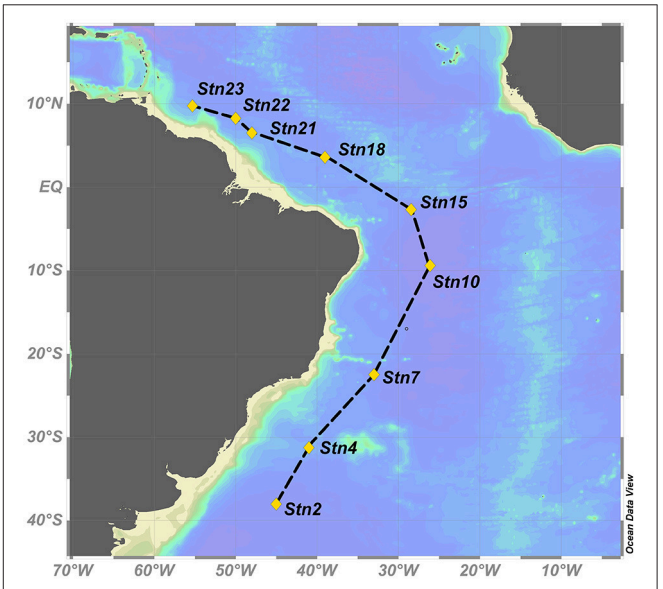

FIGURE 1 | Map of DeepDOM cruise track from 38S to 9N in the South Atlantic. Figure made in Ocean Data View Schlitzer, 2015.

Physical and Chemical Parameters

Temperature, salinity, oxygen, and fluorescence were measured via CTD (Supplementary Figure 1), and used to calculate potential temperature (θ), potential density (σ_θ), and buoyancy frequency (N^2) (Supplementary Figure 2). CTD data for every cast throughout the cruise, and nutrient data collected from discrete depths and analyzed by K. Longnecker, are available through the BCO-DMO database (Supplementary Figure 1, Kujawinski, 2013). CTD and nutrient data used for analysis in this study are provided through the associated BCO-DMO repository (Hoarfrost and Arnosti, 2016), and can be reproduced using scripts provided at the associated Github repository (Hoarfrost, 2016).

α-Glucosidase and Leucine Aminopeptidase Activities

Two substrate proxies, α- glucose linked to 4-methylumbelliferone (α-Glu; Chem Impex 21676) and leucine linked to 4-methylcoumarinyl-7-amide (L-MCA; Sigma 62480-44-8), were used to measure the activities of α-glucosidase and leucine aminopeptidase, respectively, after the method of Hoppe (1983). The enzymes hydrolyzing these substrates act on the α-1→4-linked terminal glucose of oligo- and polysaccharides, and N-terminal leucine residues of peptides or proteins, respectively. Recent work has demonstrated that L-MCA can also be hydrolyzed by enzymes other than leucine aminopeptidase (Steen et al., 2015), but this widely-used method still provides a measure of peptidase activity in the environment. For each substrate, triplicate aliquots of 4mL of live seawater and one autoclaved seawater killed control were incubated in plastic cuvettes at as close to *in situ* temperature as possible. Available incubation temperatures were 3, 12, 15, 18, 25, and 28°C. Two cuvettes with 4 mL of live or autoclaved seawater and no added substrate served as live and killed blank incubations, respectively.

Saturating concentrations were determined at each station via a saturation curve conducted over 24 h using surface water, testing increasing concentrations of substrate. The saturating concentration was identified as the concentration of substrate at which addition of higher concentrations of substrate does not induce higher rates of activity. Since enzymatic activity is typically highest in surface or near-surface waters (e.g., Baltar et al., 2009; Steen et al., 2012), and leucine aminopeptidase activity is typically higher than α-glucosidase activity (Baltar et al., 2010, 2013), saturation concentrations determined for leucine-MCA in surface waters were used for all depths and substrates at each station. Substrates were added at saturating concentrations 100 μM at stations 2, 4, and 7; 75 μM at stations 10, 15, 18, 22, and 23; and 50 μM at station 21.

Incubations were sampled at four timepoints, and fluorescence was measured in a Turner Biosystems spectrophotometer (TBS-380). Later timepoints were chosen based on the rate of activity at earlier timepoints. A typical timecourse for a rapidly-hydrolyzed substrate was 6, 12, and 24 h; for a low- to no-hydrolysis substrate, 24, 48, and 72 h. No incubation was sampled later than 72 h. All incubations were sampled at 24 h to provide a common timepoint reference.

Rates reported here are maximum hydrolysis rates, typically at T3 for α-glucosidase and at T1 for leucine aminopeptidase. T3 for α-glucosidase was typically sampled at 36–48 h in shallow, more active waters, or 60–72 h in deeper, less active waters. T1 for leucine aminopeptidase was typically sampled at 4–6 h in shallow waters, or 24 h in deeper waters. α-glucosidase activities sampled at later timepoints may include a growth response, whereas the shorter timecourse of leucine aminopeptidase incubations likely does not include a growth response. In all cases, rates represent potential hydrolysis rates, since added substrate competes with naturally-occurring substrate for enzyme active sites.

Polysaccharide Hydrolysis Measurements

Activities of extracellular enzymes that hydrolyze six different fluorescently labeled polysaccharides were measured at all six depths between 38°S and 3.5°N. These substrates—arabinogalactan, chondroitin sulfate, fucoidan, laminarin, pullulan, and xylan—were chosen for their diverse monosaccharide compositions and macromolecular structures. All of these polysaccharides are found in marine environments, and/or enzymes and genes corresponding to their hydrolysis have been identified in marine prokaryotes (e.g., Alderkamp et al., 2007; Wegner et al., 2013; Xing et al., 2015). Furthermore, the activities of enzymes hydrolyzing these substrates have been detected in a wide variety of marine environments (e.g., Arnosti, 2008; Arnosti et al., 2009, 2011).

Fluorescently-labeled polysaccharides were prepared after the method of Arnosti (1996, 2003). Each polysaccharide was incubated in triplicate live incubations in 17 mL sterilized glass vials, and one killed control incubation using autoclaved seawater. In addition, incubations without substrate with live seawater and autoclaved seawater were used as live and killed blank controls, respectively. Seawater was sterilized for 20 min in an autoclave upon recovery and incubations initiated after autoclaved water had cooled in an ice bath. Substrate was added at concentrations sufficient to detect fluorescence of the substrate, at 3.5 μM monomer-equivalent concentrations in all cases, except for fucoidan, which was added at a concentration of 5 μM due to its lower fluorescence intensity. Substrate addition is kept to the lowest concentration that is technically feasible in order to minimize growth responses due to added substrate. All samples were incubated at as close to *in situ* temperature as possible.

Each incubation was sampled at four timepoints: 0, 5, 12, and 21 days. Kill and live blank controls were sampled at T_0 and T_{final} only. Due to time constraints, at Station 15 the final timepoint was taken at day 20 instead of 21, and at Station 18 only three timepoints were collected, at 0, 5, and 12 days. At each timepoint, ∼1.8 mL was withdrawn from each incubation, filtered through a 0.2 μm pore-size syringe filter and stored at −20°C until analysis.

Enzyme activity was measured by tracking hydrolysis of the high-molecular-weight substrate into lower-molecular-weight hydrolysis products over time, as determined using gel permeation chromatography with fluorescence detection (Arnosti, 1996, 2003). Hydrolysis rates were calculated from these shifts in molecular size distribution over time

from the size-separated chromatograms using the scripts hosted at the associated Github repository (Hoarfrost, 2016). Chromatograms were manually curated after processing to verify chromatographic changes and to identify incubations with zero activity or non-hydrolytic fluorescence of the free fluorophore label, which can produce artificially high hydrolysis rates. Those incubation sets were tagged and their calculated rates adjusted by setting the activity to zero, or recalculating the rate while neglecting the free fluorophore portion of the chromatogram, respectively.

Statistical Analyses

Polysaccharide Hydrolytic Diversity Using Shannon Diversity Indices

Shannon indices, which reflect both the number of substrates hydrolyzed as well as the evenness of hydrolysis rates, were used to calculate hydrolytic diversity at all sites (Steen et al., 2010). The Shannon index is expressed as $H = -\sum_{i=1}^{n} p_i \ln(p_i)$, where n is the total number of substrates and p_i is the hydrolysis rate of the ith substrate normalized to the summed hydrolysis rate of all substrates at that site. H is equal to zero when only one substrate is hydrolyzed, and is maximal at 1.79 when all six substrates are hydrolyzed at equal rates.

Hydrolytic Compositional Dissimilarity among Sampling Sites Using Bray-Curtis Dissimilarity

The Bray-Curtis Dissimilarity, BC, is used to describe the compositional dissimilarity between two sites (Bray and Curtis, 1957). As applied here, "composition" is defined as the hydrolytic composition, or the assemblage of substrates hydrolyzed and their relative rates of hydrolysis. BC is a unitless index between 0 and 1, with a minimum of 0 when the two sites have exactly the same composition (e.g., all the same substrates are hydrolyzed at the same rate), and a maximum of 1 when none of the same substrates are hydrolyzed at the two sites. The pairwise BC dissimilarity matrix was calculated between every site with every other site.

The Bray-Curtis Dissimilarity between two sites i and j is calculated as $BC_{ij} = 1 - \frac{2C_{ij}}{S_i + S_j}$, where C_{ij} is the sum of the lesser hydrolysis rates for only those substrates that were hydrolyzed at both sites i and j, and S_i and S_j are the total hydrolysis rates at site i and site j respectively.

Multiple Regression Analysis of Environmental Parameters vs. Hydrolytic Activity

Multivariate linear regression models between polysaccharide hydrolysis rates and up to ten environmental parameters—*in situ* potential temperature, incubation temperature, salinity, oxygen, chlorophyll a, buoyancy frequency, phosphate, total nitrogen, DOC, and silicate—were generated. By testing several permutations of models considering different combinations of environmental parameters, the best fit multiple regression model was selected by manually maximizing correlation coefficient values (Supplementary Table 1).

Reproducibility

The scripts to process the GPC chromatograms and calculate rates, manipulate physicochemical data, perform statistical analyses, and generate the figures in this paper were all written in the R programming language (R Core Team, 2014), and can be reproduced using the scripts hosted at the associated Github repository (Hoarfrost, 2016). The raw data is hosted on BCO-DMO (Hoarfrost and Arnosti, 2016), and instructions to download raw data and run scripts can also be found in the Readme for the Github repository.

RESULTS

Physical Context and Water Masses

The transect covered a broad range of latitude and physicochemical conditions, as well as several distinct water masses (Supplementary Figures 1, 3). Antarctic Intermediate Water (AAIW) flowing south to north was detectable as a minimum in salinity at ca. 750–850 m depth throughout the transect. North Atlantic Deep Water (NADW) flowing north to south was identified as a maximum in oxygen between ca. 1500–4,000 m water depth. A large circulation-driven oxygen minimum zone encompassed stations 10–23. At the southernmost station sampled, station 2, the influence of Antarctic circulation was still apparent, with circumpolar deep waters bounding NADW above and below, and Antarctic Bottom Water (AABW, detectable as a temperature minimum) in the bottom water sample (Supplementary Figures 1, 3). At the northernmost station (station 23), the Amazon River plume was sampled in surface waters, detectable by a sharp halocline. The strength of the pycnocline generally increased from south to north, such that the southernmost stations were less stratified than the northernmost stations (Supplementary Figures 2, 4). A south to north gradient in chlorophyll a concentrations was also evident at the deep chlorophyll maximum, which increased from ca. 0.242 mg m^{-3} at station 2 to over 1 mg m^{-3} at station 15 (Kujawinski, 2013). DOC concentrations ranged from ca. 70–82 μM in surface, ca. 62–77 μM in DCM, and ca. 47–58 μM in mesopelagic depths, and did not directly track chlorophyll a concentrations (Kujawinski, 2013).

Polysaccharide Hydrolysis Rates and Patterns

Polysaccharide hydrolysis rates and patterns varied across depths as well as stations, as evident for individual substrates (**Figure 2**), by the summed hydrolysis rates (Supplementary Figure 5), and by the diversity of substrates hydrolyzed at a given depth (**Figure 3**). Some polysaccharides—such as laminarin—were hydrolyzed at nearly every station and depth, whereas fucoidan was not measurably hydrolyzed at any site, and arabinogalactan was hydrolyzed only in surface waters of station 15. Chondroitin, pullulan, and xylan were hydrolyzed only at particular stations and depths: chondroitin was the only substrate other than laminarin hydrolyzed below 250 m, but at some stations it was not hydrolyzed at any depths. Pullulan was hydrolyzed only

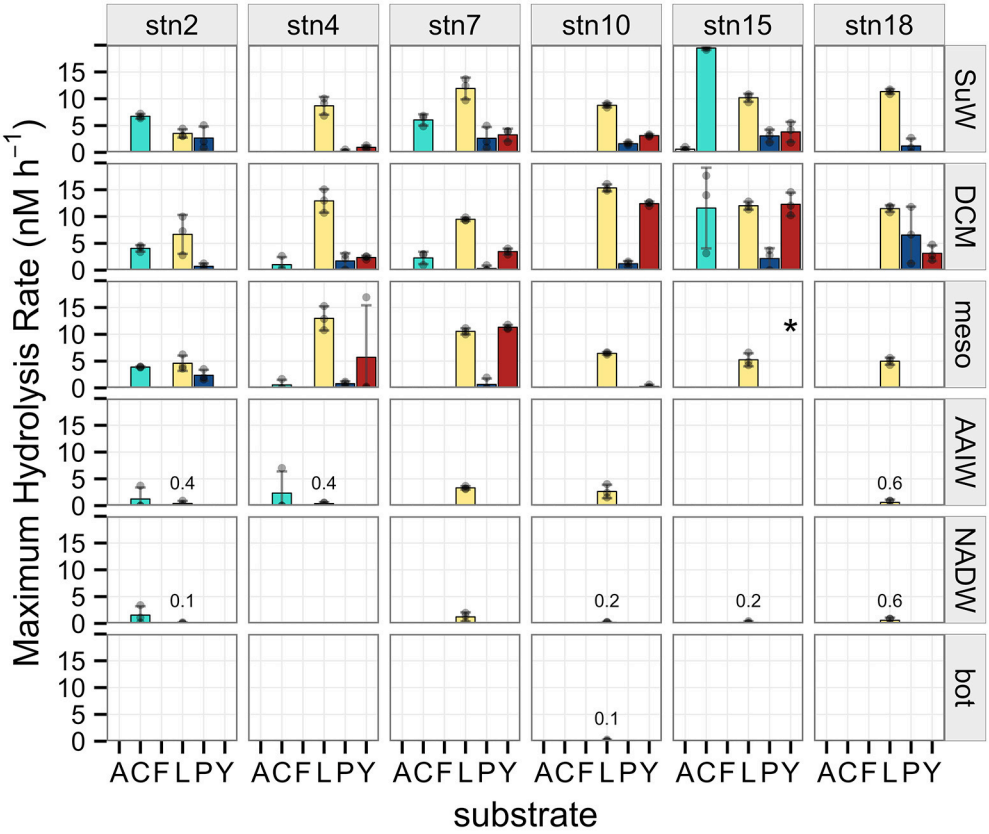

FIGURE 2 | Maximum potential hydrolysis rate (nM h^{-1}) of the six polysaccharide substrates arabinogalactan (A), chondroitin sulfate (C), fucoidan (F), laminarin (L), pullulan (P), and xylan (Y) at each station (vertical panels) and each depth (horizontal panels). Error bars indicate standard deviation of experimental triplicates. Missing data at stn 15, mesopelagic depth for the xylan substrate indicated by asterisk. Low, non-zero hydrolysis rates in deep waters indicated by numbers in the figure panel.

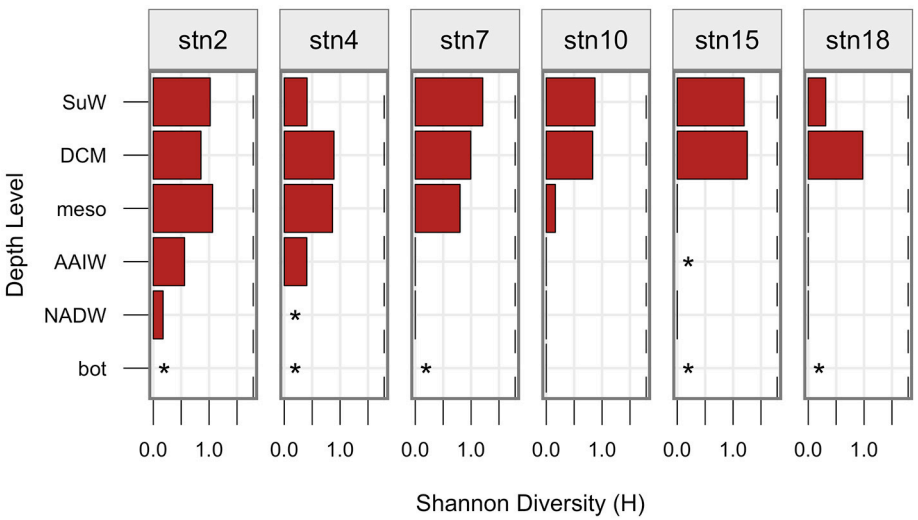

FIGURE 3 | Shannon diversity, H, at each station (vertical panels) and each depth surface to bottom (y axis). A shannon diversiy of zero is indicated by a straight line, whereas asterisks indicate H was not calculated due to no detectable hydrolysis at that site. The maximum possible value of H, 1.79, is shown as a dashed line.

above the pycnocline, while xylan was also hydrolyzed in shallow waters but only at some stations (**Figure 2**).

Hydrolysis rates (**Figure 2**) and summed hydrolysis rates (Supplementary Figure 5) decreased with depth. This decrease was more abrupt and occurred at shallower depths at more stratified stations, with most hydrolytic activity occurring in the surface and DCM depths. At less stratified stations (where maximum buoyancy frequency in the water column was lower), hydrolytic activities decreased more gradually with depth (**Figure 2**), and a greater proportion of summed activity occurred below the pycnocline (**Figure 4**, $R^2 = 0.66$, $P = 0.048$).

The transect covered a gradient in water column productivity (as represented by chlorophyll a fluorescence) and in water column stratification. At the more northerly stations where stratification was stronger and chlorophyll a concentrations were higher, the highest hydrolytic diversity and rates of enzymatic activity were measured. Additionally, the depth at which the highest hydrolysis rate was observed at a particular station was at shallower depths at northerly, more stratified stations than at southerly, less stratified stations (**Figure 4**, **Figure 2**, Supplementary Figure 5).

Hydrolytic diversity also decreased with depth from shallow to deeper waters (**Figure 3**), and sites with higher overall rates of activity also had higher hydrolytic diversity (Supplementary Figure 6). Maximum hydrolytic diversity was typically measured at the surface or DCM, although station 2 exhibited highest hydrolytic diversity at mesopelagic depths, probably because the same assemblage of substrates was hydrolyzed at surface, DCM, and mesopelagic depths at station 2, but with different degrees of evenness.

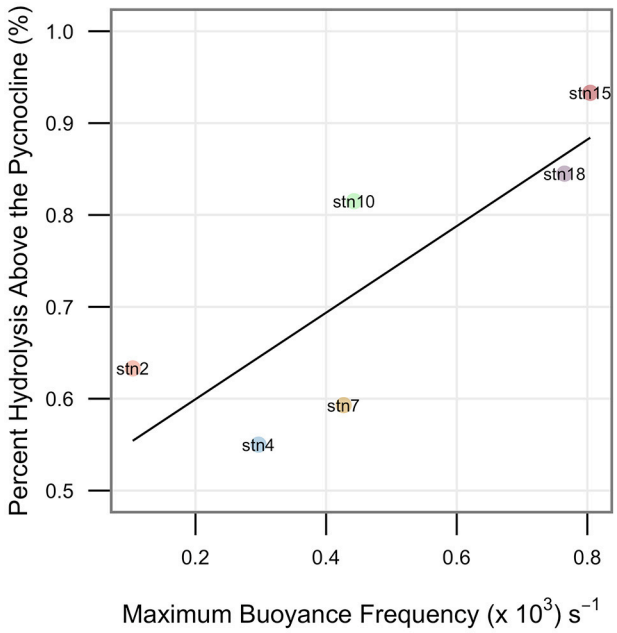

FIGURE 4 | Percent of hydrolysis occurring above the pycnocline at each station is positively correlated with the maximum buoyancy frequency at that station. $R^2 = 0.66$, $P = 0.048$.

In the upper 250 m of the water column, the assemblage of polysaccharide substrates hydrolyzed at a given station followed distinct patterns. Comparing Bray-Curtis dissimilarities among surface, DCM, and mesopelagic depths for each station, hydrolytic assemblages clustered strongly when grouped by station (**Figure 5A**, PERMANOVA $P = 0.007$). This result contrasted with grouping by depth sampled, which did not produce any distinguishable effect on Bray-Curtis distances between assemblages (**Figure 5B**, PERMANOVA $P = 0.399$). A similar analysis could not be done for the full depth range due to the lack of any detectable hydrolytic activity at many of the deeper depths.

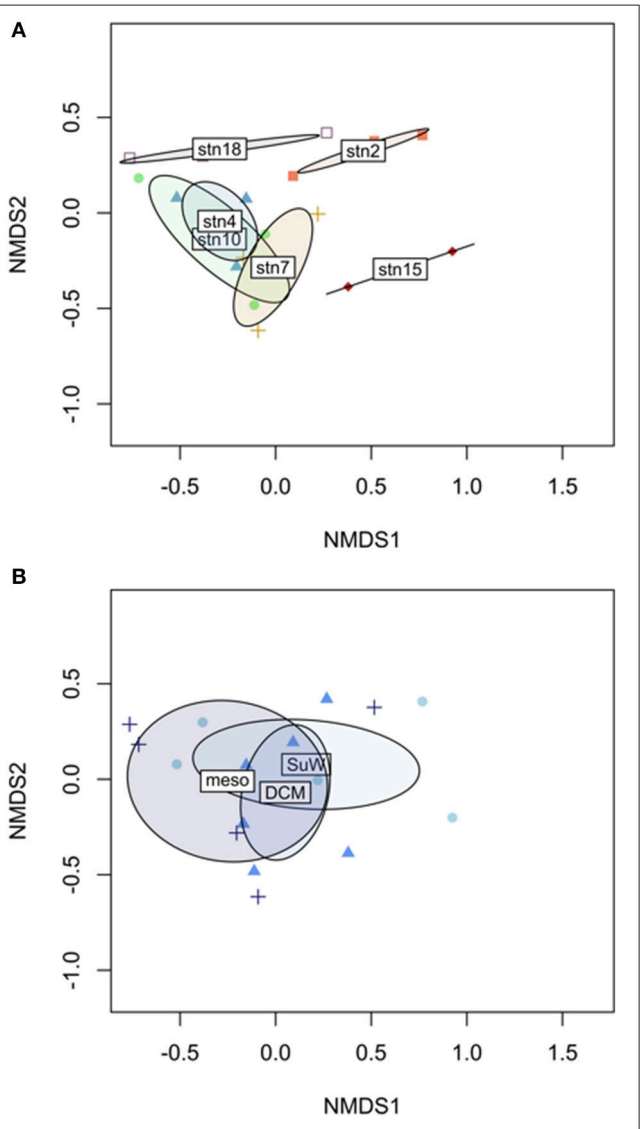

FIGURE 5 | Non-metric multidimensional scaling (NMDS) representation of Bray-Curtis dissimilarities of hydrolytic compositions among sampling sites in the upper 250 m of the water column. Sites grouped by **(A)** station show significant hydrolytic compositional differences distinct from other stations (PERMANOVA $P = 0.007$), whereas the hydrolytic composition of sites grouped by **(B)** depth are not significantly different (PERMANOVA $P = 0.399$).

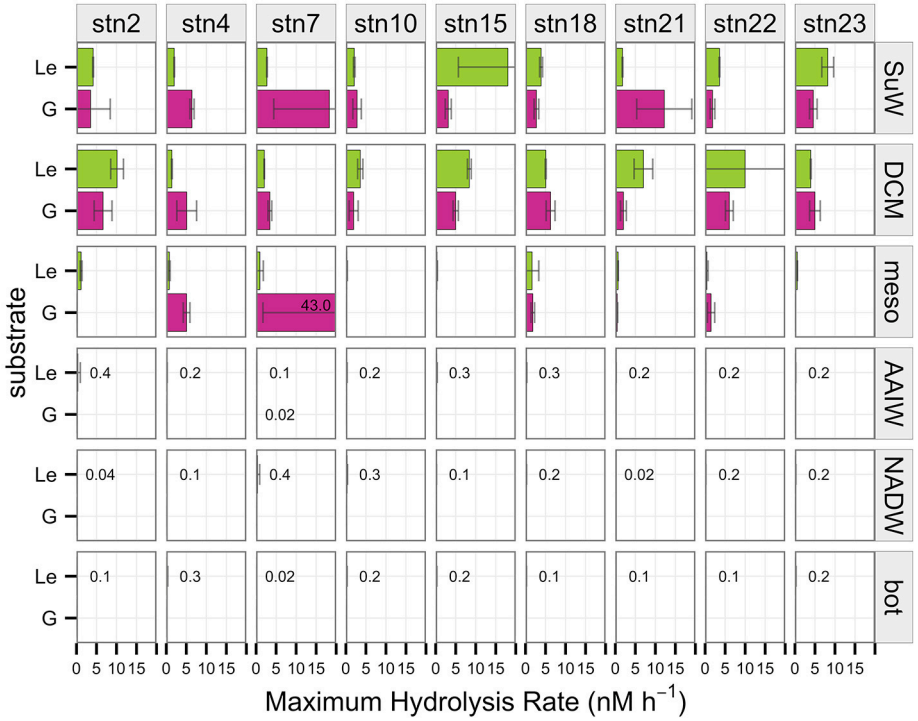

FIGURE 6 | Maximum potential hydrolysis rate (nM h^{-1}) of the monomeric substrates leucine (Le) and α-glucose (G) at each station (vertical panels) and depth (horizontal panels). Error bars indicate standard deviation of experimental triplicates. A particularly high hydrolysis rate of α-glucose at stn 7, mesopelagic depth indicated by the number in the panel. Low, non-zero hydrolysis rates in deep waters indicated by numbers in the figure panel.

Monomeric Substrate Hydrolysis Rates

Hydrolysis rates of monomeric substrates also varied by station, with maximal activity at the surface or DCM, and decreasing activity with depth (**Figure 6**), with the exception of a single replicate for α-glucose at station 7 where high activity was observed at mesopelagic depths. Depth-related decreases in α-glucosidase and leucine aminopeptidase activities, unlike the polysaccharide hydrolase activities, did not correspond to the degree of water column stratification. Below 250 m, α-glucosidase activity was undetectable at all sites even after 72 h of incubation, whereas leucine activities were very low in deep water, but nonzero.

Relationship between Polysaccharide Hydrolysis and Environmental Parameters

The strength of the relationship between polysaccharide hydrolysis rates and up to 10 environmental parameters was investigated by fitting the multiple regression model that maximized R^2-values (Supplementary Table 1). Overall, environmental parameters poorly explained the observed variation in hydrolysis rates ($R^2 = 0.22$). Since many of these parameters co-correlate with each other, one or two of these parameters generally explained as much or nearly as much of the variation in hydrolysis rates as all ten environmental variables. Temperature and chlorophyll a accounted for most of the relationship in the overall model ($R^2 = 0.19$), while the inclusion of the additional eight environmental variables only slightly improved the model ($R^2 = 0.22$). This result is mainly due to the difference in temperature and chlorophyll a in shallow vs. deep waters corresponding with higher rates of hydrolysis in shallower waters, since models using samples from just shallow or just deep water yielded very poor fits. The high frequency of zero hydrolysis rates did not appear to bias the model, however, since models using only non-zero rates yielded similar fits as the overall model (Supplementary Table 1).

When broken down by individual substrate, models were generally better fitted than the model of aggregated hydrolysis rates (Supplementary Table 1). However, the combination of environmental variables that best fit the data differed by substrate: for chondroitin, temperature only; for laminarin, temperature and chlorophyll a; for pullulan, temperature and buoyancy frequency; for xylan, chlorophyll a and salinity. Arabinogalactan and fucoidan were not modeled individually due to the lack of non-zero hydrolysis rates across all sites.

DISCUSSION

Microbial communities rely on extracellular enzymes to hydrolyze high molecular weight organic matter prior to uptake. The structural specificities of the enzymes active at a given site and depth determine which substrates are available for

further metabolism, while relative rates of hydrolysis reflect the potential speed of substrate processing. Site- and depth-related differences in hydrolysis rates and capacities imply differential remineralization of organic matter across latitude and depth in the ocean. The overall patterns of enzyme activities observed along this transect—spatial differences in hydrolytic diversity in surface waters and a decrease in the spectrum of polysaccharides hydrolyzed with depth—are consistent with studies of surface waters from other parts of the world's oceans (e.g., Arnosti et al., 2011), and add considerably to the very few other depth profiles of polysaccharide hydrolase activities in the ocean (Steen et al., 2012; D'Ambrosio et al., 2014).

Distinct functional assemblages characterized individual stations along the latitudinal gradient, such that the diversity of substrates hydrolyzed was more similar from surface to mesopelagic depths at a single station than at similar depth levels across different stations (**Figure 5**). These spatial and depth-related patterns in hydrolytic diversity, hydrolysis rate, and functional similarity together suggest that the vertical transfer of enzymatic capabilities through the upper depths of the water column—whether through cells, cellular material, or active enzymes—influences the hydrolytic signature of a station, but that this vertical transfer may be more limited at more stratified stations.

Patterns in hydrolytic assemblages among deeper water masses remain to be investigated, since activities were low or not measurable over the timescale of incubation at many of the deeper depths. A lack of measurable polysaccharide hydrolysis at deep sites may indicate that the heterotrophic community had no capacity to detect or to hydrolyze the substrates tested, or that the 21-day incubation timescale was insufficient to measure hydrolysis. In particular, low hydrolytic activities, or activities that require the growth of potentially slow-growing and/or rare members of the microbial community might not be detectable over a 21-day time course (Arnosti, 2008), since a sufficient fraction of the total added polysaccharide pool must be hydrolyzed to detect activity. The observation that leucine aminopeptidase was hydrolyzed—albeit at low rates—in bottom waters at almost all stations, however, demonstrates that an active heterotrophic community was present at these depths.

Measurable hydrolysis of leucine-MCA and MUF-α-glucose in deep waters has also been reported at other sites in the South and Equatorial Atlantic Ocean (Baltar et al., 2009, 2010, 2013). The leucine-aminopeptidase activities of 1–4 nM h^{-1} reported by Baltar and colleagues in deep water are considerably higher than the 0–0.35 nM h^{-1} in the present study, although the range of leucine-aminopeptidase activities measured in surface waters are similar between this study and previous studies (Baltar et al., 2009, 2010, 2013). The range of α-glucosidase activities measured in the present study in surface water (0–20 nM h^{-1}) are much greater than reported in previous studies (∼0–0.25 nM h^{-1}), perhaps because of a growth response during the extended timecourse of our incubations (maximum of 72 h, vs. maximum of 48 h in Baltar et al., 2009, 2010, 2013). No α-glucosidase activity was detected at any depths below 250 m in this study, even after 72 h incubation, whereas previous investigations measured low but non-zero α-glucose hydrolysis rates in deep water (∼0–0.8 nM/h, Baltar et al., 2009, 2010, 2013). For both leucine aminopeptidase and α-glucosidase activities, the subtraction of killed control fluorescence from live incubation fluorescence may have contributed to the lower rates measured in deep water in our experiments.

Multiple factors may contribute to the patterns of enzyme activities we measured. Environmental parameters alone are not likely to be the principal drivers for these patterns: the environmental variables measured at these stations poorly predicted observed rates, in univariate as well as multivariate models (Supplementary Table 1). While the specific environmental variable(s) that best fit each model varied by individual substrate (Supplementary Table 1), a causal explanation for the correlation strengths between hydrolysis rates of individual substrates and specific environmental factors is not obvious in most cases.

Instead, the patterns of enzymatic activities observed along this transect may be tied to the biogeography of the underlying microbial communities (Rusch et al., 2007; Fuhrman et al., 2008; Zinger et al., 2011; Sunagawa et al., 2015) and their functional capacities (DeLong et al., 2006; Shi et al., 2011). For example, the capacity to produce three extracellular enzymes (alkaline phosphatase, chitinase, and β-N-acetyl-glucosaminidase) commonly measured in field studies varies on very fine phylogenetic scales across all annotated prokaryotic genomes (Zimmerman et al., 2013). The heterogeneous distribution of heterotrophic genetic capacities among microbial phylogenies, and a varying distribution of these capabilities among surface water and subsurface environments (DeLong et al., 2006; Elifantz et al., 2008; Shi et al., 2011; Gomez-Pereira et al., 2012) results in functional stratification and resource partitioning along depth- and horizontal gradients. Differences in community composition and function are driven by a complex combination of factors that may include organic carbon composition and concentration (McCarren et al., 2010), distribution limitation (Follows et al., 2007; Hellweger et al., 2014), environmental selection (Ladau et al., 2013), or a confluence of interacting factors that defy simple categorization (Hanson et al., 2012).

Irrespective of the underlying factors, the relationship between water column stratification and the fraction of hydrolysis occurring in the shallow surface or DCM relative to deeper mesopelagic waters potentially has implications for the location of nutrient regeneration and for carbon export in the ocean. This point can be illustrated with a simple conceptual box model showing hypothetical DOC generation from particles sinking through the water column at the different stations along the transect (**Figure 7**). While there are many interacting factors that affect carbon export (De La Rocha and Passow, 2007), for the purposes of this discussion we consider only the degree of stratification and the spatial patterns of hydrolysis measured in this study. Assuming that particles are being hydrolyzed at the summed hydrolysis rates measured at our sites, DOC will be generated from particles during their passage through the water column at a rate related to the depth-integrated hydrolytic capacities at that location and the sinking rate of particles. For the purpose of this conceptual calculation, we assume a constant particle sinking rate of 100 m day^{-1} and divide the upper water column into three boxes: DCM—centered at the DCM sampling depth for that station and arbitrarily set at

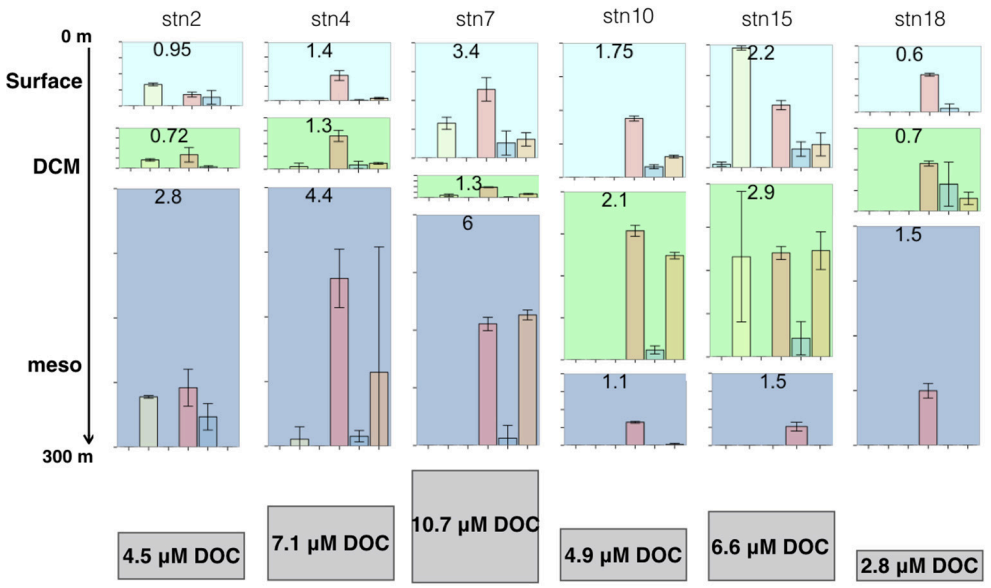

FIGURE 7 | Conceptual model of DOC generation under varying hydrolytic capacities and rates observed in this study, at each station from southernmost to northernmost (vertical panels). The amount of DOC generated, in µM, at the surface (top), DCM (middle), and mesopelagic (bottom) is shown at the top of each panel, and varies according to the relative hydrolytic capacities and rates, and the degree of stratification at that site. The total amount of DOC generated throughout the upper water column is shown below each station, and varies by station.

a thickness of 50 m; surface–all depths above the DCM; and upper mesopelagic—from below the DCM to 300 m. To estimate carbon remineralization, carbohydrates hydrolyzed from the particulate to the dissolved phase are then converted to DOC generated, assuming 6 C per monosaccharide produced. In this scenario, the total quantity of DOC generated in the upper 300 m of the water column, as well as the depth at which this DOC would be generated, varies greatly along the transect (**Figure 7**). At the productive and more strongly stratified station 15 (2.7°S), for example, most of the DOC would be generated in the surface and DCM, and labile DOC would likely quickly be respired to CO_2 which would remain in the surface ocean. The highest overall quantity of DOC, however, would be produced at station 7 (22.5°S), where more than half of the total generated DOC would be in the mesopelagic zone, and thus below the permanent thermocline. Labile DOC that is respired to CO_2 would likely remain below the thermocline, and would not exchange with surface waters or with the atmosphere on short timescales (Kheshgi, 2004).

The efficiency with which the biological pump removes surface-derived carbon from the upper ocean thus depends in part on the quantity of carbon remineralized from a sinking particle while it is still above the permanent thermocline (De La Rocha and Passow, 2007). This calculation in turn depends on the relative lability of the organic carbon in the sinking particles (Engel et al., 2009), the hydrolytic capacities of the microbial communities acting on them as they sink, the extent of water column stratification, and the residence time of the particle at different depths (Prairie et al., 2015). Holding all other factors constant, the biological pump would be more efficient at less stratified stations—such as stations 2, 4, and 7—where a larger proportion of the hydrolytic capacity occurs in the mesopelagic zone, below the permanent thermocline (**Figure 7**).

Biogeographical patterns in carbon cycling activities, and their relationship to oceanographic features, are of crucial significance to our ability to predict future conditions. For example, if increasing global temperatures result in a more stratified ocean (Capotondi et al., 2012), the quantity of organic matter sequestered by the biological pump below the thermocline may decrease. Such a decrease in turn would place greater influence on the relative hydrolytic capacities of microbial communities in the surface ocean, rather than in deeper waters, in determining the overall efficiency of the biological pump. The effects of an increase in stratification on carbon export will also depend on its impact on the biogeography of microbial communities and hydrolytic activities themselves. Increased stratification may in turn have complex downstream consequences for higher trophic levels that function in both shallow and deep waters, and depend on the availability of particulate organic carbon in both depth regions. Disentangling the roles of environmental characteristics, microbial community composition, functional capacities, and activities in regulating the marine carbon cycle is a prerequisite for a better understanding of the modern ocean, and of its sensitivity to perturbations in the future.

AUTHOR CONTRIBUTIONS

AH and CA designed experiments. AH conducted field experiments, collected and processed samples, and

processed data. AH and CA analyzed results and wrote the manuscript.

FUNDING

The authors would like to thank Liz Kujawinski for the invitation to join the DeepDOM cruise, and Krista Longnecker for providing nutrient measurements. Funding for this work was provided by the National Science Foundation (OCE-1332881 to CA).

SUPPLEMENTARY MATERIAL

The Supplementary Material for this article can be found online at: http://journal.frontiersin.org/article/10.3389/fmars.2017.00200/full#supplementary-material

REFERENCES

Alderkamp, A.-C., van Rijssel, M., and Bolhuis, H. (2007). Characterization of marine bacteria and the activity of their enzyme systems involved in degradation of the algal storage glucan laminarin. *FEMS Microbiol. Ecol.* 59, 108–117. doi: 10.1111/j.1574-6941.2006.00219.x

Arnosti, C. (1996). A new method for measuring polysaccharide hydrolysis rates in marine environments. *Org. Geochem.* 25, 105–115. doi: 10.1016/S0146-6380(96)00112-X

Arnosti, C. (2003). Fluorescent derivatization of polysaccharides and carbohydrate-containing biopolymers for measurement of enzyme activities in complex media. *J. Chromatogr. B Analyt. Technol. Biomed. Life Sci.* 793, 181–191. doi: 10.1016/S1570-0232(03)00375-1

Arnosti, C. (2008). Functional differences between Arctic seawater and sedimentary microbial communities: contrasts in microbial hydrolysis of complex substrates. *FEMS Microbiol. Ecol.* 66, 343–351. doi: 10.1111/j.1574-6941.2008.00587.x

Arnosti, C. (2011). Microbial extracellular enzymes and the marine carbon cycle. *Ann. Rev. Mar. Sci.* 3, 401–425. doi: 10.1146/annurev-marine-120709-142731

Arnosti, C., Fuchs, B. M., Amann, R., and Passow, U. (2012). Contrasting extracellular enzyme activities of particle-associated bacteria from distinct provinces of the North Atlantic Ocean. *Front. Microbiol.* 3:425. doi: 10.3389/fmicb.2012.00425

Arnosti, C., Steen, A. D., Ziervogel, K., Ghobrial, S., and Jeffrey, W. H. (2011). Latitudinal gradients in degradation of marine dissolved organic carbon. *PLoS ONE* 6:e28900. doi: 10.1371/journal.pone.0028900

Arnosti, C., Ziervogel, K., Ocampo, L., and Ghobrial, S. (2009). Enzyme activities in the water column and in shallow permeable sediments from the northeastern Gulf of Mexico. *Estuar. Coast. Shelf Sci.* 84, 202–208. doi: 10.1016/j.ecss.2009.06.018

Aspeborg, H., Coutinho, P. M., Wang, Y., Brumer, H., and Henrissat, B. (2012). Evolution, substrate specificity and subfamily classification of glycoside hydrolase family 5 (GH5). *BMC Evol. Biol.* 12:186. doi: 10.1186/1471-2148-12-186

Azam, F., and Malfatti, F. (2007). Microbial structuring of marine ecosystems. *Nat. Rev. Microbiol.* 5, 782–791. doi: 10.1038/nrmicro1747

Baltar, F., Arístegui, J., Gasol, J. M., Yokokawa, T., and Herndl, G. (2013). Bacterial versus archaeal origin of extracellular enzymatic activity in the Northeast Atlantic deep waters. *Microb. Ecol.* 65, 277–288. doi: 10.1007/s00248-012-0126-7

Baltar, F., Arístegui, J., Gasol, J., Sintes, E., van Aken, H., and Herndl, G. (2010). High dissolved extracellular enzymatic activity in the deep central Atlantic Ocean. *Aquat. Microb. Ecol.* 58, 287–302. doi: 10.3354/ame01377

Baltar, F., Arístegui, J., Sintes, E., van Aken, H. M., Gasol, J. M., and Herndl, G. (2009). Prokaryotic extracellular enzymatic activity in relation to biomass production and respiration in the meso- and bathypelagic waters of the (sub)tropical Atlantic. *Environ. Microbiol.* 11, 1998–2014. doi: 10.1111/j.1462-2920.2009.01922.x

Bray, J. R., and Curtis, J. T. (1957). An Ordination of the upland forest community of southern Wisconsin.pdf. *Ecol. Monogr.* 27, 325–349. doi: 10.2307/1942268

Capotondi, A., Alexander, M. A., Bond, N. A., Curchitser, E. N., and Scott, J. D. (2012). Enhanced upper ocean stratification with climate change in the CMIP3 models. *J. Geophys. Res.* 117, C04031. doi: 10.1029/2011JC007409

D'Ambrosio, L., Ziervogel, K., Macgregor, B., Teske, A., and Arnosti, C. (2014). Composition and enzymatic function of particle-associated and free-living bacteria: a coastal/offshore comparison. *ISME J.* 8, 1–13. doi: 10.1038/ismej.2014.67

De La Rocha, C. L., and Passow, U. (2007). Factors influencing the sinking of POC and the efficiency of the biological carbon pump. *Deep Sea Res.* 54, 5–7. doi: 10.1016/j.dsr2.2007.01.004

DeLong, E. F., Preston, C. M., Mincer, T., Rich, V., Hallam, S. J., Frigaard, N. U., et al. (2006). Community genomics among stratified microbial assemblages in the ocean's interior. *Science* 311, 496–503. doi: 10.1126/science.1120250

Elifantz, H. A., Waidner, L., Michelou, V. K., Cottrell, M. T., and Kirchman, D. L. (2008). Diversity and abundance of glycosyl hydrolase family 5 in the North Atlantic Ocean. *FEMS Microbiol. Ecol.* 63, 316–327. doi: 10.1111/j.1574-6941.2007.00429.x

Engel, A., Abramson, L., Szlosek, J., Liu, Z., Stewart, G., Hirschberg, D., et al. (2009). Investigating the effect of ballasting by $CaCO_3$ in *Emiliania huxleyi*, II: Decomposition of particulate organic matter. *Deep. Res. Part II Top. Stud. Oceanogr.* 56, 1408–1419. doi: 10.1016/j.dsr2.2008.11.028

Follows, M. J., Dutkiewicz, S., Grant, S., and Chisholm, S. W. (2007). Emergent biogeography of microbial communities in a model ocean. *Science* 315, 1843–1846. doi: 10.1126/science.1138544

Fuhrman, J. A., Steele, J. A., Hewson, I., Schwalbach, M. S. V., Brown, M., and Brown, J. H. (2008). A latitudinal diversity gradient in planktonic marine bacteria. *Proc. Natl. Acad. Sci. U.S.A.* 105, 7774–7778. doi: 10.1073/pnas.0803070105

Gomez-Pereira, P. R., Schuler, B. M., Fuchs, C. M., Bennke, H., Teeling, H., Waldmann, J., et al. (2012). Genomic content of uncultured Bacteroidetes from contrasting oceanic provinces in the North Atlantic Ocean. *Environ. Microbiol.* 14, 52–66. doi: 10.1111/j.1462-2920.2011.02555.x

Hanson, C. A., Fuhrman, J. A., Horner-Devine, M. C., and Martiny, J. B. H. (2012). Beyond biogeographic patterns: processes shaping the microbial landscape. *Nat. Rev. Microbiol.* 10, 497–506. doi: 10.1038/nrmicro2795

Hedges, J. (1992). Global biogeochemical cycles: progress and problems. *Mar. Chem.* 39, 67–93. doi: 10.1016/0304-4203(92)90096-S

Hellweger, F. L., van Sebille, E., and Fredrick, N. D. (2014). Biogeographic patterns in ocean microbes emerge in a neutral agent-based model. *Science* 345, 1346–1349. doi: 10.1126/science.1254421

Hoarfrost, A. (2016). *DeepDOM Github Repository*. Available online at: https://github.com/ahoarfrost/DeepDOM

Hoarfrost, A., and Arnosti, C. (2016). Investigating microbial activities driving organic matter transformations in the deep subsurface. *Biol. Chem. Oceanogr. Data Manag. Off.* Available online at: http://www.bco-dmo.org/project/662055

Hoppe, H. (1983). Significance of exoenzymatic activities in the ecology of brackish water: measurements by means of methylumbelliferyl-substrates. *Mar. Ecol. Prog. Ser.* 11, 299–308. doi: 10.3354/meps011299

Jiao, N., Herndl, G. J. A., Hansell, D., Benner, R., Kattner, G., Wilhelm, S. W., et al. (2010). Microbial production of recalcitrant dissolved organic matter: long-term carbon storage in the global ocean. *Nat. Rev. Microbiol.* 8, 593–599. doi: 10.1038/nrmicro2386

Kheshgi, H. S. (2004). Ocean carbon sink duration under stabilization of atmospheric CO 2: A 1, 000-year timescale. *Clim. Dyn.* 31, 1–5. doi: 10.1029/2004GL020612

Kujawinski, L. (2013). KN210-04. *Biol. Chem. Oceanogr. Data Manag. Off.* Available online at: http://www.bco-dmo.org/deployment/59057

Ladau, J., Sharpton, T. J., Finucane, M. M., Jospin, G., Kembel, S. W., O'Dwyer, J., et al. (2013). Global marine bacterial diversity peaks at high latitudes in winter. *ISME J.* 7, 1669–1677. doi: 10.1038/ismej.2013.37

McCarren, J., Becker, J. W., Repeta, D. J., Shi, Y., Young, C. R., Malmstrom, R., et al. (2010). Microbial community transcriptomes reveal microbes and metabolic pathways associated with dissolved organic matter turnover in the sea. *Proc. Natl. Acad. Sci. U.S.A.* 107, 16420–16427. doi: 10.1073/pnas,.1010732107

Prairie, J. C., Ziervogel, K., Camassa, R., McLaughlin, R. M., White, B. L., Dewald, C., et al. (2015). Delayed settling of marine snow: Effects of density gradient and particle properties and implications for carbon cycling. *Mar. Chem.* 175, 28–38. doi: 10.1016/j.marchem.2015.04.006

R Core Team (2014). *R: A Language and Environment for Statistical Computing*. Vienna: R Foundation for Statistical Computing. Available online at: http://www.R-project.org/

Rusch, D. B., Halpern, A. L., Sutton, G., Heidelberg, K. B., Williamson, S., Yooseph, S., et al. (2007). The Sorcerer II global ocean sampling expedition: Northwest Atlantic through eastern tropical Pacific. *PLoS Biol.* 5:e77. doi: 10.1371/journal.pbio.0050077

Schlitzer, R. (2015). *Ocean Data View*. Available online at: http://odv.awi.de

Shi, Y., Tyson, G. W., Eppley, J. M., and DeLong, E. F. (2011). Integrated metatranscriptomic and metagenomic analyses of stratified microbial assemblages in the open ocean. *ISME J.* 5, 999–1013. doi: 10.1038/ismej.2010.189

Steen, A. D., Ziervogel, K., and Arnosti, C. (2010). Comparison of multivariate microbial datasets with the Shannon index: an example using enzyme activity from diverse marine environments. *Org. Geochem.* 41, 1019–1021. doi: 10.1016/j.orggeochem.2010.05.012

Steen, A. D., Ziervogel, K., Ghobrial, S., and Arnosti, C. (2012). Functional variation among polysaccharide-hydrolyzing microbial communities in the Gulf of Mexico. *Mar. Chem.* 138–139, 13–20. doi: 10.1016/j.marchem.2012.06.001

Steen, A., Vazin, J., Hagen, S., Mulligan, K., and Wilhelm, S. (2015). Substrate specificity of aquatic extracellular peptidases assessed by competitive inhibition assays using synthetic substrates. *Aquat. Microb. Ecol.* 75, 271–281. doi: 10.3354/ame01755

Sunagawa, S., Coelho, L. P., Chaffron, S., Kultima, J. R., Labadie, K., Salazar, G., et al. (2015). Structure and function of the global ocean microbiome. *Science* 348, 1–10. doi: 10.1126/science.1261359

Teeling, H., Fuchs, B. M., Becher, D., Klockow, C., Gardebrecht, A., Bennke, C. M., et al. (2012). Substrate-controlled succession of marine bacterioplankton populations induced by a phytoplankton bloom. *Science* 336, 608–611. doi: 10.1126/science.1218344

Warren, R. A. (1996). Microbial hydrolysis of polysaccharides. *Annu. Rev. Microbiol.* 50, 183–212. doi: 10.1146/annurev.micro.50.1.183

Wegner, C.-E., Richter-Heitmann, T., Klindworth, A., Klockow, C., Richter, M., Achstetter, T., et al. (2013). Expression of sulfatases in *Rhodopirellula baltica* and the diversity of sulfatases in the genus Rhodopirellula. *Mar. Genomics* 9, 51–61. doi: 10.1016/j.margen.2012.12.001

Xing, P., Hahnke, R. L., Unfried, F., Markert, S., Huang, S., Barbeyron, T., et al. (2015). Niches of two polysaccharide-degrading Polaribacter isolates from the North Sea during a spring diatom bloom. *ISME J.* 9, 1410–1422. doi: 10.1038/ismej.2014.225

Zimmerman, A. E., Martiny, A. C., and Allison, S. D. (2013). Microdiversity of extracellular enzyme genes among sequenced prokaryotic genomes. *ISME J.* 7, 1187–1199. doi: 10.1038/ismej.2012.176

Zinger, L., Amaral-Zettler, L. A., Fuhrman, J. A., Horner-Devine, M. C., Huse, S. M., Mark Welch, B. A., et al. (2011). Global patterns of bacterial beta-diversity in seafloor and seawater ecosystems. *PLoS ONE* 6:e24570. doi: 10.1371/journal.pone.0024570

Conflict of Interest Statement: The authors declare that the research was conducted in the absence of any commercial or financial relationships that could be construed as a potential conflict of interest.

frontiers in Microbiology

ORIGINAL RESEARCH
published: 07 March 2017
doi: 10.3389/fmicb.2017.00353

Different Bacterial Communities Involved in Peptide Decomposition between Normoxic and Hypoxic Coastal Waters

*Shuting Liu[1], Boris Wawrik[2] and Zhanfei Liu[1]**

[1] Marine Science Institute, The University of Texas at Austin, Port Aransas, TX, USA, [2] Department of Microbiology and Plant Biology, The University of Oklahoma, Norman, OK, USA

Proteins and peptides are key components of the labile dissolved organic matter pool in marine environments. Knowing which types of bacteria metabolize peptides can inform the factors that govern peptide decomposition and further carbon and nitrogen remineralization in marine environments. A ^{13}C-labeled tetrapeptide, alanine-valine-phenylalanine-alanine (AVFA), was added to both surface (normoxic) and bottom (hypoxic) seawater from a coastal station in the northern Gulf of Mexico for a 2-day incubation experiment, and bacteria that incorporated the peptide were identified using DNA stable isotope probing (SIP). The decomposition rate of AVFA in the bottom hypoxic seawater (0.018–0.035 μM h^{-1}) was twice as fast as that in the surface normoxic seawater (0.011–0.017 μM h^{-1}). SIP experiments indicated that incorporation of ^{13}C was highest among the Flavobacteria, Sphingobacteria, Alphaproteobacteria, Acidimicrobiia, Verrucomicrobiae, Cyanobacteria, and Actinobacteria in surface waters. In contrast, highest ^{13}C-enrichment was mainly observed in several Alphaproteobacteria (*Thalassococcus*, *Rhodobacteraceae*, *Ruegeria*) and Gammaproteobacteria genera (*Colwellia*, *Balneatrix*, *Thalassomonas*) in the bottom water. These data suggest that a more diverse group of both oligotrophic and copiotrophic bacteria may be involved in metabolizing labile organic matter such as peptides in normoxic coastal waters, and several copiotrophic genera belonging to Alphaproteobacteria and Gammaproteobacteria and known to be widely distributed may contribute to faster peptide decomposition in the hypoxic waters.

Keywords: peptide, bacteria, DNA stable isotope probing, nitrogen, hypoxia, Gulf of Mexico

OPEN ACCESS

Edited by:
Andrew Decker Steen, University of Tennessee, USA

Reviewed by:
Xavier Mayali, Lawrence Livermore National Laboratory, USA
Craig E. Nelson, University of Hawaii at Manoa, USA
Nagissa Mahmoudi, Harvard University, USA

****Correspondence:***
Zhanfei Liu
zhanfei.liu@utexas.edu

Specialty section:
This article was submitted to Aquatic Microbiology, a section of the journal Frontiers in Microbiology

Received: *16 November 2016*
Accepted: *20 February 2017*
Published: *07 March 2017*

Citation:
Liu S, Wawrik B and Liu Z (2017) Different Bacterial Communities Involved in Peptide Decomposition between Normoxic and Hypoxic Coastal Waters. Front. Microbiol. 8:353. doi: 10.3389/fmicb.2017.00353

INTRODUCTION

Proteins and peptides are key components of labile dissolved organic matter (DOM) that supports bacterial growth (Azam, 1998). Small peptides (ca. <600 Da) are key immediate products of microbial protein decomposition owing to the size constraints of bacterial cell membrane transport systems, i.e., porins (Weiss et al., 1991). After proteins are degraded to small peptides, these small peptides can be either taken up directly by bacteria, or hydrolyzed further to individual amino acids via extracellular enzymes with subsequent uptake. The interaction between peptide decomposition and bacteria plays an important role in the cycling of carbon and nitrogen, regeneration of nutrients, and preservation of refractory dissolved organic nitrogen (DON) in marine environments (Aluwihare et al., 2005; Nagata, 2008).

Our previous studies have demonstrated that small peptides decompose more quickly in bottom hypoxic than surface normoxic (normal oxygen-saturated) waters in the northern Gulf of Mexico (nGOM), and that the growth of certain bacterial genera such as *Vibrio*, *Marinobacterium*, *Neptuniibacter*, *Pseudoalteromonas*, *Thalassomonas, Amphritea*, *Roseobacter* and *Ruegeria*, appears to respond to peptide addition (Liu et al., 2013; Liu and Liu, 2016). These results suggest that some bacterial groups may be more effective at metabolizing peptide-derived organic matter in hypoxic seawater, but direct evidence linking specific bacterial lineages to peptide decomposition has not been reported. Knowing which types of bacteria metabolize peptides may be useful in the assessment of factors that control hypoxia formation, as decomposition of labile organic matter leads to consumption of dissolved oxygen (DO) (Wright et al., 2012; Liu et al., 2013). As succession of microbial communities often occurs along with development of oxygen minimum zones (Crump et al., 2007; Zaikova et al., 2010; Parsons et al., 2015), studying the response of microbial communities to labile organic matter at different DO levels can also provide clues about linkages between microbial niche specialization and their resource utilization (Nelson and Wear, 2014).

Previous studies have demonstrated that some bacterial groups can outcompete others during the utilization of labile DOM (Eilers et al., 2000; Teske et al., 2011; Liu et al., 2015). For instance, the bacterial community shifted to Alphaproteobacteria and Betaproteobacteria dominated phylotypes in mesocosm tanks with diatom blooms that produced labile proteins, peptides and polysaccharides exudates (Murray et al., 2007). After bovine serum albumin (BSA) amendment, Gammaproteobacteria became the dominant bacterial class in the Chesapeake Bay water, while Bacteroidetes became dominant in the lower Delaware Bay water (Harvey et al., 2006). However, phylogeny-based incubation studies provide only indirect evidence of the role that different bacterial groups play in labile DOM mineralization, and only a few studies to date have linked specific bacteria groups with labile DOM decomposition directly using radioisotope-labeled substrate and microautoradiography combined with fluorescent *in situ* hybridization (MAR-FISH) technique (Tabor and Neihof, 1982; Ouverney and Fuhrman, 1999). For example, Cottrell and Kirchman (2000) identified that Bacteroidetes and Gammaproteobacteria actively utilized ^{3}H-labeled protein in two estuarine waters. While powerful, hybridization techniques such as MAR-FISH are a targeted approach and require the design of unique probes to detect individual phylogenetic groups. These techniques often do not allow the identification of active bacteria beyond limited taxonomic depth due to probe hybridization constraints. In contrast, DNA-stable isotope probing (SIP) techniques provide an opportunity to interrogate activity *in situ* and to identify bacteria at several phylogenetic levels without *a priori* selection of specific phylotypes. SIP techniques were initially applied to identify bacteria that can degrade one-carbon (C_1) compounds or specific pollutants in many environmental studies, such as discovering novel bacteria that degrade methanol, toluene, or alkanes in soils, sediments or marine seeps (Radajewski et al., 2000; Neufeld et al., 2007b; Luo et al., 2009; Redmond et al., 2010; Kleindienst et al., 2014). More recently, the application of DNA-SIP has been extended to marine environments. Examples include studies of urea uptake by marine pelagic bacteria and archaea in Arctic water, comparing bacteria incorporating glucose and cyanobacteria exudates in the Sargasso Sea, and exploring acetate-utilizing bacteria at the oxic–anoxic interface in the Baltic Sea (Gihring et al., 2009; Wawrik et al., 2009; Nelson and Carlson, 2012; Wawrik et al., 2012a; Berg et al., 2013; Connelly et al., 2014), demonstrating the utility of SIP to understand the marine C and N cycles.

The objective of this study was to gain insight into the identities of bacteria that utilize peptides in seawater. In particular, nGOM normoxic and hypoxic waters were targeted because they are characterized by contrasting biogeochemical processes and are known to harbor different bacterial communities that differentially respond to peptide addition. The^{13}C-labeled tetrapeptide alanine-valine-phenylalanine-alanine (AVFA) was used as a model compound and incubated in both surface normoxic and bottom hypoxic seawater in the nGOM. The AVFA sequence is derived from the protein sequence of the large subunit of ribulose-1,5-biphosphate carboxylase/oxygenase (RuBisCO) that is ubiquitous in photosynthesis and has been used to investigate peptide hydrolysis (Liu et al., 2010, 2015; Orellana and Hansell, 2012; Liu and Liu, 2014, 2015). Although individual peptides are often undetectable in natural seawater due to their rapid turnover, they play an important role in supporting bacterial growth as intermediates released from sloppy-feeding or lysis of cells (Nagata, 2008; Sipler and Bronk, 2015).

MATERIALS AND METHODS

Seawater Sampling

Surface (2 m) and bottom (16 m) seawater were collected at Sta. C6 (28°52′ N, 90°30′ W) in the nGOM during a May 2013 cruise on the R/V *Pelican*. This station, with a depth of 18 m and ca. 20 km offshore, is heavily influenced by Mississippi River discharge and often subjected to hypoxia during summer (Rabalais et al., 2001). Seawater was sampled using 10 L Niskin bottles mounted on a conductivity-temperature-depth (CTD) rosette (Seabird 911). Temperature, salinity, DO and chlorophyll *a* of seawater were monitored through the CTD device (**Table 1**). Seawater was filtered immediately onboard through a 0.2 μm Nylon filter (diameter 47 mm, Whatman) and preserved under −20°C for the analysis of dissolved organic carbon (DOC), total dissolved nitrogen (TDN), total dissolved amino acids (TDAAs), dissolved combined amino acids (DCAAs), dissolved free amino acids (DFAAs) and nutrients.

Peptide Incubation

Peptides ^{12}C-AVFA and ^{13}C-AVFA were custom-synthesized (C.S Bio, Menlo Park, CA, USA), and had a >95% compound purity (Liu et al., 2013). In ^{13}C-AVFA, 17 (all three carbons in A, all five carbons in V and six carbons of the aromatic ring in F) out of total 20 carbon atoms were labeled isotopically. As DNA of specific bacteria groups might only be partially

TABLE 1 | Chemical parameters of initial surface (2 m) and bottom (16 m) seawater at Sta. C6.

Depth	Temp (°C)	Salinity (ppt)	DO ($mg \cdot L^{-1}$)	Chl *a* ($\mu g \cdot L^{-1}$)	DOC (μM)	TDN (μM)	DCAA (μM)	DFAA (μM)	NO_3^- (μM)	NO_2^- (μM)	P_i (μM)
2 m	25.5	27	7.9	1.51	233.3	14.3	1.79	0.18	0.54	ud	0.11
16 m	22.3	35	0.4	0.63	200.0	10.7	0.56	0.07	6.85	0.54	0.89

ud, under detection limit (ca. 0.03 μM).

labeled (<100%) with ^{13}C, bacteria groups incorporating ^{13}C can be spread through all SIP fractions with different density (see related method below). The unlabeled ^{12}C-AVFA incubation was thus included as a reference for comparison with ^{13}C-AVFA incubation to confirm isotopic enrichment in DNA. The unlabeled SIP gradient should contain less DNA in the more dense fractions than that in the samples incubated with ^{13}C substrates (Neufeld et al., 2007a). AVFA was incubated onboard in the surface normoxic and bottom hypoxic seawater. Briefly, either ^{12}C-AVFA or ^{13}C-AVFA was respectively amended in a series of 125 mL amber round bottles filled with 120 mL seawater at final concentrations of 0.25–0.47 μM. Duplicate incubations were conducted in the dark for 48 h at 24°C, close to the ambient seawater temperature (**Table 1**). At different time points (0, 8, 13, 24, and 48 h), 1 mL aliquots of unfiltered water were collected and fixed with formaldehyde at a final concentration of 3% and stored at 4°C for bacterial abundance analysis. The remaining 119 mL were filtered through the 0.2 μm Nylon filter and preserved at −20°C for the analysis of peptides, amino acids, ammonium, and orthophosphate (P_i). The filters were preserved in 750 μL 1× STE (10 mM Tris-HCl [pH 8.0], 0.1 M NaCl, 1 mM EDTA [pH 8.0]) buffer at −20°C for DNA extraction and sequencing. DO was not monitored throughout the incubation, but the parallel incubation experiment showed that it remained relatively constant throughout the 72 h (Liu and Liu, 2016). Two kinds of controls were included for the incubation experiment: a seawater control without peptide amendment and a killed control with 0.48–0.58 μM ^{12}C-AVFA and 180 μM $HgCl_2$ to inhibit bacterial activity (Lee et al., 1992). The incubation and aliquot sampling for the controls followed the same procedures as described above, but only AVFA was analyzed in the killed control.

Chemical Analyses

DOC and TDN of the filtered initial seawater were analyzed using a Shimadzu total organic carbon (TOC-V) analyzer coupled with a TNM-1 TDN analyzer with <6% error between duplicates (**Table 1**). DFAA were calculated as sum of individual amino acids analyzed in high performance liquid chromatography (HPLC, Shimadzu Prominence) equipped with a fluorescence detector after pre-column *o*-phthaldialdehyde (OPA) derivatization (Lindroth and Mopper, 1979; Lee et al., 2000). TDAA were analyzed in the same way as DFAA but after hydrolysis in 6 N HCl under nitrogen at 110°C for 20 h (Kuznetsova and Lee, 2002). DCAA were calculated as TDAA subtracting DFAA. Nitrate, nitrite and orthophosphate (P_i) were measured following established protocols (Strickland and Parsons, 1968; Jones, 1984).

Alanine-valine-phenylalanine-alanine was analyzed in an HPLC-mass spectrometry (HPLC-MS) system (Shimadzu Prominence) following the method in Liu and Liu (2014). In brief, the mobile phase A was 10 mM ammonium acetate and mobile phase B was methanol. Samples were eluted through a C_{18} column (Alltima 5 μm, 150 mm × 4.6 mm) and a six-way valve was programmed to direct the sea salt peak to waste before introducing the AVFA peak to the MS detector that is equipped with an electrospray ionization (ESI) source and a quadrupole mass analyzer. ^{12}C-AVFA and ^{13}C-AVFA were quantified in positive ion mode under selective ion monitoring (SIM) at m/z = 407 and 424, respectively.

Alanine-valine-phenylalanine-alanine hydrolysis products including peptide fragments (AV, VF, FA, VFA) and amino acids (A, V, F) were analyzed by HPLC after pre-column OPA derivatization (Liu et al., 2013). Standard deviations of amino acid analysis among replicates were 10–20%. Ammonium, a main metabolite of AVFA, was analyzed using HPLC with post-column OPA derivatization (Gardner and St. John, 1991).

Bacterial Abundance Analysis

Bacterial cells in the formaldehyde-preserved samples were stained with SYBR Green II (Molecular Probes, 1:100 v/v) and enumerated in a flow cytometer (BD Accuri C6) under blue laser excitation at 488 nm (Marie et al., 1997; Liu et al., 2013). Bacterial cells were counted in a fixed volume mode with a flow rate below 300 events per second and cell counts were determined in a dot plot of side scatter (SSC-H) vs. green fluorescence signal (FL1-H) on a logarithmic scale.

DNA Extraction and Ultracentrifugation in CsCl Gradients

DNA was extracted from filtered cells using MoBio PowerSoil® DNA isolation kits (MoBio Laboratories, Carlsbad, CA, USA). Leftover STE buffer was spun in a centrifuge and the supernatant was discarded. The pellet was re-dissolved in 100 μL lysis solution from MoBio Powerbead tube and then combined with filter in the tube for DNA extraction. A subsample (ca. 10 μL) at each incubation time point was saved for microbial community structure analysis (unamended control 0 h, one duplicate of ^{12}C-AVFA 2 m 0 h, and one duplicate of ^{12}C-AVFA 16 m 0 h samples were lost during DNA extraction), and the remainder (ca. 80 μL) was for the ultracentrifugation in CsCl gradients. Duplicate DNA samples (each account for ca. 89% (80 μL out of 90 μL) of extracted DNA) from all three time points (13, 24, and 48 h)

for surface and bottom seawater incubations respectively were pooled (i.e., six samples were pooled) to obtain sufficient DNA for ultracentrifugation and fractionation. The pooled DNA was precipitated using isopropanol, and the DNA pellet was then re-suspended in 50 μL TE buffer (50 mM Tris-HCl, 15 mM EDTA [pH 8.0]) as previously described (Wawrik et al., 2009). Four pooled DNA samples (^{12}C-AVFA surface, ^{13}C-AVFA surface, ^{12}C-AVFA bottom, ^{13}C-AVFA bottom) were prepared for ultracentrifugation. Note that ultracentrifugation and following fractionation were not performed on killed control samples and unamended samples. CsCl gradient ultracentrifugation and fractionation followed protocols as described previously (Buckley et al., 2007; Luo et al., 2009; Wawrik et al., 2012a). In brief, 61–170 ng DNA, quantified through a Qubit® 2.0 Fluorometer (Life Technologies), were mixed with 0.26 mL TE buffer and 4.45 mL of 1.295 g mL^{-1} CsCl in gradient buffer A (15 mM Tris-HCl [pH 8.0], 15 mM KCl, 15 mM EDTA [pH 8.0], 2 mg mL^{-1} ethidium bromide) in 4.7 mL polyallomer Optiseal tubes (Beckman). The tubes were centrifuged in a Beckman rotor VTi 65.2 at ca. 140,000 × *g* for 48 h. After ultracentrifugation, 30 150 μL fractions were collected from each tube in a Beckman fraction recovery system by replacing samples with mineral oil on top of the tubes at a constant rate using a peristaltic pump. The density of each fraction was calculated based on the refractive index that was measured in a Reichert AR200 refractometer (Wawrik et al., 2009). DNA was purified from each CsCl fraction by isopropanol precipitation and dissolved in 50 μL sterile nuclease-free water.

Quantitative PCR (qPCR) of 16S rRNA Gene

The purified DNA from each SIP fraction was used to determine 16S rRNA gene copy numbers of bacteria via quantitative polymerase chain reaction (qPCR). Primers were 27F (5′-AGA GTT TGA TCM TGG CTC AG-3′) and 519R (5′-GWA TTA CCG CGG CKG CTG-3′) (Nakatsu and Marsh, 2007). Every 30 μL reaction mix for qPCR included 13.9 μL 2X Power SYBR Green PCR master mix (Applied Biosystems), 13.9 μL nuclease-free water, 200 nM (final concentration) of each primer, and 2 μL DNA template. qPCR was conducted in a real-time PCR system (Applied Biosystems, ABI 7300) followed the program: 2 min at 50°C, 8 min at 95°C, 40 cycles of 30 s at 95°C, 1 min at 55°C and 1 min at 72°C. Genomic DNA of *Roseobacter denitrificans* Och 114 (DSMZ 7001) was used as the standard DNA for bacteria (standard concentrations ranging from 10^{-4} to 10 ng μL^{-1}). The qPCR detection limit for bacteria was ca. 0.002 ng (corresponding gene copy number of 442) and cycle threshold was ca. 31. The qPCR data was then normalized to the highest quantities of 16S rRNA gene copy numbers observed among all fractions in that gradient, in order to account for the differential abundances and distributions of their DNA in gradients (Wawrik et al., 2009; Connelly et al., 2014). These normalized numbers were named as ratios of quantities in which the highest normalized frequency measured equaled 1.

16S rRNA Gene PCR, Barcoding, and Illumina Sequencing

DNA from each incubation time point and each fraction collected from SIP gradients was amplified by PCR using Phusion high-fidelity DNA polymerase (Thermo Scientific) and barcoded for Illumina sequencing. PCR reactions utilized the universal forward primer 519F containing a 5′ M13 tag (5′-GTA AAA CGA CGG CCA GCA CMG CCG C-3′) and the reverse primer Bac-785R (5′-TAC NVG GGT ATC TAA TCC-3′) as previously described (Wawrik et al., 2012b; Klindworth et al., 2013). PCR started with 94°C for 2 min, followed by 28–32 cycles of 95°C for 30 s, 52.8°C for 30 s, and 72°C for 30 s, then 72°C for 5 min. The number of PCR cycles was optimized based on qPCR results and agarose gel check of PCR products to make sure enough PCR products were obtained but not reaching PCR plateau. PCR products were purified by QIAquick PCR purification kit (Qiagen) and barcoded using a unique M13-contianing primer for each sample that contained a 12 bp barcode for bioinformatical parsing of data (Wawrik et al., 2012b). Barcode tagging was checked by gel electrophoresis, amplifications were mixed at equimolar ratios, and sent to the Oklahoma Medical Research Foundation for MiSeq PE250 Illumina sequencing. Sequence reads were trimmed to a quality score of Q30 and adapter and primer sequences were trimmed from raw Illumina sequences. Overlapping forward and reverse reads were stitched and all non-overlapping sequence reads were discarded. Processed sequences were clustered into OTUs using UCLUST, checked for chimeras using USEARCH and classified into taxonomy through the QIIME pipeline (Caporaso et al., 2010b). A randomly chosen set of representative sequences from each OTU was aligned to the SILVA small-subunit rRNA reference alignment[1] using the PyNAST algorithm (Caporaso et al., 2010a). Sequences were assigned to the genus level at the 95% identity as a compromise between resolution and conservative interpretation due to the short reads (250 bp) used here (Connelly et al., 2014). Sequences were deposited in National Center for Biotechnology Information (NCBI) GenBank under BioProject accession number PRJNA297372.

Bacterial community structures (relative abundance of genera presented in percentage) of the initial samples were assumed to be the same among unamended control, ^{12}C-AVFA and ^{13}C-AVFA samples. As unamended control and one duplicate of the ^{12}C-AVFA 0 h samples were lost, initial bacterial community data of ^{13}C-AVFA samples was more reliable to represent the initial bacterial community structure of all. To be consistent with the pooled SIP samples, results of the bacterial community structures from the three time points (13, 24, and 48 h) were also pooled and compared with others by non-metric multidimensional scaling (NMDS) using Matlab®. Analysis of similarity (ANOSIM) was applied to compare the bacterial community structures between surface and bottom seawater and between unamended control and AVFA treatment time-point samples using vegan package in R (Oksanen et al., 2016).

[1] http://www.arb-silva.de

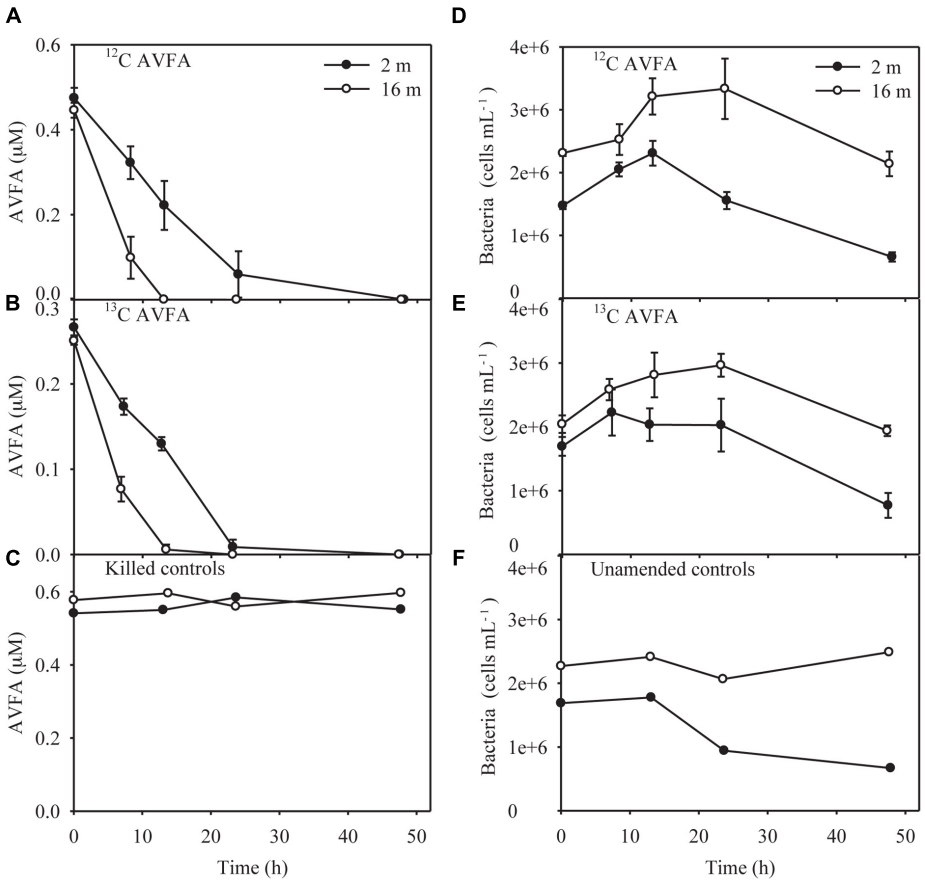

FIGURE 1 | Alanine-valine-phenylalanine-alanine (AVFA) concentrations (A–C) and bacterial abundance counted in flow cytometer **(D–F)** with incubation time in the surface 2 m and bottom 16 m seawater of ^{12}C-AVFA, ^{13}C-AVFA, and control samples. Note controls samples in **(C)** are killed controls, and in **(F)** are unamended (no-AVFA) controls. Data points were presented as average ± absolute error of duplicate samples except control samples.

Calculating percentage enrichment of each bacterial taxa in the ^{13}C-AVFA samples relative to the ^{12}C-AVFA SIP samples followed the protocol of Bell et al. (2011). In brief, 16S rRNA gene copy numbers for each SIP fraction were quantified through qPCR. Then the proportion of each bacterial taxonomic group sequences in a given density range was multiplied by the 16S rRNA gene copy number in that same density range, and the derived copy number of each bacterial taxonomic group was normalized to total gene copy number within that density range to correct for the slight difference in total DNA between the ^{12}C-AVFA and ^{13}C-AVFA samples and this normalized gene copy number was referred as relative gene copy number. Percentage enrichment of a certain bacterial taxonomic group was defined as dividing the difference of the relative copy number summed in the heavy density fractions between the ^{13}C-AVFA samples and the ^{12}C-AVFA samples by the relative copy number in the ^{12}C-AVFA samples within the same density range. The percentage enrichment was used as an indicator of the relative amount of ^{13}C enrichment among bacterial groups. A higher percentage enrichment in one bacterial taxa relative to other taxa indicates increased cell replication responding to amended ^{13}C-AVFA. For example, 100% enrichment of a given taxonomic group in the same density range indicates that its 16S rRNA gene copy number in the ^{13}C treatment is twice as abundant as that in the ^{12}C treatment. To estimate the error/noise level of the percentage enrichment, 95% confidence interval was calculated from all positive percentage enrichment values among bacterial taxa for both surface and bottom samples.

RESULTS

Peptide Decomposition

The ^{12}C- and ^{13}C-AVFA decomposition patterns were nearly identical during the 48 h incubation, as expected (**Figures 1A,B**). The AVFA concentrations decreased linearly with time in both the surface (2 m) and bottom (16 m) seawater, but the decomposition rate in the bottom seawater (0.018–0.035 μM h^{-1}) was twice as high as in the surface seawater (0.011–0.017 μM h^{-1}). The decomposition rate of AVFA in the bottom seawater was significantly higher than that in the surface seawater (*t*-test, $p < 0.03$). AVFA was completely degraded within 24–48 h in the surface water and within 13–24 h in the bottom water. In contrast, AVFA concentration in the killed

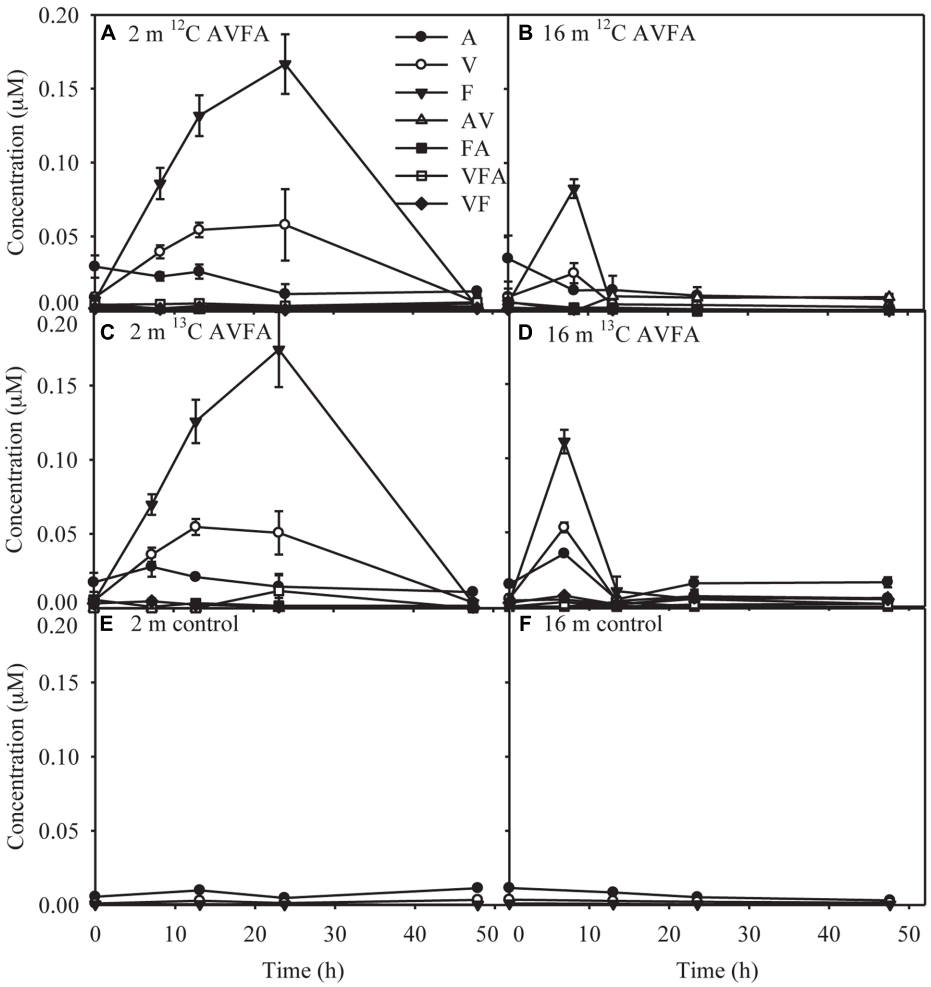

FIGURE 2 | Concentrations of produced amino acids and peptide fragments with incubation time in the (A) surface 2 m seawater of ^{12}C-AVFA incubation, **(B)** bottom 16 m seawater of ^{12}C-AVFA incubation, **(C)** surface 2 m seawater of ^{13}C-AVFA incubation, **(D)** bottom 16 m seawater of ^{13}C-AVFA incubation samples, and amino acid concentrations with time in the **(E)** surface 2 m seawater of no-AVFA control and **(F)** bottom 16 m seawater of no-AVFA control samples. Data points were presented as average ± absolute error of duplicate samples except control samples.

control remained nearly unchanged during the 48 h incubation (**Figure 1C**), indicating that the peptide disappearance in the seawater was due to microbial activity.

AV, FA, VF, and VFA produced during hydrolysis of AVFA (Liu et al., 2013) remained at low levels <0.012 μM throughout the incubation, but more amino acids and peptide fragments were produced in the surface than in the bottom incubation (**Figure 2**). Concentrations of amino acid F were significantly higher in the surface than in the bottom seawater (*t*-test, $p = 0.04$). Concentrations of free amino acids (A, V, and F) were 2–30 times greater than those of peptide fragments. As individual amino acids have been shown in similar incubations to be taken up at different rates (Liu et al., 2013), particularly amino acid A was taken up much faster than V and F, production of amino acids might not follow the stoichiometry of added peptides. F was the dominant amino acid, reaching up to 0.17 μM in the surface at 24 h and 0.082–0.11 μM in the bottom at 8 h, and then decreased to the background level at the end of the incubation. V and A followed a similar pattern to F, but with smaller changes, indicating they were taken up faster than F, consistent with a previous study at this station (Liu et al., 2013). Compared to the AVFA treatment, concentrations of amino acids in the control without peptide amendment remained relatively low (<0.011 μM) and constant throughout the incubation.

Ammonium is a key metabolite of peptides (Liu et al., 2013). During the first 24 h in the surface seawater incubation, ammonium concentrations increased by 0.66–1.45 μM in the ^{12}C- and ^{13}C-AVFA samples (Supplementary Figures S1A–C). In contrast, ammonium concentrations in the bottom seawater changed little before AVFA was completely degraded (0–13 h). However, the difference of produced ammonium between surface and bottom seawater was not significant (*t*-test, $p = 0.38$). After 13 h, ammonium concentrations kept increasing to 2.6–2.9 μM in the surface seawater and remained constant at

about 2.8 μM or increased by 1.5 μM to reach 4.1 μM in the bottom seawater. In the control without AVFA, ammonium concentrations increased by 0.97 μM in the surface seawater and decreased by 0.63 μM in the bottom seawater during the 48 h incubation.

P_i is an essential element for bacterial growth (Elser et al., 2000; Karl, 2014; Liu and Liu, 2016). However, P_i concentrations remained relatively constant throughout the 48-h incubation in both the peptide and control treatments (Supplementary Figures S1D–F). P_i concentrations in the bottom water (1.1–1.5 μM) were more than one order of magnitude higher than those in the surface water (0.02–0.09 μM).

Bacterial Abundance and Community Structure

In the surface ^{12}C- and ^{13}C-AVFA incubations, bacterial abundance increased by 31–57% within the initial 8–13 h, and then decreased afterward, while in the bottom, bacterial abundance increased by 44–45% during the initial 24 h and then decreased afterward (**Figures 1D,E**). Bacterial abundances in the control either decreased over time in the surface seawater or remained nearly constant in the bottom seawater (**Figure 1F**). Ambient surface water bacterial communities were dominated by *Synechococcus* (15–49%), whereas bottom samples were more evenly populated by *Rhodobacteraceae* (11–13%), *Acidimicrobiaceae* OCS155 marine group (3–8%), *Saprospiraceae* (5–7%), *Planctomycetaceae* (2–7%), SAR11 clade Surface 1 (3–6%), and *Acidimicrobiales* TM214 (3–5%) (Supplementary Figures S2A,B). Different initial surface community structures between ^{12}C-AVFA and ^{13}C-AVFA samples might be related to the loss of one duplicate ^{12}C-AVFA DNA sample or contamination of *Synechococcus* in one sample. Thus, initial surface community structure of the ^{13}C-AVFA duplicate samples might be more reliable than that of the ^{12}C-AVFA samples. Throughout the incubation, the relative abundance of *Rhodobacteraceae*, *Thalassococcus*, and *Ruegeria* increased by 6–14, 7–13, and 1–3%, respectively, in both surface and bottom seawater, while other bacterial genera developed differently in the surface and bottom seawater incubations. For instance, OTUs classified within the *Roseovarius* clade increased by 7% only in the surface seawater, whereas *Colwellia* increased by 3% only in the bottom seawater. The surface and bottom bacterial community structures were well-separated in the NMDS plot (Supplementary Figure S2C); ANOSIM showed significant difference between the surface and bottom bacterial community structures ($p = 0.002$), further suggesting that bacterial community structures developed differently between the two water layers. To further evaluate the bacterial community development in unamended controls vs. AVFA treatments, NMDS was also plotted separately on surface and bottom bacterial communities (**Figure 3**). At the later incubation time points, unamended treatments and AVFA treatments formed separate clusters especially at NMDS1 axis, but this separation was not significant as shown in ANOSIM analysis ($p > 0.05$), indicating peptide amendement did not significantly change bacterial community structures during the 48-h incubation as compared to controls.

Identifying Bacteria that Incorporated Peptides through DNA-SIP

Quantitative polymerase chain reaction of SIP fractions indicates that the density distribution of the 16S genes in bulk DNA of the ^{13}C-AVFA samples shifted to heavier densities as compared to the ^{12}C-AVFA samples in both the surface and bottom incubations (**Figures 4A,B**). The 16S PCR products from respective fractions were bar-coded and sequenced using Illumina Miseq to generate sequence libraries. A positive percentage enrichment is an indicator of the bacterial potential in incorporating ^{13}C (Bell et al., 2011). Estimated error/noise of percentage enrichment was 46 and 65% at the class and genus level, respectively, as calculated from the 95% confidence interval. From this error/noise estimate, percentage enrichment above 84% at the class level and above 168% at the genus level was above the 95% confidence interval. ^{13}C uptake, as suggested by SIP, was more evenly distributed among the bacterial classes in the surface seawater than in the bottom seawater (**Figures 4C,D**). Flavobacteria, Sphingobacteria, Alphaproteobacteria, Acidimicrobiia, Verrucomicrobiae, Cyanobacteria, and Actinobacteria showed highest enrichment ranging from 96 to 275% in the surface water, whereas Alphaproteobacteria and Gammaproteobacteria showed highest enrichment ranging from 175 to 279% in the bottom water.

Communities taking up ^{13}C in the surface and bottom seawater also differed at the level of dominant genera (>0.1% of the total bacterial community) (**Figures 4E,F**). In the surface seawater, *Saprospiraceae*, *Tropicibacter*, *Roseovarius*, *Owenweeksia*, *Formosa, Flavobacteria* NS4 marine group, and *Microbacteriaceae* SV1-8 dominated the ^{13}C uptake. In the bottom samples, major ^{13}C enriched groups included *Thalassococcus*, *Rhodobacteraceae*, *Ruegeria*, *Colwellia*, *Balneatrix*, and *Thalassomonas*. The extent of taxonomic enrichment in the heavier fractions varied widely among different bacterial genera, ranging from 86 to 498% in the surface incubation and from 4 to 646% in the bottom incubation. Within the same class, the enrichment of *Roseovarius* and *Thalassococcus* was almost twice as high as that of other genera in Alphaproteobacteria, and the enrichment of *Colwellia* was more than three times higher than that of other genera in Gammaproteobacteria.

DISCUSSION

Faster AVFA Decomposition in the Hypoxic than in the Normoxic Seawater

Peptide decomposition in the bottom incubation was twice as fast as that in the surface incubation (**Figures 1A,B**). Normalized to initial bacterial abundance, cell-specific rate of peptide decomposition in the bottom incubation (9.0×10^{-9}–1.5×10^{-8} nM h^{-1}) was 1.3–1.4 times as high as that in the surface incubation (6.4×10^{-9}–1.2×10^{-8} nM h^{-1}). Also, AVFA decomposition produced less hydrolyzed

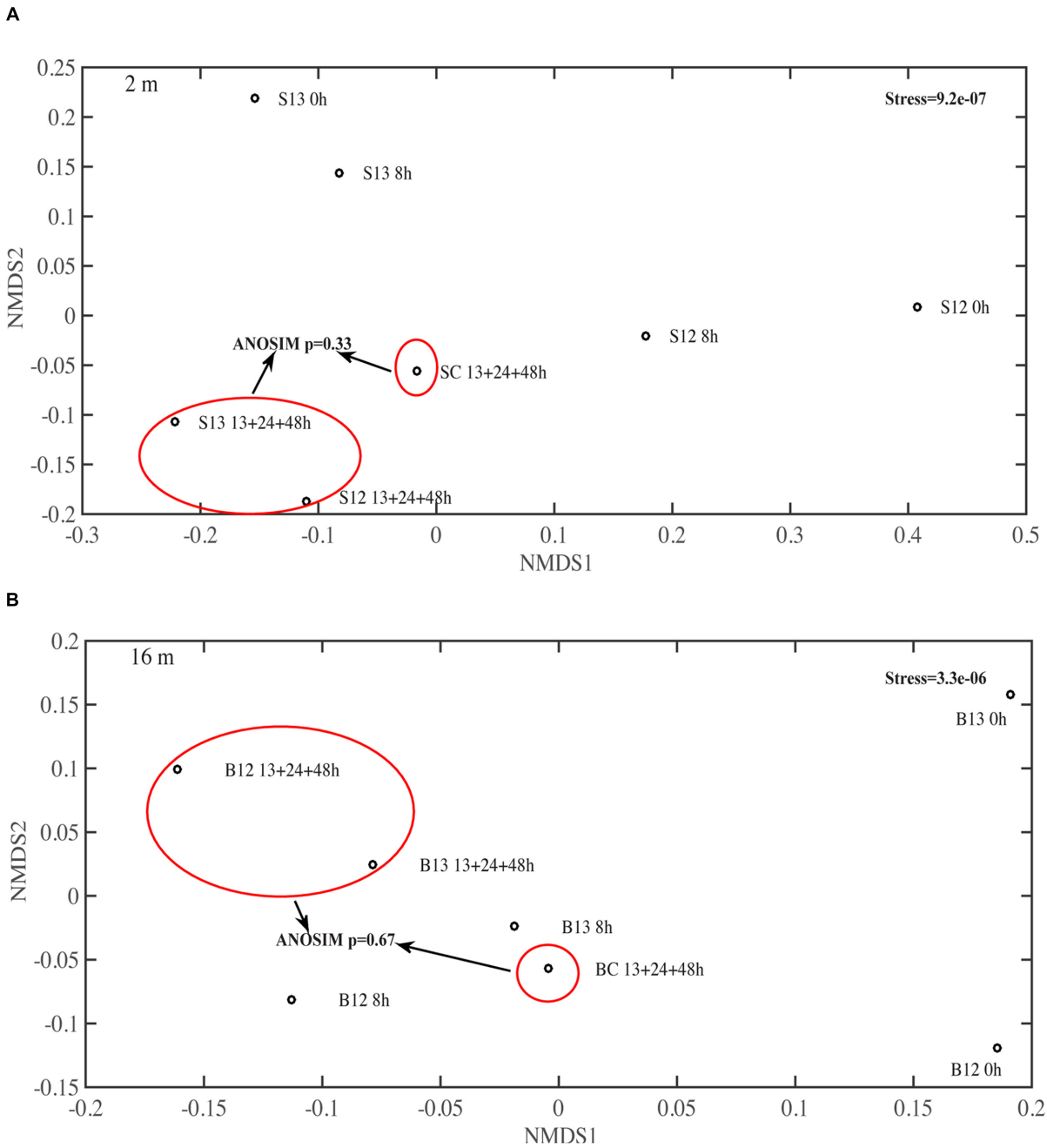

FIGURE 3 | Non-metric multidimensional scaling (NMDS) on the bacterial community structure at genera level in (A) surface 2 m and **(B)** bottom 16 m time-point samples. 13, 24, and 48 h samples were pooled to be consistent with SIP data. S12, surface 2 m ^{12}C-AVFA samples; S13, surface 2 m ^{13}C-AVFA samples; SC, surface 2 m no-AVFA control samples; B12, bottom 16 m ^{12}C-AVFA samples; B13, bottom 16 m ^{13}C-AVFA samples; BC, bottom 16 m no-AVFA control samples. Stress was 9.2e-07 at 2 m and 3.3e-06 at 16 m, indicating excellent fitting of solution to recreate the dissimilarity (stress < 0.02). Bacterial composition formed separate clusters between unamended control and AVFA incubations at the later time points at both 2 and 16 m as shown in red circles, but ANOSIM showed this separation was not significant ($p > 0.05$).

fragments, including amino acids and peptides, in the bottom than surface incubations (**Figure 2**), indicating direct uptake of AVFA or tightly coupled hydrolysis-uptake in the bottom water but extracellular hydrolysis in the surface water. In contrast to previous studies, which used relatively high concentrations of added peptides (5–10 μM) (Liu et al., 2013; Liu and Liu, 2016), the much lower concentrations of AVFA (0.25–0.47 μM) added here accounted for only 14–84% of ambient DCAA that consist of all hydrolyzable proteins and peptides in seawater (**Table 1**).

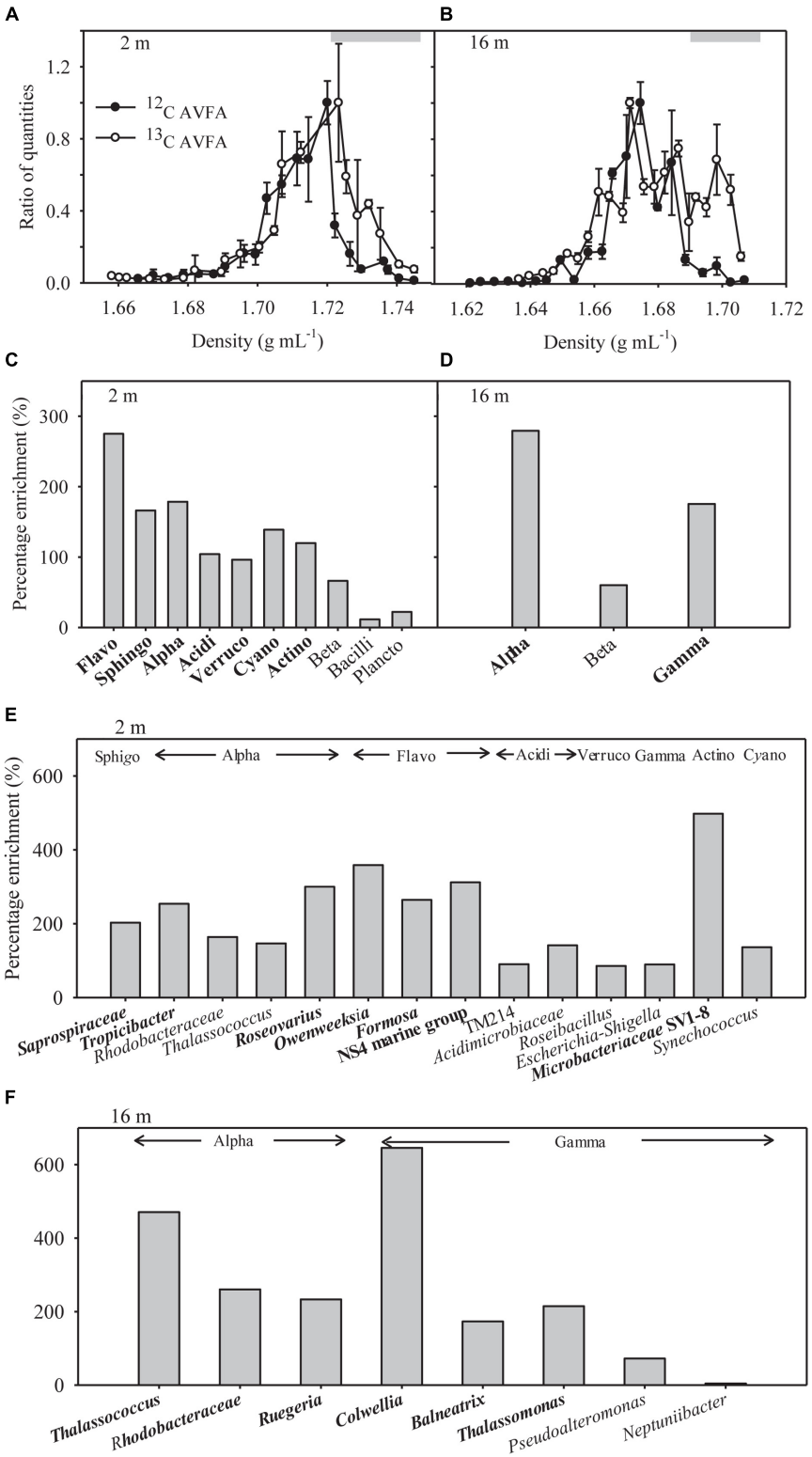

FIGURE 4 | (A,B) Quantitative polymerase chain reaction (qPCR) analysis results shown as relative quantities vs. density of SIP gradient fractions for bacterial 16S rRNA gene copies in the surface 2 m and bottom 16 m samples. The ratio of quantities was calculated as 16S rRNA gene copy numbers in specific fraction normalized to the highest quantities of 16S rRNA gene copy numbers observed among all fractions in that sample, and 1 equals the highest value observed. Data

(Continued)

FIGURE 4 | Continued
points were presented as average ± standard deviation of three replicate qPCR measurements. Gray bars indicate heavy density ranges used for percentage enrichment calculations in **(C–F)**. **(C,D)** Percentage enrichment of major bacterial classes in the heavy density range in the ^{13}C-AVFA SIP fractions compared to the ^{12}C-AVFA SIP fractions. The 13, 24, and 48 h DNA samples were pooled together for SIP results. Bacterial class chosen were at least 0.1% abundance of the community. Flavo, Flavobacteria; Sphingo, Sphingobacteria; Alpha, Alphaproteobacteria; Acidi, Acidimicrobiia; Verruco, Verrucomicrobiae; Cyano, Cyanobacteria subsection I; Actino, Actinobacteria; Beta, Betaproteobacteria; Plancto, Planctomycetacia; Gamma, Gammaproteobacteria. Class with percentage enrichment >84% at 95% confidence interval was in bold. **(E,F)** Percentage enrichment of major bacterial genera within each class (listed above the bars) in the heavy density range of the ^{13}C AVFA sample SIP fractions compared to the ^{12}C AVFA sample SIP fractions in the surface 2 m and bottom 16 m seawater. Bacterial genera chosen were at least 0.1% abundance of the community. Bacterial class abbreviation was same as before. Genus with percentage enrichment >168% at 95% confidence interval was in bold.

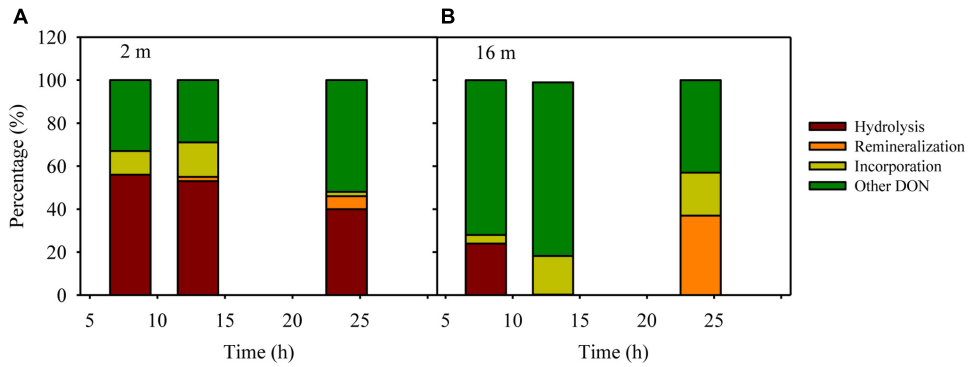

FIGURE 5 | An example of mass balance (including percentages of decreased peptide due to hydrolysis, remineralization to ammonium, incorporation into bacterial biomass and other unaccounted transformation to DON besides AVFA and amino acids) throughout the ^{12}C-AVFA decomposition in the (A) surface (2 m) and **(B)** bottom (16 m) seawaters.

As individual peptides may exist only at trace levels in ambient seawater, adding low concentration of peptides may simulate natural processes better. However, the low concentration amendments conducted here resulted in uptake patterns generally consistent with previous studies (Liu et al., 2013; Liu and Liu, 2016). Peptide decomposition all followed zero-order reaction with a linear decrease of concentration with time, indicating that the peptide decomposition in this study and previous studies was limited by the availability of enzymes produced by bacteria and the added peptide concentrations were probably all above a threshold of enzyme capacity in the ambient seawater. Faster peptide decomposition and less fragments produced in the bottom than in the surface incubations at both high and low added concentrations suggest that added peptides within this concentration range (0.25–10 μM) may trigger similar peptide decomposition mechanisms and bacterial response.

The peptide decomposition mechanism can be interrogated through a mass balance of the fate of added nitrogen, which may include: (1) extracellular hydrolysis to produce peptide fragments and amino acids, (2) remineralization to ammonium, and (3) incorporation into bacterial biomass. The percentage of extracellular hydrolysis can be estimated using the amino acid F and peptide fragments containing F, as bacterial uptake of F is limited within 24 h (Liu et al., 2013). The degree of remineralization can be estimated via changes in ammonium concentrations in peptide treatments compared to controls assuming nitrification is negligible during the 24 h (Liu et al., 2013). To calculate the incorporation percentage to microbial biomass, we assume a carbon conversion value of 20 fg C per bacterial cell and a C/N ratio of 4 for bacteria (Lee and Fuhrman, 1987). Based on these parameters, extracellular hydrolysis (40–56%) dominated the decomposition of AVFA in the surface water, whereas biomass production (4–20%) dominated in the bottom water throughout the incubation, leaving a major fraction (29–81%) of the AVFA nitrogen uncounted for in both layers, possibly in other forms of DON (**Figure 5**), which might be semi-labile and refractory DON formed via microbial production or transformation processes (Jiao et al., 2010; Benner and Amon, 2015; Walker et al., 2016). For example, at 24 h, ca. 40% of decreased AVFA in the surface seawater was hydrolyzed to peptide fragments and amino acids, ca. 6% was converted to ammonium, 2–11% to bacterial biomass (8.1×10^4–3.3×10^5 cells per mL), and about 50% to other DON. In contrast, in the bottom seawater, less than 5% was hydrolyzed to peptide fragments and amino acids, hardly any ammonium was produced, and 18–28% was incorporated into bacterial biomass (7.7×10^5–9.0×10^5 cells per mL) at 13 h when AVFA disappeared, resulting in about 70–80% of AVFA nitrogen as other DON. This contrasting pattern suggests that the fast disappearance of AVFA in the bottom water incubation may relate to the higher percentage of peptide incorporation into bacterial biomass, i.e., bacterial growth. The efficiency of AVFA decomposition may depend on the fraction of nitrogen allocated to those fast-growing bacteria.

Uptake of Peptide in the Normoxic vs. Hypoxic Seawater

In the surface seawater incubation, the incorporation of ^{13}C was greatest for Flavobacteria, Sphingobacteria, Alphaproteobacteria, Cyanobacteria, Acidimicrobiia, Verrucomicrobiae, and Actinobacteria (**Figure 4C**), indicating that both oligotrophic (such as Cyanobacteria) and copiotrophic bacteria were involved in peptide decomposition in the surface seawater. Copiotrophic, perhaps *r*-selected, bacteria use labile organic matter in nutrient-enriched environments. This is in contrast to more *K*-selected oligotrophic species that maintain efficient metabolism by growing more slowly on complex refractory substrates (Fierer et al., 2007; Wang et al., 2015). At the genus level, *Saprospiraceae* (Sphingobacteria), *Tropicibacter* (Alphaproteobacteria), *Roseovarius* (Alphaproteobacteria), *Owenweeksia* (Flavobacteria), *Formosa* (Flavobacteria), Flavobacteria NS4 marine group (Flavobacteria), and *Microbacteriaceae* SV1-8 (Actinobacteria) took up the most ^{13}C in the surface seawater (**Figure 4E**). Sphingobacteria showed a responsive role during peptone incubation in the seawater (Simon et al., 2012). The *Roseobacter* clade is often associated with plankton aggregates (Moran et al., 2007; Teeling et al., 2012; Yau et al., 2013), so *Tropicibacter* and *Roseovarius* belonging to the *Roseobacter* clade may be opportunistic in nutrient exploitation. Therefore, the observation that these populations can utilize the added peptide is expected. Flavobacteria are often effective in degrading high-molecular-weight DOM including proteins (Cottrell and Kirchman, 2000). Some Actinobacteria can produce a wide range of bioactive metabolites including extracellular peptidases that are sometimes involved in pathogenic processes (Ventura et al., 2007; Chen et al., 2011), suggesting their potential in peptide utilization. Consistent with our results, Orsi et al. (2016) also found that diverse bacterial taxa, such as Flavobacteria, Verrucomicrobia, Gammaproteobacteria, Alphaproteobacteria, Actinobacteria, and Planctomycetes, utilized added dissolved proteins in coastal California waters. The phylogenetic widespread of bacterial classes incorporating peptides in this study agrees with ecological theory and previous studies indicating that heterogeneity of the coastal oceans favors generalist bacteria in DOC utilization (Mou et al., 2008). Alternatively, this diverse bacterial pattern may result from the significant production of individual amino acids from extracellular hydrolysis (**Figures 2A,C**). Since uptake of amino acids is generally constitutive among marine bacterial taxa (Payne and Gilvarg, 1971; Poretsky et al., 2010) and uptake of amino acids is also part of peptide metabolizing process, bacterial groups possessing the ability to take up amino acids A, V, and F should be widespread, thus increasing the range of bacteria taxa showing positive percentage enrichment in the surface seawater.

In contrast to the surface seawater incubation, bacteria incorporating ^{13}C in bottom waters were associated with fewer taxonomic groups, primarily belonging to the Alphaproteobacteria and Gammaproteobacteria (**Figure 4D**). The bacteria that metabolized the peptide differed between the surface normoxic and bottom hypoxic seawater. This depth-differential response was strikingly consistent with the study of Nelson and Carlson (2012), showing that while both oligotrophic and copiotrophic bacteria incorporated amended DOC sources such as Synechococcus exudate, Synechococcus lysate, and gluconic acid in the euphotic seawater, no oligotrophic bacteria showed evidence of incorporation of amended DOC sources in the mesopelagic seawater. This concomitant pattern in different seawater systems implies that different water parameters between depths are likely to be the driving force in bacterial response to DOM sources. The dominant percentage enrichment of Alphaproteobacteria and Gammaproteobacteria in the bottom seawater suggested they can outcompete other bacteria in incorporating AVFA, thus leading to the faster decomposition of the peptide in the bottom seawater. This result is consistent with previous studies in DOM utilization, which quantified this process either directly through tracing radioisotope incorporation by bacteria or indirectly via analyzing changes of bacterial community structure (Gihring et al., 2009; McCarren et al., 2010; Carney et al., 2015). For example, the percentage of Gammaproteobacteria consuming proteins was higher than their abundance percentage among all bacterial phylogenetic groups in estuarine and coastal environments, indicating they are efficient at metabolizing proteins (Cottrell and Kirchman, 2000). Alphaproteobacteria or Gammaproteobacteria can dominate the bacterial community during DOM incubation in certain marine environments, indicating they can outcompete other bacteria in using DOM substrates (Harvey et al., 2006).

At the genus level, the highest percentage enrichment in the bottom seawater occurred to the *Thalassococcus* (Alphaproteobacteria), *Rhodobacteraceae* (Alphaproteobacteria), *Ruegeria* (Alphaproteobacteria), *Colwellia* (Gammaproteobacteria), *Balneatrix* (Gammaproteobacteria), and *Thalassomonas* (Gammaproteobacteria) (**Figure 4F**). *Thalassococcus* has been shown to be capable of utilizing phthalate (Iwaki et al., 2012), but its ability to metabolize peptides, as suggested here, has not yet been explored. Previous studies have shown that *Rhodobacterales* are often one of the dominant groups in coastal seawaters, accounting for as high as 75% of the Alphaproteobacteria (Dong et al., 2014). Their abundance is thought to be related to DOC concentrations in nutrient-enriched habitats and they are frequently involved in taking up labile organic molecules, such as peptides and amino acids, as detected by metaproteomics (Dong et al., 2014; Fodelianakis et al., 2014). Our previous study also showed that populations of *Ruegeria*, *Thalassomonas*, *Pseudoalteromonas,* and *Neptuniibacter* grew rapidly when AVFA was amended to the same Sta. C6 bottom water (Liu et al., 2013). These genera contain many copiotrophs. Copiotrophs, such as *Ruegeria*, *Vibrio*, *Alteromonas*, and *Colwellia*, grow rapidly when substrates are available, but also maintain growth potential under starvation conditions. This is akin to a "feast or famine" strategy that allows adaptation to rapidly changing environments (Eilers et al., 2000; Christie-Oleza et al., 2012). Their high capability to assimilate peptide is thus consistent with their ecology strategy. The growth of *Pseudoalteromonadaceae* and *Colwellia* increased when peptone was incubated in the Southern Ocean seawater (Simon et al., 2012). Consistently, copiotrophic bacteria, such as *Vibrio*, *Roseobacter*, *Pseudoalteromonas*, *Photobacterium*, *Marinomonas*, *Marinobacter*, and *Alteromonas*, dominated the incorporation of

DOC sources from *Synechococcus* exudate or lysate in seawater culture incubations (Nelson and Carlson, 2012). Particle-attached *Colwellia* and *Pseudoalteromonas* also showed high incorporation of proteins in marine microcosms (Mayali et al., 2015). DOC-related transporter genes, such as amino acids, oligopeptides, carbohydrates, carboxylic acids, polyamines, and lipids transporters, in coastal seawater were associated with *Rhodobacterales* (p*rimarily Roseobacter*), *Rickettsiales*, *Flavobacteriales*, and five orders of *Gammaproteobacteria*, including *Alteromonadales*, *Oceanospirallales*, *Pseudomonadales*, *Vibrionales*, and an uncharacterized taxon related to sulfur-oxidizing symbionts (Poretsky et al., 2010). Most of these bacteria also assimilated the peptide used in our study.

Changes in bacterial community structure that developed through incubations were not significantly different among the peptide treatment and control samples (**Figure 3**, ANOSIM $p > 0.05$, Supplementary Figure S2). These data suggest that peptide addition at relatively low concentrations had a minimal effect on the overall community structure. This also highlights that bacterial community structure cannot necessarily be used to infer roles of individual bacterial populations in incubation experiments. In contrast, the SIP technique directly links bacterial taxa with a metabolic function such as peptide decomposition. A direct comparison between the relative change in bacterial community structure and AVFA utilizing taxa, as determined via SIP, points to the interpretation that abundant bacterial taxa are not necessarily the most active ones (**Table 2**). For instance, *Saprospricaea*, *Escherichia–Shigella*, *Balneatrix*, and *Thalassomonas* accounted for <2% of communities and changed only <1% throughout the incubation while their abundance enrichment in heavy SIP fractions was 90–215%. *Microbacteriaceae* remained below 5% and their abundance did not increase with time during incubations, while frequencies increase by nearly 500% in heavy SIP fractions from surface seawater incubations. Similar observations have been reported elsewhere (Zemb et al., 2012), and indicate that some bacteria can be highly enriched in ^{13}C, but they may represent only a small proportion of the overall community. These rare bacteria may have long generation time with 10s of hour or more (Brock, 1971). During our short 48 h incubation, certain bacteria might be at lag phase of growth, which changed little in the community structure. For example, if these rare bacteria only doubled once during 48 h, their increase from ca. <1% to ca. <2% would not contribute much the overall community structure. Alternatively, these rare bacteria might have utilized the assimilated peptides mostly for respiration instead of for biomass building, leading to the mismatch between abundance and SIP incorporation. These data showed the potential role of some rare and uncultivable bacteria in peptide utilization, which is often overlooked based on bacterial community structure analysis. This uncoupling between microbial abundance and activity is also consistent with other studies showing uncoupled pattern between rDNA and rRNA for some bacterial populations (Campbell and Kirchman, 2013; Caruso et al., 2013; Hunt et al., 2013), reflecting bacterial activity

TABLE 2 | Comparison between the relative percentage change of bacteria genera (average percentage at 13+24+48 h relative to percentage at 0 h in quasi-replicates ($n = 4$) of ^{12}C-AVFA and ^{13}C-AVFA treatments) in the bacterial community structure and the percentage enrichment of bacteria genera showing positive enrichment in the SIP heavy fractions.

Depth	Bacteria genus	Percentage change in community structure (%)	Percentage enrichment in SIP (%)
2 m	*Saprospiraceae*	0.3	**203**
	Tropicibacter	1.7	**254**
	Rhodobacteraceae	12.6	164
	Thalassococcus	12.0	147
	Roseovarius	1.6	**300**
	Owenweeksia	−3.6	**359**
	Formosa	−0.4	**264**
	Flavobacteria NS4 marine group	−0.7	**312**
	Acidimicrobiia TM214	−0.9	91
	Acidimicrobiaceae	−1.8	142
	Roseibacillus	1.7	86
	Escherichia–Shigella	0.1	90
	Microbacteriaceae SV1-8	−0.7	**498**
	Synechococcus	−1.5	136
16 m	*Thlassococcus*	8.0	**471**
	Rhodobacteraceae	10.2	**261**
	Ruegeria	2.2	**233**
	Colwellia	3.2	**646**
	Balneatrix	0.2	**173**
	Thalassomonas	1.0	**215**
	Pseudoalteromonas	0.2	72
	Neptuniibacter	0.5	4

Percentage enrichment above 168 at 95% confidence interval was in bold.

rates are not necessarily correlated to their abundance and these two parameters may be controlled by different factors.

Factors Leading to the Development of Different Bacterial Communities

It is intriguing that bacterial communities that incorporated the added peptide differed in surface and bottom incubations. The two layers differed in chemical and biological parameters (**Table 1**, **Figures 1D–F**, **3**, and Supplementary Figure S2), such as DO, DOC, and initial bacterial community structure, which probably contributed to the development of different bacterial communities, but the role of these factors seems to be limited (Liu et al., 2013; Liu and Liu, 2016). Other than these parameters, high levels of P_i (>0.4 μM) in the bottom seawater may stimulate the growth of fast-growing bacteria with high RNA content (Liu and Liu, 2016), such as Alphaproteobacteria and Gammaproteobacteria, consistent with the Growth Rate Hypothesis (Elser et al., 2000; Makino et al., 2003). The fast-growing bacteria may lead to faster peptide decomposition observed in the bottom than in the surface seawater. Assuming 0.2 pg dry mass bacterial cells and a P content of 1.3% (Sterner and Elser, 2002), the bacterial abundance increase observed here would have required 0.01–0.08 μM P_i. These small values are close to the standard deviation (ca. 0.02 μM) of P_i measurement, which may explain why no obvious decrease of P_i was observed during our incubations (Supplementary Figures S1D,E). On the other hand, these results further suggest that the level of P_i, rather than its absence, is the key factor limiting the development of fast-growing bacteria, supporting our previous hypothesis (Liu and Liu, 2016). The unique development of certain alphaproteobacterial and gammaproteobacterial genera may also explain the much lower production of AVFA fragments during the bottom water incubation compared to the surface water incubation (**Figures 2B,D**). Either these bacteria directly took up the peptide, or the hydrolysis and subsequent uptake of the fragments were tightly coupled (Fuhrman, 1987; Kuznetsova and Lee, 2002; Liu et al., 2013). These two processes cannot be differentiated with these data, but regardless, both pathways differ from that of the surface incubation, where hydrolysis and uptake seem uncoupled.

Factors to be Considered for the DNA-SIP Approach

A successful DNA-SIP experiment depends on the amount of isotopically labeled substrate being assimilated and the length of the incubation time (Radajewski et al., 2003; Neufeld et al., 2007a). The substrate concentration must be high enough to ensure sufficient isotopic labeling of nucleic acids relative to unlabeled background substrates that are relatively abundant. However, if the substrate concentrations are too high, the incubation may deviate from the *in situ* situation. In our incubations, we added relatively low concentrations (0.25–0.47 μM) of AVFA to minimize disturbance to the natural substrates. qPCR results support the notion that sufficient isotope was incorporated into bacterial DNA. Successful uptake of peptide by bacteria is also indicated through the increased bacterial abundance in peptide treatments compared to control. Longer incubation time often results in greater isotope incorporation, but may also lead to cross-feeding, such as bacterial assimilation of labeled byproducts, intermediates or dead cells, produced from substrate metabolism (Neufeld et al., 2007a,c; Wang et al., 2015). To reduce cross-feeding, we applied relatively short incubation time (48 h) that was nonetheless sufficient to allow complete peptide loss.

A potential limitation of the DNA-SIP approach is that the buoyant density of DNA varies with G+C content. As G+C content may vary among different bacteria, this may result in a loss of power to identify bacteria that have incorporated the labeled substrate based on density shift (Buckley et al., 2007). However, it is more problematic for ^{15}N than for ^{13}C substrates given the greater buoyant density differential for nucleic acids labeled with ^{13}C. The density shift in our results was >0.01 g mL^{-1}, equating to ca. 28% of ^{13}C incorporation, which is more than the minimum percentage (20%) that is typically required for separating ^{13}C and unlabeled organisms (Uhlik et al., 2009). Note that the overall buoyant density differed somewhat between the surface and bottom DNA fractions (**Figures 4A,B**). It is unclear why this difference was observed, but may be related to the different bacterial community composition in the surface and bottom incubations, as %G+C contents of DNA vary among different bacterial taxa and higher %G+C leads to heavier density (Buckley et al., 2007; Holben, 2011). However, it is presumed that this density difference will not affect our ability to identify bacteria incorporating ^{13}C, because the taxonomic percentage enrichment was derived relative to the corresponding ^{12}C-AVFA incubations within the surface or bottom samples. We note that DNA from three incubation time points (13, 24, 48 h) was pooled. This approach results in 'smearing' of the signal by spreading the DNA of active bacterial taxa across the gradient density range to a greater degree than for a single time point. However, this smearing should not be problematic with respect to the objectives of this study, because major bacterial taxa in the bacterial community structure were similar at all these three time points and the chemistry data showed a continuous pattern among these three time points. AVFA were completely degraded during 24–48 h in the surface seawater and during 13–24 h in the bottom seawater. Bacterial cell replication and DNA synthesis may have time lag after peptide incorporation due to their 9–12 h generation time (Eilers et al., 2000). Bacterial abundance was still increasing after 13 h in the bottom seawater (**Figures 1D,E**), indicating bacteria were still utilizing peptides for their growth shortly after peptide was completely degraded. To be consistent between two depths and make sure enough ^{13}C signal is obtained, pooling the last three time points seems an appropriate choice. As surface and bottom incubations were treated in the same way for SIP samples, the comparison between two waters still holds with pooled samples. While the exact degree of isotopic labeling or peptide incorporation may therefore not be attainable from our experiments, the high degree of enrichment observed for some bacteria (**Figures 4C–F**) supports the notion of active ^{13}C incorporation.

CONCLUSION

Work presented here builds on prior observations with respect to the inferred role of bacteria in peptide decomposition (Liu et al., 2013; Liu and Liu, 2016). Here, we directly linked specific bacterial taxa with peptide decomposition in surface and bottom waters in the hypoxic region of northern Gulf of Mexico. Major conclusions and implications from this study are as follows:

(1) Bacterial groups metabolizing peptide appear to differ between the surface normoxic and bottom hypoxic seawater. A more diverse group of bacteria including both oligotrophs and copiotrophs might be involved in peptide decomposition in the surface normoxic seawater, while peptide substrates appear to favor several copiotrophic marine bacterial lineages in the bottom hypoxic seawater. With a combination of detailed chemical and biological data in an isolation-independent way, this study expands our understanding of linkage between peptide decomposition and bacterial communities, especially with low concentrations of peptide amendment, and sheds new light on microbial behavior as single cells, populations and communities in microbial ecology.

(2) Peptide decomposition efficiency, pathway and fate differed between the surface normoxic and bottom hypoxic seawater, which might be related to the energy and element allocation to different bacterial taxa under distinct marine environments. By combining these chemical analyses with SIP results, the role of bacteria in contributing to this difference can thus be inferred. This serves as the first step to explore marine C and N cycle efficiency and mechanisms in various marine environments.

(3) This study further implies that some bacteria taxa can rapidly metabolize peptide in the context of high P_i concentration in the hypoxic seawater. It provides insights into the interactions among bacteria, labile DOM, nutrient, and DO in seawater, which stimulates more ecological hypotheses about diverse microbial groups and their functions in marine environments. As hypoxia may be intensified in the future scenario, investigating bacterial decomposition of labile DOM under different nutrient conditions is necessary to pinpoint the factors controlling hypoxia formation.

AUTHOR CONTRIBUTIONS

All authors listed have made substantial, direct and intellectual contributions to the work and approved its final version for publication.

FUNDING

This work is funded by the Chemical and Biological Oceanography Programs of the National Science Foundation (OCE-1129659 & OCE-1634630).

ACKNOWLEDGMENTS

We thank the help from the crew of R/V *Pelican*. We appreciate J. Liu for his help with the incubation experiment, Dr. C. Shank for analyzing DOC samples and Dr. T. Villareal for his help with bacterial abundance analysis. We thank comments from Dr. W. Gardner, Dr. D. Erdner, Dr. J. McClelland and Dr. D. Kirchman. We are grateful for the DNA sequencing by the Oklahoma Medical Research Foundation.

SUPPLEMENTARY MATERIAL

The Supplementary Material for this article can be found online at: http://journal.frontiersin.org/article/10.3389/fmicb.2017.00353/full#supplementary-material

REFERENCES

Aluwihare, L. I., Repeta, D. J., Pantoja, S., and Johnson, C. G. (2005). Two chemically distinct pools of organic nitrogen accumulate in the ocean. *Science* 308, 1007–1010. doi: 10.1126/science.1108925

Azam, F. (1998). Microbial control of oceanic carbon flux: the plot thickens. *Science* 280, 694–696. doi: 10.1126/science.280.5364.694

Bell, T. H., Yergeau, E., Martineau, C., Juck, D., Whyte, L. G., and Greer, C. W. (2011). Identification of nitrogen-incorporating bacteria in petroleum-contaminated Arctic soils by using [15N]DNA-based stable isotope probing and pyrosequencing. *Appl. Environ. Microbiol.* 77, 4163–4171. doi: 10.1128/AEM.00172-11

Benner, R., and Amon, R. M. W. (2015). The size-reactivity continuum of major bioelements in the ocean. *Ann. Rev. Mar. Sci.* 7, 185–205. doi: 10.1146/annurev-marine-010213-135126

Berg, C., Beckmann, S., Jost, G., Labrenz, M., and Jurgens, K. (2013). Acetate-utilizing bacteria at an oxic-anoxic interface in the Baltic Sea. *FEMS Microbiol. Ecol.* 85, 251–261. doi: 10.1111/1574-6941.12114

Brock, T. D. (1971). Microbial growth rate in nature. *Bacteriol. Rev.* 35, 39–58.

Buckley, D. H., Huangyutitham, V., Hsu, S. F., and Nelson, T. A. (2007). Stable isotope probing with 15N achieved by disentangling the effects of genome G+C content and isotope enrichment on DNA density. *Appl. Environ. Microbiol.* 73, 3189–3195. doi: 10.1128/AEM.02609-06

Campbell, B. J., and Kirchman, D. L. (2013). Bacterial diversity, community structure and potential growth rates along an estuarine salinity gradient. *ISME J.* 7, 210–220. doi: 10.1038/ismej.2012.93

Caporaso, J. G., Bittinger, K., Bushman, F. D., DeSantis, T. Z., Andersen, G. L., and Knight, R. (2010a). PyNAST: a flexible tool for aligning sequences to a template alignment. *Bioinformatics* 26, 266–267. doi: 10.1093/bioinformatics/btp636

Caporaso, J. G., Kuczynski, J., Stombaugh, J., Bittinger, K., Bushman, F. D., Costello, E. K., et al. (2010b). QIIME allows analysis of high-throughput community sequencing data. *Nat. Methods* 7, 335–336. doi: 10.1038/NMETH.F.303

Carney, R. L., Mitrovic, S. M., Jeffries, T., Westhorpe, D., Curlevski, N., and Seymour, J. R. (2015). River bacterioplankton community responses to a high inflow event. *Aquat. Microb. Ecol.* 75, 187–205. doi: 10.3354/ame01758

Caruso, G., Azzaro, F., Azzaro, M., Decembrini, F., Ferla, R. L., Maimone, G., et al. (2013). Environmental variability in a transitional Mediterranean system (OlivierieTindari, Italy): focusing on the response of microbial activities and prokaryotic abundance. *Estuar. Coast. Shelf Sci.* 135, 158–170. doi: 10.1016/j.ecss.2013.10.002

Chen, Y. Q., Ntai, I., and Kelleher, N. L. (2011). A proteomic survey of nonribosomal peptide and polyketide biosynthesis in Actinobacteria. *J. Proteome Res.* 11, 85–94. doi: 10.1021/pr2009115

Christie-Oleza, J. A., Fernandez, B., Nogales, B., Bosch, R., and Armengaud, J. (2012). Proteomic insights into the lifestyle of an environmentally relevant marine bacterium. *ISME J.* 6, 124–135. doi: 10.1038/ismej.2011.86

Connelly, T. L., Baer, S. E., Cooper, J. T., Bronk, D. A., and Wawrik, B. (2014). Urea uptake and carbon fixation by marine pelagic bacteria and archaea during the Arctic summer and winter seasons. *Appl. Environ. Microbiol* 80, 6013–6022. doi: 10.1128/AEM.01431-14

Cottrell, M. T., and Kirchman, D. L. (2000). Natural assemblages of marine proteobacteria and members of the *Cytophaga-Flavobacter* cluster consuming low- and high-molecular-weight dissolved organic matter. *Appl. Environ. Microbiol.* 66, 1692–1697. doi: 10.1128/AEM.66.4.1692-1697.2000

Crump, B. C., Peranteau, C., Beckingham, B., and Cornwell, J. C. (2007). Respiratory succession and community succession of bacterioplankton in seasonally anoxic estuarine waters. *Appl. Environ. Microbiol.* 73, 6802–6810. doi: 10.1128/AEM.00648-07

Dong, H. P., Hong, Y. G., Lu, S. H., and Xie, L. Y. (2014). Metaproteomics reveals the major microbial players and their biogeochemical functions in a productive coastal system in the northern South China Sea. *Environ. Microbiol. Rep.* 6, 683–695. doi: 10.1111/1758-2229.12188

Eilers, H., Pernthaler, J., and Amann, R. (2000). Succession of pelagic marine bacteria during enrichment: a close look at cultivation-induced shifts. *Appl. Environ. Microbiol.* 66, 4634–4640. doi: 10.1128/AEM.66.11.4634-4640.2000

Elser, J. J., Sterner, R. W., Gorokhova, E., Fagan, W. F., Markow, T. A., Cotner, J. B., et al. (2000). Biological stoichiometry from genes to ecosystems. *Ecol. Lett.* 3, 540–550. doi: 10.1111/j.1461-0248.2000.00185.x

Fierer, N., Bradford, M. A., and Jackson, R. B. (2007). Toward an ecological classification of soil bacteria. *Ecology* 88, 1354–1364. doi: 10.1890/05-1839

Fodelianakis, S., Papageorgiou, N., Pitta, P., Kasapidis, P., Karakassis, I., and Ladoukakis, E. D. (2014). The pattern of change in the abundances of specific bacterioplankton groups is consistent across different nutrient-enriched habitats in Crete. *Appl. Environ. Microbiol.* 80, 3784–3792. doi: 10.1128/AEM.00088-14

Fuhrman, J. A. (1987). Close coupling between release and uptake of dissolved free amino-acids in seawater studied by an isotope-dilution approach. *Mar. Ecol. Prog. Ser.* 37, 45–52. doi: 10.3354/meps037045

Gardner, W. S., and St. John, P. A. (1991). High-performance liquid chromatographic method to determine ammonium ion and primary amines in seawater. *Anal. Chem.* 63, 537–540. doi: 10.1021/ac00005a032

Gihring, T. M., Humphrys, M., Mills, H. J., Huettel, M., and Kostka, J. E. (2009). Identification of phytodetritus-degrading microbial communities in sublittoral Gulf of Mexico sands. *Limnol. Oceanogr.* 54, 1073–1083. doi: 10.4319/lo.2009.54.4.1073

Harvey, H. R., Dyda, R. Y., and Kirchman, D. L. (2006). Impact of DOM composition on bacterial lipids and community structure in estuaries. *Aquat. Microb. Ecol.* 42, 105–117. doi: 10.3354/ame042105

Holben, W. E. (2011). "GC fractionation allows comparative total microbial community analysis, enhances diversity assessment, and facilitates detection of minority populations of bacteria," in *Handbook of Molecular Micorbial Ecology: Metagenomics and Complementary Approaches*, Vol. I, ed. F. J. de Bruijn (Hoboken, NJ: Wiley-Blackwell), 183–196.

Hunt, D. E., Lin, Y., Church, M. J., Karl, D. M., Tringe, S. G., Izzo, L. K., et al. (2013). Relationship between abundance and specific activity of bacterioplankton in open ocean surface waters. *Appl. Environ. Microbiol.* 79, 177–184. doi: 10.1128/AEM.02155-12

Iwaki, H., Nishimura, A., and Hasegawa, Y. (2012). Isolation and characterization of marine bacteria capable of utilizing phthalate. *World J. Microbiol. Biot.* 28, 1321–1325. doi: 10.1007/s11274-011-0925-x

Jiao, N., Herndl, G. J., Hansell, D. A., Benner, R., Kattner, G., Wilhelm, S. W., et al. (2010). Microbial production of recalcitrant dissolved organic matter: long-term carbon storage in the global ocean. *Nat. Rev. Microbiol.* 8, 593–599. doi: 10.1038/nrmicro2386

Jones, M. N. (1984). Nitrate reduction by shaking with Cadmium – alternative to Cadmium columns. *Water Res.* 18, 643–646. doi: 10.1016/0043-1354(84)90215-X

Karl, D. M. (2014). Microbially mediated transformations of phosphorus in the sea: new views of an old cycle. *Ann. Rev. Mar. Sci.* 6, 279–337. doi: 10.1146/annurev-marine-010213-135046

Kleindienst, S., Herbst, F. A., Stagars, M., von Netzer, F., von Bergen, M., Seifert, J., et al. (2014). Diverse sulfate-reducing bacteria of the *Desulfosarcina/Desulfococcus* clade are the key alkane degraders at marine seeps. *ISME J.* 8, 2029–2044. doi: 10.1038/ismej.2014.51

Klindworth, A., Pruesse, E., Schweer, T., Peplies, J., Quast, C., Horn, M., et al. (2013). Evaluation of general 16S ribosomal RNA gene PCR primers for classical and next-generation sequencing-based diversity studies. *Nucleic Acids Res.* 41, e1. doi: 10.1093/nar/gks808

Kuznetsova, M., and Lee, C. (2002). Dissolved free and combined amino acids in nearshore seawater, sea surface microlayers and foams: influence of extracellular hydrolysis. *Aquat. Sci.* 64, 252–268. doi: 10.1007/s00027-002-8070-0

Lee, C., Hedges, J. I., Wakeham, S. G., and Zhu, N. (1992). Effectiveness of various treatments in retarding microbial activity in sediment trap material and their effects on the collection of swimmers. *Limnol. Oceanogr.* 37, 117–130. doi: 10.4319/lo.1992.37.1.0117

Lee, C., Wakeham, S. G., and Hedges, J. I. (2000). Composition and flux of particulate amino acids and chloropigments in equatorial Pacific seawater and sediments. *Deep Sea Res. I* 47, 1535–1568. doi: 10.1016/S0967-0637(99)00116-8

Lee, S., and Fuhrman, J. A. (1987). Relationships between biovolume and biomass of naturally derived marine bacterioplankton. *Appl. Environ. Microbiol.* 53, 1298–1303.

Lindroth, P., and Mopper, K. (1979). High-performance liquid-chromatographic determination of subpicomole amounts of amino-acids by precolumn fluorescence derivatization with o-phthaldialdehyde. *Anal. Chem.* 51, 1667–1674. doi: 10.1021/ac50047a019

Liu, S., and Liu, Z. (2014). A new method to measure small peptides amended in seawater using high performance liquid chromatography coupled with mass spectrometry. *Mar. Chem.* 164, 16–24. doi: 10.1016/j.marchem.2014.05.006

Liu, S., and Liu, Z. (2015). Comparing extracellular enzymatic hydrolysis between plain peptides and their corresponding analogs in the northern Gulf of Mexico Mississippi River plume. *Mar. Chem.* 177, 398–407. doi: 10.1016/j.marchem.2015.06.021

Liu, S., Riesen, A., and Liu, Z. (2015). Differentiating the role of different-sized microorganisms in peptide decomposition during incubations using size-fractioned coastal seawater. *J. Exp. Mar. Biol. Ecol.* 472, 97–106. doi: 10.1016/j.jembe.2015.07.004

Liu, Z., Kobiela, M. E., McKee, G. A., Tang, T. T., Lee, C., Mulholland, M. R., et al. (2010). The effect of chemical structure on the hydrolysis of tetrapeptides along a river-to-ocean transect: AVFA and SWGA. *Mar. Chem.* 119, 108–120. doi: 10.1016/j.marchem.2010.01.005

Liu, Z., and Liu, S. (2016). High phosphate concentrations accelerate bacterial peptide degradation in hypoxic bottom waters of the northern Gulf of Mexico. *Environ. Sci. Technol.* 50, 676–684. doi: 10.1021/ac50047a019

Liu, Z., Liu, S., Liu, J., and Gardner, W. S. (2013). Differences in peptide decomposition rates and pathways in hypoxic and oxic coastal environments. *Mar. Chem.* 157, 67–77. doi: 10.1016/j.marchem.2013.08.003

Luo, C. L., Xie, S. G., Sun, W. M., Li, X. D., and Cupples, A. M. (2009). Identification of a novel toluene-degrading bacterium from the candidate phylum TM7, as determined by DNA stable isotope probing. *Appl. Environ. Microbiol.* 75, 4644–4647. doi: 10.1128/AEM.00283-09

Makino, W., Cotner, J. B., Sterner, R. W., and Elser, J. J. (2003). Are bacteria more like plants or animals? Growth rate and resource dependence of bacterial C : N : P stoichiometry. *Funct. Ecol.* 17, 121–130. doi: 10.1046/j.1365-2435.2003.00712.x

Marie, D., Partensky, F., Jacquet, S., and Vaulot, D. (1997). Enumeration and cell cycle analysis of natural populations of marine picoplankton by flow cytometry using the nucleic acid stain SYBR Green I. *Appl. Environ. Microbiol.* 63, 186–193.

Mayali, X., Stewart, B., Mabery, S., and Weber, P. K. (2015). Temporal succession in carbon incorporation from macromolecules by particle-attached bacteria in marine microcosms. *Environ. Microbiol. Rep.* 8, 68–75. doi: 10.1111/1758-2229.12352

McCarren, J., Becker, J. W., Repeta, D. J., Shi, Y., Young, C. R., Malmstrom, R. R., et al. (2010). Microbial community transcriptomes reveal microbes and metabolic pathways associated with dissolved organic matter turnover in

the sea. *Proc. Natl. Acad. Sci. U.S.A.* 107, 16420–16427. doi: 10.1073/pnas.1010732107

Moran, M. A., Belas, R., Schell, M. A., Gonzalez, J. M., Sun, F., Sun, S., et al. (2007). Ecological genomics of marine roseobacters. *Appl. Environ. Microbiol.* 73, 4559–4569. doi: 10.1128/AEM.02580-06

Mou, X., Sun, S., Edwards, R. A., Hodson, R. E., and Moran, M. A. (2008). Bacterial carbon processing by generalist species in the coastal ocean. *Nature* 451, 708–712. doi: 10.1038/nature06513

Murray, A. E., Arnosti, C., De La Rocha, C. L., Grossart, H. P., and Passow, U. (2007). Microbial dynamics in autotrophic and heterotrophic seawater mesocosms. II. Bacterioplankton community structure and hydrolytic enzyme activities. *Aquat. Microb. Ecol.* 49, 123–141. doi: 10.3354/ame01139

Nagata, T. (2008). "Organic matter-bacteria interactions in seawater," in *Microbial Ecology of the Oceans*, ed. D. L. Kirchman (New York, NY: Wiley-Blackwell), 207–242.

Nakatsu, C. H., and Marsh, T. L. (2007). "Analysis of microbial communities with denaturing gradient gel eletrophoresis and terminal restriction fragment length polymorphism," in *Methods for General and Molecular Microbiology*, eds C. A. Reddy, T. J. Beveridge, J. A. Breznak, G. A. Marzluf, T. M. Schmidt, and L. R. Snyder (Wahsington, DC: ASM Press), 909–923.

Nelson, C. E., and Carlson, C. A. (2012). Tracking differential incorporation of dissolved organic carbon types among diverse lineages of Sargasso Sea bacterioplankton. *Environ. Microbiol.* 14, 1500–1516. doi: 10.1111/j.1462-2920.2012.02738.x

Nelson, C. E., and Wear, E. K. (2014). Microbial diversity and the lability of dissolved organic carbon. *Proc. Natl. Acad. Sci. U.S.A.* 111, 7166–7167. doi: 10.1073/pnas.1405751111

Neufeld, J. D., Dumont, M. G., Vohra, J., and Murrell, J. C. (2007a). Methodological considerations for the use of stable isotope probing in microbial ecology. *Microb. Ecol.* 53, 435–442. doi: 10.1007/s00248-006-9125-x

Neufeld, J. D., Schafer, H., Cox, M. J., Boden, R., McDonald, I. R., and Murrell, J. C. (2007b). Stable-isotope probing implicates *Methylophaga* spp and novel *Gammaproteobacteria* in marine methanol and methylamine metabolism. *ISME J.* 1, 480–491. doi: 10.1038/ismej.2007.65

Neufeld, J. D., Wagner, M., and Murrell, J. C. (2007c). Who eats what, where and when? Isotope-labelling experiments are coming of age. *ISME J.* 1, 103–110. doi: 10.1038/ismej.2007.30

Oksanen, J., Blanchet, F. G., Kindt, R., Legendre, P., Minchin, P. R., O'Hara, R. B., et al. (2016). *Package 'Vegan'*. Available at: http://cran.r-project.org

Orellana, M. V., and Hansell, D. A. (2012). Ribulose-1,5-bisphosphate carboxylase/oxygenase (RuBisCO): a long-lived protein in the deep ocean. *Limnol. Oceanogr.* 57, 826–834. doi: 10.4319/lo.2012.57.3.0826

Orsi, W. D., Smith, J. M., Liu, S., Liu, Z., Sakamoto, C. M., Wilken, S., et al. (2016). Diverse, uncultivated bacteria and archaea underlying the cycling of dissolved protein in the ocean. *ISME J.* 10, 2158–2173. doi: 10.1038/ismej.2016.20

Ouverney, C. C., and Fuhrman, J. A. (1999). Combined Microautoradiography-16S rRNA probe technique for determination of radioisotope uptake by specific microbial cell types in situ. *Appl. Environ. Microbiol.* 65, 3264–3264.

Parsons, R. J., Nelson, C. E., Carlson, C. A., Denman, C. C., Andersson, A. J., Kledzik, A. L., et al. (2015). Microbial bacterioplankton community turnover within seasonally hypoxic waters of a subtropical sound: Devil's Hole, Bermuda. *Environ. Microbiol.* 17, 3481–3499. doi: 10.1111/1462-2920.12445

Payne, J. W., and Gilvarg, C. (1971). Peptide transport. *Adv. Enzymol. Relat. Areas Mol. Biol.* 350, 187–244. doi: 10.1002/9780470122808.ch5

Poretsky, R. S., Sun, S. L., Mou, X. Z., and Moran, M. A. (2010). Transporter genes expressed by coastal bacterioplankton in response to dissolved organic carbon. *Environ. Microbiol.* 12, 616–627. doi: 10.1111/j.1462-2920.2009.02102.x

Rabalais, N. N., Turner, R. E., and Wiseman, W. J. (2001). Hypoxia in the gulf of Mexico. *J. Environ. Qual.* 30, 320–329. doi: 10.2134/jeq2001.302320x

Radajewski, S., Ineson, P., Parekh, N. R., and Murrell, J. C. (2000). Stable-isotope probing as a tool in microbial ecology. *Nature* 403, 646–649. doi: 10.1038/35001054

Radajewski, S., McDonald, I. R., and Murrell, J. C. (2003). Stable-isotope probing of nucleic acids: a window to the function of uncultured microorganisms. *Curr. Opin. Biotechnol.* 14, 296–302. doi: 10.1016/S0958-1669(03)00064-8

Redmond, M. C., Valentine, D. L., and Sessions, A. L. (2010). Identification of novel methane-, ethane-, and propane-oxidizing bacteria at marine hydrocarbon seeps by stable isotope probing. *Appl. Environ. Microbiol.* 76, 6412–6422. doi: 10.1128/AEM.00271-10

Simon, M., Billerbeck, S., Kessler, D., Selje, N., and Schlingloff, A. (2012). Bacterioplankton communities in the Southern Ocean: composition and growth response to various substrate regimes. *Aquat. Microb. Ecol.* 68, 13–28. doi: 10.3354/ame01597

Sipler, R. E., and Bronk, D. A. (2015). "Dynamics of dissolved organic nitrogen," in *Biogeochemistry of Marine Dissolved Organic Matter*, eds D. A. Hansell and C. A. Carlson (San Diego, CA: Academic Press), 127–232.

Sterner, R. W., and Elser, J. J. (2002). *Ecological Stoichiometry: The biology of Elements from Molecules to the Biosphere*. Princeton, NJ: Princeton University Press.

Strickland, J. D. H., and Parsons, T. R. (1968). *A Practical Handbook of Seawater Analysis*. Ottawa, ON: Queen's Printer.

Tabor, P. S., and Neihof, R. A. (1982). Improved microautoradiographic method to determine individual microorganisms active in substrate uptake in natural waters. *Appl. Environ. Microbiol.* 44, 945–953.

Teeling, H., Fuchs, B. M., Becher, D., Klockow, C., Gardebrecht, A., Bennke, C. M., et al. (2012). Substrate-controlled succession of marine bacterioplankton populations induced by a phytoplankton bloom. *Science* 336, 608–611. doi: 10.1126/science.1218344

Teske, A., Durbin, A., Ziervogel, K., Cox, C., and Arnosti, C. (2011). Microbial community composition and function in permanently cold seawater and sediments from an Arctic fjord of Svalbard. *Appl. Environ. Microbiol.* 77, 2008–2018. doi: 10.1128/AEM.01507-10

Uhlik, O., Jecna, K., Leigh, M. B., Mackova, M., and Macek, T. (2009). DNA-based stable isotope probing: a link between community structure and function. *Sci. Total Environ.* 407, 3611–3619. doi: 10.1016/j.scitotenv.2008.05.012

Ventura, M., Canchaya, C., Tauch, A., Chandra, G., Fitzgerald, G. F., Chater, K. F., et al. (2007). Genomics of *Actinobacteria*: tracing the evolutionary history of an ancient phylum. *Microbiol. Mol. Biol. Rev.* 71, 495–548. doi: 10.1128/MMBR.00005-07

Walker, B. D., Beaupré, S. R., Guilderson, T. P., McCarthy, M. D., and Druffel, E. R. M. (2016). Pacific carbon cycling constrained by organic matter size, age and composition relationships. *Nat. Geosci.* 9, 888–891. doi: 10.1038/ngeo2830

Wang, X., Sharp, C. E., Jones, G. M., Grasby, S. E., Brady, A. L., and Dunfield, P. F. (2015). Stable-isotope probing identifies uncultured *Planctomycetes* as primary degraders of a complex heteropolysaccharide in soil. *Appl. Environ. Microbiol.* 81, 4607–4615. doi: 10.1128/AEM.00055-15

Wawrik, B., Boling, W. B., Van Nostrand, J. D., Xie, J. P., Zhou, J. Z., and Bronk, D. A. (2012a). Assimilatory nitrate utilization by bacteria on the West Florida Shelf as determined by stable isotope probing and functional microarray analysis. *FEMS Microbiol. Ecol.* 79, 400–411. doi: 10.1111/j.1574-6941.2011.01226.x

Wawrik, B., Callaghan, A. V., and Bronk, D. A. (2009). Use of inorganic and organic nitrogen by *Synechococcus* spp. and diatoms on the West Florida Shelf as measured using stable isotope probing. *Appl. Environ. Microbiol.* 75, 6662–6670. doi: 10.1128/AEM.01002-09

Wawrik, B., Mendivelso, M., Parisi, V. A., Suflita, J. M., Davidova, I. A., Marks, C. R., et al. (2012b). Field and laboratory studies on the bioconversion of coal to methane in the San Juan Basin. *FEMS Microbiol. Ecol.* 81, 26–42. doi: 10.1111/j.1574-6941.2011.01272.x

Weiss, M. S., Abele, U., Weckesser, J., Welte, W., Schiltz, E., and Schulz, G. E. (1991). Molecular architecture and electrostatic properties of a bacterial porin. *Science* 254, 1627–1630. doi: 10.1126/science.1721242

Wright, J. J., Konwar, K. M., and Hallam, S. J. (2012). Microbial ecology of expanding oxygen minimum zones. *Nat. Rev. Microbiol.* 10, 381–394. doi: 10.1038/nrmicro2778

Yau, S., Lauro, F. M., Williams, T. J., DeMaere, M. Z., Brown, M. V., Rich, J., et al. (2013). Metagenomic insights into strategies of carbon conservation and

unusual sulfur biogeochemistry in a hypersaline Antarctic lake. *ISME J.* 7, 1944–1961. doi: 10.1038/ismej.2013.69

Zaikova, E., Walsh, D. A., Stilwell, C. P., Mohn, W. W., Tortell, P. D., and Hallam, S. J. (2010). Microbial community dynamics in a seasonally anoxic fjord: Sannich Inlet, British Columbia. *Environ. Microbiol.* 12, 172–191. doi: 10.1111/j.1462-2920.2009.02058.x

Zemb, O., Lee, M., Gutierrez-Zamora, M. L., Hamelin, J., Coupland, K., Hazrin-Chong, N. H., et al. (2012). Improvement of RNA-SIP by pyrosequencing to identify putative 4-n-nonylphenol degraders in activated sludge. *Water Res.* 46, 601–610. doi: 10.1016/j.watres.2011.10.047

Conflict of Interest Statement: The authors declare that the research was conducted in the absence of any commercial or financial relationships that could be construed as a potential conflict of interest.

frontiers in Microbiology

ORIGINAL RESEARCH
published: 06 March 2018
doi: 10.3389/fmicb.2018.00368

Potential Activities of Freshwater Exo- and Endo-Acting Extracellular Peptidases in East Tennessee and the Pocono Mountains

*Lauren Mullen[1], Malcolm X Shabazz High School Aquatic Biogeochemistry Team[2], Kim Boerrigter[2,3], Nicholas Ferriero[2], Jeff Rosalsky[4], Abigail van Buren Barrett[1], Patrick J. Murray[2] and Andrew D. Steen[1]**

[1] Department of Earth and Planetary Sciences, University of Tennessee, Knoxville, Knoxville, TN, United States, [2] Malcolm X Shabazz High School, Newark, NJ, United States, [3] Harvard College, Cambridge, MA, United States, [4] Pocono Environmental Education Center, Dingmans Ferry, PA, United States

Proteins constitute a particularly bioavailable subset of organic carbon and nitrogen in aquatic environments but must be hydrolyzed by extracellular enzymes prior to being metabolized by microorganisms. Activities of extracellular peptidases (protein-degrading enzymes) have frequently been assayed in freshwater systems, but such studies have been limited to substrates for a single enzyme [leucyl aminopeptidase (Leu-AP)] out of more than 300 biochemically recognized peptidases. Here, we report kinetic measurements of extracellular hydrolysis of five substrates in 28 freshwater bodies in the Delaware Water Gap National Recreation Area in the Pocono Mountains (PA, United States) and near Knoxville (TN, United States), between 2013 and 2016. The assays putatively test for four aminopeptidases (arginyl aminopeptidase, glyclyl aminopeptidase, Leu-AP, and pyroglutamyl aminopeptidase), which cleave *N*-terminal amino acids from proteins, and trypsin, an endopeptidase, which cleaves proteins mid-chain. Aminopeptidase and the trypsin-like activity were observed in all water bodies, indicating that a diverse set of peptidases is typical in freshwater. However, ratios of peptidase activities were variable among sites: aminopeptidases dominated at some sites and trypsin-like activity at others. At a given site, the ratios remained fairly consistent over time, indicating that they are driven by ecological factors. Studies in which only Leu-AP activity is measured may underestimate the total peptidolytic capacity of an environment, due to the variable contribution of endopeptidases.

Keywords: extracellular enzymes, aminopeptidase, endopeptidase, freshwater, trypsin, protein

OPEN ACCESS

Edited by:
George S. Bullerjahn, Bowling Green State University, United States

Reviewed by:
Kaarina Sivonen, University of Helsinki, Finland
Izabela Marques Dourado Bastos, University of Brasília, Brazil

****Correspondence:***
Andrew D. Steen
asteen1@utk.edu

Specialty section:
This article was submitted to Aquatic Microbiology, a section of the journal Frontiers in Microbiology

Received: *29 September 2017*
Accepted: *16 February 2018*
Published: *06 March 2018*

Citation:
Mullen L, Malcolm X Shabazz High School Aquatic Biogeochemistry Team, Boerrigter K, Ferriero N, Rosalsky J, Barrett AB, Murray PJ and Steen AD (2018) Potential Activities of Freshwater Exo- and Endo-Acting Extracellular Peptidases in East Tennessee and the Pocono Mountains. Front. Microbiol. 9:368. doi: 10.3389/fmicb.2018.00368

INTRODUCTION

Kinetics of extracellular enzymes can give insight into the rates and pathways of organic matter processing in the environment (Schimel and Weintraub, 2003; Arnosti et al., 2014; Sinsabaugh et al., 2014). Diverse classes of extracellular enzymes have been observed in freshwaters, including peptidases, polysaccharide hydrolases, phosphatases, lipases, peroxidases, and laccases (Findlay and Sinsabaugh, 1999). Peptidases can be particularly valuable to microbial communities, because proteins provide organic N as well as C, and because protein-like organic matter is on

average more bioavailable than bulk natural organic matter (Fellman et al., 2010). The peptidases are a highly diverse class of enzymes: more than 300 distinct peptidases have been identified by function (McDonald et al., 2009) and many more have been identified by structure (Rawlings et al., 2016). Nevertheless, environmental studies have focused almost exclusively on the activity of a single extracellular peptidase, leucyl aminopeptidase (Leu-AP), which preferentially cleaves leucine from the *N*-terminus of proteins or peptides (Arnosti et al., 2014). In seawater, a diverse suite of aminopeptidases and endopeptidases (which cleave peptide bonds within proteins; Hooper, 2002), from bacteria as well as protists, are required for complete breakdown of proteins (Thao et al., 2014). Ratios of LeuAP and other aminopeptidases to endopeptidases can vary widely (Obayashi and Suzuki, 2005, 2008; Steen and Arnosti, 2013). The extent of this variation in freshwaters, and therefore the extent to which potential LeuAP activities represent total peptidolytic potential of freshwater ecosystems, remains unknown.

In order to constrain the degree to which LeuAP activities represent the total range of extracellular peptidases active in freshwaters, we assayed the potential activities of five different classes of extracellular peptidases in 28 freshwater bodies in southwest Pennsylvania (PA) and east Tennessee (TN) between 2013 and 2016. In addition to Leu-AP, we used substrates that putitively assay arginyl aminopeptidase (ArgAP), prolyl aminopeptidase, glycyl aminopeptidase (GlyAP), pyroglutamyl aminopeptidase, and trypsin. The first four of these are aminopeptidases while trypsin is an endopeptidase. Uniquely among amino acids in the substrates assayed here, pyroglutamic acid is not directly encoded by DNA and is not typically abundant in biomass. However, it does exist in low quantities in some environmentally relevant biomolecules, for instance, bacteriorhodopsin (Gerber et al., 1979). Freshwater organic matter contains a complex mixture of proteins and protein-like molecules that require a diverse suite of extracellular enzymes to efficiently remineralize (Arnosti et al., 2014). A better understanding of the nature of extracellular peptidases in aquatic environments could therefore shed light on the mechanisms by which organic matter is oxidized in such systems.

MATERIALS AND METHODS

Sites and Sample Collection

Samples were collected from 28 locations in and around Knoxville, TN, United States, and in the Pocono Mountains of eastern PA near the Pocono Environmental Education Center in 2013, 2015, and 2016 (PEEC; **Figure 1** and **Table 1**). Water samples were collected by hand in acid-rinsed, 1-L polyethylene bottles. *In situ* water temperature was measured at the time of sampling. For the Knoxville samples, pH was measured by electronic pH meter (Accumet AB150) upon return to the University of TN. For the PEEC samples, pH was measured using pH strips (2013–2015, 2016 YSI Pro DSS Sonde). A portion of the collected samples have missing pH values; these samples have been recorded as n.m in **Table 1**. Methods were developed through progressive years of the study and evolved to be more efficient; pH data were collected for most samples but were neglected in the early studies. Samples were kept at *in situ* temperature in the dark and returned to the lab within 1 h for enzyme assays. To assess temporal variability in peptidase activities, a short time series of six samples each was collected from the Third Creek (3rd) and Volunteer Landing (VL) sites during the period from June 8 to July 6, 2015.

Enzyme Assays

Enzyme assays were performed using fluorogenic substrates (Hoppe, 1983) according to a modified version of the protocol described by Steen and Arnosti (2011). The following

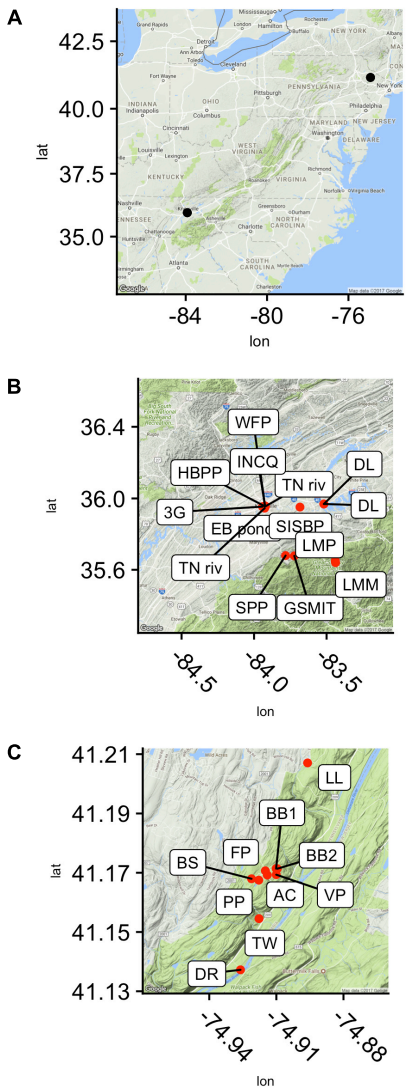

FIGURE 1 | Sampling sites in reference to the east coast of the United states **(A)** and seen in higher resolution, in the Delaware Water Gap National Recreation Area, Dingmans Ferry, PA, United States **(C)** and near Knoxville, TN, United States **(B)**.

TABLE 1 | Selected sampling sites and their corresponding GPS coordinates, temperature, pH, date, and time.

Site initials	Site name	Latitude	Longitude	Temperature	pH	Sample date	Sample time	State
TN	Tennessee River	35.956201	83.920999	30	6.81	5/13/15	13:30	TN
EB	Estabrook Fish Pond	35.955863	83.923597	29	7.88	5/14/15	13:20	TN
GSMIT	Great Smokey Mountain Institute at Tremont	35.678246	83.722413	26	7.11	5/15/15	11:00	TN
SPP	Special People's Park	35.67984	83.782517	26	7.19	5/15/15	11:20	TN
DL	Douglas Lake	35.969042	83.518601	32	7.43	5/18/15	8:00	TN
HBPP	Hesler Biology Plant Pond	35.956517	83.926578	30	6.86	5/18/15	9:00	TN
DL2	Douglas Lake 2	35.969042	83.518601	30	7.45	5/19/15	8:00	TN
SISBP	Seven Islands State Birding Park	35.951805	83.683438	28	7.38	5/19/15	8:47	TN
3G	Third Creek Greenway	35.954235	83.942073	29	7.55	5/20/15	9:10	TN
TN2	Tennessee River Water Plant	35.945633	83.926757	25	8.16	5/21/15	8:30	TN
WFP	World's Fair Park	35.958352	83.924428	20	7.66	5/21/15	8:40	TN
ECD	Eastman Chemical Dam	36.511133	82.537032	20	7.81	5/22/15	5:00	TN
INCQ	Ijams Nature Center Quarry	35.958352	83.924428	26	8.04	5/22/15	8:20	TN
BS	Briscoe Swamp	41.16796667	−74.9211	21	n.m	5/28/13	8:55	PA
BS2	Briscoe Swamp	41.16796667	−74.9211	21	8.11	6/01/16	18:20	PA
BW	Birchwood Lakes	41.242638	74.920148	23	n.m	5/28/13	n.m	PA
DR	Delaware River	41.13724	74.926029	25	7.21	5/28/15	12:35	PA
FP	Front Pond	41.170668	−74.91492	25	7	5/27/15	12:10	PA
FP2	Front Pond 2	41.170668	−74.91492	25	7	6/01/16	14:30	PA
LL	Loch Lomond	41.20705	−74.89605	23	7	5/28/15	9:40	PA
PP	Pickerel Pond	41.167504	−74.91786	27	7	5/27/15	14:06	PA
PP2	Pickerel Pond 2	41.167504	−74.91786	27	7.5	6/01/16	13:42	PA
RR	Raritan River	40.511438	−74.30216	27	8.0	5/28/15	11:00	PA
RR2	Raritan River 2	40.511438	−74.30216	27	8.0	6/02/16	10:00	PA
SI	Shark River Inlet	40.187105	−74.00984	25	n.m	5/27/13	n.m	PA
SW	Scenic Waters	41.171494	−74.90971	24	7	5/27/15	n.m	PA
SW2	Scenic Waters 2	41.171494	−74.90971	24	7	6/02/16	15:00	PA
TW	Tumbling Waters Creek	41.15451667	−74.91775	18	n.m	5/28/15	9:16	PA
AC	Alicia's Creek	41.16923333	−74.91406	20	7	5/27/15	13:58	PA
BB1	Basketball Court Pond 1	41.171401	−74.90943	23	7.12	5/28/15	13:53	PA
BB2	Basketball Court Pond 2	41.171371	−74.90930	23	7	6/02/16	10:38	PA
VP	Vernal Pool	41.16935	74.914066	23	n.m	5/28/13	10:38	PA

n.m. indicates 'not measured'.

substrates were used: Arg-7-aminomethylcoumarin (AMC), Gly-AMC, Leu-AMC, Pyr-AMC, and Z-GlyGlyArg-AMC. Details of substrates are given in **Table 2**.

The four aminopeptidase substrates were chosen to represent a broad range of amino R group chemistries, including non-polar (Leu), polar (Arg), small (Gly), and pyroglutamic acid, which is non-proteinogenic and which has an unusual cyclic R group. Z-GlyGlyArg-AMC, the only endopeptidase substrate used due to cost constraints, was chosen because hydrolysis of it was consistently observed (Obayashi and Suzuki, 2005, 2008). We note that the Z-(carboxybenzyl-) group on this substrate is a bulky protecting group that prevents sequential hydrolysis of the substrate by aminopeptidases. Throughout this manuscript, we use the Enzyme Commission (EC) system to refer to the enzymes that hydrolyze these substrates, in which enzymes are classified according to their function without regard to structure (Webb, 1992) because we lack any data (e.g., nucleic acid sequences) on enzyme structure. This is a shortcut: multiple peptidases are capable of catalyzing the hydrolysis of each of these substrates, as discussed below. For instance, both trypsin (EC 3.4.21.4) and oligopeptidase B (EC 3.4.21.83) are capable of catalyzing the hydrolysis of peptide bonds with *N*-adjacent Arg, despite major structural differences. The enzyme names used here are therefore consistent with specific enzyme classes, but not necessarily diagnostic of them.

In 2013, saturation curves (measurements of substrate hydrolysis rate as a function of substrate concentration at 0, 50, 100, 150, 200, 250, 300, and 400 μM) were measured at each site, with a single live replicate and matching killed control (boiled for ca. 5 min) at each concentration, plus triplicate live measurements at 400 μM. In 2014–2016, triplicate, saturating concentrations of 400 μM substrate were used in each incubation as well as a single killed control; 40 μL of substrate (10 mM stock concentration, dissolved in 90% MilliQ-H_2O/10% DMSO) was added to 100 μL of phosphate buffer (100 mM, pH 7.5) and 860 μL unfiltered sample, in a 1-mL methacrylate cuvette.

TABLE 2 | Substrates used.

Substrate	Abbreviation	Supplier	Product number
L-Arginine-7-amido-4-methylcoumarin HCl	Arg-AMC	Sigma-Aldrich	A2027
Glycine 7-amido-4-methylcoumarin (Gly-AMC)	Gly-AMC	Bachem	03351
L-Leucine 7-amido-4-methylcoumarin (Leu-AMC)	Leu-AMC	Chem-Impex International	06122
L-Pyroglutamic acid 7-amido-4-methylcoumarin	Pyr-AMC	Biosynth Chemistry and Biology	P-8500
Carboxybenzoyl-glycine-glycine-arginine 7-amido-4-methylcoumarin HCl	Z-GlyGlyArg-AMC	Bachem	I1140.0025

Suppliers and product numbers are examples. Different suppliers for identical molecules were used over the course of the study.

The cuvette was capped and mixed by hand. Measurements were taken approximately every 20 min for 2 h using a Promega Glomax Jr. (Ex 365 nm, Em 410–460 nm), Promega Quantifluor ST (Ex 365–395 nm, Em 440–470 nm), or Turner Biosystems TBS-380 fluorescence detector (Ex 365–395 nm, Em 440–470 nm), each set to UV mode. Samples were incubated at *in situ* temperature (PA samples; *in situ* temperatures ranged from 21.4 to 25.6°C or at room temperature (20–21°C; TN samples). For every sample, a calibration curve was made using AMC standard dissolved in MilliQ-H_2O mixed with 860 μL sample, 100 μL phosphate buffer, and an addition of MilliQ-H_2O to bring the total volume to 1000 μL.

pH dependence for Gly-AMC and Leu-AMC hydrolysis was measured at Ardena Brook and Belmar Inlet in 2016. For pH optimum measurements, the procedure was the same, but the buffer was phosphate-citrate universal buffer, and the pH was manipulated from 5.0 to 9.0. For these measurements, a standard curve was created at each pH, and each sample was calibrated with the corresponding calibration curve.

Data Analysis and Quality Control

Enzyme activities were calculated using R. All data and scripts are included as supplemental data, and deposited at http://github.com/adsteen/PEEC_MXSHS. Data were manually checked for linearity, and obvious outlier fluorescence data points were removed from the dataset based on the observation that our fluorescence detectors sometimes exhibit shot noise. Samples with outlier v_o values were not removed. V_{max} and K_m were calculated using the non-linear least-squares fitting algorithm implemented by the nls() function in base R. Fits for which estimated V_{max} and K_m were both greater than 0, and for which the standard error of estimated K_m was less than the estimated value of K_m, were considered valid. As a second quality control step, fits meeting those criteria but which qualitatively did not appear to fit the data well were omitted from analysis. Note that measured K_ms are effective K_ms, since multiple enzymes almost certainly hydrolyzed each substrate.

RESULTS

Potential Kinetics of Extracellular Peptidases

Collectively, potential enzyme activities were distributed approximately log-normally, with a geometric mean V_{max} of 91 nM h^{-1}, a median of 73 nM h^{-1}, and an interquartile range from 21 to 520 nM h^{-1} (**Supplementary Figure S1**). In Knoxville, activities were highest in Douglas Lake (DL), the TN River at VL, and a small outdoor, constructed goldfish pond (EBF). DL showed high activity both times that it was sampled. The highest activities of LeuAP were observed in the EBF and at VL. At PEEC, the highest activity was measured at sites BB1, BB2, and BS (two approximately 30-m diameter, shallow catchment ponds, and a highly turbid wetland, respectively) which were characterized by high potential ArgAP and LeuAP activities. Trypsin-like activities were consistently high in DL and at the Hesler Biology Plant Pond. One-way repeated-measures ANOVA of log-transformed V_{max} ($n = 188$) revealed significant differences in V_{max} among substrates ($p < 0.001$). Pairwise paired t-tests of difference in V_{max} means among samples revealed statistically significant differences in V_{max} among each pair of substrates except ArgAP and trypsin-like enzymes, which were indistinguishable ($p > 0.05$; p-values corrected for multiple comparisons by the Bonferroni–Holm algorithm). V_{max} of LeuAP was greatest, followed by ArgAP and trypsin-like enzymes, and then by GlyAP, and finally PyrAP (**Figure 2**).

Of the 50 sample/substrate combinations for which saturation curves were created in 2013, 20 were able to be fit to the

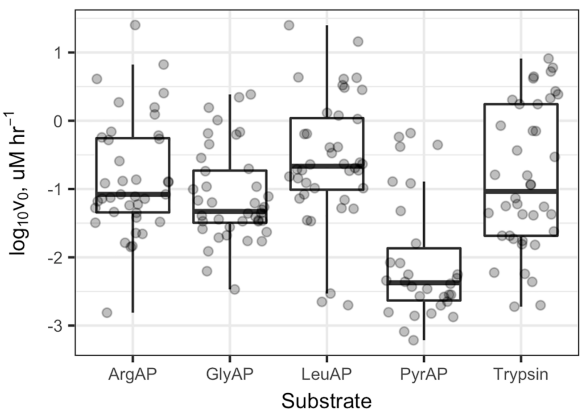

FIGURE 2 | V_{max} values for each enzyme and sample. ArgAP, GlyAP, LeuAP, and PyrAP refer to argingine aminopeptidase, glycine aminopeptidase, leucine aminopeptidase, and pyroglutamic aminopeptidase, respectively. Horizontal lines in the boxplot boxes indicate medians and 25th and 75th percentiles. Vertical whiskers extend to the most extreme data point that is no further than 1.5× the interquartile range from the 25th or 75th percentile.

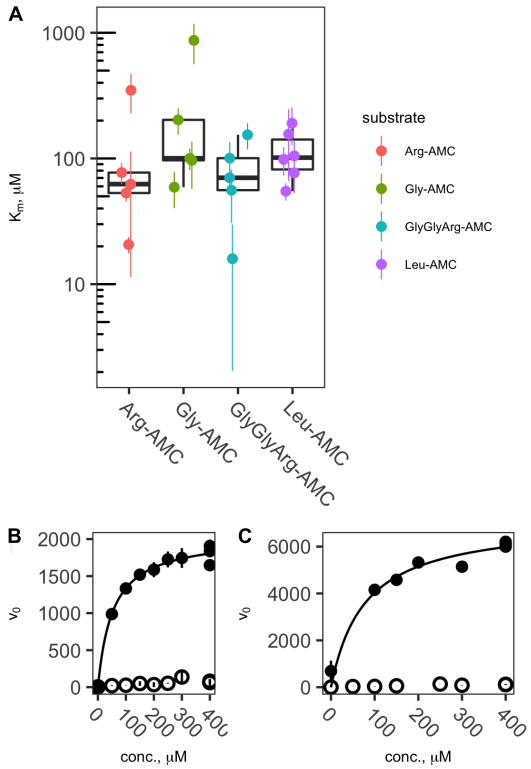

FIGURE 3 | Effective K_ms (**A**) and representative saturation curves **(B,C)** showing the relationship between substrate concentration and hydrolysis rate. Abbreviations are as in **Figure 2**. Saturation curves are for Arg-AMC at site DR **(B)** and Leu-AMC at site LL **(C)**.

Michaelis–Menten function, $v_o = \frac{V_{max}[S]}{K_m + [S]}$, where v_o is the observed rate of reaction, $[S]$ is the substrate concentration, V_{max} is the theoretical maximum rate of reaction at infinite substrate concentration, and K_m is the effective half-saturation constant. In general, samples for which v_0 in live samples was considerably greater than boiled controls yielded valid Michaelis–Menten fits, whereas those in which v_0 was low did not. Thus, effective K_m values could be estimated for each peptidase except Pyr-AP, which exhibited consistently low v_0. Effective K_m values ranged from a minimum of 15.6 μM to a maximum of 869 μM with a median of 101 μM and interquartile range from 66.3 to 273 μM (**Figure 3**).

All potential peptidase activities were significantly intercorrelated after log transformation (**Figure 4**; ArgAP-LeuAP: slope = 0.93 ± 0.05, $n = 39$, $r^2 = 0.90$, $p < < 0.01$; GlyAP-LeuAP: slope = 0.69 ± 0.04, $n = 40$, $r^2 = 0.87$, $p < < 0.01$; trypsin-like enzyme-LeuAP: 0.94 ± 0.10, $n = 40$, $r^2 = 0.68$, $p < < 0.01$; PyrAP-LeuAP: slope = 0.63 ± 0.11, $r^2 = 0.54$, $n = 30$). At individual sites, ratios of potential trypsin-like enzymes:LeuAP ranged from 0.037 to 9.3. These ratios were roughly log-normally distributed with a geometric mean of 0.53, a median of 0.46, and an interquartile range from 0.18 to 1.4 (**Supplementary Figure S2**). GlyAP and LeuAP pH dependences were indistinguishable at each site, although they were different among sites (**Supplementary Figure S3**). At Ardena Brook, both aminopeptidases were most active at pH 7.5, while at Belmar Inlet, both aminopeptidases were most active at or above pH 8.5. Potential peptidase activities were not significantly correlated to *in situ* temperature, probably because cell density or other ecological factors exerted stronger control over enzyme activity than temperature in the relatively narrow temperature range (18–32°C) sampled here.

Intertemporal Stability of Peptidase Activity Ratios

Time-series measurements from Third Creek (an urban, anthropogenically impacted creek in Knoxville, TN, United States; Im et al., 2014) and in the TN River at VL (upstream of most of Knoxville's drainage basin) indicated that patterns of enzyme activity were relatively stable on a timescale of weeks (**Figure 5**). Third Creek consistently displayed higher activity of ArgAP and trypsin-like enzymes than the TN River, which displayed higher activities of LeuAP and GlyAP. PyrAP was always negligible (but sometimes detectable) at both sites. Sites BB1 and BB2 were also sampled over multiple years and consistently showed higher LeuAP than trypsin-like potential activity.

DISCUSSION

The shape of the saturation curves and the fact that substrate hydrolysis rates in untreated samples were generally substantially higher than those in boiled samples indicate that the substrate hydrolysis observed here reflects activities of enzymes rather than abiotic processes. The median K_m value here, 101 μM, is somewhat higher than the median hydrolase K_m reported in a meta-analysis of extracellular enzyme kinetics, suggesting a moderately high concentration of enzyme-labile proteinaceous organic matter in the systems assayed here (Sinsabaugh et al., 2014). Potential peptidase activities (V_{max}) in this study varied over four orders of magnitude among environments and were all mutually inter-correlated. V_{max} values were not significantly correlated to *in situ* temperature, likely because ecological factors (e.g., cell density and organic matter concentration) were more important than the kinetic effect of temperature in driving enzyme activity, and because the range of temperatures sampled (18–32°C) was relatively narrow. Those correlations could indicate that the assays used here report activities of two distinct enzymes, expression of which is correlated at the community level. Alternately, correlations between two substrate hydrolysis rates could indicate that the same enzyme or set of enzymes hydrolyzes multiple fluorogenic substrates. Both factors likely led to the observed data. Extracellular aminopeptidases in freshwater are relatively promiscuous, and multiple classes of aminopeptidase can hydrolyze the same substrates (Steen et al., 2015). In that study, ArgAPs were responsible for more hydrolysis of LeuAMC than were Leu-APs. The tight inter-correlation between hydrolysis rates of LeuAMC, ArgAMC, and GlyAMC, combined

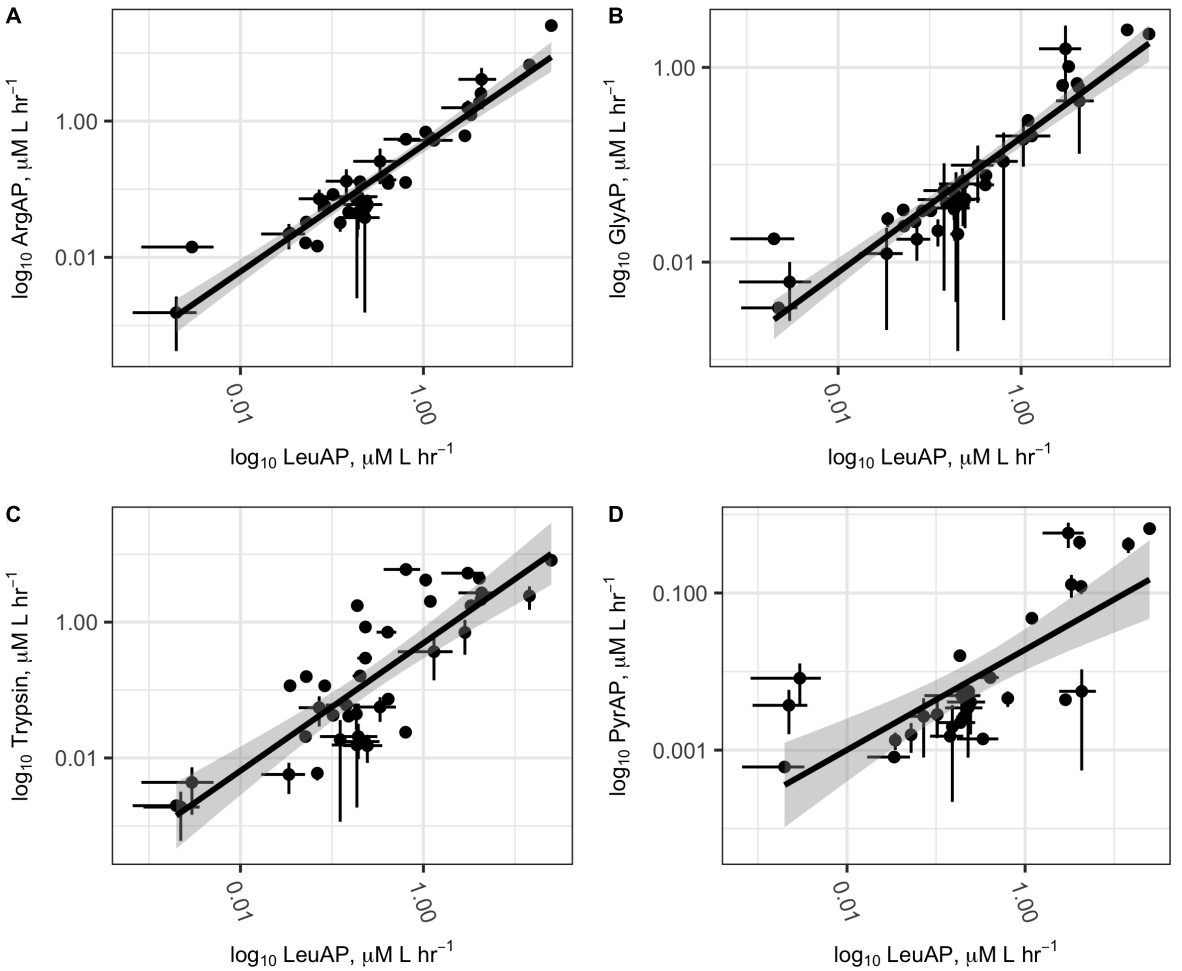

FIGURE 4 | Log–log plots of potential ArgAP **(A)**, GlyAP **(B)**, Trypsin **(C)**, and PyrAP **(D)** activity as a function of potential LeuAP activity at all sites. Abbreviations are as in **Figure 2**. Dark lines represent linear regression of log-transformed potential activities, and shaded areas represent the standard error. Error bars on individual points represent the standard deviation of three replicate measurements from each site.

with the evidence for promiscuity among aminopeptidases, suggests that those substrates may have been hydrolyzed by the same enzyme or set of enzymes. This is further supported by the fact that pH dependence of GlyAP and LeuAP, which were indistinguishable from each other at two different sites, despite varying among sites (**Supplementary Figure S3**). The fact that Leu-AMC was consistently the fastest hydrolyzed substrate suggests that LeuAP, rather than GlyAP or ArgAP, was responsible for most of that hydrolysis.

The correlations between Leu-AMC and Z-GlyGlyArg-AMC hydrolysis rates and between Leu-AMC and Pyr-AMC hydrolysis rates (r^2 = 0.68 and 0.63, respectively) were considerably looser than the correlations between Leu-AMC and Arg-AMC or Gly-AMC hydrolysis rates (r^2 = 0.90 and 0.87, respectively). Correspondingly, the ratios of Z-GlyGlyArg-AMC and Pyr-AMC to Leu-AMC hydrolysis rates at individual sites were significantly more variable than ratios of Arg-AMC and Gly-AMC to Leu-AMC hydrolysis rates (**Figure 4** and **Supplementary Figure S2**). These facts suggest that, while Leu-AMC, Gly-AMC, and Arg-AMC were likely hydrolyzed by the same set of enzymes, different sets of enzymes hydrolyzed Z-GlyGlyArg-AMC and Pyr-AMC. This makes sense from a biochemical perspective: the unusual cyclic lactam structure of pyroglutamc acid is a poor fit for the active site of a typical aminopeptidase, and indeed *N*-terminal pyroglutamic acid acts to protect peptides from intracellular hydrolysis by aminopeptidases (Kumar and Bachhawat, 2012). Aminopeptidases specific for pyroglutamic acid have been identified (EC 3.4.19.3, Awadé et al., 1994), and pyroglutamic acid is a minor component of some proteins relevant to aquatic systems, such as bacteriorhodopsin (Blanck et al., 1989). Thus, it is plausible that the hydrolysis of Pyr-AMC observed in these samples was due to pyroglutamic aminopeptidase, but given the low activities observed, we cannot exclude the possibility that Pyr-AMC hydrolysis was primarily due to some other set of peptidases, possibly including peptidases that were not directly assayed here.

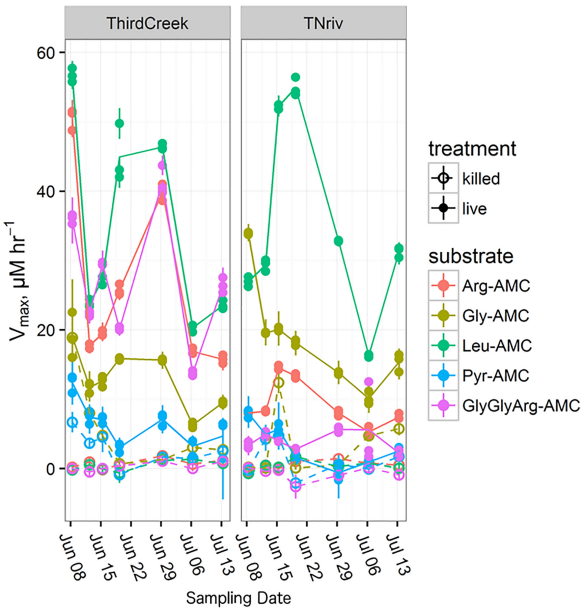

FIGURE 5 | Time series over the course of a month and a half following the trends in V_{max} for each measured substrate at the Third Creek (ThirdCreek) and the Tennessee River at Volunteer Landing (TNriv) sampling sites. Abbreviations are as in **Figure 2**. Open circles ("killed") represent the boiled control. Error bars represent the standard error of the estimation of V_{max} for each replicate. Lines are plotted through the mean of the three replicates.

Z-GlyGlyArgAMC is a nominally a substrate for trypsin, a broad-spectrum endopeptidase (i.e., peptidase that hydrolyzes proteins from the middle rather than the ends) (Obayashi and Suzuki, 2005). The bulky Z- group effectively prevents hydrolysis by aminopeptidases (Nakadai and Nasuno, 1977), and given the broad range of observed ratios of Z-GlyGlyArg-AMC:Leu-AMC hydrolysis rates, it is likely that that Z-GlyGlyArg-AMC and the single-amino acid substrates were hydrolyzed by distinct enzymes. Thus, the broad correlation in hydrolysis rates between those two substrates is probably due to community-level co-expression of trypsin-like enzymes and the common set of aminopeptidases that hydrolyzed Leu-AMC, Arg-AMC, and Gly-AMC.

It has long been recognized that a variety of peptidases are potentially present in aquatic environments (Christian and Karl, 1998). Early evidence suggested that assays of a single peptidase substrate provide a reasonable approximation of the total peptidolytic potential of a microbial community, because extracellular peptidases are frequently capable of acting on a wide range of peptides (Nomoto et al., 1960). The promiscuity of aquatic peptidases was used as justification for fluorogenic substrate-based enzyme assays when that technique was first adopted for aquatic samples (Hoppe, 1983), and indeed it appears that Leu-AMC hydrolysis is caused by a range of aminopeptidases in aquatic environments (Steen et al., 2015).

The results presented here place further constraint on the degree to which measurement of the hydrolysis rate of a single substrate is a useful measure of the total peptidolytic capacity of an ecosystem. LeuAP potential activity does correlate well with the activity of other aminopeptidases across a broad range of systems. For studies that examine systems in which activity varies by several orders of magnitude (for instance, studies that use LeuAP as a proxy for N demand across diverse environments, e.g., Sinsabaugh et al., 2009), LeuAP activity correlates well enough with endopeptidase activity that the additional information, time, and expense required to assay multiple peptidases are not justified given the novel information those measurements yield. In studies that have a narrower domain, for instance, time-series analyses in which LeuAP activity might vary within an order of magnitude (Allison et al., 2012; Mahmoudi et al., 2017) – this assumption is more dangerous, as changes in the ratio of endopeptidases : aminopeptidases could obscure patterns observed in just one peptidase. In this study, the ratio of trypsin-like potential activity to LeuAP potential activities ranged from 0.037 to 9.3. If the sum of trypsin-like activity and LeuAP activity places a lower bound on the total peptidolytic capacity of a system, then LeuAP could represent anywhere from 9.7 to 96% of total peptidolytic capacity, representing about an order of magnitude of potential error. Furthermore, since the endopeptidase:aminopeptidase activity appears to be a non-stochastic feature of ecosystems, this error would be systematic rather than random. Studies in which the range of LeuAP activities is narrower than an order of magnitude or so, assaying a broader set of peptidases, including endopeptidases and aminopeptidases, may yield a more complete picture of the potential for protein degradation.

Heterotrophic processes in aquatic systems are often described in chemically non-specific terms, such as "N acquisition" or "protein degradation." This is a useful way to distill important ecological patterns from the tremendously complex set of biochemical pathways that may be active in a system. It also flows from the limitations of organic geochemistry analytical technology: at present, it is relatively straightforward to measure the concentration of "hydrolysable amino acids" (i.e., protein-like material) in aquatic systems, but very challenging to measure concentrations of specific proteins (Moore et al., 2012). Microorganisms sense and interact with the world at much finer chemical resolution. Those fine-scale interactions with the environment are reflected in the expression of specific extracellular enzymes. Measuring a broader set of extracellular enzymes can therefore yield insight into how microorganisms interact with their chemical environment. These results indicate that Leu-AMC hydrolysis is an acceptable proxy for total peptidolytic capacity of an environment only when the potential LeuAP activities vary over several orders of magnitude. When potential LeuAP activities span about an order of magnitude or less, variability in the aminopeptidase:endopeptidase ratio may cause total peptidolytic capacity to become decoupled from potential LeuAP activity. In such a data set, assays for multiple peptidases should be included to capture variability in total community peptidolytic potential.

MEMBERS OF THE MALCOLM X SHABAZZ HIGH SCHOOL AQUATIC BIOGEOCHEMISTRY TEAM

Ivy Adu-Poku, Saskieya Anderson, Kiara Amore, Tequan Anderson, Elmy Antonio, Delvon Artis, Monai Barnes, Manusha Bearfield, Kim Boerrigter, Antwon Bowman, Zion Brummel, Abdul Bryant, Tyre Bush, Clervens Clerjuste, Latonya Coates, Ameena Corney, Jamie Crosby, Abdul Crowley, Michelle Culver, Leon Cummings, Zyion Eastmond, Genaro Falcon, Ciara Gilette, Lexus Gonzalez, Brianna Grant, Dequan Graves, Christian Hardy, Jamar Harris, Kevin Harrison, Deshawn Hart, Ismail Hinds, Latifa Hinds, Samantha Hunter, Imade Igiebor, Teniyjaa Jacobs, Malachi Jefferson, Shani Ketema, Zack Ketema, Ahmad Lancaster, Camille Laurel, Ferard Majette, Imani McCray, Francis Mensa, Elizabeth Mensah, Justin Mestre, Tai-Xian Mitchell, Davon Moody, Ivana Negron, Zaire O'Neill, Okoye Onyebuchi, Nasir Parham-Sanders, Madelyn Perez, Chris Pitt, Briana Racine, Acestra Robinson-Williams, Elvis Sanchez, Jabryant Vines, Jacelyn Valenciano, Nadira Wilkins, Anzunai Williams, Ma-Lisa Winborne, Henasia Wilson, and Yasmiah Wilson.

AUTHOR CONTRIBUTIONS

LM and ABB helped design the sampling plan, performed experiments, analyzed the data, and helped write the manuscript. MXSHS-ABT (a group author) and NF performed experiments and analyzed the data. KB designed and performed experiments and analyzed the data. JR helped design the sampling plan. PM initiated the project, helped design the sampling plan, and performed experiments. AS initiated the project, helped design the sampling plan, performed experiments, analyzed the data, and helped write the manuscript.

FUNDING

Funding was provided by the National Science Foundation (OCE-1357242), the Geraldine R. Dodge Foundation, the Foundation for Newark's Future, and Newark Public Schools. Additionally, the Malcolm X Shabazz Aquatic Geochemistry Team was funded by Wilma Baldridge Schwades, Christopher Cerf, Jacob Etter, Dianna Thompson, Bob and Ruth Steen, Erika Amir-Lin, Suzy Schmidt, Ben Cady, Ben Bond-Lamberty, Franklin Parker, gofundme.com, Elnardo Webster, Olivier Humblet, Robert Tortoriello, Rosa Leon, Nancy Ferguson, Jenna Schmidt, Cameron Huges, Rachel Yoho, Rebecca Ghent, Adam Sobel, Vivian McNeill, Liz Kujawinski, Carol Arnosti, Bill Armbruster, Elliot and Natalia Ikheloa, Yvette Jordan, Morgan Wurch, Keith Britt, Nagissa Mahmoudi, Monika Kopacz, Danielle Lee, Jordan Bird, Dug Steen, Agnes Taylor, Steven Hauck, Clark Short, Susan Cheng, Mel Goldsipe, Katrina Carter, Laura Newsome, Jill Marshall, Helena Pound, Naupaka Zimmerman, Amparo Jiminez, Moses Olivia, Dorothea Boerrigter, Patricia MacQueen, Sarah Sheffield, Mohammad Moniruzzaman, Liz Agee, Lori Fenton, Max Czapanskiy, Orlando Campos, Zena Cardman, Paula Gagliardi, Camille Thomas, Richard Lewis, James Hodges, Cecilia Kruczek, and 28 anonymous donors.

ACKNOWLEDGMENTS

We gratefully acknowledge logistical support from the staff of the Pocono Environmental Education Center, the faculty and administration of Malcolm X Shabazz High School. Karen Lloyd cofounded the Malcolm X Shabazz Aquatic Geochemistry Team and provided key operational support. Mr. Jamal Hall created amazing graphics.

SUPPLEMENTARY MATERIAL

The Supplementary Material for this article can be found online at: https://www.frontiersin.org/articles/10.3389/fmicb.2018.00368/full#supplementary-material

FIGURE S1 | Density plot of all Vmax values measured in this study, showing the approximate log-normal distribution of activities.

FIGURE S2 | Distribution of ratios of trypsin-like potential activity to LeuAP potential activity, showing the approximate log-normal distribution of activities.

FIGURE S3 | pH dependence of LeuAP (marked LeuAMC) and GlyAP (marked GlyAMC) at Ardena Brook (ARD) and Belmar Inlet (BLMR).

REFERENCES

Allison, S. D., Chao, Y., Farrara, J. D., Hatosy, S., and Martiny, A. C. (2012). Fine-scale temporal variation in marine extracellular enzymes of coastal southern California. *Front. Microbiol.* 3:301. doi: 10.3389/fmicb.2012.00301

Arnosti, C., Bell, C., Moorhead, D. L., Sinsabaugh, R. L., Steen, A. D., Stromberger, M., et al. (2014). Extracellular enzymes in terrestrial, freshwater, and marine environments: perspectives on system variability and common research needs. *Biogeochemistry* 117, 5–21. doi: 10.1007/s10533-013-9906-5

Awadé, A. C., Cleuziat, P., GonzalèS, T., and Robert-Baudouy, J. (1994). Pyrrolidone carboxyl peptidase (Pcp): an enzyme that removes pyroglutamic acid (pGlu) from pGlu-peptides and pGlu-proteins. *Proteins Struct. Funct. Genet.* 20, 34–51. doi: 10.1002/prot.340200106

Blanck, A., Oesterhelt, D., Ferrando, E., Schegk, E. S., and Lottspeich, F. (1989). Primary structure of sensory rhodopsin I, a prokaryotic photoreceptor. *EMBO J.* 8, 3963–3971.

Christian, J., and Karl, D. (1998). Ectoaminopeptidase specificity and regulation in Antarctic marine pelagic microbial communities. *Aquat. Microb. Ecol.* 15, 303–310. doi: 10.3354/ame015303

Fellman, J. B., Hood, E., and Spencer, R. G. M. (2010). Fluorescence spectroscopy opens new windows into dissolved organic matter dynamics in freshwater ecosystems: a review. *Limnol. Oceanogr.* 55, 2452–2462. doi: 10.4319/lo.2010.55.6.2452

Findlay, S., and Sinsabaugh, R. L. (1999). Unravelling the sources and bioavailability of dissolved organic matter in lotic aquatic ecosystems. *Mar. Freshw. Res.* 50, 781–790. doi: 10.1071/MF99069

Gerber, G. E., Anderegg, R. J., Herlihy, W. C., Gray, C. P., Biemann, K., and Khoranat, H. G. (1979). Partial primary structure of bacteriorhodopsin:

sequencing methods for membrane proteins. *Proc. Natl. Acad. Sci. U.S.A.* 76, 227–231. doi: 10.1073/pnas.76.1.227

Hooper, N. M. (2002). Proteases: a primer. *Essays Biochem.* 38, 1–8. doi: 10.1042/bse0380001

Hoppe, H.-G. (1983). Significance of exoenzymatic activities in the ecology of brackish water: measurements by means of methylumbelliferyl-substrates. *Mar. Ecol. Prog. Ser.* 11, 299–308. doi: 10.3354/meps011299

Im, J., Walshe-Langford, G. E., Moon, J.-W., and Löffler, F. E. (2014). Environmental fate of the next generation refrigerant 2,3,3,3-tetrafluoropropene (HFO-1234yf). *Environ. Sci. Technol.* 48, 13181–13187. doi: 10.1021/es5032147

Kumar, A., and Bachhawat, A. K. (2012). Pyroglutamic acid: throwing light on a lightly studied metabolite. *Curr. Sci.* 102, 288–297.

Mahmoudi, N., Beaupré, S. R., Steen, A. D., and Pearson, A. (2017). Sequential bioavailability of sedimentary organic matter to heterotrophic bacteria. *Environ. Microbiol.* 19, 2629–2644. doi: 10.1111/1462-2920.13745

McDonald, A. G., Boyce, S., and Tipton, K. F. (2009). ExplorEnz: the primary source of the IUBMB enzyme list. *Nucleic Acids Res.* 37, D593–D597. doi: 10.1093/nar/gkn582

Moore, E. K., Nunn, B. L., Goodlett, D. R., and Harvey, H. R. (2012). Identifying and tracking proteins through the marine water column: insights into the inputs and preservation mechanisms of protein in sediments. *Geochim. Cosmochim. Acta* 83, 324–359. doi: 10.1016/j.gca.2012.01.002

Nakadai, T., and Nasuno, S. (1977). Purification and properties of leucine aminopeptidase IV from *Aspergillus oryzae*. *Agric. Biol. Chem.* 41, 1657–1666. doi: 10.1271/bbb1961.41.1657

Nomoto, M., Narahashi, Y., and Murakami, M. (1960). A proteolytic enzyme of *Streptomyces griseus* VII. Substrate specificity of *Streptomyces griseus* protease. *J. Biochem.* 48, 906–918. doi: 10.1093/oxfordjournals.jbchem.a127244

Obayashi, Y., and Suzuki, S. (2005). Proteolytic enzymes in coastal surface seawater: significant activity of endopeptidases and exopeptidases. *Limnol. Oceanogr.* 50, 722–726. doi: 10.4319/lo.2005.50.2.0722

Obayashi, Y., and Suzuki, S. (2008). Occurrence of exo- and endopeptidases in dissolved and particulate fractions of coastal seawater. *Aquat. Microb. Ecol.* 50, 231–237. doi: 10.3354/ame01169

Rawlings, N. D., Barrett, A. J., and Finn, R. (2016). Twenty years of the *MEROPS* database of proteolytic enzymes, their substrates and inhibitors. *Nucleic Acids Res.* 44, D343–D350. doi: 10.1093/nar/gkv1118

Schimel, J. P., and Weintraub, M. N. (2003). The implications of exoenzyme activity on microbial carbon and nitrogen limitation in soil: a theoretical model. *Soil Biol. Biochem.* 35, 549–563. doi: 10.1016/S0038-0717(03)00015-4

Sinsabaugh, R. L., Belnap, J., Findlay, S. G., Shah, J. J. F., Hill, B. H., Kuehn, K. A., et al. (2014). Extracellular enzyme kinetics scale with resource availability. *Biogeochemistry* 121, 287–304. doi: 10.1007/s10533-014-0030-y

Sinsabaugh, R. L., Hill, B. H., and Follstad Shah, J. J. (2009). Ecoenzymatic stoichiometry of microbial organic nutrient acquisition in soil and sediment. *Nature* 462, 795–798. doi: 10.1038/nature08632

Steen, A. D., and Arnosti, C. (2011). Long lifetimes of β-glucosidase, leucine aminopeptidase, and phosphatase in Arctic seawater. *Mar. Chem.* 123, 127–132. doi: 10.1016/j.marchem.2010.10.006

Steen, A. D., and Arnosti, C. (2013). Extracellular peptidase and carbohydrate hydrolase activities in an Arctic fjord Smeerenburgfjord, Svalbard. *Aquat. Microb. Ecol.* 69, 93–99. doi: 10.3354/ame01625

Steen, A. D., Vazin, J. P., Hagen, S. M., Mulligan, K. H., and Wilhelm, S. W. (2015). Substrate specificity of aquatic extracellular peptidases assessed by competitive inhibition assays using synthetic substrates. *Aquat. Microb. Ecol.* 75, 271–281. doi: 10.3354/ame01755

Thao, N. V., Obayashi, Y., Yokokawa, T., and Suzuki, S. (2014). Coexisting protist-bacterial community accelerates protein transformation in microcosm experiments. *Front. Mar. Sci.* 1:69. doi: 10.3389/fmars.2014.00069

Webb, E. C. (1992). *Enzyme Nomenclature 1992: Recommendations of the Nomenclature Committee of the International Union of Biochemistry and Molecular Biology on the Nomenclature and Classification of Enzymes*. Cambridge, MA: Academic Press.

Conflict of Interest Statement: The authors declare that the research was conducted in the absence of any commercial or financial relationships that could be construed as a potential conflict of interest.

frontiers in Microbiology

ORIGINAL RESEARCH
published: 22 December 2017
doi: 10.3389/fmicb.2017.02589

A Multi-season Investigation of Microbial Extracellular Enzyme Activities in Two Temperate Coastal North Carolina Rivers: Evidence of Spatial but Not Seasonal Patterns

*Avery Bullock, Kai Ziervogel†, Sherif Ghobrial, Shannon Smith, Brent McKee and Carol Arnosti**

Department of Marine Sciences, University of North Carolina, Chapel Hill, NC, United States

OPEN ACCESS

Edited by:
Maria Montserrat Sala, Consejo Superior de Investigaciones Científicas (CSIC), Spain

Reviewed by:
Michael J. Wilkins, The Ohio State University, United States
Nina Welti, Commonwealth Scientific and Industrial Research Organisation (CSIRO), Australia

***Correspondence:**
Carol Arnosti
arnosti@email.unc.edu

†Present Address:
Kai Ziervogel, Institute for the Study of Earth, Oceans, and Space, University of New Hampshire, Durham, NH, United States

Specialty section:
This article was submitted to Aquatic Microbiology, a section of the journal Frontiers in Microbiology

Received: *12 August 2017*
Accepted: *12 December 2017*
Published: *22 December 2017*

Citation:
Bullock A, Ziervogel K, Ghobrial S, Smith S, McKee B and Arnosti C (2017) A Multi-season Investigation of Microbial Extracellular Enzyme Activities in Two Temperate Coastal North Carolina Rivers: Evidence of Spatial but Not Seasonal Patterns. Front. Microbiol. 8:2589. doi: 10.3389/fmicb.2017.02589

Riverine systems are important sites for the production, transport, and transformation of organic matter. Much of the organic matter processing is carried out by heterotrophic microbial communities, whose activities may be spatially and temporally variable. In an effort to capture and evaluate some of this variability, we sampled four sites—two upstream and two downstream—at each of two North Carolina rivers (the Neuse River and the Tar-Pamlico River) ca. twelve times over a time period of 20 months from 2010 to 2012. At all of the sites and dates, we measured the activities of extracellular enzymes used to hydrolyze polysaccharides and peptides, and thus to initiate heterotrophic carbon processing. We additionally measured bacterial abundance, bacterial production, phosphatase activities, and dissolved organic carbon (DOC) concentrations. Concurrent collection of physical data (stream flow, temperature, salinity, dissolved oxygen) enabled us to explore possible connections between physiochemical parameters and microbial activities throughout this time period. The two rivers, both of which drain into Pamlico Sound, differed somewhat in microbial activities and characteristics: the Tar-Pamlico River showed higher β-glucosidase and phosphatase activities, and frequently had higher peptidase activities at the lower reaches, than the Neuse River. The lower reaches of the Neuse River, however, had much higher DOC concentrations than any site in the Tar River. Both rivers showed activities of a broad range of polysaccharide hydrolases through all stations and seasons, suggesting that the microbial communities are well-equipped to access enzymatically a broad range of substrates. Considerable temporal and spatial variability in microbial activities was evident, variability that was not closely related to factors such as temperature and season. However, Hurricane Irene's passage through North Carolina coincided with higher concentrations of DOC at the downstream sampling sites of both rivers. This DOC maximum persisted into the month following the hurricane, when it continued to stimulate bacterial protein production and phosphatase activity in the Neuse River, but not in the Tar-Pamlico River. Microbial community activities are related to a complex array of factors, whose interactions vary considerably with time and space.

Keywords: enzyme activities, bacterial production, DOC, Hurricane Irene, peptidase, glucosidase, Neuse River, Tar River

INTRODUCTION

Riverine systems are important sources of organic carbon and nutrients for coastal and estuarine systems (Paerl et al., 1998; Stow et al., 2001; Lin et al., 2007). The availability of organic matter that can be processed within rivers is dependent on multiple physical, biological, and chemical factors, including the nature and extent of allochthonous input via runoff and groundwater, as well as autochthonous production within the system (Spencer et al., 2012). The quantity and quality of organic carbon and nutrients ultimately delivered to estuaries and coasts is partially the outcome of organic matter processing by heterotrophic microbial communities within the rivers. These communities facilitate the transformation and respiration of organic matter, and regeneration of nutrients (Blackburn et al., 1996). The extent to which organic matter is processed and transformed within a riverine system is thus dependent in part on the capabilities of heterotrophic microbial communities. The initial step of organic matter transformation is typically hydrolysis via extracellular enzymes, since high molecular weight organic matter is too large to be transported directly into microbial cells. The heterotrophic microbial community therefore must utilize extracellular enzymes to hydrolyze high molecular weight organic matter to sizes sufficiently small for uptake (see Arnosti et al., 2014 for a review). Though not the sole sources of extracellular enzymes, bacterioplankton are assumed to be the major producers of extracellular enzymes in aquatic systems (Hoppe et al., 2002; Vrba et al., 2004). Only a sub-fraction of a microbial community may produce specific extracellular enzymes, but the products of hydrolysis potentially might be accessed by a wider range of organisms. The activities of extracellular enzymes may therefore benefit a wider community, and measurement of extracellular enzyme activities can represent the potential to initiate organic matter remineralization at the community-level.

A number of biological, chemical, and physical factors can influence the production of extracellular enzymes (Allison and Vitousek, 2005; Artigas et al., 2009), while the degradation of organic matter can be dependent upon such factors as substrate type (McCallister et al., 2006), availability (Sinsabaugh and Moorhead, 1994), and community nutrient demands (Rier et al., 2011). In addition, studies have shown that organic matter concentration and type change seasonally in freshwater watersheds (Singh et al., 2013). These seasonal changes are due largely to sorption of DOM on mineral soil surfaces and/or microbial breakdown of leaf litter. Singh et al. (2013) found that stormflow in summer contained DOM that was more humic in character than in spring and winter, as a result of more influence from the watershed during higher discharge periods. Therefore, changes in organic matter supply, environmental conditions, or microbial community composition across spatiotemporal scales may be reflected in the enzymatic profiles and activities of a microbial community.

Since organic matter type, concentration, and microbial community composition likely influence enzymatic activities, spatial and temporal variability of enzymatic activities could vary widely. Freshwater systems such as creeks and streams have been shown to be a medley of different microbial community activities, responding to temporally-changing environmental gradients (Frossard et al., 2012). Capturing these varying dynamics is challenging; prior studies typically have focused on sampling a range of stations over a limited timescale or on sampling a few sites over a longer period of time (e.g., Artigas et al., 2009; Millar et al., 2015).

We investigated spatial and as well as seasonal variations in microbial activities and organic matter remineralization in two distinct river systems in central and eastern North Carolina: the Neuse River and the Tar-Pamlico River. These rivers were each sampled at four different sites (two upstream sites, two downstream sites) ∼12 times over a 20-month period. We carried out this extended sampling program in an effort to capture temporal variability over a range of sites. Part of this temporal variability was caused by Hurricane Irene's passage over eastern North Carolina (August 2011), an event that provided the opportunity to measure changes in microbial activities in the rivers in response to a large-scale influx of precipitation and laterally-flowing water. In order to investigate a greater range of heterotrophic capabilities, we measured the activities of enzymes capable of hydrolyzing small substrate proxies typically used to assess glucosidase and leucine aminopeptidase activities, and also used a suite of polysaccharide substrates that can measure the endo-acting activities of enzymes that cleave specific polysaccharides mid-chain. We sought to investigate the manner in which changing biological, physical, and chemical parameters may affect organic carbon cycling, as measured via activities of extracellular enzymes.

MATERIALS AND METHODS

Study Sites

The Neuse and Tar-Pamlico Rivers, extending from central to eastern North Carolina, feed into Pamlico Sound (Paerl et al., 2010; **Figure 1**). The Albemarle-Pamlico Sound estuary system is the second largest estuary system in the United States (Paerl et al., 2010), and provides significant nursery area for commercially-important fisheries on the U.S. Atlantic coast (Burkholder et al., 2006). Although the Albemarle-Pamlico Sound, as well as other estuary systems, serves as an important link between terrestrial/riverine systems and the marine environment (Paerl et al., 1998), the dynamics of organic matter processing occurring in the Neuse and Tar-Pamlico Rivers are not well-studied.

The two river systems have contrasting watersheds (Burgess, 2013a,b). The Neuse River is heavily urbanized upstream, with a population of over 1.5 million residing within its watershed (Burgess, 2013a), and is also subject to heavy industrialized agricultural use. The Tar-Pamlico River is a smaller, less developed river both in terms of agricultural and urban development, but it is the largest tributary of the Pamlico River Estuary (Overton et al., 2012; **Table 1**). The mean discharge to the Albemarle-Pamlico estuarine system is 190 m^3 s^{-1} for the Neuse River and 148 m^3 s^{-1} for the Tar-Pamlico River (Lin et al., 2007). Downstream salinities also differ between rivers: the Tar-Pamlico endmember salinities are close to zero (compared to the

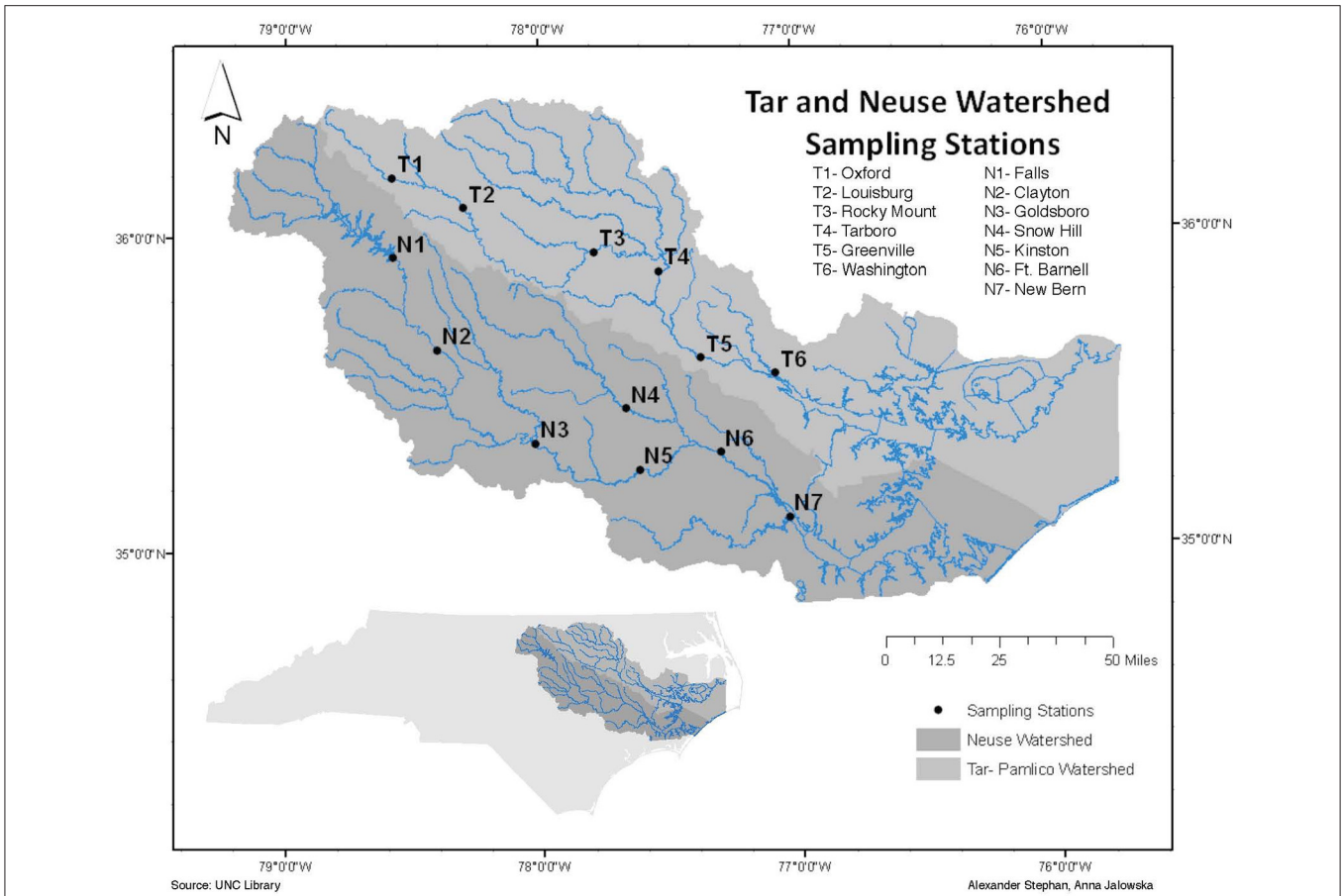

FIGURE 1 | Location of sampling stations in the Tar-Pamlico and Neuse Rivers.

TABLE 1 | Characteristics of the Neuse and Tar-Pamlico Rivers (O'Driscoll et al., 2010).

	Neuse river	Tar-Pamlico river
Maximum elevation (m)	183	218
River length (km)	443	346
Basin area (km^2)	15,700	15,923
Population	1,687,462	472,629
Land use (%)		
Forested	30	36
Grassland	4	3
Agriculture	26	22
Urban	15	5
Wetland	19	18

Neuse) because the Tar-Pamlico estuary is relatively narrow and the influence of ocean waters due to wind mixing is much more limited relative to that in the Neuse estuary, which has a more open morphology.

Surface water samples were collected from four stations in each river: N1, N2, N6, and N7 in the Neuse River, and T1, T2, T5, and T6 in the Tar River (**Figure 1**). These stations were chosen to include the different land-use impacts of the rivers (urbanization of upstream stations; agricultural effects on downstream stations), as well as the transition from a freshwater to an estuarine ecosystem. Collection dates (**Supplementary Table 1**) varied slightly among sites, due to the complex logistics of sampling eight different locations spread across a considerable distance. Due to the timing of our study, we also partially captured the influence of a major storm event (Hurricane Irene) on the lower stations of the Tar-Pamlico and Neuse Rivers in August 2011.

Sample Collection

Surface water samples were collected over a 20-month period (November 2010 to June 2012) from each of the four stations in the Neuse and Tar-Pamlico Rivers (**Figure 1**). Samples were collected in 33 L Nalgene carboys and stored at *in-situ* temperatures during transportation back to UNC-Chapel Hill. Measurements of enzyme activities and bacterial productivity were initiated upon return to the lab, and samples for cell counts were preserved (see below). Dissolved oxygen, temperature, salinity, and pH data were collected on site using a YSI (YSI Inc. 556MPS) (**Supplementary Table 1**). River discharge and

gage height for most stations was obtained from the USGS's monitoring website (http://waterdata.usgs.gov/nc/nwis/rt). Note that the USGS does not have a monitoring site at T6, and USGS data collection was ended at N7 in 2009, so for the downstream stations we used gage height (**Supplementary Figure 1**) and discharge data from T4 and T5 for the Tar River, and N5 and N6 for the Neuse River (**Figure 1**; **Supplementary Table 4**). Hurricane Irene struck eastern North Carolina on 27–28 August 2011. Post-hurricane sampling of the Tar-Pamlico River occurred at Stns. 5 and 6 on August 29, 2011. Somewhat later post-hurricane sampling was carried out at Stns. T5 and T6 and Stn. N7 on Sept. 14th (Stns. T1 and T2 and Stns. N1 and N2 were sampled on Sept. 12th); all sampling dates are shown in **Supplementary Table 1**.

Extracellular Enzyme Activities

Activities of exo-acting (terminal-unit cleaving) as well as endo-acting (mid-chain cleaving) enzymes were measured using two different methods. Low molecular weight substrate proxies [4-methylumbelliferone- (MUF-) and 4-methylcoumarinyl-7-amide- (MCA-) labeled substrates] were used to measure α- and β-glucosidase, leucine aminopeptidase, and phosphatase activities, after the method of Hoppe (1983; Hoppe et al., 1988). Triplicate water samples from each station were amended with substrate proxies to a final concentration of 400 μM (this concentration was chosen at the start of the project, from a saturation curve made to determine the appropriate saturation concentration of each substrate in the river water). Killed controls consisted of autoclaved water to which substrate was added. Samples were incubated for a period of 3–5 h at *in situ* or near *in-situ* temperature; an initial time-zero measurement was taken at the start of this period, and two to three subsequent time points were measured during this period. For each measurement, a 1-ml aliquot was taken from the incubating sample and combined with 1 ml of 20 mM borate buffer, and fluorescence was measured using single-cell fluorometers (Turner Biosystem TBS-380 or a Promega Quantifluor-ST). A dilution curve was made with each fluorophore in autoclaved river water to determine a fluorescence-hydrolysis rate conversion factor for each river. Hydrolysis rates were then calculated using the conversion factors and fluorescence measurements.

The activities of extracellular enzymes responsible for endo-acting (mid-chain cleaving) hydrolysis of a specific set of polysaccharides were measured using six distinct fluorescently labeled (FLA) polysaccharides (Arnosti, 1996, 2003). Arabinogalactan, chondroitin, fucoidan, laminarin, pullulan, and xylan (all obtained from Sigma-Aldrich USA) were labeled with fluoresceinamine as described in Arnosti (2003). These polysaccharides were selected because they are derived from a range of terrestrial (xylan, arabinogalactan) and marine (laminarin, xylan, fucoidan, pullulan, chondroitin) sources, and/or enzymes hydrolyzing these polysaccharides have been identified in marine bacteria and in marine bacterial genomes (for details, see e.g., Bold, 1985; Arnosti, 2000; Alderkamp et al., 2007; Wegner et al., 2013). In addition, the activities of enzymes hydrolyzing all of these polysaccharides have been measured in marine (Arnosti et al., 2011) as well as freshwater systems (Ziervogel et al., 2014). Because of the time and resources required for measurements with FLA-polysaccharides, polysaccharide hydrolysis rates were measured in duplicate, only at the upriver-most and downriver-most station in each river. At these stations (Stns. T1, T6; N1, and N7), duplicate live water samples, as well as an autoclaved control water sample for each station, were separately amended with one of each of the six substrates to a final concentration of 3.5 nM monosaccharide equivalent. A time-zero measurement was immediately taken, and the samples were then incubated in the dark at near *in-situ* temperature, with subsamples withdrawn periodically. After processing the samples, we found that, with very few exceptions, all polysaccharides were hydrolyzed at 3 days, the first time-point after the zero-time sample, so the data reported are all from this time point. Inconsistencies in sampling timepoints after 3 days in any case preclude use of later timepoints across the dataset.

Samples for measurement of polysaccharide hydrolase activities were collected by filtering 1–3 ml of sample water through a 0.2 μm cellulose acetate-membrane + GF-prefilter syringe filter (Sartorius Stedim Biotech, Germany), and freezing samples at −20°C until analysis. Hydrolysis was measured via changes in the molecular weight distribution of the FLA-labeled polysaccharide using gel permeation chromatography, as described in detail in Arnosti (2003). Several samples were lost prior to analysis from the Stn. T1 sample set: (date/substrate): 01/11 (fucoidan), 04/11 (pullulan), 06/11 (fucoidan), and 06/12 (xylan). At Stn. T6, missing samples were as follows: 09/11 (fucoidan), 11/11 (fucoidan), and 06/12 (laminarin).

Bacterial Cell Counts and Production

Aliquots of water were fixed for bacterial cell counts, following Porter and Feig (1980). Staining was carried out with 4′, 6-diamidino-2-phenylindole (Sigma-Aldrich USA), and slides were counted under an epifluorescence microscope (Olympus U-RFL, Olympus USA) using MetaMorph Microscopy software (Molecular Devices USA). 10 fields of view were counted per slide, with duplicate slides made for each river station.

Bacterial production was measured using ^{3}H-leucine incorporation (Kirchman, 2001). These measurements were only initiated in January 2011, so no data are available for samples collected during November/December 2010. Water from the upstream- and downstream-most stations (the same stations used to measure polysaccharide hydrolysis) in each river, plus autoclaved control water, was amended with ^{3}H-leucine to a final concentration of 20 nM. Samples were incubated for 1–2 h; following this incubation period, reactions were terminated using 100% trichloroacetic acid (TCA). Samples were then concentrated and washed with 80% ethanol before drying over night. Samples were then amended with scintillation liquid and allowed to sit for a 2-day period before analysis in a scintillation counter (Perkin Elmer TriCarb 3110 TR).

Dissolved Organic Carbon

Water samples from each station were filtered through 0.2 μm cellulose acetate-membrane + GF-prefilter syringe filter (Sartorius Stedim Biotech, Germany) into pre-combusted glass scintillation vials and frozen at −20°C until further analysis.

Dissolved organic carbon concentrations from these samples was measured via high temperature catalytic oxidation and non-dispersive infrared detection on a Shimazdu TOC-L series instrument (Shimadzu Corp. Kyoto). Samples were acidified to a pH < 2 and sparged with commercially obtained CO_2 free, zero-grade air for 10 min for inorganic carbon removal. Standards were generated from dilution of commercially prepared potassium hydrogen phthalate [KHP] (La-Mar-Ka Inc., Baton Rouge, LA) with 18.2 MΩ ultrapure water.

Statistical Analyses

Environmental data and microbial activity measurements described above were analyzed to look for correlations using the corrplot package in R (R Core Team, 2014), run in R version 3.3.3. The same package was used to look for correlations among activities of individual polysaccharide hydrolases. *T*-test analyses of potential effects of season, station, and the effects of Hurricane Irene on microbial activity measurements were also analyzed using R.

RESULTS

Environmental and Hydrological Characteristics

Environmental data including dissolved oxygen (DO), pH, and salinity (**Supplementary Table 1**), as well as river discharge (**Figure 2**), were used establish a picture of the seasonal environmental characteristics and dynamics of both rivers, and to investigate potential connections between community activity and river characteristics. River discharge indicated that the upstream and downstream stations were hydrologically decoupled (**Figure 2**). Discharge volume for Stns. T1 and T2 tracked together, and were distinctly separated from discharge volume at Stns. T4 and T5. Discharge data from the Neuse River likewise showed decoupling of upstream (Stns. N1 and N2) stations from the downstream-most station for which discharge data are available (Stn. N6). These patterns were supported by other chemical and physical data (**Supplementary Table 1**): in the Neuse River, salinity remained near zero upstream (Stns. N1, N2); the downstream stations exhibited greater fluctuations in salinity, varying between freshwater and estuarine conditions. Salinity of the Tar-Pamlico River, however, remained close to zero, even at the station farthest downriver (Stn. T6; **Supplementary Table 1**). Temperature ranges changed seasonally in both rivers, with the annual variations in the Neuse River between 4 and 30°C, and near 0 to 29°C in the Tar-Pamlico River. At each sampling point, temperatures were broadly comparable among stations, although downriver stations were frequently slightly warmer than upriver stations, and the temperature difference between Stns. T1 and T6 was typically a few degrees greater than between Stns. N1 and N7 (**Supplementary Table 1**). Dissolved oxygen (DO) followed an inverse relationship with temperature in both rivers. The range of DO for both downstream stations was greater than the DO ranges upstream.

DOC concentrations showed broad patterns across spatial and temporal scales. In the Neuse River, DOC was consistently highest (near or above 1,200 μmol C L^{-1}) at the downstream-most station, Stn. N7 (**Figure 3**; **Table 2**), while DOC concentrations at Stns. N1, N2, and N6 ranged from ∼400 to 800 μmol C L^{-1}. Stn. N2 exhibited the least temporal variation in concentration. No seasonal trends were evident, but the highest DOC measured at Stn. N7 (1,861 μmol C L^{-1}) was in September 2011, following Hurricane Irene in August 2011. In the Tar-Pamlico River, DOC concentrations at most stations and seasons exhibited wider temporal variability than in the Neuse River, ranging from ca. 300 to 1,000 μmol C L^{-1}. There was no distinct seasonal trend (**Figure 3**; **Table 2**), but DOC concentrations were higher downstream than upstream (**Table 2**), and the highest DOC concentrations (exceeding 1,700 μmol C L^{-1}) were also recorded at the downriver stations, Stns. T5 and T6, in September 2011, following Hurricane Irene (**Figure 3**).

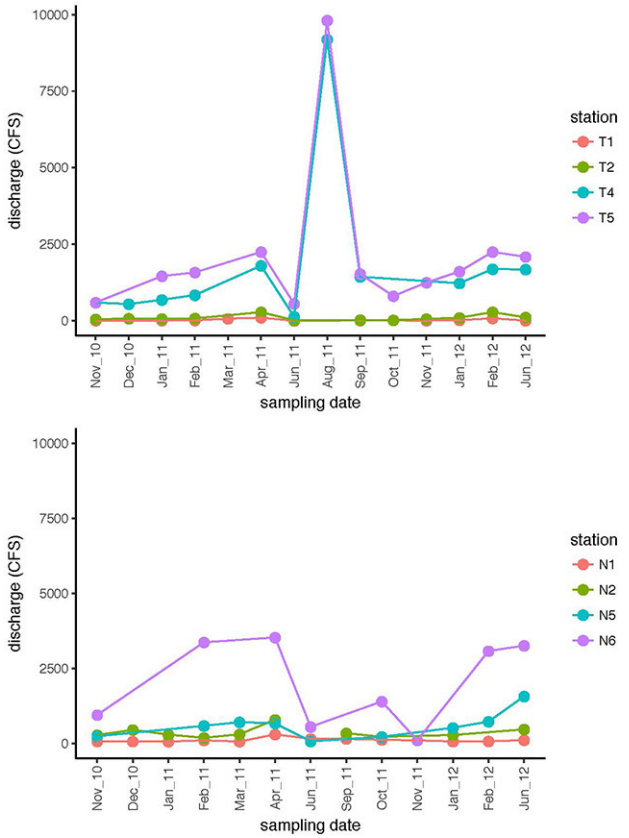

FIGURE 2 | Discharge (cubic feet per second) at four stations in the Tar-Pamlico River and the Neuse River on dates when samples were collected. Filled circles are from the dates at which samples were collected; lines connect consecutive sampling dates.

Microbial Cell Counts and Leucine Incorporation

Seasonally, bacterial numbers were highest in the late winter and early spring (Feb.–April) of 2011 (*t*-test; $p < 0.01$). In both rivers, months sampled in the winter and late spring of 2012 had

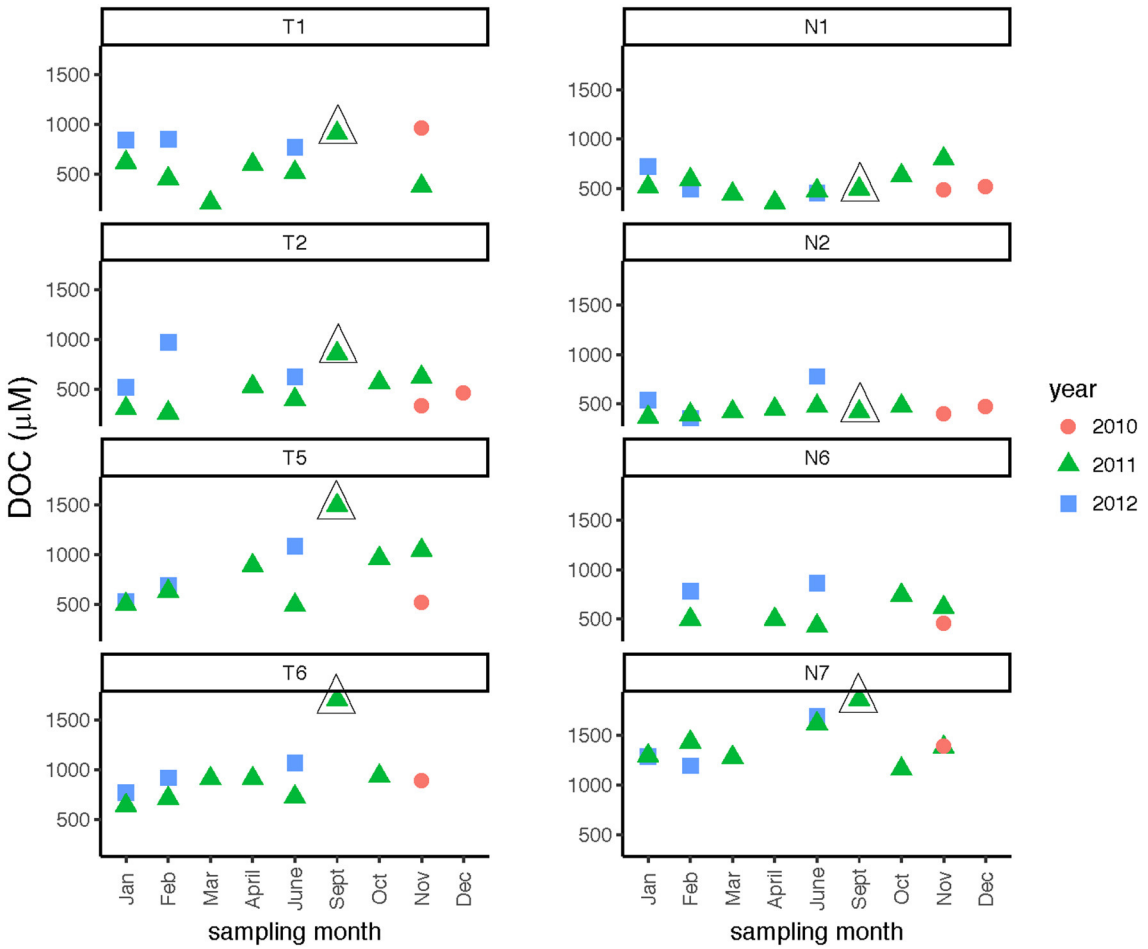

FIGURE 3 | Dissolved organic carbon concentrations at four stations each in the Tar-Pamlico and Neuse River. "T" corresponds to Tar-Pamlico stations, "N" corresponds to Neuse stations. Symbols outlined with triangles show sampling carried out in the month post Hurricane Irene.

lower bacterial abundance than their 2011 counterparts. Bacterial abundance (**Supplementary Table 2**) varied by a factor of 10 over the time course of the study. Bacterial protein production (**Figure 4**) showed slight increases during the spring through fall months, with minima occurring during the winter months (Jan/Feb) for both rivers (**Table 2**). When normalized on a per-cell basis (**Supplementary Table 2**), the summer and late fall months showed highest bacterial production. For most months, bacterial protein production rates normalized to cell abundance were higher downstream (Stns. T6, N7) compared to upstream (Stns. T1, N1) in both rivers (**Supplementary Table 2**). The highest bacterial protein production measured during the study (per cell, as well as on a volume basis) was measured in the Neuse River at Stn. N7 in Sept. 2011, after the passage of Hurricane Irene (**Figure 4**).

Activities of Glucosidase, Peptidase, and Phosphatase Enzymes

Leucine amino peptidase (Leu-MCA), glucosidase (α- and β-glu), and phosphatase activities were measured immediately upon return of the samples to the lab to assess microbial heterotrophic activities across locations and seasons. Leu-MCA hydrolysis rates were highest at the downstream-most station for the Tar-Pamlico River (**Figure 5**; **Table 2**). Averaged across all timepoints, Leu-MCA hydrolysis rates were 182, 147, 156 nmol L^{-1} h^{-1} for Stns. T1, T2, and T5, respectively, and approximately double-—324 nmol L^{-1} h^{-1}–at Stn. T6. For the Neuse River, averaged across all timepoints, Leu-MCA hydrolysis was 137, 144, and 93 nmol L^{-1} h^{-1} at Stns. N1, N2, and N6, respectively, and considerably higher (239 nmol L^{-1} h^{-1}) for Stn. N7. Although in both cases minimum rates occurred during winter months (**Table 2**), there were no overall seasonal trends for either river.

Glucosidase hydrolysis rates were generally higher in the Tar-Pamlico than the Neuse River, although this difference was statistically significant only for β-glu activities (**Table 2**). Glucosidase hydrolysis rates averaged close to 30 nmol L^{-1} h^{-1} in the Tar-Pamlico River and ∼10 nmol L^{-1} h^{-1} in the Neuse River. In both rivers, β-glu activities were generally a factor of 2–3 higher than α-glu activities (**Figures 6**, **7**; **Supplementary Table 5**); β-glu activities also showed a greater dynamic range (difference between lowest and highest rates). In both rivers, glucosidase activities were lowest in January and

TABLE 2 | *P*-values (*T*-tests) to determine statistical significance (as shown by $P < 0.05$; bold font) of microbial activities, cell counts, and DOC concentration by location and time.

	β-glu	α-glu	Leu	Phosph.	Sum FLA	DOC	Bact prod	Cell counts
Jan/Feb vs. other months	**8.33E-04**	**9.96E-03**	**6.76E-04**	**8.18E-08**	**1.60E-16**	0.341	**3.44E-07**	0.867
Tar/Neuse	**0.004**	0.051	0.187	**0.009**	0.937	0.738	0.554	0.446
Upriver/downriver	0.642	0.537	0.056	0.177	0.937	**4.31E-08**	**0.033**	0.440
Tar: T6 vs. other Tar stns	0.752	0.411	**0.049**	0.936	0.937	**0.014**	0.819	
Neuse: N7 vs. other Neuse stns	0.860	0.343	0.089	0.572	0.184	**0.001**	**0.014**	0.965
T6/N7 differences	0.089	0.300	0.374	0.089	0.432	**2.57E-04**	0.091	0.577
Hurricane Irene	0.090	0.435	0.292	**0.001**	0.057	**0.006**	0.488	**0.017**

β-glu, β-glucosidase activities; α- glu, α-glucosidase activities; Leu, leucine aminopeptidase activities; phosph, phosphatase activities; sum FLA, summed polysaccharide hydrolase activities; bact prod, bacterial protein production; DOC, dissolved organic carbon concentration. Hurricane Irene-affected times and locations were defined as Stations T5/T6 and N6/N7 in Sept 2011 (and for T5/T6, also in Aug 2011) compared to all other months at the same stations.

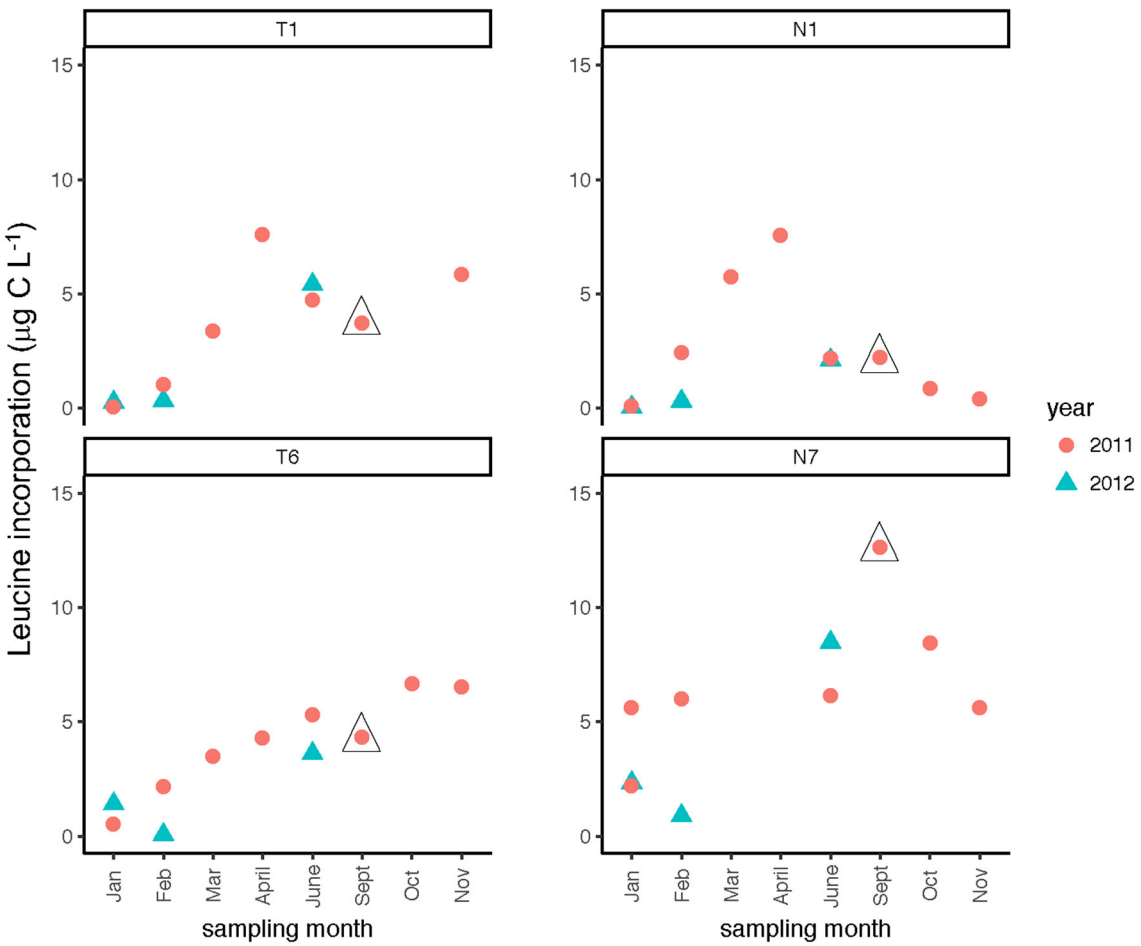

FIGURE 4 | Bacterial protein production measured at two stations each in the Tar-Pamlico and Neuse River. "T" corresponds to Tar-Pamlico stations, "N" corresponds to Neuse stations. Symbols outlined with triangles show sampling carried out in the month post Hurricane Irene.

February (**Table 2**), but otherwise varied considerably by month and station.

Phosphatase activities typically were higher in the Tar-Pamlico than in the Neuse River (**Figure 8**; **Table 2**). In both rivers, phosphatase activities were typically low in January and February, and were considerably higher during other months of the year (**Table 2**). Activities did not differ systematically between upstream and downstream locations (**Table 2**). At Stn. N7, however, a notably high maximum (ca. 500 nmol L^{-1} h^{-1}) was measured in Sept. 2011, the month after Hurricane Irene, when bacterial productivity and the DOC concentration at this station also reached maxima (**Figures 3**, **4**).

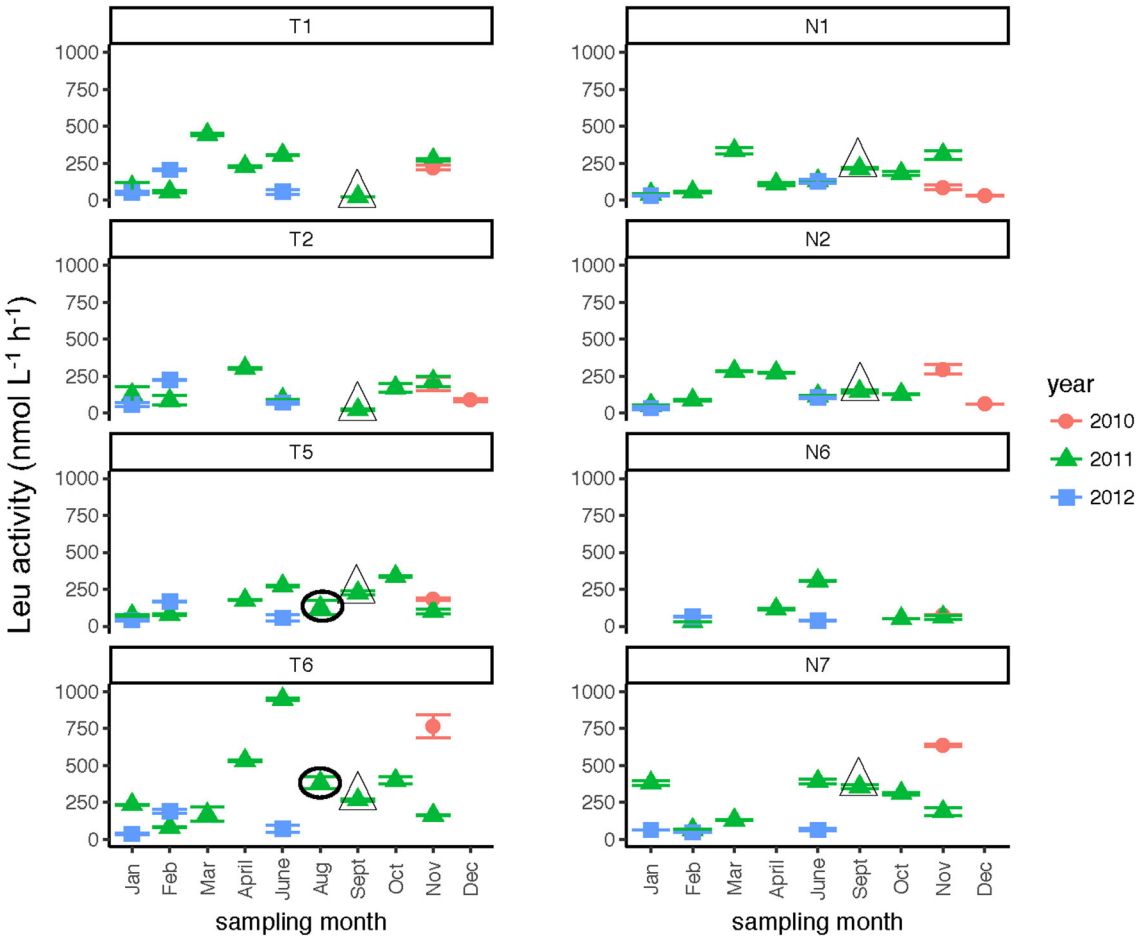

FIGURE 5 | Leu-MCA activities (average and standard deviations) at four stations in the Neuse and Tar-Pamlico Rivers from 2010 to 2012. "T" corresponds to Tar-Pamlico stations, "N" corresponds to Neuse stations. Symbols outlined with triangles show sampling carried out in the month post Hurricane Irene. Circled symbols (Stns. T5 and T6 only) show samples collected in August 2011, shortly after Hurricane Irene crossed through eastern North Carolina.

Activities of Polysaccharide-Hydrolyzing Enzymes

In both rivers, a broad spectrum of polysaccharide hydrolase activities was measured, with all six polysaccharides hydrolyzed at many sampling dates and stations (**Supplementary Table 3**). Summed polysaccharide hydrolysis rates were frequently lowest in the winter months (**Table 2**), but otherwise varied considerably (**Figure 9**). The relative contribution of each polysaccharide hydrolase activity to summed activities was quite dissimilar, however. Chondroitin and xylan hydrolysis together averaged 58–65% of the total contributions to the summed polysaccharide hydrolysis rates across all seasons and stations in both rivers, irrespective of whether summed activities were high or low (**Supplementary Table 3**). For most stations, hydrolysis rates generally decreased in the order xylan, chondroitin >> laminarin > arabinogalactan with smaller contributions from fucoidan and pullulan (**Supplementary Table 3**). The annual range of summed hydrolysis rates was similar among all stations, from 3 to 65 nmol monomer L^{-1} h^{-1} at Stn. N1, 6–87 nmol monomer L^{-1} h^{-1} at Stn. N7, 3–81 nmol monomer L^{-1} h^{-1} at Stn. T1, and 4–71 nmol monomer L^{-1} h^{-1} at Stn. T6 (**Figure 9**).

Correlations among Microbial Activities and Environmental Parameters

Correlation analysis of environmental parameters and microbial activities (**Figure 10**; *p*-values in **Supplementary Table 6**) showed some expected as well as unexpected correlations. Unsurprisingly, dissolved oxygen (DO) was strongly inversely correlated with temperature, and discharge, conductivity, and gage height also showed moderate correlation. Summed polysaccharide hydrolase activities (FLA; **Figure 10**) were positively correlated with temperature, and thus also inversely correlated with DO, although other enzyme activities did not show a notable correlation with temperature (or DO). Correlations among the other enzyme activities varied: β- and α-glu were strongly correlated with each other, and were more weakly correlated with Leu-MCA and phosphatase.

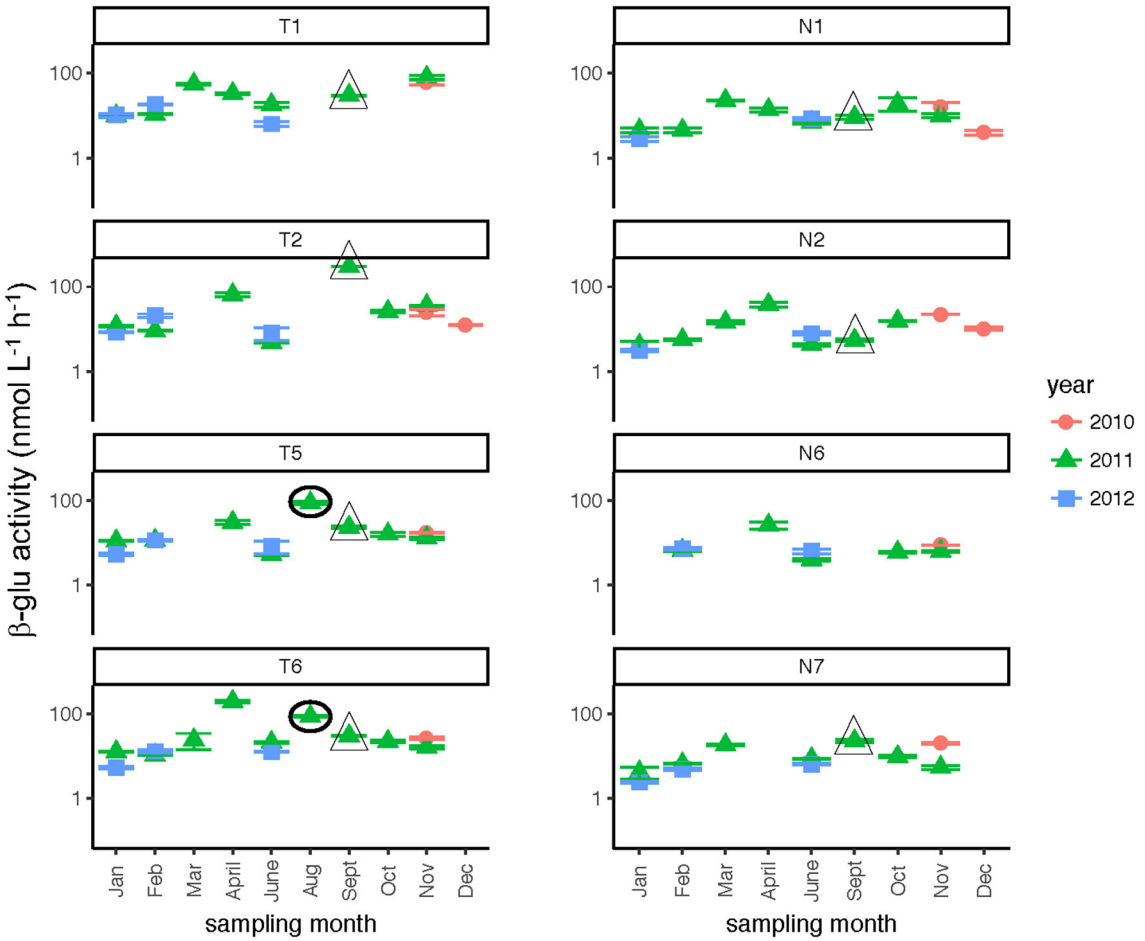

FIGURE 6 | β-glucosidase activities (average and standard deviations) at four stations each in the Neuse and Tar-Pamlico Rivers from 2010 to 2012. "T" corresponds to Tar-Pamlico stations, "N" corresponds to Neuse stations. Symbols outlined with triangles show sampling carried out in the month post Hurricane Irene. Circled symbols (Stns. T5 and T6 only) show samples collected in August 2011, shortly after Hurricane Irene crossed through eastern North Carolina. y-axis is a logarithmic scale.

Cell counts were inversely correlated with DOC, but leucine incorporation (bacterial protein production) showed only a strong inverse correlation with DO. Correlation analysis among the individual polysaccharide hydrolase activities (**Figure 11**; *p*-values in **Supplementary Table 7**) showed that summed activities were most strongly correlated with xylan and chondroitin hydrolysis, followed by arabinogalactan and laminarin hydrolysis.

Effects of Hurricane Irene

Post-Hurricane Irene sampling (September 2011, plus August 2011 for Stns. T5 and T6) showed that phosphatase activities and DOC concentrations were considerably elevated compared to other sampling dates at the downriver stations (T5, T6, N6, N7; **Table 2**; **Figures 3**, **8**). Although bacterial protein productivity was greatly elevated at Stn. N7 in September 2011 (**Figure 4**), the statistical significance of this measurement could not be calculated due to the small number of observations.

DISCUSSION

Microbial processing of organic matter in riverine systems can be influenced by a variety of physical, chemical, and biological factors that vary across a range of spatial and temporal scales (Singh et al., 2013). Most previous studies of microbially-driven carbon cycling in rivers have focused on either sampling a range of sites across a limited time period, or have investigated fewer sites over an annual cycle (e.g., Artigas et al., 2009; Tiquia, 2011; Frossard et al., 2012; Millar et al., 2015). In an effort to investigate some of the complexities of these interactions in rivers, we sampled both the Neuse and Tar-Pamlico Rivers across multiple seasons and sites. The range of Leu-MCA, β-glu, and phosphatase activities measured across sites and seasons in the Tar-Pamlico and Neuse Rivers proved to be similar to or slightly higher than rates measured across a broad range of riverine sites sampled at one season (e.g., Williams et al., 2012; Millar et al., 2015), as well as seasonal studies at fewer locations (Wilczek et al., 2005), suggesting that the Tar-Pamlico and Neuse Rivers

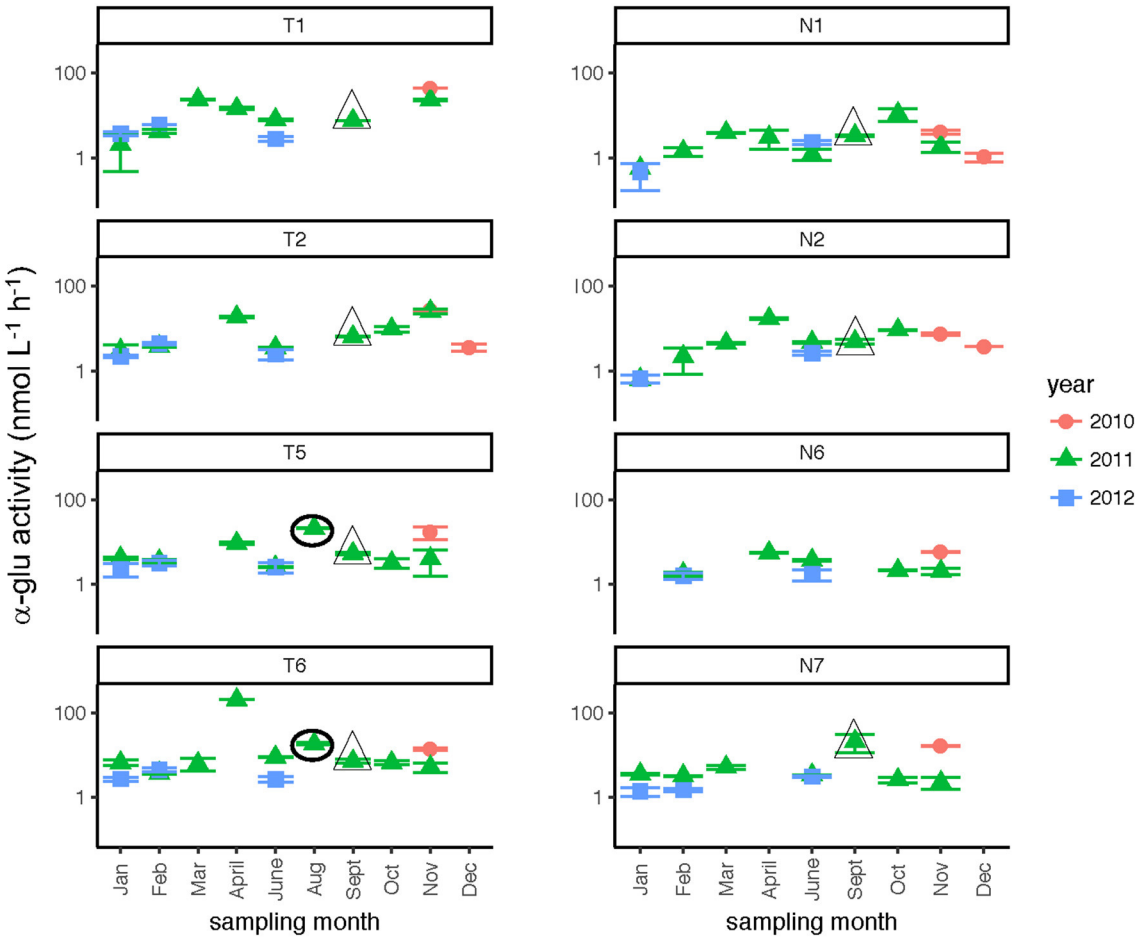

FIGURE 7 | α-glucosidase activities (average and standard deviations) at four stations each in the Neuse and Tar-Pamlico Rivers from 2010 to 2012. "T" corresponds to Tar-Pamlico stations, "N" corresponds to Neuse stations. Symbols outlined with triangles show sampling carried out in the month post Hurricane Irene. Circled symbols (Stns. T5 and T6 only) show samples collected in August 2011, shortly after Hurricane Irene crossed through eastern North Carolina. y-axis is a logarithmic scale.

are not atypical in their enzymatic activities. Cell counts were also generally similar to those reported from other riverine locations (Wilczek et al., 2005; Williams et al., 2012; Millar et al., 2015).

Two broad-scale spatial patterns in microbial enzyme activities emerged over the course of the study: higher peptidase activities at T6 compared to the other stations in the Tar-Pamlico River, and higher β-glucosidase and phosphatase activities in the Tar-Pamlico River compared to the Neuse River (**Table 2**; **Figures 5**, **6**, **8**). These spatial patterns in microbial enzyme activities contrast in particular with a lack of spatial patterns for microbial cell counts, and bacterial productivity that showed a different spatial pattern: upriver/downriver contrasts, and higher values at Stn. N7 than N1 (**Table 2**). Moreover, bacterial protein production correlated (inversely) only with dissolved oxygen, but not with any of the other activity measurements (**Figure 10**).

Microbial sources likely account for most of the enzymes active in the water column, but individual microbes can differ considerably in terms of activity, as exemplified by the differences in cell-count normalized bacterial production (**Supplementary Table 2**), which also demonstrated no distinct spatial patterns. Moreover, the capabilities of distinct members of microbial communities to carry out specific enzymatic function differs substantially, even among closely-related microbes (Xing et al., 2014). Since the measured enzyme activities are also an outcome of the kinetic characteristics of enzymes and their active lifetimes in the water column, as well as the quantity of enzymes produced, a lack of correlation between microbial cell numbers or bacterial productivity and enzyme activities is not entirely surprising. A lack of correlation between either cell counts or bacterial productivity and glucosidase and Leu-MCA activities has also been observed in other freshwater environments (e.g., Sieczko et al., 2015). The observation that summed polysaccharide hydrolase activities do not demonstrate the same spatial patterns seen for β-glucosidase activities—there is no difference between the activities measured in the Tar-Pamlico and in the Neuse River (**Table 2**)—is likely due to the fact that the overall ability to produce specific extracellular enzymes is non-uniformly distributed among members of microbial

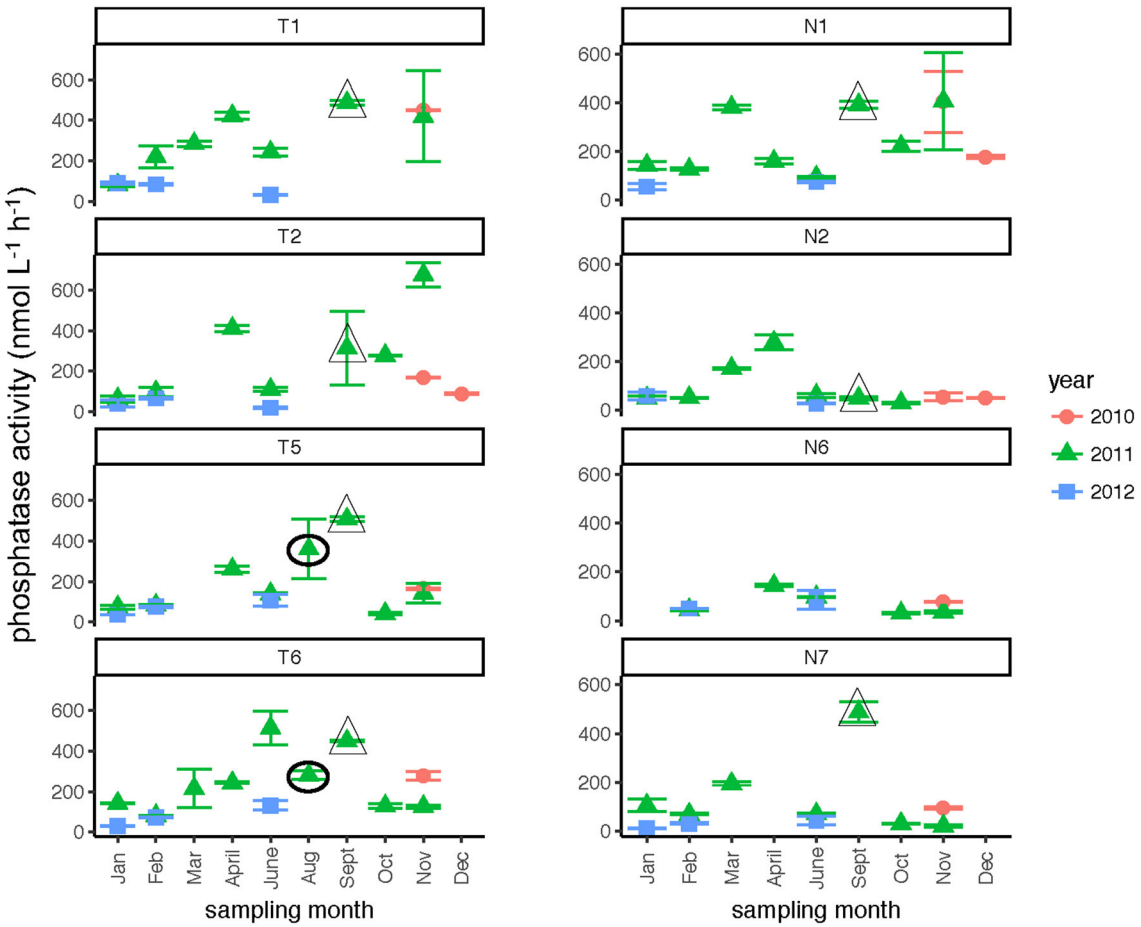

FIGURE 8 | Phosphatase activities (average and standard deviations) at four stations each in the Neuse and Tar-Pamlico Rivers from 2010 to 2012. "T" corresponds to Tar-Pamlico stations, "N" corresponds to Neuse stations. Symbols outlined with triangles show sampling carried out in the month post Hurricane Irene. Circled symbols (Stns. T5 and T6 only) show samples collected in August 2011, shortly after Hurricane Irene crossed through eastern North Carolina.

communities (Zimmerman et al., 2013). Furthermore, the longer incubation times for the polysaccharide hydrolase measurements (3 days, compared to hours for the β-glucosidase activities) allows time for growth and induction responses to polysaccharide addition, which may have masked any initial differences among sites.

Given prior observations of a limited spectrum of polysaccharide-hydrolyzing enzyme activities in aquatic systems (e.g., Ziervogel and Arnosti, 2009; Arnosti et al., 2011; Ziervogel et al., 2014), the hydrolysis of all six polysaccharide substrates at every station in the Neuse and Tar-Pamlico Rivers at timepoints throughout the year was remarkable (**Supplementary Table 3**). This breadth of hydrolytic capabilities has seldom been observed in other locations; even nutrient addition has not led to hydrolysis of some polysaccharides in some locations (Steen and Arnosti, 2014). Typically, over time-courses of incubations lasting well over 3 days, only a subset of polysaccharides was hydrolyzed (e.g., Steen et al., 2008; Arnosti et al., 2011; Ziervogel et al., 2014). Moreover, this broad range of hydrolytic capabilities in the Neuse and Tar-Pamlico Rivers was observed at timepoints when summed hydrolysis rates were low, as well as at times when summed hydrolysis rates were high, as at Stn. N1 in February and June 2012, when summed hydrolysis rates were 6 and 65 nmol monomer L^{-1} h^{-1}, respectively (**Figure 9**; **Supplementary Table 3**).

The broad hydrolytic capabilities of microbial communities in the Neuse and Tar-Pamlico Rivers may be due to the extensive and diverse watersheds of both rivers, as well as the occurrence of seasonal flooding events, leading to substantial terrestrial input into the systems, which provides the microbial community with a greater quantity and diversity of organic matter sources. In particular, the lower reaches of both rivers are subject to frequent overbank flooding because there are no large dams to control flooding and because these low-elevation coastal plain rivers have low banks that help facilitate frequent flooding (Peng et al., 2004; Reed et al., 2008). Although previous studies in other riverine systems have suggested that freshwater and estuarine organic matter of autochthonous, as opposed to allochthonous, origin is of greater importance to the microbial community for uptake

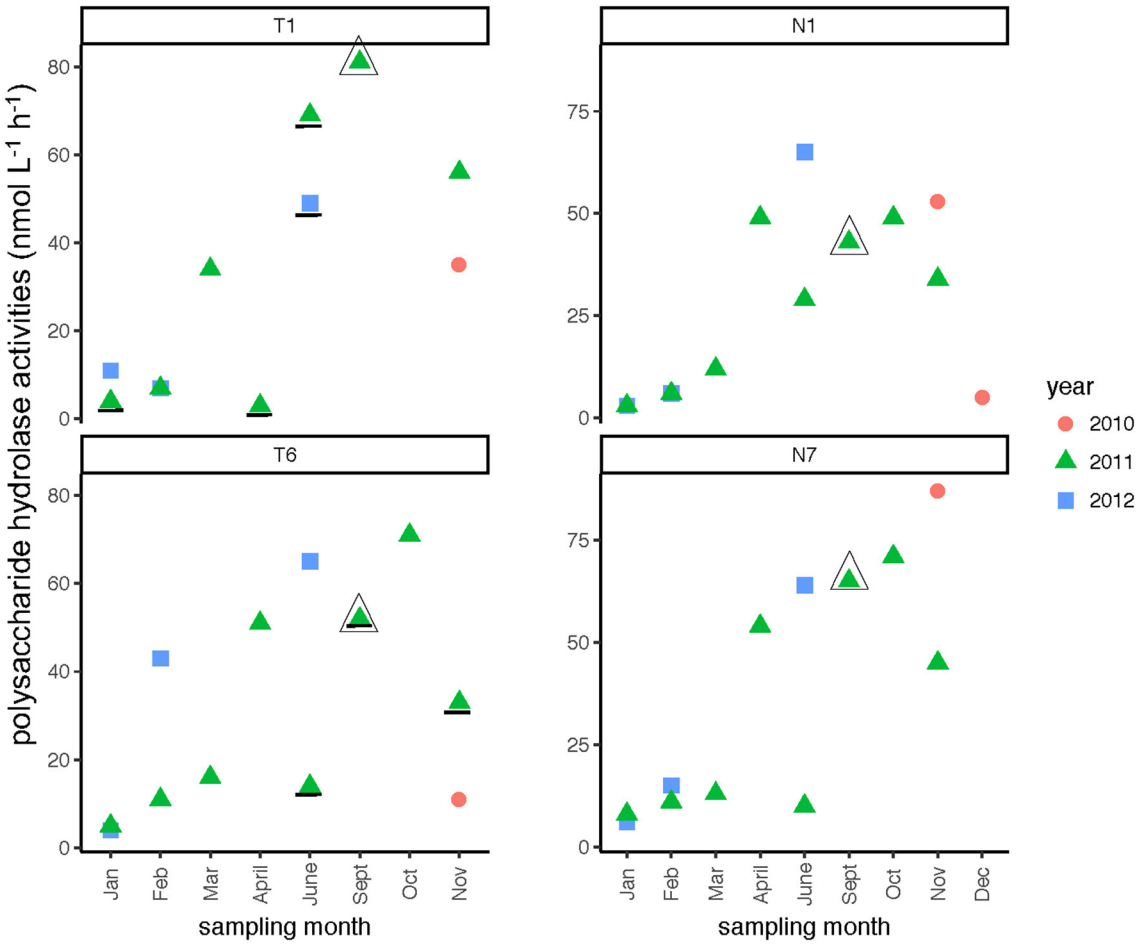

FIGURE 9 | Summed polysaccharide hydrolase activities in the Neuse and Tar-Pamlico Rivers from 2010 to 2012. "T" corresponds to Tar-Pamlico stations, "N" corresponds to Neuse stations. Plot shows the average of summed activities; note that hydrolysis of each individual polysaccharide was measured in duplicate. Symbols that are underlined for Stns. T1 and T6 indicate dates for which specific polysaccharide hydrolase samples were missing (see Methods). All polysaccharide hydrolase data are shown in **Supplementary Table 3**.

(McCallister et al., 2006), significant input of terrestrial organic matter may well influence, and possibly increase, hydrolytic capabilities. Such a broad range of DOM sources may also account for the observation that a site within Pamlico Sound also showed hydrolysis of all six polysaccharide substrates, in contrast to a nearby site on the continental shelf, where only four of the substrates were hydrolyzed (D'Ambrosio et al., 2014). Throughout all seasons, the comparatively high contributions of xylan hydrolysis to summed hydrolysis rates may be an additional indication of the importance of terrestrial sources of organic matter to both rivers, since xylan is a major constituent of land plants (Ebringerova and Heinze, 2000), as well as some algae. High xylan hydrolysis rates have also been measured in the Chesapeake Bay (Steen et al., 2008) and Delaware River (Ziervogel and Arnosti, 2009). Comparably high contributions of both chondroitin and xylan to summed hydrolysis rates have to date been observed in the Delaware River (Ziervogel and Arnosti, 2009), and in the Gulf of Mexico, at sites that presumably also have the potential to be influenced by terrigenous input from the Mississippi River (Arnosti et al., 2011; Steen et al., 2012).

Spatial differences in DOC concentrations were evident—most notably elevated downstream DOC concentrations, particularly at Stn. N7—but this pattern is not reflected in most of the enzyme activities measured in the two rivers (**Table 2**). The elevated DOC concentration particularly at Stn. N7 may in part reflect lateral input at the downstream locations, as well as the hydrologic disconnect shown by discharge and gage height (**Figure 2**; **Supplementary Figure 1**) of upstream and downstream stations. DOC contributed via different hydrologic flow paths can differ considerably in source as well as composition (Singh et al., 2013). Moreover, lateral input of DOC may include comparatively more microbially recalcitrant organic matter that survives photochemical and microbiological processing, and does not enhance bacterial activity. A lack of clear relationships between DOC and enzyme activities was also reported for the large tributaries of the lower Mississippi

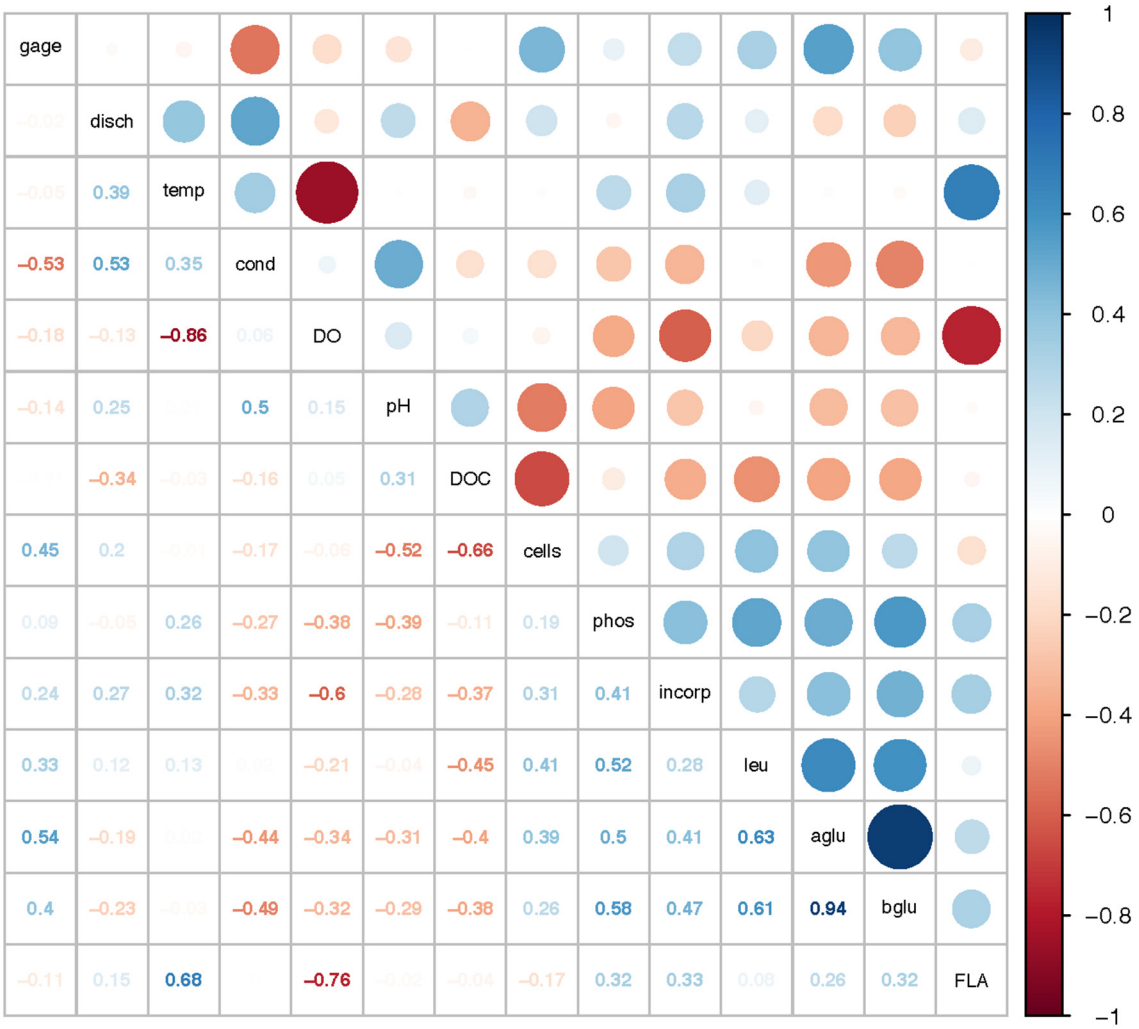

FIGURE 10 | Correlation plot for physical/chemical and microbial activity data. Gage, gage height; disch, discharge; temp, temperature; cond, conductivity; DO, dissolved oxygen; pH, pH; DOC, dissolved organic carbon; cells, cell counts; phos, phosphatase activities; incorp, bacterial protein production (leucine incorporation); leu, leucine-aminopeptidase (Leu-MCA); aglu, a-glucosidase; bglu, b-glucosidase; FLA, summed polysaccharide hydrolase activities. Colors show intensity of positive (blue) and negative (red) correlations; numbers show corresponding correlation coefficients.

River, where site-to-site differences for a single river were as large as between-river variations in enzyme activities (Millar et al., 2015). A similar lack of relationship between the origin and optical properties of DOM and glucosidase or Leu-MCA activities was reported for the Danube floodplain (Sieczko et al., 2015). The Danube floodplain sites also showed little systematic variation in bacterial abundance or productivity, despite differences in glucosidase and peptidase activities (Sieczko et al., 2015).

The lack of broad seasonal trends in microbial activities and abundance was something of a surprise. Although glucosidase, peptidase, and phosphatase activities were lowest in Jan/Feb (**Table 2**), when temperatures were also lowest (**Supplementary Table 1**), low activities were at times also measured in other months—for example, in June—when seasonal temperatures were near or at their maximum. Across the entire study period, temperature correlated with summed polysaccharide hydrolase activities (**Table 2**), but summed activities were sometimes low at times when water temperatures were high (e.g., June 2011 at Stn. N7; **Figure 9**) Other studies have shown seasonality to be an important factor associated with changes in microbial community activities (Artigas et al., 2009), with temperature as an important controlling variable (Wilczek et al., 2005). A high-resolution investigation of enzyme activities at a single site in the coastal Pacific, however, demonstrated that substantial variations in enzyme activities occurred on timescales shorter than 1 month, and that seasonal patterns were not clearly evident (Allison et al., 2012).

An investigation of microbial community composition along the salinity gradient of the Columbia River and its estuary, extending into the coastal ocean, also found that strong spatial patterns overwhelmed seasonal patterns, which were more

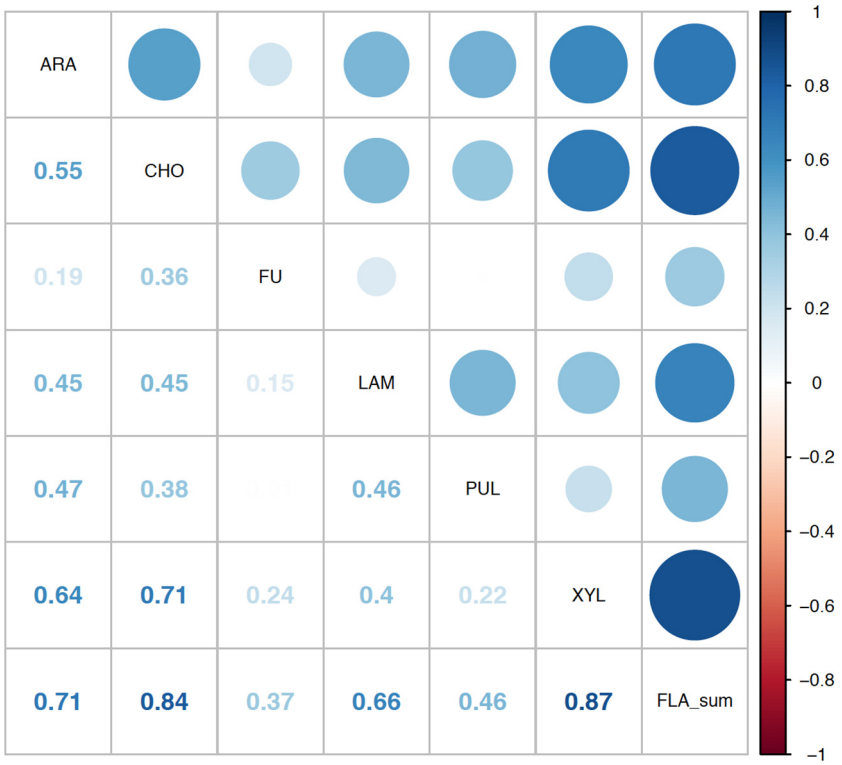

FIGURE 11 | Correlation plot for the polysaccharide hydrolase activities contributing to the summed activity. ARA, arabinogalactan; CHON, chondroitin sulfate; FU, fucoidan; LAM, laminarin; PUL, pullulan; XYL, xylan; FLA_sum, summed polysaccharide hydrolase activities. Colors show intensity of correlations; numbers show corresponding correlation coefficients.

evident within individual groups of bacteria (Fortunato et al., 2012). Metabolic potential, as represented by metagenomes, varied comparatively little along this same gradient, but metatranscriptomic data showed considerable variability that was unrelated to season or salinity (Fortunato and Crump, 2015), suggesting that the communities were reacting to localized environmental conditions. In the case of the Tar-Pamlico and Neuse Rivers, factors that are unrelated to season—such as land use, and abundance of natural land cover (**Table 1**)—may correlate more strongly with enzyme activities (Williams et al., 2012). The interplay between factors that do and do not have consistent seasonal trends may thus help drive enzymatic activities, and obscure seasonal correlations. However, evidence suggests that microbial communities in freshwater, estuarine, and marine systems are able to respond rapidly to increased organic matter inputs (Williams and Jochem, 2006; Allison et al., 2012). Such rapid responses may be the reason that consistent, long-term seasonality is not evident in the Neuse and Tar-Pamlico Rivers, as microbial communities may respond to factors that change on timescales different than the length of time between sampling dates.

The passage of Hurricane Irene across the eastern half of North Carolina in August 2011, however, is an example of an event that left a signature discernable in the lower reaches of the Tar-Pamlico and Neuse Rivers even two-plus weeks post-event. Phosphatase activities, DOC concentrations, and cell counts showed significant differences in September 2011 (and August, for Stns. T5 and T6) compared to other sampling months at these sites (**Table 2**). (Note that the August sampling was a day after Hurricane Irene passed through North Carolina; the September samplings were ca. 2 weeks post-hurricane). DOC concentrations at Stns. T5, T6, and N7 all were far higher in September 2011 than in any other month at the same location (**Figure 3**), despite the probability that the concentrations measured 2 weeks post-event were lower than the maximum concentrations. Maximal DOC input into the Neuse estuary lagged maximum discharge by ∼1 week (Brown et al., 2014), presumably due to lateral inputs into the upper reaches of the Neuse River in response to extensive flooding. Flooding and elevated discharge were likely responsible for changes in microbial community composition in the Tar-Pamlico River, where microbial community composition downstream (Stn. T6) shifted considerably post-hurricane (Balmonte et al., 2016). Prior to the hurricane, the community composition of Stns. T1 and T6 were notably dissimilar. Immediately post-hurricane (August 2011) as well as 2 weeks later (Sept. 2011), there was evidence of coupling between upstream and downstream stations, as well as post-hurricane microbial input from terrestrial sources. These distinct microbial signatures were less evident by November 2011 (Balmonte et al., 2016).

Although DOC concentrations measured in Sept. 2011 were similar in the Neuse and Tar-Pamlico Rivers (**Figure 3**), the composition of this DOC was likely different, given the difference in watersheds (**Figure 1**; **Table 1**) and the notable differences in responses of the microbial communities in the two rivers to this DOC. Bacterial production on a cell-specific basis reached a maximum in Sept. 2011 at Stn. N7 more than an order of magnitude higher than otherwise measured at this station, and more than four times greater than at Stn. T6 at the same time (**Supplementary Table 2**); bacterial production at Stn. N7 was also maximal at this station on volume-specific basis (**Figure 4**). Phosphatase activities were also greatly elevated at Stn. N7, but not at Stn. T6 (**Figure 8**). In the Tar-Pamlico River, by contrast, bacterial production, glucosidase, and Leu-MCA activities at Stn. T6 were not notably elevated even during the August 2011 sampling (**Figures 5**–**7**), the day after the passage of Hurricane Irene. Although no data on the chemical characteristics of Hurricane-Irene associated DOC are available from the Tar-Pamlico and Neuse Rivers, Hurricane Irene-associated water collected within a Maryland watershed showed distinct spectroscopic characteristics compared to water collected at other times, likely due to differences in sources and flow-paths (Singh et al., 2013). The differences in land use, drainage, and flow paths thus may have led to considerable compositional differences in the DOC added to the Neuse and Tar-Pamlico Rivers as a consequence of Hurricane Irene. Together, these data suggest that there was a microbial response to the DOC added to the Neuse River, but not the Tar-Pamlico River, post Hurricane Irene, but this response did not involve the glucosidase, Leu-MCA, or polysaccharide hydrolase enzymes whose activities we measured, or (alternatively), any enzymatic response in the Neuse River was shorter-lived than the elevation of DOC concentration, two-plus weeks post-event.

Complex trends of organic carbon remineralization characterize microbial activities in the Tar-Pamlico and Neuse River systems. Broad-scale spatial patterns—in particular, higher β-glucosidase and phosphatase activities in the Tar-Pamlico compared to the Neuse River, as well as higher downstream Leu-MCA activities in the Tar-Pamlico River—are evident in this study, but no single factor can be pinpoint as the most influential in shaping community activities; even large-scale events such as a hurricane's passage elicited different responses in the two rivers. Future studies of similar spatiotemporal scales, ideally including focused investigation of DOC characteristics and flow paths, will be necessary for clearer understanding of the factors that drive microbial community activities and organic matter remineralization across aquatic gradients.

AUTHOR CONTRIBUTIONS

CA and BM designed the study. AB, KZ, SG, and SS collected the samples, carried out the incubations, and collected the data. AB, KZ, SG, SS, and CA analyzed the data. AB and CA wrote the manuscript, with input from all co-authors. We are very grateful to the two reviewers, whose thoughtful comments considerably improved the manuscript.

FUNDING

This project was initiated and carried out with funding from the Eddie and Jo Allison Smith Family Foundation, with matching funding from UNC's Institute for the Environment and the Wallace Genetic Foundation. Additional support was provided by NSF (OCE-1332881 and OCE-1736772) to CA.

ACKNOWLEDGMENTS

We thank JP Balmonte, Kim DeLong, Sarah Underwood, and Benjamin Rhodes for assistance with lab and fieldwork. We also thank Anna Jalowska and Alexander Stephan for creating the map used as **Figure 1**.

SUPPLEMENTARY MATERIAL

The Supplementary Material for this article can be found online at: https://www.frontiersin.org/articles/10.3389/fmicb.2017.02589/full#supplementary-material

Supplementary Figure 1 | Gage height (ft) for the Tar-Pamlico and Neuse rivers. Solid circle show time points at which were collected; lines connect consecutive sampling dates.

Supplementary Table 1 | Temperature, salinity, dissolved oxygen, and pH at the date and time of sampling for all stations and sites.

Supplementary Table 2 | Leucine incorporation, cell counts, leucine incorporation per cell, and DOC concentration for all stations and sites.

Supplementary Table 3 | Polysaccharide hydrolase activities (nmol monomer L^{-1} h^{-1}) for all stations and sites. Ara, arabinogalactan; cho, chondroitin sulfate; fu, fucoidan; lam, laminarin; pul, pullulan; xyl, xylan.

Supplementary Table 4 | Gage height and discharge on the date of sampling for each station and date.

Supplementary Table 5 | α-glucosidase, β-glucosidase, and leu-aminopeptidase activities (nmol L^{-1} h^{-1}) for each station and date.

Supplementary Table 6 | Data shown in **Figure 10**; *P*-values as calculated using the corrplot package in R. Values where $P < 0.05$ are shown in bold font.

Supplementary Table 7 | Data shown in **Figure 11**. *P*-values as calculated using the corrplot package in R. Values where $P < 0.05$ are shown in bold font.

REFERENCES

Alderkamp, A.-C., van Rijssel, M., and Bolhuis, H. (2007). Characterization of marine bacteria and the activity of their enzyme systems involved in degradation of the algal storage glucan laminarin. *FEMS Microbiol. Ecol.* 59, 108–117. doi: 10.1111/j.1574-6941.2006.00219.x

Allison, S. D., and Vitousek, P. M. (2005). Responses of extracellular enzymes to simple and complex nutrient inputs. *Soil Biol. Biochem.* 37, 937–944. doi: 10.1016/j.soilbio.2004.09.014

Allison, S. D., Chao, Y., Farrara, J. D., Hatosy, S., and Martiny, A. C. (2012). Fine-scale temporal variation in marine extracellular enzymes of coastal southern California. *Front. Microbiol.* 3:301. doi: 10.3389/fmicb.2012.00301

Arnosti, C. (1996). A new method for measuring polysaccharide hydrolysis rates in marine environments. *Organ. Geochem.* 25, 105–115. doi: 10.1016/S0146-6380(96)00112-X

Arnosti, C. (2000). Substrate specificity in polysaccharide hydrolysis: contrasts between bottom water and sediments. *Limnol. Oceanogr.* 45, 1112–1119. doi: 10.4319/lo.2000.45.5.1112

Arnosti, C. (2003). Fluorescent derivatization of polysaccharides and carbohydrate-containing biopolymers for measurement of enzyme activities in complex media. *J. Chromatogr. B* 793, 181–191. doi: 10.1016/S1570-0232(03)00375-1

Arnosti, C., Bell, C., Moorhead, D. L., Sinsabaugh, R. L., Steen, A. D., Stromberger, M., et al. (2014). Extracellular enzymes in terrestrial, freshwater, and marine environments: perspectives on system variability and common research needs. *Biogeochemistry* 117, 5–21. doi: 10.1007/s10533-013-9906-5

Arnosti, C., Steen, A. D., Ziervogel, K., Ghobrial, S., and Jeffrey, W. H. (2011). Latitudinal gradients in degradation of marine dissolved organic carbon. *PLoS ONE* 6:e28900. doi: 10.1371/journal.pone.0028900

Artigas, J., Romani, A. M., Gaudes, A., Munoz, I., and Sabater, S. (2009). Organic matter availability structures microbial biomass and activity in a Mediterranean stream. *Freshw. Biol.* 54, 2025–2036. doi: 10.1111/j.1365-2427.2008.02140.x

Balmonte, J. P., Arnosti, C., Underwood, S., McKee, B. A., and Teske, A. (2016). Riverine bacterial communities reveal environmental disturbance signatures within the Betaproteobacteria and Verrucomicrobia. *Front. Microbiol.* 7:1441. doi: 10.3389/fmicb.2016.01441

Blackburn, N., Zweifel, U., and Hagström, Å. (1996). Cycling of marine dissolved organic matter. II. a model analysis. *Aquat. Microb. Ecol.* 11, 79–90. doi: 10.3354/ame011079

Bold, H. C. (1985). *Algae*. Englewood Cliffs, NJ: Prentice Hall.

Brown, M. M., Mulligan, R. P., and Miller, R. L. (2014). Modeling the transport of freshwater and dissolved organic carbon in the Neuse River Estuary, NC, USA following Hurricane Irene (2011). *Estuar. Coastal Shelf Sci.* 139, 148–158. doi: 10.1016/j.ecss.2014.01.005

Burgess, C. (ed.). (2013a). *Neuse River Basin.* North Carolina Department of Education; Office of Environmental Education and Public Affairs, Raleigh, NC.

Burgess, C. (ed.). (2013b). *Tar-Pamlico River Basin*. North Carolina Department of Education; Office of Environmental Education and Public Affairs, Raleigh, NC.

Burkholder, J. M., Dickey, D. A., Kinder, C. A., Reed, R. E., Mallin, M. A., McIver, M. R., et al. (2006). Comprehensive trend analysis of nutrients and related variables in a large eutrophic estuary: a decadal study of climatic and anthropogenic influences. *Limnol. Oceanogr.* 51, 463–487. doi: 10.4319/lo.2006.51.1_part_2.0463

D'Ambrosio, L., Ziervogel, K., MacGregor, B., Teske, A., and Arnosti, C. (2014). Composition and enzymatic function of particle-associated and free-living bacteria: a coastal/offshore comparison. *ISME J.* 8, 2167–2179. doi: 10.1038/ismej.2014.67

Ebringerova, A., and Heinze, T. (2000). Naturally occurring xylan structures, isolation procedures and properties. *Macromol. Rapid Commun.* 21, 542–556. doi: 10.1002/1521-3927(20000601)21:9<542::AID-MARC542>3.0.CO;2-7

Fortunato, C. S., and Crump, B. C. (2015). Microbial gene abundance and expression patterns across a river to ocean salinity gradient. *PLoS ONE* 10:e0140578. doi: 10.1371/journal.pone.0140578

Fortunato, C. S., Herfort, L., Zuber, P., Baptista, A. M., and Crump, B. C. (2012). Spatial variability overwhelms seasonal patterns in bacterioplankton communities across a river to ocean gradient. *ISME J.* 6, 554–563. doi: 10.1038/ismej.2011.135

Frossard, A., Gerull, L., Mutz, M., and Gessner, M. O. (2012). Disconnect of microbial structure and function: enzyme activities and bacterial communities in nascent stream corridors. *ISME J.* 6, 680–691. doi: 10.1038/ismej.2011.134

Hoppe, H. G. (1983). Significance of exoenzymatic activities in the ecology of brackish water-measurements by means of methylumbelliferyl-substrates. *Mar. Ecol. Prog. Ser.* 11, 299–308. doi: 10.3354/meps011299

Hoppe, H. G., Arnosti, C., and Herndl, G. J. (2002). *Ecological Significance of Bacterial Enzymes in the Marine Environment*. New York, NY: Marcel Dekker.

Hoppe, H. G., Kim, S. J., and Gocke, K. (1988). Microbial decomposition in aquatic environments: combined process of extracellular enzyme activity and substrate uptake. *Appl. Environ. Microbiol.* 54, 784–790.

Kirchman, D. (2001). Measuring bacterial biomass production and growth rates from leucine incorporation in natural aquatic environments. *Methods Microbiol.* 30, 227–238. doi: 10.1016/S0580-9517(01)30047-8

Lin, J., Xie, L., Pietrafesa, L. J., Ramus, J. S., and Paerl, H. W. (2007). Water quality gradients across Albemarle-Pamlico estuarine system: seasonal variations and model applications. *J. Coastal Res.* 23, 213–229. doi: 10.2112/05-0507.1

McCallister, S., Bauer, J. E., and Canuel, E. A. (2006). Bioreactivity of estuarine dissolved organic matter: a combined geochemical and microbiological approach. *Limnol. Oceanogr.* 51, 94–100. doi: 10.4319/lo.2006.51.1.0094

Millar, J. J., Payne, J. T., Ochs, C. A., and Jackson, C. R. (2015). Particle-associated and cell-free extracellular enzyme activity in relation to nutrient status of large tributaries of the lower mississippi River. *Biogeochemistry* 124:255. doi: 10.1007/s10533-015-0096-1

O'Driscoll, M., Johnson, P., and Mallinson, D. (2010). Geological controls and effects of floodplain asymmetry on river-groundwater interactions in the southeastern coastal Plain, USA. *Hydrogeol. J.* 18, 1265–1279. doi: 10.1007/s10040-010-0595-z

Overton, A. S., Jones, N. A., and Rulifson, R. (2012). Spatial and temporal variability in instantaneous growth, mortality, and recruitment of Larval River Herring in Tar–Pamlico River, North Carolina. *Mar. Coastal Fish.* 4, 218–227. doi: 10.1080/19425120.2012.675976

Paerl, H. W., Pinckney, J. L., Fear, J. M., and Peierls, B. L. (1998). Ecosystem responses to internal and watershed organic matter loading: consequences for hypoxia in the eutrophying Neuse River Estuary, North Carolina, USA. *Mar. Ecol. Prog. Ser.* 166:17. doi: 10.3354/meps166017

Paerl, H. W., Rossignol, K. L., Hall, S. N., Peierls, B. L., and Wetz, M. S. (2010). Phytoplankton community indicators of short-and long-term ecological change in the anthropogenically and climatically impacted Neuse River Estuary, North Carolina, USA. *Estuar. Coasts* 33, 485–497. doi: 10.1007/s12237-009-9137-0

Peng, M., Xie, L., and Pietrafesa, L. (2004). A numerical study of storm surge and inundation in the croatan-albemarle-pamlico estuary system. *Estuar. Coastal Shelf Sci.* 59, 121–137. doi: 10.1016/j.ecss.2003.07.010

Porter, K. G., and Feig, Y. S. (1980). Use of DAPI for identifying and counting aquatic microflora. *Limnol. Oceanogr.* 25, 943–948.

R Core Team (2014). *R: A Language and Environment for Statistical Computing*. Vienna: R Foundation for Statistical Computing.

Reed, R., Dickey, D., Burkholder, J., Kinder, C., and Brownie, C. (2008). Water level variations in the Neuse and Pamlico Estuaries, North Carolina due to local and remote forcing. *Estuar. Coastal Shelf Sci.* 76, 431–446. doi: 10.1016/j.ecss.2007.05.049

Rier, S. T., Nawrocki, K. S., and Whitley, J. C. (2011). Response of biofilm extracellular enzymes along a stream nutrient enrichment gradient in an agricultural region of north central Pennsylvania, USA. *Hydrobiologia* 669, 119–131. doi: 10.1007/s10750-011-0654-z

Sieczko, A., Maschek, M., and Peduzzi, P. (2015). Algal extracellular release in river-floodplain dissolved organic matter: response of extracellular enzymatic activities during a post-flood period. *Front. Microbiol.* 6:80. doi: 10.3389/fmicb.2015.00080

Singh, S., Inamdar, S., Mitchell, M., and McHale, P. (2013). Seasonal pattern of dissolved organic matter (DOM) in watershed sources: influence of hydrologic flow paths and autumn leaf fall. *Biogeochemistry* 118, 321–337. doi: 10.1007/s10533-013-9934-1

Sinsabaugh, R. L., and Moorhead, D. L. (1994). Resource allocation to extracellular enzyme production: a model for nitrogen and phosphorus control of litter decomposition. *Soil Biol. Biochem.* 26, 1305–1311. doi: 10.1016/0038-0717(94)90211-9

Spencer, R. G., Butler, K. D., and Aiken, G. R. (2012). Dissolved organic carbon and chromophoric dissolved organic matter properties of rivers in the USA. *J. Geophys. Res. Biogeosci.* 117:G03001. doi: 10.1029/2011JG001928

Steen, A. D., and Arnosti, C. (2014). Picky, hungry eaters in the cold: persistent substrate selectivity among polar pelagic microbial communities. *Front. Microbiol.* 5:527. doi: 10.3389/fmicb.2014.00527

Steen, A. D., Hamdan, L. J., and Arnosti, C. (2008). Dynamics of dissolved carbohydrates in the Chesapeake Bay: insights from enzyme activities, concentrations, and microbial metabolism". *Limnol. Oceanogr.* 53, 936–947. doi: 10.4319/lo.2008.53.3.0936

Steen, A. D., Ziervogel, K., Ghobrial, S., and Arnosti, C. (2012). Functional variation among polysaccharide-hydrolyzing communities in the Gulf of Mexico. *Mar. Chem*. 138, 13–20. doi: 10.1016/j.marchem.2012.06.001

Stow, C. A., Borsuk, M. E., and Stanley, D. W. (2001). Long-term changes in watershed nutrient inputs and riverine exports in the Neuse River, North Carolina. *Water Res.* 35, 1489–1499. doi: 10.1016/S0043-1354(00)00402-4

Tiquia, S. M. (2011). Extracellular hydrolytic enzyme activities of the heterotrophic microbial communities of the Rouge river: an approach to evaluate ecosystem response to urbanization. *Microb. Ecol*. 62, 679–689. doi: 10.1007/s00248-011-9871-2

Vrba, J., Callieri, C., Bittl, T., Šimek, K., Bertoni, R., Filandr, P., and Nedoma, J. (2004). Are bacteria the major producers of extracellular glycolytic enzymes in aquatic environments?. *Int. Rev. Hydrobiol*. 89, 102–117. doi: 10.1002/iroh.200310673

Wegner, C.-E., Richter-Heitmann, T., Klindworth, A., Klockow, C., Richter, M., Achstetter, T., et al. (2013). Expression of sulfatases in *Rhodopirellula baltica* and the diversity of sulfatases in the genus Rhodopirellula. *Mar. Genomics* 9, 51–61. doi: 10.1016/j.margen.2012.12.001

Wilczek, S., Fischer, H., and Pusch, M. T. (2005). Regulation and seasonal dynamics of extracellular enzyme activities in the sediments of a large lowland river. *Microb. Ecol.* 50, 253–267. doi: 10.1007/s00248-004-0119-2

Williams, C. J., Scott, A. B., Wilson, H. F., and Xenopoulos, M. A. (2012). Effects of land use on water column bacterial activity and enzyme stoichiometry in stream ecosystems. *Aquat. Sci.* 74, 483–494. doi: 10.1007/s00027-011-0242-3

Williams, C. J., and Jochem, F. J. (2006). Ectoenzyme kinetics in Florida Bay: implications for bacterial carbon source and nutrient status. *Hydrobiology* 569, 113–127. doi: 10.1007/s10750-006-0126-z

Xing, P., Hahnke, R. L., Unfried, F., Markert, S., Hugang, S., Barbeyron, T., et al. (2014). Niches of two polysaccharide-degrading Polaribacter isolates from the North Sea during a spring diatom bloom. *ISME J.* 9, 1410–1422. doi: 10.1038/ismej.2014.225

Ziervogel, K., and Arnosti, C. (2009). Enzyme activities in the Delaware estuary affected by elevated suspended sediment load. *Estuar. Coastal Shelf Sci*. 84, 253–258. doi: 10.1016/j.ecss.2009.06.022

Ziervogel, K., Leech, D., and Arnosti, C. (2014). Differences in the substrate spectrum of extracellular enzymes in shallow lakes of differing trophic status. *Biogeochemistry* 117, 143–151. doi: 10.1007/s10533-013-9874-9

Zimmerman, A. E., Martiny, A. C., and Allison, S. D. (2013). Microdiversity of extracellular enzyme genes among sequenced prokaryotic genomes. *ISME J.* 7, 1187–1199. doi: 10.1038/ismej.2012.176

Conflict of Interest Statement: The authors declare that the research was conducted in the absence of any commercial or financial relationships that could be construed as a potential conflict of interest.

frontiers in Microbiology

ORIGINAL RESEARCH
published: 09 March 2017
doi: 10.3389/fmicb.2017.00351

The Effect of Increased Loads of Dissolved Organic Matter on Estuarine Microbial Community Composition and Function

*Sachia J. Traving[1], Owen Rowe[2,3†], Nina M. Jakobsen[4], Helle Sørensen[4], Julie Dinasquet[5†], Colin A. Stedmon[6], Agneta Andersson[2,3] and Lasse Riemann[1,5]**

[1] Centre for Ocean Life, Marine Biological Section, University of Copenhagen, Helsingør, Denmark, [2] Umeå Marine Sciences Centre, Umeå University, Hörnefors, Sweden, [3] Department of Ecology and Environmental Science, Umeå University, Umeå, Sweden, [4] Laboratory for Applied Statistics, Department of Mathematical Sciences, University of Copenhagen, Copenhagen, Denmark, [5] Marine Biological Section, University of Copenhagen, Helsingør, Denmark, [6] Centre for Ocean Life, National Institute of Aquatic Resources, Technical University of Denmark, Charlottenlund, Denmark

Increased river loads are projected as one of the major consequences of climate change in the northern hemisphere, leading to elevated inputs of riverine dissolved organic matter (DOM) and inorganic nutrients to coastal ecosystems. The objective of this study was to investigate the effects of elevated DOM on a coastal pelagic food web from the coastal northern Baltic Sea, in a 32-day mesocosm experiment. In particular, the study addresses the response of bacterioplankton to differences in character and composition of supplied DOM. The supplied DOM differed in stoichiometry and quality and had pronounced effects on the recipient bacterioplankton, driving compositional changes in response to DOM type. The shifts in bacterioplankton community composition were especially driven by the proliferation of Bacteroidetes, Gemmatimonadetes, Planctomycetes, and Alpha- and Betaproteobacteria populations. The DOM additions stimulated protease activity and a release of inorganic nutrients, suggesting that DOM was actively processed. However, no difference between DOM types was detected in these functions despite different community compositions. Extensive release of re-mineralized carbon, nitrogen and phosphorus was associated with the bacterial processing, corresponding to 25–85% of the supplied DOM. The DOM additions had a negative effect on phytoplankton with decreased Chl *a* and biomass, particularly during the first half of the experiment. However, the accumulating nutrients likely stimulated phytoplankton biomass which was observed to increase towards the end of the experiment. This suggests that the nutrient access partially outweighed the negative effect of increased light attenuation by accumulating DOM. Taken together, our experimental data suggest that parts of the future elevated riverine DOM supply to the Baltic Sea will be efficiently mineralized by microbes. This will have consequences for bacterioplankton and phytoplankton community composition and function, and significantly affect nutrient biogeochemistry.

Keywords: bacterioplankton community composition, community functions, extracellular enzymes, 16S rRNA, climate change, dissolved organic matter, generalized linear models, Baltic Sea

OPEN ACCESS

Edited by:
Anna M. Romaní, University of Girona, Spain

Reviewed by:
Hans-Peter Grossart, Leibniz Institute of Freshwater Ecology and Inland Fisheries, Germany
Guang Gao, Nanjing Institute of Geography and Limnology (CAS), China

****Correspondence:***
Lasse Riemann
lriemann@bio.ku.dk

†Present address:
Owen Rowe, Department of Food and Environmental Sciences, University of Helsinki, Helsinki, Finland;
Julie Dinasquet, Laboratoire d'Océanographie Microbienne, Observatoire de Banyuls sur mer, Banyuls sur mer, France

Specialty section:
This article was submitted to Aquatic Microbiology, a section of the journal Frontiers in Microbiology

Received: *24 November 2016*
Accepted: *20 February 2017*
Published: *09 March 2017*

Citation:
Traving SJ, Rowe O, Jakobsen NM, Sørensen H, Dinasquet J, Stedmon CA, Andersson A and Riemann L (2017) The Effect of Increased Loads of Dissolved Organic Matter on Estuarine Microbial Community Composition and Function. Front. Microbiol. 8:351. doi: 10.3389/fmicb.2017.00351

INTRODUCTION

Climate change is projected to increase precipitation in the northern hemisphere, by as much as 30% in the Baltic region (Andersson et al., 2015). This will lead to a 15–20% increase in freshwater runoff (Meier et al., 2012) and parallel increases in loadings of riverine dissolved organic matter (DOM) and nutrients to coastal systems. The input of DOM and nutrients will conceivably affect the composition, function and activity of the recipient microbial communities and thereby impact the entire ecosystem (Sandberg et al., 2004; Wikner and Andersson, 2012). The elevated riverine DOM supply will likely increase bacterial respiration, as humic material is typically carbon rich and fuels bacterial respiration (Benner, 2003; Fasching et al., 2014). In coastal systems riverine DOM may support a significant fraction of bacterioplankton activity, thereby decoupling the activity of heterotrophic bacteria from phytoplankton production (Kemp et al., 1997; Sandberg et al., 2004; Wikner and Andersson, 2012; Figueroa et al., 2016). Moreover, an increased allochthonous carbon load supporting bacterial activity may lead to increased competition for inorganic nutrients between bacteria and phytoplankton (Thingstad et al., 2008; Wikner and Andersson, 2012), which may further weaken the link between phytoplankton production and bacterial activity and expand zones of net heterotrophy.

Bacterial communities are tightly coupled to the concentration and composition of DOM, with shifts in DOM composition inducing changes in bacterial community composition and functionality (e.g., Gasol et al., 2002; Kritzberg et al., 2004; Judd et al., 2006; Alonso-Sáez and Gasol, 2007). Therefore, the concentration and characteristics of riverine DOM may be important for the ultimate fate of this additional organic matter, such as the partitioning between local remineralization, passage through the food web or export to adjacent shelf seas. In addition, the increases in DOM will likely lead to "brownification" of the recipient waters and increased light attenuation due to higher concentrations of humic substances in DOM (Roulet and Moore, 2006), which is commonly observed in coastal regions (Sanden and Håkansson, 1996; Aksnes and Ohman, 2009; Frigstad et al., 2013). This may affect phytoplankton biomass and productivity ultimately leading to carbon limitation of bacterioplankton growth (Thingstad et al., 2008).

The Baltic Sea consists of basins characterized by distinct hydrology and differing land usage. The consequences of climate change are therefore expected to vary regionally (Rönnberg and Bonsdorff, 2004). The north receives large inputs of riverine DOM rich in humic substances (Andersson et al., 2015), while the south receives a comparatively nutrient rich riverine DOM inflow (Stepanauskas et al., 2002). The riverine loadings differ significantly in C:N:P stoichiometry depending on region and can potentially have very different effects on the recipient ecosystem. However, it remains unclear how the character and concentration of DOM supplied by rivers will influence the bacterioplankton and thereby the fate of carbon and nutrients in the system.

The objective of this study was to experimentally investigate the effects of elevated DOM on a recipient coastal microbial community and examine the impact on functional activity and population structures. Specifically, we focused on the response of the microbial community to differences in DOM characteristics.

MATERIALS AND METHODS

Collection Site and Mesocosm Setup

The experiment was performed from May 21–June 25 2012 at Umeå Marine Sciences Centre (UMF), Sweden, in 12 indoor mesocosm tanks of 4.87 m height (water column) and a diameter of 0.76 m. The water was collected on May 21 and 22 from a regularly sampled station in the Bothnian Sea (63°32′05.2″ N 19°56′09.6″ E) at 4 m depth, using a rotating pump (Flygt DS 3057.181 MT-230), with a 1.5 mm mesh pre-filter. The salinity of the water was 3.8 (Seaguard CTD, Aanderaa) and *in situ* temperature was 6°C. The water was transported in 1 m^3 polythene containers to the field station and thereafter carefully pumped into the mesocosms, ensuring an equal distribution of the water between tanks. All mesocosms received inorganic nutrients on May 21, at concentrations of 0.7 μmol l^{-1} nitrogen and 0.09 μmol l^{-1} phosphorus, to prevent nutrient exhausting during a 4 days acclimation period. During this period the temperature was incrementally increased to 15°C. To prevent stratification, a constant and gentle bubbling was applied at 0.6 m depth and convective stirring was generated by maintaining the upper section of each mesocosm tank at 14.8°C, the middle section at 15.0°C, and the lower section at 15.2°C, the latter supported by a 250 W electrical heater. Light was provided on a 12 h light:dark cycle, using 150 W halogen lamps (MASTERColour CDM-T 150W/942 G12 1CT. Phillips©), yielding a photosynthetically active radiation (PAR) light level of ∼400 μmol photons m^{-2} s^{-1} immediately below the surface.

Treatments

The 12 mesocosm tanks received one of four treatments, each replicated in triplicate. Two treatments (North and South) received additions of soil extracted DOM (**Table 1**), prepared from soil samples collected along the riverbanks of two contrasting rivers that discharge into the Baltic Sea. The North treatment was collected from the Öre river in northern Sweden (63°32′40.7″ N 19°42′35.6″ E), the catchment area of this river being predominantly characterized by coniferous and deciduous forest. The South treatment was collected from the riverbanks

TABLE 1 | Daily supplements in carbon (C), nitrogen (N), and phosphorus (P) to the mesocosms after addition of soil extracted dissolved organic matter.

Treatment	C μmol l^{-1}	N μmol l^{-1}	P μmol l^{-1}
North	10 (83)	1.1 (8.8)	0.03 (0.2)
South	20 (166)	2.3 (20)	0.13 (1.1)
$Ctrl_N$	–	0.001 (0.01)	0.0008 (0.007)
$Ctrl_S$	–	0.009 (0.08)	0.005 (0.04)

In parentheses, the increase after the initial ∼22% addition; Section "Materials and Methods." $Ctrl_N$ and $Ctrl_S$ received inorganic N and P in the stoichiometry and concentrations supplied with the DOM in the North and South treatments.

of the Reda river, Poland (54°38′35.80″ N, 18°27′41.28″ E), with a catchment area characterized by agricultural activities and some broad-leaf forest. Soil extracts were prepared and stored according to the procedure described in Lefebure et al. (2013). In brief, soil extracts were mixed with Milli-Q water and ion exchange resin (Amberlite IRC 7481) for 48 h at 4°C, and then filtered through a 90 μm mesh. The carbon (C), nitrogen (N), and phosphorus (P) content of the extracts were determined using a Shimadzu TOC-5000 carbon analyzer and a Braan and Luebbe TRAACS 800 autoanalyzer. The experiment was designed to simulate future predictions of increased riverine DOM load to the Baltic (Eriksson Hägg et al., 2010). The DOM treatments aimed to increase dissolved organic carbon (DOC) in the water with roughly 50% (North) and 100% (South) relative to the DOC concentration (∼333 μmol l^{-1}) in the Bothnian Sea. Two additional treatments were set up as controls for the DOM addition, receiving only inorganic N and P (**Table 1**), corresponding to the inorganic N and P concentrations in the North and South, from here on referred to as "$Ctrl_N$" and "$Ctrl_S$," respectively.

Three days prior to first sampling DOM treatments received an initial large DOM addition, corresponding to ∼22% of the total amount of DOC added during the experiment, and this was then followed by smaller daily doses (**Table 1**). Control treatments also received corresponding N:P additions. The experiment had a duration of 32 days and sampling was initiated on May the 28th by the addition of seven equally sized young-of-the-year perch (*Perca fluviatilis*) to each mesocosm. The fish were added in order to complete a pelagic food web, encompassing bacteria to zooplanktivorous fish. Every second day 40 l of water from 2 m depth was removed, and replaced with 40 l of 0.2 μm filtered Bothnian Sea water pumped into the marine research station from a point ∼2 km offshore (63°33′15.6″ N 19°50′08.4″ E). Samples were collected on days: 0, 3, 7, 10, 14, 17, 21, 24, and 28. The majority of parameters were sampled/processed on all days and extracellular enzymes were measured on two additional occasions, days 5 and 12.

Water Chemistry, Phytoplankton Biomass, and Community Composition

Colored dissolved organic matter (CDOM) samples were filtered through pre-combusted Whatman® GF/F filters, and the filtrate was immediately frozen at −20°C until further processing. Samples were measured within 2 months of the experiment on a Horiba Scientific Aqualog according to Murphy et al. (2011). CDOM absorption properties were characterized by calculating the spectral slope across 300–650 nm (Stedmon et al., 2000). Samples for inorganic nutrients and DOC were filtered through 0.22 μm cellulose-acetate filters (Gelman Supor®) and immediately measured. Inorganic nutrients (NH_4^+, NO_3^-, NO_2^-, and PO_4^{3-}) were measured in whole water samples using continuous flow analysis on a Quaatro system (Seal Analytical), following methods outlined in Grasshoff et al. (1983) and Helcom guidelines (HELCOM, 2014). Samples for measurement of total dissolved nitrogen (TDN), total dissolved phosphorus (TDP), and DOC were filtered through 0.2 μm Acrodisk (Supor®) filters (Pall Corporation). TDN and TDP samples were subjected to oxidative digestion using the peroxodisulfate/boric acid system (Koroleff, 1983), and then analyzed using the same method as for nitrate and phosphate. DOC was approximated as Non Purgeable Organic Carbon and analyzed using high temperature catalytic oxidation followed by non-dispersive infrared sensor detection of the gaseous CO_2. The instrument used was a Shimadzu TOC-L Total Organic Carbon Analyzer (Shimadzu Corporation). Dissolved organic nitrogen (DON) was calculated by subtracting NH_4^+, NO_3^-, NO_2^- from TDN, and total dissolved phosphorus (DOP) was calculated by subtracting PO_4^{3-} from TDP.

Chlorophyll *a* (Chl *a*) and phytoplankton community composition were measured as detailed in Lefebure et al. (2013). In brief, Chl *a* samples were filtered onto Whatman® GF/F filters (100 ml in duplicates), extracted in 95% ethanol for 24 h in the dark, and measured on a Perkin Elmer LS 30 fluorometer. Samples for phytoplankton community composition were preserved in Lugol's solution and later counted using microscopy and converted to biomass (μg C l^{-1}) using carbon conversion (Menden-Deuer and Lessard, 2000).

Bacterial Functions

Bacterial production was assayed using ^{3}H-thymidine incorporation (Fuhrman and Azam, 1982). Samples were incubated with thymidine (final concentration of 24 nM, and an activity of 84.4 Ci $mmol^{-1}$) at 15°C for ∼1 h, and analyzed using a Beckman 6500 scintillation counter. Bacterial production was estimated using a conversion factor of 1.4×10^{18} cells μmol^{-1} thymidine (Wikner and Hagström, 1999) and 20.4 fg C $cell^{-1}$ (Lee and Fuhrman, 1987). Samples for bacterial abundance were preserved in a 4% final concentration of formaldehyde, stained with acridine orange, and enumerated using an epifluorescence microscope (Zeiss Axiovert 100, Thornwood, NY, USA) and image analysis (Blackburn et al., 1998).

Extracellular enzyme activities were assayed using fluorogenic 4-methylumbelliferone (MUF) and 7-amino-4-methylcoumarin (MCA) substrates (Sigma-Aldrich, St. Louis, MO, USA). The enzyme assays were prepared according to Hoppe (1983), modified to a reaction volume of 200 μl with 400 μM substrate (final concentration). The enzymes assayed and substrates used were: protease (L-Leucine-MCA), alkaline phosphatase (MUF-phosphate disodium salt), β-NAGase (MUF-*N*-acetyl-β-D-glucosaminide), lipase (MUF-oleate) and α- and β-glucosidases (MUF-α-D-glycopyranoside and MUF-β-D-glycopyranoside. respectively). Assays were measured in triplicates at 355 nm excitation and 460 nm emission on a FLUOstar OPTIMA plate reader (BMG, Labtech GmbH, Ortenberg, Germany). Assays were incubated at 15°C in the dark and followed for 5 h.

Bacterial Community – Extraction of Nucleic Acids and 16S rRNA Amplicon Sequencing

Samples (500 ml) for DNA and RNA extraction were filtered onto separate 0.22 μm cellulose-acetate filters (Gelman Supor®), except for the South treatment which clogged at 300 ml. DNA

filters were stored in 1 ml Tris-EDTA buffer (VWR, Radnor, PA, USA) at −20°C, while RNA filters were covered with 1 ml RNA*later*® (Ambion®, Life Technologies, Carlsbad, CA, USA), flash frozen in liquid nitrogen, and stored at −80°C until further processing. Extractions of DNA and RNA were done using the E.Z.N.A® Tissue DNA kit (OMEGA biotek, USA) and PowerWater® RNA isolation kit (MO BIO Laboratories, Inc., USA), respectively. Synthesis of cDNA was done according to Bentzon-Tilia et al. (2015) using TaqMan reverse-transcription reagents (Applied Biosystems, Foster City, CA, USA) and the 806r primer listed below. 16S ribosomal RNA (cDNA) and DNA amplicons of the V4 region of bacterial and archaeal communities were obtained using the primers 515f (5′-126 GTGCCAGCMGCCGCGGTAA) and 806r (5′-GGACTACHVGGGTWTCTAAT) (Caporaso et al., 2012). Polymerase chain reactions (PCRs) were performed in 25 μl reaction volume containing 1 (DNA) and 10 (cDNA) ng template, primers, MyTaq DNA polymerase reagents (Saveen & Verner AB, Limhamn, Sweden), 0.07 nmol BSA (Sigma-Aldrich, St. Louis, MO, USA) and 2 nmol $MgCl_2$ (DNA Diagnostic, Risskov, Denmark). The PCR conditions included an initial denaturing step at 94°C for 3 min followed by 29 cycles of 94°C for 45 s, 50°C for 1 min, 72°C for 1 min 30 s, and a final step of elongation at 72°C for 10 min. Triplicate PCR reactions were pooled for each sample, purified using the Agencourt AMPure XP purification kit (Beckman Coulter, Inc., Brea, CA, USA), and quantified using the Quant-iT^{TM} PicoGreen® quantification kit (Invitrogen, Waltham, MA, USA) and a FLUOstar OPTIMA plate reader (BMG Labtech GmbH, Ortenberg, Germany). PCR amplicons were pooled at equimolar concentrations and submitted for commercial paired-end sequencing on an Illumina MiSeq.

Sequence reads were assembled, trimmed to a mean length of 252 nucleotides, and de-multiplexed using QIIME v1.9 (Caporaso et al., 2010). Removal of singletons and clustering of operational taxonomic units (OTUs) at 97% similarity was done in USEARCH v1.8 (Edgar, 2010) using the UPARSE-OTU algorithm (Edgar, 2013) with implicit chimera check. Taxonomy was assigned in QIIME using uclust (Edgar, 2010) and the Greengenes v.13.8 reference database (McDonald et al., 2012). Chloroplasts and mitochondrial reads were removed before downstream analysis. OTUs only occurring once in the dataset and/or including < 10 reads in total were excluded. Henceforth, 16S rRNA and rRNA gene amplicons are referred to as rRNA and rDNA, respectively. Sequences were deposited in GenBank NCBI (accession numbers KX178204-KX179464). In the rRNA dataset three samples were lost during processing – (day, tank): (21, 4), (17, 5), (28, 10).

Data Analysis

All data and statistical analyses were carried out in R (R Core Team, 2016) using the R packages mvabund v. 3.11.7 (Wang et al., 2012), pgirmess v. 1.6.4 (Giraudoux, 2016), FactoMineR v. 1.31.4 (Husson et al., 2015), and vegan v. 2.3-2 (Oksanen et al., 2015). For testing differences between treatments, linear mixed models were used; with day, treatment, and their interaction as fixed effects and mesocosm tank as a random effect. Data were log-transformed if appropriate. The average outcome over time was compared for North and $Ctrl_N$, South and $Ctrl_S$, and for North and South. A total of 45 tests were carried out, and the *p*-values were Bonferroni–Holm adjusted in order to ensure a family wise error rate of at most 5%. Patterns of bacterial community compositions were analyzed using Bray–Curtis distances and visualized by non-metric multidimensional scaling (NMDS). Specifically for the NMDS and descriptions of relative composition of communities, samples were subsampled to a depth of 2280 reads per sample to accommodate for the smallest sample in the set.

Generalized linear models (GLM) were applied to identify the OTUs contributing most to the differences between the four treatments at the beginning (day 0) and end (day 28) of the experiment. The aim of the GLM approach described here is similar to that of the SIMilarity PERcentages analysis (SIMPER, Clarke, 1993), but also takes the mean-variance relationship in the rDNA and rRNA data, into account (Warton et al., 2012). For this analysis, datasets were filtered to include only OTUs with a relative abundance > 1% in at least one observation, leaving 87 and 95 OTUs in the rDNA and rRNA datasets, respectively. For each of these OTUs, and separately for days 0 and 28, univariate negative binomial regression models were fitted with abundance as the response variable. In each model, treatment was included as an explanatory variable while the logarithm of the total abundance of OTUs in each observation was included as an offset variable, in order to take into account the varying sample sizes. The models were fitted using a log link function and assuming an unknown over-dispersion parameter in each model, which was estimated from the data. Likelihood ratio (LR) test statistics for the hypothesis of no treatment effect were computed for each of the univariate models. Corresponding *p*-values adjusted for the multiple tests performed within the rDNA and rRNA datasets, respectively, for each of the days 0 and 28, were computed by means of a step-down resampling procedure using residual permutation (as implemented in Wang et al., 2012). These *p*-values were further adjusted by multiplication with a factor four (a Bonferroni-type correction) to ensure a family-wise error rate of <5% among all tests pertaining to the GLM models. OTUs with the largest LR test statistics are interpreted as the OTUs that exhibit the most notable difference in relative abundance between treatments. For an adjusted *p*-value of less than 0.05, the difference between treatments is considered statistically significant.

RESULTS

DOM and Nutrients

Dissolved organic carbon increased significantly during the experiment (**Figure 1A**) in both North and South compared to their controls (adjusted $p << 0.0001$) and also differed between North and South (adjusted $p < 0.002$). However, the increase was less than expected based on the added DOC (**Figure 1A**). The total amount of DOC removed corresponded to 25 and 37% of the added DOC in the North and South treatments, respectively (**Figure 1B**), calculated as the difference between added and measured DOC. In comparison, 12 and 13% of the

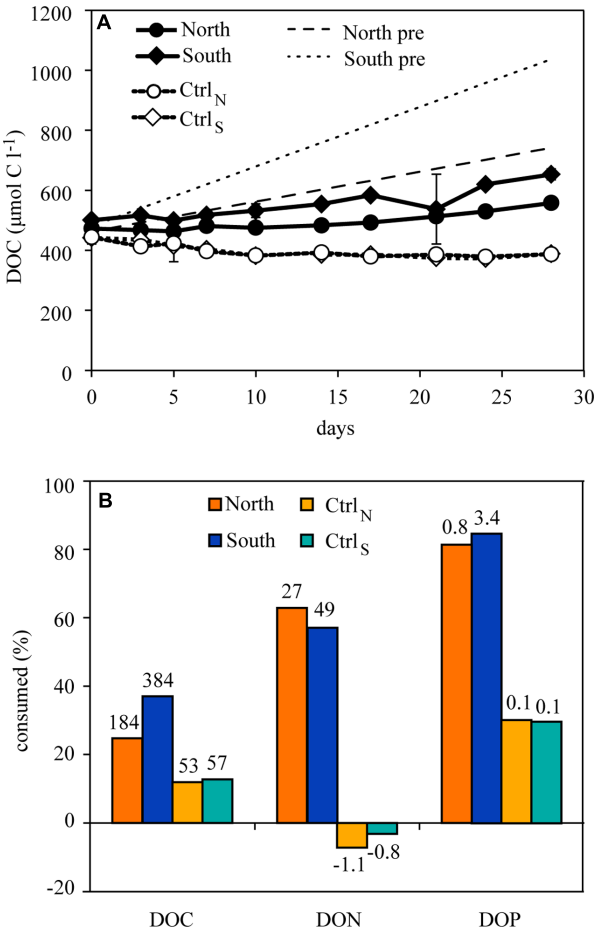

FIGURE 1 | (A) Concentrations of dissolved organic carbon (DOC) over time in the four treatments. The dotted lines ("North pre" and "South pre") represent predictions of accumulated DOC calculated from the respective DOM additions assuming no biological consumption, in North and South, respectively. Error bars represent standard deviations ($n = 3$). **(B)** The stoichiometry of the consumed DOM in the treatments. In the DOM treatments, consumption of DOC is calculated as % difference between the predicted DOC accumulation and measured DOC concentrations, and in the controls the consumption is calculated as the difference between measured start and end concentrations. Consumption of dissolved organic nitrogen (DON) and phosphorus (DOP) was calculated as for DOC. Values above each bar are the consumed concentrations (µmol l^{-1}).

DOC was removed in the $Ctrl_N$ and $Ctrl_S$, respectively (calculated as the difference between measured DOC at start and end). For DON and DOP, the communities in both treatments appeared to effectively mineralize a large fraction. In the North treatment 63 and 81% of the added DON and DOP, respectively, was removed and similar high removal was observed in the South treatment (57 and 85% DON and DOP, respectively), despite the higher DOM additions in South. Small amounts of DON accumulated in $Ctrl_N$ and $Ctrl_S$, corresponding to 7 and 3%, respectively, while 30% of the DOP was removed. The C:N:P stoichiometry of the removed DOM was 239:36:1 and 114:15:1 for North and South, respectively. This corresponded roughly to the stoichiometry of the added DOM, 387:41:1 for North and 156:18:1 in South.

Inorganic nutrients were also affected by the DOM additions, which caused significantly higher concentration of NH_4^+ (adjusted $p < 0.02$), NO_3^- (adjusted $p < 0.001$), total N (adjusted $p << 0.0001$), and total P (adjusted $p << 0.0001$) in North and South, when compared to their respective controls (**Figure 2**). In addition, NO_2^- (adjusted $p < 0.001$) and PO_4^{3-} (adjusted $p < 0.0001$) were also significantly higher in South compared to $Ctrl_S$, an effect not detected in the North treatment. Between North and South PO_4^{3-}, total N and P (adjusted $p < 0.0001$) were significantly different.

The CDOM slope (S) for the UVA-visible wavelength range (300–650 nm) was used as an indicator of differences in DOM quality between treatments. The UVA-visible range was used due to the direct link between organic matter and light attenuation. Other CDOM parameters measured behaved as expected based on the S values, e.g., short wavelength slopes correlated positively with S, and SUVA was inversely correlated to S. Hence, these were not included in further analyses. For both DOM treatments the slopes decreased with time while the controls showed little systematic change and no noteworthy differences. The DOM additions resulted in lower S values with the lowest values in South (**Figure 3A**). The increases in CDOM absorption over time in the DOM treatments resulted in decreasing PAR levels at 1 m depth during the experiment (**Figure 3B**).

Phyto-and protozooplankton Biomass and Community Composition

Concentrations of Chl *a* and phytoplankton biomass decreased over time in all treatments accompanied by shifts in phytoplankton community composition (**Figures 4**, **5**). Initially diatoms, chlorophytes and ciliates made up the majority of the community in all treatments. On day 17, $Ctrl_N$ and $Ctrl_S$ were dominated by cyanobacteria whereas North and South were dominated by cryptophytes, prasinophytes and a group of unidentified flagellates. On day 28, total biomass had increased again being highest in North and South treatments with diatoms, chlorophytes and prasinophytes being the dominant groups, whereas chrysophytes, prymnesiophytes, and cyanobacteria dominated in the control treatments.

Bacterial Response to DOM Additions

Patterns of bacterial abundance and production followed similar trends in the four treatments (**Figure 6**), with no significant differences in the bacterial abundance or production between DOM treatments, and compared to their respective controls.

Extracellular enzyme activities responded to DOM additions, but only protease had significantly higher activity (adjusted $p < 0.0002$), in North and South, compared to their controls (**Figure 7**). Furthermore, protease activity was not significantly different between North and South.

Shifts in Bacterial Community Composition

A total of 1,866,318 high quality reads remained after quality and chimera check, with 1,637 reads assigned to *Archaea*.

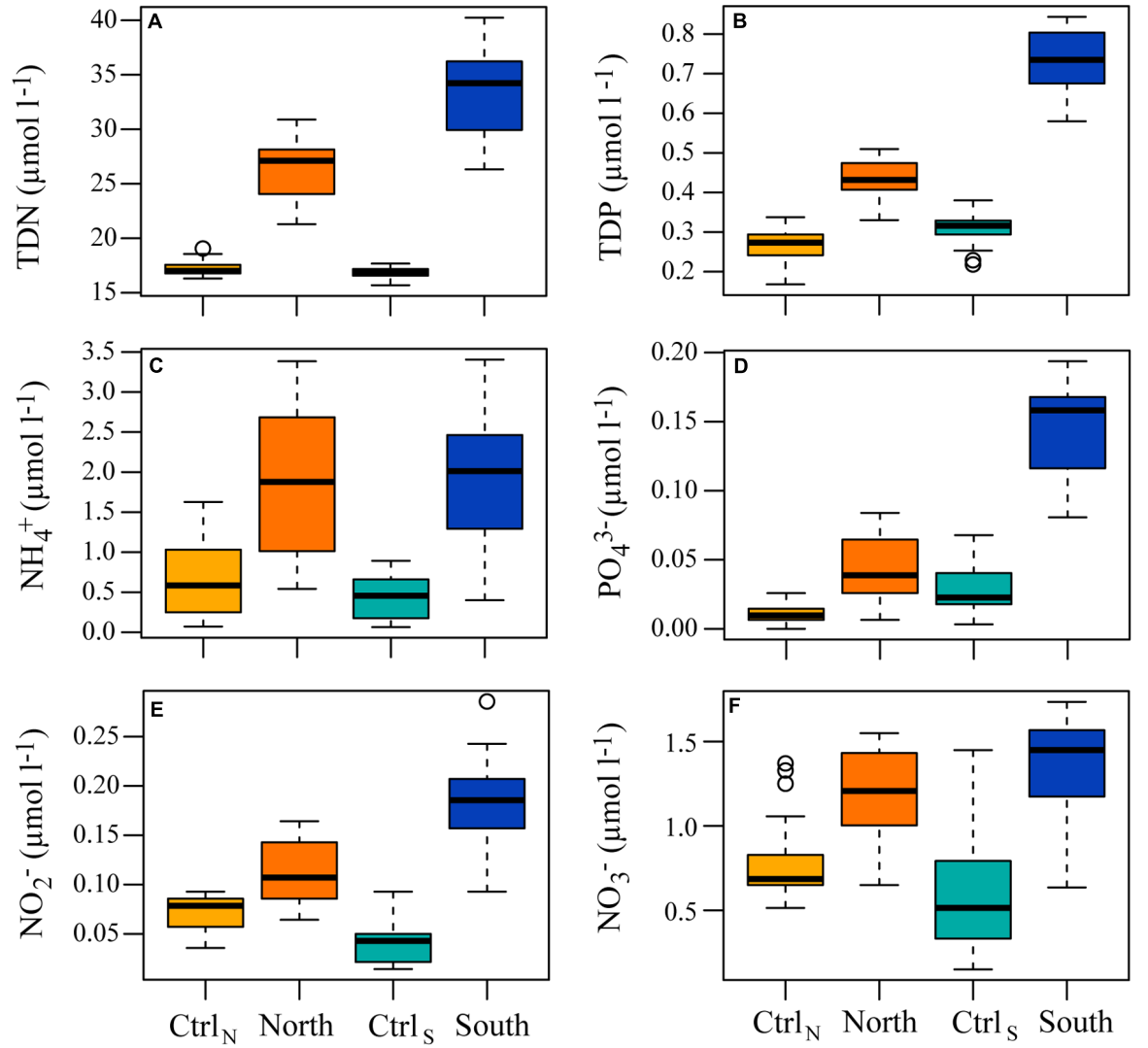

FIGURE 2 | Box and whisker plots indicating the median concentrations for the whole experiment, with the lower 25th and upper 75th percentile, of total dissolved (A) nitrogen (TDN), **(B)** phosphorus (TDP), **(C)** NH_4^+, **(D)** PO_4^{3-}, **(E)** NO_2^-, and **(F)** NO_3^- in the four treatments.

Clustering at 97% similarity resulted in a total of 1,261 OTUs. The composition in the total community (rDNA) changed in response to treatment and time, becoming more dissimilar over time and resulting in North and South communities shifting apart from each other, and from the two controls (**Figure 8A**). A similar shift in composition was observed in the active community (**Figure 8B**).

To further investigate the observed relative changes in community composition, a GLM analysis was applied to identify the OTUs for which relative abundance differed between the four treatments. This was done for the beginning (day 0) and the end (day 28) of the experiment. The OTUs with the most notable and significant differences between treatments, as indicated by the size of their LR test statistics and adjusted *p*-values, are reported together with their relative abundances (**Table 2** and **Figure 9**). At day 0 in the total communities the relative abundance of six OTUs were significantly different between treatments, five Bacteroidetes OTUs (OTU_19, 36, 51, 55, and 761) and one Alphaproteobacteria (OTU_7). In the active communities at day 0, two OTUs (OTU_280 and 19, from Betaproteobacteria and Bacteroidetes, respectively) exhibited significant differences between treatments.

By the end of the experiment the community composition had changed, and the OTUs showing significant differences between treatments in the GLM models had also changed. On day 28, four OTUs were significant in the total communities, two OTUs from Gemmatimonadetes (OTU_46 and 61) and two OTUs from Bacteroidetes and Planctomycetes (OTU_ 29 and 154, respectively). In the active communities on day 28 only a single OTU from Bacteroidetes (OTU_761) showed a significant difference between treatments.

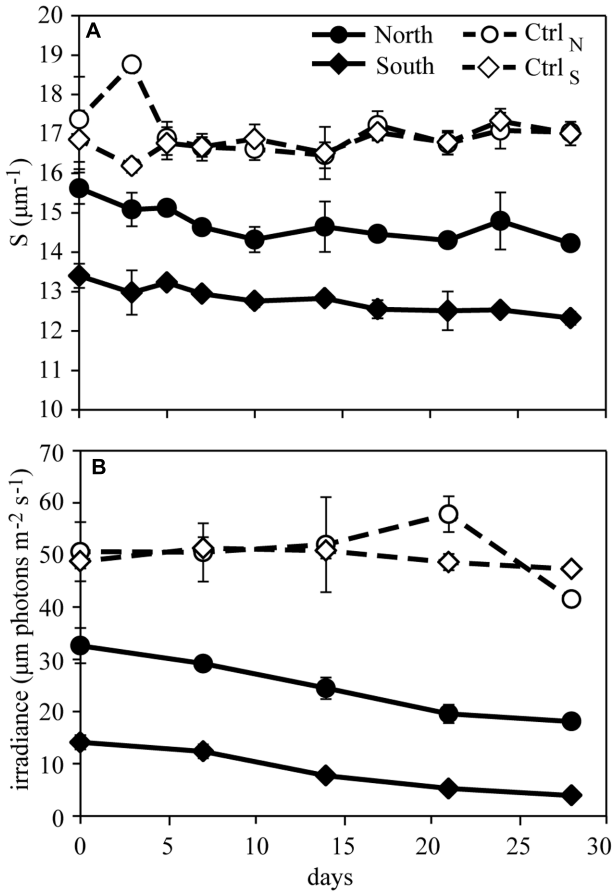

FIGURE 3 | Development in optical properties during the experiment. **(A)** the spectral slope (300–650 nm) of CDOM indicating differences in DOM character between treatments and **(B)** the irradiance of PAR indicating the influence of DOM additions on light penetration. The two controls $Ctrl_N$ and $Ctrl_S$ remained relatively stable over time. Error bars represent the standard deviations ($n = 3$).

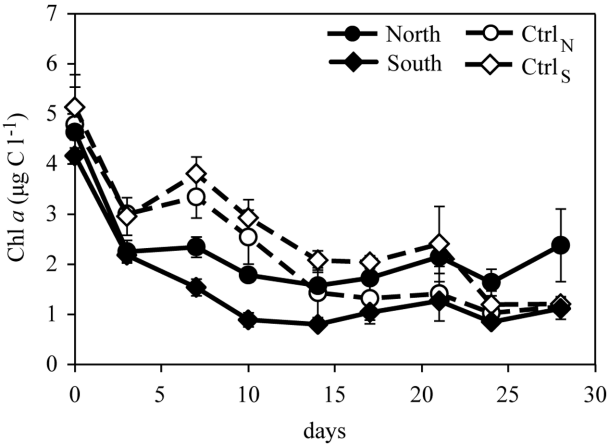

FIGURE 4 | Concentration of Chl *a* over time in the four treatments. Error bars represent standard deviation ($n = 3$).

DISCUSSION

Elevated inputs of riverine DOM have been predicted for the future Baltic Sea (Andersson et al., 2015). The present experiment suggests that a fraction of the terrestrial DOM supplied was available to the microbial community over timescales similar to that of mixing in coastal waters. The organic matter addition was processed by the microbial community and resulted in an accumulation of inorganic nutrients, and this bacterioplankton mediated change in resource utilization stimulated phytoplankton biomass despite the simultaneous decrease in light penetration due to light absorption by CDOM.

Fate of DOM

Dissolved organic matter flocculation can be an important removal process in estuarine systems (Sholkovitz, 1976; Sholkovitz et al., 1978). However, the majority of studies suggest that this is highly salinity-dependent. DOM flocculation is low at salinities < 5 and a minor factor in systems with relatively stable salinities (Sholkovitz et al., 1978; Søndergaard et al., 2003). As salinities were constant at 3.8 in this experiment it is unlikely that abiotic flocculation contributed significantly to DOM removal. Microbial activity has also been suggested to contribute to DOC flocculation in freshwater with estimated removal rates between 0.3 and 1.2 $\mu mol\ C\ l^{-1}\ d^{-1}$ (Wachenfeldt et al., 2009). That would correspond to flocculation causing a C removal of 2 to 18% in our experiment, a relatively small fraction of the total C removed from the North and South treatments. We therefore interpret the removed DOM in the mesocosms to be primarily caused by microbial activity. The microbial communities in the DOM treatments consumed organic resources in ratios reflecting the C, N, P – stoichiometry of the input DOM, suggesting a relatively flexible consumption, as observed in bacterial isolates and natural aquatic assemblages (Makino et al., 2003; Godwin and Cotner, 2015). The observed differences in bacterial processing of DOM did not translate into differences in bacterial production or abundances between treatments. This suggests that the additional DOM consumption in North and South was not channeled into the bacterial biomass. However, grazing by hetero- and mixotrophic protists and viral lysis are the major processes controlling bacterial removal, unfortunately neither group was quantified so the fate of the DOM that was channeled into the bacterial commmunity remains speculative.

As a consequence of bacterial degradation the stoichiometry of the input DOM will affect the resource landscape of the recipient water due to the flexible consumption of the bacterioplankton. This seems to be supported by the significantly higher inorganic nutrient concentrations in the DOM treatments compared to the controls, likely causing the increased phytoplankton biomass towards the end of the experiment. The accumulated DOM, i.e., the fraction not utilized by bacteria, was rich in organic C, causing an increased coloration of the water and decreasing levels of PAR, and the CDOM characteristics (S values) in the DOM

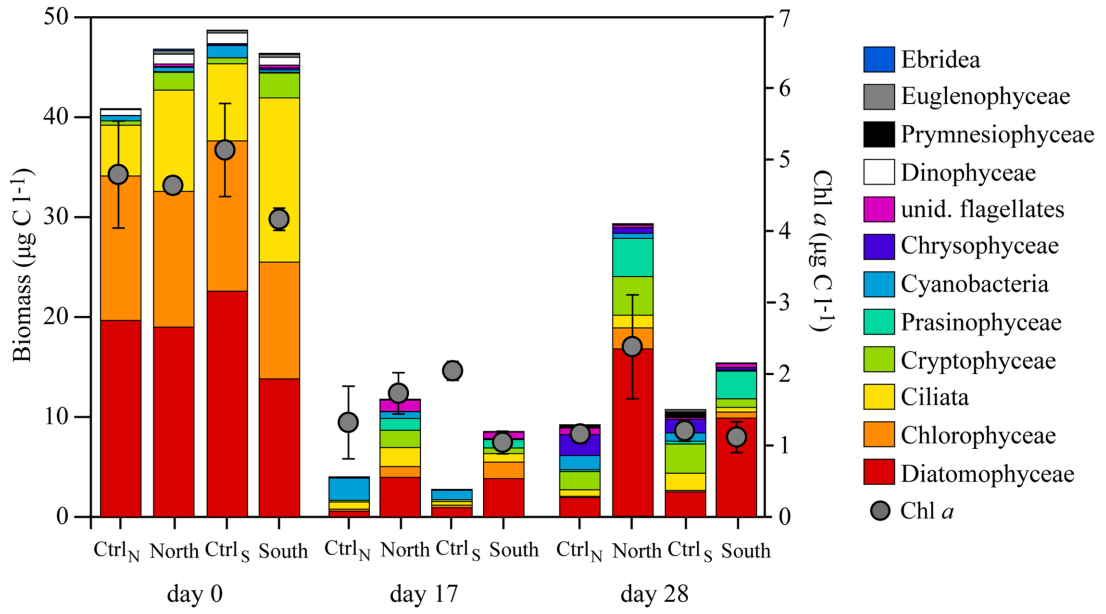

FIGURE 5 | Phyto- and protozooplankton community composition shown as stacked bars, indicating the total biomass. Chl *a* is indicated by gray dots. All values are averages from the triplicate mesocosms.

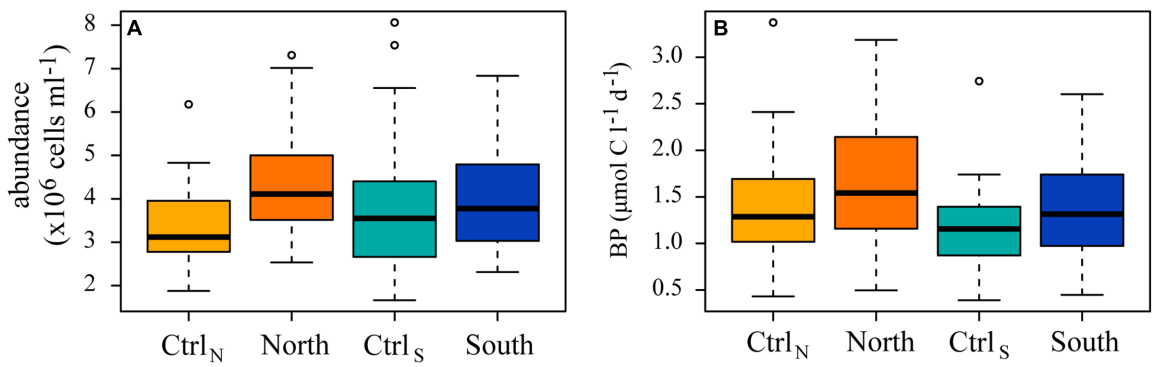

FIGURE 6 | Box and whisker plots indicating the median (A) bacterial abundance and **(B)** production (BP) for the whole experiment, with the lower 25th and upper 75th percentile.

treatments were lower, typical of terrestrial DOM (Stedmon et al., 2000). In our experiment, the increased light attenuation likely opposed more extensive phytoplankton growth induced by the available re-mineralized inorganic nutrients. Hence, a future elevated outflow of DOM may affect the relative importance of inorganic nutrients and light in the Baltic Sea – the two main factors controlling local phytoplankton growth and structure (Andersson et al., 1996).

The DOM additions stimulated protease activity with significantly higher activities measured in the presence of the terrestrial DOM. This is similar to findings in previous studies demonstrating strong protease stimulation by humic-rich DOM (Stepanauskas et al., 1999). The increased protease activity was consistent with the efficient consumption of DON, and lead to a release and accumulation of inorganic nitrogen. Alkaline phosphatase activity was not significantly different between treatments suggesting that the microbial communities in all four treatments were deficient in P. Indeed total P concentrations in all four treatments were relatively low (<0.9 µmol l^{-1}) with more than 80% bound in the organic fraction. Extracellular phosphatases are expressed by both prokaryotes and eukaryotes, and the activity is controlled by external dissolved inorganic P concentrations and intracellular P demand (Hoppe, 2003). Natural P concentrations in the Northern parts of the Baltic are low due to relatively little anthropogenic activity and removal of inorganic P through flocculation and sedimentation (Andersson et al., 1996; Forsgren et al., 1996). The activity of the proteases and alkaline phosphatases was likely the primary drivers in generating inorganic nutrients. No difference was detected in the activities of the glucosidases or β-NAGase, which suggests that

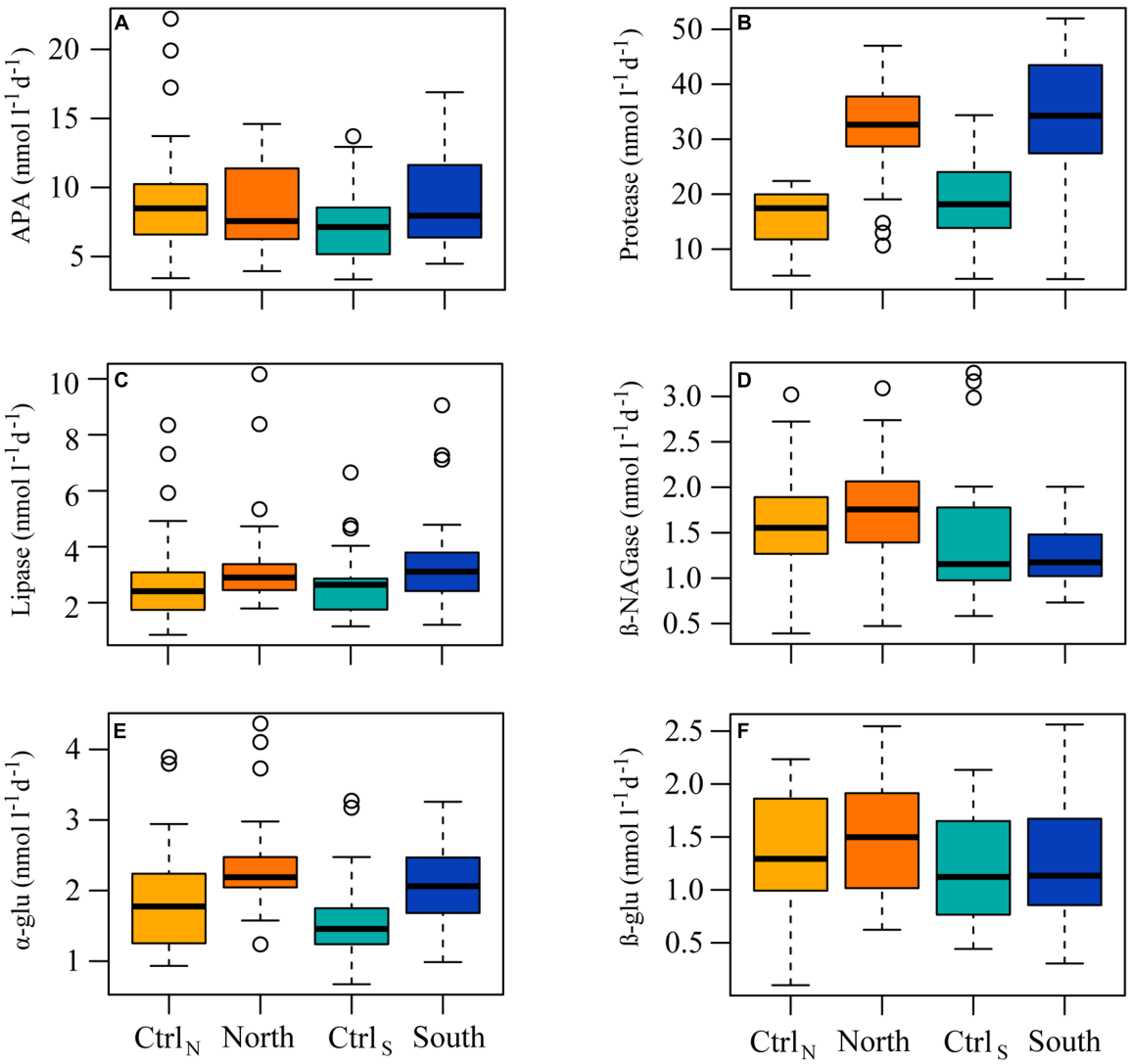

FIGURE 7 | Box and whisker plots indicating the median rates for the whole experiment, with the lower 25th and upper 75th percentile, of the enzymatic activity of (A) alkaline phosphatase (APA), **(B)** protease, **(C)** lipase, **(D)** β-NAGase, **(E)** α-glucosidase (α-glu), and **(F)** β-glucosidase (β-glu) in the four treatments.

the C sources being hydrolyzed were similar in the treatments and that the added organic C did not stimulate the activities of these enzyme groups. Similarly, no difference was detected in lipase activity. This interpretation disregards the effect of time, and the variability in activities did indicate distinct enzyme responses. Extracellular enzymes vary in how their synthesis is controlled, as evident from the protease and alkaline phosphatase activities measured here, and to which environmental cues they respond (Arnosti, 2011). Moreover, they have a variable distribution and phylogenetic placement in natural bacterial communities (Elifantz et al., 2008; Zimmerman et al., 2013). It may therefore be hard to discern clear-cut responses in extracellular enzyme activities to environmental perturbations when working with natural bacterial communities, like in the present experiment.

The bacterial community composition changed in response to treatment, causing the North and South communities to separate from the two controls, which were indistinguishable. There was also a large effect of incubation on the composition patterns, evident as a relatively uniform temporal trend in all four treatments, a common observation in incubation experiments (Piquet et al., 2010). The active communities had a similar response pattern, suggesting that the DOM additions exerted selective pressure on the present (DNA) as well as the active (RNA) bacterial communities in the DOM treatments. The divergence between the North and South communities was likely driven by the different DOM stoichiometry and concentration. Changes in community composition may influence bacterial C:N:P stoichiometry due to differences in growth and cellular content, and likewise the input stoichiometry of resources

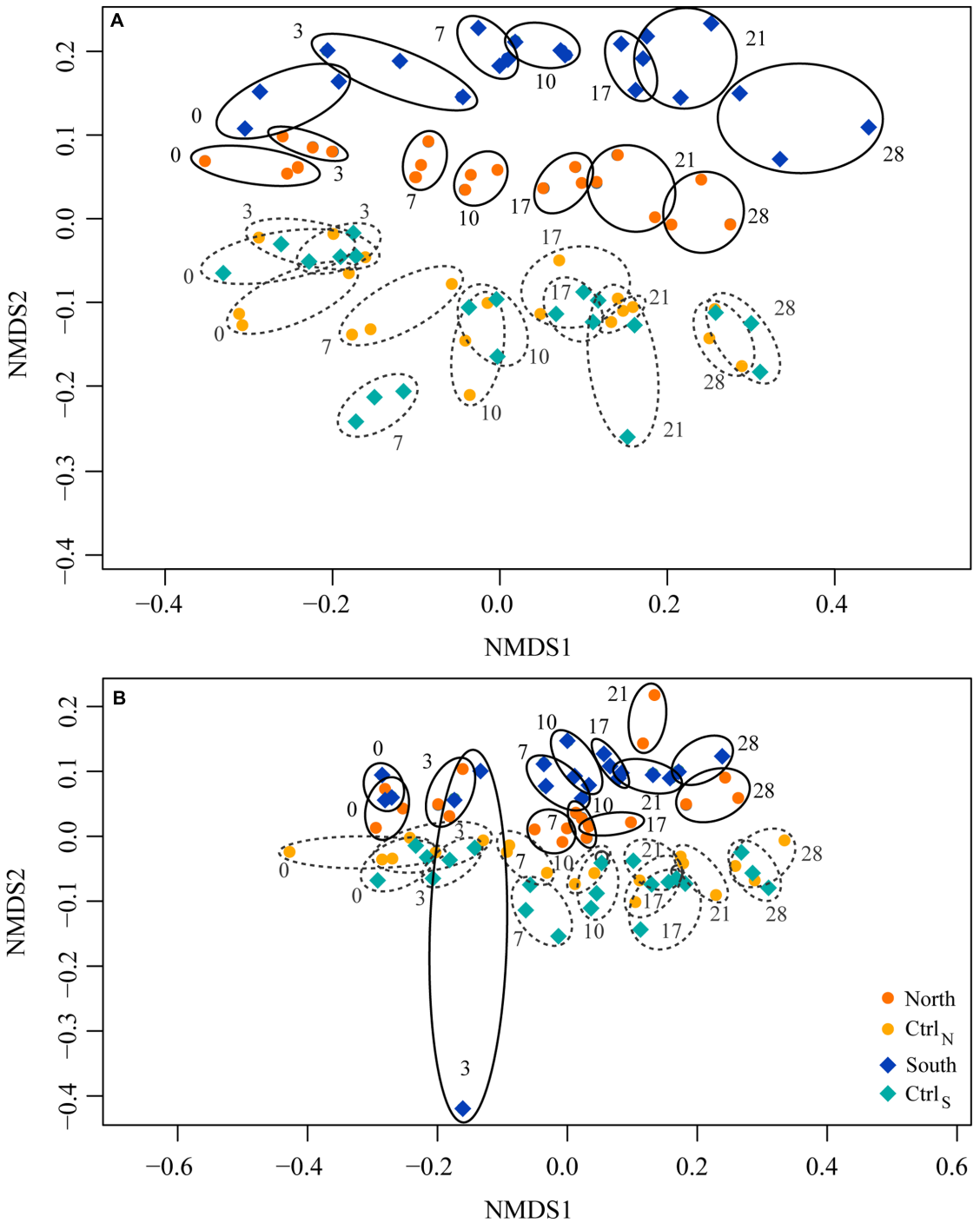

FIGURE 8 | Non-metric multidimensional scaling (NMDS) plots of changes in (A) total (rDNA) and **(B)** active (rRNA) community composition in the four treatments over time. Similarities were based on the Bray–Curtis distance. Rings indicate replicate communities from the same day. Numbers indicate days of sampling.

influence community composition (Makino et al., 2003). Furthermore, community composition and succession may be linked to functionality (Kirchman et al., 2004; Teira et al., 2008). However, we did not observe any significant differences between North and South in the protease activities or bacterial production despite large differences in community composition. Hence, with respect to these functionalities the communities of the two treatments were functionally redundant.

TABLE 2 | A list of the operational taxonomic units (OTUs) that contributed significantly to the community composition differences between the four treatments, ordered according to the size of their likelihood-ratio (LR) test statistics and adjusted *p*-value from the generalized linear model (GLM) analyses.

OTU#	Phylum	Taxon	LR statistics	Adjusted *p*-value
Day 0 rDNA				
OTU_51	Bacteroidetes	*Flavobacterium*	44.521	0.001
OTU_7	Alphaproteobacteria	*Rhodobacter*	40.985	0.002
OTU_19	Bacteroidetes	Flavobacteriaceae	39.757	0.002
OTU_36	Bacteroidetes	Flavobacteriaceae	33.300	0.004
OTU_55	Bacteroidetes	Flavobacteriales	29.159	0.021
OTU_761	Bacteroidetes	*Fluviicola*	27.911	0.028
Day 0 rRNA				
OTU_280	Betaproteobacteria	*Delftia*	34.690	0.003
OTU_19	Bacteroidetes	Flavobacteriaceae	33.440	0.005
Day 28 rDNA				
OTU_61	Gemmatimonadetes	KD8-87	38.773	0.003
OTU_29	Bacteroidetes	Sphingobacteriales	36.143	0.004
OTU_46	Gemmatimonadetes	*Gemmatimonas*	35.273	0.006
OTU_154	Planctomycetes	*Pirellulaceae*	30.669	0.038
Day 28 rRNA				
OTU_761	Bacteroidetes	*Fluviicola*	31.744	0.025

Only OTUs which were significant are reported here. Taxonomy was assigned using Greengenes v. 13.8.

To examine the communities and identify putative bacterial populations responding to DOM load, individual populations (i.e., OTUs), which contributed significantly to the differences in community composition between the treatments, were identified for the start and end of the experiment. In the day 0 communities, five Bacteroidetes populations and one Alphaproteobacteria population (*Rhodobacter*) were identified, and all except OTU_761 had the highest relative abundance in North or South. Bacteroidetes are common and widespread in marine and coastal bacterioplankton communities (DeLong et al., 1993; Cottrell and Kirchman, 2000; Kirchman, 2002). They are often linked to the degradation of high molecular weight organic matter (Covert and Moran, 2001; Gómez-Pereira et al., 2012) and enriched in carbohydrate-active hydrolases and other functions compliant with a lifestyle of utilizing high molecular weight DOM (Davey et al., 2001; Cottrell et al., 2005; Teeling et al., 2012). Most of the Bacteroidetes populations were assigned to Flavobacteriaceae, a widespread group commonly found in soil, fresh and marine waters, and many isolates are known enzyme producers (Bernardet and Nakagawa, 2006). Another Bacteroidetes was a *Fluviicola* population which dominated in the control treatments. Known *Fluviicola* strains are from freshwater environments and they utilize carbohydrates for growth (Muramatsu et al., 2012). Alphaproteobacteria also contributed to the difference between communities with a *Rhodobacter* population. These are also common members of coastal bacterioplankton and often observed as particle-colonizers (González and Moran, 1997; Crump et al., 1999). In the active communities two populations contributed to the differences between treatments. One of these populations also appeared in the total community (OTU_19) while the other population was related to *Delftia* (Betaproteobacteria). Both populations were highest in the South community. Previous studies have linked members of Betaproteobacteria, including a relative to Comamonadaceae which *Delftia* is grouped in, to the utilization of riverine DOM (Kisand and Wikner, 2003). Consequently, the DOM had dramatically altered the community structure, just 3 days after the initial DOM additions.

At the end of the experiment community compositions had changed, and the populations contributing to the differences between treatments also differed. Two populations from Gemmatimonadetes were present in the DOM treatments, with the highest abundances in North. A single population in the active communities contributed significantly to the treatment differences at the end, the Bacteroidetes population OTU_761 (*Fluviicola*). This population was the only one occurring both at the start and end, where it had increased its relative abundance in North and decreased in the two controls, suggesting it responded to the DOM. Both Gemmatimonadetes and Planctomycetes inhabit aquatic and terrestrial ecosystems (Ward et al., 2006). Gemmatimonadetes are one of the major phyla in soil communities (DeBruyn et al., 2011), and the populations occurring at the end of the experiment may well originate from the added DOM as the soil extracts were not sterile. However, estuarine communities constantly receive an inflow of terrestrial and freshwater bacteria from surrounding sources, and the brackish conditions and long water retention times (>5 years) in the Northern Baltic Sea has previously been hypothesized to promote relatively stable bacterioplankton communities of uniquely adapted bacteria (Riemann et al., 2008). Furthermore, all the populations responding to the treatments during the experiment, represent phylogenetic groups which have previously been linked to the

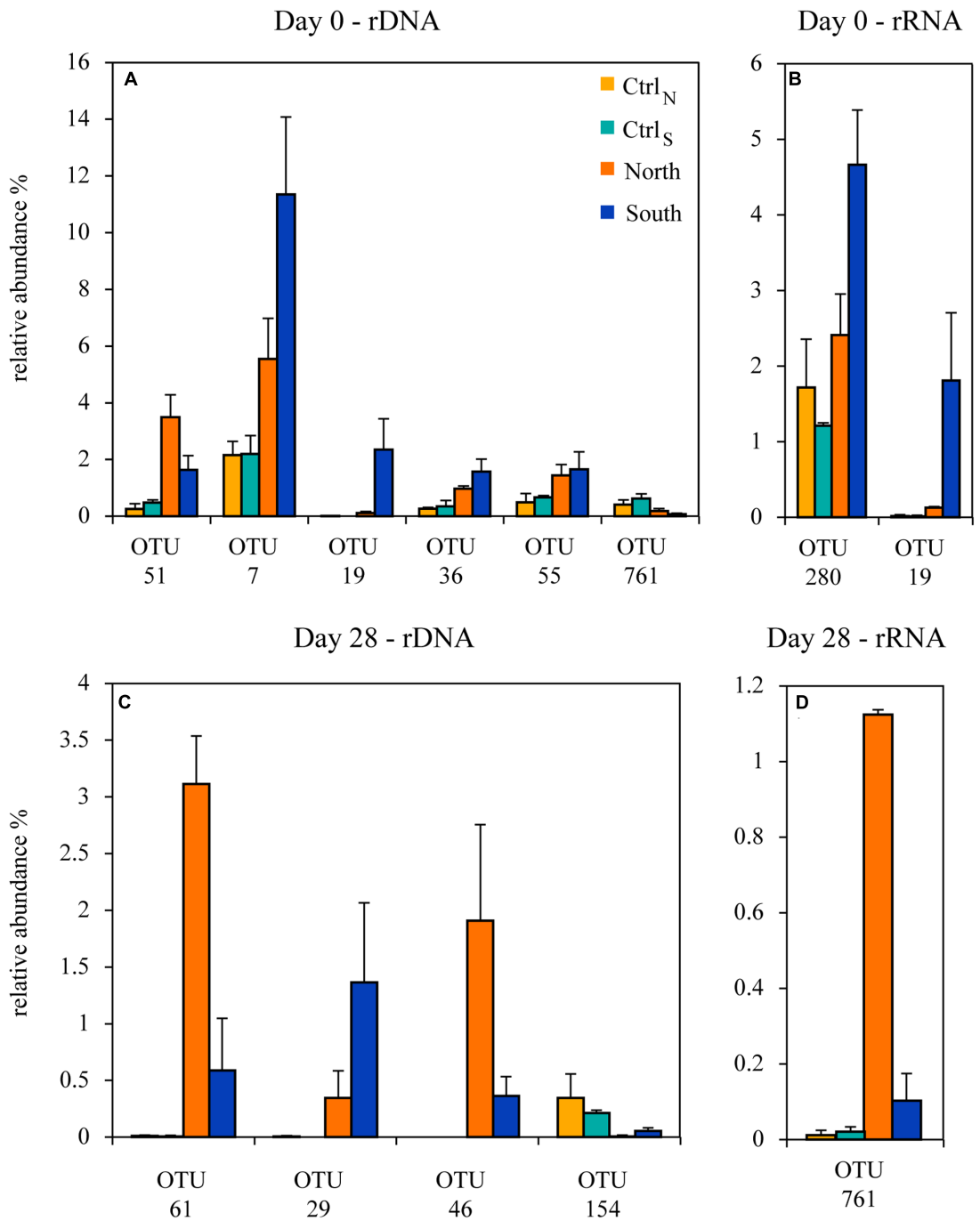

FIGURE 9 | The relative abundance of operational taxonomic units (OTUs) from the GLM models which contributed significantly to the difference between the four treatments, on day 0 in the (A) total and **(B)** active communities, and at day 28 in the **(C)** total and **(D)** active communities. Error bars represent standard deviation (*n* = 3).

degradation of riverine DOM (Kisand et al., 2002; Kisand and Wikner, 2003), and which are commonly identified as responsive in experiments amended with DOM (Pinhassi et al., 2004; Teeling et al., 2012; Lindh et al., 2015). Moreover, the dominance of Bacteroidetes in the GLM analysis suggests that this phylum is particularly responsive to elevated levels of DOM. Moreover, the different response patterns in OTUs contributing to the day 0 and day 28 community differences, suggest that bacterial populations may respond to the particular DOM composition, and that the continued treatment differences over time, were maintained by underlying shifts within each community.

CONCLUSION

The results presented here indicate that increased DOM inflow will have a major effect on the recipient ecosystem. The DOM caused shifts in bacterioplankton community composition and stimulated protease activity and bacterial DOM consumption. Despite that the different types of DOM selected for distinct communities, only some functions responded, and these did not differ between the DOM treatments. The bacterioplankton utilization of DOM corresponded to approximately 25–85% of the supplied DOM depending on type (DON, DOP, or DOC), and the microbial activity caused a release of inorganic nutrients. This conceivably stimulated a succession in phytoplankton community composition as well as increasing biomass towards the end of the experiment. The increased phytoplankton biomass indicates that access to mineralized inorganic nutrients partially outweighs the detrimental effect of extensive light attenuation associated with the high DOM levels. Our experimental data suggest that a large fraction of future elevated DOM inflow to the Baltic Sea will be mineralized by bacterioplankton with consequences for nutrient biogeochemistry and primary production in coastal regions.

AUTHOR CONTRIBUTIONS

ST, OR, AA, and LR conceived the study. ST, OR, and AA carried out the experimental work. ST, NJ, HS, CS, JD, and LR performed the analyses and interpretations. ST and LR wrote the paper including the comments and revisions from all co-authors. All authors have read and approved the submitted version.

FUNDING

This project was funded by the EU project MESOAQUA (No. 228224), the Marine Strategic Environment initiative EcoChange – Ecosystems dynamics in the Baltic Sea in a climate change perspective (FORMAS), the VKR Centre of Excellence in Ocean Life funded by the Villum foundation, the BONUS BLUEPRINT and COCOA projects that have received funding from BONUS, the joint Baltic Sea research and development program (Art 185), funded jointly from the European Union's Seventh Program for research, technological development and demonstration, and The Danish Council for Strategic Research.

ACKNOWLEDGMENTS

The authors would like to thank H. Larsson, A. Brutemark, R. Lefébure, F. Miranda, J. Paczkowska, F. Chiriboga, P. Byström, U. Båmstedt, E. Lindehoff, B. Deutsch, and the staff at Umeå Marine Sciences Centre (UMF), Umeå University, for providing their help and expertise to accomplish this mesocosm experiment.

REFERENCES

Aksnes, D. L., and Ohman, M. D. (2009). Multi-decadal shoaling of the euphotic zone in the southern sector of the California Current System. *Limnol. Oceanogr.* 54, 1272–1281. doi: 10.4319/lo.2009.54.4.1272

Alonso-Sáez, L., and Gasol, J. M. (2007). Seasonal variations in the contributions of different bacterial groups to the uptake of low-molecular-weight compounds in northwestern mediterranean coastal waters. *Appl. Environ. Microbiol.* 73, 3528–3535. doi: 10.1128/AEM.02627-06

Andersson, A., Hajdu, S., Haecky, P., Kuparinen, J., and Wikner, J. (1996). Succession and growth limitation of phytoplankton in the Gulf of Bothnia (Baltic Sea). *Mar. Biol.* 126, 791–801. doi: 10.1007/BF00351346

Andersson, A., Meier, H. M., Ripszam, M., Rowe, O., Wikner, J., Haglund, P., et al. (2015). Projected future climate change and Baltic Sea ecosystem management. *Ambio* 44, 345–356. doi: 10.1007/s13280-015-0654-8

Arnosti, C. (2011). Microbial extracellular enzymes and the marine carbon cycle. *Annu. Rev. Mar. Sci.* 3, 401–425. doi: 10.1146/annurev-marine-120709-142731

Benner, R. (2003). "Molecular indicators of the bioavailability of dissolved organic matter," in *Aquatic Ecosystems: Interactivity of Dissolved Organic Matter*, eds S. Findlay and R. L. Sinsabaugh (Cambridge, MA: Academic Press), 121–137.

Bentzon-Tilia, M., Traving, S. J., Mantikci, M., Knudsen-Leerbeck, H., Hansen, J. L. S., Markager, S., et al. (2015). Significant N2 fixation by heterotrophs, photoheterotrophs and heterocystous cyanobacteria in two temperate estuaries. *ISME J.* 9, 273–285. doi: 10.1038/ismej.2014.119

Bernardet, J.-F., and Nakagawa, Y. (2006). "An introduction to the family Flavobacteriaceae," in *The Prokaryotes*, eds M. Dworkin, S. Falkow, E. Rosenberg, K. H. Schleifer, and E. Stackebrandt (New York. NY: Springer), 455–480.

Blackburn, N., Fenchel, T., and Mitchell, J. (1998). Microscale nutrient patches in planktonic habitats shown by chemotactic bacteria. *Science* 282, 2254–2256. doi: 10.1126/science.282.5397.2254

Caporaso, J. G., Kuczynski, J., Stombaugh, J., Bittinger, K., Bushman, F. D., Costello, E. K., et al. (2010). QIIME allows analysis of high-throughput community sequencing data. *Nat. Methods* 7, 335–336. doi: 10.1038/nmeth.f.303

Caporaso, J. G., Lauber, C. L., Walters, W. A., Berg-Lyons, D., Huntley, J., Fierer, N., et al. (2012). Ultra-high-throughput microbial community analysis on the Illumina HiSeq and MiSeq platforms. *ISME J.* 6, 1621–1624. doi: 10.1038/ismej.2012.8

Clarke, K. R. (1993). Non-parametric multivariate analyses of changes in community structure. *Aust. J. Ecol.* 18, 117–143. doi: 10.1111/j.1442-9993.1993.tb00438.x

Cottrell, M. T., and Kirchman, D. L. (2000). Community composition of marine bacterioplankton determined by 16S rRNA gene clone libraries and fluorescence in situ hybridization. *Appl. Environ. Microbiol.* 66, 5116–5122. doi: 10.1128/AEM.66.12.5116-5122.2000

Cottrell, M. T., Yu, L., and Kirchman, D. L. (2005). Sequence and expression analyses of *Cytophaga*-like hydrolases in a Western arctic metagenomic library and the Sargasso Sea. *Appl. Environ. Microbiol.* 71, 8506–8513. doi: 10.1128/AEM.71.12.8506-8513.2005

Covert, J. S., and Moran, M. A. (2001). Molecular characterization of estuarine bacterial communities that use high- and low-molecular weight fractions of dissolved organic carbon. *Aquat. Microb. Ecol.* 25, 127–139. doi: 10.3354/ame025127

Crump, B. C., Armbrust, E. V., and Baross, J. A. (1999). Phylogenetic analysis of particle-attached and free-living bacterial communities in the Columbia River, its estuary, and the adjacent coastal ocean. *Appl. Environ. Microbiol.* 65, 3192–3204.

Davey, K. E., Kirby, R. R., Turley, C. M., Weightman, A. J., and Fry, J. C. (2001). Depth variation of bacterial extracellular enzyme activity and population diversity in the northeastern North Atlantic Ocean. *Deep Sea Res. Part II Top. Stud. Oceanogr.* 48, 1003–1017. doi: 10.1016/S0967-0645(00)00106-5

DeBruyn, J. M., Nixon, L. T., Fawaz, M. N., Johnson, A. M., and Radosevich, M. (2011). Global biogeography and quantitative seasonal dynamics of Gemmatimonadetes in soil. *Appl. Environ. Microbiol.* 77, 6295–6300. doi: 10.1128/AEM.05005-11

DeLong, E. F., Franks, D. G., and Alldredge, A. L. (1993). Phylogenetic diversity of aggregate-attached vs. free-living marine bacterial assemblages. *Limnol. Oceanogr.* 38, 924–934. doi: 10.1111/j.1574-6941.2010.00914.x

Edgar, R. C. (2010). Search and clustering orders of magnitude faster than BLAST. *Bioinformatics* 26, 2460–2461. doi: 10.1093/bioinformatics/btq461

Edgar, R. C. (2013). UPARSE: highly accurate OTU sequences from microbial amplicon reads. *Nat. Methods* 10, 996–998. doi: 10.1038/nmeth.2604

Elifantz, H., Waidner, L. A., Cottrell, M. T., and Kirchman, D. L. (2008). Diversity and abundance of glycosyl hydrolase family 5 in the North Atlantic Ocean. *FEMS Microbiol. Ecol.* 63, 316–327. doi: 10.1111/j.1574-6941.2007.00429.x

Eriksson Hägg, H., Humborg, C., Mörth, C.-M., Medina, M. R., and Wulff, F. (2010). Scenario analysis on protein consumption and climate change effects on riverine N export to the Baltic Sea. *Environ. Sci. Technol.* 44, 2379–2385. doi: 10.1021/es902632p

Fasching, C., Behounek, B., Singer, G. A., and Battin, T. J. (2014). Microbial degradation of terrigenous dissolved organic matter and potential consequences for carbon cycling in brown-water streams. *Sci. Rep.* 4:4981. doi: 10.1038/srep04981

Figueroa, D., Rowe, O. F., Paczkowska, J., Legrand, C., and Andersson, A. (2016). Allochthonous carbon–a major driver of bacterioplankton production in the subarctic northern Baltic Sea. *Microb. Ecol.* 71, 789–801. doi: 10.1007/s00248-015-0714-4

Forsgren, G., Jansson, M., and Nilsson, P. (1996). Aggregation and sedimentation of iron, phosphorus and organic carbon in experimental mixtures of freshwater and estuarine water. *Estuar. Coast. Shelf Sci.* 43, 259–268. doi: 10.1006/ecss.1996.0068

Frigstad, H., Andersen, T., Hessen, D. O., Jeansson, E., Skogen, M., Naustvoll, L.-J., et al. (2013). Long-term trends in carbon, nutrients and stoichiometry in Norwegian coastal waters: evidence of a regime shift. *Prog. Oceanogr.* 111, 113–124. doi: 10.1016/j.pocean.2013.01.006

Fuhrman, J., and Azam, F. (1982). Thymidine incorporation as a measure of heterotrophic bacterioplankton production in marine surface waters: evaluation and field results. *Mar. Biol.* 66, 109–120. doi: 10.1007/BF00397184

Gasol, J. M., Comerma, M., García, J. C., Armengol, J., Casamayor, E. O., Kojecká, P., et al. (2002). A transplant experiment to identify the factors controlling bacterial abundance, activity, production, and community composition in a eutrophic canyon-shaped reservoir. *Limnol. Oceanogr.* 47, 62–77. doi: 10.4319/lo.2002.47.1.0062

Giraudoux, P. (2016). *pgirmess: Data Analysis in Ecology. R Package Version* 1.6.4. Available at: https://CRAN.R-project.org/package=pgirmess.

Godwin, C. M., and Cotner, J. B. (2015). Aquatic heterotrophic bacteria have highly flexible phosphorus content and biomass stoichiometry. *ISME J.* 9, 2324–2327. doi: 10.1038/ismej.2015.34

Gómez-Pereira, P. R., Schüler, M., Fuchs, B. M., Bennke, C., Teeling, H., Waldmann, J., et al. (2012). Genomic content of uncultured Bacteroidetes from contrasting oceanic provinces in the North Atlantic Ocean. *Environ. Microbiol.* 14, 52–66. doi: 10.1111/j.1462-2920.2011.02555.x

González, J. M., and Moran, M. A. (1997). Numerical dominance of a group of marine bacteria in the alpha-subclass of the class *Proteobacteria* in coastal seawater. *Appl. Environ. Microbiol.* 63, 4237–4242.

Grasshoff, K., Kremling, K., and Ehrhardt, M. (1983). *Methods of Seawater Analysis*, 2nd Edn. Weinheim: Verlag Chemie.

HELCOM (2014). *Manual for Marine Monitoring in the COMBINE Programme of HELCOM. Part C Programme for monitoring of eutrophication and its effects. Baltic Marine Environment Protection Commission – Helsinki Commission*. Available at: http://www.helcom.fi/action-areas/monitoring-and-assessment/manuals-and-guidelines/combine-manual/

Hoppe, H.-G. (1983). Significance of exoenzymatic activities in the ecology of brackish water: measurements by means of methylumbelliferyl-substrates. *Mar. Ecol. Prog. Ser.* 11, 299–308. doi: 10.3354/meps011299

Hoppe, H.-G. (2003). Phosphatase activity in the sea. *Hydrobiologia* 493, 187–200. doi: 10.1023/A:1025453918247

Husson, F., Josse, J., Le, S., and Mazet, J. (2015). *Package 'FactoMineR'. R Package Version* 1.31.4. Available at http://CRAN.R-project.org/package=FactoMineR

Judd, K. E., Crump, B. C., and Kling, G. W. (2006). Variation in dissolved organic matter controls bacterial production and community composition. *Ecology* 87, 2068–2079. doi: 10.1890/0012-9658(2006)87[2068:VIDOMC]2.0.CO;2

Kemp, W., Smith, E., Marvin-DiPasquale, M., and Boynton, W. (1997). Organic carbon balance and net ecosystem metabolism in Chesapeake Bay. *Mar. Ecol. Prog. Ser.* 150, 229–248. doi: 10.3354/meps150229

Kirchman, D. L. (2002). The ecology of *Cytophaga*–Flavobacteria in aquatic environments. *FEMS Microbiol. Ecol.* 39, 91–100. doi: 10.1016/s0168-6496(01)00206-9

Kirchman, D. L., Dittel, A. I., Findlay, S. E., and Fischer, D. (2004). Changes in bacterial activity and community structure in response to dissolved organic matter in the Hudson River, New York. *Aquat. Microb. Ecol.* 35, 243–257. doi: 10.3354/ame035243

Kisand, V., Cuadros, R., and Wikner, J. (2002). Phylogeny of culturable estuarine bacteria catabolizing riverine organic matter in the northern Baltic Sea. *Appl. Environ. Microbiol.* 68, 379–388. doi: 10.1128/AEM.68.1.379-388.2002

Kisand, V., and Wikner, J. (2003). Combining culture-dependent and-independent methodologies for estimation of richness of estuarine bacterioplankton consuming riverine dissolved organic matter. *Appl. Environ. Microbiol.* 69, 3607–3616. doi: 10.1128/AEM.69.6.3607-3616.2003

Koroleff, F. (1983). "Determination of nutrients," in *Method of Seawater Analysis*, eds K. Grasshof, M. Ehrhardt, and K. Kremling (Weinheim: Verlag Chemie).

Kritzberg, E. S., Cole, J. J., Pace, M. L., Granéli, W., and Bade, D. L. (2004). Autochthonous versus allochthonous carbon sources of bacteria: results from whole-lake 13C addition experiments. *Limnol. Oceanogr.* 49, 588–596. doi: 10.4319/lo.2004.49.2.0588

Lee, S., and Fuhrman, J. A. (1987). Relationships between biovolume and biomass of naturally derived marine bacterioplankton. *Appl. Environ. Microbiol.* 53, 1298–1303.

Lefebure, R., Degerman, R., Andersson, A., Larsson, S., Eriksson, L. O., Båmstedt, U., et al. (2013). Impacts of elevated terrestrial nutrient loads and temperature on pelagic food-web efficiency and fish production. *Glob. Chang Biol.* 19, 1358–1372. doi: 10.1111/gcb.12134

Lindh, M. V., Figueroa, D., Sjöstedt, J., Baltar, F., Lundin, D., Andersson, A., et al. (2015). Transplant experiments uncover Baltic Sea basin-specific responses in bacterioplankton community composition and metabolic activities. *Front. Microbiol.* 6:223. doi: 10.3389/fmicb.2015.00223

Makino, W., Cotner, J., Sterner, R., and Elser, J. (2003). Are bacteria more like plants or animals? Growth rate and resource dependence of bacterial C: N: P stoichiometry. *Funct. Ecol.* 17, 121–130. doi: 10.1046/j.1365-2435.2003.00712.x

McDonald, D., Price, M. N., Goodrich, J., Nawrocki, E. P., DeSantis, T. Z., Probst, A., et al. (2012). An improved Greengenes taxonomy with explicit ranks for ecological and evolutionary analyses of bacteria and archaea. *ISME J.* 6, 610–618. doi: 10.1038/ismej.2011.139

Meier, H., Hordoir, R., Andersson, H., Dieterich, C., Eilola, K., Gustafsson, B. G., et al. (2012). Modeling the combined impact of changing climate and changing nutrient loads on the Baltic Sea environment in an ensemble of transient simulations for 1961–2099. *Clim. Dyn.* 39, 2421–2441. doi: 10.1007/s00382-012-1339-7

Menden-Deuer, S., and Lessard, E. J. (2000). Carbon to volume relationships for dinoflagellates, diatoms, and other protist plankton. *Limnol. Oceanogr.* 45, 569–579. doi: 10.4319/lo.2000.45.3.0569

Muramatsu, Y., Takahashi, M., Kamakura, Y., Suzuki, K.-I., and Nakagawa, Y. (2012). Salinirepens amamiensis gen. nov., sp. nov., a member of the family Cryomorphaceae isolated from seawater, and emended descriptions of the genera Fluviicola and Wandonia. *Int. J. Syst. Evol. Microbiol.* 62, 2235–2240. doi: 10.1099/ijs.0.032029-0

Murphy, K. R., Hambly, A., Singh, S., Henderson, R. K., Baker, A., Stuetz, R., et al. (2011). Organic matter fluorescence in municipal water recycling schemes: toward a unified PARAFAC model. *Environ. Sci. Technol.* 45, 2909–2916. doi: 10.1021/es103015e

Oksanen, J., Blanchet, F. G., Kindt, R., Legendre, P., Minchin, P. R., O'Hara, R., et al. (2015). *vegan: Community Ecology Package. R package version* 2.3-2, 2.2-1. Available at: https://CRAN.R-project.org/package=vegan.

Pinhassi, J., Sala, M. M., Havskum, H., Peters, F., Guadayol, O., Malits, A., et al. (2004). Changes in bacterioplankton composition under different phytoplankton regimens. *Appl. Environ. Microbiol.* 70, 6753–6766. doi: 10.1128/AEM.70.11.6753-6766.2004

Piquet, A. M.-T., Bolhuis, H., Davidson, A. T., and Buma, A. G. (2010). Seasonal succession and UV sensitivity of marine bacterioplankton at an Antarctic

coastal site. *FEMS Microbiol. Ecol.* 73, 68–82. doi: 10.1111/j.1574-6941.2010.00882.x

R Core Team (2016). *R: A Language and Environment for Statistical Computing*. Austria: R Foundation for Statistical Computing. Available at: https://www.R-project.org/

Riemann, L., Leitet, C., Pommier, T., Simu, K., Holmfeldt, K., Larsson, U., et al. (2008). The native bacterioplankton community in the central Baltic Sea is influenced by freshwater bacterial species. *Appl. Environ. Microbiol.* 74, 503–515. doi: 10.1128/AEM.01983-07

Rönnberg, C., and Bonsdorff, E. (2004). Baltic Sea eutrophication: area-specific ecological consequences. *Hydrobiologia* 514, 227–241. doi: 10.1023/B:HYDR.0000019238.84989.7f

Roulet, N., and Moore, T. R. (2006). Environmental chemistry: browning the waters. *Nature* 444, 283–284. doi: 10.1038/444283a

Sandberg, J., Andersson, A., Johansson, S., and Wikner, J. (2004). Pelagic food web structure and carbon budget in the northern Baltic Sea: potential importance of terrigenous carbon. *Mar. Ecol. Prog. Ser.* 268, 13–29. doi: 10.3354/meps268013

Sanden, P., and Håkansson, B. (1996). Long-term trends in Secchi depth in the Baltic Sea. *Limnol. Oceanogr.* 41, 346–351. doi: 10.4319/lo.1996.41.2.0346

Sholkovitz, E. R. (1976). Flocculation of dissolved organic and inorganic matter during the mixing of river water and seawater. *Geochim. Cosmochim. Acta* 40, 831–845. doi: 10.1016/0016-7037(76)90035-1

Sholkovitz, E. R., Boyle, E. A., and Price, N. B. (1978). The removal of dissolved humic acids and iron during estuarine mixing. *Earth Planet. Sci. Lett.* 40, 130–136. doi: 10.1016/0012-821X(78)90082-1

Søndergaard, M., Stedmon, C. A., and Borch, N. H. (2003). Fate of terrigenous dissolved organic matter (DOM) in estuaries: aggregation and bioavailability. *Ophelia* 57, 161–176. doi: 10.1080/00785236.2003.10409512

Stedmon, C. A., Markager, S., and Kaas, H. (2000). Optical properties and signatures of chromophoric dissolved organic matter (CDOM) in Danish coastal waters. *Estuar. Coast. Shelf Sci.* 51, 267–278. doi: 10.1006/ecss.2000.0645

Stepanauskas, R., Leonardson, L., and Tranvik, L. J. (1999). Bioavailability of wetland-derived DON to freshwater and marine bacterioplankton. *Limnol. Oceanogr.* 44, 1477–1485. doi: 10.4319/lo.1999.44.6.1477

Stepanauskas, R. N., JØrgensen, N. O., Eigaard, O. R., Žvikas, A., Tranvik, L. J., and Leonardson, L. (2002). Summer inputs of riverine nutrients to the Baltic Sea: bioavailability and eutrophication relevance. *Ecol. Monogr.* 72, 579–597. doi: 10.1890/0012-9615(2002)072[0579:SIORNT]2.0.CO;2

Teeling, H., Fuchs, B. M., Becher, D., Klockow, C., Gardebrecht, A., Bennke, C. M., et al. (2012). Substrate-controlled succession of marine bacterioplankton populations induced by a phytoplankton bloom. *Science* 336, 608–611. doi: 10.1126/science.1218344

Teira, E., Gasol, J. M., Aranguren-Gassis, M., Fernández, A., González, J., Lekunberri, I., et al. (2008). Linkages between bacterioplankton community composition, heterotrophic carbon cycling and environmental conditions in a highly dynamic coastal ecosystem. *Environ. Microbiol.* 10, 906–917. doi: 10.1111/j.1462-2920.2007.01509.x

Thingstad, T., Bellerby, R., Bratbak, G., Børsheim, K., Egge, J., Heldal, M., et al. (2008). Counterintuitive carbon-to-nutrient coupling in an Arctic pelagic ecosystem. *Nature* 455, 387–390. doi: 10.1038/nature07235

Wachenfeldt, E. V., Bastviken, D., and Tranvika, L. J. (2009). Microbially induced flocculation of allochthonous dissolved organic carbon in lakes. *Limnol. Oceanogr.* 54, 1811–1818. doi: 10.4319/lo.2009.54.5.1811

Wang, Y., Naumann, U., Wright, S. T., and Warton, D. I. (2012). mvabund– an R package for model-based analysis of multivariate abundance data. *Methods Ecol. Evol.* 3, 471–474. doi: 10.1111/j.2041-210X.2012.00190.x

Ward, N., Staley, J. T., Fuerst, J. A., Giovannoni, S., Schlesner, H., and Stackebrandt, E. (2006). *The Order Planctomycetales, Including the Genera Planctomyces, Pirellula, Gemmata and Isosphaera and the Candidatus Genera Brocadia, Kuenenia and Scalindua*. Berlin: Springer. doi: 10.1007/0-387-30747-8_31

Warton, D. I., Wright, S. T., and Wang, Y. (2012). Distance-based multivariate analyses confound location and dispersion effects. *Methods Ecol. Evol.* 3, 89–101. doi: 10.1111/j.2041-210X.2011.00127.x

Wikner, J., and Andersson, A. (2012). Increased freshwater discharge shifts the trophic balance in the coastal zone of the northern Baltic Sea. *Glob. Change Biol.* 18, 2509–2519. doi: 10.1111/j.1365-2486.2012.02718.x

Wikner, J., and Hagström, Å. (1999). Bacterioplankton intra-annual variability: importance of hydrography and competition. *Aquat. Microb. Ecol.* 20, 245–260. doi: 10.3354/ame020245

Zimmerman, A. E., Martiny, A. C., and Allison, S. D. (2013). Microdiversity of extracellular enzyme genes among sequenced prokaryotic genomes. *ISME J.* 7, 1187–1199. doi: 10.1038/ismej.2012.176

Conflict of Interest Statement: The authors declare that the research was conducted in the absence of any commercial or financial relationships that could be construed as a potential conflict of interest.

frontiers in Marine Science

ORIGINAL RESEARCH
published: 04 January 2018
doi: 10.3389/fmars.2017.00430

Formation of Chromophoric Dissolved Organic Matter by Bacterial Degradation of Phytoplankton-Derived Aggregates

Joanna D. Kinsey[1], Gabrielle Corradino[1], Kai Ziervogel[2], Astrid Schnetzer[1] and Christopher L. Osburn[1]*

[1] Department of Marine, Earth, and Atmospheric Sciences, North Carolina State University, Raleigh, NC, United States, [2] Ocean Process Analysis Laboratory, Institute for the Study of Earth, Oceans, and Space, University of New Hampshire, Durham, NH, United States

Organic matter produced and released by phytoplankton during growth is processed by heterotrophic bacterial communities that transform dissolved organic matter into biomass and recycle inorganic nutrients, fueling microbial food web interactions. Bacterial transformation of phytoplankton-derived organic matter also plays a poorly known role in the formation of chromophoric dissolved organic matter (CDOM) which is ubiquitous in the ocean. Despite the importance of organic matter cycling, growth of phytoplankton and activities of heterotrophic bacterial communities are rarely measured in concert. To investigate CDOM formation mediated by microbial processing of phytoplankton-derived aggregates, we conducted growth experiments with non-axenic monocultures of three diatoms (*Skeletonema grethae*, *Leptocylindrus hargravesii*, *Coscinodiscus* sp.) and one haptophyte (*Phaeocystis globosa*). Phytoplankton biomass, carbon concentrations, CDOM and base-extracted particulate organic matter (BEPOM) fluorescence, along with bacterial abundance and hydrolytic enzyme activities (α-glucosidase, β-glucosidase, leucine-aminopeptidase) were measured during exponential growth and stationary phase (∼3–6 weeks) and following 6 weeks of degradation. Incubations were performed in rotating glass bottles to keep cells suspended, promoting cell coagulation and, thus, formation of macroscopic aggregates (marine snow), more similar to surface ocean processes. Maximum carbon concentrations, enzyme activities, and BEPOM fluorescence occurred during stationary phase. Net DOC concentrations (0.19–0.46 mg C L^{-1}) increased on the same order as open ocean concentrations. CDOM fluorescence was dominated by protein-like signals that increased throughout growth and degradation becoming increasingly humic-like, implying the production of more complex molecules from planktonic-precursors mediated by microbial processing. Our experimental results suggest that at least a portion of open-ocean CDOM is produced by autochthonous processes and aggregation likely facilitates microbial reprocessing of organic matter into refractory DOM.

Keywords: excitation-emission matrix (EEM), base-extracted particulate organic matter (BEPOM), marine snow, aggregates, hydrolytic enzyme activities, phytoplankton, fluorescence

OPEN ACCESS

Edited by:
Judith Piontek, GEOMAR Helmholtz Centre for Ocean Research Kiel (HZ), Germany

Reviewed by:
Teresa S. Catalá, University of Oldenburg, Germany
Yumiko Obayashi, Ehime University, Japan

****Correspondence:***
Joanna D. Kinsey
jdkinsey@ncsu.edu

Specialty section:
This article was submitted to Aquatic Microbiology, a section of the journal Frontiers in Marine Science

Received: *07 July 2017*
Accepted: *14 December 2017*
Published: *04 January 2018*

Citation:
Kinsey JD, Corradino G, Ziervogel K, Schnetzer A and Osburn CL (2018) Formation of Chromophoric Dissolved Organic Matter by Bacterial Degradation of Phytoplankton-Derived Aggregates. Front. Mar. Sci. 4:430. doi: 10.3389/fmars.2017.00430

INTRODUCTION

Oceanic primary production (PP) contributes between 35 and 65 petagrams (Pg) of carbon annually to global net PP (Field et al., 1998; del Giorgio and Duarte, 2002; Carr et al., 2006; Chavez et al., 2011), mainly through autochthonous production by photosynthetic phytoplankton. Phytoplankton release 2–50% of photosynthetically fixed carbon as dissolved organic matter (DOM) through active exudation and passive leakage (Thornton, 2014), contributing to the largest reservoir of reduced carbon on earth (662 Pg C) (Hansell et al., 2009). Additional phytoplanktonic DOM is released through viral infection, sloppy feeding by predators such as zooplankton, and cell death, with zooplankton contributing their own DOM through excretion of organic matter and fecal pellets (Urban-Rich et al., 2006; Steinberg et al., 2008; Saba et al., 2011). A significant, yet poorly characterized, portion of primary production is exported out of the euphotic zone and into the twilight zone (Siegel et al., 2016). The vertical export has been estimated to range from 5 to more than 12 Pg C y^{-1} (e.g., Boyd and Trull, 2007; Henson et al., 2011) spanning annual anthropogenic CO_2 emissions (∼7.0 Pg C y^{-1}) (Siegenthaler and Sarmiento, 1993). Sinking aggregates (or marine snow) are an amalgam of intact phytoplankton cells, detritus, fecal pellets, silica and/or carbonate frustules (that provide ballast) and transparent exopolymeric material (TEP) (Alldredge and Silver, 1988). These aggregates exhibit a wide variability with respect to chemical composition (Wakeham and Lee, 1989, 1993; Minor et al., 2003) and may result in significant export of organic matter to depth (e.g., Hansell et al., 2009; Carlson et al., 2010) and contribution to refractory DOM (RDOM) formation (Lechtenfeld et al., 2015).

DOM is a complex mixture of organic compounds that play an important role in marine biogeochemical cycling. The optically active fraction, chromophoric DOM (CDOM), is essential in both physical and biological processes, controlling light attenuation and photochemical reactions in the surface ocean, impacting the depth of primary production and screening out harmful ultraviolet light (e.g., Arrigo and Brown, 1996; Blough and Del Vecchio, 2002; Mopper et al., 2015). A small fraction of DOM fluoresces, allowing for the identification of DOM sources using excitation-emission matrices (EEMs). Two types of fluorescence are typically described, amino acid-like compounds and humic-like compounds (Coble, 2007), and have been attributed to autochthonous (e.g., primary production) and allochthonous (e.g., terrestrial) production, respectively (Coble, 1996; Yamashita and Tanoue, 2003). Fluorescence of base-extracted particulate organic matter (BEPOM), has been established as a relatively new technique that allows for the optical properties and sources of intracellular fluorophores in POM to be determined (Brym et al., 2014). This work has suggested strong discrete fluorophores including amino acids in estuarine and coastal ocean POM, while studies investigating CDOM production from phytoplankton have confirmed strong amino acid-like fluorescence in axenic cultures with additional fluorescence in the region of humic-like fluorescence for some species (Romera-Castillo et al., 2010; Fukuzaki et al., 2014). Additionally, humic-like fluorescence has been found to increase in degradation studies (Rochelle-Newall and Fisher, 2002; Stedmon and Markager, 2005; Biers et al., 2007; Shimotori et al., 2009; Romera-Castillo et al., 2011) and with apparent oxygen utilization (AOU), especially in the Pacific and Southern oceans (Chen and Bada, 1992; Yamashita et al., 2007; Yamashita and Tanoue, 2008; Jørgensen et al., 2011; Catalá et al., 2015). This suggests a linkage to microbial oxidation and organic matter degradation (Hayase and Shinozuka, 1995; Yamashita et al., 2007; Jørgensen et al., 2011) and may be especially important as an indicator for biogeochemical cycling since DOM serves as a substrate for heterotrophic microbial remineralization of carbon and other trace elements. Microbes utilize extracellular enzymes to catalyze high-molecular weight DOM into smaller compounds that can be transported across cell membranes of bacteria (Arnosti, 2011) or through osmotic uptake by fungi and labyrinthulomycetes (Bochdansky et al., 2017). The carbon is then incorporated into biomass, respired to CO_2, or excreted as dissolved organic carbon (DOC) in the form of metabolically transformed products (Arnosti, 2011).

Given the potential importance of heterotrophic bacterial processing of organic matter for both biogeochemical cycling and contribution to deep-sea fluorescence, we aimed to investigate the role of microbes in the formation of open-ocean CDOM from phytoplankton-derived POM to better understand sources of open-ocean fluorescence. Our study builds upon previous culture studies that investigated CDOM production by incorporating fluorescence of base-extracted POM and hydrolytic enzyme activities in addition to traditional CDOM fluorescence measurements. Roller bottle incubations were used to form planktonic aggregates of four monocultures, sampling at initial, exponential, and stationary growth phases, and after 6 weeks of degradation in the dark. Bacterial abundance and two classes of hydrolytic extracellular enzymes indicative of carbohydrate and peptide hydrolysis (glucosidase and leucine-aminopeptidase, respectively) were measured in conjunction with carbon concentrations and CDOM and BEPOM fluorescence. We demonstrate that the production of CDOM fluorescence is directly related to microbial processing of phytoplankton-derived material.

MATERIALS AND METHODS

Phytoplankton Growth Experiments and Sample Collection

Growth experiments were conducted with four phytoplankton taxa commonly found in coastal waters. Three strains were obtained from the NCMA Bigelow collection (https://ncma.bigelow.org/) including diatoms *Skeletonema grethae* (CCMP2801, isolated May 2004 off North Carolina) and *Leptocylindrus hargravesii* (CCMP1856, isolated Feb 1997 in the Gulf of Mexico), and one haptophyte *Phaeocystis globosa* (CCMP2754, isolated Aug 2003 in the Atlantic Bight). The fourth was a coastal non-axenic isolate of *Coscinodiscus* sp. (COS1, isolated April 2015 off North Carolina). Two growth experiments were conducted, one with *Skeletonema*, *Leptocylindrus*, and *Phaeocystis* spp. grown in parallel and the other with only *Coscinodiscus* sp. All cultures were grown

in optically clear 0.2 μm-filtered artificial seawater (ASW) prepared with baked (550°C, 6 h) or ultrapure salts to minimize background CDOM fluorescence. A total of twelve 1.9 L borosilicate bottles per organism were inoculated with an initial concentration of ~21,000–66,000 cells mL^{-1} with the exception of the much slower growing *Coscinodiscus* sp. with ~5 cells mL^{-1}. All inoculated bottles, along with control bottles of ASW containing no phytoplankton, were amended with f/20 growth media (one-tenth of f/2 media, Guillard and Ryther, 1962). Inoculated bottles and controls were grown on a Wheaton roller culture apparatus rotating at ~1 rpm (Shanks and Edmondson, 1989). Cultures were maintained at 18°C and a 12:12 L:D cycle at ~90 μEinstein m^{-2} s^{-1} under cool white fluorescent light in a culture incubator (Percival Scientific, Iowa).

Growth was monitored every other day by *in vivo* fluorescence and cell counts until particles formed. This information guided more comprehensive sampling for additional chemical and biological parameters (see further detail below) during each growth phase. *Skeletonema* sp., *Leptocylindrus* sp., and *Phaeocystis* sp. were grown for 3–4 weeks under the above conditions, sampling at the beginning of the experiment (T_0), during exponential growth (T_1), and early stationary phase (particle formation; T_2). Immediately after sampling for T_2, the remaining culture and control bottles were placed in the dark for 6 weeks to promote bacterial degradation of particles (T_3). The *Coscinodiscus* sp. experiment lasted 6 weeks with no degradation phase and was sampled at the beginning of the experiment (T_0), twice during exponential growth [early-exponential and late-exponential (T_1)], and early stationary phase (particle formation; T_2). Changes in cell densities were used to calculate specific growth rates of phytoplankton during exponential phases (Brand et al., 1981). Cell counts (mL^{-1}) were conducted using an Olympus BX53 compound microscope after preservation with acid Lugol's solution (5%) with settling volumes depending on growth phase (Utermöhl, 1958).

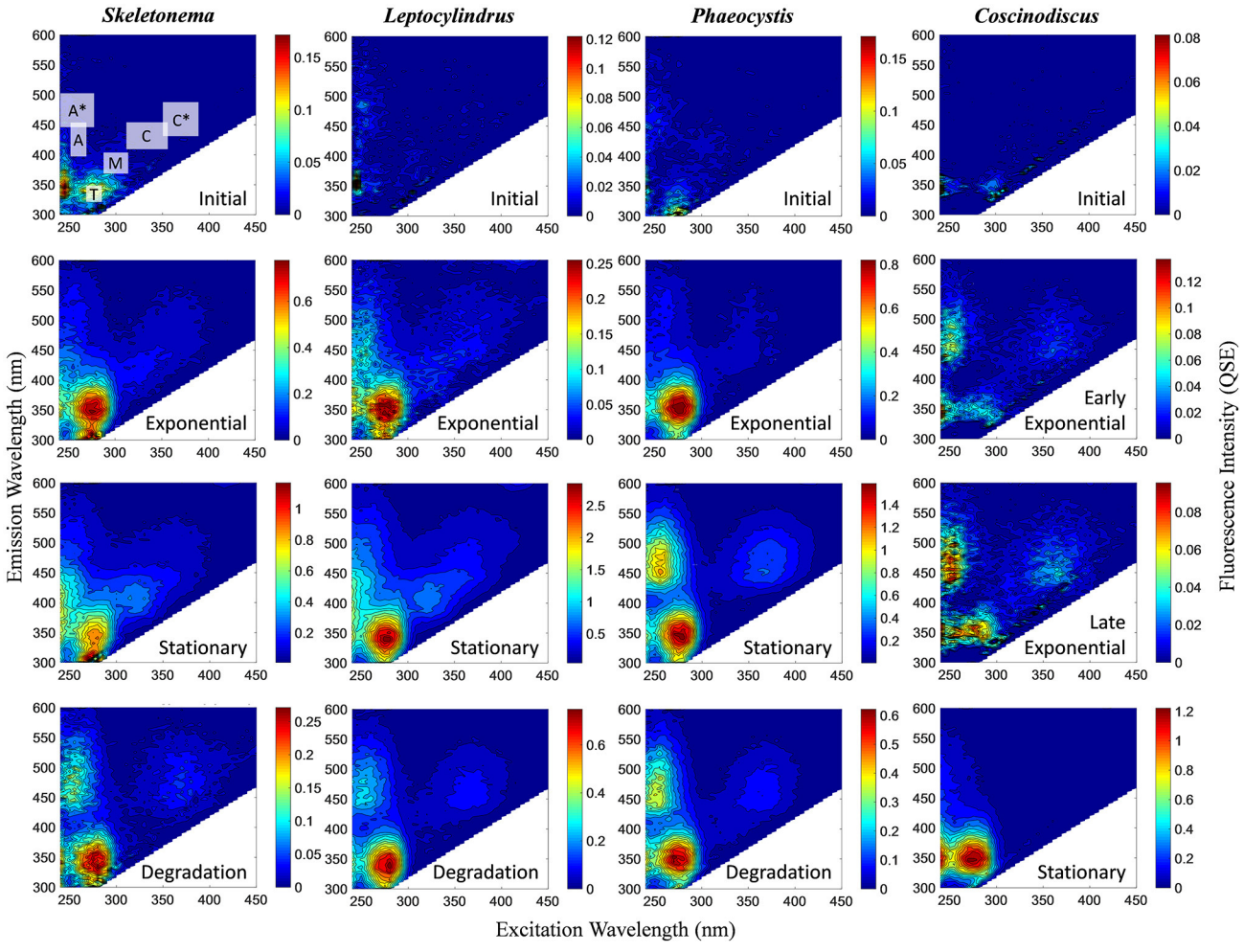

FIGURE 1 | Representative excitation-emission matrices (EEMs) of BEPOM fluorescence for genera *Skeletonema*, *Leptocylindrus*, and *Phaeocystis* at initial, exponential, stationary, and degradation phases and for *Coscinodiscus* sp. at initial, early exponential, late exponential, and stationary growth phases. Color bars are presented in quinine sulfate equivalence (QSE) where 1 QSE = 1 ppb quinine sulfate equivalents. Note different scales for color bars for each EEM. Major peak regions of EEMs are indicated in the initial time point for *Skeletonema* sp.

At each time point, three culture bottles of each organism and one control bottle (0.2 μm filtered ASW with f/20 nutrients) were sacrificed. Sample aliquots were gently vacuum filtered through pre-combusted (450°C, minimum 6 h) 0.7 μm (nominal mesh size) glass fiber filters. Filters were stored at −20°C until analyzed for particulate organic carbon (POC), POC/PON, and base-extracted POM (BEPOM) fluorescence followed by base-extracted POC (BEPOC). Filtrate was collected in polycarbonate bottles for absorbance and fluorescence and analyzed within 24 h or in pre-combusted borosilicate vials, acidified with 85% phosphoric acid (H_3PO_4) to pH 2, and stored at 4°C for dissolved organic carbon (DOC) analysis.

Optical Measurements

POM filters were base-extracted (BEPOM) in 10 mL of 0.1 M sodium hydroxide (NaOH) for 24 h at 4°C in the dark. After 24 h, extracts were neutralized with concentrated hydrochloric acid, then filtered using a 0.2 μm porosity Sterivex-GP polyethersulfone filter (EMD) (Brym et al., 2014). The filtrate was analyzed for absorbance and fluorescence in the same manner as CDOM.

Absorbance of CDOM and BEPOM was measured from 200 to 800 nm in a 1 or 10 cm quartz cell (Starna Cells, Inc.) on a Varian 300 UV spectrophotometer with ultrapure water as the reference blank for DOM samples and neutralized 0.1 M NaOH solution as the reference blank for BEPOM samples. Blank-corrected absorbance values were converted to Napierian absorption coefficients (α_λ) (Osburn et al., 2012).

CDOM and BEPOM fluorescence were measured using a Varian Eclipse spectrophotometer with excitation (Ex) from 240 to 450 nm at 5 nm intervals and emission (Em) from 300 to 600 nm every 2 nm. Samples were run with slit widths set at 5 nm for both Ex and Em modes, an integration time of 0.0125 s, scan rate of 2,400 nm m^{-1}, and at either 800 or 950 V, depending on sample response. Fluorescence measurements were corrected for excitation energy and emission detector response using correction factors supplied by the manufacturer and any inner-filter effects were corrected following Tucker et al. (1992). Final

TABLE 1 | Central regions of EEM fluorescence attributed to different sources of organic matter, modified from Coble (2007) by Stedmon and Nelson (2015).

Region	Type	Ex (nm)	Em (nm)
A	Humic-like; often characterized as terrestrial	260	400–460
M	Humic-like; often attributed to microbial processing of organic matter	290–310	370–410
C	Humic-like; often characterized as terrestrial; also found in sedimentary pore waters	320–360	420–460
T	Protein-like; spectrally similar to the amino acid tryptophan	275	340
B	Protein-like; spectrally similar to the amino acid tyrosine	275	305
N	Protein-like; spectrally similar to indole acetic acid	280	370

Ex, peak excitation wavelength(s); Em, peak emission wavelength(s).

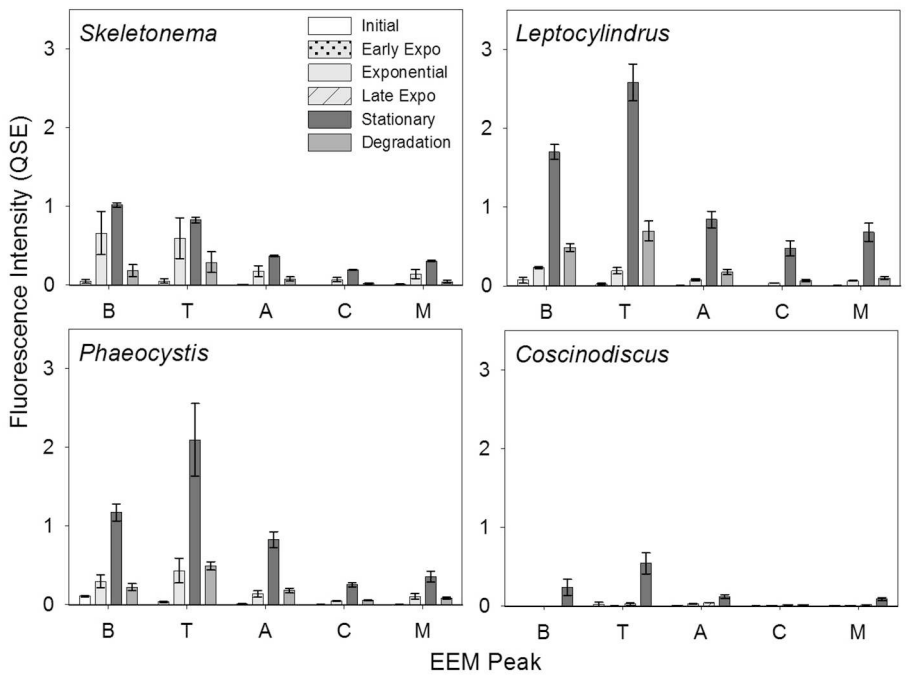

FIGURE 2 | BEPOM fluorescence intensity of Coble EEM peaks over growth and degradation for genera *Skeletonema* ($n = 3$), *Leptocylindrus* ($n = 2$–4), *Phaeocystis* ($n = 3$), and *Coscinodiscus* ($n = 3$–4). Note the different growth stages for *Coscinodiscus* sp. All data are presented as mean ± standard error.

BEPOM fluorescence values were corrected for dilution and filtration volumes and both BEPOM and CDOM values were calibrated in quinine sulfate equivalents (QSE, where 1 QSE = 1 ppb quinine sulfate) (Lawaetz and Stedmon, 2009). Fluorescence results were concatenated into excitation-emission matrices (EEMs) for visualization as contour plots. The humification index (HIX) was determined by dividing the emission intensity in the 435–480 nm region by the intensity in the 300–345 nm region (Ohno, 2002).

Carbon Concentrations and POC/PON

DOC and BEPOC (from BEPOM samples) concentrations were measured on an OI Analytical 1030D TOC analyzer in combustion mode (Lalonde et al., 2014). Prior to analysis all acidified samples were sparged with ultrahigh purity argon. DOC concentrations were blank corrected using 18.2 MΩ ultrapure Milli-Q (Millipore) water and calibrated with caffeine standards (0–5 mg C L^{-1}) and Hansell deep sea reference (DSR) water. BEPOC concentrations were blank-corrected against ultrapure water and caffeine standards ranging from 0 to 20 mg C L^{-1}. Final BEPOC concentrations were corrected for extraction volume and initial filtration volume. Filters for POC concentrations and POC/PON ratios were dried overnight at 60°C followed by flash combustion to CO_2 and N_2 using a Thermo Flash 1112 elemental analyzer with acetanilide as a standard and corrected for volume filtered.

Bacteria Abundance

Bacterial cells were enumerated by flow cytometry (Gasol and Del Giorgio, 2000). At each sampling point 1 mL of experimental or control water was fixed with 0.1% glutaraldehyde (final concentration) for 10 min at room temperature in the dark, and stored at −80°C. Prior to analysis, thawed samples were pipetted through a cell strainer (Flowmi, 70 μm porosity) and stained with SYBR Green I for 15 min on ice in the dark. Counts were performed with a FACSCalibur flow cytometer (Becton-Dickinson) using fluorescent microspheres (Molecular Probes) of 1 μm in diameter as internal size standard. Cells were enumerated according to their right angle scatter and green fluorescence using the FloJo 7.6.1 software. This method quantifies free bacteria and does not account for bacteria attached to the aggregate particles.

Hydrolytic Enzyme Activity

Hydrolytic enzyme activities were determined using L-leucine-4-methylcoumarinyl-7-amide (MCA) hydrochloride, 4-methylumbelliferyl α-D-glucopyranoside, and 4-methylumbelliferone (MUF) β-D-glucopyranoside (Sigma-Aldrich) as substrate proxies for leucine-aminopeptidase, α-glucosidase, and β-glucosidase activities, respectively (Hoppe, 1983). For each bottle and substrate proxy, 196 μL of unfiltered experimental or control water was added in duplicate to a pure-grade black 96-well plate (Brand Life Sciences) containing a single substrate proxy at saturation levels (final concentration 200 μM). Fluorescence (excitation 370 nm, emission 440 nm) was measured in a Tecan Infinite 200 Pro microplate reader immediately following the addition of the substrate and several more times over 7–20 h. The well plates were incubated in the dark at ∼20°C. MCA and MUF standard solutions prepared in ASW were used to determine hydrolysis rates. Killed controls (boiled sample water) and ultrapure water samples showed little change over the incubations.

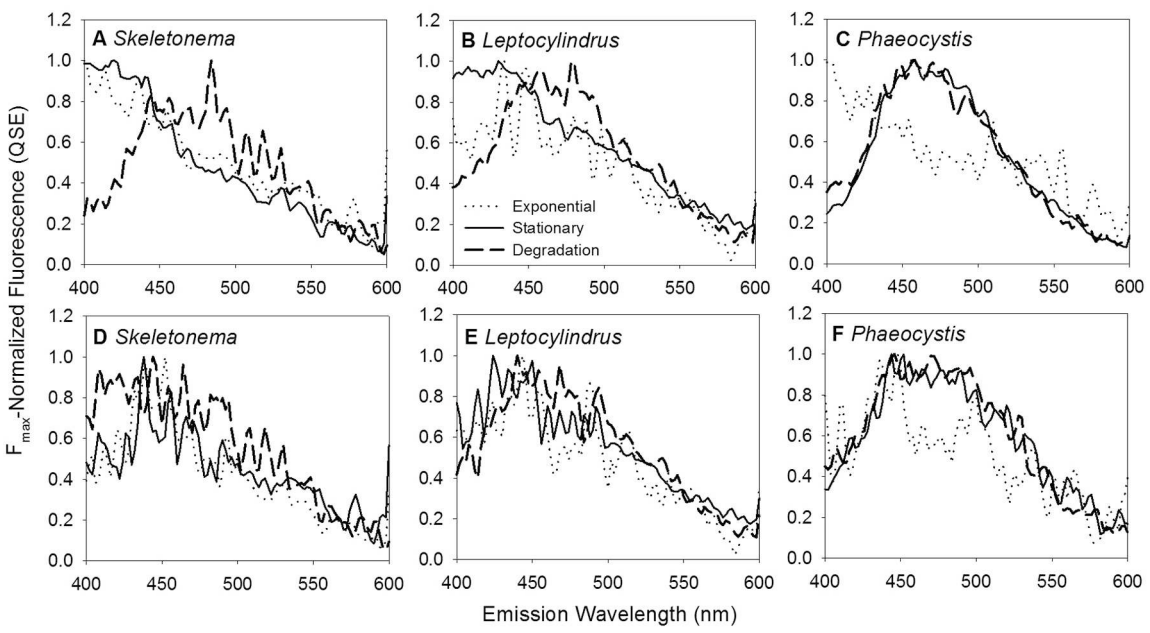

FIGURE 3 | BEPOM **(A–C)** and CDOM **(D–F)** F_{max}-normalized emission spectra at 250 nm excitation for genera *Skeletonema*, *Leptocylindrus*, and *Phaeocystis* at exponential (dotted line), stationary (solid line), and degradation (dashed line) growth phases.

Statistical Analysis

All statistical analyses were performed using SigmaPlot Version 12.5 (Systat Software Inc.). Results were not normally distributed thus non-parametric Spearman correlation coefficients (r) were computed to examine relationships between all variables. An α-value of $\leq$0.05 was used for all statistical analyses.

RESULTS

Phytoplankton Growth

Exponential growth (T_1) was reached within 15–23 days in all experiments. Specific growth rates (μ) for each of the strains were 0.25 d^{-1} for *Skeletonema* sp., 0.21 d^{-1} for *Leptocylindrus* sp., 0.17 d^{-1} for *Phaeocystis* sp., and 0.11 d^{-1} for *Coscinodiscus* sp. Macroscopic particles formed within 3–8 days of the onset of exponential growth. Particle characteristics varied for each organism, from lightly aggregated particles for *Skeletonema* sp., to small well suspended particles for *Leptocylindrus* and *Phaeocystis* spp. *Coscinodiscus* sp. aggregates started out stringy and suspended becoming rounded, dense aggregates over time.

Fluorescence Characteristics

BEPOM samples for genera *Skeletonema*, *Leptocylindrus*, and *Phaeocystis* during exponential growth (T_1) were dominated by low-intensity fluorescence (<0.15 QSE) in the region of 275/340 (excitation/emission, peak T) with additional diffuse secondary emission occurring in the regions of 260/400–460 (peak A) and 320–360/420–460 (peak C) (**Figures 1**, **2**, **Table 1**). BEPOM peaks A and C became more distinct and shifted to longer wavelengths over the duration of the experiment (**Figure 3**). Peak A red-shifted in emission wavelengths to 260/440–500 (peak A*) and peak C red-shifted in both excitation and emission to 350–400/450–500 (peak C*), resulting in a

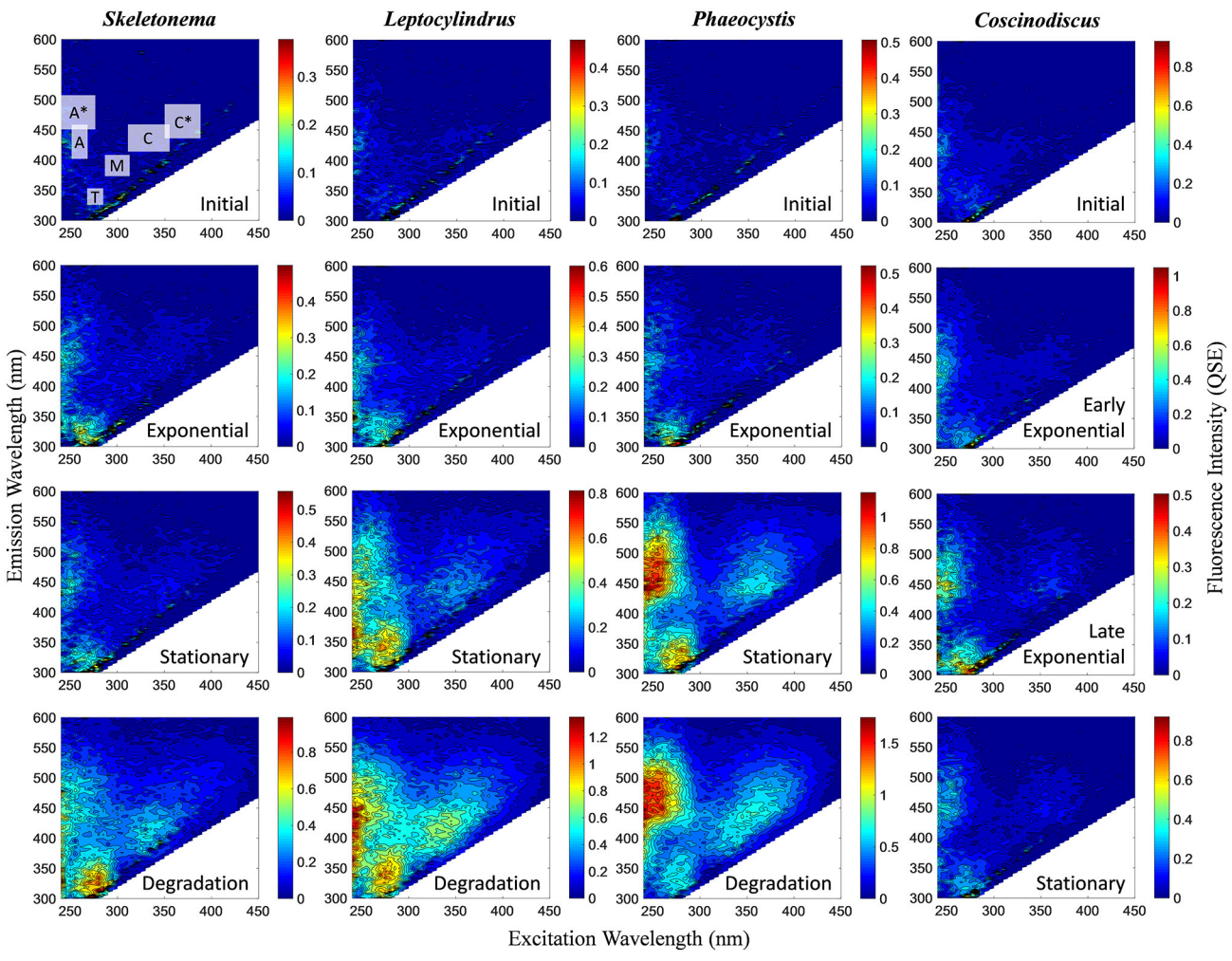

FIGURE 4 | Representative excitation-emission matrices (EEMs) of CDOM fluorescence for genera *Skeletonema*, *Leptocylindrus*, and *Phaeocystis* at initial, exponential, stationary, and degradation phases and for *Coscinodiscus* sp. at initial, early exponential, late exponential, and stationary growth phases. Color bars are presented in quinine sulfate equivalence (QSE) where 1 QSE = 1 ppb quinine sulfate equivalents. Note different scales for color bars for each EEM. Major peak regions of EEMs are indicated in the initial time point for *Skeletonema* sp.

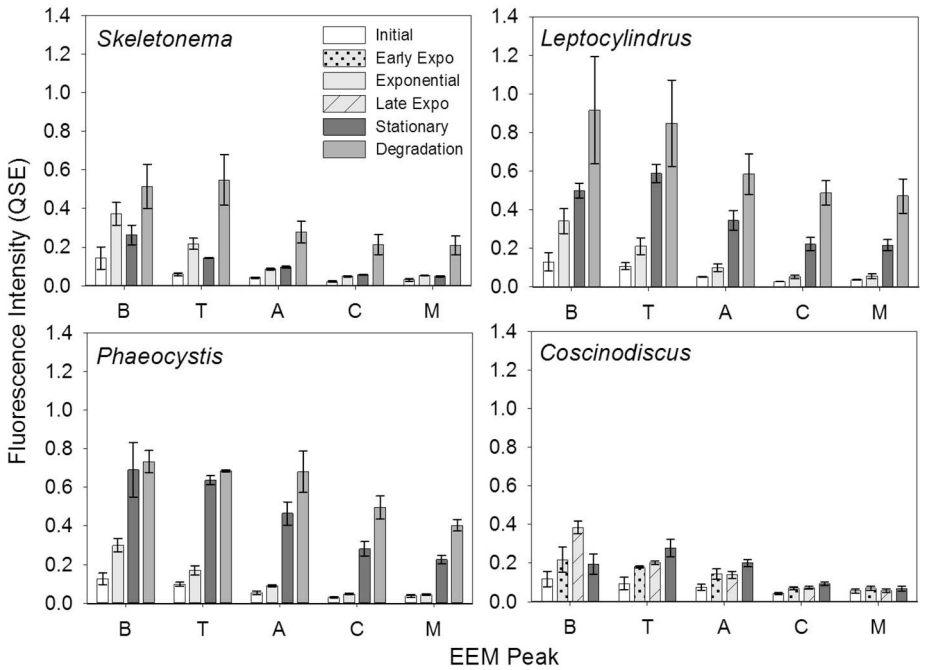

FIGURE 5 | CDOM fluorescence intensity of Coble EEM peaks over growth and degradation for genera *Skeletonema* ($n = 3$), *Leptocylindrus* ($n = 2$–4), *Phaeocystis* ($n = 3$), and *Coscinodiscus* ($n = 3$–4). Note the different growth stages for *Coscinodiscus* sp. All data are presented as mean ± standard error.

TABLE 2 | Spearman correlation coefficient (r) between select CDOM fluorescence peaks and select BEPOM fluorescence peaks (T, M, A, and C) for all data ($n = 12$) and excluding degradation phase data in parenthesis ($n = 9$).

	CDOM							
	T		**M**		**A**		**C**	
	r	***p***	***r***	***p***	***r***	***p***	***r***	***p***
SKELETONEMA								
BEPOM T	0.29 (**0.67**)	0.35 (**0.04**)	0.20 (0.53)	0.53 (0.12)	0.30 (0.63)	0.33 (0.06)	0.38 (**0.77**)	0.22 (**0.01**)
BEPOM M	0.20 (0.45)	0.53 (0.20)	0.18 (0.48)	0.57 (0.17)	0.44 (**0.82**)	0.22 (**0.00**)	0.45 (**0.93**)	0.14 (**0.00**)
BEPOM A	0.25 (0.45)	0.42 (0.20)	0.23 (0.48)	0.46 (0.17)	0.44 (**0.82**)	0.14 (**0.00**)	0.50 (**0.93**)	0.09 (**0.00**)
BEPOM C	0.28 (0.48)	0.36 (0.17)	0.23 (0.43)	0.46 (0.22)	0.44 (**0.82**)	0.11 (**0.00**)	0.55 (**0.93**)	0.06 (**0.00**)
LEPTOCYLINDRUS								
BEPOM T	**0.82** (**0.97**)	**0.00** (**0.00**)	**0.69** (**0.97**)	**0.01** (**0.00**)	**0.74** (**0.93**)	**0.00** (**0.00**)	**0.66** (**0.90**)	**0.02** (**0.00**)
BEPOM M	**0.79** (**0.90**)	**0.00** (**0.00**)	**0.64** (**0.85**)	**0.02** (**0.00**)	**0.66** (**0.78**)	**0.02** (**0.01**)	**0.60** (**0.77**)	**0.04** (**0.01**)
BEPOM A	**0.77** (**0.88**)	**0.00** (**0.00**)	**0.59** (**0.83**)	**0.04** (**0.00**)	**0.62** (**0.77**)	**0.03** (**0.01**)	0.55 (**0.75**)	0.06 (**0.02**)
BEPOM C	**0.76** (**0.83**)	**0.00** (**0.00**)	**0.57** (**0.78**)	**0.05** (**0.01**)	**0.65** (**0.82**)	**0.02** (**0.00**)	**0.59** (**0.83**)	**0.04** (**0.00**)
PHAEOCYSTIS								
BEPOM T	**0.68** (**0.88**)	**0.01** (**0.00**)	0.56 (**0.70**)	0.05 (**0.03**)	**0.65** (**0.85**)	**0.02** (**0.00**)	**0.66** (**0.88**)	**0.02** (**0.00**)
BEPOM M	**0.70** (**0.90**)	**0.01** (**0.00**)	**0.62** (**0.73**)	0.03 (**0.02**)	**0.70** (**0.88**)	**0.01** (**0.00**)	**0.70** (**0.90**)	**0.01** (**0.00**)
BEPOM A	**0.71** (**0.93**)	**0.01** (**0.00**)	**0.65** (**0.82**)	**0.02** (**0.00**)	**0.72** (**0.92**)	**0.01** (**0.00**)	**0.71** (**0.93**)	**0.01** (**0.00**)
BEPOM C	**0.66** (**0.90**)	**0.02** (**0.00**)	0.57 (**0.73**)	0.05 (**0.02**)	**0.65** (**0.88**)	**0.02** (**0.00**)	**0.66** (**0.90**)	**0.02** (**0.00**)
COSCINODISCUS								
BEPOM T	0.46	0.11	−0.06	0.84	0.54	0.05	**0.56**	**0.05**
BEPOM M	**0.70**	**0.01**	0.16	0.59	**0.78**	**0.00**	**0.77**	**0.00**
BEPOM A	**0.71**	**0.01**	0.18	0.55	**0.82**	**0.00**	**0.84**	**0.00**
BEPOM C	**0.62**	**0.02**	0.06	0.84	**0.71**	**0.01**	**0.72**	**0.00**

Values of r are significant at p-values ≤ 0.05 (values in bold). Coscinodiscus sp. data only for initial through stationary phase, no degradation phase data available.

three-peak pattern with peak T over growth and degradation. For example, BEPOM peak A emission fluorescence in *Skeletonema* sp. occurred at 400–410 nm for exponential and stationary growth phases but shifted to longer wavelengths (∼490 nm) after 6 weeks of degradation (**Figure 3**). *Coscinodiscus* sp. showed only faint secondary emission during both exponential growth samplings, but still followed the three-peak pattern observed in the other cultures. By stationary phase (T_2), *Coscinodiscus* sp. had minimal secondary emission in the region of peaks C and C*. Maximum fluorescence for all fluorescent peaks occurred during stationary phase (T_2) with a sharp decrease (ca. 70%) over the 6 weeks of degradation (T_3, **Figures 1**, **2**).

In contrast to the distinct fluorophores in the BEPOM samples, CDOM samples from exponential growth (T_1) had low (<0.3 QSU), unstructured fluorescence with slightly enhanced fluorescence in the region of peak T and B (275/305), most commonly associated with protein-like fluorescence (**Figures 4**, **5**, **Table 1**). Higher overall fluorescence intensities occurred during stationary (T_2) and degradation (T_3) phases and demonstrated a three-peak pattern similar to the BEPOM samples, though CDOM maximum fluorescence intensities were about half of BEPOM maximum fluorescence intensities. While CDOM shared the three-peak features observed in the BEPOM, the three peaks were much broader and less distinct in CDOM than in BEPOM and increased in fluorescence throughout growth and degradation for all areas of fluorescence (**Figures 4**, **5**). Overall, CDOM fluorescence patterns were similar between all the phytoplankton species, with peaks A and T being the most prominent. CDOM peaks A and C were significantly correlated with BEPOM peaks A and C for many of the cultures, and all were significantly correlated when degradation (T_3) time points were excluded (**Table 2**).

The humification index (HIX) is a florescence index of the degree of organic matter degradation, with higher values characteristic of higher molecular weight, aromatic compounds (Huguet et al., 2009). CDOM HIX values increased over the duration of the experiment for all of the cultures, whereas BEPOM HIX values were more variable with no clear trend among the cultures (**Figure 6**).

Carbon Concentrations and POC/PON

Carbon concentrations were similar between all three carbon pools (particulate, base-extracted, and dissolved) for all four cultures (**Figure 7**, **Table 3**). In general all carbon concentrations increased through stationary phase and decreased over the 6 weeks of degradation. The exception to this was *Phaeocystis* sp. DOC concentrations that leveled off between stationary and degradation phases, and for *Coscinodiscus* sp. which did not include a degradation stage. The largest increase occurred in the particulate pool with POC increasing between initial (T_0) and stationary phase (T_2) by 1.56 mg C L^{-1} for genera *Skeletonema* and 5.08 mg C L^{-1} for *Leptocylindrus*. For base-extracted POC, *Phaeocystis* sp. had the smallest increase (0.33 mg C L^{-1}) compared to *Leptocylindrus* sp. (1.33 mg C L^{-1}) over the experiment. DOC concentrations had a similar range, with *Coscinodiscus* sp. increasing by 0.29 mg C L^{-1} and *Leptocylindrus* sp. increasing by 1.14 mg C L^{-1} between initial (T_0) and stationary phase (T_2).

Base-extraction efficiencies (BEPOC concentration divided by POC concentration times 100) varied between 4 and 88%, with *Leptocylindrus* sp. having a slightly narrower range (4–36%) (**Table 3**). These extraction efficiencies were consistent with those reported in Brym et al. (2014). Greater extraction efficiencies occurred earlier in growth (e.g., exponential phase 21–78%) and decreased with the duration of the experiment with the lowest extraction efficiencies occurring after 6 weeks of degradation (4–24%, T_3). Overall BEPOC concentration was correlated to POC concentration ($r = 0.75$, $p < 0.001$).

POC/PON ratios ranged from 5.2 to 10.9 for time points between exponential (T_1) and degradation growth phases (T_3) (**Table 3**). Higher POC/PON ratios occurred for *Leptocylindrus* sp. (6.9–9.6) and *Coscinodiscus* sp. (6.9–10.9), while *Skeletonema* sp. (6.7–7.2) and *Phaeocystis* sp. (5.2–6.8) had slightly lower POC/PON ratios; however, these differences were not significant.

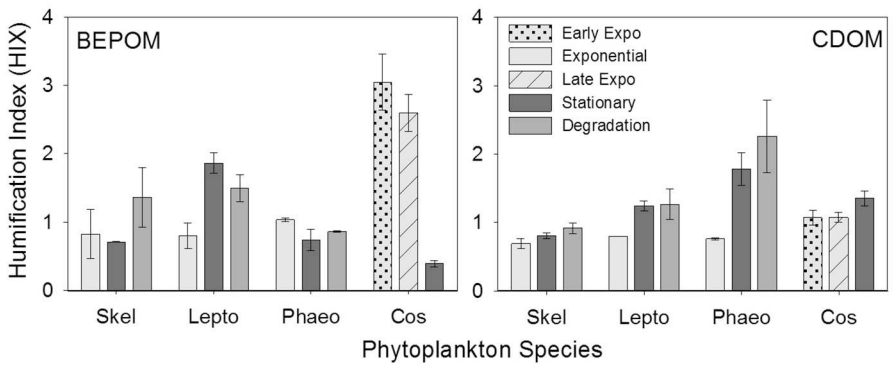

FIGURE 6 | Humification index (HIX) for BEPOM and CDOM for genera *Skeletonema* (Skel, $n = 3$), *Leptocylindrus* (Lepto, $n = 2$–4), *Phaeocystis* (Phaeo, $n = 3$), and *Coscinodiscus* (Cos, $n = 3$–4). Note the different growth stages for *Coscinodiscus*. All data are presented as mean ± standard error. Ratios from the initial time point were excluded due to low fluorescence at this stage.

Bacterial Abundance and Activities

Bacterial Cell Counts

The greatest increase in bacterial cell numbers occurred for genera *Phaeocystis* and *Leptocylindrus*, which had maximum bacterial cell numbers during stationary phase of growth (T_2), reaching 5.5 ± 2.4 × 10^6 cells mL^{-1} and 4.3 ± 1.0 × 10^6 cells mL^{-1}, respectively (**Figure 8**, **Table 3**). By the end of the 6 weeks of degradation (T_3), bacterial cell numbers decreased by nearly half to 3.6 ± 0.7 × 10^6 cells mL^{-1} and 2.4 ± 0.5 × 10^6 cells mL^{-1}, respectively. Bacterial cell numbers in the *Skeletonema* culture increased throughout the growth experiment, but only increased from 0.02 × 10^6 at the initial sampling (T_0) to 1.0 × 10^6 during degradation (T_3). The *Coscinodiscus* culture had the lowest overall bacterial cell numbers, only reaching 0.2 × 10^6 cells mL^{-1} during stationary growth (T_2).

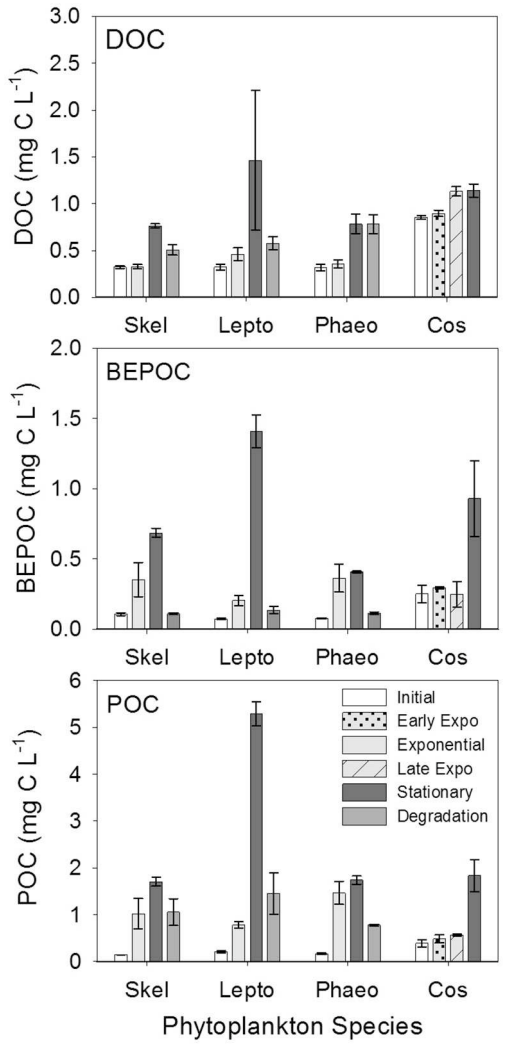

FIGURE 7 | Dissolved (DOC), base-extracted particulate (BEPOC), and particulate (POC) organic carbon concentrations for genera *Skeletonema* (Skel, $n = 3$), *Leptocylindrus* (Lepto, $n = 2$–4), *Phaeocystis* (Phaeo, $n = 3$), and *Coscinodiscus* (Cos, $n = 3$–4). Samples were collected at initial, exponential, stationary, and after 6 weeks of degradation, except for *Coscinodiscus* sp. which had time points collected at initial, early exponential, late exponential, and stationary phases of growth. All data are presented as mean ± standard error.

Hydrolytic Enzyme Activities

Aminopeptidase enzyme activities were typically three to five orders of magnitude higher than either glucosidase activities, with the *Phaeocystis* culture having the highest activities during stationary phase (T_2, **Figure 8**, **Table 3**). Activities of β-glucosidase were typically a factor of two greater than α-glucosidase activities, except for *Phaeocystis* sp. which had β-glucosidase activities a factor of six to seven higher than α-glucosidase. Due to sampling constraints, no data was available for late-exponential (second T_1) or stationary (T_2) phases for *Coscinodiscus* spp.

Enzyme activities were highly correlated to fluorescent components, especially for glucosidase activities with genera *Leptocylindrus* and *Phaeocystis* and for aminopeptidase with *Skeletonema* sp. (**Table 4**). α- and β-glucosidase activities were also correlated to all carbon concentrations for genera *Leptocylindrus* and *Phaeocystis*.

DISCUSSION

Formation of CDOM by Marine Plankton in Culture

Previous laboratory experiments have relied on high nutrients (e.g., Rochelle-Newall and Fisher, 2002; Romera-Castillo et al., 2010) or additions of carbon substrates (e.g., Gruber et al., 2006; Goto et al., 2017) to observe CDOM formation by phytoplankton and/or bacteria. In our experiments, we produced CDOM fluorescence and phytoplankton densities on the same magnitude as open ocean waters using moderate nutrient additions and rotating bottles to keep cells in suspension. Using this approach, our maximum CDOM fluorescence for all cultures was low and ranged between 0.5 and 2 QSE (**Figure 4**), comparable to fluorescence intensities in several oceanic regions (0.5–6 QSE) (Nelson and Gauglitz, 2016; Netburn et al., in press). Additionally, trans-oceanic Pacific and Atlantic CDOM fluorescence ranged between 0.1 and 1 QSE for humic-like components and 0.1 to 11 QSE for protein-like components when data was modeled by parallel factor analysis (PARAFAC) (Murphy et al., 2008). Together, our results and previously published data, demonstrate that fluorescence intensities produced in culture experiments are similar to oceanic fluorescence intensities, even allowing for instrument variability. The low fluorescence intensities produced further suggest future culture experiments should use media with minimal background fluorescence to observe the low CDOM production by plankton.

Base-extraction of chromophoric and fluorophoric material from marine particles is a relatively new way to analyze POM and allowed for direct comparison between the two organic matter pools. The available field studies have been conducted in estuaries and coastal waters, but show remarkable consistency in BEPOM fluorescence. Overall fluorescence was low, typically

TABLE 3 | Bacteria abundance, hydrolytic enzyme activities (α-glucosidase, β-glucosidase, and aminopeptidase), dissolved (DOC), base-extracted (BEPOC), and particulate (POC) organic carbon concentrations, particulate organic carbon to nitrogen ratios (POC/PON), and BEPOM extraction efficiencies for the four phytoplankton cultures and associated controls.

Phytoplankton, time point (day)	*n*	Bacteria abundance ($\times 10^5$ cells mL^{-1})	α-Glu (nM h^{-1})	β-Glu (nM h^{-1})	Aminopeptidase (nM h^{-1})	DOC (mg C L^{-1})	BEPOC (mg C L^{-1})	POC (mg C L^{-1})	POC/PON	BEPOM extraction efficiency (%)
SKELETONEMA										
Initial (0)	3	0.2 ± 0.0*	0.001 ± 0.000†	0.001 ± 0.000†	21 ± 0**	0.32 ± 0.01	0.11 ± 0.01	0.15 ± 0.00	7.0 ± 0.0*	73 ± 7
Exponential (15)	3	4.0 ± 0.2	0.011 ± 0.000†	0.019 ± 0.001	207 ± 7	0.33 ± 0.02	0.35 ± 0.12	1.03 ± 0.33	6.7 ± 0.1	33 ± 2
Stationary (23)	3	8.0 ± 0.2	0.007 ± 0.000†	0.013 ± 0.000†	419 ± 10	0.77 ± 0.02	0.69 ± 0.03	1.71 ± 0.10	7.2 ± 0.3	40 ± 2
Degradation (65)	3	9.5 ± 1.4	0.041 ± 0.001	0.111 ± 0.000†	428 ± 6	0.51 ± 0.05	0.11 ± 0.01	1.06 ± 0.29	6.8 ± 0.3	12 ± 4
LEPTOCYLINDRUS										
Initial (0)	3	0.8 ± 0.0*	0.009 ± 0.001	0.013 ± 0.001	127 ± 4	0.32 ± 0.03	0.07 ± 0.01	0.22 ± 0.02	8.0 ± 1.0	34 ± 1
Exponential (23)	2	4.2 ± 0.4	0.011 ± 0.000†	0.027 ± 0.000†	133 ± 1	0.46 ± 0.07	0.21 ± 0.04	0.78 ± 0.07	7.3 ± 0.6	26 ± 2
Stationary (31)	4	43.0 ± 4.9	0.579 ± 0.009	1.092 ± 0.008	262 ± 10	1.46 ± 0.75	1.41 ± 0.12	5.30 ± 0.26	9.6 ± 0.2	27 ± 2
Degradation (72)	3	23.7 ± 3.0	0.208 ± 0.003	0.316 ± 0.020	690 ± 5	0.58 ± 0.07	0.14 ± 0.03	1.45 ± 0.44	6.9 ± 0.8	13 ± 6
PHAEOCYSTIS										
Initial (0)	3	1.2 ± 0.0	0.011 ± 0.000†	0.063 ± 0.001	103 ± 1	0.32 ± 0.04	0.08 ± 0.00	0.17 ± 0.01	10.4 ± 0.6	45 ± 1
Exponential (15)	3	4.2 ± 0.02	0.051 ± 0.000†	0.302 ± 0.002	863 ± 6	0.36 ± 0.04	0.36 ± 0.10	1.47 ± 0.25	6.8 ± 0.4	24 ± 2
Stationary (23)	3	55.1 ± 13.8	0.324 ± 0.009	1.802 ± 0.011	5593 ± 53	0.78 ± 0.11	0.41 ± 0.01	1.74 ± 0.09	5.2 ± 0.3	24 ± 1
Degradation (65)	3	36.3 ± 4.0	0.108 ± 0.004	0.728 ± 0.005	558 ± 5	0.78 ± 0.10	0.11 ± 0.01	0.78 ± 0.02	5.7 ± 0.0*	15 ± 1
***SKELETONEMA, LEPTOCYLINDRUS*, AND *PHAEOCYSTIS* CONTROLS**										
Initial (0)	1	0.2	0.000 ± 0.000†	0.000 ± 0.000†	8 ± 1	0.31	0.12	0.30	14.0	40
Exponential (15)	1	0.5	0.000 ± 0.000†	0.000 ± 0.000†	11 ± 0**	0.30	0.08	0.18	12.9	47
Expo/Stat (23)	1	1.8	0.003 ± 0.003	0.000 ± 0.000†	21 ± 2	0.35	0.10	0.20	10.4	47
Stationary (31)	1	2.7	0.001 ± 0.000†	0.000 ± 0.000†	0 ± 0**	0.37	0.12	0.23	9.3	52
Degradation (65)	1	2.0	0.001 ± 0.000†	0.002 ± 0.000†	42 ± 1	0.28	0.19	0.22	13.3	89
Degradation (72)	1	3.3	0.003 ± 0.000†	0.008 ± 0.000†	76 ± 3	0.39	0.07	0.16	8.0	44
COSCINODISCUS										
Initial (0)	3	0.2 ± 0.0*	0.001 ± 0.000†	0.001 ± 0.000†	16 ± 1	0.85 ± 0.02	0.25 ± 0.06	0.39 ± 0.08	16.3 ± 4.0	72 ± 23
Early Expo (21)	3	1.5 ± 0.2	0.017 ± 0.001	0.022 ± 0.001	150 ± 12	0.90 ± 0.03	0.30 ± 0.01	0.48 ± 0.09	8.9 ± 2.2	65 ± 11
Late Expo (25)	3	1.1 ± 0.1	ND	ND	ND	1.13 ± 0.05	0.25 ± 0.09	0.57 ± 0.02	6.9 ± 0.5	43 ± 16
Stationary (42)	4	1.9 ± 0.1	ND	ND	ND	1.14 ± 0.07	0.93 ± 0.27	1.84 ± 0.34	10.9 ± 2.2	48 ± 6
***COSCINODISCUS* CONTROLS**										
Initial (0)	1	0.2	0.008 ± 0.001	0.011 ± 0.000†	0 ± 0**	0.89	0.22	0.33	15.3	68
Early Expo (21)	1	4.0	0.000 ± 0.001	0.000 ± 0.000†	4 ± 1	0.90	0.20	0.31	5.9	66
Late Expo (25)	1	2.5	ND	ND	ND	0.84	0.35	0.39	7.6	90
Stationary (42)	1	0.4	ND	ND	ND	0.94	0.34	0.36	9.1	95

All data are presented as mean ± standard error.

Controls were single bottles for each time point for either the Skeletonema, Leptocylindrus, and Phaeocystis experiment or the Coscinodiscus experiment so no standard error is presented for those measurements.

**Value < 0.05; † value < 0.0005; **value < 0.5; ‡ value < 0.005.*

less than 0.25 QSE, with maximum fluorescence corresponding to chlorophyll maxima and decreasing with depth (Brym et al., 2014; Ziervogel et al., 2016; Netburn et al., in press). For our cultures, maximum BEPOM fluorescence ranged between 0.4 and 3 QSE during stationary phase and decreased to 0.1–0.9 QSE during degradation (**Figure 1**). The elevated BEPOM fluorescence in cultures relative to natural samples was likely the result of measuring the cultures at the peak of phytoplankton biomass in a controlled environment compared to natural phytoplankton blooms that have more complex growth dynamics and influenced by other processes such as aggregation, grazing, and hydrodynamics.

Spectral Properties of Phytoplankton-Derived CDOM and BEPOM

All four monocultures produced a three-peak pattern that was dominated by discrete BEPOM fluorophores, suggestive of distinct compounds such as aromatic amino acids (**Figure 1**). This three-peak pattern has been described previously in natural BEPOM samples of estuarine (Brym et al., 2014) and oceanic (Ziervogel et al., 2016; Netburn et al., in press) origin. The prominence of the protein-like peak strongly resembles tryptophan, which has been shown to be dominant during phytoplankton growth (Stedmon and Markager, 2005; Murphy et al., 2008; Jørgensen et al., 2011). Distinct fluorescence in the region of peaks A and C have been attributed to fluorophores present in derivatives of benzoic acids (including phenols) and flavins, respectively (Wolfbeis, 1985; Wünsch et al., 2015). Other possibilities include siderophores (Fukuzaki et al., 2014). More generally, peaks A and C have previously been attributed to, and are abundant in, terrestrially-derived humic substances. Given our algal growth medium lacked material of terrestrial origin, as it was prepared with artificial seawater with f/20 nutrients, the observed formation and subsequent red-shift of peaks A and C were likely the result of microbially-transformed planktonic material rather than terrestrially-derived fluorescence.

CDOM fluorescence showed similar peak regions to BEPOM, but were generally broader and unstructured in emission and increased through growth and degradation phases (**Figure 4**). We interpret these findings to suggest that degradation processes occurred on the algal-derived material once in the dissolved phase. In previous studies, CDOM generated in phytoplankton and bacterial cultures showed similar fluorescence patterns to those presented here. Culture work on diatoms, dinoflagellates, and prasinophytes illustrated CDOM production by phytoplankton at intensities observed in the ocean (Romera-Castillo et al., 2010). Fukuzaki et al. (2014) presented EEM spectra measured on DOM from axenic diatoms, dinoflagellates, chlorophytes, cryptophytes, haptophytes, and raphidophytes monocultures. Though the dominant fluorophores differed between individual species, the ubiquitous fluorescence patterns produced overall by a range of genera further supports planktonic-sources of open

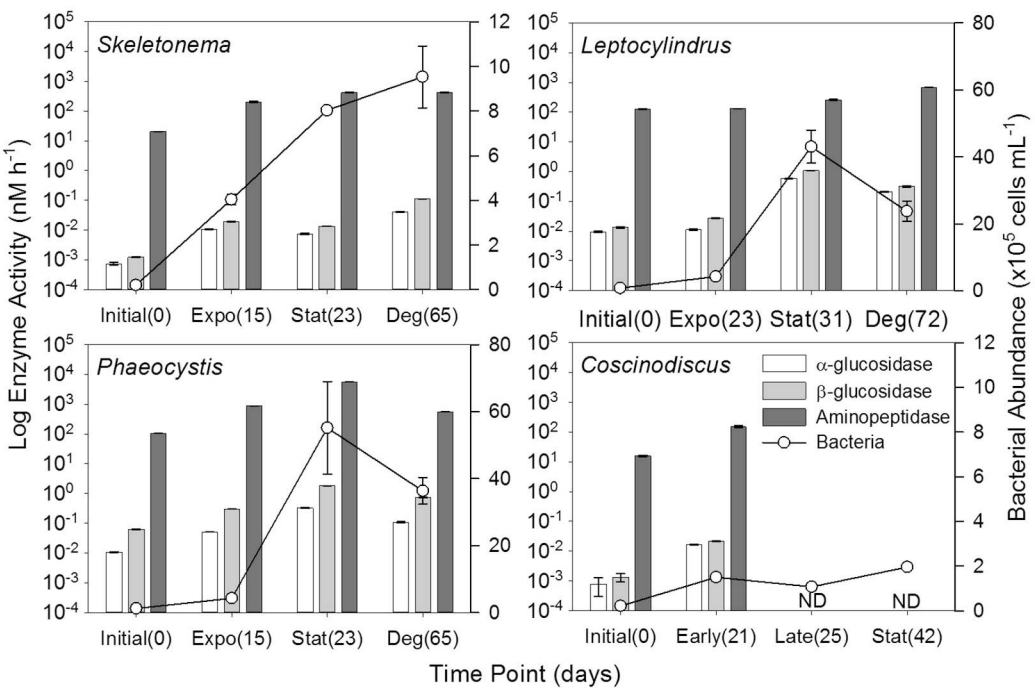

FIGURE 8 | Hydrolytic enzyme activities (α-glucosidase, β-glucosidase, and aminopeptidase) and bacterial abundance for genera *Skeletonema* ($n = 3$), *Leptocylindrus* ($n = 2$–4), *Phaeocystis* ($n = 3$), and *Coscinodiscus* ($n = 3$–4). Samples were collected at initial, exponential (Expo), stationary (Stat), and after 6 weeks of degradation (Deg), except for *Coscinodiscus* sp. which had time points collected at initial and early exponential (Early); no enzyme activity data (ND) were available for late exponential (Late) and stationary. The number of days following inoculation are given in parentheses. All data are presented as mean ± standard error.

TABLE 4 | Spearman correlation coefficient (*r*) between bacterial abundance or enzyme activity and DOC, BEPOC, POC and select BEPOM and CDOM fluorescence peaks (T, M, A, and C).

	DOC		BEPOC		POC		BEPOM								CDOM							
							T		M		A		C		T		M		A		C	
	r	*p*	*r*	*p*	*r*	*p*	*r*	*p*	*r*	*p*	*r*	*p*	*r*	*p*	*r*	*p*	*r*	*p*	*r*	*p*	*r*	*p*
BACTERIAL ABUNDANCE																						
Skeletonema	**0.76**	**0.00**	0.34	0.26	**0.71**	**0.01**	0.41	0.17	0.50	0.09	0.57	0.05	**0.60**	**0.04**	0.57	0.05	**0.63**	**0.03**	**0.85**	**0.00**	**0.88**	**0.00**
Leptocylindrus	**0.84**	**0.00**	**0.76**	**0.00**	**0.81**	**0.00**	**0.92**	**0.00**	**0.84**	**0.00**	**0.84**	**0.00**	**0.84**	**0.00**	**0.84**	**0.00**	**0.74**	**0.00**	**0.83**	**0.00**	**0.76**	**0.00**
Phaeocystis	**0.77**	**0.00**	**0.57**	**0.05**	**0.59**	**0.04**	**0.82**	**0.00**	**0.83**	**0.00**	**0.85**	**0.00**	**0.86**	**0.00**	**0.80**	**0.00**	**0.76**	**0.00**	**0.79**	**0.00**	**0.80**	**0.00**
Coscinodiscus	0.54	0.05	**0.56**	**0.04**	**0.76**	**0.00**	**0.60**	**0.03**	**0.69**	**0.01**	**0.84**	**0.00**	**0.77**	**0.00**	0.65	0.02	0.41	0.16	**0.80**	**0.00**	**0.76**	**0.00**
α-GLUCOSIDASE																						
Skeletonema	0.36	0.23	0.14	0.65	0.41	0.18	0.37	0.22	0.32	0.31	0.38	0.22	0.42	0.17	**0.91**	**0.00**	**0.88**	**0.00**	**0.87**	**0.00**	**0.88**	**0.00**
Leptocylindrus	**0.84**	**0.00**	**0.75**	**0.00**	**0.83**	**0.00**	**0.92**	**0.00**	**0.85**	**0.00**	**0.83**	**0.00**	**0.83**	**0.00**	**0.83**	**0.00**	**0.73**	**0.01**	**0.81**	**0.00**	**0.76**	**0.00**
Phaeocystis	**0.77**	**0.00**	**0.69**	**0.01**	**0.67**	**0.02**	**0.93**	**0.00**	**0.94**	**0.00**	**0.95**	**0.00**	**0.94**	**0.00**	**0.73**	**0.01**	**0.65**	**0.02**	**0.73**	**0.01**	**0.73**	**0.01**
Coscinodiscus	0.66	0.18	0.09	0.92	0.26	0.66	0.37	0.50	0.54	0.30	**0.99**	**0.00**	**1.00**	**0.00**	0.66	0.18	0.43	0.42	0.77	0.10	0.83	0.06
β-GLUCOSIDASE																						
Skeletonema	0.42	0.17	0.12	0.70	0.49	0.10	0.44	0.14	0.37	0.22	0.42	0.17	0.43	0.15	**0.89**	**0.00**	**0.83**	**0.00**	**0.85**	**0.00**	**0.87**	**0.00**
Leptocylindrus	**0.84**	**0.00**	**0.76**	**0.00**	**0.81**	**0.00**	**0.92**	**0.00**	**0.84**	**0.00**	**0.81**	**0.00**	**0.81**	**0.00**	**0.84**	**0.00**	**0.74**	**0.00**	**0.83**	**0.00**	**0.76**	**0.00**
Phaeocystis	**0.78**	**0.00**	**0.69**	**0.01**	**0.66**	**0.02**	**0.94**	**0.00**	**0.94**	**0.00**	**0.96**	**0.00**	**0.95**	**0.00**	**0.74**	**0.00**	**0.66**	**0.02**	**0.73**	**0.01**	**0.74**	**0.00**
Coscinodiscus	0.66	0.18	0.09	0.92	0.26	0.66	0.37	0.50	0.54	0.30	**0.99**	**0.00**	**1.00**	**0.00**	0.66	0.18	0.43	0.42	0.77	0.10	0.83	0.06
AMINOPEPTIDASE																						
Skeletonema	**0.79**	**0.00**	0.50	0.09	**0.80**	**0.00**	**0.66**	**0.02**	**0.72**	**0.01**	**0.73**	**0.01**	**0.72**	**0.01**	**0.63**	**0.03**	**0.66**	**0.02**	**0.83**	**0.00**	**0.86**	**0.00**
Leptocylindrus	0.48	0.11	0.01	0.97	0.11	0.72	0.10	0.75	0.27	0.39	0.20	0.53	0.13	0.68	0.34	0.26	0.51	0.08	0.51	0.08	**0.59**	**0.04**
Phaeocystis	0.50	0.09	**0.85**	**0.00**	**0.84**	**0.00**	**0.91**	**0.00**	**0.90**	**0.00**	**0.87**	**0.00**	**0.87**	**0.00**	0.50	0.09	0.33	0.28	0.47	0.12	0.48	0.11
Coscinodiscus	0.49	0.36	0.60	0.24	0.14	0.80	−0.09	0.92	0.14	0.80	**0.90**	**0.02**	0.83	0.06	0.83	0.06	0.83	0.06	**0.94**	**0.02**	**1.00**	**0.00**

Values of r are significant at p-values ≤ 0.05 (values in bold). For all relationships n = 12, except for Coscinodiscus enzyme activities, where n = 6 since no data were available for the last two time points of that experiment.

ocean CDOM. However, these studies were only able to suggest that CDOM was formed contemporaneously with plankton growth as no fluorescence measurements on POM material were performed (Romera-Castillo et al., 2010; Fukuzaki et al., 2014). Additionally, these previous studies as well as our own still show elevated fluorescence in the regions of peaks A, C, and T, unlike open-ocean fluorescence which is low overall with maximum fluorescence in the area of peak A (Jørgensen et al., 2011). This suggests longer degradation experiments than performed in the present study and others (e.g., Gruber et al., 2006; Fukuzaki et al., 2014) are required to fully transform the protein and humic-like fluorescence into the low CDOM fluorescence observed in the ocean.

Results from our phytoplankton growth experiments, viewed through BEPOM to represent the particle phase, in addition to CDOM, strongly indicate that the unstructured CDOM fluorescence signal was a direct product of the microbial loop operating on planktonic biomass. Correlations between CDOM and BEPOM fluorescence peaks A and C (**Table 2**) were strongest when samples from degradation time points were excluded, due to the continual increase in CDOM fluorescence and concurrent decrease in BEPOM fluorescence (**Figures 4**, **5**, **Tables 1**, **2**). The overall increase in CDOM fluorescence and humification index (**Figure 6**), along with general decreases in all three carbon pools (**Figure 7**) and high microbial activities (**Figure 8**) between stationary and degradation time points, suggest microbial alteration of the DOM pool resulted in its compositional alteration to more fluorescent components. CDOM fluorescence increased in all peak regions throughout growth and degradation, including peaks A and C that have previously been described as humic-like substances arising from terrestrial material (Coble, 2007; Stedmon and Nelson, 2015). However, with no terrestrial material in our culture experiments, the humic-like fluorescence has to be a direct product of autochthonous production and microbial transformation. Similar processes occurring in the open-ocean water column would explain the global observations of elevated fluorescence and correlations with AOU in the deep ocean (Chen and Bada, 1992; Yamashita et al., 2007; Yamashita and Tanoue, 2008; Jørgensen et al., 2011; Catalá et al., 2015) that has been linked to the remineralization of organic matter and formation of RDOM (Yamashita et al., 2007; Jiao et al., 2010; Hansell, 2013; Lechtenfeld et al., 2015).

One advantage of incorporating BEPOM measurements into field sampling would be to observe subtle fluorescence shifts that are more distinct than in the dissolve phase and indicate microbial transformation of autochthonous material (**Figure 3**). A few previous studies have observed red-shifts in peaks A and C in CDOM, but these signals could easily be misinterpreted as terrestrial humic-like material or overshadowed by strong terrestrial influence, especially in coastal and freshwater systems. Murphy et al. (2008) hypothesized degradation of their coastal and open-ocean CDOM samples resulted in a PARAFAC component (C3) with excitation maxima at 260 and 370 nm and an emission maxima at 490 nm, similar to the locations of our red-shifted peaks A and C. Additionally, a similar PARAFAC component (C2, Ex 240 and 370 nm, Em 480) was determined from a meridional transect in the Atlantic Ocean by Kowalczuk et al. (2013), with its intensities doubling below the mixed layer. Burdige et al. (2004) also observed red-shifts in humic-like fluorescence of peaks A (239/429) and M (328/422) to longer wavelengths, resulting in peaks A' (248/461) and C (360/460) in sediment pore waters, and attributed the red-shift to diagenetic transformations of the original fluorophores. The red-shift in natural samples were all explained as a result of microbial degradation processes and most were at locations in the open ocean, far removed from terrigenous inputs of DOM. Thus, these studies support our interpretation that the appearance of red-shifted peaks in our plankton experiments were due to microbial degradation and that structurally complex substances were formed from planktonic precursors. The structural complexity may arise as a direct result of marine snow formation and microbial processing. Aggregation during particle formation could bring aromatic aldehydes and ketones in close proximity with hydroxylated benzoic acid derivatives through the microbial reprocessing into more complex molecules such as RDOM (Lechtenfeld et al., 2015). The presence of these molecules in the same moiety could facilitate charge transfer interactions between electron acceptors and donors, which has been suggested for lignin derivatives (Del Vecchio and Blough, 2004; Baluha et al., 2013; Sharpless and Blough, 2014). While the biochemical pathways and ecological ramifications of the planktonic CDOM phenomenon remain elusive, we can be certain that not all oceanic CDOM is terrestrially-derived and plankton are important sources of RDOM to the deep ocean.

Organic Matter Remineralization

Positive correlations between bacterial cell numbers and the different carbon pools (**Table 4**) suggest a close link between bacterial growth and activities in our experiments, with the microbes actively transforming organic matter compounds, such as carbohydrates, to shape the CDOM and BEPOM pools. Furthermore, decreases in BEPOM fluorescence (ca. 70%), BEPOM extraction efficiencies, and BEPOC concentrations during the 6 weeks of degradation suggest that substantial amounts of base-extractable POM components were degraded or solubilized to the dissolved phase by bacteria. This solubilized material was then rapidly removed from the dissolved phase, likely though organic matter remineralization to CO_2, resulting in net increases in DOC concentrations ranging between 0.19 and 0.46 mg C L^{-1}, regardless of the maximum carbon concentrations produced in each culture (**Figure 7**). This net DOC production was on the same order of magnitude as RDOC concentrations observed in the deep ocean (0.41–0.96 mg C L^{-1}) (Hansell et al., 2009).

Strong correlations between bulk glucosidase activities and organic matter fluorescence indicate that either carbohydrate hydrolysis products were a major source of CDOM likely resulting from POM sources, or that bacterial formation of CDOM is an energetically demanding process. Goto et al. (2017) demonstrated that a strain of *Alteromonas* grown solely on glucose produced humic-like CDOM fluorescence with emission properties similar to what we measured in our cultures. In contrast, amino acids and other nitrogen compounds apparently played a minor role

in the formation of the pool of fluorescing organic matter as indicated by fewer correlations between aminopeptidase activities and organic matter parameters (**Table 4**). Rather, intermediate reactions, such as the reaction of aldehydes with organic amines may incorporate N into structures that can produce charge transfer, thus creating "humic-like" CDOM fluorescence on these purely planktonic precursors (Kieber et al., 1997; Brandes et al., 2004; Del Vecchio and Blough, 2004). Furthermore, the overall high rates of aminopeptidase (**Figure 8**, **Table 3**) indicate rapid turnover of nitrogen compounds and recycling of nutrients throughout the phytoplankton growth experiments. The coupling of BEPOM analysis of fluorescence along with measurements of enzyme activities has clearly opened a new dimension of observation of processes by which CDOM in the ocean may be formed by plankton.

CONCLUSIONS

Overall, our study demonstrates that phytoplankton-derived organic matter directly results in the formation of unstructured "humic-like" CDOM fluorescence, facilitated by aggregation and microbial processing of precursor POM biomolecules containing discrete, yet unidentified, fluorophores. We have demonstrated the ability to measure fluorescence from the cellular biomass of POM, extracted into dilute base, but without the need to use resin extraction techniques to concentrate the signal, which may alter the composition (and optical properties) of CDOM. The overall trends in growth and production of fluorescent CDOM follows global ocean observations in fluorescence patterns and intensity, as well as, net production of DOC. Furthermore, the significant correlations between BEPOM and CDOM fluorescence, especially peaks A and C, challenges the paradigm that humic-like fluorescence in the open ocean is the result of terrestrially-derived material (Andrew et al., 2013; Jørgensen et al., 2014). Finally, hydrolytic enzymatic rates suggest that the bacterial community actively transforms organic matter with significant turnover of carbon and nitrogen, making bacterially-mediated production of RDOM from planktonic biomass a key pathway in global element cycles (e.g., Jiao et al., 2010; Lechtenfeld et al., 2015; Moran et al., 2016).

AUTHOR CONTRIBUTIONS

All authors contributed to the design of the study and data interpretation. JK and GC performed the incubation experiment. JK, GC, and KZ ran sample analyses. JK wrote the initial draft of the manuscript and all authors contributed to its revision.

FUNDING

Financial support for this work was provided by the National Science Foundation Chemical Oceanography award 1459406.

ACKNOWLEDGMENTS

The authors thank Daniel Wiltsie, Mackenzie Fiss, and Alexandra Gizzi for their assistance in sample collection and analyses.

REFERENCES

Alldredge, A. L., and Silver, M. W. (1988). Characteristics, dynamics and significance of marine snow. *Prog. Oceanogr*. 20, 41–82. doi: 10.1016/0079-6611(88)90053-5

Andrew, A. A., Del Vecchio, R., Subramaniam, A., and Blough, N. V. (2013). Chromophoric dissolved organic matter (CDOM) in the equatorial atlantic ocean: optical properties and their relationship to CDOM structure and source. *Mar. Chem*. 148, 33–43. doi: 10.1016/j.marchem.2012.11.001

Arnosti, C. (2011). Microbial extracellular enzymes and the marine carbon cycle. *Ann. Rev. Mar. Sci*. 3, 401–425. doi: 10.1146/annurev-marine-120709-142731

Arrigo, K. R., and Brown, C. W. (1996). Impact of chromophoric dissolved organic matter on UV inhibition of primary productivity in the sea. *Mar. Ecol. Prog. Ser*. 140, 207–216. doi: 10.3354/meps140207

Baluha, D. R., Blough, N. V., and Del Vecchio, R. (2013). Selective mass labeling for linking the optical properties of chromophoric dissolved organic matter to structure and composition via ultrahigh resolution electrospray ionization mass spectrometry. *Environ. Sci. Technol*. 47, 9891–9897. doi: 10.1021/es402400j

Biers, E. J., Zepp, R. G., and Moran, M. A. (2007). The role of nitrogen in chromophoric and fluorescent dissolved organic matter formation. *Mar. Chem*. 103, 46–60. doi: 10.1016/j.marchem.2006.06.003

Blough, N. V., and Del Vecchio, R. (2002). "Chromophoric DOM in the coastal environment," in *Biogeochemistry of Marine Dissolved Organic Matter*, eds D. A. Hansell and C. A. Carlson (San Diego, CA: Academic Press), 509–546.

Bochdansky, A. B., Clouse, M. A., and Herndl, G. J. (2017). Eukaryotic microbes, principally fungi and labyrinthulomycetes, dominate biomass on bathypelagic marine snow. *ISME J*. 11, 362–373. doi: 10.1038/ismej.2016.113

Boyd, P. W., and Trull, T. W. (2007). Understanding the export of biogenic particles in oceanic waters, Is there a consensus. *Prog. Oceanogr*. 72, 276–312. doi: 10.1016/j.pocean.2006.10.007

Brand, L. E., Guillard, R. R. L., and Murphy, L. S. (1981). A method for the rapid and precise determination of acclimated phytoplankton reproduction rates. *J. Plankton Res*. 3, 193–201. doi: 10.1093/plankt/3.2.193

Brandes, J. A., Lee, C., Wakeham, S., Peterson, M., Jacobson, C., Wirick, S., et al. (2004). Examining marine particulate organic matter at sub-micron scales using scanning transmission X-ray microscopy and carbon X-ray absorption near edge structure spectroscopy. *Mar. Chem*. 92, 107–121. doi: 10.1016/j.marchem.2004.06.020

Brym, A., Paerl, H. W., Montgomery, M. T., Handsel, L. T., Ziervogel, K., and Osburn, C. L. (2014). Optical and chemical characterization of base-extracted particulate organic matter in coastal marine environments. *Mar. Chem*. 162, 96–113. doi: 10.1016/j.marchem.2014.03.006

Burdige, D. J., Kline, S. W., and Chen, W. (2004). Fluorescent dissolved organic matter in marine sediment pore waters. *Mar. Chem*. 89, 289–311. doi: 10.1016/j.marchem.2004.02.015

Carlson, C. A., Hansell, D. A., Nelson, N. B., Siegel, D. A., Smethie, W. M., Khatiwala, S., et al. (2010). Dissolved organic carbon export and subsequent remineralization in the mesopelagic and bathypelagic relms of the North Atlantic basin. *Deep-Sea Res. II* 57, 1433–1445. doi: 10.1016/j.dsr2.2010.02.013

Carr, M.-E., Friedrichs, M. A. M., Schmeltz, M., Aita, M. N., Antoine, D., Arrigo, K. R., et al. (2006). A comparison of global estimates of marine primary production from ocean color. *Deep-Sea Res. II* 53, 741–770. doi: 10.1016/j.dsr2.2006.01.028

Catalá, T. S., Reche, I., Fuentes-Lema, A., Romera-Castillo, C., Nieto-Cid, M., Ortega-Retuerta, E., et al. (2015). Turnover time of fluorescent dissolved organic matter in the dark global ocean. *Nat. Comm*. 6:5986. doi: 10.1038/ncomms6986

Chavez, F. P., Messié, M., and Pennington, J. T. (2011). Marine primary production in relation to climate variability and change. *Ann. Rev. Mar. Sci*. 3, 227–260. doi: 10.1146/annurev.marine.010908.163917

Chen, R. F., and Bada, J. L. (1992). The fluorescence of dissolved organic matter in seawater. *Mar. Chem.* 37, 191–221. doi: 10.1016/0304-4203(92)90078-O

Coble, P. G. (1996). Characterization of marine and terrestrial DOM in seawater using excitation-emission matrix spectroscopy. *Mar. Chem.* 51, 325–346.

Coble, P. G. (2007). Marine optical biogeochemistry: the chemistry of ocean color. *Chem. Rev.* 107, 402–418. doi: 10.1021/cr050350+

del Giorgio, P. A., and Duarte, C. M. (2002). Respiration in the open ocean. *Nature* 420, 379–384. doi: 10.1038/nature01165

Del Vecchio, R., and Blough, N. V. (2004). On the origin of the optical properties of humic substances. *Environ. Sci. Technol.* 38, 3885–3891. doi: 10.1021/es049912h

Field, C. B., Behrenfeld, M. J., Randerson, J. T., and Falkowski, P. (1998). Primary production of the biosphere: integrating terrestrial and oceanic components. *Science* 281, 237–240.

Fukuzaki, K., Imai, I., Fukushima, K., Ishii, K.-I., Sawayama, S., and Yoshioka, T. (2014). Fluorescent characteristics of dissolved organic matter produced by bloom-forming coastal phytoplankton. *J. Plank. Res.* 36, 685–694. doi: 10.1093/plankt/fbu015

Gasol, J. M., and Del Giorgio, P. A. (2000). Using flow cytometry for counting natural planktonic bacteria and understanding the structure of planktonic bacterial communities. *Sci. Mar.* 64, 197–224. doi: 10.3989/scimar.2000.64n2197

Goto, S., Tada, Y., Suzuki, K., and Yamashita, Y. (2017). Production and reutilization of fluorescent dissolved organic matter by a marine bacterial strain, Alteromonas macleodii. *Front. Microbiol.* 8:507. doi: 10.3389/fmicb.2017.00507

Gruber, D. F., Simjouw, J.-P., Seitzinger, S. P., and Taghon, G. L. (2006). Dynamics and characterization of RDOM produced by a pure bacterial culture in an experimental predator-prey system. *Appl. Environ. Microbiol.* 72, 4184–4191. doi: 10.1128/AEM.02882-05

Guillard, R. R., and Ryther, J. H. (1962). Studies of marine planktonic diatoms. I. Cyclotella nana Hustedt and Detonula confervacea (cleve) Gran. *Can. J. Microbiol.* 8, 229–239.

Hansell, D. A. (2013). Recalcitrant dissolved organic carbon fractions. *Annu. Rev. Mar. Sci.* 5, 421–445. doi: 10.1146/annurev-marine-120710-100757

Hansell, D. A., Carlson, C. A., Repeta, D. J., and Schlitzer, R. (2009). Dissolved organic matter in the ocean: a controversy stimulates new insights. *Oceanography* 22, 202–211. doi: 10.5670/oceanog.2009.109

Hayase, K., and Shinozuka, N. (1995). Vertical distribution of fluorescent organic matter along with AOU and nutrients in the equatorial Central Pacific. *Mar. Chem.* 48, 283–290. doi: 10.1016/0304-4203(94)00051-E

Henson, S. A., Sanders, R., Madsen, E., Morris, P. J., Moigne, F. L., and Quartly, G. D. (2011). A reduced estimate of the strength of the ocean's biological carbon pump. *Geophy. Res. Lett.* 38:L04606. doi: 10.1029/2011GL046735

Hoppe, H.-G. (1983). Significance of exoenzymatic activities in the ecology of brackish water: measurements by means of methylumbelliferyl-substrates. *Mar. Ecol. Progr. Ser.* 11, 299–308. doi: 10.3354/meps011299

Huguet, A., Vacher, L., Relexans, S., Saubusse, S., Froidefond, J. M., and Parlanti, E. (2009). Properties of fluorescent dissolved organic matter in the gironde estuary. *Org. Geochem.* 40, 706–719. doi: 10.1016/j.orggeochem.2009.03.002

Jiao, N., Herndl, G. J., Hansell, D. A., Benner, R., Kattner, G., Wilhelm, S. W., et al. (2010). Microbial production of recalcitrant dissolved organic matter: Long-term carbon storage in the global ocean. *Nat. Rev. Microbiol.* 8, 593–599. doi: 10.1038/nrmicro2386

Jørgensen, L., Stedmon, C. A., Granskog, M. A., and Middelboe, M. (2014). Tracing the long-term microbial production of recalcitrant fluorescent dissolved organic matter in seawater. *Geophys. Res. Lett.* 41, 2481–2488. doi: 10.1002/2014GL059428

Jørgensen, L., Stedmon, C. A., Kragh, T., Markager, S., Middelboe, M., and Søndergaard, M. (2011). Global trends in the fluorescence characteristics and distribution of marine dissolved organic matter. *Mar. Chem.* 126, 139–148. doi: 10.1016/j.marchem.2011.05.002

Kieber, R. J., Hydro, L. H., and Seaton, P. J. (1997). Photooxidation of triglycerides and fatty acids in seawater: implication toward the formation of marine humic substances. *Limnol. Oceanogr.* 42, 1454–1462. doi: 10.4319/lo.1997.42.6.1454

Kowalczuk, P., Tilstone, G. H., Zabłocka, M., Röttgers, R., and Thomas, R. (2013). Composition of dissolved organic matter along an Atlantic meridional Transect from fluorescence spectroscopy and parallel factor analysis. *Mar. Chem.* 157, 170–184. doi: 10.1016/j.marchem.2013.10.004

Lalonde, K., Middlestead, P., and Gélinas, Y. (2014). Automation of 13C/12C ratio measurement for freshwater and seawater DOC using high temperature combustion. *Limnol. Oceanogr. Methods* 12, 816–829. doi: 10.4319/lom.2014.12.816

Lawaetz, A. J., and Stedmon, C. A. (2009). Fluorescence intensity calibration using the raman scatter peak of water. *Appl. Spectrosc.* 63, 936–940. doi: 10.1366/000370209788964548

Lechtenfeld, O. J., Hertkorn, N., Shen, Y., Witt, M., and Benner, R. (2015). Marine sequestration of carbon in bacterial metabolites. *Nat. Commun.* 6:6711. doi: 10.1038/ncomms7711

Minor, E. C., Wakeham, S. G., and Lee, C. (2003). Changes in the molecular-level characteristics of sinking marine particles with water column depth. *Geochim. Cosmochim. Ac.* 67, 4277–4288. doi: 10.1016/S0016-7037(00)00263-1

Mopper, K., Kieber, D. J., and Stubbins, A. (2015). "Marine photochemistry of organic matter: processes and impacts," in *Biogeochemistry of Marine Dissolved Organic Matter*, eds D. A. Hansell and C. A. Carlson (San Diego, CA: Academic Press), 390–450.

Moran, M. A., Kujawinski, E. B., Stubbins, A., Fatland, R., Aluwihare, L. I., Buchan, A., et al. (2016). Deciphering ocean carbon in a changing world. *Proc. Natl. Acad. Sci. U.S.A.* 113, 3143–3151. doi: 10.1073/pnas.1514645113

Murphy, K. R., Stedmon, C. A., Waite, T. D., and Ruiz, G. M. (2008). Distinguishing between terrestrial and autochthonous organic matter sources in marine environments using fluorescence spectroscopy. *Mar. Chem.* 108, 40–58. doi: 10.1016/j.marchem.2007.10.003

Nelson, N. B., and Gauglitz, J. M. (2016). Optical signatures of dissolved organic matter transformation in the global ocean. *Front. Mar. Sci.* 2:118. doi: 10.3389/fmars.2015.00118

Netburn, A. N., Kinsey, J. D., Bush, S., Djurhuus, A., Fernandez, J., Hoffman, C. L., et al. (in press). First HOV *Alvin* study of the pelagic environment at Hydrographer Canyon (NW Atlantic). *Deep Sea Res. II.* doi: 10.1016/j.dsr2.2017.10.001

Ohno, T. (2002). Fluorescence inner-filtering correction for determining the humification index of dissolved organic matter. *Environ. Sci. Tech.* 36, 742–746. doi: 10.1021/es0155276

Osburn, C. L., Handsel, L. T., Mikan, M. P., Paerl, H. W., and Montgomery, M. T. (2012). Fluorescence tracking of dissolved and particulate organic matter in a river-dominated estuary. *Environ. Sci. Technol.* 46, 8628–8636. doi: 10.1021/es3007723

Rochelle-Newall, E. J., and Fisher, T. R. (2002). Production of chromophoric dissolved organic matter fluorescence in marine and estuarine environments: an investigation into the role of phytoplankton. *Mar. Chem.* 77, 7–21. doi: 10.1016/S0304-4203(01)00072-X

Romera-Castillo, C., Sarmento, H., Álvarez-Salgado, X. A., Gasol, J. M., and Marrasé, C. (2010). Production of chromophoric dissolved organic matter by marine phytoplankton. *Limnol. Oceanogr.* 55, 446–454. doi: 10.4319/lo.2010.55.3.1466

Romera-Castillo, C., Sarmento, H., Alvarez-Salgado, X. A., Gasol, J. M., and Marrasé, C. (2011). Net production and consumption of fluorescent colored dissolved organic matter by natural bacterial assemblages growing on marine phytoplankton exudates. *Appl. Environ. Microbiol.* 77, 7490–7498. doi: 10.1128/AEM.00200-11

Saba, G. K., Steinberg, D. K., and Bronk, D. A. (2011). The relative importance of sloppy feeding, excretion, and fecal pellet leaching in the release of dissolved carbon and nitrogen by *Acartia tonsa* copepods. *J. Exp. Mar. Bio. Ecol.* 404, 47–56. doi: 10.1016/j.jembe.2011.04.013

Shanks, A. L., and Edmondson, E. W. (1989). Laboratory-made artificial marine snow: a biological model of the real thing. *Mar. Biol.* 101, 463–470. doi: 10.1007/BF00541648

Sharpless, C. M., and Blough, N. V. (2014). The importance of charge-transfer interactions in determining CDOM optical and phtoochemical properties. *Environ. Sci. Proc. Impacts* 16, 654–671. doi: 10.1039/c3em00573a

Shimotori, K., Omori, Y., and Hama, T. (2009). Bacterial production of marine humic-like fluorescent dissolved organic matter and its biogeochemical importance. *Aquat. Microb. Ecol.* 58, 55–66. doi: 10.3354/ame01350

Siegel, D. A., Buesseler, K. O., Behrenfeld, M. J., Benitez-Nelson, C. R., Boss, E., Brzezinski, M. A., et al. (2016). Prediction of the export and fate of global ocean net primary production: the EXPORTS science plan. *Front. Mar. Sci.* 3:22. doi: 10.3389/fmars.2016.00022

Siegenthaler, U., and Sarmiento, J. L. (1993). Atmospheric carbon dioxide and the ocean. *Nature* 365, 119–125.

Stedmon, C. A., and Markager, S. (2005). Tracing the production and degradation of autochthonous fractions of dissolved organic matter by fluorescence analysis. *Limnol. Oceanogr.* 50, 1415–1426. doi: 10.4319/lo.2005.50.5.1415

Stedmon, C. A., and Nelson, N. B. (2015). "The optical properties of DOM in the ocean," in *Biogeochemistry of Marine Dissolved Organic Matter*, eds Dennis A. Hansell and Craig A. Carlson (San Diego, CA: Academic Press), 481–508.

Steinberg, D. K., Mooy, B. A. V., Buesseler, K. O., Boyd, P. W., Kobari, T., and Karl, D. M. (2008). Bacterial vs. zooplankton control of sinking particle flux in the ocean's twilight zone. *Limnol. Oceanogr.* 53, 1327–1338. doi: 10.4319/lo.2008.53.4.1327

Thornton, D. C. O. (2014). Dissolved organic matter (DOM) release by phytoplankton in the contemporary and future ocean. *Eur. J. Phycol.* 49, 20–46. doi: 10.1080/09670262.2013.875596

Tucker, S. A., Amszi, V. L., and Acree, W. E. (1992). Primary and secondary inner filtering: effect of K2Cr2O7 on fluorescence emission intensities of quinine sulfate. *J. Chem. Educ.* 69, A8–A12. doi: 10.1021/ed069pA8

Urban-Rich, J., McCarty, J. T., Fernández, D., and Acua, J. L. (2006). Larvaceans and copepods excrete fluorescent dissolved organic matter (FDOM). *J. Exp. Mar. Bio. Ecol.* 332, 96–105. doi: 10.1016/j.jembe.2005.11.023

Utermöhl, H. (1958). Zur Vervollkommung der quantitativen Phytoplankton Methodik. *Mitt. Iinternat. Verin. Limnol.* 9, 1–38.

Wakeham, S. G., and Lee, C. (1989). Organic geochemistry of particulate matter in the ocean: the role of particles in oceanic sedimentary cycles. *Org. Geochem.* 14, 83–96. doi: 10.1016/0146-6380(89)90022-3

Wakeham, S. G., and Lee, C. (1993). "Production, transport, and alteration of particulate organic matter in the marine water column," in *Organic Geochemistry*, eds M. H. Engel and S. A. Macko (Boston, MA: Springer), 145–169. doi: 10.1007/978-1-4615-2890-6_6

Wolfbeis, O. S. (1985). "The fluorescence of organic natural products," in *Molecular Luminescence Spectroscopy – Methods and Applications*; *Part 1*, ed S. G. Schulman (New York, NY: John Wiley and Sons), 167–370.

Wünsch, U. J., Murphy, K. R., and Stedmon, C. A. (2015). Fluorescence quantum yields of natural organic matter and organic compounds: implications for the fluorescence-based interpretation of organic matter composition. *Front. Mar. Sci.* 2:98. doi: 10.3389/fmars.2015.00098

Yamashita, Y., and Tanoue, E. (2003). Chemical characterization of protein-like fluorophores in DOM in relation to aromatic amino acids. *Mar. Chem.* 82, 255–271. doi: 10.1016/S0304-4203(03)00073-2

Yamashita, Y., and Tanoue, E. (2008). Production of bio-refractory fluorescent dissolved organic matter in the ocean interior. *Nat. Geosci.* 1, 579–582. doi: 10.1038/ngeo279

Yamashita, Y., Tsujasaki, A., Nishida, T., and Tanoue, E. (2007). Vertical and horizontal distribution of fluorescent dissolved organic matter in the Southern Ocean. *Mar. Chem.* 106, 498–509. doi: 10.1016/j.marchem.2007.05.004

Ziervogel, K., Osburn, C., Brym, A., Battles, J., Joye, S., D'souza, N., et al. (2016). Linking heterotrophic microbial activities with particle characteristics in waters of the Mississippi River Delta in the aftermath of hurricane Isaac. *Front. Mar. Sci.* 3:8. doi: 10.3389/fmars.2016.00008

Conflict of Interest Statement: The authors declare that the research was conducted in the absence of any commercial or financial relationships that could be construed as a potential conflict of interest.

frontiers in Microbiology

ORIGINAL RESEARCH
published: 24 April 2018
doi: 10.3389/fmicb.2018.00798

Extracellular Enzyme Activity Profile in a Chemically Enhanced Water Accommodated Fraction of Surrogate Oil: Toward Understanding Microbial Activities After the Deepwater Horizon Oil Spill

Manoj Kamalanathan[1], Chen Xu[2], Kathy Schwehr[2], Laura Bretherton[1], Morgan Beaver[2], Shawn M. Doyle[3], Jennifer Genzer[1], Jessica Hillhouse[1], Jason B. Sylvan[3], Peter Santschi[2,3] and Antonietta Quigg[1,3]*

[1] Department of Marine Biology, Texas A&M University at Galveston, Galveston, TX, United States, [2] Department of Marine Science, Texas A&M University at Galveston, Galveston, TX, United States, [3] Department of Oceanography, Texas A&M University, College Station, TX, United States

OPEN ACCESS

Edited by:
Andrew Decker Steen, University of Tennessee, Knoxville, United States

Reviewed by:
Zhanfei Liu, University of Texas at Austin, United States
John Paul Balmonte, University of North Carolina at Chapel Hill, United States

***Correspondence:**
Manoj Kamalanathan
manojka@tamug.edu;
manojkamalanathan711@gmail.com

Specialty section:
This article was submitted to Aquatic Microbiology, a section of the journal Frontiers in Microbiology

Received: *21 November 2017*
Accepted: *10 April 2018*
Published: *24 April 2018*

Citation:
Kamalanathan M, Xu C, Schwehr K, Bretherton L, Beaver M, Doyle SM, Genzer J, Hillhouse J, Sylvan JB, Santschi P and Quigg A (2018) Extracellular Enzyme Activity Profile in a Chemically Enhanced Water Accommodated Fraction of Surrogate Oil: Toward Understanding Microbial Activities After the Deepwater Horizon Oil Spill. Front. Microbiol. 9:798. doi: 10.3389/fmicb.2018.00798

Extracellular enzymes and extracellular polymeric substances (EPS) play a key role in overall microbial activity, growth and survival in the ocean. EPS, being amphiphilic in nature, can act as biological surfactant in an oil spill situation. Extracellular enzymes help microbes to digest and utilize fractions of organic matter, including EPS, which can stimulate growth and enhance microbial activity. These natural processes might have been altered during the 2010 Deepwater Horizon oil spill due to the presence of hydrocarbon and dispersant. This study aims to investigate the role of bacterial extracellular enzymes during exposure to hydrocarbons and dispersant. Mesocosm studies were conducted using a water accommodated fraction of oil mixed with the chemical dispersant, Corexit (CEWAF) in seawater collected from two different locations in the Gulf of Mexico and corresponding controls (no additions). Activities of five extracellular enzymes typically found in the EPS secreted by the microbial community – α- and β-glucosidase, lipase, alkaline phosphatase, leucine amino-peptidase – were measured using fluorogenic substrates in three different layers of the mesocosm tanks (surface, water column and bottom). Enhanced EPS production and extracellular enzyme activities were observed in the CEWAF treatment compared to the Control. Higher bacterial and micro-aggregate counts were also observed in the CEWAF treatment compared to Controls. Bacterial genera in the order *Alteromonadaceae* were the most abundant bacterial 16S rRNA amplicons recovered. Genomes of *Alteromonadaceae* commonly have alkaline phosphatase and leucine aminopeptidase, therefore they may contribute significantly to the measured enzyme activities. Only *Alteromonadaceae* and *Pseudomonadaceae* among bacteria detected here have higher percentage of genes

for lipase. *Piscirickettsiaceae* was abundant; genomes from this order commonly have genes for leucine aminopeptidase. Overall, this study provides insights into the alteration to the microbial processes such as EPS and extracellular enzyme production, and to the microbial community, when exposed to the mixture of oil and dispersant.

Keywords: enzymes, aggregates, EPS, oil, corexit, bacteria

INTRODUCTION

The Deepwater Horizon (DwH) oil spill in the Gulf of Mexico was a catastrophic event that released 4.9 million barrels of oil (Turner et al., 2014). This was followed by the use of ∼2.9 million liters of the dispersing agent Corexit in an attempt to clear the oil from the surface of the ocean and protect coastal ecosystems (Kujawinski et al., 2011). Months after this event, the oil disappeared from the surface ocean, with factors such as natural light induced photo-oxidation, volatilization, sedimentation, and microbial degradation playing an important role (Mendelssohn et al., 2012). The ability of some bacterial taxa to degrade oil has been well established (Bailey et al., 1973), and oil biodegradation during the DwH spill has been extensively reported (Hazen et al., 2010; Valentine et al., 2010; Kostka et al., 2011). Following the oil spill, extracellular polymeric substances (EPS) combined with particulates and other materials, operationally defined as marine snow (Quigg et al., 2016), were observed in large amounts (Passow et al., 2012). Much of this marine snow was also found to have oil included in the aggregated material, so that it was referred to as 'marine oil snow' (MOS) by Passow et al. (2012). Enhanced EPS production in the form of transparent exopolymer particles (TEP) was observed in the presence of oil; this material might have acted as a bio surfactant (Kleindienst et al., 2015b).

Given that EPS production by phytoplankton can vary from 3 to 40% of the total primary productivity (Engel, 2002), and considering primary productivity accounts for 45–50 Pg C yr^{-1} in the ocean (Longhurst et al., 1995; Field et al., 1998), the amount of carbon released as EPS could range between 1.5 and 20 Pg C yr^{-1}. Furthermore, bacteria are also known to produce EPS (Manivasagan and Kim, 2014), and these EPS have been implicated to play a protective role against adverse environmental condition (Poli et al., 2010). EPS is heterogeneous in composition, consisting mainly of carbohydrates, proteins, monomers of sugars, amino acids, and uronic acids (Underwood et al., 2004; Xu et al., 2011a,b; Quigg et al., 2016). EPS can act as a carbon, nitrogen and phosphorus substrate that assists the growth of bacteria and mixotrophic phytoplankton, thereby boosting microbial activity (Decho, 1990). Several studies have shown that extracellular enzymes facilitate breakdown of complex polymers in EPS to less complex molecules (Jones and Lock, 1993; Romaní and Sabater, 2000; Espeland et al., 2001), which heterotrophic microbes would otherwise not be able to use. Heterotrophic microbes secrete several types of extracellular enzymes (exoenzymes) that assist them in degrading the various components of EPS (Decho, 1990) such as α- and β-glucosidase, alkaline phosphatase, leucine amino-peptidase, and lipase (Yamada and Suzumura, 2010). As enzymes are specific to the substrates they act upon and microbes vary in their ability to produce different kinds of enzymes, the differences in activities between enzymes can be used as an indirect indicator of microbial functional diversity in the system and/or the nutrient composition of the system (Caldwell, 2005).

In addition to the EPS, the oil and Corexit can act as a source of carbon to the microbes during the DwH oil spill, which may have affected EPS production and enzyme activities. Oil and Corexit has also known to cause a significant change in the microbial community, favoring hydrocarbon degraders (Bacosa et al., 2015b; Kleindienst et al., 2015a; Doyle et al., 2018). Therefore, how the addition of oil and Corexit can affect EPS production, extracellular enzyme production, microbial community and aggregate formation needs to be examined. In this study, we conducted mesocosm scale experiments with seawater from two sites in the Gulf of Mexico. A chemically enhanced water accommodated fraction of oil (CEWAF) prepared from a mixture of oil and Corexit (ratio of 20:1) in seawater and Controls (no additions) were used to test the effects of oil/dispersant mixture on the microbial community, their enzymatic activity and EPS production in three different layers within the mesocosm tanks (surface, water column, and bottom).

MATERIALS AND METHODS

Mesocosm Study

Two mesocosm studies were carried out using seawater collected from the Gulf of Mexico during July 2016. The first site located at 27°53N, 94°2W (salinity: 30.77 ppt, pH: 8.38, temperature: 30.8°C) was chosen as an offshore, open ocean site (∼174 km from shore) while the second site at 29°22N, 93°23W (salinity: 31.13 ppt, pH: 8.02, temperature: 30.5°C) was chosen as a coastal site (∼20 km from shore). These will be referred to as offshore and coastal respectively. The seawater was supplemented with nutrients at f/20 concentrations (Guillard and Ryther, 1962) before starting the six mesocosms (3 controls, 3 CEWAF). The seawater was used directly as a Control treatment (87 L each mesocosm). Macondo surrogate oil (25 ml) and dispersant in the ratio of 20:1 were combined to produce a chemically enhanced water accommodated fraction (CEWAF) of oil according to Wade et al. (2017). Briefly, the oil and Corexit were added together before being transferred to the corresponding seawater and mixed in 130 L circulating baffled tanks for 24 h under low light and ambient temperature (∼21°C). At the end of this period, the 87 L of CEWAF was transferred to the mesocosm tanks by pumping from the bottom of the baffled tank in order to avoid the surface slick. The initial nitrate and phosphate concentration were 97 (±4.7) $\mu Mol.L^{-1}$ and 11.2 (±0.3) $\mu Mol.L^{-1}$ in the Control and 119 (±1.9) $\mu Mol.L^{-1}$ and

5.5 (±0.4) μMol.L^{-1} in the CEWAF of the offshore mesocosm. Whereas, the initial nitrate and phosphate concentration were 133.3 (±33.8) μMol.L^{-1} and 10.2 (±0.2) μMol.L^{-1} in the Control and 130.0 (±7.4) μMol.L^{-1} and 11.0 (±0.3) μMol.L^{-1} in the CEWAF of the coastal mesocosm respectively. The initial estimated oil equivalent (EOE) concentration in the offshore and coastal CEWAF treatment were 39.06 (±0.77) mg.L^{-1} and 81.06 (±20.50) mg.L^{-1}, respectively. The incubation time for the offshore and coastal mesocosms were 96 hrs and 72 h respectively. The incubation time for both the mesocosm were decided based on the percentage of oil consumed/remaining in the CEWAF tanks. Due to technical issues associated with replicating CEWAF with the same initial oil concentration, the percentage oil concentration was chosen as the deciding parameter over actual oil concentration in terminating the study. The offshore mesocosms took 96 h to reach ∼20% of the initial oil concentration, whereas it only took 72 h in the coastal mesocosm.

Sample Collection

Samples for enzyme activity, EPS composition, and total organic carbon (TOC), dissolved organic carbon (DOC), and particulate organic carbon (POC) analysis were collected from three different layers of the mesocosm tanks on the last day. The mesocosm tanks were 74.5 cm long and 43 cm wide. Samples collected in the top 2–5 cm of the tanks were designated as the surface. Samples collected through a spigot mounted on the side of the tanks were designated as water column. Finally, samples collected from the floor of the tanks were designated as the bottom. A syringe was used to collect the samples from the surface and bottom respectively. The samples were collected from these three layers in order to account for the differences in aggregation (higher in the bottom layer for Control and in the surface for CEWAF treatment) observed during the experiment. Samples for bacterial community composition and micro-aggregate counts/sizes were collected concurrently from the water column layer.

Enzyme Assays

Enzyme activities for α- and β-glucosidase, alkaline phosphatase, leucine amino-peptidase, and lipase were measured on the last day according to Yamada and Suzumura (2010). The enzymes and the substrates used in this study are listed in **Table 1**. The substrates were dissolved in milli-Q water so that the final stock solutions were 1 mM. The substrate for 4-Methylumbelliferyl oleate was dissolved in minute volume (250 µl) of DMSO and the concentration was adjusted with milli-Q water to a final concentration of 1 mM, Substrates were then added to Control and CEWAF samples in triplicate to a final concentration of 0.2 mM. The samples were then incubated at room temperature in the dark for 3 h. After incubation, the reactions were stopped by the addition of 1 mL of borate buffer solution (0.4 M) adjusted to pH 8.0 for 7-amido-4-methylcoumarin (AMC)-tagged substrates or pH 10.0 for 4-methylumbelliferyl (MUF)-tagged substrates. The fluorescence intensity was then measured at excitation/emission wavelengths (nm) of 380/440 (AMC) or 365/448 (MUF) using a spectrofluorometer (Shimadzu RF-5300). The measurements were then corrected with the blank values obtained using heated seawater samples (80°C for 15 min) in duplicate at the beginning of the incubation. Respective substrates corresponding to the different enzymes were added to the blank samples prior to incubation and measurement.

EPS Analysis

Extracellular polymeric substances composition was measured in terms of carbohydrate, protein, and uronic acid content and total EPS was calculated by summing these parameters. Particles were collected with a polycarbonate filter (0.4 µm, Millipore, United States), and the attached EPS from the particles was then extracted with 0.35 M EDTA followed by an ultrafiltration step to remove the salts and excessive EDTA (Xu et al., 2009, 2011a,b). EPS from the dissolved phase was directly obtained by concentrating and desalting using an Amicon Ultra-15 centrifugal filter unit with ultracel-3 membrane (Millipore, 3 kDa). The carbohydrate concentration in the EPS was determined by anthrone method with glucose as the standard (Yemm and Willis, 1954). The protein content of EPS was determined with the help of a Pierce BCA protein assay kit based on a modified bicinchoninic acid method with bovine serum albumin as the standard (Smith et al., 1985). Uronic acids in the EPS were estimated by the addition of sodium borate (75 mM) in concentrated sulfuric acid and *m*-hydroxydiphenyl according to Blumenkrantz and Asboe-Hansen (1973) with glucuronic acid as the standard for this assay.

TOC, DOC, and POC Analysis

TOC and DOC were determined using a Shimadzu TOC-L analyzer (Xu et al., 2011b). For POC analysis, water sample was filtered through a pre-combusted GF/F membrane (0.7 µm, Whatman, United States), and then quantified using a Perkin Elmer Series II CHNS 2400 analyzer, after HCl-fuming to remove the carbonates. Acetanilide (71.09%) was used as the analytical standard (Xu et al., 2011a). Samples from the offshore mesocosm were limited, therefore only samples from the coastal mesocosm were analyzed.

Dissolved Oxygen (DO) Concentration

A calibrated 556 MPS YSI meter (Yellow Springs, OH, United States) fitted with a DO/Temperature sensor (5563-10) was used to measure the DO (mg L^{-1}) directly in the surface and

TABLE 1 | List of enzymes with fluorescent substrate used in this study.

Enzyme	Substrate	Catalog number
α-*Glucosidase*	4-Methylumbelliferyl α-D-glucopyranoside	M9766 (Sigma-Aldrich)
β-*Glucosidase*	4-Methylumbelliferyl β-D-glucopyranoside	M3633 (Sigma-Aldrich)
Lipase	4-Methylumbelliferyl oleate	M2639 (Sigma-Aldrich)
Alkaline phosphatase (AP)	4-Methylumbelliferyl phosphate	M8883 (Sigma-Aldrich)
Leucine amino-peptidase (LAP)	Leu-AMC hydrochloride	ab145346 (Abcam)

bottom of each mesocosm tank on the last day of each mesocosm experiment.

Microbial and Micro-Aggregate Counts/Sizes

Direct cell counts were performed on the samples collected from the water column on the last day in three replicate tanks per treatment. Samples were visualized with an epifluorescence microscope (Zeiss Axio Imager.M2) after staining the fixed samples with DAPI (45 μM final concentration) for 5 min in the dark and filtering them onto 25 mm, 0.2 μm black polycarbonate filters, according to Doyle et al. (2018). Microbial cell counts were performed at 1000× magnification and, due to their much larger size, micro-aggregates were quantified at 400× magnification. For micro-aggregate abundance, the presence of a micro-aggregate was counted, not the number of cells present per micro-aggregate. Micro-aggregates were defined as groups of cells in clumps 10–200 μm in diameter, often found gathered around drops of oil.

Size fraction analysis of aggregates was also performed using Z1 dual-threshold Coulter counter (Beckman Coulter). It should be noted that these aggregates do not exactly correspond to the microbial micro-aggregates measured above, and likely include those as well as other particles in that size fraction. Samples (15 mL) from the water column were taken on the last day and analyzed immediately. Particles of four different size ranges (5–10, 10–20, 20–50, and >50 μm) were counted with a 100 μm aperture. A sample of filtered seawater was used as blank (typically less than 10 particles were counted). Samples were diluted with filtered seawater (0.2 μm) if the particle coincidence at the aperture exceeded 5%, where particle coincidence is the chance of more than one particle passing through the aperture at once.

Bacterial Community Composition

Prokaryotic community composition (Bacteria and Archaea) was analyzed as described in detail in Doyle et al. (2018). Briefly, samples (150 ml) collected from the water column in three replicate tanks per treatment concurrently with other samples were pre-filtered through 10 μm filters to remove most eukaryotic cells followed by filtration onto 47 mm 0.22 μm Supor PES filter membranes (Pall). Total DNA was extracted from filters using FastDNA Spin kits (MP Biomedical). 16S rRNA gene (hyper-variable V4 region) was PCR amplified with GoTaq Flexi DNA Polymerase (Promega) according to Caporaso et al. (2012), with specifics in Doyle et al. (2018). Amplifications were performed using the 515F-806R universal primer pair according to recent revisions (Apprill et al., 2015; Parada et al., 2016), which included Golay barcodes and adapters for Illumina MiSeq sequencing. The products were combined and quantified with the QuantiFluor dsDNA System (Promega), pooled and purified with an UltraClean PCR Clean-Up Kit (MoBio Laboratories). The library, along with the three sequencing primers, were sent to the Georgia Genomics Facility (Athens, GA, United States) for MiSeq sequencing (v2 chemistry, 2 × 250 bp). Sequence processing was carried out using mothur v.1.36.1 (Schloss et al., 2009) following a modified version of the protocol described in Kozich et al. (2013). Analysis of rarefaction curves was conducted using all available reads. Generation of operational taxonomic units (OTUs) and analysis of alpha and beta diversity was conducted using a dataset subsampled to 39,054 samples per read (Supplementary Table S1). Goods coverage was >0.99 for all samples.

Raw DNA sequence data used in this project can be found in the NCBI Genbank database under accession numbers SAMN07795505-SAMN07795510 (Offshore) and SRR6176504, SRR6176505, SRR6176497, SRR6176488, SRR6176473 and SRR6176442 (Coastal).

Screening of Microbial Genomes

To determine which of the most relatively abundant bacterial families detected are potentially capable of extracellular enzyme production, we searched the Integrated Microbial Genomes (IMG) database (Markowitz et al., 2006) for genomes within these orders using the "Find Functions" search and the "Enzymes (list)" filters for each bacterial order searched, similar to previous work (Jacobson Meyers et al., 2014). EC 3.4.11.1 was used to search for the gene(s) encoding leucine aminopeptidase, EC 3.1.3.1 was used to search for the gene(s) encoding alkaline phosphatase, EC 3.1.1.3 was used to search for genes encoding for lipase, EC 3.2.1.20 was used to search for genes encoding α-glucosidase, and EC 3.2.1.21 was used to search for genes encoding β-glucosidase. Genomes were scored as positive if they contained a gene that encoded for an exoenzyme, and then the number of genes within the family was tallied to calculate the percentage of genomes within that family capable of producing each enzyme. This analysis depends on a few assumptions: (a) if an organism is a member of a clade in which a specific enzyme is more abundant, then that organism is more likely to have the enzyme, (b) the annotations in IMG are reliable, and (c) that the exoenzymes assayed are expressed extracellularly, rather than intracellularly.

Statistical Analysis

The results were statistically analyzed by using one-way ANOVA with multiple comparisons of the mean of each group with the mean of every other group using a Tukey test. These statistical analyses were performed using GraphPad Prism software (version 7.0f).

RESULTS

Measurement of α-glucosidase activities in different layers of the CEWAF tanks revealed highest activity at the surface in both the offshore and the coastal mesocosms (One way ANOVA: $p < 0.02$; **Figure 1A**). Similar patterns were seen for both β-glucosidase and alkaline phosphatase, although the differences in alkaline phosphatase were not statistically significant (**Figures 1B,C**). In the Control tanks, the activities of α-glucosidase, β-glucosidase and alkaline phosphatase were significantly higher at the bottom than in other layers in the offshore mesocosm (One way ANOVA: $p < 0.0005$; **Figure 1**). While the activities were similarly higher at the bottom layer in the Control tanks of the coastal mesocosm, the differences

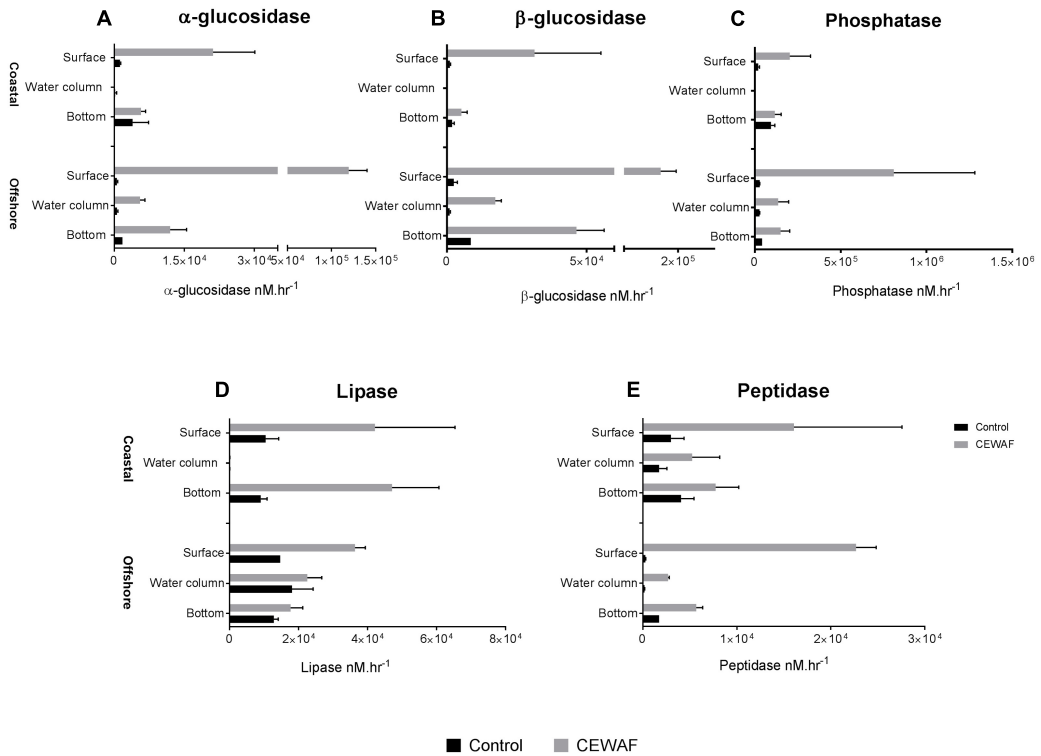

FIGURE 1 | Average enzyme activities (±SD) of **(A–E)** α- and β-glucosidase, alkaline phosphatase, lipase, leucine amino-peptidase measured in the surface, water column and bottom of the offshore and coastal mesocosms.

were statistically significant only for alkaline phosphatase (One way ANOVA: $p < 0.0015$). Comparison of Control vs. CEWAF tanks in the coastal mesocosm revealed significant differences for α-glucosidase, β-glucosidase and alkaline phosphatase only at the surface (Two way ANOVA: $p < 0.004$). However, for the offshore mesocosm, α-glucosidase and β-glucosidase activities were significantly higher in CEWAF compared to Control in all three layers (Two way ANOVA: $p < 0.0001$), whereas alkaline phosphatase was significantly higher only at the surface (Two way ANOVA: $p = 0.0011$).

Measurement of lipase activities revealed slightly different profile compared to α-glucosidase, β-glucosidase and alkaline phosphatase (**Figure 1D**). For CEWAF tanks, lipase activities were highest in the surface compared to other layers in the offshore mesocosm (Two way ANOVA: $p < 0.002$), similar to that observed for α-glucosidase, β-glucosidase and alkaline phosphatase. However, in the coastal mesocosm, lipase activities were the lowest in the water column (Two way ANOVA: $p < 0.002$), and similar between surface and bottom layer in CEWAF tanks. Comparison of Control vs. CEWAF tanks in the offshore mesocosm revealed significant differences only at the surface for the offshore mesocosm (Two way ANOVA: $p < 0.0001$). However, in the coastal mesocosm, lipase activities were significantly higher in CEWAF than Control in both surface and bottom layers (Two way ANOVA: $p < 0.004$).

Measurement of leucine aminopeptidase activities in different layers of the CEWAF tanks revealed highest activity at the surface in the offshore mesocosm (One way ANOVA: $p < 0.0001$; **Figure 1E**). A similar pattern was observed for leucine aminopeptidase in the coastal mesocosm, however the differences were not statistically significant (**Figure 1**). In Control tanks, the activities were higher at the bottom for leucine aminopeptidase in the offshore mesocosm (One way ANOVA: $p < 0.0001$), whereas the activities were similar in the coastal mesocosm. CEWAF had significantly higher leucine aminopeptidase activities than the Control in all the layers for the offshore mesocosm (Two way ANOVA: $p < 0.02$), however, significant differences were only seen at the surface for the coastal mesocosm (Two way ANOVA: $p = 0.02$). Overall, most of the enzymes showed higher activities at the surface for CEWAF treatments and at the bottom for Control treatment in the offshore and/ or coastal mesocosms (**Figure 1**). In addition, overall enzyme activities were significantly higher in CEWAF treatment than in the Control for both offshore (Unpaired *t*-test: $p = 0.0057$) and coastal (Unpaired *t*-test: $p = 0.0312$) experiment (Supplementary Figure S1).

EPS Composition Across the Layers

The polysaccharide, protein, and uronic acid content was measured to determine the overall EPS composition (**Figure 2**). Total EPS concentration was highest in the water column in both treatments for both mesocosms (Two-way ANOVA: $p < 0.0001$). In Control tanks, significantly higher concentration of EPS was observed at the bottom layer compared to the surface layer in the offshore mesocosm (Unpaired *t*-test: $p = 0.009$). Similar trends

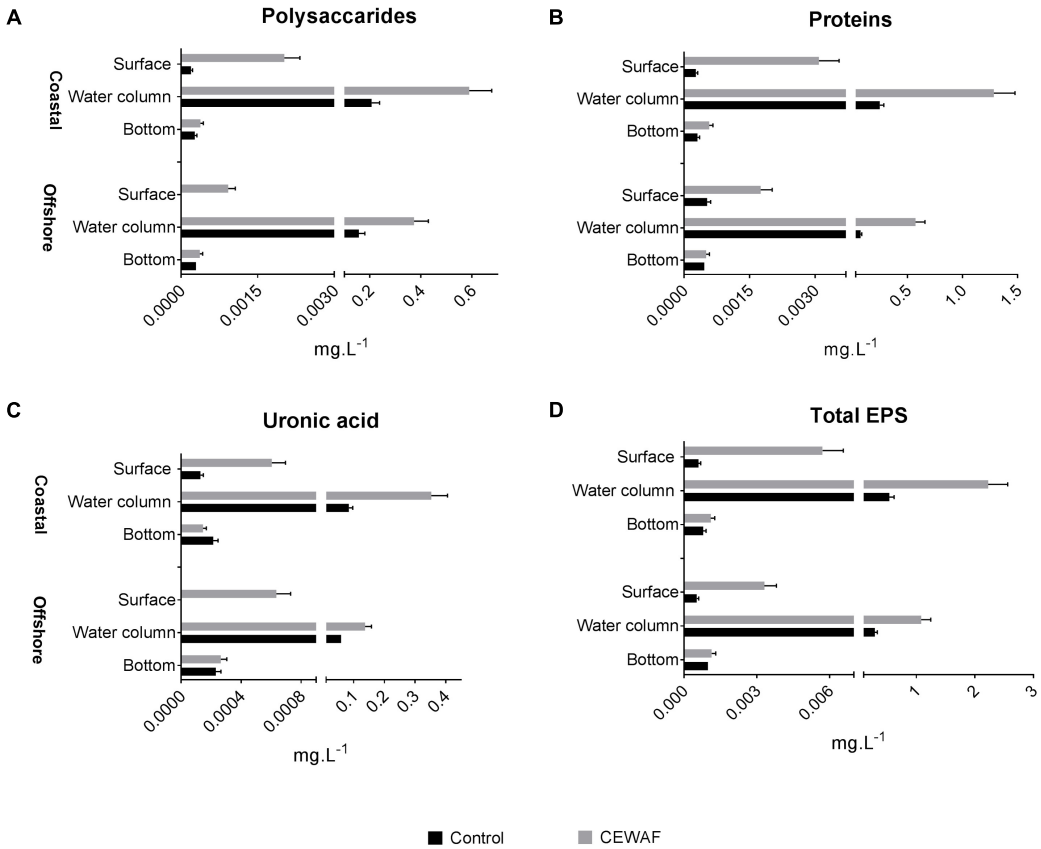

FIGURE 2 | (A–D) Average polysaccharide, protein and uronic acid content (±SD) of EPS at measured in the surface, water column and bottom layers of offshore and coastal mesocosms.

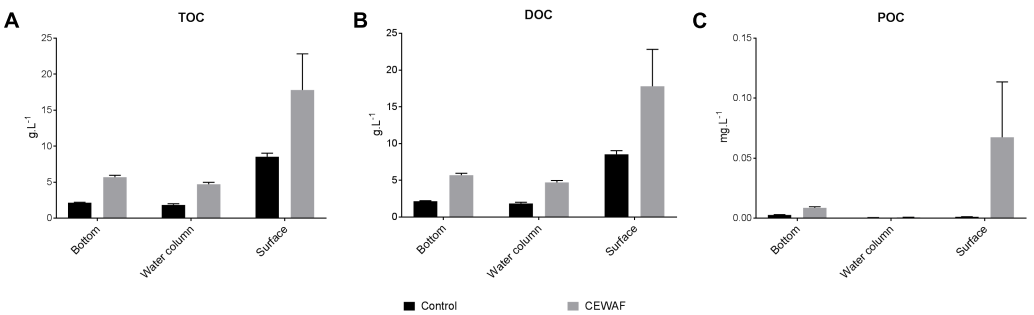

FIGURE 3 | (A–C) Average TOC, DOC, and POC levels (±SE) of water samples from surface, water column and the bottom of the coastal mesocosms.

were observed in the coastal mesocosm samples, however, the differences were not statistically significant (**Figure 2D**). In the CEWAF tanks, there was more EPS in the surface than the bottom layer in both the mesocosms (Unpaired *t*-test: $p < 0.003$). Exposure to CEWAF treatment significantly increased the amount of polysaccharide, proteins and uronic acids produced in the water column and in the surface (Two-way ANOVA: $p < 0.0001$; **Figure 2**). Comparison of EPS composition in the water column of CEWAF relative to the Control, showed higher production of proteins in both the coastal (5.3 fold) and offshore (8.1 fold) mesocosms followed by uronic acids (4.4 and 2.6 fold) and carbohydrates (2.9 and 2.4 fold). Comparison of EPS composition in the surface of CEWAF relative to the Control showed similar patterns to that observed in the water column.

TOC, DOC, and POC

In the coastal mesocosm, TOC and DOC concentrations were highest in the surface layers in both treatments (Two-way ANOVA: $p < 0.0025$) (**Figure 3A**). Overall, there was significantly

TABLE 2 | Average dissolved oxygen concentration (±SD) at the surface and bottom in control and CEWAF treatments of the offshore and coastal mesocosm tanks.

	Control		CEWAF	
	Surface mg L^{-1}	Bottom mg L^{-1}	Surface mg L^{-1}	Bottom mg L^{-1}
Offshore	6.31 (±0.06)	5.67 (±0.65)	0.33 (±0.12)	0.16 (±0.04)
Coastal	7.54 (±1.09)	7.51 (±1.14)	0.39 (±0.01)	0.22 (±0.04)

more TOC and DOC in the CEWAF tanks than in the Control tanks at all layers (**Figure 3B**) (Two-way ANOVA: $p = 0.0007$). POC concentrations were significantly higher in the CEWAF treatment in the surface layer than in the Control (Unpaired *t*-test: $p < 0.00001$) (**Figure 3C**). The bottom POC concentration was higher than both the water column (Two-way ANOVA: $p = 0.0007$) and surface layers (Two-way ANOVA: $p = 0.0056$) in the Control treatment. In the CEWAF treatment, the POC was higher at the surface than in the water column and bottom (**Figure 3C**), although these differences were not statistically significant (One-way ANOVA: $p > 0.2571$).

Dissolved Oxygen Concentration

The DO concentration in the CEWAF mesocosms was very low on the last day, decreasing to almost zero at the bottom of the offshore and coastal tanks (**Table 2**). A decrease in DO in the CEWAF treatments from 0.3 (±0.12) mg L^{-1} at the surface to 0.1 (±0.04) mg L^{-1} at the bottom of the tanks was observed in offshore and 0.4 (±0.01) mg L^{-1} to 0.22 (±0.04) mg L^{-1} in coastal tanks (**Table 2**). These concentrations are considered to be hypoxic to anoxic. By comparison, the Control treatments had a significantly higher dissolved oxygen concentration throughout the tank with an average value of 6 (±0.37) mg L^{-1} in offshore and 7.5 (±1.11) mg L^{-1} in the coastal mesocosms from surface to bottom.

Microbial and Aggregate Counts

Compared to the Control, bacterial counts in the CEWAF treatments were approximately 3.3 fold higher in offshore and nearly 2 fold higher in coastal seawater (**Figure 4**). Similarly, the micro-aggregate counts in CEWAF were nearly 14 fold higher in offshore and 12 fold higher in coastal as compared to Control treatments (Two-way ANOVA: $p < 0.0001$). Further analysis of the aggregates based on size showed significantly higher particle concentrations in 5–10, 10–20, and 20–50 μm size range in the CEWAF treatment compared to the Control (Two-way ANOVA: $p < 0.0001$) (**Figure 5**). Control tanks had significantly higher number of particles than CEWAF treatments in the size range of >50 μm in the coastal mesocosm (Two-way ANOVA: $p < 0.0001$); however, no differences were observed for the same size range in offshore tanks. Particles abundance was more similar between coastal and offshore tanks across all the size ranges except for 10–20 μm, where it was higher in the coastal mesocosm (Two-way ANOVA: $p < 0.0001$) (**Figure 5**).

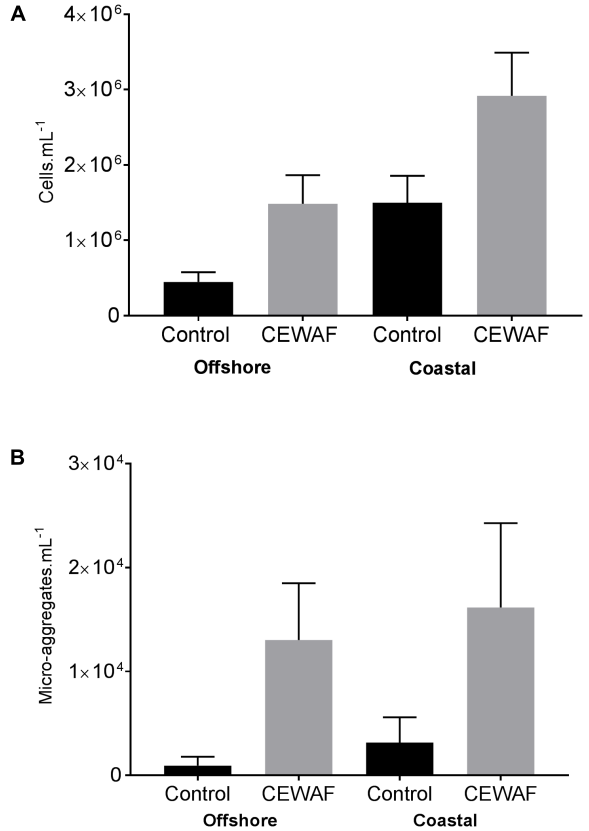

FIGURE 4 | (A,B) Average bacterial and micro-aggregate numbers (±SD) in Control and CEWAF treatments from the offshore and coastal mesocosms.

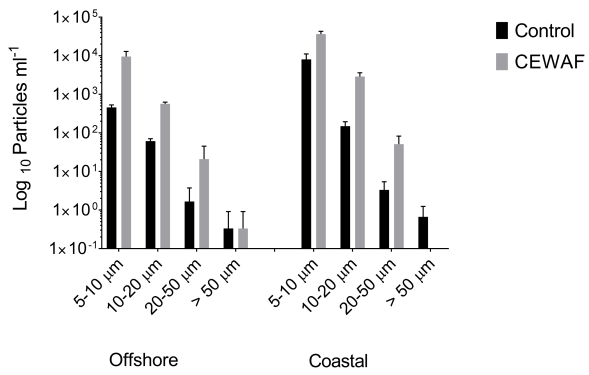

FIGURE 5 | Average $\log_{10}$ particle number determined using a coulter counter (±SD) in the size ranges 5–10, 10–20, 20–50, and >50 μm in Control and CEWAF treatment from the offshore and coastal mesocosms.

Microbial Community Composition

Prokaryotic communities in Control treatments were more diverse in both mesocosms than in the CEWAF treatments (Supplementary Figure S2 and Supplementary Table S1). Based on 16S rRNA amplicon sequence data, Bacteria were detected at much higher relative proportion than Archaea in both mesocosm experiments (**Figure 6**). Microbial community

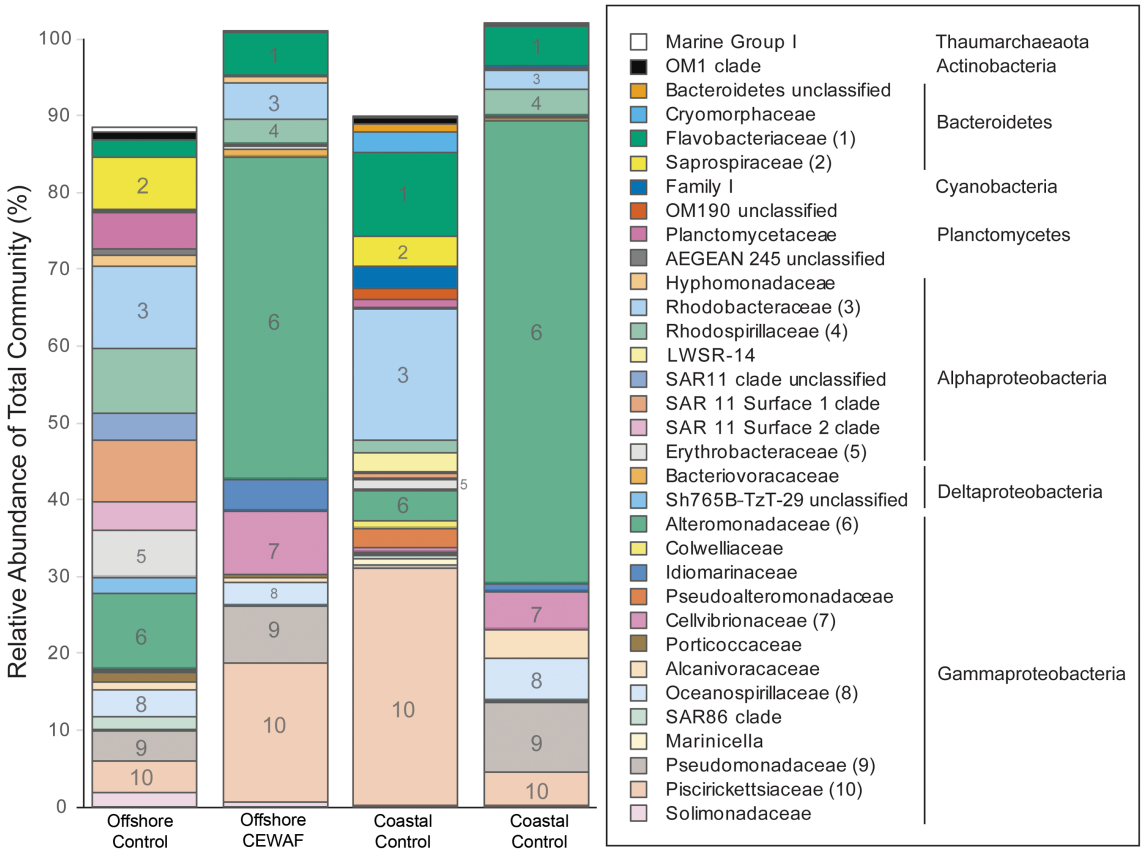

FIGURE 6 | Prokaryotic relative abundance assessed via Illumina sequencing of the V4 region of 16S rRNA. Results are mean of three replicate tanks per treatment. Only taxa representative of >0.5% of the total community in *at least* one sample are shown. The 10 families shown in Figure are indicated by number in the bars and in parentheses after the family name in the key. Phylum and Class (for Proteobacteria) are given for the families identified in the key at right.

composition was dramatically different between the Control and CEWAF samples for both the coastal and offshore mesocosms. The mean relative abundance of the family *Alteromonadaceae* was highest, followed by *Piscirickettsiaceae*, *Rhodobacteraceae*, *Flavobacteriaceae*, *Pseudomonadaceae*, and *Rhodospirillaceae*. Among these abundant families, the genera with the highest relative abundances was *Marinobacter*, followed by *Alteromonas* (both belonging to the family *Alteromonadaceae*), *Methylophaga* (*Piscirickettsiaceae*), unclassified *Oceanospirillales*, *Cycloclasticus* (*Piscirickettsiaceae*), *Aestuariibacter* (*Alteromonadaceae*) and *Tenacibaculum* (*Flavobacteriaceae*). Three different OTUs of *Marinobacter* (family *Alteromonadaceae*), OTU3, OTU8 and OTU11, represented 21% of the CEWAF community in the offshore and 45% of the CEWAF community in the coastal experiments, respectively (Supplementary Table S2). OTU level responses were not always uniform within a genus. For example, the relative abundance of the two most abundant OTUs of *Methylophaga* (family *Piscirickettsiaceae*) was different between treatments, with OTU2 having highest relative abundance in CEWAF in the offshore mesocosm and OTU5 exhibiting higher relative abundance in the Control for both mesocosm experiments.

Compared to all the extracellular enzymes, α-glucosidase was present in the lowest percentage (<75%) of genomes amongst all the abundant bacterial orders (**Figure 7**). β-glucosidase was 100% positive in *Cellvibrionaceae*, members of which were abundant in both the CEWAF treatments. In addition, β-glucosidase was highly positive (76-99%) in *Pseudomonadaceae*, which was abundant in both CEWAF treatments and the offshore Control treatments (**Figure 7**). Lastly, *Erythrobacteraceae*, which had higher relative abundance in the offshore mesocosm than the coastal mesocosm were highly positive for β-glucosidase as well (**Figure 7**). *Alteromonadaceae* and *Pseudomonadaceae* had the highest percentage of genomes positive for lipase (51–75%) (**Figure 7**). Both these orders, especially *Alteromonadaceae*, were significantly abundant in both the CEWAF treatments. Relative to other extracellular enzymes, leucine amino-peptidase was highly positive (76–100%) amongst all the abundant bacterial orders with the exception of *Flavobacteriaceae* and *Saprospiraceae* (**Figure 7**). Alkaline phosphatase was highly positive (76–99%) amongst *Alteromonadaceae*, *Pseudomonadaceae* and *Cellvibrionaceae*, which were abundant in both the CEWAF treatments (**Figure 7**). Amongst bacterial orders abundant in the Control treatments, alkaline phosphatase were 100% positive in

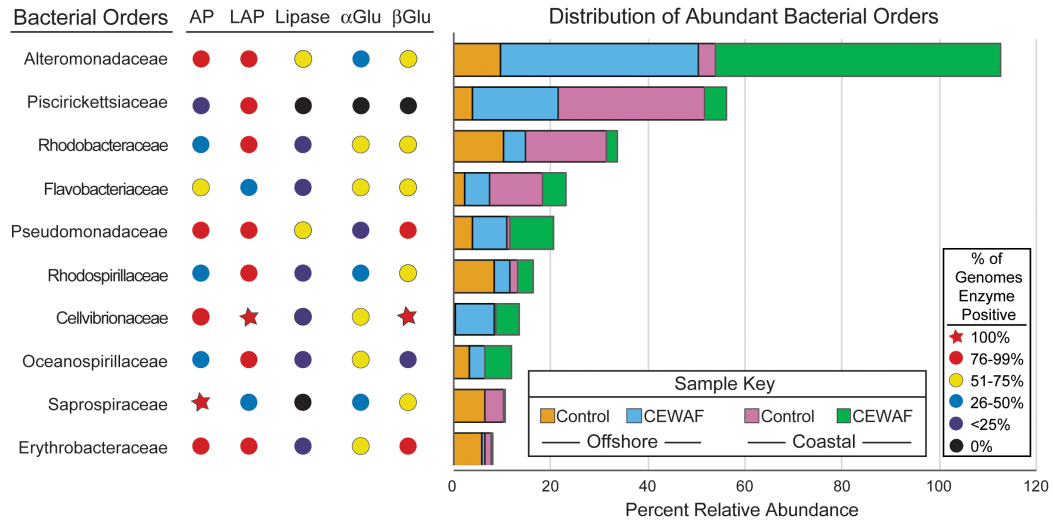

FIGURE 7 | Distribution of bacterial orders with high relative abundance (defined as orders which are present at ≥1% relative abundance in two or more samples) and percentages of sequenced genomes containing exoenzymes assayed. The *x*-axis measures the relative abundance of taxa. AP, alkaline phosphatase; LAP, leucine aminopeptidase; αGlu, α-Glucosidase; βGlu, β-Glucosidase. The sequence of the genes coding for these enzymes were obtained from IMG database.

Saprospiraceae and highly positive in *Erythrobacteraceae* (**Figure 7**).

DISCUSSION

The goal of this study is to better understand the role of extracellular enzymes, EPS production, and microbial community composition in the presence of a mixture of oil and dispersant. Five different enzymes: α- and β-glucosidase, lipase, alkaline phosphatase and leucine amino-peptidase were studied in the surface, water column and bottom of the mesocosm tanks filled with either coastal or offshore water from the Gulf of Mexico with and without CEWAF. Elevated extracellular enzyme activities have been previously reported in oil containing aggregates (Ziervogel et al., 2012). Also dense microbial colonization and active degradation of oil and components of EPS have been reported (Ziervogel et al., 2012, 2016; Arnosti et al., 2016), suggesting a link between extracellular enzymes and microbial aggregates.

α and β-glucosidase help in the digestion of complex polysaccharides (Reese et al., 1968). These enzymes help in cleavage of glycosidic bonds with α and β-glucosidase acting at α and β -linkages allowing the release of glucose molecule from polysaccharides (de Melo et al., 2006). In the Control treatments, highest α and β-glucosidase activity was seen in layers whereby the polysaccharide concentration in the EPS was lower and vice-versa. Similar patterns but relatively higher levels of activity, were observed in CEWAF treatments as well. This inverse relationship between glucosidase activity and EPS polysaccharide concentration across the three layers is indicative of active breakdown of polysaccharides by these enzymes.

α and β-glucosidase have been shown to help the turnover of polysaccharides secreted by phytoplankton and bacteria, as EPS fueling heterotrophic metabolism in the ocean (Piontek et al., 2010). We therefore hypothesize that the increased activity of these enzymes at the bottom for the Control and surface for CEWAF might help breakdown of the EPS, thereby enhancing the availability of simple carbon in the form of glucose. In addition, compared to the Control, a relatively higher glucosidase activity was observed in CEWAF in both the offshore and coastal mesocosms. Enhanced polysaccharide degradation by extracellular enzymes, especially laminarin, which are targets of glucosidase was observed by Arnosti et al. (2016) in oil associated aggregates. In addition, the polysaccharide concentrations decreased in the Control treatments from ∼0.15 mg.L^{-1} at 0 hrs (data not shown) to ∼0.0003 mg.L^{-1} at 96 h in the bottom of offshore and ∼0.18 mg.L^{-1} (data not shown) to 0.0002 mg.L^{-1} in the coastal mesocosm. Similarly in the CEWAF tanks, the polysaccharide concentrations decreased from ∼0.19 mg.L^{-1} (data not shown) at 0 h to ∼0.0009 mg.L^{-1} at 72 h in the surface of offshore and ∼0.36 mg.L^{-1} (data not shown) to 0.002 mg.L^{-1} for the coastal mesocosm. We therefore hypothesize that CEWAF induced enhanced EPS secretion in the form of polysaccharide at an earlier time point of this experiment that may have been rapidly degraded by these glucosidases.

Ziervogel et al. (2012) previously showed a correlation between lipase activity and oil degradation. Therefore, the higher lipase enzyme activity at the surface and at the bottom of the mesocosm tanks for the CEWAF treatments, along with other hydrocarbon degrading enzymes (not measured in this study), might have played a role in breakdown of the oil components. Analysis of relative prokaryotic abundance showed the presence of lipase producing families, such as *Alteromonadaceae*, *Oceanospirillaceae*, and *Pseudomonadaceae*, in relatively higher numbers. Several other studies focusing on DwH oil spill have reported the presence of these families in samples containing high concentrations of oil

(Dubinsky et al., 2013; Lamendella et al., 2014; King et al., 2015; Campeão et al., 2017). Additionally, the lipase producing genomic capabilities detected among members of the families *Altermonadaceae*, and *Pseudomonadaceae* suggest that these taxa might have played a significant role in the degradation of oil in the CEWAF treatment. The products of these extracellular hydrocarbon degrading enzymes might have led to increased carbon availability in the CEWAF treatment.

Leucine aminopeptidase (LAP) helps microbes acquire nitrogen by breaking down proteins and peptide molecules (Fruton and Mycek, 1956). Likewise, alkaline phosphatase is responsible for degradation of organic phosphates, providing a source of phosphorus to microbes (Martínez, 1968). Both leucine amino-peptidase and alkaline phosphatase activity patterns had higher activities at the surface than in the water column and the bottom of the mesocosm tanks for CEWAF treatments. EPS protein content was higher in the water column of the mesocosms than at the surface or bottom, similar to that observed for polysaccharides. Moreover, the higher leucine amino-peptidase and alkaline phosphatase activities at the surface for the CEWAF treatment pattern matches well with α- and β-glucosidase activities. This suggests active assimilation of nitrogen and phosphorus through leucine amino peptidase and alkaline phosphatase along with carbon through α and β-glucosidase from the EPS, which could have contributed in the generation of microbial biomass. There are other reports where enzyme activities have been shown to correlate with the C:N:P requirements of microbes (Sinsabaugh et al., 2008, 2009). Therefore, we hypothesize that the products of these extracellular enzyme activities observed in our mesocosm tanks may have supported microbial requirements that lead to increased microbial biomass observed in the CEWAF tanks.

Analysis of alkaline phosphatase, leucine amino-peptidase and β-glucosidase in whole water and <10 μm size fractions were statistically indistinguishable (Whitaker, personal communication), indicating that at least large eukaryotes > 10 μm are not responsible for the vast majority of activity measured. These assumptions aside, similar to other studies (Gutierrez et al., 2013; Kleindienst et al., 2015b; Yang et al., 2016a,b), our observations showed that *Alteromonadaceae*, represented largely by *Marinobacter*, *Alteromonas*, and *Aestuariibacter*, are the most abundant bacterial order detected and also very commonly have alkaline phosphatase and leucine aminopeptidase. This indicates a potentially large contribution to overall enzyme activity from these genera to alkaline phosphatase and leucine aminopeptidase enzyme activity rates. In particular, for AP and Lipase, the percentages of enzyme positive genomes are highly uneven, indicating that a consortia of microbes is necessary to efficiently hydrolyze EPS *in situ*.

It is also interesting that the family *Piscirickettsiaceae* is abundant but seems to only use leucine amino-peptidase out of the five enzymes in any significant proportion. All other abundant prokaryotes potentially contribute to 3–4 of the measured enzymes in a similar proportion within the family, but *Piscirickettsiaceae* operate outside this trend. This may indicate that this abundant family gets its phosphorus and carbon through other means. The two genera common in our mesocosm experiments, *Methylophaga* and *Cycloclasticus*, are putative hydrocarbon degraders (Gutierrez and Aitken, 2014). Therefore, they may have used hydrocarbons for carbon and enzymes other than lipase or glucosidases to metabolize that carbon-source.

Some members of the most abundant families in our mesocosms are known as "cheaters"; abundant community members that have minimal to no contribution in terms of enzyme activity (Allison, 2005). For example, members of the family *Planctomycetaceae* and SAR11 clades (Unclassified, Surface 1, and Surface 2) were abundant in the Control treatments but genomes from these lineages do not harbor abundant exoenzymes: < 10% of *Pelagibactereaceae* genomes have any of the enzymes assayed here, with the exception of leucine aminopeptidase, which is present in 47% of the genomes queried. Interestingly, there were almost no families lacking extracellular enzyme producing ability (cheaters) in the CEWAF treatments. This could be due to the potential toxicity of oil and Corexit, or the hypoxic environment in the CEWAF treatments restraining the microbial community exclusively to a few dominant families that are being selected due to their ability to tolerate and degrade hydrocarbons (Hamdan and Fulmer, 2011; Bacosa et al., 2012, 2015b; Liu et al., 2017). Such reduced microbial diversity limited to fewer families such as *Alteromonadaceae*, *Pseudomonadaceae*, *Oceanospirillaceae*, *Piscirickettsiaceae,* and *Idiomarinaceae* has been reported in other studies focusing of DwH oil spill (Kleindienst et al., 2015b; Yang et al., 2016a,b).

The overall abundance of potential oil degraders such as members of *Alteromonadaceae*, *Pseudomonadaceae*, *Cellvibrionaceae*, and *Piscirickettsiaceae* in the CEWAF treatments suggests oil may have acted as the primary carbon source. However, since the glucosidase were higher in CEWAF treatments, we hypothesize the products of glucosidases may have provided additional carbon source as well. Moreover, the heavy supply of carbon also increases the demand for other elements such as nitrogen and phosphorus, which are not present in oil. We assume, some portions (in addition to the supplemented nutrients in the mesocosm tanks) of the required high levels of nitrogen and phosphorus to support the growth may have been provided by means of extracellular enzyme reactions such as alkaline phosphatase and leucine amino-peptidase. The overall activities of enzymes were relatively higher in CEWAF treatments than Control, and similar observations were made by Kleindienst et al. (2015b). Therefore, the products of these enzymes may have played a role in the high cell numbers seen in this treatment relative to Control. Several reports indeed have shown that the products of these extracellular enzyme can support the growth of bacteria (Frankenberger and Dick, 1983; Vetter and Deming, 1999). Apart from higher cell counts, statistically higher micro-aggregate counts was also observed in the CEWAF treatments compared to Control. This can be explained by relatively higher protein content of the EPS produced in response to CEWAF. We hypothesize that increase in proteins content may have enhanced the amphiphilic nature of the EPS, which may have facilitated better interaction of the EPS with the oil. This in-turn may lead to formation of

more micro-aggregates in CEWAF treatment. Such role of EPS interaction with oil in the formation of aggregates has been previously suggested (Passow et al., 2012; Kleindienst et al., 2016; Quigg et al., 2016). Although, the enzyme activities and EPS production were higher in the CEWAF treatments than in Control, any interpretation on the effect of dispersant addition alone has to be taken with caution as the study did not compare CEWAF to WAF or a Corexit only treatment. Kleindienst et al. (2015b) suggested Corexit could suppress microbial activity, on the other hand, Bacosa et al. (2015a,b) showed positive effect on growth and alkane degradation in the presence of the dispersant Corexit. There were many differences between the experimental conditions used in Bacosa et al. (2015a,b) and Kleindienst et al. (2015b) such as temperature (8°C vs. ambient temperature similar to our study) and site of sampling depth (1500 m vs. surface similar to our study). Kleindienst et al. (2015b) worked with a closed bottle system in the dark for 6 weeks while our study lasted a few days in an open system. These differences and others in experimental conditions may have influenced the outcome of dispersant addition on microbial activity. Therefore, despite the observation of higher microbial activity in our CEWAF treatments, further studies are essential to gain a more detailed understanding the effects of dispersant addition alone. Different levels of enzyme activities, EPS production, cell and aggregate counts were observed in response CEWAF of the offshore relative the coastal mesocosm. We hypothesize that these differences could be primarily due to the different initial conditions in the offshore and coastal waters.

CONCLUSION

Our study shows that addition of oil and dispersant Corexit enhances extracellular enzyme activity and EPS production in relative to Control, and a similar comparison between oil and dispersant mixture with oil only treatment is needed. Microbial community in CEWAF treatment was mostly dominated by hydrocarbon degraders such as members of *Alteromonadaceae*, *Pseudomonadaceae* and *Cellvibrionaceae*. The higher protein content of EPS in response to CEWAF may have facilitated increased aggregation. However, further studies comparing CEWAF treatment with WAF with time course measurements are needed to discern the effect of dispersant addition on extracellular enzyme and EPS production and aggregation.

AUTHOR CONTRIBUTIONS

MK designed the experiment, conducted the enzyme measurements and data analysis, and wrote the manuscript. CX helped in conducting the EPS and carbon analysis and manuscript preparation. KS helped in designing the experiment and writing of the manuscript. LB helped in measurements of the particle size and manuscript preparation. MB helped in conducting the EPS and carbon analysis. SD conducted the genomic and associated data analysis and manuscript preparation. JG and JH helped in conducting the experiment. JS helped in genomic data analysis and manuscript preparation. PS helped in designing the experiment and manuscript preparation. AQ mentored the study and helped in designing the experiment and manuscript preparation.

FUNDING

This research was made possible by a grant from The Gulf of Mexico Research Initiative to support consortium research entitled ADDOMEx (Aggregation and Degradation of Dispersants and Oil by Microbial Exopolymers) Consortium. Data are publicly available through the Gulf of Mexico Research Initiative Information and Data Cooperative (GRIIDC) at http://data.gulfresearchinitiative.org (doi: 10.7266/N7348HTQ, doi: 10.7266/N7C53JDP, and doi: 10.7266/N77D2SPZ).

ACKNOWLEDGMENTS

We thank Terry Wade, Gopal Bera, and Tony Knap for making the CEWAF, Kendra Dean in assisting in the collection of the water from the Gulf of Mexico, Julia Sweet for collecting the aggregates, Gen Mei Lin for cell counts, and Jocelyn Simmons for help with enzyme activity measurements.

SUPPLEMENTARY MATERIAL

The Supplementary Material for this article can be found online at: https://www.frontiersin.org/articles/10.3389/fmicb.2018.00798/full#supplementary-material

REFERENCES

Allison, S. D. (2005). Cheaters, diffusion and nutrients constrain decomposition by microbial enzymes in spatially structured environments. *Ecol. Lett.* 8, 626–635. doi: 10.1111/j.1461-0248.2005.00756.x

Apprill, A., McNally, S., Parsons, R., and Weber, L. (2015). Minor revision to V4 region SSU rRNA 806R gene primer greatly increases detection of SAR11 bacterioplankton. *Aquat. Microb. Ecol.* 75, 129–137. doi: 10.3354/ame01753

Arnosti, C., Ziervogel, K., Yang, T., and Teske, A. (2016). Oil-derived marine aggregates–hot spots of polysaccharide degradation by specialized bacterial communities. *Deep Sea Res. Part II* 129, 179–186. doi: 10.1016/j.dsr2.2014.12.008

Bacosa, H. P., Erdner, D. L., and Liu, Z. (2015a). Differentiating the roles of photooxidation and biodegradation in the weathering of light louisiana sweet crude oil in surface water from the deepwater horizon site. *Mar. Pollut. Bull.* 95, 265–272. doi: 10.1016/j.marpolbul.2015.04.005

Bacosa, H. P., Liu, Z., and Erdner, D. L. (2015b). Natural sunlight shapes crude oil-degrading bacterial communities in Northern Gulf of Mexico surface waters. *Front. Microbiol.* 6:1325. doi: 10.3389/fmicb.2015.01325

Bacosa, H. P., Suto, K., and Inoue, C. (2012). Bacterial community dynamics during the preferential degradation of aromatic hydrocarbons by a microbial consortium. *Int. Biodeterior. Biodegradation* 74, 109–115. doi: 10.1016/j.ibiod.2012.04.022

Bailey, N. J. L., Jobson, A. M., and Rogers, M. A. (1973). Bacterial degradation of crude oil: comparison of field and experimental data. *Chem. Geol.* 11, 203–221. doi: 10.1016/0009-2541(73)90017-X

Blumenkrantz, N., and Asboe-Hansen, G. (1973). New method for quantitative determination of uronic acids. *Anal. Biochem.* 54, 484–489. doi: 10.1016/0003-2697(73)90377-1

Caldwell, B. A. (2005). Enzyme activities as a component of soil biodiversity: a review. *Pedobiologia* 49, 637–644. doi: 10.1016/j.pedobi.2005.06.003

Campeão, M. E., Reis, L., Leomil, L., de Oliveira, L., Otsuki, K., Gardinali, P., et al. (2017). The deep-sea microbial community from the amazonian basin associated with oil degradation. *Front. Microbiol.* 8:1019. doi: 10.3389/fmicb.2017.01019

Caporaso, J. G., Lauber, C. L., Walters, W. A., Berg-Lyons, D., Huntley, J., Fierer, N., et al. (2012). Ultra-high-throughput microbial community analysis on the Illumina HiSeq and MiSeq platforms. *ISME J.* 6, 1621–1624. doi: 10.1038/ismej.2012.8

de Melo, E. B., da Silveira Gomes, A., and Carvalho, I. (2006). α-and β-Glucosidase inhibitors: chemical structure and biological activity. *Tetrahedron* 62, 10277–10302. doi: 10.1016/j.tet.2006.08.055

Decho, A. W. (1990). Microbial exopolymer secretions in ocean environments: their role (s) in food webs and marine processes. *Oceanogr. Mar. Biol. Annu. Rev.* 28, 73–153.

Doyle, S. M., Whitaker, E. A., De Pascuale, V., Wade, T. L., Knap, A. H., Santschi, P. H., et al. (2018). Rapid formation of microbe-oil aggregates and changes in community composition in coastal surface water following exposure to oil and corexit. *Front. Microbiol.* 9:689. doi: 10.3389/fmicb.2018.00689

Dubinsky, E. A., Conrad, M. E., Chakraborty, R., Bill, M., Borglin, S. E., Hollibaugh, J. T., et al. (2013). Succession of hydrocarbon-degrading bacteria in the aftermath of the deepwater horizon oil spill in the Gulf of Mexico. *Environ. Sci. Technol.* 47, 10860–10867. doi: 10.1021/es401676y

Engel, A. (2002). Direct relationship between CO2 uptake and transparent exopolymer particles production in natural phytoplankton. *J. Plankton Res.* 24, 49–53. doi: 10.1093/plankt/24.1.49

Espeland, E. M., Francoeur, S. N., and Wetzel, R. G. (2001). Influence of algal photosynthesis on biofilm bacterial production and associated glucosidase and xylosidase activities. *Microb. Ecol.* 42, 524–530. doi: 10.1007/s00248-001-1022-8

Field, C. B., Behrenfeld, M. J., Randerson, J. T., and Falkowski, P. (1998). Primary production of the biosphere: integrating terrestrial and oceanic components. *Science* 281, 237–240. doi: 10.1126/science.281.5374.237

Frankenberger, W., and Dick, W. A. (1983). Relationships between enzyme activities and microbial growth and activity indices in soil. *Soil Sci. Soc. Am. J.* 47, 945–951.

Fruton, J. S., and Mycek, M. J. (1956). Proteolytic enzymes. *Annu. Rev. Biochem.* 25, 57–78. doi: 10.1146/annurev.bi.25.070156.000421

Guillard, R. R., and Ryther, J. H. (1962). Studies of marine planktonic diatoms: I. Cyclotella Nana Hustedt, and Detonula Confervacea (CLEVE) Gran. *Can. J. Microbiol.* 8, 229–239. doi: 10.1139/m62-029

Gutierrez, T., and Aitken, M. D. (2014). Role of methylotrophs in the degradation of hydrocarbons during the Deepwater Horizon oil spill. *ISME J.* 8, 2543–2545. doi: 10.1038/ismej.2014.88

Gutierrez, T., Singleton, D. R., Berry, D., Yang, T., Aitken, M. D., and Teske, A. (2013). Hydrocarbon-degrading bacteria enriched by the Deepwater Horizon oil spill identified by cultivation and DNA-SIP. *ISME J.* 7, 2091–2104. doi: 10.1038/ismej.2013.98

Hamdan, L. J., and Fulmer, P. A. (2011). Effects of COREXIT® EC9500A on bacteria from a beach oiled by the Deepwater Horizon spill. *Aquat. Microb. Ecol.* 63, 101–109. doi: 10.3354/ame01482

Hazen, T. C., Dubinsky, E. A., DeSantis, T. Z., Andersen, G. L., Piceno, Y. M., Singh, N., et al. (2010). Deep-sea oil plume enriches indigenous oil-degrading bacteria. *Science* 330, 204–208. doi: 10.1126/science.1195979

Jacobson Meyers, M. E., Sylvan, J. B., and Edwards, K. J. (2014). Extracellular enzyme activity and microbial diversity measured on seafloor exposed basalts from Loihi seamount indicate the importance of basalts to global biogeochemical cycling. *Appl. Environ. Microbiol.* 80, 4854–4864. doi: 10.1128/AEM.01038-14

Jones, S. E., and Lock, M. A. (1993). Seasonal determinations of extracellular hydrolytic activities in heterotrophic and mixed heterotrophic/autotrophic biofilms from two contrasting rivers. *Hydrobiologia* 257, 1–16. doi: 10.1007/BF00013991

King, G. M., Kostka, J. E., Hazen, T. C., and Sobecky, P. A. (2015). Microbial responses to the Deepwater Horizon oil spill: from coastal wetlands to the deep sea. *Annu. Rev. Mar. Sci.* 7, 377–401. doi: 10.1146/annurev-marine-010814-015543

Kleindienst, S., Paul, J. H., and Joye, S. B. (2015a). Using dispersants after oil spills: impacts on the composition and activity of microbial communities. *Nat. Rev. Microbiol.* 13, 388–396. doi: 10.1038/nrmicro3452

Kleindienst, S., Seidel, M., Ziervogel, K., Grim, S., Loftis, K., Harrison, S., et al. (2015b). Chemical dispersants can suppress the activity of natural oil-degrading microorganisms. *Proc. Natl. Acad. Sci. U.S.A.* 112, 14900–14905. doi: 10.1073/pnas.1507380112

Kostka, J. E., Prakash, O., Overholt, W. A., Green, S. J., Freyer, G., Canion, A., et al. (2011). Hydrocarbon-degrading bacteria and the bacterial community response in Gulf of Mexico beach sands impacted by the Deepwater Horizon oil spill. *Appl. Environ. Microbiol.* 77, 7962–7974. doi: 10.1128/AEM.05402-11

Kozich, J. J., Westcott, S. L., Baxter, N. T., Highlander, S. K., and Schloss, P. D. (2013). Development of a dual-index sequencing strategy and curation pipeline for analyzing amplicon sequence data on the MiSeq Illumina sequencing platform. *Appl. Environ. Microbiol.* 79, 5112–5120. doi: 10.1128/AEM.01043-13

Kujawinski, E. B., Kido Soule, M. C., Valentine, D. L., Boysen, A. K., Longnecker, K., and Redmond, M. C. (2011). Fate of dispersants associated with the Deepwater Horizon oil spill. *Environ. Sci. Technol.* 45, 1298–1306. doi: 10.1021/es103838p

Lamendella, R., Strutt, S., Borglin, S., Chakraborty, R., Tas, N., Mason, O. U., et al. (2014). Assessment of the Deepwater Horizon oil spill impact on Gulf coast microbial communities. *Front. Microbiol.* 5:130. doi: 10.3389/fmicb.2014.00130

Liu, J., Bacosa, H. P., and Liu, Z. (2017). Potential environmental factors affecting oil-degrading bacterial populations in deep and surface waters of the northern Gulf of Mexico. *Front. Microbiol.* 7:2131. doi: 10.3389/fmicb.2016.02131

Longhurst, A., Sathyendranath, S., Platt, T., and Caverhill, C. (1995). An estimate of global primary production in the ocean from satellite radiometer data. *J. Plankton Res.* 17, 1245–1271. doi: 10.1093/plankt/17.6.1245

Manivasagan, P., and Kim, S. K. (2014). "Extracellular polysaccharides produced by marine bacteria," in *Advances in Food and Nutrition Research*, Vol. 72, ed. N. A. Michael Eskin (Cambridge, MA: Academic Press), 79–94.

Markowitz, V. M., Korzeniewski, F., Palaniappan, K., Szeto, E., Werner, G., Padki, A., et al. (2006). The integrated microbial genomes (IMG) system. *Nucleic Acids Res.* 34, D344–D348. doi: 10.1093/nar/gkj024

Martínez, J. R. (1968). Organic phosphorus mineralization and phosphatase activity in soils. *Folia Microbiol.* 13, 161–174. doi: 10.1007/BF02868220

Mendelssohn, I. A., Andersen, G. L., Baltz, D. M., Caffey, R. H., Carman, K. R., Fleeger, J. W., et al. (2012). Oil impacts on coastal wetlands: implications for the Mississippi River Delta ecosystem after the Deepwater Horizon oil spill. *Bioscience* 62, 562–574. doi: 10.1525/bio.2012.62.6.7

Parada, A. E., Needham, D. M., and Fuhrman, J. A. (2016). Every base matters: assessing small subunit rRNA primers for marine microbiomes with mock communities, time series and global field samples. *Environ. Microbiol.* 18, 1403–1414. doi: 10.1111/1462-2920.13023

Passow, U., Ziervogel, K., Asper, V., and Diercks, A. (2012). Marine snow formation in the aftermath of the Deepwater Horizon oil spill in the Gulf of Mexico. *Environ. Res. Lett.* 7:035301. doi: 10.3389/fmicb.2017.00676

Piontek, J., Lunau, M., Händel, N., Borchard, C., Wurst, M., and Engel, A. (2010). Acidification increases microbial polysaccharide degradation in the ocean. *Biogeosciences* 7, 1615–1624. doi: 10.5194/bg-7-1615-2010

Poli, A., Anzelmo, G., and Nicolaus, B. (2010). Bacterial exopolysaccharides from extreme marine habitats: production, characterization and biological activities. *Mar. Drugs* 8, 1779–1802. doi: 10.3390/md8061779

Quigg, A., Passow, U., Chin, W. C., Xu, C., Doyle, S., Bretherton, L., et al. (2016). The role of microbial exopolymers in determining the fate of oil and chemical dispersants in the ocean. *Limnol. Oceanogr. Lett.* 1, 3–26. doi: 10.1002/lol2.10030

Reese, E. T., Maguire, A. H., and Parrish, F. W. (1968). Glucosidases and exo-glucanases. *Can. J. Biochem.* 46, 25–34. doi: 10.1139/o68-005

Romaní, A. M., and Sabater, S. (2000). Influence of algal biomass on extracellular enzyme activity in river biofilms. *Microb. Ecol.* 40, 16–24. doi: 10.1007/s002480000041

Schloss, P. D., Westcott, S. L., Ryabin, T., Hall, J. R., Hartmann, M., Hollister, E. B., et al. (2009). Introducing mothur: open-source, platform-independent, community-supported software for describing and comparing microbial communities. *Appl. Environ. Microbiol.* 75, 7537–7541. doi: 10.1128/AEM.01541-09

Sinsabaugh, R. L., Hill, B. H., and Shah, J. J. F. (2009). Ecoenzymatic stoichiometry of microbial organic nutrient acquisition in soil and sediment. *Nature* 462, 795–798. doi: 10.1038/nature08632

Sinsabaugh, R. L., Lauber, C. L., Weintraub, M. N., Ahmed, B., Allison, S. D., Crenshaw, C., et al. (2008). Stoichiometry of soil enzyme activity at global scale. *Ecol. Lett.* 11, 1252–1264. doi: 10.1111/j.1461-0248.2008.01245.x

Smith, P. K., Krohn, R. I., Hermanson, G., Mallia, A., Gartner, F., Provenzano, M., et al. (1985). Measurement of protein using bicinchoninic acid. *Anal. Biochem.* 150, 76–85. doi: 10.1016/0003-2697(85)90442-7

Turner, R., Overton, E., Meyer, B., Miles, M., and Hooper-Bui, L. (2014). Changes in the concentration and relative abundance of alkanes and PAHs from the Deepwater Horizon oiling of coastal marshes. *Mar. Pollut. Bull.* 86, 291–297. doi: 10.1016/j.marpolbul.2014.07.003

Underwood, G. J., Boulcott, M., Raines, C. A., and Waldron, K. (2004). Environmental effects on exopolymer production by marine benthic diatoms: dynamics, changes in composition, and pathways of production1. *J. Phycol.* 40, 293–304. doi: 10.1111/j.1529-8817.2004.03076.x

Valentine, D. L., Kessler, J. D., Redmond, M. C., Mendes, S. D., Heintz, M. B., Farwell, C., et al. (2010). Propane respiration jump-starts microbial response to a deep oil spill. *Science* 330, 208–211. doi: 10.1126/science.1196830

Vetter, Y., and Deming, J. (1999). Growth rates of marine bacterial isolates on particulate organic substrates solubilized by freely released extracellular enzymes. *Microb. Ecol.* 37, 86–94. doi: 10.1007/s002489900133

Wade, T. L., Morales-McDevitt, M., Bera, G., Shi, D., Sweet, S., Wang, B., et al. (2017). A method for the production of large volumes of WAF and CEWAF for dosing mesocosms to understand marine oil snow formation. *Heliyon* 3:e00419. doi: 10.1016/j.heliyon.2017.e00419

Xu, C., Santschi, P. H., Hung, C. C., Zhang, S. J., Schwehr, K. A., Roberts, K. A., et al. (2011a). Controls of (234)Th removal from the oligotrophic ocean by polyuronic acids and modification by microbial activity. *Mar. Chem.* 123, 111–126. doi: 10.1016/j.marchem.2010.10.005

Xu, C., Santschi, P. H., Schwehr, K. A., and Hung, C. C. (2009). Optimized isolation procedure for obtaining strongly actinide binding exopolymeric substances (EPS) from two bacteria (*Sagittula stellata* and *Pseudomonas fluorescens* Biovar II). *Bioresour. Technol.* 100, 6010–6021. doi: 10.1016/j.biortech.2009.06.008

Xu, C., Zhang, S. J., Chuang, C. Y., Miller, E. J., Schwehr, K. A., and Santschi, P. H. (2011b). Chemical composition and relative hydrophobicity of microbial exopolymeric substances (EPS) isolated by anion exchange chromatography and their actinide-binding affinities. *Mar. Chem.* 126, 27–36. doi: 10.1016/j.marchem.2011.03.004

Yamada, N., and Suzumura, M. (2010). Effects of seawater acidification on hydrolytic enzyme activities. *J. Oceanogr.* 66, 233–241. doi: 10.1007/s10872-010-0021-0

Yang, T., Nigro, L. M., Gutierrez, T., Joye, S. B., Highsmith, R., and Teske, A. (2016a). Pulsed blooms and persistent oil-degrading bacterial populations in the water column during and after the Deepwater Horizon blowout. *Deep Sea Res. Part II* 129, 282–291. doi: 10.1016/j.dsr2.2014.01.014

Yang, T., Speare, K., McKay, L., MacGregor, B. J., Joye, S. B., and Teske, A. (2016b). Distinct bacterial communities in surficial seafloor sediments following the 2010 Deepwater Horizon blowout. *Front. Microbiol.* 7:1384. doi: 10.3389/fmicb.2016.01384

Yemm, E., and Willis, A. (1954). The estimation of carbohydrates in plant extracts by anthrone. *Biochem. J.* 57, 508–514. doi: 10.1042/bj0570508

Ziervogel, K., Joye, S. B., and Arnosti, C. (2016). Microbial enzymatic activity and secondary production in sediments affected by the sedimentation pulse following the Deepwater Horizon oil spill. *Deep Sea Res. Part II* 129, 241–248. doi: 10.1016/j.dsr2.2014.04.003

Ziervogel, K., McKay, L., Rhodes, B., Osburn, C. L., Dickson-Brown, J., Arnosti, C., et al. (2012). Microbial activities and dissolved organic matter dynamics in oil-contaminated surface seawater from the Deepwater Horizon oil spill site. *PLoS One* 7:e34816. doi: 10.1371/journal.pone.0034816

Conflict of Interest Statement: The authors declare that the research was conducted in the absence of any commercial or financial relationships that could be construed as a potential conflict of interest.

frontiers in Microbiology

ORIGINAL RESEARCH
published: 10 October 2017
doi: 10.3389/fmicb.2017.01952

Methodological Considerations and Comparisons of Measurement Results for Extracellular Proteolytic Enzyme Activities in Seawater

Yumiko Obayashi[1]*, *Chui Wei Bong*[1,2,3] and *Satoru Suzuki*[1]

[1] Center for Marine Environmental Studies, Ehime University, Matsuyama, Japan, [2] Institute of Biological Sciences, Faculty of Science, University of Malaya, Kuala Lumpur, Malaysia, [3] Institute of Ocean and Earth Sciences (IOES), University of Malaya, Kuala Lumpur, Malaysia

Microbial extracellular hydrolytic enzymes that degrade organic matter in aquatic ecosystems play key roles in the biogeochemical carbon cycle. To provide linkages between hydrolytic enzyme activities and genomic or metabolomic studies in aquatic environments, reliable measurements are required for many samples at one time. Extracellular proteases are one of the most important classes of enzymes in aquatic microbial ecosystems, and protease activities in seawater are commonly measured using fluorogenic model substrates. Here, we examined several concerns for measurements of extracellular protease activities (aminopeptidases, and trypsin-type, and chymotrypsin-type activities) in seawater. Using a fluorometric microplate reader with low protein binding, 96-well microplates produced reliable enzymatic activity readings, while use of regular polystyrene microplates produced readings that showed significant underestimation, especially for trypsin-type proteases. From the results of kinetic experiments, this underestimation was thought to be attributable to the adsorption of both enzymes and substrates onto the microplate. We also examined solvent type and concentration in the working solution of oligopeptide-analog fluorogenic substrates using dimethyl sulfoxide (DMSO) and 2-methoxyethanol (MTXE). The results showed that both 2% (final concentration of solvent in the mixture of seawater sample and substrate working solution) DMSO and 2% MTXE provide similarly reliable data for most of the tested substrates, except for some substrates which did not dissolve completely in these assay conditions. Sample containers are also important to maintain the level of enzyme activity in natural seawater samples. In a small polypropylene containers (e.g., standard 50-mL centrifugal tube), protease activities in seawater sample rapidly decreased, and it caused underestimation of natural activities, especially for trypsin-type and chymotrypsin-type proteases. In conclusion, the materials and method for measurements should be carefully selected in order to accurately determine the activities of microbial extracellular hydrolytic enzymes in aquatic ecosystems; especially, low protein binding materials should be chosen to use at overall processes of the measurement.

Keywords: extracellular hydrolytic enzyme, protease, activity measurement, microbial loop, organic matter degradation, low protein binding microplate, MCA substrate

OPEN ACCESS

Edited by:
Andrew Decker Steen,
University of Tennessee, United States

Reviewed by:
Zhanfei Liu,
University of Texas at Austin, United States
Jason B. Sylvan,
Texas A&M University, United States

***Correspondence:**
Yumiko Obayashi
obayashi.yumiko.nn@ehime-u.ac.jp

Specialty section:
This article was submitted to Aquatic Microbiology, a section of the journal Frontiers in Microbiology

Received: *31 March 2017*
Accepted: *22 September 2017*
Published: *10 October 2017*

Citation:
Obayashi Y, Wei Bong C and Suzuki S (2017) Methodological Considerations and Comparisons of Measurement Results for Extracellular Proteolytic Enzyme Activities in Seawater. Front. Microbiol. 8:1952. doi: 10.3389/fmicb.2017.01952

INTRODUCTION

In aquatic ecosystems, heterotrophic prokaryotes play important roles in organic matter cycling, including the transformation and remineralization of organic molecules and in its transfer to other organisms via trophic interactions. In order for heterotrophic bacteria that are osmotrophs to obtain nutrients from polymeric biomolecules such as proteins, these high molecular weight organic molecules must be hydrolyzed extracellularly to smaller sizes (approx. <600 Da, Nikaido and Vaara, 1985) prior to their transport across the bacterial outer membrane (Weiss et al., 1991). Thus, hydrolytic activities of extracellular enzymes in aquatic environment are investigated from the standpoint of microbial ecology, biogeochemistry, and organic geochemistry (Arnosti, 2011).

Hydrolytic enzyme activities, such as protease, glucosidase, phosphatase, and chitinase, have been detected and estimated in natural seawaters (reviewed in Hoppe et al., 2002; Arnosti, 2003) using model substrates as proxies of natural substrates. Model substrates added to the sample for measuring potential hydrolytic activities in seawater may be unlabeled oligomers (Liu et al., 2010; Liu and Liu, 2015) or labeled molecules that can be detected as hydrolytic derivatives (e.g., Arnosti, 1996; Pantoja et al., 1997; Steen et al., 2006). Among fluorogenic model substrates, which have fluorophores liberated by enzymatic hydrolysis, 4-methylumbelliferyl (MUF) substrates for α-glucosidase, β-glucosidase, and alkaline phosphatase, and 4-methylcoumaryl-7-amide (MCA) substrate for leucine-aminopeptidase are the most commonly used proxies of natural substrates for measuring individual enzymatic activities in seawater samples (Hoppe, 1993). Although, using these proxies to assess natural hydrolytic activities of enzymes in environmental samples results in some theoretical limitations and uncertainties (e.g., Steen et al., 2015), important information on biogeochemical processes in aquatic ecosystems can be obtained.

Estimating more than two hydrolytic activities in the same sample permits consideration of the nutritional mode of the bacteria and the biochemical composition of available polymeric substrates in marine systems (Nagata, 2008). For example, Fukuda et al. (2000) investigated the ratio of activities by leucine-aminopeptidase and β-glucosidase along the east-west transect of the North Pacific and suggested that there is a difference in microbial biochemical conditions between the eastern and western parts of the northern North Pacific. Sala et al. (2001) suggested that the ratio of alkaline phosphatase and aminopeptidase activities could be an indicator of nitrogen and phosphate limitation in the microbial community.

Enzyme activity in bulk seawater samples are often operationally divided into fractions such as "particle-associated" and "dissolved (cell-free)" activities by taking measurements separately on seawater that passes through filters of a specified pore size, as well as unfiltered samples. These fractionations may provide insights into the natural forms of hydrolytic enzymes in seawater and the ecological roles that each play (Arnosti, 2003). Smith et al. (1992) and Karner and Herndl (1992) showed that particle (marine snow)-associated hydrolytic activities were much higher than those in the surrounding seawater at least for their tested enzyme types. Meanwhile, dissolved (free) enzymes have been reported to make substantial contributions to the total activity (e.g., Keith and Arnosti, 2001; Obayashi and Suzuki, 2008a; Baltar et al., 2016), although their ratios vary depending on the sampling conditions and enzyme type.

Proteins and peptides should be good nutrition for heterotrophic prokaryotes after suitable hydrolysis by extracellular enzymes, and thus extracellular proteases are one of the most important hydrolytic enzymes in aquatic microbial ecosystems. Measurements of extracellular proteolytic enzyme activity in aquatic samples using fluorogenic model substrates have been popular since their introduction (e.g., Hoppe, 1993), especially for leucine aminopeptidase, because of their high sensitivity and easiness of the method. Not only aminopeptidase activity but a number of diverse proteolytic enzymes and the importance of trypsin-type endopeptidases, which cleave peptide bonds within a peptide, in natural seawater were also reported using 16 different MCA substrates (Obayashi and Suzuki, 2005). To discuss the relationships or interactions with physical and chemical environmental conditions, or to link those with genomic or metabolomic information on microbial communities, high-resolution reliable measurement data on extracellular proteolytic enzyme activities are required. High-resolution analysis requires many samples to be measured at one time, such as collecting samples at many depth layers at each sampling site, many size fractionations, or testing with different kinds of model substrates. To get reliable activity data, many samples should be analyzed as soon as possible after sampling (German et al., 2011) and each sample measurement should be performed in replicate. Moreover, for reliable estimation of the potential activity of microbial extracellular hydrolytic enzymes in the aquatic environment, many factors should be considered. For example, Obayashi and Suzuki (2008b) pointed out that adsorption effects to the filter for size fractionation could lead underestimation of the enzyme activity in the filtrates depending on the type of filter material and that the effects were different among the type of enzymes. Recently, not only a standard spectrofluorometer with a cuvette, a fluorometric microplate reader with a micro-well plate has been also applied as a device to read fluorescent intensity during a measurement of activity (e.g., Baltar et al., 2010). Microplate reader offers considerable advantage to get measurement data for many samples at one time, however, using 96-well microplates, water sample volume is small and the ratio of the area touching plate material (the wall and bottom of each well) to the sample volume is relatively large. Considering a kind of adsorption effect likely to filters for size fractionation, samples in a microplate might be more susceptible to some kinds of artifact than in a larger volume cuvette. However, many researches might be performed with microplate not always taking care about the types of microplate materials, and to our knowledge, systematic comparison between data obtained from microplates and cuvettes has not been reported so far regarding the measurement of extracellular enzyme activity in a natural seawater sample. Here, we examine several concerns regarding to achieve high-resolution reliable estimations of extracellular proteolytic enzyme activities in seawater using

many kinds of MCA substrates and a fluorometric microplate reader.

MATERIALS AND METHODS

Seawater Samples

Seawater samples for each test were collected by bucket or Van Dorn water sampler along the coast of Ehime Prefecture, Japan, and filtered through nylon mesh (150 or 50 μm) into bottles to remove large particles. Polycarbonate 500 mL bottles were used as a sample container, except for the experiment to compare several types of containers. Samples were immediately placed on ice for transport to the laboratory where the samples were refrigerated at 4°C until proceeding with the assays within several hours. In general, to assess the extracellular enzyme activities in natural aquatic samples the activities should be measured as soon as possible after sampling, to minimize the possible alteration after sampling such as degradation of dissolved enzymes and changing of microbial community and their activity. Even though the main purpose of each experiment in this study was to compare the data for the same water sample using different methodological conditions, we conducted each experiment as soon as possible after seawater sampling (within several hours), except for the preservation test in different sample containers. When we kept water samples for a short time before measurement, samples were kept cool and in the dark for the least degradation of enzymes possible, although there were still unavoidable possibilities of microbial cell lysis at 4°C.

For some experiments, an aliquot of sample was filtered through a 0.2 μm pore size polycarbonate Nuclepore filter (Whatman), then both unfiltered and filtered (<0.2 μm) seawater samples were used.

Enzyme Activities Measurement

The potential activities of extracellular proteolytic enzymes in seawater samples were measured using 17 MCA substrates (**Table 1**, Peptide Institute): 5 for aminopeptidase, 10 for trypsin, and 2 for chymotrypsin. Enzyme activities measurement was conducted as follows with modifications for the different methods tested, as noted below.

MCA substrates were dissolved in solvents dimethyl sulfoxide (DMSO) or 2-methoxyethanol (MTXE) to prepare stock solutions (10 or 20 mM). For assay, 10× substrate working solutions were prepared from the stock solutions in autoclaved artificial seawater and solvent to control for solvent concentration in the solution, with substrate and solvent concentrations 10 times higher than the target final concentrations in assay. Seawater samples and 10× substrate solutions were mixed in disposable cuvettes or 96-well microplates and incubated at 25°C in the dark to measure potential enzyme activities. The fluorescence of the hydrolytic product, 7-amino-4-methylcoumarin (AMC), was measured several times at intervals (t0, t1, t2, t3; typically 1 h interval) during the incubation. The excitation/emission wavelengths for fluorescence measurements were 380/460 nm on a spectrofluorometer (Hitachi F-2500) or 380/440 nm on a microplate reader (Corona SH8100Lab). A solvent blank (seawater sample with solvent but without substrate) was also prepared and subjected to fluorescence measurements along with samples. After subtracting the solvent fluorescence blank, the concentration of AMC generated during the incubation was calculated using a calibration curve prepared by measuring fluorescence intensity of AMC solutions at seven concentrations (0–1 μM) under the same conditions as the sample measurements. To measure the non-enzymatic produced AMC during incubation, collected seawater was autoclaved and prepared and assayed as an inactivated control under the same conditions as the intact sample. The hydrolysis rate of the substrate in the seawater sample, namely, extracellular enzyme activity in seawater, was calculated by determining the increase in AMC concentration with time after subtracting the concentration of non-enzymatic produced AMC estimated in autoclaved seawater.

Every assay was performed in triplicate using three cuvettes or three wells in a microplate for each sample and substrate pair.

Comparison Methods for Protease Activities Measurement

Extracellular proteolytic enzyme activities in natural seawater samples were measured using different assay methods (Methods A, B, and C) simultaneously with the same working solutions. In Method A, we used a spectrofluorometer with disposable cuvettes, while Methods B and C were conducted on a fluorometric microplate reader with regular and low protein binding microplates, respectively. The excitation/emission wavelengths recommended by the supplier of MCA substrates (Peptide Institute) for the assay were 380/460 nm; however, to obtain a higher intensity fluorescence signal from smaller sample volumes used on microplates (Methods B and C), we set the emission wavelength at 440 nm, the wavelength of maximum fluorescence intensity for AMC. We confirmed that readings taken at 440 and 460 nm provided equivalent results when the corresponding calibration curve was applied. Following are brief overviews of Methods A, B, and C:

Method A (cuvette) was conducted with a reaction volume of 1 mL in a disposable cuvette made from polymethylmethacrylate (PMMA). Fluorescence was measured by a spectrofluorometer at excitation/emission wavelengths of 380/460 nm.

Method B (regular microplate) was conducted with a reaction volume of 300 μL in regular 96-well black microplates made from polystyrene (Nunc #237107). Fluorescence was measured by a microplate reader in fluorescence mode at an excitation/emission wavelength of 380/440 nm.

Method C (low protein binding microplate) was conducted as for Method B except with a low protein binding, black, 96-well microplate made from polystyrene coated with methacryloyloxyethyl phosphorylcholine (MPC) (Nunc #245393).

Pearson's correlation coefficient and simple regression were used to compare data obtained from different methods in pairwise comparisons (Methods A vs. B, Methods A vs. C, Methods C vs. B). Regression analyses of pairs of methods were performed with combined dataset from unfiltered and

TABLE 1 | List of fluorogenic substrates used in the present study.

Substrate		Experiment						
Name	**Substrate for**	**Method comparison**	**Kinetics**	**Microplate comparison**	**Solvent**			**Sample container**
		Methods A,B,C	**Methods B,C**	**3 Suppliers**	**DMSO 10% vs. 2%**	**DMSO 2% vs. 1%**	**DMSO 2% vs. MTXE 2%**	
Arg-MCA	Aminopeptidase	+		+		*	*	
Leu-MCA	Aminopeptidase	+	+	+	+	+	+	+
Ala-MCA	Aminopeptidase	+	+	+	+	+	+	+
Lys-MCA	Aminopeptidase	+		+		+	+	
Phe-MCA	Aminopeptidase	+		+		+	+	
Bz-Arg-MCA	Trypsin	+		+		+	+	
Z-Phe-Arg-MCA	Trypsin	+				*	*	
Glt-Gly-Arg-MCA	Trypsin	+		+		+	+	
Boc-Leu-Gly-Arg-MCA	Trypsin	+		+		+	+	
Boc-Leu-Thr-Arg-MCA	Trypsin	+		+		+	+	
Boc-Phe-Ser-Arg-MCA	Trypsin	+	+	+	+	*	+	+
Boc-Val-Pro-Arg-MCA	Trypsin	+		+		+	+	
Boc-Leu-Ser-Thr-Arg-MCA	Trypsin	+	+	+	+	+	+	+
Boc-Val-Leu-Lys-MCA	Trypsin	+		+		+	+	
Boc-Glu-Lys-Lys-MCA	Trypsin	+		+		+	+	
Suc-Ala-Ala-Pro-Phe-MCA	Chymotrypsin	+	+	+	+	+	+	+
Suc-Leu-Leu-Val-Tyr-MCA	Chymotrypsin	+			*	*	*	
MUF-phosphate	Phosphatase		+					

*+Substrate used in experiment; *Substrate not soluble in one or both concentrations of solvent. MCA, 4-methylcoumaryl-7-amide; Bz, Benzoyl; Z, Carbobenzoxy; Boc, t-Butyloxycarbonyl; Suc, Succinyl; MUF, 4-Methylumbelliferyl.*

filtered seawater samples for "all estimated activities" and for the "aminopeptidase activities," "trypsin-type activities," and "chymotrypsin-type activities."

Kinetic Experiments

Using selected MCA substrates for proteases (**Table 1**), kinetic experiments were performed, and the Michaelis plots obtained by Method B (regular microplate) and Method C (low protein binding microplate) were compared. For the kinetic experiments, MCA substrates were added to samples at final concentrations of 0, 10, 20, 50, 100, 150, 200, and 250 μM. Hydrolysis rates of substrates were measured by Methods B and C with the protocol given above.

To determine whether differences in results between Methods B and C are proteolytic enzyme-specific, the same experiment was conducted using MUF substrate for phosphatase (MUF-phosphate, Wako Chemicals) at a final concentration of 0, 10, 30, 60, 100, 160, and 200 μM. Measurement of the hydrolysis rate of the MUF substrates was conducted by the same method as for the MCA substrates, except that the excitation/emission wavelengths of 365/445 nm were used to detect the 4-methylumbelliferon product.

Based on the measured hydrolytic activities, V, and the substrate concentrations, [S], the theoretical maximum activity, V_{max}, and the Michaelis constant, K_m, were estimated by curve fitting using software OriginPro 9.1 to the Michaelis–Menten equation:

$$V = V_{\max} \times [S]/(K_m + [S]) \quad (1)$$

Comparison of Low Protein Binding Microplates from Different Suppliers

Low protein binding 96-well black microplates from different suppliers were tested using seawater collected by bucket and strained through 50 μm nylon mesh into polycarbonate bottles. An aliquot of seawater (180 μL) was mixed with 20 μL of each of 15 MCA substrate solutions (**Table 1**; final concentration, 200 μM substrate, 2% DMSO) in three different microplates. Nunc low protein binding plate (Nunc #245393, as described above), Greiner Bio-one No-binding plate (Greiner 655900), and SUMILON Proteosave plate (Sumitomo Bakelite MS-8296K) were used to measure proteases activities in the same seawater sample with the same substrate solution, and the results were compared. Enzyme activities were measured using the protocol described above.

Examination of Solvent

The manufacturer of the MCA substrates (Peptide Institute) recommends using DMSO to prepare stock solutions. Considering the possibility of solvent bias in activities measurement, a lower concentration of solvent in assay is

better. However, lower solvent concentration may result in reduced solubility of the substrate in seawater. To examine the effect of DMSO, two experiments were conducted with different DMSO concentrations: (1) kinetic experiments comparing 10% (v/v) and 2% (v/v) DMSO, and (2) comparison of the activities measurement with 2 and 1% DMSO with 200 μM substrate final concentration.

Substrate working solution (10×) were prepared for each substrate concentration with 100% DMSO for final 10% DMSO in the assay, while those were prepared with autoclaved artificial seawater containing 20% DMSO for final 2% in the assay. Using low protein binding, 96-well microplates (Nunc), natural seawater sample 270 μL and 10× substrate working solution 30 μL were mixed in each well of the microplate. For this experiment, five MCA substrates (2 for aminopeptidase, 2 for trypsin, and 1 for chymotrypsin) were used (**Table 1**). Calibration curves of AMC were generated for each assays conducted with 10 and 2% DMSO.

Activity measurements were compared between 2 and 1% DMSO concentrations with 200 μM final substrate concentration. For this experiment, 15 substrates (**Table 1**) and low protein binding microplates from three suppliers (Nunc, Greiner, Sumitomo, as described above) were used. The seawater sample (180 μL) and 20 μL of 2 mM substrate working solution with 20 or 10% DMSO were mixed in each well of the microplate. Calibration curves of AMC were generated for each the assays conducted with 2 and 1% DMSO.

Previous studies used 2-methoxyethanol (MTXE, methylcellosolve) as a solvent of substrates to measure potential activities of extracellular hydrolytic enzymes in seawater (e.g., Fukuda et al., 2000). We also tested MTXE instead of DMSO as a solvent to dissolve the MCA substrates for protease assay. Substrate stock solutions (20 mM) were prepared with MTXE, and working solutions (10×) of each substrate, which contain 2 mM substrate and 20% MTXE, were prepared from the stock solution and autoclaved artificial seawater. A calibration curve of AMC with 2% MTXE was also prepared, and other procedures for fluorescence measurement and activities estimations were conducted as described above.

Significance of differences between 1 and 2% DMSO concentrations and different solvents (2% MTXE and 2% DMSO) were tested by Student's *t*-test.

Sample Containers for Seawater Collection

To test the effect of sampling container material, the following five types of containers were used: 500 mL polycarbonate bottles (PC500) (Nalgene), 50 mL polypropylene tubes supplied by Corning (PPC) and Eppendorf (PPE), 50 mL polyethylene terephthalate tubes (PET) (Corning), and low protein binding ProteosaveSS 50 mL tubes (SS) (Sumitomo Bakelite Co., Ltd.). The four 50 mL tubes had a similar shape of ordinary plastic centrifugal tubes. Natural seawater samples were collected by a bucket and immediately transferred to these containers through 50 μm nylon mesh. All seawater samples were kept cool until measurements of proteases activities. Proteases activities were measured using five MCA substrates (2 for aminopeptidase, 2 for trypsin, and 1 for chymotrypsin) at several hours after sampling, and at 1 day (26 h) and 2 days (47 h) after sampling. Reaction volume for the assay was 200 μL (180 μL seawater sample + 20 μL substrate solution) in low protein binding microplate (Nunc), and the final concentrations in the mixture were 200 μM substrate with 2% DMSO. Other procedures for fluorescence measurement and enzyme activities estimation were the same as described above.

RESULTS AND DISCUSSION

Microplates for Enzyme Activities Measurement in Seawater

Comparison of Activity Estimation by Methods A (Cuvette), B (Regular Microplate), and C (Low Protein Binding Microplate)

Figure 1 shows the relationship hydrolytic activities measurements obtained by each method for the same samples. Data from unfiltered and 0.2 μm filtered seawater samples were indicated as filled and opened symbols, respectively. Different shapes of the symbols in **Figure 1** refer to different types of enzyme activities estimated by using different substrates.

The protease activities measured by Method B (microplate reader with regular polystyrene microplates) were systematically lower than those by Method A (spectrofluorometer with cuvette; **Figure 1A**) and Method C (microplate reader with low protein binding microplates; **Figure 1C**). For the comparison of Method B to Method A, the linear relationship between measured activity for the two methods on all samples was significant [$n = 64$ (unfiltered and filtered samples were combined), $r = 0.953$, $p < 0.0001$] with a regression coefficient of 0.394 ± 0.015 (regression line for all data not shown in **Figure 1A**) indicated that the measured values obtained by Method B were only about 39% of those measured by Method A. The linear relationships between the results of Methods B and A were significant for both aminopeptidase activity ($n = 20$, $r = 0.988$, $p < 0.0001$) and trypsin-type activity ($n = 36$, $r = 0.972$, $p < 0.0001$). Regression line was not shown for chymotrypsin-type activity in **Figure 1A** because of the limited number of data points comparing with aminopeptidase and trypsin-type activity. The regression coefficient for trypsin-type activity (0.361 ± 0.014) was significantly smaller ($t = 4.12$, $p < 0.0005$) than that for aminopeptidase activity (0.643 ± 0.023). Although, there is not absolute evidence that higher estimation is more accurate, these results seem to suggest that Method B (microplate reader with regular polystyrene microplates) resulted in an underestimation of extracellular enzyme activity in natural seawater, and this effect was greater for trypsin-type activity than for aminopeptidase activity. Similarly, for the comparison of activities measurements by Method B and Method C (**Figure 1C**) shows that aminopeptidase activity and trypsin-type activities measured by Method B are 85 and 41%, respectively, of the measured values by Method C. For this comparison, the analytical methods of Methods B and C are identical and the

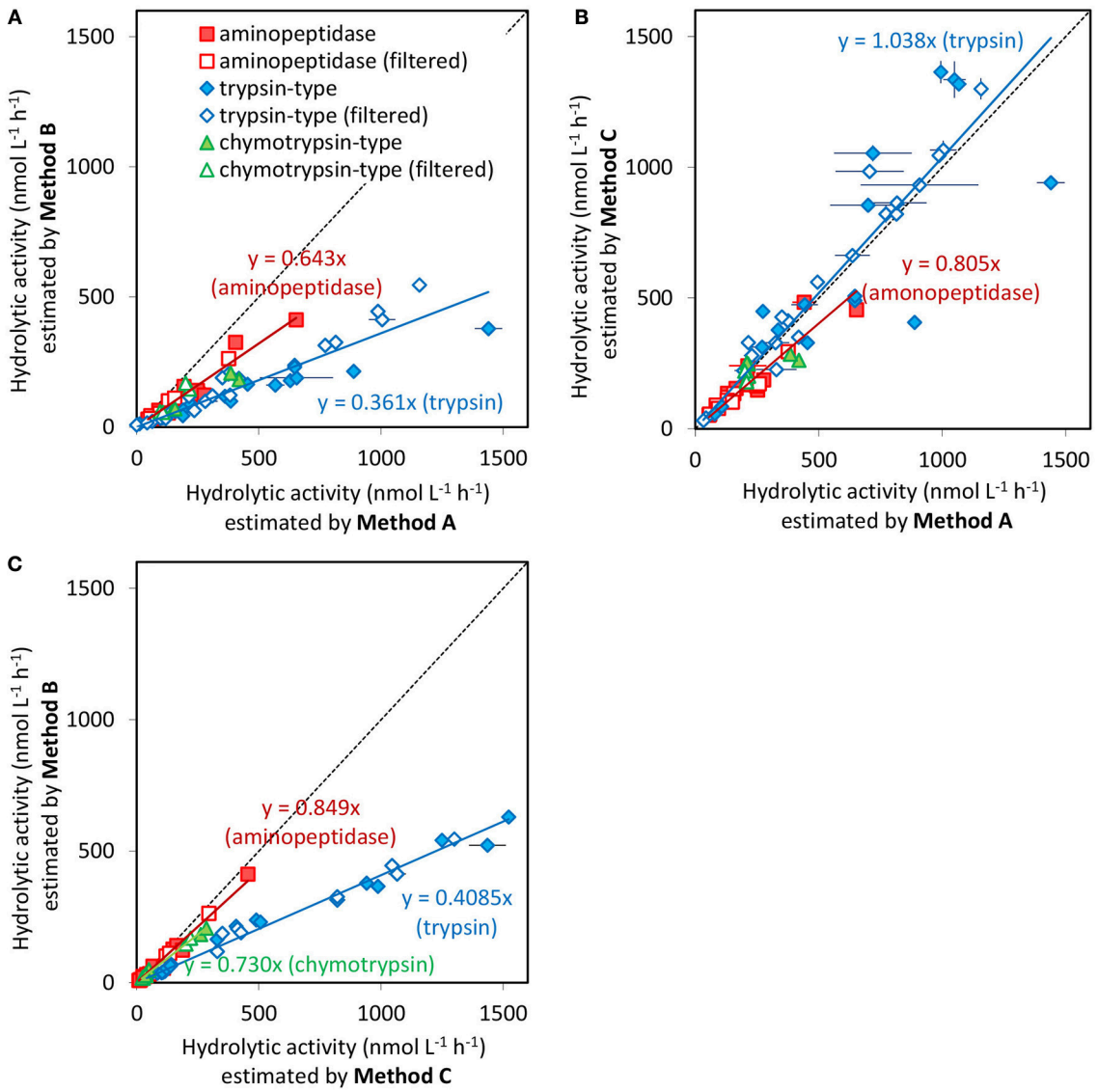

FIGURE 1 | Scatter plots of hydrolytic activities measured by **(A)** Method A (spectrofluorometer with disposable cuvettes) and Method B (fluorometric microplate reader with regular polystyrene microplate), **(B)** Method A and Method C (fluorometric microplate reader with low protein binding microplate), and **(C)** Method C and Method B. Activities measured for all samples by each of the two methods are plotted. The shapes of symbols indicate enzymes type, and filled and opened symbols indicate unfiltered seawater samples and <0.2 μm filtered seawater (dissolved fraction), respectively. Samples from different dates are not differentiated. Error bars are the standard deviations of triplicate sample preparations. Regression lines for aminopeptidase and trypsin-type endopeptidase and their equations are also shown. These regression analyses were performed with combined dataset from unfiltered and filtered samples. Dashed line indicates 1:1.

differences in measurement are attributable to the material of the microplates.

The linear relationship between the enzyme activities measurements obtained by Methods A and C was significant ($n = 64$, $r = 0.968$, $p < 0.0001$) and the regression coefficient was near 1 (1.015 ± 0.031), indicating that proteases activities measurements by these two methods are equivalent. Separate analyses for each of the enzyme types also were significant with regression coefficients for aminopeptidase and trypsin-type activity of 0.805 ± 0.039 and 1.038 ± 0.044, respectively (**Figure 1B**); the difference between these two coefficients was not significant ($t = 0.95$, $p > 0.35$). These results indicated that the systematic underestimation of enzyme activities using Method B can be avoided by using low protein binding microplates.

Factors Causing Reduced Enzyme Activities Measurements with Regular Polystyrene Microplates

To clarify the discrepancies between the results obtained using regular microplates and low protein binding microplates, kinetic experiments were conducted based on the following hypotheses. If the observed underestimation is due solely to the adsorption of the artificial substrate and not due

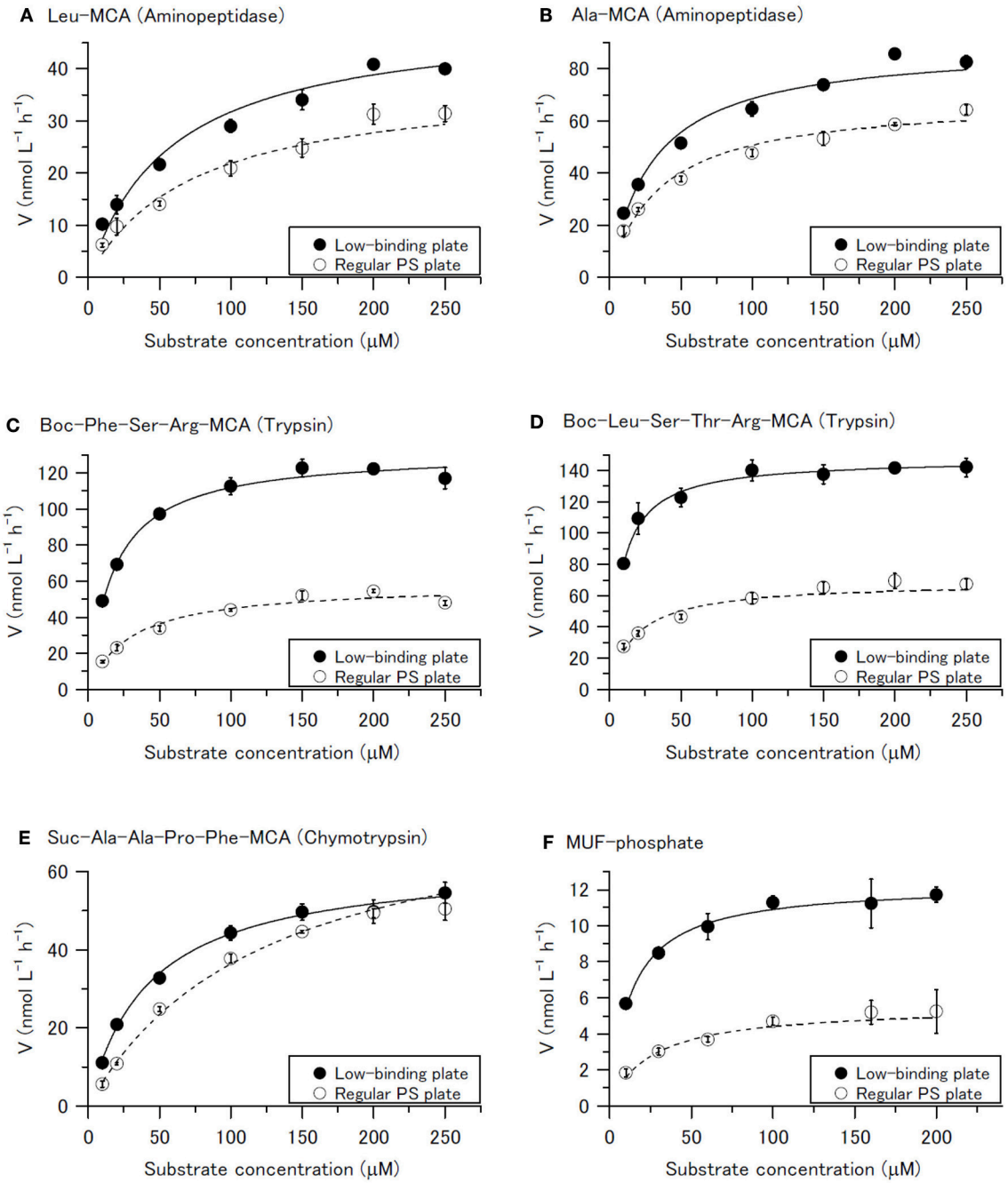

FIGURE 2 | Michaelis plot of hydrolysis of **(A)** Leu-MCA (substrate for aminopeptidase), **(B)** Ala-MCA (substrate for aminopeptidase), **(C)** Boc-Phe-Ser-Arg-MCA (substrate for trypsin), **(D)** Boc-Leu-Ser-Thr-Arg-MCA (substrate for trypsin), **(E)** Suc-Ala-Ala-Pro-Phe-MCA (substrate for chymotrypsin), and **(F)** MUF-phosphate (substrate for phosphatase) measured by Method C (low protein binding microplate) and Method B (regular polystyrene microplate). Error bars are the standard deviation of triplicate sample preparations (each sample and substrate pair was incubated and measured in 3 wells separately). Solid lines and dashed lines indicate curves fitting data from the low protein binding microplates and regular polystyrene microplates, respectively, to the Michaelis-Menten equation.

to the adsorption and deactivation of enzymes onto the surface of the polystyrene microplates, the measured activity by Method B should become saturated at higher level of the substrate than by Method C, and the differences between the measurements by Methods B and C should diminish at higher concentrations of substrate. On the other hand, if the reduced measurements are due to adsorption/deactivation of enzymes, the activities measurement by Method B should become saturated at almost the same level of substrate concentration as for Method C; namely, the Michaelis constant,

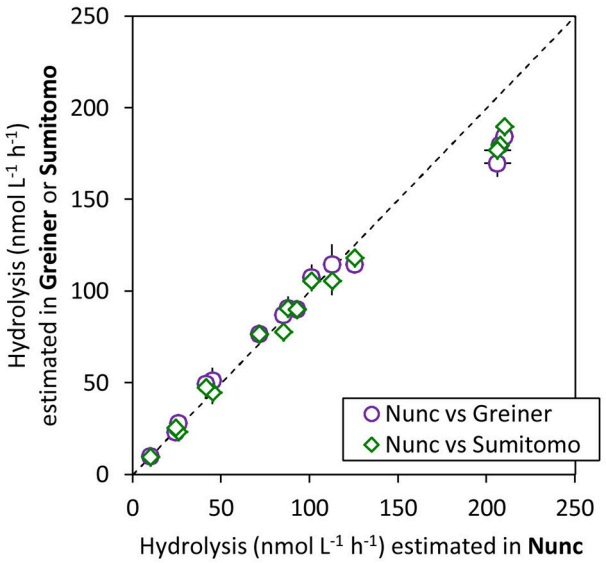

FIGURE 3 | Comparison between hydrolytic activities measured in Greiner Bio-one No-binding microplate (Greiner) and SUMILON Proteosave microplate (Sumitomo) to Nunc low binding microplate (Nunc), for the same seawater samples, using the same analytical method except for the microplates. Error bars are the standard deviation of triplicate sample preparations (same sample incubated in 3 wells). Dashed line indicates 1:1.

K_m, should be at a similar value, and the maximum activity, V_{max}, estimated by Method B should be smaller than that for Method C.

Our results show that aminopeptidase and trypsin-type activities estimated by Method B were lower than those by Method C even at higher substrate concentrations (**Figure 2**), although not much differences in chymotrypsin-type activity at the highest substrate concentration for Methods B and C. By curve fitting to the Michaelis–Menten equation, V_{max} of aminopeptidase by Methods B and C was estimated to be 38.0 ± 5.6 and 50.1 ± 3.9 nmol L^{-1} h^{-1}, respectively, for hydrolysis of Leu-MCA and 68.7 ± 3.0 and 89.3 ± 2.0 nmol L^{-1} h^{-1}, respectively, for Ala-MCA. V_{max} estimation of trypsin-type activity by Methods B and C was 58.2 ± 1.9 and 131.8 ± 4.6 nmol L^{-1} h^{-1}, respectively, for hydrolysis of Boc-Phe-Ser-Arg-MCA and 68.3 ± 3.0 and 147.4 ± 2.5 nmol L^{-1} h^{-1}, respectively, for hydrolysis of Boc-Leu-Ser-Thr-Arg-MCA. Thus, for aminopeptidase (**Figures 2A,B**) and trypsin-type activity (**Figures 2C,D**), V_{max} by Method B were 76–77% and 44–46% of those by Method C, respectively. These results indicate that significant adsorption of enzyme itself onto the surface of the regular polystyrene microplate occurred and that it could result in the underestimation of protease activity in seawater, especially for trypsin-type enzymes.

If the reason for lower enzyme activity is due solely to adsorption of the enzyme, the Michaelis constant (half-saturation constant) should be the same for a sample by both assay methods. However, the K_m estimated by curve fitting the trypsin-type activity data obtained by Methods B and C to the Michaelis–Menten equation were different: 30.1 ± 3.8 and 17.9 ± 1.6 μM, respectively, for hydrolysis of Boc-Phe-Ser-Arg-MCA and 18.1 ± 2.6 and 8.4 ± 0.4 μM, respectively, for hydrolysis of Boc-Leu-Ser-Thr-Arg-MCA. These differences could be explained by the adsorption of the substrates onto the regular polystyrene microplates and the available substrate concentration becoming lower than expected.

We also conducted the same kinetic experiment for phosphatase activity in terms of hydrolysis of MUF-phosphate to determine whether the discrepancy in measurement results between Methods B and C was specific to proteolytic enzymes, which is estimated by hydrolysis of oligopeptide analog MCA substrates. The results of phosphatase activity assays were almost the same as those of trypsin-type proteases activity tests with Boc-Phe-Ser-Arg-MCA and Boc-Leu-Ser-Thr-Arg-MCA. The phosphatase activity, V_{max} of hydrolysis of MUF-phosphate, was 5.5 ± 0.4 nmol L^{-1} h^{-1} by Method B, which is 45% of that measured by Method C (12.3 ± 0.4 nmol L^{-1} h^{-1}) for the same seawater sample (**Figure 2F**). The K_m estimated by curve fitting to the data obtained from a regular plate and a low protein binding plate was 25.2 ± 6.2 and 12.8 ± 1.3 μM, respectively.

From these results, we conclude that the reduced enzyme activities measurements with the use of regular polystyrene microplates (Method B) are attributable to the adsorption of both enzymes and substrates to the microplate surface. Although, the relationship between enzyme adsorption (binding) onto the polystyrene surface and deactivation of the adsorbed enzymes was not determined, Calliou et al. (2008) reported that adsorbed enzymes could be deactivated based on their model experiments. Among the proteases tested in our study, adsorption effects appeared to be more severe for trypsin-type enzymes than for aminopeptidases. A similar suppression of enzymatic activities measurements in seawater was previously reported during filtration (Obayashi and Suzuki, 2008b). In that case, trypsin-type enzyme appeared to be much more readily adsorbed onto the mixed cellulose esters filter (0.22 μm pore size) than aminopeptidase; as a result, not only particles in the sample but also much of the dissolved trypsin were removed by filtration. Taking the results of previous and present studies together, we suppose that trypsin-type enzymes in seawater are more easily adsorbed on some kinds of solid surfaces and/or deactivated on solid surfaces than are aminopeptidases. These results imply that enzyme behaviors and characteristics in natural environment are different for extracellular aminopeptidases and trypsin-type endopeptidases.

Low Protein Binding 96-Well Microplates

Figure 3 shows a comparison of estimated proteases activities in the same seawater sample using low protein binding, black, 96-well microplates from three suppliers. All three low protein binding microplates tested here gave similar measurements of hydrolytic activities of all tested substrates. Although, most experiments in present study were conducted using Nunc low binding microplates, Greiner Bio-one No-binding black 96-well

microplates and SUMILON ProteosaveSS black microplates can provide equivalent results.

Solvent for Substrates

DMSO Concentration in the Assay

Most MCA substrates need to be dissolved in organic solvent prior to mixing with the seawater sample. DMSO is a good solvent for dissolving MCA substrates; however, toxic effects to microbial cells in seawater and other unexpected effects could occur during the incubation and affect the measurement of extracellular enzyme activities in seawater samples. To minimize these types of artifacts, a lower concentration of organic solvent in the assay mixture is preferred. However, too low of a solvent concentration with a high concentration of substrate might result in solubility difficulties during the assay.

Michaelis plots for assays conducted with 10 and 2% DMSO with various substrate concentrations of five selected substrates (2 for aminopeptidase, 2 for trypsin, and 1 for chymotrypsin) are shown in **Figure 4**. Aminopeptidase and chymotrypsin-type activities were estimated lower in 10% DMSO than in 2% DMSO, irrespective of substrate type. In the case of the trypsin-type activity, hydrolysis rates in 2% DMSO were higher than in 10% DMSO for lower concentration of substrate, while rates of both were at the same level (hydrolysis of Boc-Leu-Ser-Thr-Arg-MCA, **Figure 4D**), or the rate in 2% DMSO was lower than that in 10% DMSO condition (hydrolysis of Boc-Phe-Ser-Arg-MCA, **Figure 4C**) at higher concentration of substrate. Previous studies have reported that a large proportion of aminopeptidase activity in seawater was detected from the bacterial cell size fraction as ectoenzymes, while trypsin-type activities were mostly detected in the dissolved (<0.2 μm filtered) fraction (Karner and Rassoulzadegan, 1995; Hoppe et al., 2002; Obayashi and Suzuki, 2008a; Bong et al., 2013). Higher contributions of bacterial cell-associated fractions of chymotrypsin-type activity were reported in some cases (Bong et al., 2013). The difference in the apparent DMSO effects between trypsin-type and other enzymes could be due to predominant state of existence in seawater: Lower activity of aminopeptidase and chymotrypsin-type enzymes in 10% DMSO in this study might reflect the toxic effects of DMSO to microbial cells during the incubation. Taking the Michaelis plot for the assay with Boc-Leu-Ser-Thr-Arg-MCA as a substrate (**Figure 4D**), 10% DMSO appears to act as a competitive inhibitor for dissolved trypsin-type enzyme. The reason for the discrepancy between the results of hydrolysis of two substrates for trypsin (Boc-Phe-Ser-Arg-MCA and Boc-Leu-Ser-Thr-Arg-MCA) at higher concentration of substrates was not clear; however, it might be related to the solubility of Boc-Phe-Ser-Arg-MCA as explored below.

Among the 17 tested MCA substrates listed in **Table 1**, Z-Phe-Arg-MCA (substrate for trypsin) and Suc-Leu-Leu-Val-Tyr-MCA (substrate for chymotrypsin) were not soluble enough to use with 2% DMSO, and additionally, Arg-MCA (substrate for aminopeptidase), and Boc-Phe-Ser-Arg-MCA (substrate for trypsin) could not be used with 1% DMSO. These substrates produced visible precipitates or aggregates in the 10× working solution or upon mixing with seawater samples for assay.

Excluding these four substrates, which were not sufficiently soluble, we compared the enzyme activities measurements in assays with 2 and 1% DMSO (**Figure 5**). For this test, the final concentration of each substrate was set to 200 μM, which is the saturation level for most of the tested substrates. Hydrolytic activity results for 2 and 1% DMSO were similar and the differences were not significant ($p = 0.295$ for all pairs, $n = 39$; $p = 0.274$ for aminopeptidase, $n = 12$; $p = 0.256$ for trypsin-type, $n = 24$; $p = 0.965$ for chymotrypsin-type, $n = 3$). Steen et al. (2015) examined the effect of DMSO on aminopeptidase (Leu-MCA hydrolysis) kinetics in river water samples and reported that DMSO at 4% or less did not influence the estimation of K_m but use of 5% DMSO produced different results.

Although, the actual effects of DMSO might differ among the enzymes, estimation of hydrolysis for many MCA substrates with 2% DMSO seemed to provide reliable estimation of protease activity in environmental seawater samples. For substrates with high solubility throughout the assay, a lower percentage of DMSO should be acceptable for measuring enzyme activity in seawater samples.

Comparison of Using 2% DMSO and 2% MTXE in Assay

In previous studies, MTXE was used to prepare stock solutions of hydrolytic substrates. Here, we compared the enzyme activities measurements in assays with the only difference being the use of solvents 2% DMSO and 2% MTXE. Among the MCA substrates tested, two could not be used with MTXE: Suc-Leu-Leu-Val-Tyr-MCA (for chymotrypsin) did not dissolve in MTXE for preparation of the stock solution, and Arg-MCA (for aminopeptidase) appeared as a suspension in the 10× working solution (2 mM substrate, 20% MTXE in autoclaved artificial seawater). **Figure 6** shows a comparison of hydrolytic activity for 14 MCA substrates (**Table 1**) in seawater samples with assay solutions of 2% DMSO and 2% MTXE and a 200 μM final substrate concentration. Hydrolytic activity was nearly the same by both methods, and the differences were not significant ($p = 0.948$ for all pairs, $n = 42$; $p = 0.905$ for aminopeptidase, $n = 12$; $p = 0.963$ for trypsin-type, $n = 27$; $p = 0.323$ for chymotrypsin-type, $n = 3$).

To assess the potential extracellular protease activities in natural seawater, the use of both 2% DMSO and 2% MTXE in assay give similar results for the hydrolysis of most MCA substrates with a final substrate concentration of 200 μM.

Assessment of Sample Container Material

Underestimation of hydrolytic enzyme activity in seawater using regular polystyrene microplates in the assay implies that similar concern is needed for the water sample container used to store seawater samples until assay. In general, adsorption effects are less for larger volume containers. While keeping seawater samples in smaller volume containers is convenient, the sample can be easily affected by differences among materials of the containers. For samples stored five types of container materials (**Figure 7**), the estimated activities in seawater were different among the type of sample containers. At the first measurement, several hours after seawater collection, activity in

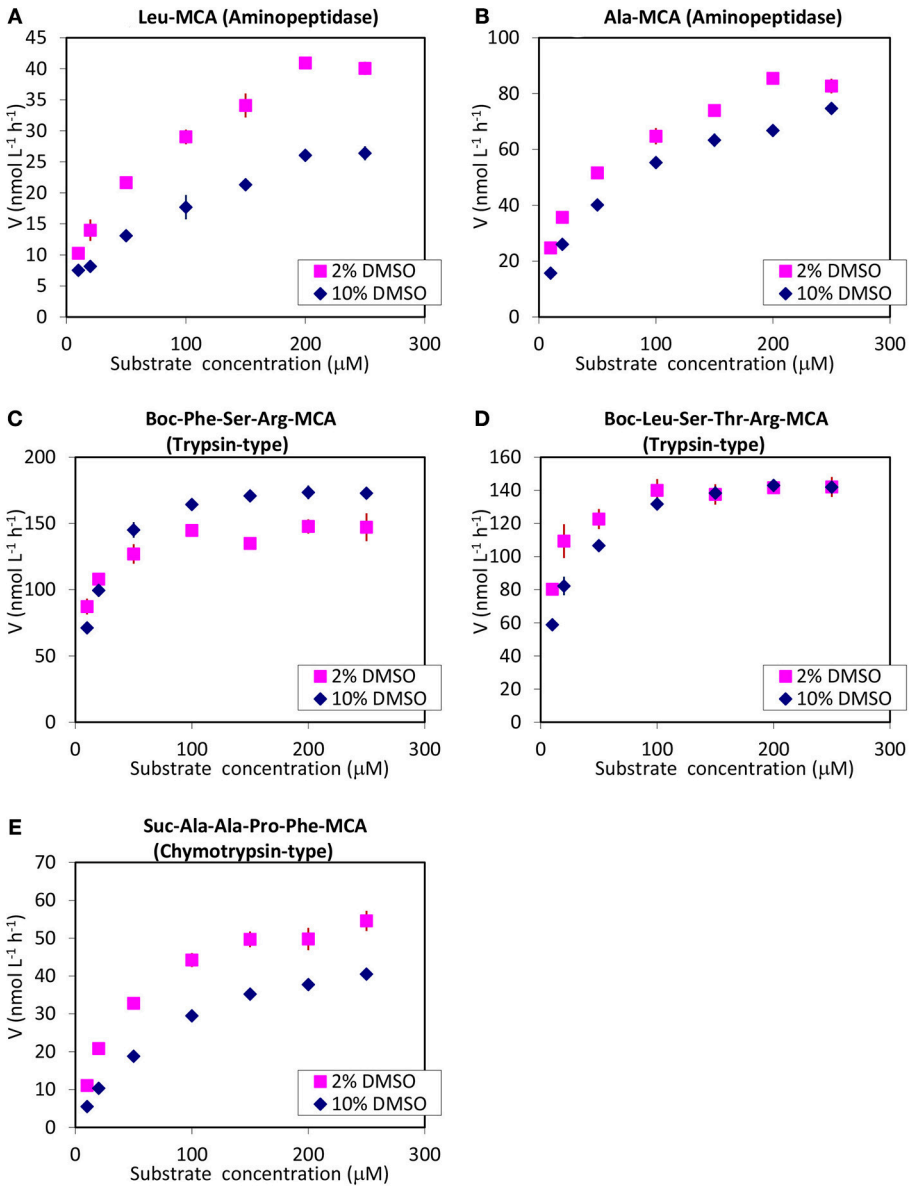

FIGURE 4 | Michaelis plots of the hydrolysis of **(A)** Leu-MCA (substrate for aminopeptidase), **(B)** Ala-MCA (substrate for aminopeptidase), **(C)** Boc-Phe-Ser-Arg-MCA (substrate for trypsin), **(D)** Boc-Leu-Ser-Thr-Arg-MCA (substrate for trypsin), and **(E)** Suc-Ala-Ala-Pro-Phe-MCA (substrate for chymotrypsin), measured in 2 and 10% DMSO. Error bars are the standard deviation of triplicate sample preparations (same sample incubated in 3 wells).

the samples kept in 50 mL regular polypropylene tubes (PPC and PPE) was already lower than in the others, and the activities continued to decrease greatly after 1 day (at 26 h) and 2 days (at 47 h). Differences in the estimated activities of trypsin-type and chymotrypsin-type enzymes among the different tubes were greater than those of the aminopeptidase, and these trends corresponded with the effects observed for microplates (**Figure 1**) and from filters for size fractionation reported in Obayashi and Suzuki (2008b). The seawater sample stored in the ProteosaveSS 50 mL tube (SS), which has a hydrophilic polymer coating designed to reduce nonspecific adsorption of protein and peptide to the inside of the tube, showed similar results with the sample stored in 500 mL polycarbonate bottle (PC500), while the sample kept in the 50 mL polyethylene terephthalate tube (PET) showed lower trypsin- and chymotrypsin-type enzyme activities than water samples stored in PC500 and SS but higher than those in polypropylene tubes (PPC and PPE).

These results show that protease activity in seawater samples stored in small polypropylene tubes decreased rapidly, causing the underestimation of natural activities, especially for trypsin-type and chymotrypsin-type endopeptidases. The choice of containers for water samples is an important consideration, even

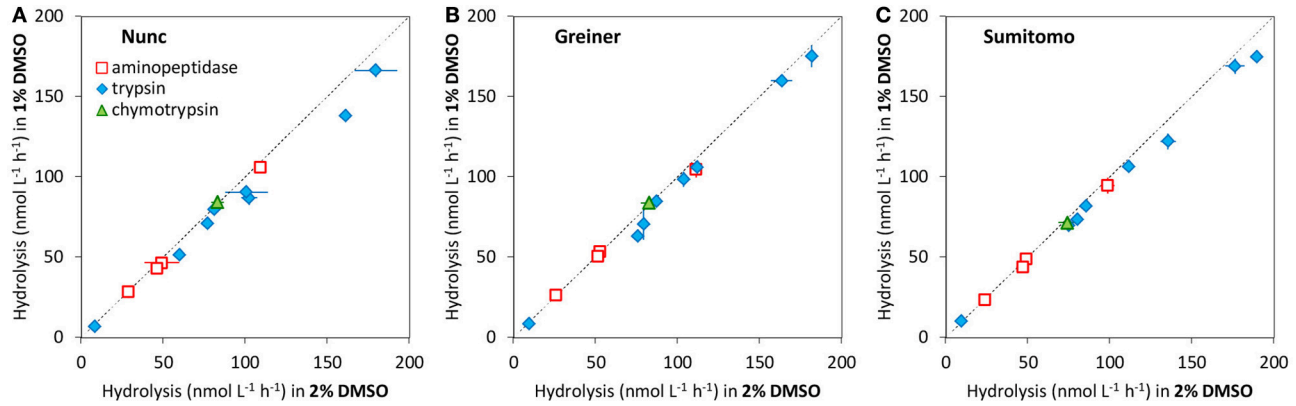

FIGURE 5 | Scatter plots of hydrolytic activities measured in 2 and 1% DMSO on **(A)** Nunc low binding microplate, **(B)** Greiner Bio-one No-binding microplate, and **(C)** SUMILON Proteosave microplate. Error bars are the standard deviation of triplicate sample preparations (same sample incubated in 3 wells). Dashed line indicates 1:1.

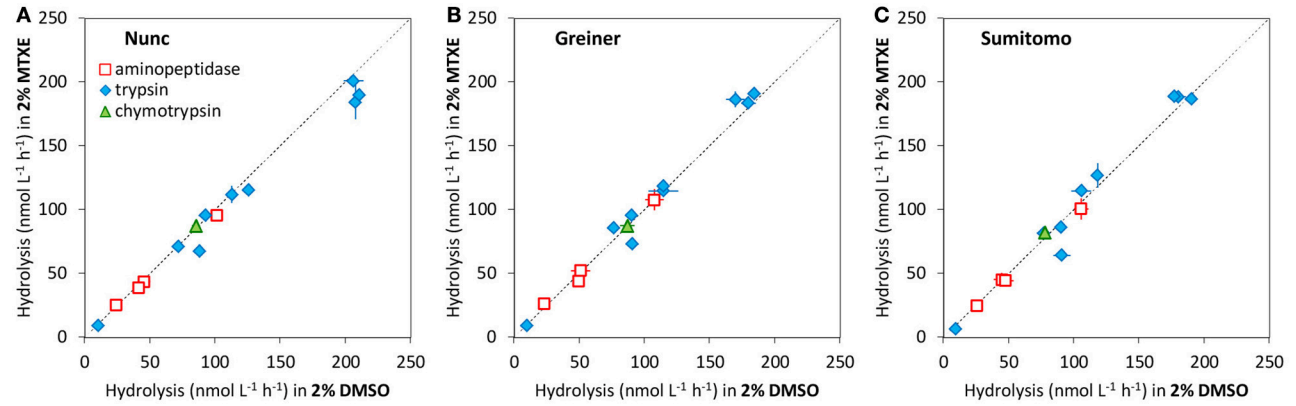

FIGURE 6 | Scatter plots of hydrolytic activities measured in 2% DMSO and 2% MTXE on **(A)** Nunc low binding microplate, **(B)** Greiner Bio-one No-binding microplate, and **(C)** SUMILON Proteosave microplate. Error bars are the standard deviation of triplicate sample preparations (same sample incubated in 3 wells). Dashed line indicates 1:1.

when assays are conducted as soon after sampling as possible, for assessing the level of enzyme activity in natural environmental seawater samples. In general, adsorption of organic molecules onto glassware is thought to be less than that on plastics, especially if the glass surfaces are silanized. We did not test glassware in this study, however, glass vials could be thought as a good sample container, depending on the research purposes.

CONCLUSIONS

It is thought that various enzymes in nature have a range of characteristics and behaviors in natural aquatic environments. Some enzymes in seawater are easily adsorbed onto the surfaces of some materials, and that may cause artificial effects or biases in the enzyme activities measurement. To assess the actual natural activities of microbial extracellular hydrolytic enzymes in aquatic ecosystems, materials used for both sampling and measurement assays should be carefully selected.

Water sample containers must maintain enzyme activity in the natural seawater samples for the short-term; protease activities in seawater decreased rapidly in small volume polypropylene tubes. Using fluorogenic substrates and a fluorometric microplate reader with low protein binding, black, 96-well microplates was effective for obtaining high-resolution and reliable measurements of hydrolytic enzyme activities in small volume (180 μL) of seawater samples, while regular polystyrene microplates showed significant underestimation of activities, especially for trypsin-type proteases.

For measuring the potential activities of extracellular proteases in seawater, a final substrate concentration at 200 μM in the assay (seawater sample with substrate solution) appeared to be a good saturation level for most of the tested oligopeptide analog MCA substrates for aminopeptidase, trypsin, and chymotrypsin. Stock solutions of MCA substrate are usually dissolved in a solvent, and both 1 or 2% DMSO and 2% MTXE in assay provided similar and reliable activities measurements, except for some

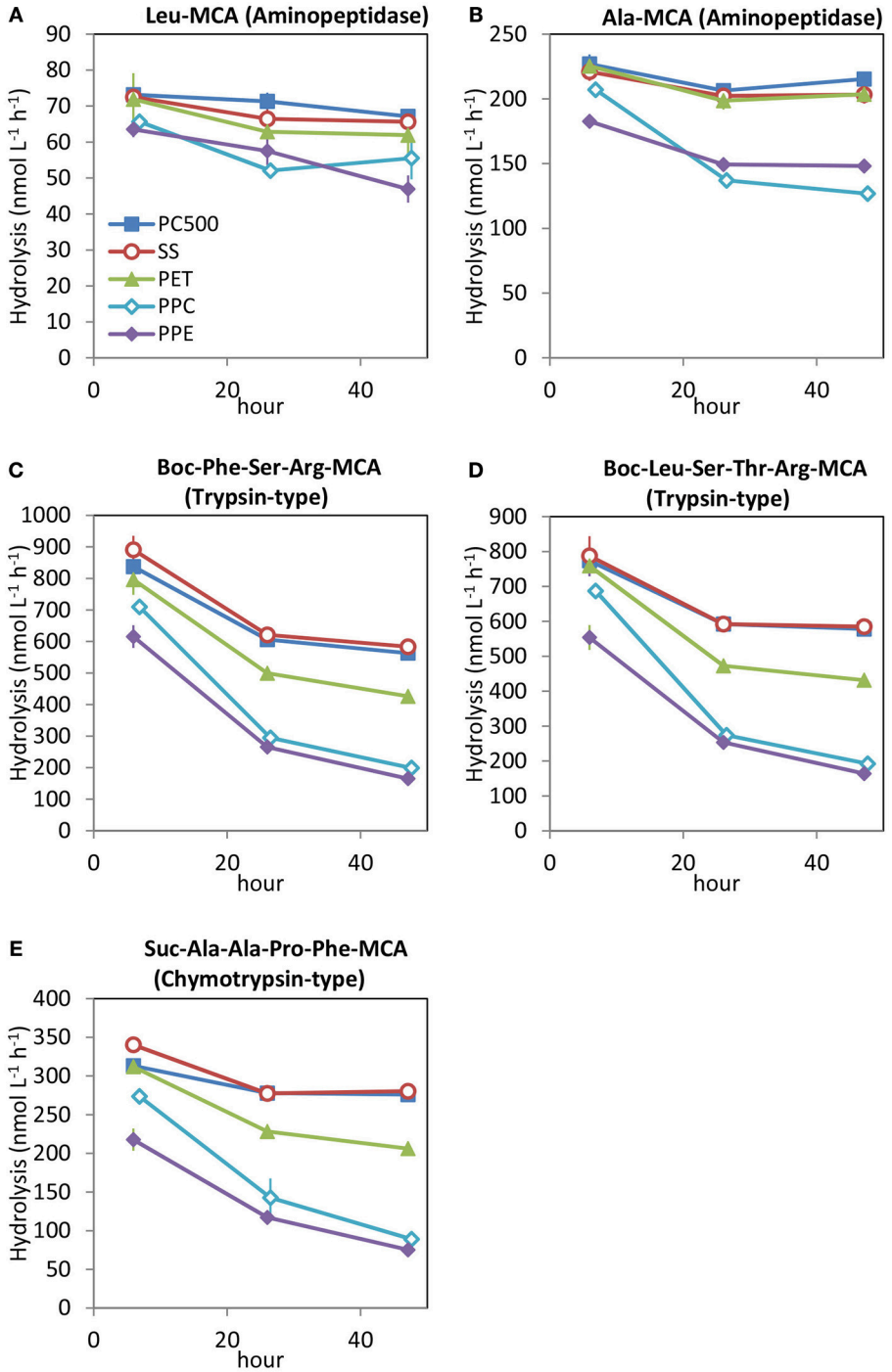

FIGURE 7 | Changes in protease activities in seawater samples kept in sample containers of different materials: PC500, 500 mL polycarbonate bottle; SS, 50 mL ProteosaveSS tube; PET, 50 mL polyethylene terephthalate tube; PP, 50 mL polypropylene tube (Corning); and PPE, 50 mL polypropylene tube (Eppendorf). The time of filling the container with seawater is taken as 0 h. Hydrolysis rates of **(A)** Leu-MCA (substrate for aminopeptidase), **(B)** Ala-MCA (substrate for aminopeptidase), **(C)** Boc-Phe-Ser-Arg-MCA (substrate for trypsin), **(D)** Boc-Leu-Ser-Thr-Arg-MCA (substrate for trypsin), and **(E)** Suc-Ala-Ala-Pro-Phe-MCA (substrate for chymotrypin).

substrates which were not sufficiently soluble. Calibration curves of AMC (product of substrate hydrolysis) should be generated under the same conditions as are used for the sample measurement. A solvent blank (sample with solvent without substrate) and an inactivated control (autoclaved seawater) should be also prepared and assayed with the samples

for reliable calculation of hydrolytic enzyme activity in the sample.

Substrate concentrations at saturation level for assay of potential activity and substrate solubility may depend on sample type, targeted enzyme, and its substrate. It is important to optimize these factors for the sample types and target enzymes to obtain data that are as reliable as possible.

AUTHOR CONTRIBUTIONS

YO designed and conducted all experiments, analyzed data, constructed discussion, and prepared the manuscript; CWB conducted portions of the experiments with YO; and SS supported all stages of the research and contributed to preparation of the manuscript.

ACKNOWLEDGMENTS

We thank H. Onishi, S. Nakano, and his colleagues for their kind cooperation in the sample collection. This work was supported in part by JSPS KAKENHI Grant Numbers JP26450245 and JP24710005, and grants from the government to national university corporations for Joint Usage/Research Center, MEXT, Japan.

REFERENCES

Arnosti, C. (1996). A new method for measuring polysaccharide hydrolysis rates in marine environments. *Organ. Geochem.* 25, 105–115. doi: 10.1016/S0146-6380(96)00112-X

Arnosti, C. (2003). "Microbial extracellular enzymes and their role in dissolved organic matter cycling," in *Aquatic Ecosystems: Interactivity of Dissolved Organic Matter*, eds S. E. G. Findlay and R. L. Sinsabaugh (San Diego, CA: Academic Press), 315–342.

Arnosti, C. (2011). Microbial extracellular enzymes and the marine carbon cycle. *Annu. Rev. Mar. Sci.* 3, 401–425. doi: 10.1146/annurev-marine-120709-142731

Baltar, F., Legrand, C., and Pinhassi, J. (2016). Cell-free extracellular enzymatic activity is linked to seasonal temperature changes: a case study in the Baltic Sea. *Biogeosciences* 13, 2815–2821. doi: 10.5194/bg-13-2815-2016

Baltar, F., Arístegui, J., Gasol, J. M., Sintes, E., Van Aken, H. M., and Herndl, G. J. (2010). High dissolved extracellular enzymatic activity in the deep central Atlantic Ocean. *Aquat. Microb. Ecol.* 58, 287–302. doi: 10.3354/ame01377

Bong, C. W., Obayashi, Y., and Suzuki, S. (2013). Succession of protease activity in seawater and bacterial isolates during starvation in a mesocosm experiment. *Aquat. Microb. Ecol.* 69, 33–46. doi: 10.3354/ame01618

Calliou, S., Gerin, P. A., Nonckreman, C. J., Fleith, S., Dupont-Gillain, C. C., Landoulsi, J., et al. (2008). Enzymes at solid surfaces: nature of the interfaces and physico-chemical processes. *Electrochim. Acta* 54, 116–122. doi: 10.1016/j.electacta.2008.02.100

Fukuda, R., Sohrin, Y., Saotome, N., Fukuda, H., Nagata, T., and Koike, I. (2000). East-west gradient in ectoenzyme activities in the subarctic Pacific: possible regulation by zinc. *Limnol. Oceanogr.* 45, 930–939. doi: 10.4319/lo.2000.45.4.0930

German, D. P., Weintraub, M. N., Grandy, A. S., Lauber, C. L., Rinkes, Z. L., and Allison, S. D. (2011). Optimization of hydrolytic and oxidative enzyme methods for ecosystem studies. *Soil Biol. Biochem.* 43, 1387–1397. doi: 10.1016/j.soilbio.2011.03.017

Hoppe, H. G. (1993). "Use of fluorogenic model substrates for extracellular enzyme activity (EEA) measurement of bacteria," in *Handbook of Methods in Aquatic Microbial Ecology*, eds P. F. Kemp, B. F. Sherr, E. B. Sherr, and J. J. Cole (Boca Raton, FL: Lewis Publishers), 423–431.

Hoppe, H. G., Arnosti, C., and Herndl, G. F. (2002). "Ecological Significance of bacterial enzymes in the marine environment," in *Enzymes in the Environment. Activity, Ecology, and Applications*, eds R. G. Burns and R. P. Dick (New York, NY: Marcel Dekker), 73–107.

Karner, M., and Herndl, G. J. (1992). Extracellular enzymatic activity and secondary production in free-living and marine-snow-associated bacteria. *Mar. Biol.* 113, 341–347.

Karner, M., and Rassoulzadegan, F. (1995). Extracellular enzyme activity: indications for high short-term variability in a coastal marine ecosystem. *Microb. Ecol.* 30, 143–156.

Keith, S. C., and Arnosti, C. (2001). Extracellular enzyme activity in a river-bay-shelf transect: variations in polysaccharide hydrolysis rates with substrate and size class. *Aquat. Microb. Ecol.* 24, 243–253. doi: 10.3354/ame024243

Liu, S., and Liu, Z. (2015). Comparing extracellular enzymatic hydrolysis between plain peptides and their corresponding analogs in the northern Gulf of Mexico Mississippi River plume. *Mar. Chem.* 177, 398–407. doi: 10.1016/j.marchem.2015.06.021

Liu, Z., Kobiela, M. E., McKee, G. A., Tang, T., Lee, C., Mulholland, M. R., et al. (2010). The effect of chemical structure on the hydrolysis of tetrapeptides along a river-to-ocean transect: AVFA and SWGA. *Mar. Chem.* 119, 108–120. doi: 10.1016/j.marchem.2010.01.005

Nagata, T. (2008). "Organic matter-bacteria interactions in seawater," in *Microbial Ecology of the Oceans*, *2 Edn*, ed D. L. Kirchman (Hoboken, NJ: John Wiley and Sons), 207–241.

Nikaido, H., and Vaara, M. (1985). Molecular basis of bacterial outer membrane permeability. *Microbiol. Rev.* 49, 1–32.

Obayashi, Y., and Suzuki, S. (2005). Proteolytic enzymes in coastal surface seawater: significant activity of endopeptidases and exopeptidases. *Limonol. Oceanogr.* 50, 722–726. doi: 10.4319/lo.2005.50.2.0722

Obayashi, Y., and Suzuki, S. (2008a). Occurrence of exo- and endopeptidases in dissolved and particulate fractions of coastal seawater. *Aquat. Microb. Ecol.* 50, 231–237. doi: 10.3354/ame01169

Obayashi, Y., and Suzuki, S. (2008b). Adsorption of extracellular proteases in seawater onto filters during size fractionation. *J. Oceanogr.* 64, 367–372. doi: 10.1007/s10872-008-0029-x

Pantoja, S., Lee, C., and Marecek, J. F. (1997). Hydrolysis of peptides in seawater and sediment. *Mar. Chem.* 57, 25–40. doi: 10.1016/S0304-4203(97)00003-0

Sala, M. M., Karner, M., Arin, L., and Marrasé, C. (2001). Measurement of ectoenyzyme activities as an indication of inorganic nutrient imbalance in microbial community. *Aquat. Microb. Ecol.* 23, 301–311. doi: 10.3354/ame023301

Smith, D. C., Simon, M., Alldredge, A. L., and Azam, F. (1992). Intense hydrolytic enzyme activity on marine aggregates an implications for rapid particle dissolution. *Nature* 359, 139–141. doi: 10.1038/359139a0

Steen, A. D., Arnosti, C., Ness, L., and Blough, N. V. (2006). Electron paramagnetic resonance spectroscopy as a novel approach to measure macromolecule–surface interactions and activities of extracellular enzymes. *Mar. Chem.* 101, 266–276. doi: 10.1016/j.marchem.2006.04.001

Steen, A. D., Vazin, J. P., Hagen, S. M., Mulligan, K. H., and Wilhelm, S. W. (2015). Substrate specificity of aquatic extracellular peptidases assessed by competitive inhibition assays using synthetic substrates. *Aquat. Microb. Ecol.* 75, 271–281. doi: 10.3354/ame01755

Weiss, M. S., Abele, U., Weckesser, J., Welte, W., Schiltz, E., and Schulz, G. E. (1991). Molecular architecture and electrostatic properties of a bacterial porin. *Science* 254, 1627–1630. doi: 10.1126/science.1721242

Conflict of Interest Statement: The authors declare that the research was conducted in the absence of any commercial or financial relationships that could be construed as a potential conflict of interest.

frontiers in Microbiology

ORIGINAL RESEARCH
published: 21 February 2018
doi: 10.3389/fmicb.2018.00271

An Experimental Insight into Extracellular Phosphatases – Differential Induction of Cell-Specific Activity in Green Algae Cultured under Various Phosphorus Conditions

Jaroslav Vrba[1,2], Markéta Macholdová[3], Linda Nedbalová[3], Jiří Nedoma[2] and Michal Šorf[1,4]*

[1] Department of Ecosystem Biology, Faculty of Science, University of South Bohemia, České Budějovice, Czechia, [2] Institute of Hydrobiology, Biology Centre CAS, České Budějovice, Czechia, [3] Department of Ecology, Faculty of Science, Charles University, Prague, Czechia, [4] Department of Zoology, Fisheries, Hydrobiology and Apiculture, Faculty of AgriSciences, Mendel University, Brno, Czechia

OPEN ACCESS

Edited by:
Sonja Endres,
Max Planck Institute for Chemistry (MPG), Germany

Reviewed by:
Monika Nausch,
Leibniz Institute for Baltic Sea Research (LG), Germany
Michael R. Twiss,
Clarkson University, United States

****Correspondence:***
Jaroslav Vrba
jaroslav.vrba@prf.jcu.cz

Specialty section:
This article was submitted to Aquatic Microbiology, a section of the journal Frontiers in Microbiology

Received: *12 October 2017*
Accepted: *06 February 2018*
Published: *21 February 2018*

Citation:
Vrba J, Macholdová M, Nedbalová L, Nedoma J and Šorf M (2018) An Experimental Insight into Extracellular Phosphatases – Differential Induction of Cell-Specific Activity in Green Algae Cultured under Various Phosphorus Conditions. Front. Microbiol. 9:271. doi: 10.3389/fmicb.2018.00271

Extracellular phosphatase activity (PA) has been used as an overall indicator of P depletion in lake phytoplankton. However, detailed insights into the mechanisms of PA regulation are still limited, especially in the case of acid phosphatases. The novel substrate ELF97 phosphate allows for tagging PA on single cells in an epifluorescence microscope. This fluorescence-labeled enzyme activity (FLEA) assay enables for autecological studies in natural phytoplankton and algal cultures. We combined the FLEA assay with image analysis to measure cell-specific acid PA in two closely related species of the genus *Coccomyxa* (Trebouxiophyceae, Chlorophyta) isolated from two acidic lakes with distinct P availability. The strains were cultured in a mineral medium supplied with organic (beta-glycerol phosphate) or inorganic (orthophosphate) P at three concentrations. Both strains responded to experimental conditions in a similar way, suggesting that acid extracellular phosphatases were regulated irrespectively of the origin and history of the strains. We found an increase in cell-specific PA at low P concentration and the cultures grown with organic P produced significantly higher (ca. 10-fold) PA than those cultured with the same concentrations of inorganic P. The cell-specific PA measured in the cultures grown with the lowest organic P concentration roughly corresponded to those of the original *Coccomyxa* population from an acidic lake with impaired P availability. The ability of *Coccomyxa* strains to produce extracellular phosphatases, together with tolerance for both low pH and metals can be one of the factors enabling the dominance of the genus in extreme conditions of acidic lakes. The analysis of frequency distribution of the single-cell PA documented that simple visual counting of 'active' (labeled) and 'non-active' (non-labeled) cells can lead to biased conclusions regarding algal P status because the actual PA of the 'active' cells can vary from negligible to very high values. The FLEA assay using image cytometry offers a strong tool in plankton ecology for exploring P metabolism.

Keywords: acid phosphatase, *Coccomyxa*, ELF97 phosphate, FLEA technique, image cytometry, inorganic phosphorus, organic phosphorus, phosphorus limitation

INTRODUCTION

Phosphorus (P) has been proven to be a limiting resource in many aquatic ecosystems (Schindler, 2012; Schindler et al., 2016). Aquatic microorganisms, except for phagotropic protists, can only assimilate dissolved inorganic P, i.e., dissolved orthophosphate (P_i) (Reynolds, 1997). Yet P_i also reacts with and adsorbs to various compounds or seston particles (e.g., clay) that may sediment and ultimately reduce the availability of P in the epilimnion and euphotic zone. Therefore, P_i is a subject of more or less severe competition in the planktonic microbial community, encompassing not only individual phytoplankton species (Sommer, 1981, 1985), but also bacterioplankton (Currie and Kalff, 1984; Cotner and Wetzel, 1992). On the other hand, plankton consumers may regenerate substantial amounts of P_i into the water column (e.g., Knoll et al., 2016). Such a consumer driven nutrient recycling often results in dissolved organic P (DOP) forms that are not readily available to microorganisms. The DOP compounds need to be cleaved by extracellular enzymes before they can be taken up by microbial cells (Cembella et al., 1984; Jansson et al., 1988; Cotner and Wetzel, 1991).

In the light of this, several artificial chromogenic or fluorogenic substrates have been used for regular measurements of the extracellular phosphatase activity (Jones, 1972; Healey and Hendzel, 1979; Hoppe, 1983), increased level of which in lake water was proposed to indicate P deficiency in lake phytoplankton (Healey and Hendzel, 1980). By adding an artificial DOP substrate to a water sample and to its cell-free filtrate, total and free (dissolved) phosphatase activities are measured, respectively. The free, or dissolved, activity represents the bulk activity of all free (dissolved) enzymes, both of microbial and metazoan origin (Boavida and Heath, 1984; Carr and Goulder, 1990). The particulate activity, calculated as the difference of total and free activity, represents the bulk activity of both microbial ectoenzymes and free enzymes adsorbed to particles (Wetzel, 1991; Nagata and Kirchman, 1992). It is sometimes possible to estimate proportions of 'bacterial' and 'algal' ectoenzymes by using a more detailed size fractionation of water samples (Vrba et al., 1993; Nedoma et al., 2006); however, none of the widely-used substrates allows for enzyme localization or detection of phosphatase producers, which is the serious methodological drawback of the bulk phosphatase assay.

A new generation of fluorogenic substrates, such as ELF® 97 phosphate (ELFP) based on 2-(2′-phosphoryloxyphenyl)-4-(3H)-quinazolinone (Huang et al., 1992), can overcome most disadvantages. Insoluble precipitates of the hydrolysis product (ELF® 97 alcohol, ELFA) at the sites of hydrolysis (under certain conditions – see below) allow for direct visualization of the active enzymes in organisms (cells) by epifluorescence microscopy. An early application of the ELF® 97 Endogenous Phosphatase Detection Kit successfully visualized phosphatase-positive cells in both algal cultures and natural phytoplankton, i.e., directly tagged the P-limited algal species (González-Gil et al., 1998; Dyhrman and Palenik, 1999; Rengefors et al., 2001), although further studies revealed some uncertainties and/or potential misinterpretations (e.g., Rengefors et al., 2003; Dignum et al., 2004; Ou et al., 2010). The principle shortcoming of the ELF® 97 method as it is applied in recent studies, including the original paper by González-Gil et al. (1998), is that only the occurrence of ELFA-labeling, i.e., merely qualitative estimates of phosphatase-positive algal cells and/or species, presence/absence of tagged phytoplankton, etc., could be reported (Štrojsová et al., 2003; Cao et al., 2005; Rychtecký et al., 2015; Ren et al., 2017). The only quantification of phosphatase activity accessible within the limits of this original method is to score a percentage of ELFA-labeled cells (e.g., Rengefors et al., 2003; Dyhrman and Ruttenberg, 2006; Litchman and Nguyen, 2008; Young et al., 2010).

This problem has been largely solved by using ELF® 97 phosphate (ELFP) according to a modified protocol (Nedoma et al., 2003b; Štrojsová et al., 2003) derived from a common fluorescence assay (e.g., Hoppe, 1983) for extracellular activity in plankton and further standardized by buffering the samples (Štrojsová and Vrba, 2006). Inhibition experiments suggested that both substrates (i.e., ELFP and 4-methylumbelliferyl phosphate) were hydrolyzed by the same extracellular phosphatases (Štrojsová et al., 2003). This protocol, referred to as fluorescence-labeled enzyme activity (FLEA) assay, allows not only for distinguishing between enzymatically active and inactive specimens in a sample, but, most essentially, for the quantification of the ELFA fluorescence at single cell or species level using image cytometry (Nedoma et al., 2003b; Nedoma and Vrba, 2006; Novotná et al., 2010). This cell-specific fluorescence intensity can be further converted to a specific rate of enzymatic ELFP hydrolysis by the particular producers.

Since decades ago, realistic interpretation and sometimes contradictory results of various phosphatase assays remains a subject of discussions in plankton ecology (e.g., Berman et al., 1990; Nedoma et al., 2003a). There is no doubt, at present, that the bulk extracellular phosphatase activity must not be interpreted as exclusively algal activity (e.g., Hoppe, 2003; Cao et al., 2005; Nedoma et al., 2006). The paradigm of phosphatase expression only under P deficiency is overly simplistic as algae may constitutively express some phosphatase activity, but also may not efficiently regulate it in response to P availability (Young et al., 2010). There is also increasing awareness that all phytoplankton species do not react uniformly to P depletion (e.g., Litchman and Nguyen, 2008) and many species indeed do not produce extracellular phosphatases at all under such circumstances, while other species can exhibit constitutive activity (e.g., Rengefors et al., 2001, 2003; Štrojsová et al., 2003, 2005, 2008; Rychtecký et al., 2015). For instance, ELFA-labeled, i.e., phosphatase-positive phytoplankton species were reported from eutrophic lakes under high concentrations of soluble reactive P (SRP) (e.g., Cao et al., 2005, 2009). Most data, however, have been obtained from field studies. Laboratory experiments focused on the influence of P form and concentration on cell-specific phosphatase activity under controlled conditions are scarce and performed entirely in batch cultures (Huang et al., 2000; Young et al., 2010; Ren et al., 2017).

In this study, we examined two closely related algal species isolated from two acidic lakes differing in their P concentrations. Each algal population had been exposed to distinct environmental conditions for decades. We tested the ability of both species to grow on inorganic or organic P in a

semi-continuous system, and the response of single algal cells to various degree of P depletion. Cell-specific acid phosphatase activity was measured using the FLEA assay according to the protocol, which enabled us to quantify more accurately its variability in individual experimental treatments. The main objectives of this study were to determine (i) if expression of algal acid phosphatases is under environmental control, (ii) if the manner of the control differs in the isolates originating from environments contrasting in P availability, and (iii) if acid phosphatase activity reflects actual needs of algal cells given by their growth rate and source of P.

MATERIALS AND METHODS

Algal Cultures

We isolated two unialgal cultures of *Coccomyxa* strains (Trebouxiophyceae, Chlorophyta) by serial dilution from the plankton of two acidic lakes of distinct trophic status in Czechia. Lake Plešné (48°46′35″ N, 13°51′55″ E; 1087 m a.s.l.) is of glacial origin and it was strongly acidified due to atmospheric sulfur and nitrogen deposition that peaked in the 1980s (Vrba et al., 2003). In this acidic (pH = 4.8–5.5) mesotrophic lake, P availability remains largely impaired by reactive aluminum (Vrba et al., 2006), with mean epilimnetic SRP concentrations as low as ∼40 nmol L^{-1} (Novotná et al., 2010). Its P-limited phytoplankton are dominated by coccoid green algae (formerly misidentified as *Monoraphidium dybowskii*; cf. Štrojsová and Vrba, 2006, 2009) that was recently described as a new species, *Coccomyxa silvae-gabretae* (Barcytė and Nedbalová, 2017). Eutrophic Lake Hromnice (49°51′03″ N, 13°26′39″ E; 330 m a.s.l.) is a former pyritic shale mine. Its lake water is characterized by extremely low pH (2.3−2.9), high concentrations of P (1−52 μmol L^{-1} SRP) and several metals (Al, Fe, Mn, Ni, Cu, Co, and Pb) (Hrdinka et al., 2013). A common phytoplankton species in Lake Hromnice is *Coccomyxa elongata* (Barcytė and Nedbalová, 2017). We maintained non-axenic cultures of the two strains in an acidified BBM medium (Bischoff and Bold, 1963), with the pH adjusted to 4, at room temperature and daylight.

For all phosphatase experiments, we cultivated both *Coccomyxa* strains in semi-continuous, turbidostatic systems, in the acidified BBM medium supplied with distinct P sources at three concentrations (see below), at room temperature and permanent light provided by fluorescent tubes (photosynthetically active radiation ∼40 μmol s^{-1} m^{-2}). We used 0.5-L conical vessels (separatory funnels with stopcock for easy sampling), filled with 200 ml of medium and inoculated with 0.5 ml of stock culture at the beginning of each experiment. The medium as well as cultivation vessels were sterilized. Continuous aeration by sterile air bubbling into the bottom of each vessel ensured both CO_2 saturation and mixing of algal suspension. To provide merely inorganic (hereafter referred as I) or organic (hereafter referred as O) P sources, we supplied the BBM medium with P_i or β-glycerol phosphate (β-GP) as the single source of P, respectively. For either source, we used one P-replete (variants I1 and O1) and two P-depleted (variants I2−I3 or O2−O3) media with the original concentrations adjusted to 858, 16 and 10 μmol L^{-1} of P.

We ran all experimental variants in triplicates for 3 weeks. We regularly screened all variants for chlorophyll *a* concentration using a fluorometer (TD-700 Laboratory Flurometer, Turner Designs, San Jose, CA, United States) and diluted the cultures by the corresponding fresh medium at regular intervals, i.e., three times during the cultivation, to maintain chlorophyll *a* concentrations close to ∼10 μg L^{-1} in P-depleted (I2/O2 and I3/O3) and to 50 μg L^{-1} in P-replete (I1/O1) variants. In addition, in the middle and at the end of each experiment, we checked all variants for residual P concentrations in cultures – SRP was determined by the molybdate method after filtering the samples through glass fiber filters (0.7 μm, Macherey-Nagel, Düren, Germany). After the 3-week cultivation, we sampled all replicates to estimate cell-specific phosphatase activity of individual *Coccomyxa* populations in each experimental variant.

For each cultivation, we further calculated a specific growth rate (μ, day^{-1}) of the individual *Coccomyxa* population for the period between the second and third dilutions according to the equation:

$$\mu = \frac{ln\mathrm{N_f} - ln\mathrm{N_i}}{\mathrm{t_f} - \mathrm{t_i}}$$

where N is the final (f) or initial (i) cell density at time (t). A conversion curve was used to calculate N from chlorophyll fluorescence values.

Cell-Specific Phosphatase Activity (FLEA Assay)

After the 3-week cultivations, we employed the protocol for FLEA assay (Nedoma et al., 2003b) to estimate extracellular cell-specific phosphatase activity of the *Coccomyxa* strains grown on different P sources. We incubated 5-ml samples with fluorogenic substrate ELFP (Molecular Probes; Invitrogen, Eugene, OR, United States). The incubation started by the addition of ELFP solution (final concentration of 20 μmol L^{-1}) and lasted 3 h at room temperature and daylight. Then, each incubation was terminated by filtering 1-ml subsamples over mild vacuum (<20 kPa) through polycarbonate membrane filters (pore size 2 μm; Osmonics, Minnetonka, MN, United States). The filter with retained algae was placed on a microscopic slide, embedded with immersion oil, covered with a coverslip, and preserved in a freezer at −20°C until the image cytometry analysis (cf. Nedoma et al., 2003b).

Image Cytometry

The image analysis system used for ELFA fluorescence quantification included the fluorescence microscope Nikon Eclipse 90i (Nikon, Tokyo, Japan; Nikon Plan Fluor 60×), monochromatic digital camera (Andor Clara, Andor Technology, Ltd., Belfast, United Kingdom), and the software NIS-Elements 4.12 (Laboratory Imaging, s.r.o., Prague, Czechia). From every slide, 30 image files corresponding to 30 randomly selected microscope fields were made. Each image file contained two types of images from two channels (**Figure 1**) – one was captured with ELFA-fluorescence-specific filter cube

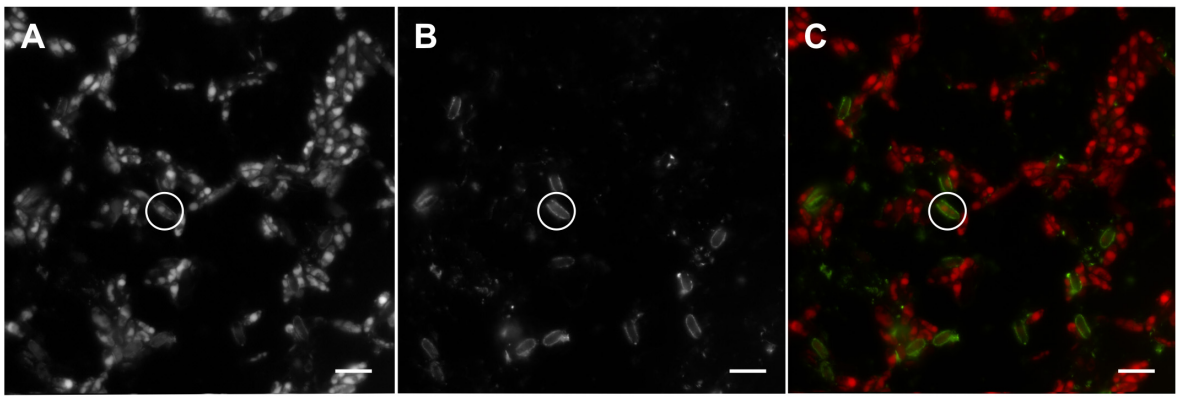

FIGURE 1 | A set of epifluorescence microphotographs of the *Coccomyxa elongata* culture with induced extracellular phosphatase activity grown in P-depleted organic medium (O3). Same image areas show: **(A)** the image captured with chlorophyll-autofluorescence-specific filter cube (excitation/emission: 510–550 nm/>590 nm) visualizing single algal cells; **(B)** the image captured with ELFA-fluorescence-specific filter cube (excitation/emission: 360–370 nm/520–540 nm) visualizing fluorescence-labeled enzyme activity (FLEA), i.e., the ELFA precipitates on surfaces of phosphatase-positive cells; and **(C)** the merged images A and B in artificial colors – red and green stand for chlorophyll autofluorescence and ELFA fluorescence, respectively. Circles indicate the same phosphatase-active cell; scale bars represent 10 μm.

(excitation/emission: 360–370 nm/520–540 nm) and served for the measurement of cell-associated ELFA fluorescence; the second image was captured with chlorophyll-autofluorescence-specific filter cube (excitation/emission: 510–550 nm/>590 nm) and served for cell localization and sizing (see below). In NIS-Elements software, 3−6 randomly chosen cells (90−180 from one slide) were demarcated (segmented) manually on the chlorophyll-fluorescence image. The system then measured cell dimensions and the mean gray level of the cell and of the ELFA image background. Cell-associated ELFA fluorescence [F_{ELFA}, in relative fluorescence units (FUs) cell^{-1}h^{-1}] was then calculated using the following equation (Nedoma et al., 2003b):

$$F_{ELFA} = \frac{\text{Area} \times (\text{MGrey} - \text{BgMGrey})}{T_{exp}} \times F_{cal}$$

where Area (μm^2) is projected area of the cell, MGrey (dimensionless) is mean gray of the cell, BgMGrey (dimensionless) is mean gray of the background, F_{cal} (dimensionless) is fluorescence calibration factor, and T_{exp} (ms) is exposure time. For rough estimation of the cell-specific phosphatase activity (in the units of fmol cell^{-1}h^{-1}), we used the conversion factor of 0.1 fmol FU^{-1}, based on experiments with Plešné Lake natural plankton (for details see Nedoma et al., 2003b).

Mean cell volumes of individual *Coccomyxa* populations in each replicate were calculated using the measured cell dimensions, i.e., cell length and area from the chlorophyll-fluorescence images, by approximation of cell shape to an ellipsoid.

Statistical Analyses

A three-way ANOVA with a *post hoc* Tukey HSD test of differences among experimental variants were performed to test the effects of P sources, P concentrations, species of *Coccomyxa*, and their interactions on algal growth rate, mean cell size, and cell-specific phosphatase activity. All data were transformed by log (x+1) to meet the assumptions of ANOVA. All analyses were performed using Statistica 13.2 (Dell Inc., 2016).

RESULTS

The two strains of *Coccomyxa* species revealed very similar results and generally responded in a consistent way to all experimental treatments. No significant differences in either of the treatments were detected between both species (**Tables 1**–**3**). Final residual concentrations averaged at around 600 μmol L^{-1} of SRP in P-replete cultures grown on inorganic medium (P_i, I1), whereas they leveled at ∼30 μmol L^{-1} of SRP in those grown on organic medium (β-GP, O1). Yet, in all P-depleted variants, these concentrations were very similar, on average 2–6 μmol L^{-1} of SRP. In the organic media, β-GP was obviously transformed into SRP in all treatments.

We found the highest growth rates (0.17–0.18 day^{-1}) in P-replete P_i medium (variants I1), whereas they were significantly lower (0.06–0.10 day^{-1}) in both P-depleted variants

TABLE 1 | Results of three-way ANOVA testing the effects of species (*C. elongata* vs. *C. silvae-gabretae*), media (inorganic vs. organic), and three P concentrations on growth rate.

Factor	df	*F*	*P*
Species (S)	1	0.02	0.9
Medium (M)	**1**	**4.69**	**0.04**
P concentration (P)	**2**	**44.0**	**<0.001**
S × M	1	0.88	0.36
S × P	2	0.88	0.43
M × P	2	0.59	0.56
S × M × P	2	1.19	0.32

Significant differences (P < 0.05) are given in bold; ×, interaction of factors.

TABLE 2 | Results of three-way ANOVA testing the effects of species (*C. elongata* vs. *C. silvae-gabretae*), media (inorganic vs. organic), and three P concentrations on cell volume.

Factor	df	*F*	*P*
Species (S)	1	0.61	0.44
Medium (M)	1	0.14	0.71
P concentration (P)	**2**	**11.3**	**<0.001**
S × M	1	0.61	0.44
S × P	2	0.55	0.58
M × P	2	0.26	0.77
S × M × P	2	0.07	0.93

Significant differences ($P < 0.05$) are given in bold; ×, interaction of factors.

TABLE 3 | Results of three-way ANOVA testing the effects of species (*C. elongata* vs. *C. silvae-gabretae*), media (inorganic vs. organic), and three P concentrations on cell-specific phosphatase activity.

Factor	df	*F*	*P*
Species (S)	1	0.02	0.88
Medium (M)	**1**	**36.3**	**<0.001**
P concentration (P)	**2**	**32.8**	**<0.001**
S × M	1	0.64	0.43
S × P	2	0.03	0.97
M × P	**2**	**9.66**	**<0.001**
S × M × P	2	0.42	0.66

Significant differences ($P < 0.05$) are given in bold; ×, interaction of factors.

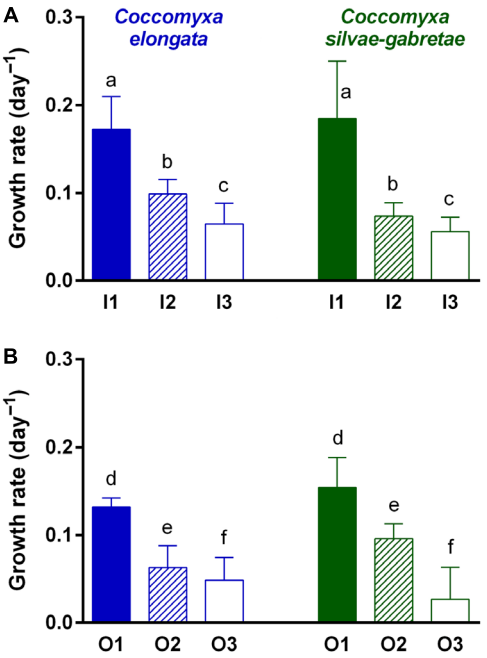

FIGURE 2 | Comparison of growth rates of the *Coccomyxa* cultures in P-replete (1) and P-depleted (2 and 3) media with either inorganic (I; top: **A**) or organic (O; bottom: **B**) P source. Columns are means, bars represent SDs; note that scales are the same. Differences among treatments were tested using three-way ANOVA with a *post hoc* Tukey HSD test; lower case letters above the columns (a–f) indicate significant differences among treatments (see **Table 1** for summary statistics).

(I2 and I3; **Figure 2**). Moreover, both the species reached significantly lower growth rates in media with β-GP (0.13–0.15 and 0.03–0.10 day^{-1}, respectively) compared to their P_i counterparts (**Table 1**), while keeping the same descending trends from P-replete to depleted variants (O1–O3; **Figure 2B**). Notwithstanding the P source and species, all P-depleted cultures revealed significantly larger mean cell volumes (38–52 μm^3) than those that were P-replete (23–31 μm^3; **Figure 3** and **Table 2**).

In both P-replete media, we detected negligible ELFA labeling (**Figures 4A,B**) in both *Cocomyxa* cultures. We therefore estimated close to zero cell-specific phosphatase activity (relative FU $cell^{-1}h^{-1}$) in every replicate of the I1 and O1 variants (**Figure 5**). On the contrary, we detected substantial phosphatase activity in all P-depleted cultures. While its increase, compared to the corresponding P-replete variant, was lower in P-depleted P_i media and significant only in the I3 variant, all P-depleted cultures grown with β-GP exhibited bright fluorescence (**Figures 4C–F**). Moreover, the cell-specific phosphatase activities in O2 and O3 treatments exceeded those in I2 by one order of magnitude (**Figure 5**). Three-way ANOVA confirmed highly significant effects of both P source and P concentration, as well as their interaction (see, respectively, factors M and P in **Table 3**). This interaction reflected different responses to the P source concertation in the P_i and β-GP cultures (cf. **Figures 5A,B**).

We further analyzed the frequency distributions of the cell-specific phosphatase activities measured in all replicates of each treatment. In general, we did not find any remarkable difference in the distribution patterns among the two *Coccomyxa* species tested (**Figure 6**). In the P-replete cultures, most of the algal cells (nearly 100% in I1 and almost 80% in O1) exhibited negligible activity (<0.02 FU $cell^{-1}h^{-1}$). Unlike in I1 variants, up to ∼20% of algae in the O1 cultures exhibited low activity (<0.64 FU $cell^{-1}h^{-1}$). On the contrary, we observed low percentage of such weakly ELFA-labeled and/or inactive cells with very similar distribution patterns in all P-depleted β-GP cultures (cf. O2 and O3 in **Figures 6C,D**). The P-depleted P_i and β-GP cultures, however, showed very different distribution patterns in two aspects: (i) the maximum in the histogram of single-cell phosphatase activities was notably shifted toward higher activities in β-GP compared to P_i cultures (peaking around 0.6 and 2.5 FU $cell^{-1}h^{-1}$, respectively), and (ii) in P_i cultures, the moderate P-depletion (I2) resulted in a flat and uniform frequency distribution limited to the region of low activities (<1.26 FU $cell^{-1}h^{-1}$), whereas the high P-depletion (I3) induced clear maximum between 0.32 and 1.26 FU $cell^{-1}h^{-1}$ (**Figures 6A,B**).

At comparable growth rates, the cell-specific phosphatase activities were roughly 5–10 times higher in the variants with β-GP compared to P_i as phosphorus source. The relationship between growth rate and phosphatase activity was similar in both *Coccomyxa* species examined (**Figure 7**).

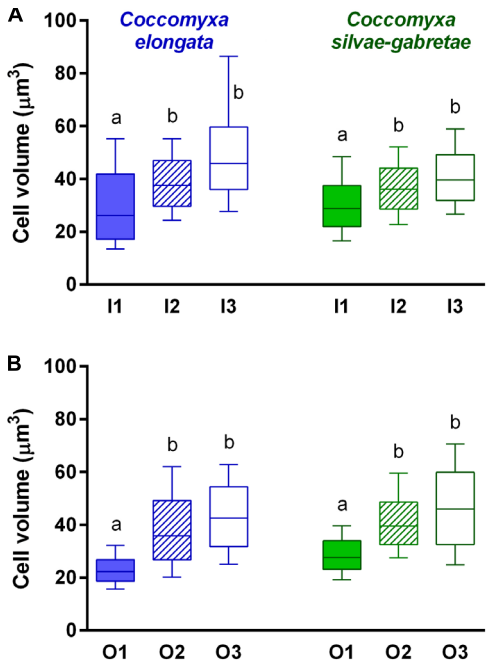

FIGURE 3 | Comparison of mean cell volume of the *Coccomyxa* cultures in P-replete (1) and P-depleted (2 and 3) media with either inorganic (I; top: **A**) or organic (O; bottom: **B**) P source. Box and whisker plots show medians (bar), 25 and 75% quartiles (box), and 10–90% percentiles (whiskers); note same scales. Differences among treatments were tested using three-way ANOVA with a *post hoc* Tukey HSD test; lower case letters above the columns (a, b) indicate significant differences among treatments (see **Table 2** for summary statistics).

DISCUSSION

Our results clearly suggest that both tested *Coccomyxa* species, although their original populations had lived in acidic lakes with the contrasting P availability for decades, possessed the same ability to produce acid extracellular phosphatases. We can speculate that the absence of a genomic adaptation to high P concentrations in *C. elongata* indicates that the production of acid phosphatases represent an evolutionarily conservative trait of vital importance for the acidotolerant algae. These phosphatases were inducible ectoenzymes (cf. Chróst, 1991), exclusively produced in all P-depleted cultures, while their production in the P-replete variants (I1 or O1) was negligible. Some early studies considered alkaline phosphatases as inducible and acid phosphatases as constitutive (Cembella et al., 1984; Jansson et al., 1988). In contrast, individual phytoplankton species exhibited, depending on circumstances, zero to extreme acid phosphatase activity per cell in chronically P limited acidic lakes, indicating that these ectoenzymes were inducible too (Štrojsová and Vrba, 2009; Novotná et al., 2010). Our results in this study suggested that acid phosphatases in *Coccomyxa* species were regulated in the same manner as it is known for alkaline phosphatases (e.g., Jansson et al., 1988).

Surprisingly, the relatively well-growing O1 cultures, grown entirely with organic P source, produced very little phosphatases. Most likely, some non-enzymatic hydrolysis of β-GP could liberate enough P_i for algal growth, as suggested by the residual SRP concentrations (~30 µmol L^{-1}) observed in this P-replete medium (O1). The high β-GP concentration could also saturate the enzymes to such a degree that the ELFP substrate was outcompeted during the assay (likewise glucose-6-phosphate and 4-methylumbelliferyl phosphate inhibited the ELFP hydrolysis; cf. Figure 1 in Štrojsová et al., 2003). Consequently, just <20% of algal cells showed weak ELFA labeling (**Figure 6**). Moreover, we could not exclude some β-GP hydrolysis by bacterial extracellular enzymes (cf. Siuda and Chróst, 2001) as the algal cultures were not axenic. Such an enzymatic activity, however, would not interfere with the FLEA assay, which specifically quantifies relative fluorescence of individual algae (**Figure 1**). Furthermore, hardly any bacterial or free activity would be retained on the filter used (2-µm pore size); indeed very few such ELFA precipitates were observed by epifluorescence microscopy (**Figure 4B**).

Cell-specific phosphatase activities were almost an order of magnitude higher with β-GP (O2 and O3) compared to those with P_i (I2 and I3) (cf. the different scales in **Figures 5A,B**) and the growth rates with P_i were slightly but significantly higher than those with β-GP (**Figure 2** and **Table 1**). Similar responses were recently reported also by Ren et al. (2017), who cultured algal (*Chlorella pyrenoidosa* and *Pseudokirchneriella subcapitata*) or cyanobacterial (*Microcystis aeruginosa*) species with various P sources in axenic batch cultures. Similarly to our study, both green algae (*C. pyrenoidosa* and *P. subcapitata*) and cyanobacteria grew faster with P_i than with β-GP or glucose-6-phosphate (Ren et al., 2017). At the same P concentrations, P_i provided apparently better support for growth than organic P sources (**Figure 7**). Hence, the production of phosphatases might represent additional investment of energy (Novotná et al., 2010) and/or the phosphatases were not able to liberate enough P_i for growth. The substantially higher phosphatase activity in the cultures grown with organic P could reflect stronger P deficiency in these cultures compared to those grown with P_i. Besides, not only the lack of P_i but also the presence of organic P could contribute to phosphatase upregulation. In other words, both *Coccomyxa* species maintained approximately twofold higher phosphatase activity to perform the growth rates lower or equal to 0.1 day^{-1} as shown in **Figure 7**.

Our results suggested fully inducible nature of acid phosphatases in the studied algae, because ELFA labeling was negligible in either P_i or β-GP excess. On the contrary, Young et al. (2010) observed certain P-insensitive component of alkaline phosphatase activity in the benthic *Cladophora*-epiphyte assemblage from Lake Michigan, cultured with P_i and α-glycerol phosphate supply, as well. Their conclusions, however, were based on an experimental study on the benthic assemblage, i.e., neither planktonic nor unialgal populations (Young et al., 2010). Moreover, their conclusions were based only on qualitative evidence (i.e., presence of ELFA-labeling) and not on quantification of the cell-specific phosphatase activity as was the case in this and other studies on *C. silvae-gabretae* (Štrojsová and Vrba, 2006, 2009; Novotná et al., 2010).

In our study, all P-depleted *Coccomyxa* cultures had significantly higher mean cell volumes compared to those that

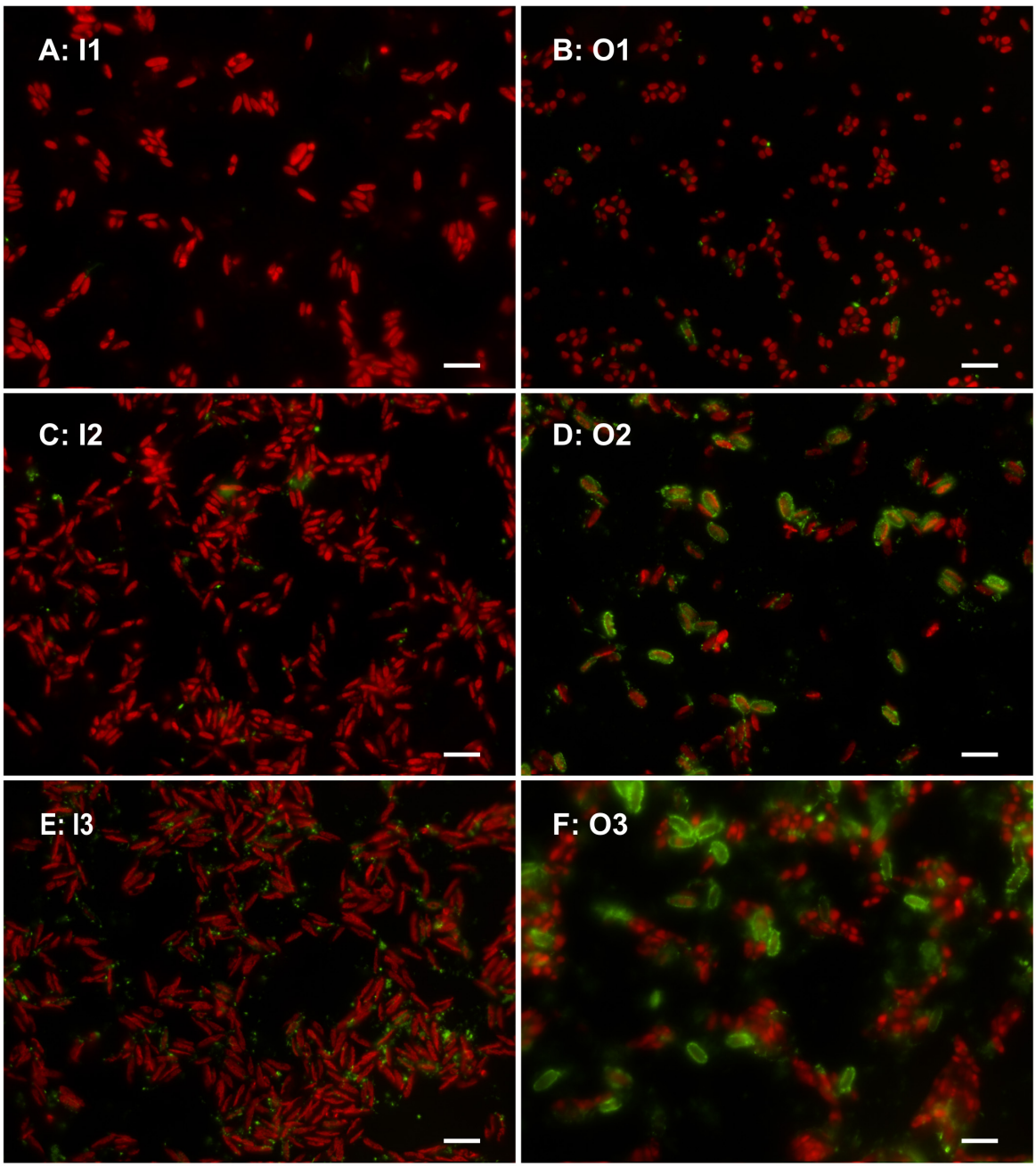

FIGURE 4 | Microphotographs of the *C. elongata* cultures grown in all experimental treatments (see variants' codes), i.e., in P-replete (top: **A,B**) and P-depleted (middle and bottom: **C–F**) media with inorganic (left) or organic (right) P sources. Combined images in artificial colors (for details, see **Figure 1**); scale bars represent 10 μm.

were P-replete (**Figure 3**). Such larger cells of P-limited algae were reported in batch cultures of *Scenedesmus quadricauda* and *Asterionella formosa* (Litchman and Nguyen, 2008), as well as in continuous cultures of *Cryptomonas phaseolus* (Mindl et al., 2005). Cells in the P-limited cultures likely divided less often due to the lack of P and, at the same time, enlarged their volume via storing photosynthates. The larger cells indeed should result in a relatively low P content, hence, in other words, in the low cellular P quota and, consequently, in high phosphatase expression (Litchman and Nguyen, 2008).

Unlike in the short-term experiments with gradually exhausting sources in the batch cultures (e.g., Ou et al., 2010; Ren et al., 2017), in the present study, we employed semi-continuous cultures, better adjusted to keep the (limiting) P concentration tested. This setup allowed us to maintain the algal cultures at a more stable P deficiency or P sufficiency

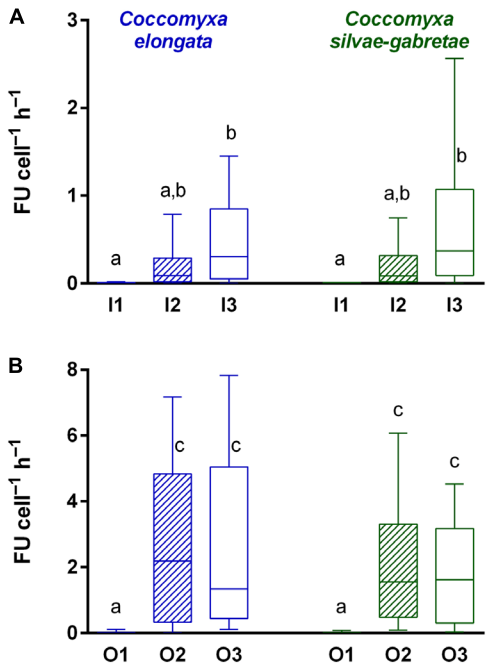

FIGURE 5 | Comparison of cell-specific phosphatase activity [in relative fluorescence units (FUs)] in the *Coccomyxa* cultures in P-replete (1) and P-depleted (2 and 3) media with either inorganic (I; top: **A**) or organic (O; bottom: **B**) P source. Box and whisker plots show medians (bar), 25 and 75% quartiles (box), and 10 and 90% percentiles (whiskers); note the different scales of y axes. Differences among treatments were tested using three-way ANOVA with a *post hoc* Tukey HSD test; lower case letters above the columns (a–c) indicate significant differences among treatments (see **Table 3** for summary statistics).

for longer periods of time, to maintain more close-to-natural conditions of both original *Coccomyxa* populations (Barcytė and Nedbalová, 2017), and to allow for their cross-comparison. While *C. elongata* dominated in the phytoplankton of the eutrophic Lake Hromnice (Hrdinka et al., 2013), *C. silvae-gabretae* (previously misdetermined as *Monoraphidium dybowskii*) prevailed in the phytoplankton biomass of the mesotrophic Lake Plešné, with enormous bulk activity of extracellular phosphatases due to impaired P availability (Vrba et al., 2006).

Our results on *C. silvae-gabretae* cultures in this study are consistent with the observed *in situ* response of this species to increasing P availability. The *in situ* phosphatase activity of *C. silvae-gabretae* gradually decreased with the progressing lake recovery from acid stress during past decades (Novotná et al., 2010). The first application of FLEA assay in Lake Plešné in 2001 showed remarkable ELFA-labeling of all bacterioplankton, as well as of most phytoplankton species, including the entire population of *C. silvae-gabretae* (Nedoma et al., 2003b). The cell-specific phosphatase activity of this species varied within four orders of magnitude (0.5–500 fmol cell^{-1}h^{-1}) in 2003 (Štrojsová et al., 2005), but averaged within a closer range (0.4–12 fmol cell^{-1}h^{-1}) in 2005 (Štrojsová and Vrba, 2009), whereas hardly any production of extracellular phosphatases, i.e., weak ELFA-labeling of *C. silvae-gabretae* cells, was detected in 2007 (Novotná et al., 2010). Using a conversion factor of 0.1 fmol FU^{-1} for our experimental results (in relative FU cell^{-1}h^{-1}), medians of phosphatase activity in the P-depleted variants I3 and O3 (**Figure 5**) were 0.04 and 0.16 fmol cell^{-1}h^{-1}, respectively, and the most frequent classes in both O2 and O3 variants (**Figure 6D**) fell between 1.3 and 5.1 fmol cell^{-1}h^{-1} for the strain of *C. silvae-gabretae*. These estimates of cell-specific phosphatase activity corresponded well to those determined for growing native populations of *C. silvae-gabretae* in Lake Plešné during the period of severe P limitation (Nedoma et al., 2003b; Štrojsová et al., 2005; Štrojsová and Vrba, 2009). The same estimates were calculated for the strain of *C. elongata* as well, although its native population in Lake Hromnice likely never experienced serious P depletion (Hrdinka et al., 2013).

The residual SRP concentrations in all P-depleted experimental variants (2–6 μmol L^{-1}) were at least by one order of magnitude higher than the threshold indicating P limitation in freshwaters (∼0.15 μmol L^{-1} of SRP; Nedoma et al., 1993; Vrba et al., 1993), whereas the epilimnetic SRP concentrations in Lake Plešné averaged seasonally as low as 0.04 μmol L^{-1} (Novotná et al., 2010). Yet in this lake, Štrojsová and Vrba (2009) documented remarkable diurnal variations in cell-specific phosphatase activity within the native population of *C. silvae-gabretae* in 2005, while Novotná et al. (2010) could not detect any measurable activity in this species at all in 2007. Both field studies suggested that single cells in the phytoplankton populations may differ remarkably in their individual cell-specific phosphatase activities due to the asynchronous character of the populations. Single algal cells likely reflected their internal needs in P, i.e., individual cellular P quota, as also suggested by Litchman and Nguyen (2008) or Ren et al. (2017). Štrojsová and Vrba (2009) proposed that distinct sub-populations (such as epilimnetic and metalimnetic) of *C. silvae-gabretae* with different life history characteristics could occur in the lake phytoplankton (e.g., due to strong mixing). Novotná et al. (2010) explained the absence of ELFA-labeling in the *C. silvae-gabretae* population by a pronounced P regeneration by grazing of abundant zooplankton, which re-colonized the lake between 2005 and 2007.

In our opinion, there is a common, but serious, methodological limitation in many recent studies employing ELFP (Rengefors et al., 2003; Dyhrman and Ruttenberg, 2006; Litchman and Nguyen, 2008; Young et al., 2010). Our analysis of frequency distribution of cell-associated ELFA fluorescences measured in this study (**Figure 6**) clearly illustrates the weakness of many studies employing ELFP that were based just on the scoring of ELFA-labeled cells (Rengefors et al., 2003; Dyhrman and Ruttenberg, 2006; Litchman and Nguyen, 2008; Young et al., 2010). For instance, our analysis showed that some ELFA-labeled cells could be found even in the P-replete culture (I1) grown on P_i (about some 40% of cells were 'positive,' i.e., with non-zero fluorescence; **Figure 6**), which could lead to a false conclusion that the population was P-deficient. Yet their actual phosphatase activity was negligible (in the range of 0–0.08 FU cell^{-1}h^{-1}; cf. **Figures 5A** and **6A** or **6B**). At

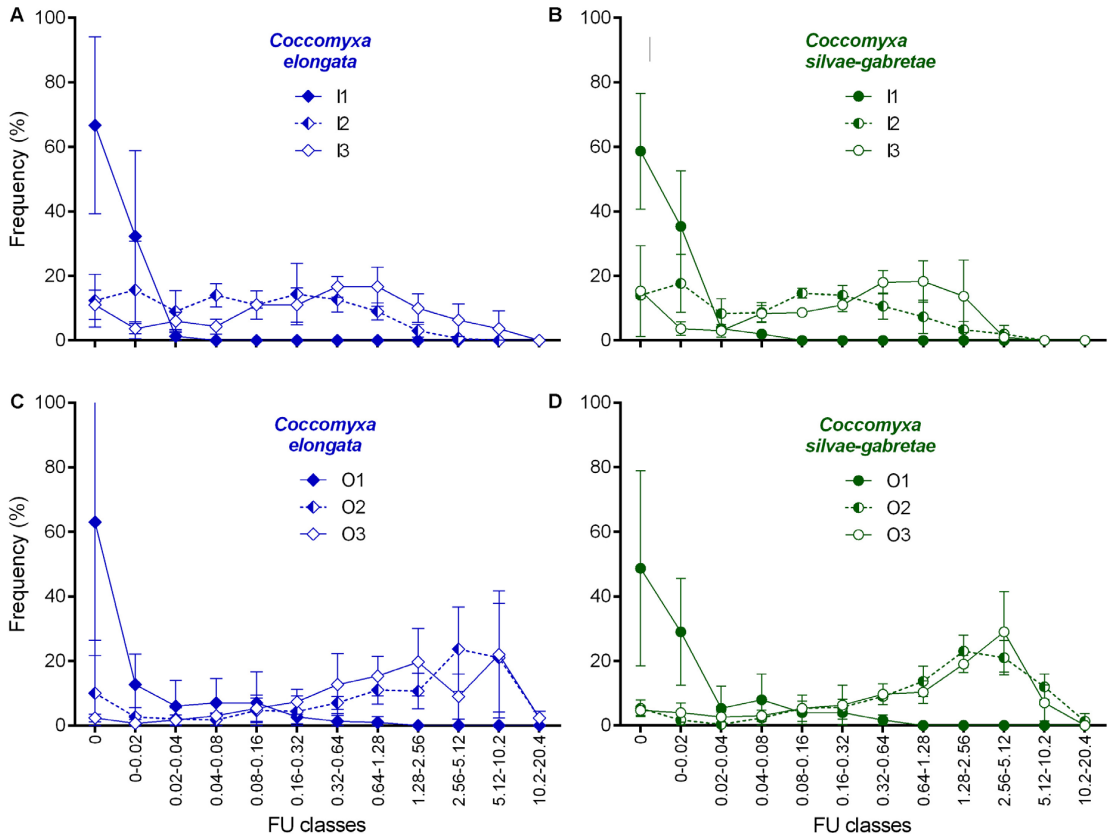

FIGURE 6 | Frequency distribution of cell-specific phosphatase activity (in relative FU cell^{-1}h^{-1}) in the *Coccomyxa* cultures in P-replete (1) and P-depleted (2 and 3) media with either inorganic (I; top: **A,B**) or organic (O; bottom**: C,D**) P source. Except for zero classes (no activity), all FU classes are expressed in a geometric progression to cover broad range of ELFA fluorescence. All symbols are means of triplicates, bars represent SDs; note same scales; 100% is the sum of means in a variant. The total cell number (in a variant) measured for *C. elongata*: 300 (I1), 360 (I2), 420 (I3), 357 (O1), 360 (O2), 360 (O3), and *C. silvae-gabretae*: 300 (I1), 360 (I2), 355 (I3), 355 (O1), 359 (O2), 360 (O3).

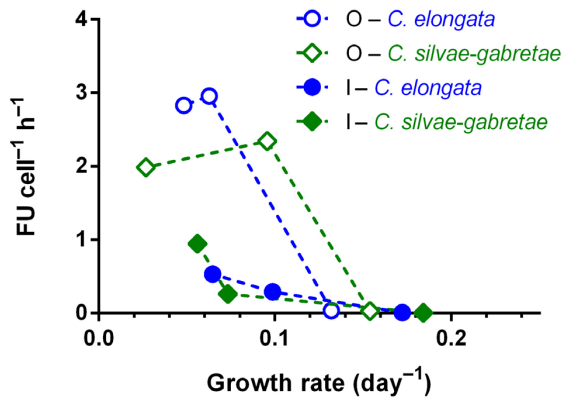

FIGURE 7 | Relationship of cell-specific phosphatase activity (in relative FUs) to the growth rates of *Coccomyxa* cultures grown with inorganic (I) or organic (O) P source. Symbols are means of triplicates.

present, the Fluorescently-Labeled Enzyme Activity assay (the true FLEA assay – Štrojsová and Vrba, 2006) is the only method available for adequate quantification of phosphatase activity at the level of individual cells or populations. The data on the percentages of ELFA-labeled cells should be interpreted with caution and considered, at the best, as semi-quantitative estimates of phosphatase activity in the assemblages (cf. Young et al., 2010).

Our experimental study suggested that the conclusions of our former field studies were plausible and confirmed the FLEA assay as a strong tool in phytoplankton ecology to explore P metabolism. To obtain reliable results, however, one should keep the following methodological recommendations: (i) Using ELF® 97 phosphate as the substrate for algal extracellular phosphatases, because an application of the ELF® 97 Endogenous Phosphatase Detection Kit likely may cause permeability of cell membranes and result in tagging of intracellular enzymes in some species (cf. Dyhrman and Palenik, 1999). (ii) Buffering phytoplankton samples, if pH *in situ* exceeds 8, to ensure the precipitation of ELFA molecules (Štrojsová and Vrba, 2006). (iii) Terminating sample incubation by gentle filtration (without application of phosphate buffered saline); only preserving samples with $HgCl_2$ before filtration is recommended for fragile flagellates (Nedoma et al., 2003b; Štrojsová et al., 2003). (iv) The ELFA-fluorescence-specific filter cube (see section "Materials

and Methods") should be used for acquiring images; another chlorophyll-autofluorescence-specific filter cube is recommended to localize algal cells (**Figure 1**). A monochromatic rather than color camera is optimal for convenient image cytometry.

CONCLUSION

The application of the FLEA assay in this experimental study confirmed the existence of environmental control of extracellular phosphatase expression in some acidotolerant algae and provided an insight into the impact of different P forms and concentrations on phosphatase activity in phytoplankton. This study represents the first evidence of inducible nature of acid phosphatases in algae. Our results further stress the importance of careful application of the FLEA method to gain reliable quantification of phosphatase activity at the single cell level.

AUTHOR CONTRIBUTIONS

JV, MM, and LN designed the experiment. MM and JN performed the image analysis. LN and MŠ performed the statistical analyses. All authors contributed to the manuscript.

FUNDING

This study was partly supported from the specific research funding of the Charles University and University of South Bohemia, as well as from the institutional funding of the Biology Centre CAS.

ACKNOWLEDGMENTS

Dagmara Sirová did a language revision of the final text.

REFERENCES

Barcytė, D., and Nedbalová, L. (2017). *Coccomyxa*: a dominant planktic alga in two acid lakes of different origin. *Extremophiles* 21, 245–257. doi: 10.1007/s00792-016-0899-6

Berman, T., Wynne, D., and Kaplan, B. (1990). Phosphatases revisited: analysis of particle-associated activities in aquatic systems. *Hydrobiologia* 207, 287–294. doi: 10.1007/BF00041467

Bischoff, H. W., and Bold, H. C. (1963). *Phycological Studies. IV. Some Soil Algae from Enchanted Rock and Related Algal Species*. Austin, TX: University of Texas Publications.

Boavida, M. J., and Heath, R. T. (1984). Are the phosphatases released by *Daphnia magna* components of its food? *Limnol. Oceanogr.* 29, 641–645. doi: 10.4319/lo.1984.29.3.0641

Cao, X., Song, C., Zhou, Y., Štrojsová, A., Znachor, P., Zapomělová, E., et al. (2009). Extracellular phosphatases produced by phytoplankton and other sources in shallow eutrophic lakes (Wuhan, China): taxon-specific versus bulk activity. *Limnology* 10, 95–104. doi: 10.1007/s10201-009-0265-9

Cao, X. Y., Štrojsová, A., Znachor, P., Zapomělová, E., Liu, G. X., Vrba, J., et al. (2005). Detection of extracellular phosphatases in natural spring phytoplankton of a shallow eutrophic lake (Donghu, China). *Eur. J. Phycol.* 40, 251–258. doi: 10.1080/09670260500192760

Carr, O. J., and Goulder, R. (1990). Fish-farm effluents in rivers. I. Effects on bacterial populations an alkaline phosphatase activity. *Water Res.* 24, 631–638. doi: 10.1016/0043-1354(90)90196-D

Cembella, A. D., Antia, N. J., and Harrison, P. J. (1984). The utilization of inorganic and organic phosphorus compounds as nutrients by eukaryotic microalgae: a multidisciplinary perspective: Part I. *Crit. Rev. Microbiol.* 10, 317–391. doi: 10.3109/10408418209113567

Chróst, R. J. (1991). "Environmental control of the synthesis and activity of aquatic microbial ectoenzymes," in *Microbial Enzymes in Aquatic Environments*, ed. R. J. Chróst (New York, NY: Springer-Verlag), 29–59.

Cotner, J. B., and Wetzel, R. G. (1991). 5′-Nucleotidase activity in a eutrophic lake and an oligotrophic lake. *Appl. Environ. Microbiol.* 57, 1306–1312.

Cotner, J. B., and Wetzel, R. G. (1992). Uptake of dissolved inorganic and organic phosphorus compounds by phytoplankton and bacterioplankton. *Limnol. Oceanogr.* 37, 232–243. doi: 10.4319/lo.1992.37.2.0232

Currie, D. J., and Kalff, J. (1984). A comparison of the abilities of freshwater algae and bacteria to acquire and retain phosphorus. *Limnol. Oceanogr.* 29, 298–310. doi: 10.4319/lo.1984.29.2.0298

Dell Inc. (2016). *Dell Statistica (Data Analysis Software System), Version 13.2*.

Dignum, M., Hoogveld, H. L., Matthijs, H. C. P., Laanbroek, H. J., and Pel, R. (2004). Detecting the phosphate status of phytoplankton by enzyme-labelled fluorescence and flow cytometry. *FEMS Microbiol. Ecol.* 48, 29–38. doi: 10.1016/j.femsec.2003.12.007

Dyhrman, S. T., and Palenik, B. (1999). Phosphate stress in cultures and field populations of the dinoflagellate *Prorocentrum minimum* detected by a single-cell alkaline phosphatase assay. *Appl. Environ. Microbiol.* 65, 3205–3212.

Dyhrman, S. T., and Ruttenberg, K. C. (2006). Presence and regulation of alkaline phosphatase activity in eukaryotic phytoplankton from the coastal ocean: implications for dissolved organic phosphorus remineralization. *Limnol. Oceanogr.* 51, 1381–1390. doi: 10.4319/lo.2006.51.3.1381

González-Gil, S., Keafer, B. A., Jovine, R. V. M., Aguilera, A., Lu, S., and Anderson, D. M. (1998). Detection and quantification of alkaline phosphatase in single cells of phosphorus-starved marine phytoplankton. *Mar. Ecol. Prog. Ser.* 164, 21–35. doi: 10.3354/meps164021

Healey, F. P., and Hendzel, L. L. (1979). Fluorometric measurement of alkaline-phosphatase activity in algae. *Freshwat. Biol.* 9, 429–439. doi: 10.1111/j.1365-2427.1979.tb01527.x

Healey, F. P., and Hendzel, L. L. (1980). Physiological indicators of nutrient deficiency in lake phytoplankton. *Can. J. Fish. Aquat. Sci.* 37, 442–453. doi: 10.1139/f80-058

Hoppe, H. G. (1983). Significance of exoenzymatic activities in the ecology of brackish water: measurements by means of methylumbelliferyl substrates. *Mar. Ecol. Prog. Ser.* 11, 299–308. doi: 10.3354/meps011299

Hoppe, H. G. (2003). Phosphatase activity in the sea. *Hydrobiologia* 493, 187–200. doi: 10.1023/A:1025453918247

Hrdinka, T., Šobr, M., Fott, J., and Nedbalová, L. (2013). The unique environment of the most acidified permanently meromictic lake in the Czech Republic. *Limnologica* 43, 417–426. doi: 10.1016/j.limno.2013.01.005

Huang, B. Q., Huang, S. Y., Wen, Y., and Hong, H. S. (2000). Effects of dissolved phosphorus on alkaline phosphatase activity in marine microalgae. *Acta Oceanol. Sin.* 19, 29–35.

Huang, Z., Terpetschnig, E., You, W., and Haugland, R. P. (1992). 2-(2′-phosphoryloxyphenyl)-4(3H)-quinazolinone derivates as fluorogenic precipitating substrates of phosphatases. *Anal. Biochem.* 207, 32–39. doi: 10.1016/0003-2697(92)90495-S

Jansson, M., Olsson, H., and Pettersson, K. (1988). Phosphatases; origin, characteristics and function in lakes. *Hydrobiologia* 170, 157–175. doi: 10.1007/BF00024903

Jones, J. G. (1972). Studies on freshwater micro-organisms: phosphatase activity in lakes of differing degrees of eutrophication. *J. Ecol.* 60, 777–791. doi: 10.2307/2258564

Knoll, L. B., Morgan, A., Vanni, M. J., Leach, T. H., Williamson, T. J., and Brentrup, J. A. (2016). Quantifying pelagic phosphorus regeneration using three methods in lakes of varying productivity. *Inland Waters* 6, 509–522. doi: 10.1080/IW-6.4.866

Litchman, E., and Nguyen, B. L. V. (2008). Alkaline phosphatase activity as a function of internal phosphorus concentration in freshwater phytoplankton. *J. Phycol.* 44, 1379–1383. doi: 10.1111/j.1529-8817.2008.00598.x

Mindl, B., Sonntag, B., Pernthaler, J., Vrba, J., Psenner, R., and Posch, T. (2005). Effects of phosphorus loading on the interactions of algae and bacteria: a reinvestigation of the "phytoplankton-bacteria paradox" in a continuous cultivation system. *Aquat. Microb. Ecol.* 38, 203–213. doi: 10.3354/ame038203

Nagata, T., and Kirchman, D. L. (1992). Release of macromolecular organic complexes by heterotrophic marine flagellates. *Mar. Ecol. Prog. Ser.* 83, 233–240. doi: 10.3354/meps083233

Nedoma, J., García, J., Comerma, M., Šimek, K., and Armengol, J. (2006). Extracellular phosphatases in a Mediterranean reservoir: seasonal, spatial and kinetic heterogeneity. *Freshwat. Biol.* 51, 1264–1276. doi: 10.1111/j.1365-2427.2006.01566.x

Nedoma, J., Padisák, J., and Koschel, R. (2003a). Utilisation of 32P-labelled nucleotide- and non-nucleotide dissolved organic phosphorus by freshwater plankton. *Arch. Hydrobiol. Adv. Limnol.* 58, 87–99.

Nedoma, J., Porcalová, A., Komárková, J., and Vyhnálek, V. (1993). Phosphorus deficiency diagnostics in the eutrophic Římov reservoir. *Water Sci. Technol.* 28, 75–84.

Nedoma, J., Štrojsová, A., Vrba, J., Komárková, J., and Šimek, K. (2003b). Extracellular phosphatase activity of natural plankton studied with ELF97 phosphate: fluorescence quantification and labelling kinetics. *Environ. Microbiol.* 5, 462–472. doi: 10.1046/j.1462-2920.2003.00431.x

Nedoma, J., and Vrba, J. (2006). Specific activity of cell-surface acid phosphatase in different bacterioplankton morphotypes in an acidified mountain lake. *Environ. Microbiol.* 8, 1271–1279. doi: 10.1111/j.1462-2920.2006.01023.x

Novotná, J., Nedbalová, L., Kopáček, J., and Vrba, J. (2010). Cell-specific extracellular phosphatase activity of dinoflagellate populations in acidified mountain lakes. *J. Phycol.* 46, 635–644. doi: 10.1111/j.1529-8817.2010.00858.x

Ou, L. J., Huang, B. Q., Hong, H. S., Qi, Y. Z., and Lu, S. H. (2010). Comparative alkaline phosphatase characteristics of the algal bloom dinoflagellates *Prorocentrum donghaiense* and *Alexandrium catenella*, and the diatom *Skeletonema costatum*. *J. Phycol.* 46, 260–265. doi: 10.1111/j.1529-8817.2009.00800.x

Ren, L. X., Wang, P. F., Wang, C., Chen, J., Hou, J., and Qian, J. (2017). Algal growth and utilization of phosphorus studied by combined mono-culture and co-culture experiments. *Environ. Pollut.* 220, 274–285. doi: 10.1016/j.envpol.2016.09.061

Rengefors, K., Pettersson, K., Blenckner, T., and Anderson, D. M. (2001). Species-specific alkaline phosphatase activity in freshwater spring phytoplankton: application of a novel method. *J. Plankton Res.* 23, 435–443. doi: 10.1093/plankt/23.4.435

Rengefors, K., Ruttenberg, K. C., Haupert, C. L., Taylor, C., and Howes, B. L. (2003). Experimental investigation of taxon-specific response of alkaline phosphatase activity in natural freshwater phytoplankton. *Limnol. Oceanogr.* 48, 1167–1175. doi: 10.4319/lo.2003.48.3.1167

Reynolds, C. S. (1997). *Vegetation Processes in the Pelagic: A Model for Ecosystem Theory*. Oldenburg: Ecology Institute.

Rychtecký, P., Řeháková, K., Kozlíková, E., and Vrba, J. (2015). Light availability may control extracellular phosphatase production in the turbid environment. *Microb. Ecol.* 69, 37–44. doi: 10.1007/s00248-014-0483-5

Schindler, D. W. (2012). The dilemma of controlling cultural eutrophication of lakes. *Proc. Biol. Sci.* 279, 4322–4333. doi: 10.1098/rspb.2012.1032

Schindler, D. W., Carpenter, S. R., Chapra, S. C., Hecky, R. E., and Orihel, D. M. (2016). Reducing phosphorus to curb lake eutrophication is a success. *Environ. Sci. Technol.* 50, 8923–8929. doi: 10.1021/acs.est.6b02204

Siuda, W., and Chróst, R. J. (2001). Utilization of selected dissolved organic phosphorus compounds by bacteria in lake water under non-limiting orthophosphate conditions. *Pol. J. Environ. Stud.* 10, 475–483.

Sommer, U. (1981). The role of r- and K-selection in the succession of phytoplankton in Lake Constance. *Acta Oecol.* 2, 327–342.

Sommer, U. (1985). Comparison between steady state and non-steady state competition: experiments with natural phytoplankton. *Limnol. Oceanogr.* 30, 335–346. doi: 10.4319/lo.1985.30.2.0335

Štrojsová, A., Nedoma, J., Štrojsová, M., Cao, X., and Vrba, J. (2008). The role of cell-surface-bound phosphatases in species competition within natural phytoplankton assemblage: an *in situ* experiment. *J. Limnol.* 67, 128–138. doi: 10.4081/jlimnol.2008.128

Štrojsová, A., and Vrba, J. (2006). Phytoplankton extracellular phosphatases: investigation using ELF (Enzyme Labelled Fluorescence) technique. *Pol. J. Ecol.* 54, 715–723.

Štrojsová, A., and Vrba, J. (2009). Short-term variation in extracellular phosphatase activity: possible limitations for diagnosis of nutrient status in particular algal populations. *Aquat. Ecol.* 43, 19–25. doi: 10.1007/S10452-007-9154-7

Štrojsová, A., Vrba, J., Nedoma, J., Komárková, J., and Znachor, P. (2003). Seasonal study on expression of extracellular phosphatases in the phytoplankton of an eutrophic reservoir. *Eur. J. Phycol.* 38, 295–306.

Štrojsová, A., Vrba, J., Nedoma, J., and Šimek, K. (2005). Extracellular phosphatase activity of freshwater phytoplankton exposed in different *in situ* phosphorus concentrations. *Mar. Freshw. Res.* 56, 417–424. doi: 10.1071/MF04283

Vrba, J., Komárková, J., and Vyhnálek, V. (1993). Enhanced activity of alkaline phosphatases – phytoplankton response to epilimnetic phosphorus depletion. *Water Sci. Technol.* 28, 15–24.

Vrba, J., Kopáček, J., Bittl, T., Nedoma, J., Štrojsová, A., Nedbalová, L., et al. (2006). A key role of aluminium in phosphorus availability, food web structure, and plankton dynamics in strongly acidified lakes. *Biologia* 61, S441–S451. doi: 10.2478/s11756-007-0077-5

Vrba, J., Kopáček, J., Fott, J., Kohout, L., Nedbalová, L., Pračáková, M., et al. (2003). Long-term studies (1871–2000) on acidification and recovery of lakes in the Bohemian Forest (central Europe). *Sci. Total Environ.* 310, 73–85. doi: 10.1016/S0048-9697(02)00624-1

Wetzel, R. G. (1991). "Extracellular enzymatic interactions: storage, redistribution, and interspecific communication," in *Microbial Enzymes in Aquatic Environments*, ed. R. J. Chróst (New York, NY: Springer-Verlag), 6–28.

Young, E. B., Tucker, R. C., and Pansch, L. A. (2010). Alkaline phosphatase in freshwater *Cladophora*-epiphyte assemblages: regulation in response to phosphorus supply and localization. *J. Phycol.* 46, 93–101. doi: 10.1111/j.1529-8817.2009.00782.x

Conflict of Interest Statement: The authors declare that the research was conducted in the absence of any commercial or financial relationships that could be construed as a potential conflict of interest.

frontiers in Microbiology

ORIGINAL RESEARCH
published: 23 March 2017
doi: 10.3389/fmicb.2017.00441

Identification and Characterization of a Novel Salt-Tolerant Esterase from the Deep-Sea Sediment of the South China Sea

*Yi Zhang[1], Jie Hao[1], Yan-Qi Zhang[1], Xiu-Lan Chen[1], Bin-Bin Xie[1], Mei Shi[1], Bai-Cheng Zhou[1], Yu-Zhong Zhang[1,2] and Ping-Yi Li[1]**

[1] State Key Laboratory of Microbial Technology, Marine Biotechnology Research Center, Institute of Marine Science and Technology, Shandong University, Jinan, China, [2] Laboratory for Marine Biology and Biotechnology, Qingdao National Laboratory for Marine Science and Technology, Qingdao, China

Marine esterases play an important role in marine organic carbon degradation and cycling. Halotolerant esterases from the sea may have good potentials in industrial processes requiring high salts. Although a large number of marine esterases have been characterized, reports on halotolerant esterases are only a few. Here, a fosmid library containing 7,200 clones was constructed from a deep-sea sediment sample from the South China Sea. A gene *H8* encoding an esterase was identified from this library by functional screening and expressed in *Escherichia coli*. Phylogenetic analysis showed that H8 is a new member of family V of bacterial lipolytic enzymes. H8 could effectively hydrolyze short-chain monoesters (C4–C10), with the highest activity toward *p*-nitrophenyl hexanoate. The optimal temperature and pH for H8 activity were 35°C and pH 10.0, respectively. H8 had high salt tolerance, remaining stable in 4.5 M NaCl, which suggests that H8 is well adapted to the marine saline environment and that H8 may have industrial potentials. Unlike reported halophilic/halotolerant enzymes with high acidic/basic residue ratios and low pI values, H8 contains a large number of basic residues, leading to its high basic/acidic residue ratio and high predicted pI (9.09). Moreover, more than 10 homologous sequences with similar basic/acidic residue ratios and predicted pI values were found in database, suggesting that H8 and its homologs represent a new group of halotolerant esterases. We also investigated the role of basic residues in H8 halotolerance by site-directed mutation. Mutation of Arg195, Arg203 or Arg236 to acidic Glu significantly decreased the activity and/or stability of H8 under high salts, suggesting that these basic residues play a role in the salt tolerance of H8. These results shed light on marine bacterial esterases and halotolerant enzymes.

Keywords: esterase, salt-tolerance, deep-sea sediment, metagenomics, basic residues

OPEN ACCESS

Edited by:
Andrew Decker Steen, University of Tennessee, Knoxville, USA

Reviewed by:
Amy Michele Grunden, North Carolina State University, USA
Wei Xie, Tongji University, China

****Correspondence:***
Ping-Yi Li
lipingyipeace@sdu.edu.cn

Specialty section:
This article was submitted to Aquatic Microbiology, a section of the journal Frontiers in Microbiology

Received: *05 December 2016*
Accepted: *03 March 2017*
Published: *23 March 2017*

Citation:
Zhang Y, Hao J, Zhang Y-Q, Chen X-L, Xie B-B, Shi M, Zhou B-C, Zhang Y-Z and Li P-Y (2017) Identification and Characterization of a Novel Salt-Tolerant Esterase from the Deep-Sea Sediment of the South China Sea. Front. Microbiol. 8:441. doi: 10.3389/fmicb.2017.00441

INTRODUCTION

Lipolytic enzymes, including esterases and lipases, are involved in catalyzing the hydrolysis and synthesis of esters. Esterases usually hydrolyze water-soluble short-chain monoesters, while lipases prefer water-insoluble long-chain triglycerides (Jaeger et al., 1999). Marine lipolytic enzymes play an important role in marine organic carbon degradation and cycling. A large number of active

microbial lipolytic enzymes have been discovered from surface and deep-sea seawater (Chu et al., 2008; Fang et al., 2014), hydrothermal vents (Placido et al., 2015), and marine sediments (Li et al., 2014), suggesting their potential roles in marine ecosystems.

Marine environments usually contain ∼3.5% (w/v) NaCl, and in some salterns, the salinity can even reach as high as 37% (w/v) (Ventosa et al., 2014). Many microbial enzymes of marine origin have evolved to be halotolerant or halophilic. Several halotolerant or halophilic lipolytic enzymes have been discovered from marine environments, including a halotolerant esterase (Est10) from *Psychrobacter pacificensis* (Wu et al., 2013), a halophilic esterase (LipC) from *Haloarcula marismortui* (Rao et al., 2009), a halotolerant esterase (ThaEst2349) from *Thalassospira* sp. (De Santi et al., 2016), and a halophilic lipase (LipBL) from *Marinobacter lipolyticus* (Perez et al., 2011). Studies on halotolerant/halophilic lipolytic enzymes and other halophilic enzymes show that these proteins have a significant increase in negatively charged acidic amino acid residues over their surfaces, which may form protective hydrated ion network and promote the adaption of the protein to salinity (Oren et al., 2005). The increase in acidity over the surface also prevents the aggregation of proteins (Elcock and Mccammon, 1998). However, there is also a report showing that an increase in positively charged basic residues on the enzyme surface may contribute to the adaption of an endonuclease *Vs*EndA from *Vibrio salmonicida* to saline habitat (Altermark et al., 2008). Thus, halotolerant and halophilic enzymes may have diverse salt-adapted strategies. The halotolerance of lipolytic enzymes can help themselves and the strains producing them well adapt to the saline environments and play a role in marine organic carbon degradation and cycling. It has been reported that halotolerant/halophilic lipolytic enzymes have potentials in industrial processes requiring high salts, low water activity, and the presence of organic solvents.

Based on amino acid sequences and biochemical properties, microbial lipolytic enzymes have been classified into eight families (families I-VIII) (Arpigny and Jaeger, 1999). Enzymes grouped in family V originates from a wide variety of bacteria, including mesophilic, psychrophilic, and thermophilic organisms (Arpigny and Jaeger, 1999). Recently, many members of family V lipolytic enzymes have been discovered (Prive et al., 2013; Sumby et al., 2013; Tchigvintsev et al., 2015). This family contains lipases and esterases, displaying diverse substrate specificities and characteristics (Peng et al., 2011; Chen et al., 2013; Pereira et al., 2015). However, studies on the salt tolerance of this family are still scarce.

Marine environments benefit the discovery of novel enzymes with special characteristics. Because more than 99% of marine microorganisms are still uncultured (Schloss and Handelsman, 2003), metagenomics, a cultivation-independent method, has been developed to discover new functional genes from both cultured and uncultured microorganisms (Handelsman, 2004). The application of functional metagenomics has led to the discovery of several new lipases and esterases from diverse marine environments, such as intertidal flat (Kim et al., 2009), tidal flat sediment (Jeon et al., 2012), and marine surface water (Chu et al., 2008).

To identify novel esterases from marine sediments, in this study, a fosmid library of a deep-sea sediment sample from the South China Sea was constructed, and functional metagenomic screening was performed to obtain novel esterases. A lipolytic enzyme gene *H8* was identified from the library, and the encoding esterase H8 was expressed and characterized. The result showed that H8 was a new member of family V of bacterial lipolytic enzymes with a substrate preference toward short-chain monoesters (C4–C10). H8 displayed high halotolerance. The sequence of H8 contains a large number of basic residues, leading to a high basic/acidic residue ratio and a high predicted isoelectric point (pI). The roles of basic residues in H8 halotolerance were investigated by site-directed mutagenesis. Sequence analysis suggests that H8 together with its homologs represent a new group of halotolerant esterases. These results shed light on marine bacterial esterases and halotolerant enzymes.

MATERIALS AND METHODS

Sample Collection and DNA Extraction

Marine sediment sample S100 was collected from the South China Sea (13.5°N, 118°E) at a water depth of 3,939 m in September 2011. Temperature and salinity of bottom water in this area was 2.4°C and 3.46% (w/v), respectively. The sample was stored at −20°C until processing. Environmental genomic DNA was extracted from the sample by following the SDS-based extraction procedure described by Zhou et al. (1996).

Metagenomic Library Construction and Screening of Lipolytic Enzymes

The DNA extract was separated by pulsed-filed gel electrophoresis (PFGE), and DNA bands of ∼35 kbp in the gel were extracted by gelase enzymolysis and ethanol precipitation. A metagenomic DNA library was constructed using the Copy-Control Fosmid Library Production Kit (Epicentre Biotechnologies, Madison, WI, USA) by following the manufacturer's instructions. A total of 7,200 fosmid clones were obtained, which were spread onto Luria-Bertani (LB) agar plates supplemented with 1% (v/v) emulsified tributyrin to screen clones with lipolytic enzyme activity. Clones exhibiting a clear zone around the colony were selected to construct their respective subcloning libraries. Fosmid DNA was extracted from positive clones and partially digested by the restriction enzyme Sau3AI. The DNA fragments of 1.5–5 kbp were recovered from an agarose gel, end-repaired and ligated into the pUC19 vector that had been digested by BamHI and pretreated by bacterial alkaline phosphatase. The ligated products were transformed into *E. coli* TOP10 cells, and the transformants were spread onto LB agar plates supplemented with 100 μg/ml ampicillin and 1% (v/v) tributyrin. Transformants forming clear zones were sequenced. The open reading frames (ORFs) in the sequenced

DNA fragments were predicted by the GeneMark program[1] and the genes encoding potential lipolytic enzymes were identified by using the blastx program against the NCBI non-redundant protein database (nr). Multiple sequence alignment was performed using MUSCLE (Edgar, 2004). Phylogenetic analysis was carried out with the neighbor-joining method using MEGA 6.0 (Tamura et al., 2013). The potential signal peptide sequence was predicted by SignalP 4.0 (Petersen et al., 2011).

Gene Cloning and Protein Expression and Purification

The gene *H8* encoding a lipolytic enzyme was amplified from the fosmid DNA using the primer pair of H8_F (5′-GGGAATTC CATATGCAGTCTGGCACGGTGAG-3′, NdeI digestion site was underlined) and H8_R (5′-CCGCTCGAGCGCCACCGCCGGT TGCGCC-3′, XhoI digestion site was underlined), and cloned into the expression vector pET-22b.

The constructed plasmid pET-22b-*H8* was transformed into *E. coli* BL21 (DE3). Transformants were cultured at 37°C and 180 rpm in LB liquid medium containing 100 μg/mL ampicillin. When the OD_{600} of cells reached approximately 0.6, 1 mM isopropyl-β-D-thiogalactopyranoside (IPTG) was added for the induction of protein expression. Then, the culture was incubated at 20°C and 110 rpm for 20 h. After incubation, the cells in the culture were harvested, resuspended in lysis buffer (50 mM Tris-HCl, 100 mM NaCl, pH 8.0) and disrupted by pressure. The recombinant His-tagged protein in the extract was first purified by Ni affinity chromatography (Qiagen, USA), and further purified by gel filtration chromatography on a Superdex 200 column (GE healthcare, Sweden). Protein concentrations were determined by using the Pierce BCA Protein Assay Kit (Thermo Scientific, USA).

Enzyme Assays

The esterase activity was measured by monitoring the hydrolysis of *p*-nitrophenyl (*p*NP) esters (Sigma, USA) using a spectrophotometric method (Shirai and Jackson, 1982). The reaction mixture contained 50 mM Tris-HCl buffer (pH 8.0), 0.02 ml of 10 mM substrate, and 0.02 ml enzyme with appropriate concentration in a final volume of 1 m1. After incubation at an indicated temperature for 5 min, the reaction was terminated by an addition of 0.1 ml 20% (w/v) SDS. The absorbance of the reaction mixture at 405 nm was measured to detect the amount of released *p*-nitrophenol (Li et al., 2014). The background hydrolysis of the substrate was determined by using a blank control with a composition identical with the reaction mixture except that the enzyme was replaced by buffer. One unit of enzyme (U) is defined as the amount of enzyme required to liberate 1 μmol *p*-nitrophenol per minute.

Biochemical Characterization of H8

The substrate specificity of H8 was investigated using the substrates *p*NP acetate (C2), *p*NP butyrate (C4), *p*NP caproate (C6), *p*NP caprylate (C8), *p*NP decanoate (C10), *p*NP laurate (C12), *p*NP myristate (C14), and *p*NP palmitate (C16) (Sigma, USA). The optimum temperature for H8 activity was measured at temperatures ranging from 0 to 60°C at pH 8.0. For thermostability assay, the enzyme was incubated at temperatures ranging from 0 to 60°C for 1 h, and then the residual activity was measured at 35°C. The optimum pH of H8 was determined at 35°C in the Britton–Robinson buffers ranging from pH 4.0 to 13.0. For pH stability assay, the enzyme was incubated in buffers with a pH range of 4.0–13.0 at 25°C for 1 h, and then the residual activity was measured at pH 8.0 and 35°C. The effect of NaCl on H8 activity was determined at NaCl concentrations ranging from 0 to 4.8 M. For salt tolerance assay, the enzyme was incubated at 0°C for 1 h in buffers containing NaCl ranging from 0 to 4.6 M before the residual activity was measured at 35°C.

The effects of metal ions (K^+, Li^+, Ba^{2+}, Ca^{2+}, Co^{2+}, Cu^{2+}, Fe^{2+}, Mg^{2+}, Mn^{2+}, Ni^{2+}, and Zn^{2+}) and potential inhibitors (β-mercaptoethanol, DTT, Thiourea, Urea, EDTA, and PMSF) on H8 activity were examined at pH 8.0 and 35°C in a final concentration of 1 mM or 10 mM. The effects of organic solvents on H8 activity were examined using methanol, ethanol, isopropanol, acetone, acetonitrile, dimethylsulfoxide (DMSO), and dimethylformamide (DMF) at final concentrations of 10% and 20% (v/v). The effects of Tween 20, Tween 80, and Triton X-100 on H8 activity were examined at final concentrations of 0.001–0.1% (v/v). The effect of SDS on enzyme activity was measured at final concentrations of 0.001–0.1% (w/v).

Site-Directed Mutagenesis of H8

Using plasmid pET-22b-*H8* as the template, site-directed mutagenesis on *H8* was performed with the QuikChange® 146 mutagenesis kit II (Agilent technologies, USA) according to the method of QuikChange site-directed mutagenesis (Liu and Naismith, 2008). After verified by DNA sequencing, mutated plasmids were transformed into *E. coli* BL21 (DE3) for protein expression. The purification of H8 mutants was performed under the same conditions as those of the wild type (WT) H8.

Enzyme Kinetic Assays

Enzyme kinetic assays of H8 and its mutants were carried out at pH 7.5 (50 mM Tris-HCl) using *p*NPC6 at concentrations from 0.02 to 2.0 mM. Kinetic parameters were calculated by non-linear regression fit directly to the Michaelis–Menten equation using the Origin8.5 software.

Circular Dichroism Spectroscopy

Circular dichroism (CD) spectra of WT H8 and its mutants were recorded at 25°C on a J-810 spectropolarimeter (JASCO, Japan). All the spectra were collected from 200 to 250 nm at a scanning speed of 200 nm/min with a path length of 0.1 cm. Proteins for CD spectroscopy assays were at a concentration of 0.3 mg/ml in 50 mM Tris-HCl buffer (pH 8.0).

Nucleotide Sequence Accession Number

The nucleotide sequence of H8 has been deposited in the GenBank database under accession number KY273927.

[1] http://topaz.gatech.edu/GeneMark/

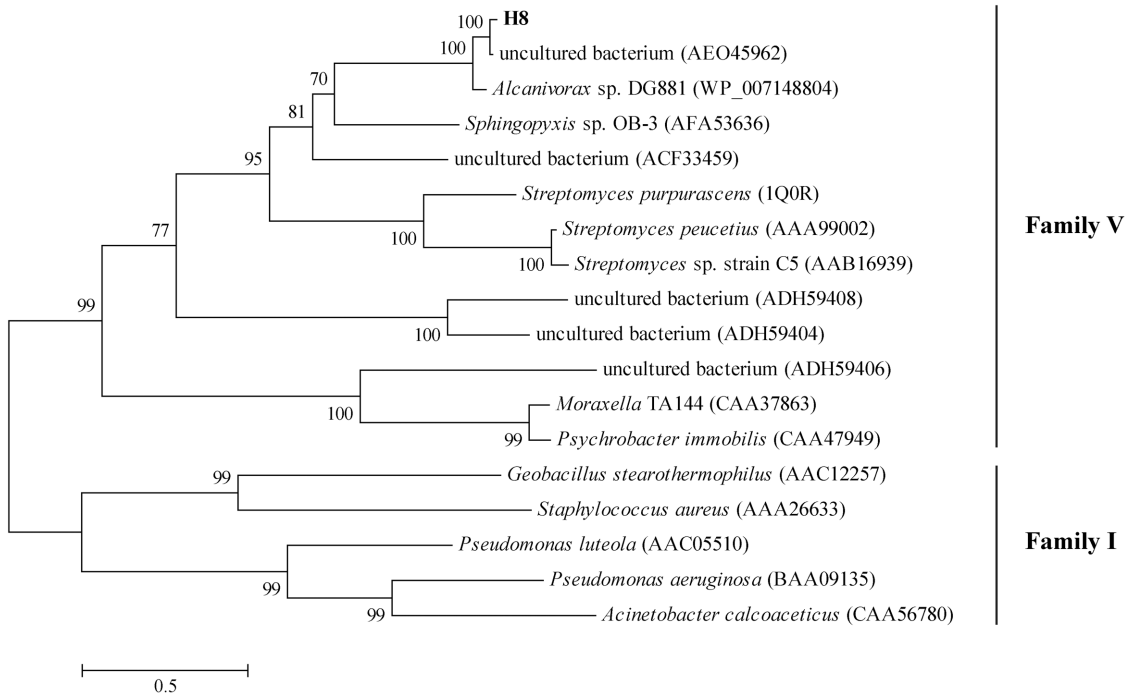

FIGURE 1 | Phylogenetic tree of esterase H8 and representative lipolytic enzyme sequences from family V. The tree was built by Neighbor-Joining method with JTT-matrix based model using 218 amino acid positions. Bootstrap analysis of 1000 replicates was executed and values above 50% are shown. The scale for branch length is shown below the tree. Lipases from family I were used as outgroups.

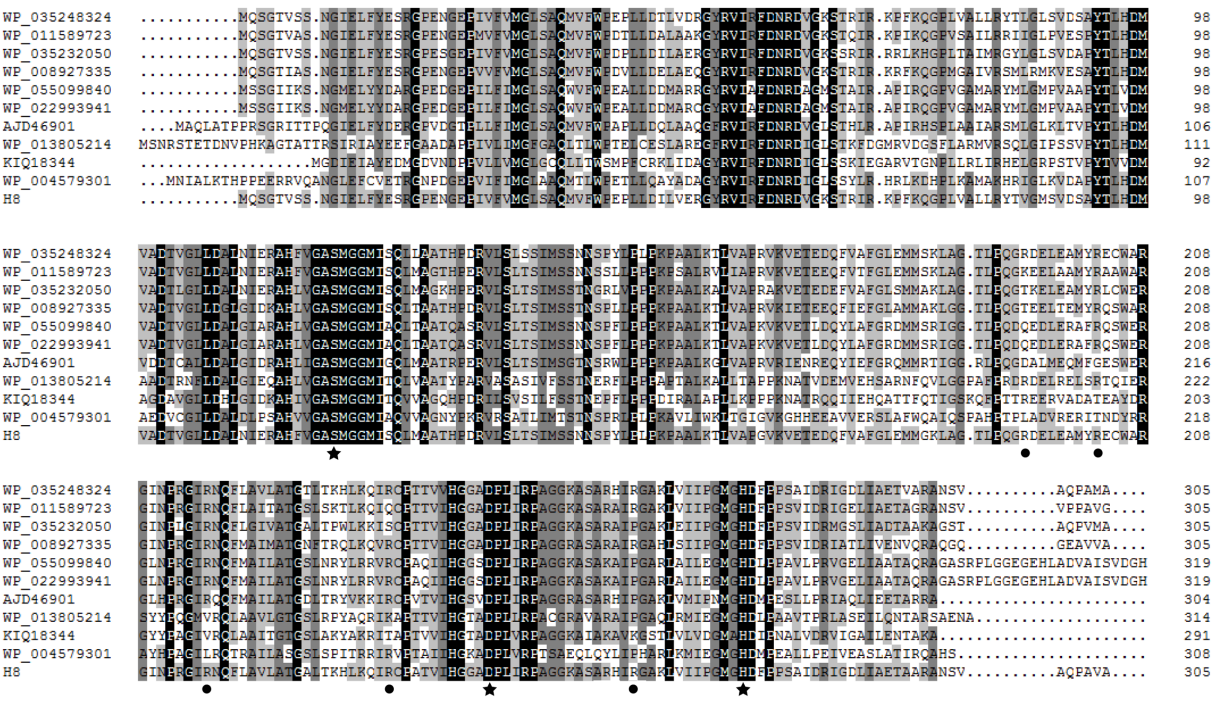

FIGURE 2 | Multiple sequence alignment of H8 and its homologs. Identical and similar amino acids are shaded in black and gray, respectively. Stars indicate amino acid residues belonging to the catalytic triad, and circles indicate basic amino acid residues (Arg195, Arg203, Arg216, Arg236, and Arg263) selected for site-directed mutation. Sequence analysis suggested that residues Arg203, Arg216, and Arg236 are highly conserved, and residues Arg195 and Arg263 are partially conserved.

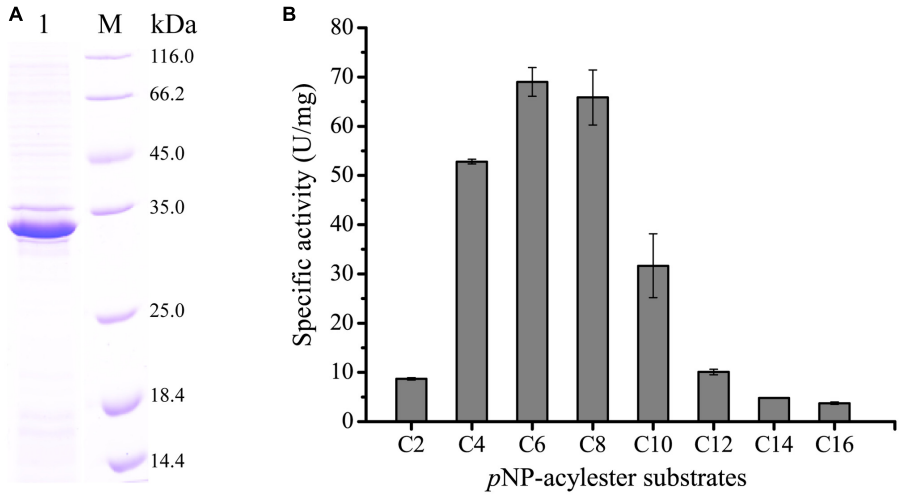

FIGURE 3 | Sodium dodecyl sulfate polyacrylamide gel electrophoresis (SDS-PAGE) analysis of purified esterase H8 and the substrate specificity of H8. (A) SDS-PAGE analysis of purified H8. Lane 1, purified H8; lane M, protein mass markers. **(B)** Substrate specificity of H8 evaluated with *p*NP esters. The graph shows data from triplicate experiments (mean ± SD).

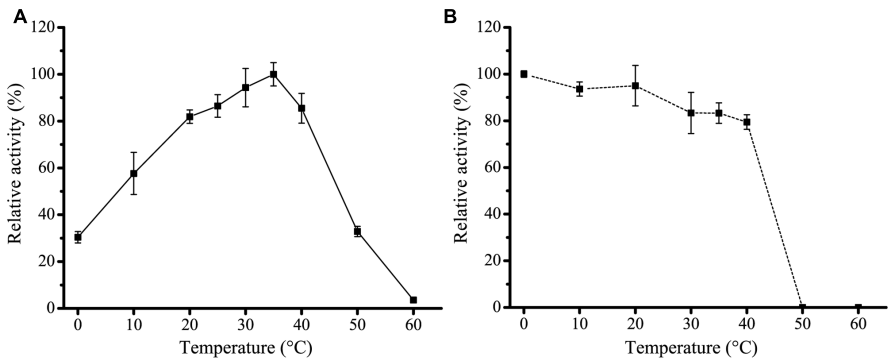

FIGURE 4 | Effect of temperature on the activity and stability of H8. (A) Effect of temperature on H8 activity. The highest activity of H8 at 35°C (69.2 U/mg) was taken as 100%. **(B)** Effect of temperature on the stability of H8. The enzyme was incubated at 0–60°C for 1 h. The remaining activity was measured under optimal conditions. The activity at 0°C (66.4 U/mg) was taken as 100%. The graphs show data from triplicate experiments (mean ± SD).

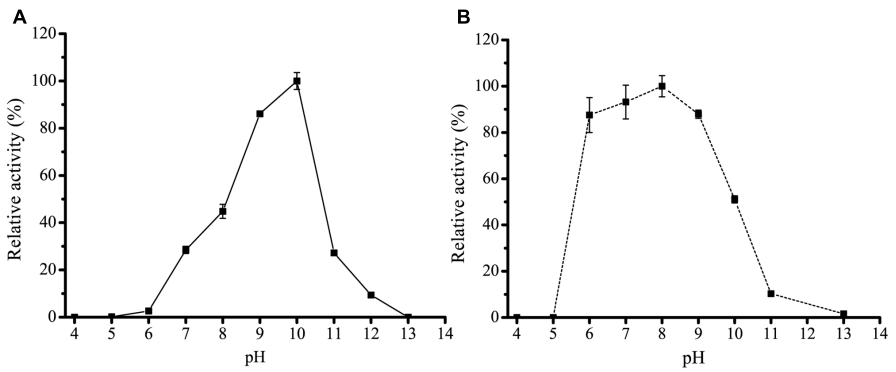

FIGURE 5 | Effect of pH on the activity and stability of H8. (A) Effect of pH on the activity of H8. The activity was measured at 35°C in Britton–Robinson buffers ranging from pH 4.0 to 13.0. The highest activity at pH 10.0 (70.2 U/mg) was taken as 100%. **(B)** Effect of pH on the stability of H8. The enzyme was incubated in buffers ranging from pH 4.0 to 13.0 at 25°C for 1 h. The remaining activity was measured under optimal conditions. The highest activity at pH 8.0 (54.4 U/mg) was taken as 100%. The graphs show data from triplicate experiments (mean ± SD).

RESULTS

Functional Metagenomic Screening of Lipolytic Enzymes

A metagenomic library was constructed from a deep-sea sediment sample from the South China Sea, which contained a total of 7,200 fosmid clones. The metagenomic library represented approximately 252 Mbp environmental DNA assuming an average insert size of 35 kbp. By functional assays, 10 fosmid clones showing lipolytic enzyme activities were screened from this library. The sequences of putative lipolytic enzyme-encoding genes in the identified fosmids were determined by subcloning library construction and subsequent sequencing. Among these genes, the gene *H8* containing 918 bp was predicted to encode a lipolytic enzyme and chosen for further analysis.

Sequence Analysis of the Lipolytic Enzyme H8

The gene *H8* encodes a lipolytic enzyme of 305 amino acid residues with a predicted molecular weight of 32.8 kDa and a predicted pI of 9.09. Prediction by SignalP 4.0 suggested that H8 may lack an N-terminal signal sequence. Among the characterized lipolytic enzymes, H8 showed the highest sequence identity (46%) to a family V esterase (Est16) from a microbial consortium specialized for diesel oil degradation (Pereira et al., 2015). Phylogenetic tree also showed that H8 belongs to the family V of bacterial lipolytic enzymes (**Figure 1**). Based on sequence alignments with other proteins from family V, the catalytic triad of H8 was identified, which is composed of Ser120, Asp247, and His275 (**Figure 2**). The catalytic Ser120 is located in the conserved GASMGGMI motif, Asp247 in the conserved DPL motif, and His275 in the conserved MG/AHD motif.

Expression and Characterization of the Esterase H8

H8 was over-expressed in *E. coli* BL21 (DE3), and the recombinant H8 protein was first purified by Ni affinity chromatography and then by gel filtration chromatography. Sodium dodecyl sulfate polyacrylamide gel electrophoresis (SDS-PAGE) analysis showed that the purified H8 displayed an apparent molecular weight of approximately 33 kDa, accordant to that predicted from its sequence (32.8 kDa) (**Figure 3A**). H8 could efficiently hydrolyze short-chain *p*NP esters (C4–C10), with the maximal activity toward *p*NPC6 (69.0 U/mg) (**Figure 3B** and Supplementary Figure 1). H8 showed a limited ability to degrade *p*NP esters longer than 10 carbon atoms, indicating that H8 is an esterase. H8 showed the highest activity at 35°C and retained 30% of its highest activity at 0°C (**Figure 4A**). H8 retained more than 80% of its highest activity after 1 h incubation at temperatures lower than 40°C, but lost all the activity after 1 h incubation at 50°C (**Figure 4B**). H8 had the highest activity at pH 10.0 (**Figure 5A**) and showed good tolerance in a range of pH 6.0–9.0, retaining over 80% of its highest activity after 1 h incubation in the buffers of pH 6.0–9.0 at 25°C (**Figure 5B**).

The effect of metal ions on the activity of H8 was also investigated (**Table 1**). H8 activity was almost unaffected by K^+, Li^+, Ca^{2+}, Co^{2+} or Mg^{2+} at 1∼10 mM, but significantly inhibited by Zn^{2+} at 1∼10 mM, and Ba^{2+}, Mn^{2+}, and Ni^{2+} at 10 mM, and fully inhibited by Cu^{2+} and Fe^{2+} at 10 mM. EDTA had no effect on H8 activity, suggesting that the catalysis by H8 may not require metal ions. H8 activity was significantly inhibited by 10 mM PMSF, indicating that H8 is most likely a serine hydrolase. H8 activity was also severely inhibited by

TABLE 1 | Effects of metal ions and potential inhibitors on H8 activity.

Compound	Relative/Residual activity (%)	
	1 mM	10 mM
K^+	107.8 ± 5.8	107.6 ± 1.5
Li^+	99.8 ± 2.1	86.1 ± 3.1
Ba^{2+}	93.4 ± 4.4	59.4 ± 2.8
Ca^{2+}	94.9 ± 8.1	90.9 ± 6.1
Co^{2+}	84.9 ± 0.8	74.3 ± 2.6
Cu^{2+}	82.2 ± 2.7	0.7 ± 0.2
Fe^{2+}	85.0 ± 1.4	LD[a]
Mg^{2+}	96.8 ± 6.1	84.1 ± 5.4
Mn^{2+}	76.0 ± 3.3	57.2 ± 2.6
Ni^{2+}	67.5 ± 1.8	57.1 ± 1.7
Zn^{2+}	25.1 ± 0.6	11.5 ± 0.4
β-Mercaptoethanol	78.6 ± 3.1	11.9 ± 2.8
DTT	31.3 ± 1.2	5.0 ± 2.7
Thiourea	111.5 ± 1.2	118.2 ± 5.1
Urea	103.5 ± 8.0	115.2 ± 4.0
EDTA	106.8 ± 1.8	114.4 ± 1.3
PMSF	96.2 ± 4.7	33.4 ± 1.1

[a] *LD indicates that the value was less than the limit of detection.*

TABLE 2 | Effects of detergents on H8 activity.

Detergent	Relative activity (%)		
	0.001% (v/v)	0.01% (v/v)	0.1% (v/v)
Tween 20	128.9 ± 5.6	112.3 ± 4.9	110.6 ± 3.4
Tween 80	102.9 ± 3.4	103.8 ± 3.0	112.3 ± 2.7
Triton X-100	113.4 ± 1.8	84.2 ± 0.5	62.8 ± 3.0
SDS[a]	33.0 ± 0.6	1.4 ± 0.2	LD[b]

[a] *The concentrations of SDS used were presented in w/v.*
[b] *LD indicates that the value was less than the limit of detection.*

TABLE 3 | Effects of organic solvents on H8 activity.

Organic solvent	Relative activity (%)	
	10% (v/v)	20% (v/v)
Methanol	122.5 ± 4.6	52.6 ± 2.2
Ethanol	120.4 ± 8.6	24.4 ± 0.9
Isopropanol	70.2 ± 6.1	4.4 ± 0.3
Acetone	82.3 ± 3.0	16.2 ± 0.5
Acetonitrile	65.6 ± 3.5	2.7 ± 0.3
DMF	109.9 ± 3.5	75.4 ± 1.9
DMSO	110.2 ± 2.1	104.7 ± 1.9

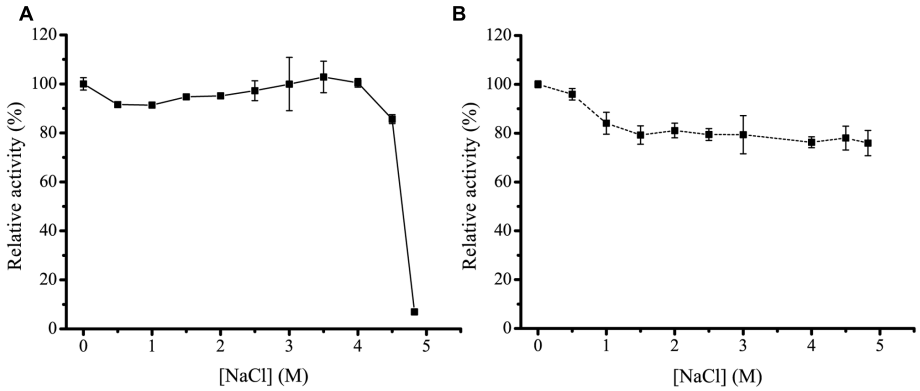

FIGURE 6 | Effect of NaCl on the activity and stability of H8. (A) Effect of NaCl on the activity of H8. The activity was measured at 35°C in 50 mM Tris-HCl buffer with different concentrations of NaCl. The activity in 0 M NaCl (70.9 U/mg) was taken as 100%. **(B)** Effect of NaCl on the stability of H8. The enzyme was incubated at 0°C for 1 h in buffers containing NaCl ranging from 0 to 4.6 M. The remaining activity was measured under optimal conditions. The activity in 0 M NaCl (68.6 U/mg) was taken as 100%. The graphs show data from triplicate experiments (mean ± SD).

TABLE 4 | Comparison of the amino acid composition of H8 and its homologs and reported halotolerant enzymes.

	Halotolerant H8	H8 homologs	Halophilic *Vs*EndA	Halotolerant PE10	Halophilic Hm EST
pI value	9.09	7.96–10.28	9.57	4.65	4.24
Arg + Lys (%)	10.49	10.00–11.84	17.06	6.45	5.8
Asp + Glu (%)	9.18	8.20–9.97	9.48	10.75	16.8
(Arg + Lys)/(Asp + Glu)	1.14	1.03–1.38	1.80	0.60	0.35
Sequence identity to H8[a]	100%	44–99%	–	–	–

[a] *–, no sequence identity detected.*

reductants DTT and β-mercaptoethanol. However, H8 showed high resistance to chaotropic agents urea and thiourea (**Table 1**). H8 activity was slightly increased by 0.001–0.1% (v/v) Tween 20, but fully inhibited by 0.01% (w/v) SDS (**Table 2**). Among all the tested organic solvents at 10% (v/v) concentration, methanol, ethanol, DMF, and DMSO slightly increased H8 activity, and other detergents slightly reduced H8 activity. At 20% (v/v) concentration, DMF and DMSO had nearly no effect on H8 activity, whereas other detergents significantly inhibited H8 activity (**Table 3**).

High Salt Tolerance of H8

Because the *H8* gene is isolated from a deep-sea sediment, we investigated the effect of NaCl of different concentrations on the activity and stability of H8. H8 still had full activity in NaCl with a concentration as high as 4.0 M (**Figure 6A**), indicating that H8 has high salt tolerance. Moreover, after 1 h incubation in 4.6 M NaCl, H8 still retained 80% activity (**Figure 6B**). These results show that H8 is a halotolerant enzyme.

High Contents of Basic Residues in H8

Unlike most reported halophilic/halotolerant enzymes that have high acidic/basic residue ratios and relatively low pI values ranging from 4.3 to 6.8 (Ng et al., 2000; Kennedy et al., 2001; Dassarma et al., 2013), H8 contains more basic residues (10.49%) than acidic residues (9.18%) (**Table 4**), leading to a high predicted pI value of 9.09. By searching NCBI nr database using the H8 sequence as a query, more than 10 homologs of H8 are found to have more basic residues than acidic residues and high pI values (**Table 4**), suggesting that H8 and its homologs may represent an uncharacterized group of lipolytic enzymes rich in basic residues.

The Role of Basic Residues in the Salt Tolerance of H8

Until now, only one halophilic enzyme, the endonuclease *Vs*EndA from *V. salmonicida*, is found to have an overwhelming number of basic residues distributed on the protein surface for its haloadaption (Altermark et al., 2008). To study the roles of the basic residues, especially the surface basic residues, in the salt tolerance of H8, we tried to obtain its crystal structure or modeled structure. Unfortunately, the crystal structure of H8 was unable to be solved due to the low resolution of the H8 crystals we obtained. In addition, due to the low sequence identity (lower than 28%) between H8 and reported proteins with resolved structures, no modeled structure of H8 could be constructed. Finally, according to multiple sequence alignment (**Figure 2**), we selected five basic residues (Arg195, Arg203, Arg216, Arg236, and Arg263) for site-directed mutation to acidic Glu to investigate their roles in H8 halotolerance. Residues Arg195 and Arg263 are partially conserved and residues Arg203, Arg216, and Arg236 are highly conserved in H8 homologs (**Figure 2**).

The effect of NaCl on the activities and stabilities of the mutants was measured and compared to WT H8 (**Figure 7**). Under their respective optimum temperatures, the effect of NaCl

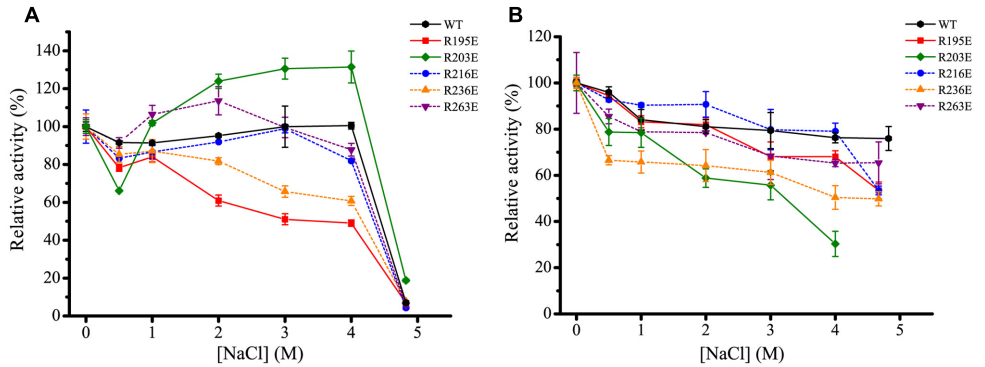

FIGURE 7 | Effect of NaCl on the activity and stability of the mutants of H8. (A) Effect of NaCl on the activity of WT H8 and its mutants. The activities of H8 and its mutants were determined at different NaCl concentrations at their respective optimum temperatures. The activities of WT H8 (70.9 U/mg), R195E (65.6 U/mg), R203E (7.5 U/mg), R216E (82.6 U/mg), R236E (53.0 U/mg), and R263E (62.0 U/mg) in 0 M NaCl were taken as 100%, respectively. **(B)** Effect of NaCl on the stability of WT H8 and its mutants. The enzymes were incubated in buffers containing different NaCl concentrations at 0°C for 1 h, and the residual activity was measured at their optimum temperatures, respectively. The activities of WT H8 (68.6 U/mg), R195E (64.5 U/mg), R203E (6.7 U/mg), R216E (72.8 U/mg), R236E (48.8 U/mg), and R263E (61.0 U/mg) in 0 M NaCl were taken as 100%, respectively. The graphs show data from triplicate experiments (mean ± SD).

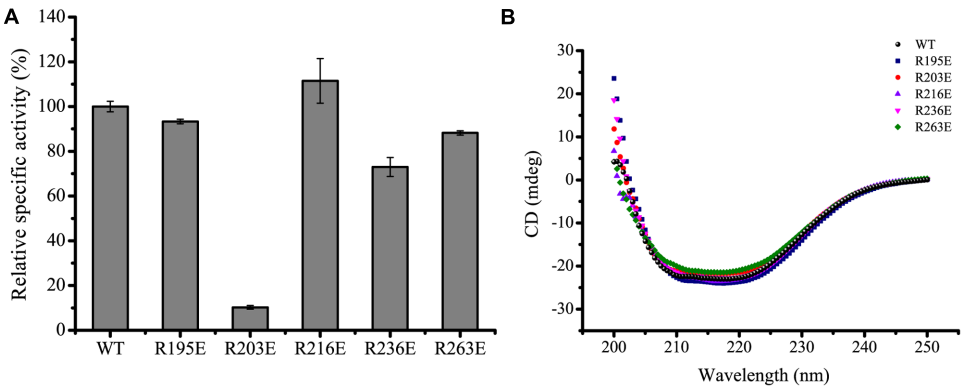

FIGURE 8 | Relative specific activities and circular dichroism (CD) spectra of WT H8 and its mutants. (A) Relative specific activities of WT H8 and its mutants. The specific activity of WT H8 (69.7 U/mg) was defined as 100%. **(B)** CD spectra of WT H8 and its mutants. All the spectra were collected from 200 to 250 nm at a scanning speed of 200 nm/min with a path length of 0.1 cm. The graphs show data from triplicate experiments (mean ± SD).

TABLE 5 | Impact of mutations on H8 stability and activity.

Enzyme	T_{opt} (°C)	V_{max} (μM/min/mg)	K_m (mM)	k_{cat} (s^{-1})	k_{cat}/K_m (mM^{-1} s^{-1})
WT	35	73.36 ± 1.91	0.074 ± 0.014	40.10 ± 1.04	539.8 (100%)
R195E	30	51.96 ± 2.92	0.052 ± 0.011	28.41 ± 1.59	546.2 (101.2%)
R203E	30	8.50 ± 1.09	0.070 ± 0.002	4.64 ± 0.59	66.6 (12.3%)
R216E	35	74.49 ± 2.63	0.072 ± 0.008	40.72 ± 2.44	546.7 (101.3%)
R236E	30	46.53 ± 1.54	0.053 ± 0.003	25.44 ± 0.84	481.8 (89.3%)
R263E	35	50.01 ± 2.37	0.058 ± 0.008	26.64 ± 1.19	459.3 (85.1%)

on the activities and stabilities of mutants R216E and R263E was similar to that of the WT (**Figures 7A,B**), suggesting that these two residues Arg216 and Arg263 may not be related to the salt tolerance of H8. In addition, mutants R216E and R263E had similar K_m and k_{cat} values and specific activities to the WT (**Figure 8A** and **Table 5**), indicating that these two mutations had little effect on the substrate binding and catalysis of H8 and that Arg216 and Arg263 are potentially surface residues.

Although the activity of mutant R203E was slightly stimulated by 1.2- to 1.3-fold in NaCl ranging from 2.0 to 4.0 M, its stability was significantly reduced in increased concentrations of NaCl. After incubated in 4.0 M NaCl for 1 h, H8 retained 80% activity, whereas R203E retained only 30% activity, indicating that mutant R203E is less tolerant than the WT under high salts. Mutation R203E had no impact on the K_m of H8, but significantly reduced its k_{cat} and specific activity (**Figure 8A** and **Table 5**). These data

suggest that Arg203 might be directly or indirectly involved in the catalysis of H8.

The effect of NaCl on the stability of mutant R195E was similar to that of the WT, whereas its activity was significantly reduced by NaCl. Compared to WT H8, the activity of mutant R195E in 4 M NaCl was reduced by 51%, suggesting its potential role in the salt tolerance of H8. Mutation R195E had no impact on the specific activity of H8 and small impact on the K_m and k_{cat} values (**Figure 8A** and **Table 5**), indicating that Arg195 is potentially located on the surface of H8 protein.

For mutant R236E, both the activity and stability was significantly reduced in increased concentrations of NaCl, suggesting that Arg236 may play an important role in the salt tolerance of H8. Mutant R236E had only small effect on the substrate binding and catalysis of H8 (**Table 5**), suggesting that residue Arg236 is potentially a surface residue.

Circular dichroism spectral analysis showed that these mutations caused no visible changes in H8 structure (**Figure 8B**), indicating that the decrease in the enzymatic activity and stability of the mutants resulted from residue substitution rather than structural changes.

DISCUSSION

In this study, a metagenomic library containing 7,200 fosmid clones was constructed from a deep-sea sediment sample from the South China Sea to functionally screen lipolytic enzyme-encoding genes, and a gene encoding an esterase H8 was identified, cloned and over-expressed. Phylogenetic analysis showed that H8 belongs to the family V of bacterial lipolytic enzymes. Among the characterized lipolytic enzymes, H8 has the highest identity (46%) to Est16 from a microbial consortium specialized for diesel oil degradation (Pereira et al., 2015). However, H8 shows different substrate specificities from Est16 (Pereira et al., 2015). H8 can efficiently hydrolyze short-chain monoesters (C4–C10), especially for *p*NPC6 and *p*NPC8, while Est16 prefers to hydrolyze *p*NPC4 and *p*NPC5 (Pereira et al., 2015). Therefore, H8 is a new family V esterase.

A few halotolerant/halophilic lipolytic enzymes have been reported. Consistent with other known halotolerant/halophilic enzymes, halotolerant/halophilic lipolytic enzymes contain more acidic residues (Asp and Glu) than basic residues in their sequences, leading to their low pI values (Ng et al., 2000; Kennedy et al., 2001; Dassarma et al., 2013). Moreover, modeled structural analysis suggests that a large number of negatively charged acidic residues are distributed over the protein surface of halotolerant/halophilic lipolytic enzymes, which may form a protective solvation shell to keep the protein surface hydrated and promote the adaption of the protein to salinity (De Santi et al., 2016; Wang et al., 2016). Until now, reports on the salt tolerance of family V lipolytic enzymes are still scarce. We studied the effect of NaCl on the activity and stability of H8. The result showed that H8 has high halotolerance. However, unlike most reported halotolerant/halophilic enzymes, H8 contains a large number of basic residues in sequence, leading to its high basic/acidic residue ratio and high pI value (9.09). In addition, more than 10 homologous sequences with similar basic/acidic residue ratios and predicted pI values to H8 are found in NCBI nr database. Therefore, H8 and its homologs may represent a new subgroup of family V halotolerant lipolytic enzymes rich in basic residues.

Up to date, only a halophilic endonuclease *V*sEndA from *V. salmonicida* is reported to contain more basic residues than acidic residues and have high pI value (9.57) (Altermark et al., 2008). Moreover, structural analysis shows that the protein surface of *V*sEndA is populated with positively charged basic residues, which may result in the haloadaption of *V*sEndA (Altermark et al., 2008). We studied the roles of five conserved basic residues in the salt tolerance of H8 by residue replacement. The results suggested that Arg195, Arg203, and Arg236 may play a role in the salt tolerance of H8, but Arg216 and Arg263 have little effect on the salt tolerance of H8. However, due to the lack of H8 structure, it is difficult to determine the exact positions and roles of these basic residues in H8, which still need further study.

In addition, H8 is also a cold-adapted enzyme. H8 had a low optimal temperature (35°C) for activity and still remained 30% of the maximal activity at 0°C. The halotolerant and cold-adapted characteristics indicate that H8 is well adapted to deep-sea sediment and may play a role in marine organic degradation and carbon cycling. Moreover, the good halotolerance of H8 implies its potentials in harsh industrial processes requiring high salts, low water activity, and the presence of organic solvents (such as DMSO).

AUTHOR CONTRIBUTIONS

YZ, JH, and Y-QZ performed all experiments. P-YL and X-LC directed the experiments. YZ and P-YL wrote the manuscript. B-BX and MS helped in data analysis. Y-ZZ and B-CZ designed the research.

ACKNOWLEDGMENTS

This work was supported by the National Science Foundation of China (grants 31290231, 91328208, 31670497, and 41676180), and the Program of Shandong for Taishan Scholars (TS200 90803).

SUPPLEMENTARY MATERIAL

The Supplementary Material for this article can be found online at: http://journal.frontiersin.org/article/10.3389/fmicb.2017.00441/full#supplementary-material

REFERENCES

Altermark, B., Helland, R., Moe, E., Willassen, N. P., and Smalas, A. O. (2008). Structural adaptation of endonuclease I from the cold-adapted and halophilic bacterium *Vibrio salmonicida*. *Acta Crystallogr. D Biol. Crystallogr.* 64(Pt 4), 368–376. doi: 10.1107/S0907444908000097

Arpigny, J. L., and Jaeger, K. E. (1999). Bacterial lipolytic enzymes: classification and properties. *Biochem. J.* 343(Pt 1), 177–183. doi: 10.1042/bj3430177

Chen, K., Liu, Y., Mao, D. M., Liu, X. M., Li, S. P., and Jiang, J. D. (2013). An essential esterase (BroH) for the mineralization of bromoxynil octanoate by a natural consortium of *Sphingopyxis* sp. strain OB-3 and *Comamonas* sp. strain 7D-2. *J. Agric. Food Chem.* 61, 11550–11559. doi: 10.1021/jf4037062

Chu, X., He, H., Guo, C., and Sun, B. (2008). Identification of two novel esterases from a marine metagenomic library derived from South China Sea. *Appl. Microbiol. Biotechnol.* 80, 615–625. doi: 10.1007/s00253-008-1566-3

Dassarma, S., Capes, M. D., Karan, R., and Dassarma, P. (2013). Amino acid substitutions in cold-adapted proteins from *Halorubrum lacusprofundi*, an extremely halophilic microbe from antarctica. *PLoS ONE* 8:e58587. doi: 10.1371/journal.pone.0058587

De Santi, C., Leiros, H. K., Di Scala, A., de Pascale, D., Altermark, B., and Willassen, N. P. (2016). Biochemical characterization and structural analysis of a new cold-active and salt-tolerant esterase from the marine bacterium *Thalassospira* sp. *Extremophiles* 20, 323–336. doi: 10.1007/s00792-016-0824-z

Edgar, R. C. (2004). MUSCLE: multiple sequence alignment with high accuracy and high throughput. *Nucleic Acids Res.* 32, 1792–1797. doi: 10.1093/nar/gkh340

Elcock, A. H., and Mccammon, J. A. (1998). Electrostatic contributions to the stability of halophilic proteins 1. *J. Mol. Biol.* 280, 731–748. doi: 10.1006/jmbi.1998.1904

Fang, Z., Li, J., Wang, Q., Fang, W., Peng, H., Zhang, X., et al. (2014). A novel esterase from a marine metagenomic library exhibiting salt tolerance ability. *J. Microbiol. Biotechnol.* 24, 771–780. doi: 10.4014/jmb.1311.11071

Handelsman, J. (2004). Metagenomics: application of genomics to uncultured microorganisms. *Microbiol. Mol. Biol. Rev.* 68, 669–685. doi: 10.1128/MMBR.68.4.669-685.2004

Jaeger, K. E., Dijkstra, B. W., and Reetz, M. T. (1999). Bacterial biocatalysts: molecular biology, three-dimensional structures, and biotechnological applications of lipases. *Annu. Rev. Microbiol.* 53, 315–351. doi: 10.1146/annurev.micro.53.1.315

Jeon, J. H., Lee, H. S., Kim, J. T., Kim, S. J., Choi, S. H., Kang, S. G., et al. (2012). Identification of a new subfamily of salt-tolerant esterases from a metagenomic library of tidal flat sediment. *Appl. Microbiol. Biotechnol.* 93, 623–631. doi: 10.1007/s00253-011-3433-x

Kennedy, S. P., Ng, W. V., Salzberg, S. L., Hood, L., and DasSarma, S. (2001). Understanding the adaptation of *Halobacterium* species NRC-1 to its extreme environment through computational analysis of its genome sequence. *Genome Res.* 11, 1641–1650. doi: 10.1101/gr.190201

Kim, E. Y., Oh, K. H., Lee, M. H., Kang, C. H., Oh, T. K., and Yoon, J. H. (2009). Novel cold-adapted alkaline lipase from an intertidal flat metagenome and proposal for a new family of bacterial lipases. *Appl. Environ. Microbiol.* 75, 257–260. doi: 10.1128/AEM.01400-08

Li, P. Y., Ji, P., Li, C. Y., Zhang, Y., Wang, G. L., Zhang, X. Y., et al. (2014). Structural basis for dimerization and catalysis of a novel esterase from the GTSAG motif subfamily of the bacterial hormone-sensitive lipase family. *J. Biol. Chem.* 289, 19031–19041. doi: 10.1074/jbc.M114.574913

Liu, H., and Naismith, J. H. (2008). An efficient one-step site-directed deletion, insertion, single and multiple-site plasmid mutagenesis protocol. *BMC Biotechnol.* 8:91. doi: 10.1186/1472-6750-8-91

Ng, W. V., Kennedy, S. P., Mahairas, G. G., Berquist, B., Pan, M., Shukla, H. D., et al. (2000). Genome sequence of *Halobacterium* species NRC-1. *Proc. Natl. Acad. Sci. U.S.A.* 97, 12176–12181. doi: 10.1073/pnas.190337797

Oren, A., Larimer, F., Richardson, P., Lapidus, A., and Csonka, L. N. (2005). How to be moderately halophilic with broad salt tolerance: clues from the genome of *Chromohalobacter salexigens*. *Extremophiles* 9, 275–279. doi: 10.1007/s00792-005-0442-7

Peng, Q., Zhang, X., Shang, M., Wang, X., Wang, G., Li, B., et al. (2011). A novel esterase gene cloned from a metagenomic library from neritic sediments of the South China Sea. *Microb. Cell Fact.* 10:95. doi: 10.1186/1475-2859-10-95

Pereira, M. R., Mercaldi, G. F., Maester, T. C., Balan, A., and Lemos, E. G. (2015). Est16, a new esterase isolated from a metagenomic library of a microbial consortium specializing in diesel oil degradation. *PLoS ONE* 10:e0133723. doi: 10.1371/journal.pone.0133723

Perez, D., Martin, S., Fernandez-Lorente, G., Filice, M., Guisan, J. M., Ventosa, A., et al. (2011). A novel halophilic lipase, LipBL, showing high efficiency in the production of eicosapentaenoic acid (EPA). *PLoS ONE* 6:e23325. doi: 10.1371/journal.pone.0023325

Petersen, T. N., Brunak, S., von Heijne, G., and Nielsen, H. (2011). SignalP 4.0: discriminating signal peptides from transmembrane regions. *Nat. Methods* 8, 785–786. doi: 10.1038/nmeth.1701

Placido, A., Hai, T., Ferrer, M., Chernikova, T. N., Distaso, M., Armstrong, D., et al. (2015). Diversity of hydrolases from hydrothermal vent sediments of the Levante Bay, Vulcano Island (Aeolian archipelago) identified by activity-based metagenomics and biochemical characterization of new esterases and an arabinopyranosidase. *Appl. Microbiol. Biotechnol.* 99, 10031–10046. doi: 10.1007/s00253-015-6873-x

Prive, F., Kaderbhai, N. N., Girdwood, S., Worgan, H. J., Pinloche, E., Scollan, N. D., et al. (2013). Identification and characterization of three novel lipases belonging to families II and V from *Anaerovibrio lipolyticus* 5ST. *PLoS ONE* 8:e69076. doi: 10.1371/journal.pone.0069076

Rao, L., Zhao, X., Pan, F., Li, Y., Xue, Y., Ma, Y., et al. (2009). Solution behavior and activity of a halophilic esterase under high salt concentration. *PLoS ONE* 4:e6980. doi: 10.1371/journal.pone.0006980

Schloss, P. D., and Handelsman, J. (2003). Biotechnological prospects from metagenomics. *Curr. Opin. Biotechnol.* 14, 303–310. doi: 10.1016/S0958-1669(03)00067-3

Shirai, K., and Jackson, R. L. (1982). Lipoprotein lipase-catalyzed hydrolysis of p-nitrophenyl butyrate. Interfacial activation by phospholipid vesicles. *J. Biol. Chem.* 257, 1253–1258.

Sumby, K. M., Grbin, P. R., and Jiranek, V. (2013). Characterization of EstCOo8 and EstC34, intracellular esterases, from the wine-associated lactic acid bacteria *Oenococcus oeni* and *Lactobacillus hilgardii*. *J. Appl. Microbiol.* 114, 413–422. doi: 10.1111/jam.12060

Tamura, K., Stecher, G., Peterson, D., Filipski, A., and Kumar, S. (2013). MEGA6: molecular evolutionary genetics analysis version 6.0. *Mol. Biol. Evol.* 30, 2725–2729. doi: 10.1093/molbev/mst197

Tchigvintsev, A., Tran, H., Popovic, A., Kovacic, F., Brown, G., Flick, R., et al. (2015). The environment shapes microbial enzymes: five cold-active and salt-resistant carboxylesterases from marine metagenomes. *Appl. Microbiol. Biotechnol.* 99, 2165–2178. doi: 10.1007/s00253-014-6038-3

Ventosa, A., Fernández, A. B., León, M. J., Sánchez-Porro, C., and Rodriguez-Valera, F. (2014). The Santa Pola saltern as a model for studying the microbiota of hypersaline environments. *Extremophiles* 18, 811–824. doi: 10.1007/s00792-014-0681-6

Wang, G., Wang, Q., Lin, X., Ng, T. B., Yan, R., Lin, J., et al. (2016). A novel cold-adapted and highly salt-tolerant esterase from *Alkalibacterium* sp. SL3 from the sediment of a soda lake. *Sci. Rep.* 6:19494. doi: 10.1038/srep19494

Wu, G., Wu, G., Zhan, T., Shao, Z., and Liu, Z. (2013). Characterization of a cold-adapted and salt-tolerant esterase from a psychrotrophic bacterium *Psychrobacter pacificensis*. *Extremophiles* 17, 809–819. doi: 10.1007/s00792-013-0562-4

Zhou, J., Bruns, M. A., and Tiedje, J. M. (1996). DNA recovery from soils of diverse composition. *Appl. Environ. Microbiol.* 62, 316–322.

Conflict of Interest Statement: The authors declare that the research was conducted in the absence of any commercial or financial relationships that could be construed as a potential conflict of interest.

frontiers in Microbiology

ORIGINAL RESEARCH
published: 22 December 2016
doi: 10.3389/fmicb.2016.02016

Characterization of a New S8 serine Protease from Marine Sedimentary *Photobacterium* sp. A5–7 and the Function of Its Protease-Associated Domain

*Hui-Juan Li[1,2†], Bai-Lu Tang[1†], Xuan Shao[1], Bai-Xue Liu[1], Xiao-Yu Zheng[1], Xiao-Xu Han[1], Ping-Yi Li[1], Xi-Ying Zhang[1], Xiao-Yan Song[1] and Xiu-Lan Chen[1]**

[1] State Key Laboratory of Microbial Technology, Marine Biotechnology Research Center, Institute of Marine Science and Technology, Shandong University, Jinan, China, [2] College of Chemical and Environmental Engineering, Shandong University of Science and Technology, Qingdao, China

Bacterial extracellular proteases are important for bacterial nutrition and marine sedimentary organic nitrogen degradation. However, only a few proteases from marine sedimentary bacteria have been characterized. Some subtilases have a protease-associated (PA) domain inserted in the catalytic domain. Although structural analysis and deletion mutation suggests that the PA domain in subtilases is involved in substrate binding, direct evidence to support this function is still absent. Here, a protease, P57, secreted by *Photobacterium* sp. A5-7 isolated from marine sediment was characterized. P57 could hydrolyze casein, gelatin and collagen. It showed the highest activity at 40°C and pH 8.0. P57 is a new subtilase, with 63% sequence identity to the closest characterized protease. Mature P57 contains a catalytic domain and an inserted PA domain. The recombinant PA domain from P57 was shown to have collagen-binding ability, and Phe349 and Tyr432 were revealed to be key residues for collagen binding in the PA domain. This study first shows direct evidence that the PA domain of a subtilase can bind substrate, which provides a better understanding of the function of the PA domain of subtilases and bacterial extracellular proteases from marine sediment.

Keywords: subtilase, protease-associated domain, marine sediment, collagen-binding, aromatic residues

OPEN ACCESS

Edited by:
Andrew Decker Steen, University of Tennessee, USA

Reviewed by:
Nina Dombrowski, Texas State University System, USA
Karolina Michalska, Argonne National Laboratory, USA

****Correspondence:***
Xiu-Lan Chen
cxl0423@sdu.edu.cn

† These authors have contributed equally to this work.

Specialty section:
This article was submitted to Aquatic Microbiology, a section of the journal Frontiers in Microbiology

Received: *08 September 2016*
Accepted: *01 December 2016*
Published: *22 December 2016*

Citation:
Li H-J, Tang B-L, Shao X, Liu B-X, Zheng X-Y, Han X-X, Li P-Y, Zhang X-Y, Song X-Y and Chen X-L (2016) Characterization of a New S8 serine Protease from Marine Sedimentary Photobacterium sp. A5–7 and the Function of Its Protease-Associated Domain. Front. Microbiol. 7:2016. doi: 10.3389/fmicb.2016.02016

INTRODUCTION

Organic nitrogen degradation is an important part of marine nitrogen cycle (Aluwihare et al., 2005). Particulate organic nitrogen (PON) that deposits to marine sediments is mainly decomposed by bacterial extracellular proteases, which is generally considered to be the initial and rate-limiting step of nitrogen cycle in marine sediments (Talbot and Bianchi, 1997; Brunnegård et al., 2004). It has been found that protease-producing bacteria and their extracellular proteases are rich and diverse in marine sediments (Olivera et al., 2007; Zhou et al., 2009, 2013). Some proteases from marine sedimentary bacteria have been characterized, most of which are shown to have special properties, such as cold adaptation (Chen et al., 2007; Yan et al., 2009; Kurata et al., 2010; Yang et al., 2013), salt tolerance (Yan et al., 2009), distinct substrate specificity and catalytic mechanism (Ran et al., 2014). Therefore, marine sediments are good resources for exploring novel proteases.

Peptidase family S8, also known as the subtilisin or subtilase family, is the second-largest family of serine proteases (Rawlings et al., 2010). Proteases in this family

are all characterized by an Asp/His/Ser catalytic triad and an α/β fold catalytic center containing a seven-stranded parallel β-sheet (Rawlings et al., 2006). Some proteases in the S8 family contain a protease-associated (PA) domain, which is inserted in the catalytic domain. This kind of proteases are reported from both plants and bacteria, such as tomato SBT3 (Ottmann et al., 2009), soybean protease C1 (Tan-Wilson et al., 2012), streptococcal C5a peptidase (Brown et al., 2005; Kagawa et al., 2009), lactococcal cell-envelope protease (Bruinenberg et al., 1994; Sadat-Mekmene et al., 2011), VapT from *Vibrio metschnikovii* RH530 (Kwon et al., 1995), Apa1 from *Pseudoalteromonas* sp. AS-11 (Dong et al., 2001), SapSh from *Shewanella* sp. Ac10 (Kulakova et al., 1999) and AcpII from *Alkalimonas collagenimarina* AC40 (Kurata et al., 2010).

The PA domains in subtilases were reported to have diverse functions. For plant subtilases, the PA domain of tomato SBT3 was suggested to be required for enzyme maturation, secretion, dimerization and activation (Cedzich et al., 2009; Ottmann et al., 2009); homology modeling and molecular simulation indicated that the PA domain of soybean protease C1 was crucial for determining the optimum length of peptide substrate (Tan-Wilson et al., 2012). For bacterial subtilases, deletion experiment indicated that the PA domain of lactococcal cell-envelope protease influenced the enzyme substrate specificity, but was unnecessary for enzyme folding or autoprocessing (Bruinenberg et al., 1994); the PA domains of AcpII from *Alkalimonas collagenimarina* AC40 and of streptococcal C5a peptidase SCPA from *Streptococcus pyogenes* were reported to restrict substrate access to the active site (Kagawa et al., 2009; Kurata et al., 2010). Although structural analyses and deletion experiments suggest that the PA domains in subtilases are involved in substrate binding, there has been no evidence showing that the PA domain of subtilase can bind substrate directly.

In a previous study, 66 protease-producing strains were screened from 6 sediment samples from Jiaozhou Bay, China, in which *Photobacterium* (39.4%), *Bacillus* (25.8%), *Vibrio* (19.7%) and *Shewanella* (7.6%) were the major groups and *Photobacterium* strains were distributed in all sediment samples. Among the strains, *Photobacterium* sp. A5–7 had the highest protease activity, which was isolated from the sediment sample from the A5 station site where the depth, temperature, pH and carbon/nitrogen ratio were 5.9 m, 24.7°C, 8.11 and 7.0, respectively (Zhang et al., 2015). In this study, we aimed to purify and characterize the protease secreted by *Photobacterium* sp. A5–7. The result showed that the protease P57 secreted by *Photobacterium* sp. A5–7 could hydrolyze casein, gelatin and collagen. We then cloned the gene encoding P57. Sequence analysis showed that P57 is a subtilase of the S8 family, containing a PA domain inserted in its catalytic domain. To study its function, the PA domain of P57 was expressed in *Escherichia coli* as a EGFP-fused protein, and its collagen-binding ability was determined by using fluorescent technology. The recombinant PA domain was shown to have collagen-binding ability, suggesting that the PA domain is likely involved in substrate binding during the hydrolysis of insoluble collagen by P57. Site-directed mutations were also performed to analyze the key residues for collagen binding in the PA domain of P57. Our results reveal a new S8 subtilase from a marine sedimentary bacterium and show direct evidence that the PA domain of a subtilase can bind substrate, which shed light on marine bacterial proteases and marine PON degradation.

MATERIALS AND METHODS

Phylogenetic Analysis of Strain A5-7

Genomic DNA of strain A5-7 was extracted using a bacterial genomic DNA isolation kit (BioTeke, China). Using the genomic DNA as template, the 16S rRNA gene of strain A5–7 was amplified by PCR with primers 27F and 1492R (Lane, 1991) and sequenced at Shanghai Biosune Biotechnology Corp. (China). The 16S rRNA gene sequence of strain A5–7, deposited in GenBank database under the accession number JX134463, was compared with those in GenBank and EzTaxon[1] (Kim et al., 2012) databases using BLASTN (Altschul et al., 1997) to determine the approximate phylogenetic affiliation and select reference sequences of related species for subsequent phylogenetic analysis. The 16S rRNA gene sequence of strain A5–7 was aligned with those of type strains of closely related species using the Clustal W program (Thompson et al., 1994) in the MEGA 5 (Tamura et al., 2011). The alignment obtained was manually trimmed to remove the uneven 5′ and 3′ ends. Phylogenetic trees were constructed using the neighbor-joining (Saitou and Nei, 1987) and maximum-likelihood (Felsenstein, 1981) methods with MEGA 5 (Tamura et al., 2011). Bootstrap analyses (1000 replications) were performed to evaluate tree topologies. Evolutionary distances were calculated using the model of Jukes and Cantor (1969).

Purification of the Protease P57 Secreted by Strain A5–7

Strain A5–7 was cultivated at 15°C for 72 h in a marine LB medium supplemented with 0.3% (w/v) casein and 0.5% (w/v) gelatin in a rotatory shaker at 180 rpm. The culture was centrifuged at 12,000 *g* and 4°C for 15 min. The cell-free supernatant was concentrated against polyethylene glycol (PEG) 20,000, and then dialyzed against 20 mM phosphate buffer (pH 7.0). The sample was loaded onto a DEAE-Sepharose Fast Flow column (GE Healthcare, USA) equilibrated with the same buffer. Bound proteins were eluted with a linear gradient of 0-1 M NaCl in 20 mM phosphate buffer (pH 7.0). The protease activity of every fraction (4 mL) was measured with casein as substrate. Fractions having protease activity were further subjected to 12.5% SDS-PAGE. Then, fractions having protease activity and displaying a single band in SDS-PAGE gel were collected for further use. The purified protease was named P57.

Analysis of the N-Terminal Amino Acid Sequence of Protease P57

The purified P57 was transferred from SDS-PAGE gel to a Sequi-Blot polyvinylidene difluoride membrane (PVDF

[1]http://eztaxon-e.ezbiocloud.net/

membrane, Bio-Rad, USA). Its N-terminal amino acid sequence was determined by the Edman degradation method with a PROCISE491 sequencer (Applied Biosystems, USA) at Peking University, China. The obtained N-terminal sequence of P57 was aligned with those of proteases in GenBank using BLASTP to determine the protease type.

Characterization of Protease P57

The activity of P57 was measured as described by Chen et al. (2003) with 2% (w/v) casein as substrate. The optimal temperature of P57 was determined over the range from 0 to 70°C in 20 mM phosphate buffer (pH 7.0). The effect of temperature on protease stability was evaluated by measuring the residual activity at 40°C after P57 was incubated at 30°C, 40°C, or 45°C for different time intervals (5, 10, 15, 20, 30, 40, or 60 min). The optimum pH of P57 was assayed at 40°C in the following buffers (20 mM): Na_2HPO_4-citric acid (pH 4.0–6.0), Na_2HPO_4-NaH_2PO_4 (pH 6.0–8.0), Tris-HCl (pH 8.0–10.0), and Na_2CO_3-$NaHCO_3$ (pH 9.0–11.0). To evaluate the effect of NaCl on enzyme activity, the assay was carried out at 40°C and pH 8.0 with different salt concentrations from 0 to 3 M. The effects of enzyme inhibitors (PMSF (phenylmethylsulfonyl fluoride), EDTA (ethylene diamine tetraacetic acid), EGTA (ethylene glycol tetraacetic acid), *o*-P (*o*-phenanthroline), and IA (iodoacetic acid)) and metal ions (K^+, Li^+, Ba^{2+}, Ca^{2+}, Co^{2+}, Cu^{2+}, Mg^{2+}, Mn^{2+}, Ni^{2+}, Sr^{2+}, Zn^{2+}, and Fe^{3+}) on the activity of P57 were evaluated by measuring the enzyme activity at 40°C and pH 8.0 after the enzyme was pre-incubated with each inhibitor or metal ion for 1 h at 4°C.

Substrate specificity of protease P57 was determined by measuring its activities toward casein, gelatin, collagen (Bovine-insoluble type I collagen fiber, Worthington Biochemical Corp., USA), elastin and synthetic peptides. The activities of protease P57 toward collagen and gelatin were measured by the method as described by Worthington Biochemical Corp. (Freehold, 1972). For collagen, the mixture of 1 mL enzyme solution (0.2 mg/mL) and 5 mg collagen was stirred at 37°C for 5 h. One unit is defined as the amount of enzyme that released 1 μmol leucine from collagen in 1 h. For gelatin, the mixture of 100 μL enzyme solution (0.04 mg/mL) and 100 μL of 2% (w/v) gelatin were incubated at 40°C for 10 min. One unit is defined as the amount of enzyme that released 1 μmol leucine from gelatin in 1 min. The activity of protease P57 toward elastin was assayed by the method of Chen et al. (2009). The activities of protease P57 toward synthetic peptides were determined in 20 mM phosphate buffer (pH 8.0) at 40°C according to Peek's method (Peek et al., 1993). One unit was defined as the amount of enzyme that catalyzed the formation of 1 μmol *p*-nitroaniline in 1 min (Chen et al., 2007). The synthetic peptides used as substrate (0.2%, w/v) were as follows, *N*-succinyl-Ala-Ala-Pro-Leu-*p*-nitroanilide (AAPL), *N*-succinyl-Ala-Ala-Pro-Phe-*p*-nitroanilide (AAPF), *N*-succinyl-Phe-Ala-Ala-Phe-*p*-nitroanilide (FAAF), *N*-succinyl-Ala-Ala-Pro-Arg-*p*-nitroanilide (AAPR), *N*-succinyl-Ala-Ala-Pro-Lys-*p*-nitroanilide (AAPK) and *N*-succinyl-Ala-Ala-Val-Ala-*p*-nitroanilide (AAVA). Protein concentrations were determined by the Bradford method (Bradford, 1976) with bovine serum albumin (BSA) as the standard.

Gene Cloning and Sequence Analysis of P57

Based on the N-terminal amino acid sequence of P57 and the conserved sequence of the catalytic center of serine proteases (Maciver et al., 1994), two degenerated primers (P57N and RM6) were designed (**Table 1**). With the degenerated primers and the genomic DNA of strain A5–7 as template, a part of the gene encoding P57 was amplified by PCR and sequenced at Shanghai Biosune Biotechnology Corp. (China). By using specific primers and general primers (**Table 1**), the neighboring sequences of the obtained gene fragment were amplified by thermal asymmetric interlaced PCR (TAIL-PCR) (Liu and Whittier, 1995). Through assembly, an entire gene sequence containing an ATG start codon and a TAA stop codon was obtained. Two specific primers (A5–7N and A5–7C) were designed (**Table 1**) according to this ORF, and the full gene encoding P57 was amplified by PCR from the genomic DNA of strain A5–7, and verified by sequencing. The gene sequence of P57 was deposited in GenBank database under the accession number KT923662.

The domain architectures of P57 were analyzed by the Conserved Domain Database (CDD) of NCBI[2] (Marchlerbauer et al., 2007). Homologous sequences to P57 were searched using the BLAST against NCBI nr database and the MEROPS database[3] (Rawlings et al., 2006) with default parameters. The representative homologs to P57 were aligned by using DNAMAN software.

Expression and Purification of the PA Domain and Its Site-directed Mutants

The DNA fragment encoding the PA domain of protease P57 with an overlapping sequence of EGFP was amplified by PCR using the genomic DNA of strain A5–7 as the template and two primers (PA-N, PA-GFP1) (**Table 1**). The DNA fragment encoding EGFP with the same overlapping sequence was also amplified by PCR using the vector p*EGFP-N1* (Clontech, USA) as the template and the primers PA-GFP2 and PA-GFP(C) (**Table 1**). The two fragments were concatenated by the overlapping extension PCR (Liu and Whittier, 1995). The chimeric gene was sub-cloned into the NdeI-XhoI site of pET-22b (+) to construct the expression vector pET-22b-*PA-EGFP*, which was then transformed into *E. coli* BL21 (DE3). The recombinant PA-EGFP was expressed as a C-terminal His_6-tagged protein. The transformant cells were cultivated in a 100 mL LB medium supplemented with 100 μg/mg ampicillin at 37°C and 180 rpm, until the absorbance at 600 nm reached 1.5. Then, isopropyl β-D-thiogalactopyranoside (IPTG) was added to a final concentration of 0.1 mM. After induction for 24 h at 15°C and 150 rpm, cells were harvested by centrifugation. Cell pellets were suspended in a 35 mL lysis buffer (50 mM Tris-HCl pH 9.0) and disrupted by sonication. After centrifugation at

[2]http://www.ncbi.nlm.nih.gov/Structure/cdd

[3]http://www.merops.ac.uk

TABLE 1 | Primers used in this study.

Gene	Primer type	Sequence
P57	Degenerated primers	P57N: 5′-TCCCAAAGCCTTCCNTGGGGNCA-3′
		RM6: 5′-GGNACNTCNATGGCNACNCC-3′
	5′-region specific primers	U1: 5′-TTACCGCTGAGATCGTTGTGTG-3′
		U2: 5′-CGTTGTGTGCAAGATCGTAGCCTG-3′
		U3: 5′-CAATGATACACACGGTGCGGTTAC-3′
	General primer	ADn: 5′-AAKYRTATG-3′
	3′-region specific primers	D1: 5′-GCAGCTACAACCTTGTTTCGG-3′
		D2: 5′-TGTTTCGGTATCTGTCGATCGCAC-3′
		D3: 5′-GCACCCTTGGTTTGGAACTGGC-3′
	General primer	ADc: 5′-GCAGCGTTA-3′
	Specific primers	A5-7N: 5′-TTCCATGAACAAGAACTATAAC-3′
		A5-7C: 5'-TTTAAAGTTGATACGCCAGC-3'
PA-EGFP	Overlapping primers	PA-N: 5′-CGCCATATGGATATTACCTTAGCAGGACAG-3′(NdeI)
		PA-GFP1: 5′-CTCCTCGCCCTTGCTCAC ACTATCGACAGTTATTG-3′
		PA-GFP2: 5′-AATAACTGTCGATAGTGTGAGCAAGGGCGAGGAG-3′
		PA-GFP(C): 5′-CGCGCTCGAGCTTGTACAGCTCGTCCATG-3′(XhoI)

Note, the underlined sequences indicate restricted enzyme sites.

4°C and 12,000 *g* for 30 min, the supernatant was collected and the recombinant PA-EGFP protein was purified with a HisBind metal chelating column.

Alignment of the PA domains from P57 and other reported S8 subtilases were performed by using Clustal W. The conserved aromatic residues and positively charged residues were chosen for mutagensis. Site-directed mutagenesis on the PA domain was carried out by overlapping extension PCR (An et al., 2005) using the vector pET-22b-*PA-EGFP* as template. Mutated sites were introduced by the primers with single-point mutations. The mutated genes were sub-cloned into pET-22b (+) and transformed into *E. coli* BL21 (DE3). All mutations were confirmed by enzyme digestion and nucleotide sequencing. The expression and purification of the mutants were performed under the same conditions as those of PA-EGFP.

Analysis of the Binding Ability of Wild P57, the PA Domain and Its Mutants to Bovine-Insoluble Type I Collagen Fiber

To analyze the binding ability of the PA domain and its mutants toward collagen, 5 mg collagen fibers were mixed with 500 μL PA-EGFP, EGFP or the mutants (0.5 mg/mL) in 50 mM Tris-HCl buffer (pH 8.0). The mixture was incubated at 37°C for 2 h, and then centrifuged at 12,000 *g* and 4°C for 10 min. The free fluorescence intensity in the supernatant before and after incubation was measured on a FP-6500 spectrofluorometer (Jasco, Japan). Fraction of fusion protein bound (%) = (B-A)/B*100%, B and A represent the free fluorescence intensity in the solution before and after a fusion protein binds to collagen, respectively.

The collagen-binding ability of wild P57 was assayed as described by Itoi et al. (2006). Purified P57 (0.2 mg/mL, 0.5 mL) in 20 mM Na_2HPO_4-NaH_2PO_4 (pH 7.0) containing 10 mM Fe^{3+} was incubated at 4°C for 1 h to inhibit the enzyme activity. Then collagen fibers (1, 5, or 10 mg) was added and the mixture was incubated at 37°C for 2 h with stirring. After incubation, the mixture was centrifuged for 10 min at 12,000 *g* and 4°C. The supernatant was analyzed by 12.5% SDS-PAGE. BSA as a negative control was treated as P57.

Analysis of the PA Domain and Its Mutants by Circular Dichroism

Circular dichroism (CD) spectra of the purified PA-EGFP and its mutants F349A-EGFP and Y432A-EGFP in 50 mM Tris-HCl buffer (0.1 mg/mL) were measured on a Jasco J810 spectropolarimeter (Japan) according to the method described by Zhao et al. (2008).

RESULTS

Phylogenetic Analysis of Strain A5–7

Strain A5–7 was isolated from marine sediment collected from A5 station in Jiaozhou Bay, China, and the nearly complete 16S rRNA gene sequence (1536 bp) of the strain was determined. Sequence comparison showed that strain A5–7 shared the highest 16S rRNA gene sequence identities with known *Photobacterium* species, suggesting an affiliation with the genus *Photobacterium*. In the neighbor-joining and maximum-likelihood trees (**Figures 1A,B**) based on the 16S rRNA gene sequences, strain A5–7 fell within the clade of the genus *Photobacterium* and formed a distinct intra-branch with type strain of *Photobacterium aplysiae* supported by high bootstrap values (>85%), indicating its close phylogenetic relationship to the latter. However, considering that strain A5–7 has only 96.8% 16S rRNA gene sequence identity to the type strain of *P. aplysiae*, strain A5–7 may represent a potential new species of the genus *Photobacterium,* which merits further study.

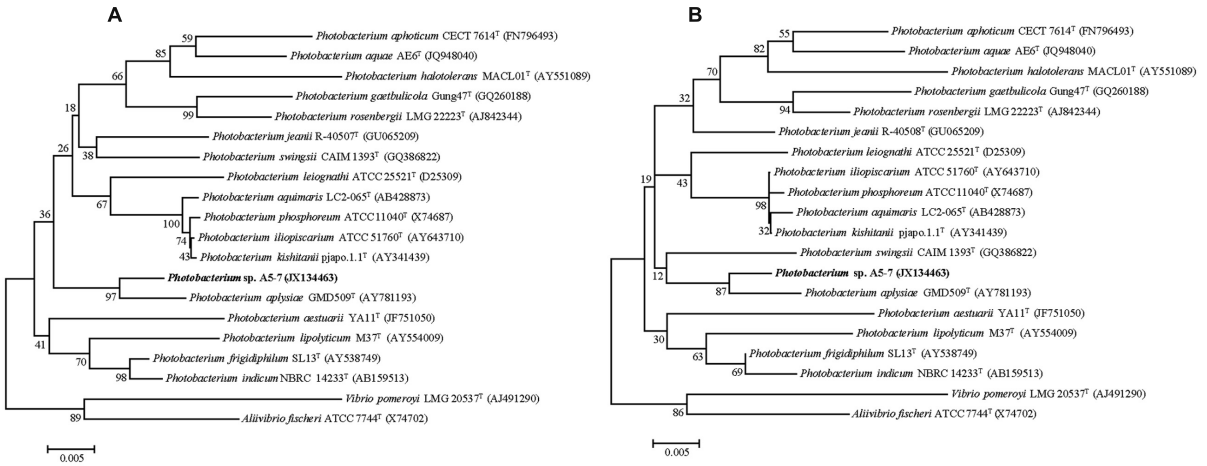

FIGURE 1 | Neighbor-joining (A) and Maximum-likelihood **(B)** phylogenetic trees based on the 16S rRNA gene sequences of strain A5–7 and type strains of species from the *Photobacterium* genus and other related genera. Bootstrap percentages from 1,000 replicates are indicated at nodes. Bar, 0.005 substitutions per nucleotide position.

Purification and Characterization of Protease P57 Secreted by *Photobacterium* sp. A5–7

A protease was purified from the culture of strain A5–7 by anion exchange chromatography with a yield of 15.9%. SDS-PAGE analysis showed that the purified protease had high purity, with an apparent molecular mass of approximately 45 kDa (**Figure 2A**). This protease was named P57 in this study.

With casein as substrate, the optimum temperature of P57 was 40°C, and 10% of the maximum activity was retained at 0°C (**Figure 2B**). P57 was stable at 30°C for at least 1 h, but unstable at temperatures higher than 30°C. The half time of its activity at 40°C and 45°C was 40 min and 7 min, respectively (**Figure 2C**). P57 was active in a wide range of pH from 5.0 to 11.0, with the maximum activity at pH 8.0 (**Figure 2D**). In the buffers containing 0–3 M NaCl, the activity of P57 peaked at 0.25 M NaCl, then declined with the increase of NaCl concentration, but still retained 50% of the maximum activity at 1.5 M NaCl (**Figure 2E**).

Effects of metal ions and inhibitors on P57 activity were shown in **Table 2**. P57 activity was not affected by Li^+, K^+, Ba^{2+}, Co^{2+}, or Sr^{2+}. At the final concentration of 8 mM, Cu^{2+}, Zn^{2+}, and Ni^{2+} obviously inhibited P57 activity, and Fe^{3+} severely inhibited P57 activity by 96.4%. While Ca^{2+} and Mg^{2+} slightly activated the enzyme activity, Mn^{2+} significantly increased P57 activity to 194.1%, showing an activating effect on P57 activity. In addition, P57 activity was strongly inhibited by PMSF, a serine protease inhibitor, indicating that P57 is likely a serine protease. The activity of P57 was also inhibited by metal chelators EDTA and EGTA, but not affected by *o*-P or IA.

Substrate specificity analysis showed that P57 could hydrolyze casein, gelatin and collagen, with the highest activity toward gelatin, the degenerated form of collagen (**Table 3**). P57 showed no activity toward elastin. Among the synthetic peptides, P57 had higher activities toward AAPL and AAPF and lower activities toward FAAF, AAPR, AAPK and AAVA (**Table 3**).

Gene Cloning and Sequence Analysis of P57

The N-terminal sequence of mature P57 was determined by protein sequencing to be Ser-Gln-Ser-Leu-Pro-Trp-Gly-Gln-Thr-Phe-Val-Gly-Ala-Thr-Leu, which shows identities to some serine proteases of the S8 family, such as SapSh (66.7%) from *Shewanella* sp. Ac10 (Kulakova et al., 1999), Apa1 (66.7%) from *Pseudoalteromonas* sp. AS-11 (Dong et al., 2001), VapT (40%) from *V. metschnikovii* RH530 (Kwon et al., 1995) and AcpII (40%) from *A. collagenimarina* AC40 (Kurata et al., 2010). This suggests that P57 is a serine protease of the S8 family. Based on the N-terminal amino acid sequence of P57 and the highly conserved sequence of the catalytic domains of the S8 serine proteases, the gene encoding protease P57 was cloned from the genomic DNA of strain A5–7 by a combination of PCR and TAIL-PCR.

The ORF of *P57* is 2,037 bp in length, including an ATG start codon and a TAA stop codon. It encodes a protein of 678 amino acid residues with a calculated molecular weight of 71,788 Da. According to BLAST analysis against CDD database (Marchlerbauer et al., 2007), the precursor of P57 contains an N-terminal pre-sequence (Met1-Leu123), an S8 catalytic domain (Asn146-Ala565), a PA domain (Asp340-Ser479) inserted in the catalytic domain, a linker (Glu566-Leu599) and a C-terminal P-proprotein (Thr600-Lys678) (**Figure 3A**). SignalP 3.0 (Bendtsen et al., 2004) prediction suggested that the pre-sequence of P57 contains an N-terminal signal peptide sequence (Met1-Ala29). According to the result of N-terminal sequencing, the first N-terminal residue of mature P57 is Ser124. The molecular mass of mature P57 was determined to be 46,016 Da by MALDI-TOF mass spectrometry. Thus, based on the sequence and the molecular mass of P57, it was

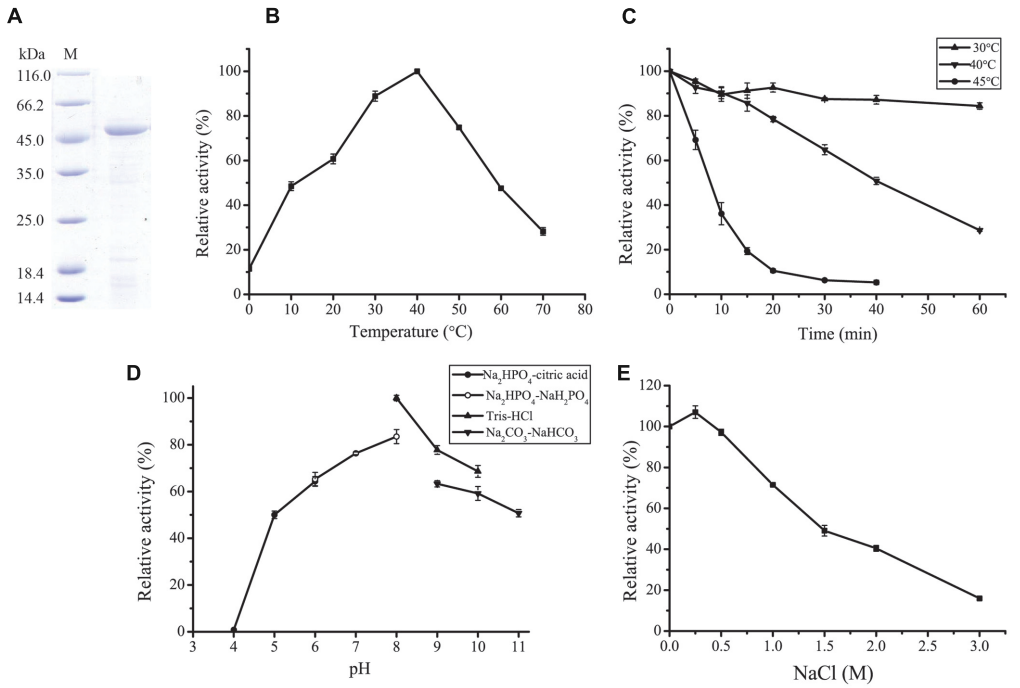

FIGURE 2 | Purification and characterization of P57. (A) SDS-PAGE analysis of the purified P57. M, protein molecular mass marker; Lane 1, the purified P57. **(B)** Effect of temperature on P57 activity. Enzyme activity was measured at 0–70°C in 20 mM phosphate buffer (pH 7.0). **(C)** Thermostability of P57. The enzyme was incubated at 30°C, 40°C, or 45°C for different time periods, and then residual activity was measured at 40°C. **(D)** Effect of pH on the activity of P57. Enzyme activity was measured at 40°C in different pH buffers (20 mM): Na_2HPO_4-citric acid (pH 4.0–6.0), Na_2HPO_4-NaH_2PO_4 (pH 6.0–8.0), Tris-HCl (pH 8.0–10.0), and Na_2CO_3-$NaHCO_3$ (pH 9.0–11.0). **(E)** Effect of NaCl on the activity of P57. Enzyme activity was measured at 40°C in different concentrations of NaCl. The graph shows data from triplicate experiments (mean ± SD).

TABLE 2 | Effects of metal ions and inhibitors on the activity of protease P57.

Metal ions	Relative activity (%)		Metal ions	Relative activity (%)		Inhibitor	Residual activity (%)
	2 mM[b]	8 mM[b]		2 mM[b]	8 mM[b]		
Control[a]	100	100				Control[a]	100
K^+	92.8 ± 1.5	95.4 ± 3.2	Mg^{2+}	98.4 ± 3.5	107.6 ± 0.4*	PMSF (1 mM[c])	2.8 ± 0.1
Li^+	99.4 ± 1.4	87.7 ± 3.0	Mn^{2+}	142.1 ± 5.1*	194.1 ± 2.1**	EDTA (1 mM[c])	11.6 ± 1.8
Ba^{2+}	101.0 ± 2.0	97.5 ± 1.3	Ni^{2+}	80.6 ± 2.7*	76.1 ± 1.5**	EGTA (1 mM[c])	17.9 ± 1.3
Ca^{2+}	92.2 ± 1.1	110.4 ± 2.1*	Sr^{2+}	97.8 ± 1.6	102.3 ± 1.9	*o*-P (5 mM[c])	79.4 ± 1.8
Co^{2+}	102.8 ± 1.3	99.0 ± 3.3	Zn^{2+}	102.3 ± 2.2	67.1 ± 1.3**	IA (5 mM[c])	82.7 ± 2.5
Cu^{2+}	103.6 ± 1.8	62.2 ± 2.1**	Fe^{3+}	99.8 ± 2.9	3.6 ± 0.3**		

[a] *The activity of P57 without any metal ion or inhibitor was taken as control.* [b] *The final concentration of metal ion in the reaction mixture.* [c] *The final concentration of inhibitor in the reaction mixture.*

**, ** stand for different significance at $p < 0.05$ and $p < 0.01$, respectively. The data shown are the means of three repeats with standard deviations. PMSF, phenylmethylsulfonyl fluoride; EDTA, ethylene diamine tetraacetic acid; EGTA, ethylene glycol tetraacetic acid; o-P, o-phenanthroline; IA, iodoacetic acid.*

predicted that mature P57 contains 442 residues from Ser124 to Ala565. Therefore, both the N-terminal pre-sequence and the C-terminal *P*-proprotein are cleaved off during enzyme maturation, and mature P57 only contains the catalytic domain and the inserted PA domain (**Figure 3A**). Multiple sequence alignment suggests that the catalytic triad of P57 is composed of Asp153, His188 and Ser492 (**Figure 3B**). The highest sequence identity of P57 with reported S8 serine proteases is 63% according to BLASTP analysis against NCBI non-redundant protein database.

Collagen Binding Ability of the PA Domain

To study the function of the PA domain in P57 catalysis, the PA domain fused with EGFP (PA-EGFP) was expressed in *E. coli* BL21 (DE3), and purified by HisBind metal chelating column with a yield of 51.7%. Because P57 could hydrolyze insoluble collagen, we investigated the binding ability of the recombinant PA domain to insoluble collagen by fluorescence analysis. After PA-EGFP was mixed with insoluble collagen fibers for 2 h at 37°C,

TABLE 3 | Substrate specificity of P57 toward various proteins and synthetic peptides[a].

Substrate	Specific activity (U/mg)	Substrate	Specific activity (U/mg)
Casein	2,460.42 ± 62.68	AAPL	3.84 ± 0.06
Gelatin	15,878.57 ± 202.51	AAPF	3.29 ± 0.15
Collagen	298.13 ± 58.31	FAAF	1.96 ± 0.05
Elastin	–	AAPR	1.75 ± 0.02
		AAPK	0.75 ± 0.01
		AAVA	0.70 ± 0.02

[a]*The data shown are the means of three repeats with standard deviations. –, No detectable activity. AAPL, N-succinyl-Ala-Ala-Pro-Leu-p-nitroanilide; AAPF, N-succinyl-Ala-Ala-Pro-Phe-p-nitroanilide; FAAF, N-succinyl-Phe-Ala-Ala-Phe-p-nitroanilide; AAPR, N-succinyl-Ala-Ala-Pro-Arg-p-nitroanilide; AAPK, N-succinyl-Ala-Ala-Pro-Lys-p-nitroanilide; AAVA, N-succinyl-Ala-Ala-Val-Ala-p-nitroanilide.*

the precipitated collagen fibers displayed a bright green color, whereas the collagen fibers mixed with EGFP still displayed its own white color (**Figure 4A**). This result suggests that the PA domain of P57 has collagen-binding ability. To further confirm this, we quantified the fluorescence intensity changes of the supernatant with different amounts of collagen in the mixture. As shown in **Figure 4B**, the fluorescence intensity in the supernatant decreased from 500 to 360 with the increase of collagen amount from 0 to 10 mg in the mixture, which indicated that the amount of PA-EGFP bound to collagen fibers increased with the increase of collagen amount in the mixture, thereby leading to a successive decrease of PA-EGFP amount in the solution. Taken together, these results indicate that the PA domain of P57 has collagen-binding ability, implying that the PA domain in P57 may be involved in substrate binding in the catalysis of P57 toward collagen.

In addition, to estimate the contribution of the PA domain to the interaction of P57 with collagen, the collagen-binding ability of P57 was assayed after the enzyme activity was inhibited by 10 mM Fe^{3+}. As shown in **Figure 4C**, after P57 was incubated with collagen at 37°C for 2 h in the presence of 10 mM Fe^{3+}, the amount of P57 protein in the supernatant significantly decreased, whereas the amount of BSA in the supernatant showed little change after incubation with collagen (**Figure 4C**). This result indicated that P57 can bind to collagen at 37°C. The PA domains probably play an important role in the interaction of P57 with collagen because it has collagen-binding ability (**Figures 4A,B**).

Key Residues for Collagen Binding in the PA Domain

To determine the key amino acid residues in the PA domain of P57 for collagen binding, site-directed mutagenesis was performed. It has been reported that aromatic residues and charged residues usually play a key role in the binding of binding domains to insoluble substrates (Bhaskaran et al., 2008; Philominathan et al., 2009). Based on sequence alignment of the PA domains from P57 and other reported proteases (**Figure 3B**), conserved aromatic residues (Phe349, Tyr412, Tyr432, Phe444 and Tyr452) and conserved positively charged residues (Lys397, Arg403 and Lys419) in the PA domain of P57 were mutated to Ala, and all the mutants were expressed as EGFP-fused proteins. The mutants R403A-EGFP and F444A-EGFP could not be expressed as soluble proteins, probably because these two residues are important for the correct folding of the proteins. The binding abilities of the mutants to collagen were measured and compared with that of PA-EGFP. While the collagen-binding abilities of mutants K397A-EGFP, Y412A-EGFP, K419A-EGFP and Y452A-EGFP were partly reduced, the collagen-binding abilities of mutants F349A-EGFP and Y432A-EGFP were severely destroyed, implying that Phe349 and Tyr432 may be essential for the PA domain to bind collagen (**Figure 5A**). In addition, CD spectra of PA-EGFP, F349A-EGFP and Y432A-EGFP were collected to analyze the structural changes that residue substitution mutation may cause in the mutants. There were few differences in the spectra of PA-EGFP, F349A-EGFP and Y432A-EGFP (**Figure 5B**), suggesting that the loss of the collagen-binding ability of F349A-EGFP and Y432A-EGFP should be caused by amino acid substitution. Altogether, these data indicate that Phe349 and Tyr432 are likely two key residues for collagen binding in the PA domain of P57. The data also suggest that hydrophobic interactions likely play an important role in the binding of the PA domain to collagen because Phe349 and Tyr432 are both aromatic amino acids.

DISCUSSION

In this study, the extracellular protease P57 from *Photobacterium* sp. A5–7 isolated from the sea sediment of Jiaozhou Bay in China was characterized. P57 is a serine protease of the S8 family. Among reported S8 serine proteases, P57 has the highest identity (63%) to VapT from *V. metschnikovii* RH530 (Kwon et al., 1995), which suggests that P57 is a new member of the S8 family. Although the precursor of P57 contains an N-terminal pre-sequence, an S8 catalytic domain, a PA domain and a C-terminal *P*-proprotein domain, mature P57 only contains the catalytic domain and the PA domain that is inserted in the catalytic domain. The N-terminal pre-sequence, which is required for protease folding and secretion (Chen and Inouye, 2008), and the C-terminal *P*-proprotein domain, which is also important in enzyme secretion through the cell membrane (Kurata et al., 2007), are all cleaved off during P57 maturation.

Our results show that P57 is a subtilase with an inserted PA domain in its catalytic domain. Some subtilases with an inserted PA domain in the catalytic domain have been reported from plants and bacteria, and structural and deletion mutational analyses have suggested that the PA domains in some subtilases are involved in substrate binding. For example, the crystal structures of C5a peptidases from *S. agalactiae* and *S. pyogenes* show that the PA domain is located near the active-site cleft of the catalytic domain (Brown et al., 2005; Kagawa et al., 2009). Three out of four residues that form the S4 subsite belong to the PA domain in soybean protease C1 (Tan-Wilson et al., 2012). Cleavage specificity toward natural casein substrate was

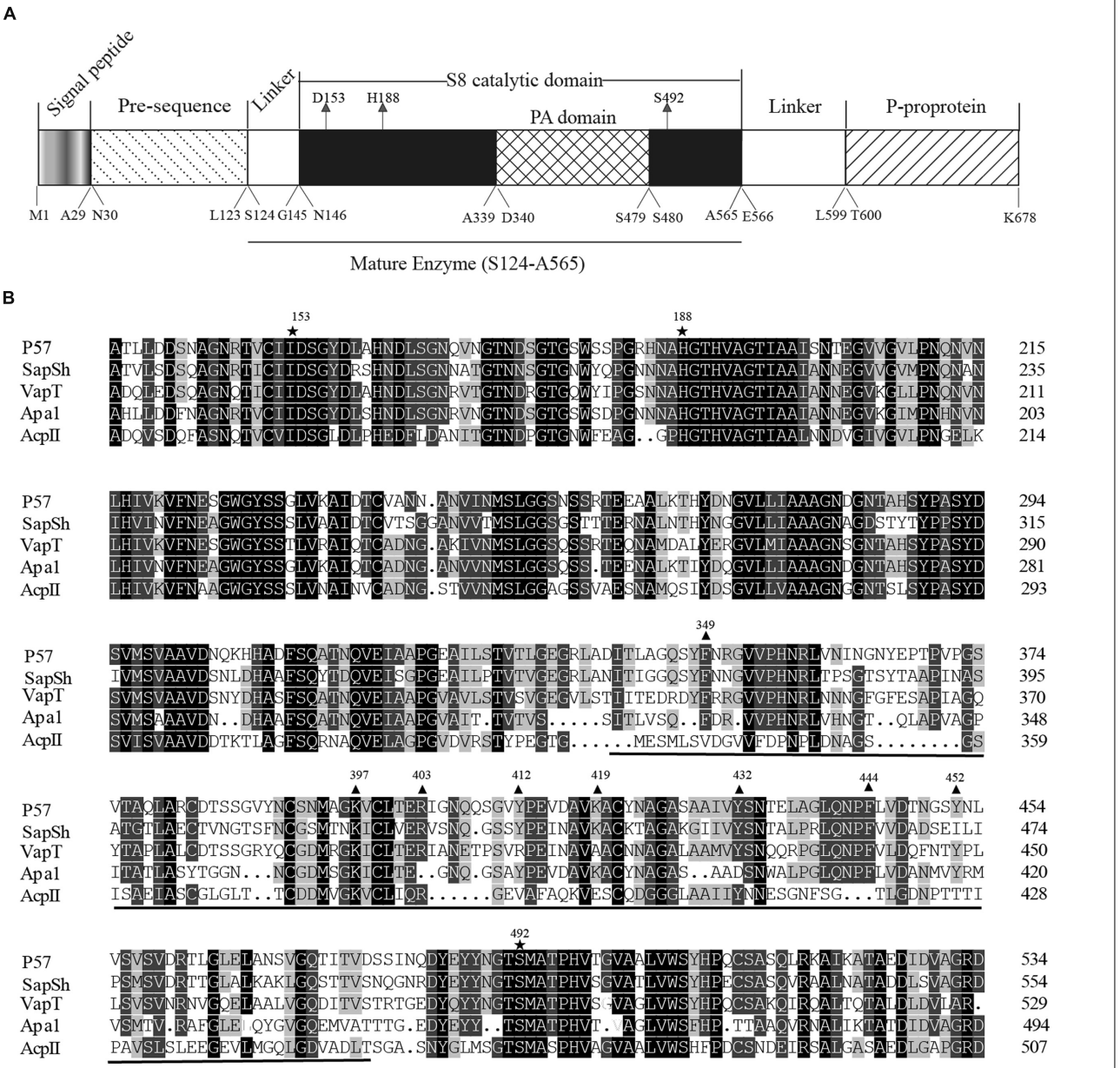

FIGURE 3 | Sequence analysis of protease P57. (A) The diagram of conserved domains of P57 based on BLAST analysis against Conserved Domain Database. **(B)** Sequence alignment of the catalytic domains of P57 and other reported S8 subtilases with a PA domain. Catalytic residues are indicated with "★", and the PA domain is underlined. Identical residues are shaded in black. Conserved amino acid residues indicated with "▲" are the residues chosen for site-directed mutations to determine the key residues for collagen binding in the PA domain. P57, from *Photobacterium*. sp. A5–7 in this study (KT923662); SapSh, from *Shewanella* sp. Ac10^T (AAC04871) (Kulakova et al., 1999); VapT, from *Vibrio metschnikovii* strain RH530^T (CAA82213) (Kwon et al., 1995); Apa1, from *Pseudoalteromonas* sp. AS-11^T (AB120714) (Dong et al., 2001); AcpII, from *Alkalimonas collagenimarina* AC40^T (BAI50017) (Kurata et al., 2010).

changed in PrtP from *Lactococcus lactis* without the PA domain (Bruinenberg et al., 1994). The activity of AcpII-ΔPA toward gelatin, casein and collagen was remarkably increased (Kurata et al., 2010). Despite these structural and deletion mutational analyses, there is no direct evidence that the PA domain from a subtilase has substrate-binding ability. In this study, the results showed that the PA domain from the subtilase P57 had collagen-binding ability, and that residues Phe349 and Tyr432 are two key residues responsible for collagen binding in the PA domain, showing direct evidence that the PA domain of a subtilase has substrate-binding ability. These results also suggest that the function of the PA domain in P57 is most likely to participate in the binding of insoluble substrate such as collagen during P57 catalysis.

While most subtilases have no collagenolytic activity, some subtilases have been reported to be serine collagenolytic

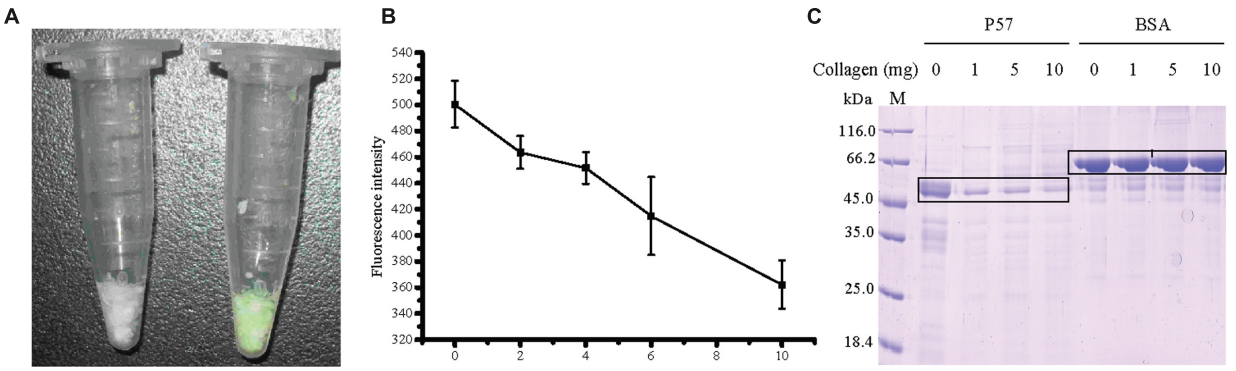

FIGURE 4 | Analysis of the collagen-binding ability of the recombinant PA domain. (A) The binding ability of EGFP (left tube) and PA-EGFP (right tube) on bovine-insoluble type I collagen. After the mixture of EGFP or PA-EGFP with 5 mg collagen was incubated at 37°C for 2 h with agitating and subsequently centrifuged, the precipitated collagen fibers were washed two times with distilled water. **(B)** Fluorescence analysis of the collagen-binding ability of the PA domain. The fusion protein PA-EGFP was incubated with various amounts of collagen at 37°C for 2 h. After centrifugation, the fluorescence intensities of the supernatants were determined at 510 nm. PA-EGFP incubated with no collagen at the same conditions was served as control. The graph shows data from triplicate experiments (mean ± SD). **(C)** SDS-PAGE analysis of the binding ability of P57 to bovine insoluble type I collagen in the presence of 10 mM Fe^{3+}. P57 in 20 mM Na_2HPO_4-NaH_2PO_4 (pH 7.0) containing 10 mM Fe^{3+} was incubated at 4°C for 1 h to inhibit the enzyme activity, and then was mixed with 0, 1, 5, or 10 mg collagen. The mixtures were incubated at 37°C for 2 h, and the unbound P57 fractions in the mixtures were analyzed by 12.5% SDS-PAGE. BSA was used as a negative control. M, protein molecular mass marker.

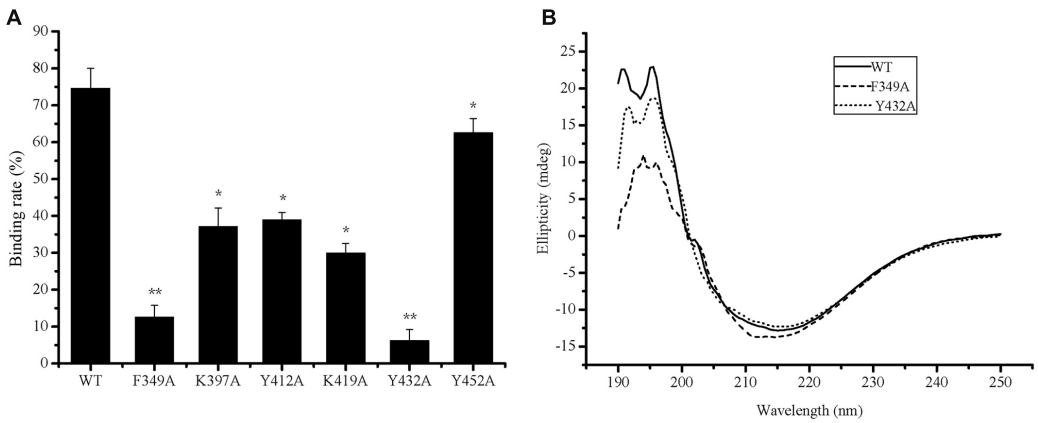

FIGURE 5 | Collagen-binding affinity and circular dichroism spectra of PA-EGFP and its mutants. (A) The collagen-binding affinity of PA-EGFP (WT) and its mutants. The graph shows data from triplicate experiments (mean ± SD). *, ** stand for different significance at $p < 0.05$ and $p < 0.01$, respectively. **(B)** Circular dichroism spectra of PA-EGFP (WT) and its mutants F349A-EGFP (F349A) and Y432A-EGFP (Y432A).

proteases that can degrade insoluble collagen, such as MCP-01 from *Pseudoalteromonas* sp. SM9913 (Zhao et al., 2008; Ran et al., 2013), the thermostable protease from *Geobacillus collagenovorans* MO-1 (Okamoto et al., 2001), AcpII from *Alkalimonas collagenimarina* AC40 (Kurata et al., 2010), and myroicolsin from *Myroides profundi* D25 (Ran et al., 2014). P57 has collagenolytic activity and its PA domain has collagen-binding ability, indicating that P57 is an S8 serine collagenolytic protease. Subtilases, such as SapSh (Kulakova et al., 1999), VapT (Kwon et al., 1995) and AcpII (Kurata et al., 2010), usually have activity toward synthetic peptides AAPL and AAPF. Consistent with this, P57 has obvious activity toward these two peptides. Metal ions have different effects on the activity of different enzymes. It was reported that Ca^{2+} could increase the enzyme activity or the thermal stability of some subtilases (Kurata et al., 2007, 2010; Zhao et al., 2008; Ran et al., 2014). However, Ca^{2+} only had a little effect on P57 activity. Previous reports showed that Mn^{2+} did not affect the enzyme activity of subtilase significantly (Kurata et al., 2007) or slightly inhibited the enzyme activity of subtilase (Zhao et al., 2008; Ran et al., 2014). Our result showed that 8 mM Mn^{2+} significantly increased P57 activity. EDTA and EGTA are ion chelators, which usually inactivate subtilase that contains metal ion and/or lower their stability by depriving the metal ion (Kurata et al., 2010). The activity of P57 was significantly reduced by EDTA and EGTA, implying that P57 may contain metal ion.

Extracellular proteases from marine sedimentary bacteria usually have some environment-adapted characters, including

cold-adaptation, salt tolerance/activation, and an optimal pH equal or near that of seawater, such as proteases MCP-01 and MCP-03 from *Pseudoalteromonas* sp. SM9913 (Chen et al., 2003; Zhao et al., 2008; Yan et al., 2009) and pseudoalterin from *Pseudoalteromonas* sp. CF6-2 (Zhao et al., 2012). Consistent with this, P57 also shows some characters adapted to marine sediment environment. *Photobacterium* sp. A5–7 was isolated from a marine sediment sample from the A5 station site in Jiaozhou Bay, China, where the depth, temperature, pH and C/N ration were 5.9 m, 24.7°C, 8.11 and 7.0, respectively (Zhang et al., 2015). P57 had low optimal temperature (40°C), and low thermostability at moderate temperatures (unstable at temperatures higher than 30°C), and displayed high activity at alkaline pH (pH 7.0–9.0) with the optimum pH of 8.0. P57 showed the highest activity at 0.25 M NaCl, and retained 50% of the maximum activity at 1.5 M NaCl. These characters reflect the adaptation of P57 to the marine sedimentary environment. Extracellular proteases of marine sedimentary bacteria play important roles in PON degradation and nitrogen cycling in marine sediments. As a bacterial extracellular protease from marine sediment can degrade proteins and peptides, P57 should be actively involved in sedimentary PON degradation.

In summary, protease P57 secreted by marine sedimentary *Photobacterium* sp. A5–7 was characterized in this study. P57 is a new S8 subtilase that can degrade casein, collagen and gelatin. P57 has a PA domain inserted in its catalytic domain. The PA domain from P57 has collagen-binding ability, which represents the first direct evidence that the PA domain of a subtilase has substrate-binding ability. Phe349 and Tyr432 were further revealed to be key residues responsible for collagen binding in the PA domain of P57 by site-directed mutational analysis. Our results provide more insight into the function of PA domain of subtilases and shed light on marine sedimentary bacterial proteases and PON degradation.

AUTHOR CONTRIBUTIONS

H-JL, B-LT, and X-XH performed the biochemical experiments. XS, B-XL, and X-YZ helped in protein purification. X-LC designed and directed the research. H-JL and X-LC wrote the manuscript. P-YL and X-YZ helped in data analysis and manuscript editing.

ACKNOWLEDGMENTS

This work was supported by the National Science Foundation of China (31290230, 31290231, 91228210, 41276149, 31270117, 31270064), the Hi-Tech Research and Development Program of China (2014AA093509), and the Fundamental Research Funds of Shandong University (2014QY006).

REFERENCES

Altschul, S. F., Madden, T. L., Schäffer, A. A., Zhang, J. H., Zhang, Z., Miller, W., et al. (1997). Gapped BLAST and PSI-BLAST: a new generation of protein database search programs. *Nucleic Acids Res.* 25, 3389–3402. doi: 10.1093/nar/25.17.3389

Aluwihare, L. I., Repeta, D. J., Pantoja, S., and Johnson, C. G. (2005). Two chemically distinct pools of organic nitrogen accumulate in the ocean. *Science* 308, 1007–1010. doi: 10.1126/science.1108925

An, Y., Ji, J., Wu, W., Lv, A., Huang, R., and Wei, Y. (2005). A rapid and efficient method for multiple-site mutagenesis with a modified overlap extension PCR. *Appl. Microbiol. Biotechnol.* 68, 774–778. doi: 10.1007/s00253-005-1948-8

Bendtsen, J. D., Nielsen, H., von Heijne, G., and Brunak, S. (2004). Improved prediction of signal peptides: signalP 3.0. *J. Mol. Biol.* 340, 783–795. doi: 10.1016/j.jmb.2004.05.028

Bhaskaran, R., Palmier, M. O., Lauer-Fields, J. L., Fields, G. B., and Van Doren, S. R. (2008). MMP-12 catalytic domain recognizes triple helical peptide models of collagen V with exosites and high activity. *J. Biol. Chem.* 283, 21779–21788. doi: 10.1074/jbc.M709966200

Bradford, M. M. (1976). A rapid and sensitive method for the quantitation of microgram quantities of protein utilizing the principle of protein-dye binding. *Anal. Biochem.* 72, 248–254. doi: 10.1016/0003-2697(76)90527-3

Brown, C. K., Gu, Z. Y., Matsuka, Y. V., Purushothaman, S. S., Winter, L. A., Cleary, P. P., et al. (2005). Structure of the streptococcal cell wall C5a peptidase. *Proc. Natl. Acad. Sci. U.S.A.* 102, 18391–18396. doi: 10.1073/pnas.0504954102

Bruinenberg, P. G., Doesburg, P., Alting, A. C., Exterkate, F. A., de Vos, W. M., and Siezen, R. J. (1994). Evidence for a large dispensable segment in the subtilisin-like catalytic domain of the Lactococcus lactis cell-envelope proteinase. *Protein Eng.* 7, 991–996. doi: 10.1093/protein/7.8.991

Brunnegård, J., Grandel, S., Ståhl, H., Tengberg, A., and Hall, P. O. J. (2004). Nitrogen cycling in deep-sea sediments of the Porcupine Abyssal Plain, NE Atlantic. *Prog. Oceanogr.* 63, 159–181. doi: 10.1016/j.pocean.2004.09.004

Cedzich, A., Huttenlocher, F., Kuhn, B. M., Pfannstiel, J., Gabler, L., Stintzi, A., et al. (2009). The protease-associated domain and C-terminal extension are required for zymogen processing, sorting within the secretory pathway, and activity of tomato subtilase 3 (SlSBT3). *J. Biol. Chem.* 284, 14068–14078. doi: 10.1074/jbc.M900370200

Chen, X. L., Xie, B. B., Bian, F., Zhao, G. Y., Zhao, H. L., He, H. L., et al. (2009). Ecological function of myroilysin, a novel bacterial M12 metalloprotease with elastinolytic activity and a synergistic role in collagen hydrolysis, in biodegradation of deep-sea high-molecular-weight organic nitrogen. *Appl. Environ. Microbiol.* 75, 1838–1844. doi: 10.1128/AEM.02285-08

Chen, X. L., Xie, B. B., Lu, J. T., He, H. L., and Zhang, Y. Z. (2007). A novel type of subtilase from the psychrotolerant bacterium *Pseudoalteromonas* sp. SM9913: catalytic and structural properties of deseasin MCP-01. *Microbiology* 153, 2116–2125. doi: 10.1099/mic.0.2007/006056-0

Chen, X. L., Zhang, Y. Z., Gao, P. J., and Luan, X. W. (2003). Two different proteases produced by a deep-sea psychrotrophic bacterial strain, *Pseudoalteromonas* sp. *SM*9913. *Mar. Biol.* 143, 989–993. doi: 10.1007/s00227-003-1128-2

Chen, Y. J., and Inouye, M. (2008). The intramolecular chaperone-mediated protein folding. *Curr. Opin. Struct. Biol.* 18, 765–770. doi: 10.1016/j.sbi.2008.10.005

Dong, D., Ihara, T., Motoshima, H., and Watanabe, K. (2001). Crystallization and preliminary X-ray crystallographic studies of a psychrophilic subtilisin-like protease Apa1 from antarctic *Pseudoalteromonas* sp. strain AS-11. *Acta Crystallogr.* 61(Pt 3), 308–311.

Felsenstein, J. (1981). Evolutionary trees from DNA sequences: a maximum likelihood approach. *J. Mol. Evol.* 17, 368–376. doi: 10.1007/BF01734359

Freehold, N. J. (1972). *Worthington Enzyme Manual*. Lakewood, CA: Worthington Biochemical Corporation, 43–45.

Itoi, Y., Horinaka, M., Tsujimoto, Y., Matsui, H., and Watanabe, K. (2006). Characteristic features in the structure and collagen-binding ability of a thermophilic collagenolytic protease from the thermophile *Geobacillus collagenovorans* MO-1. *J. Bacteriol.* 188, 6572–6579. doi: 10.1128/JB.00767-06

Jukes, T. H., and Cantor, C. R. (1969). "Evolution of protein molecules," in *Mammalian Protein Metabolism*, Vol. 3, ed. H. N. Munro (New York, NY: Academic Press), 21–132.

Kagawa, T. F., O'Connell, M. R., Mouat, P., Paoli, M., O'Toole, P. W., and Cooney, J. C. (2009). Model for substrate interactions in C5a peptidase from

Streptococcus pyogenes: a 1.9 Å crystal structure of the active form of ScpA. *J. Mol. Biol.* 386, 754–772. doi: 10.1016/j.jmb.2008.12.074

Kim, O. S., Cho, Y. J., Lee, K., Yoon, S. H., Kim, M., Na, H., et al. (2012). Introducing EzTaxon-e: a prokaryotic 16S rRNA gene sequence database with phylotypes that represent uncultured species. *Int. J. Syst. Evol. Microbiol.* 62, 716–721. doi: 10.1099/ijs.0.038075-0

Kulakova, L., Galkin, A., Kurihara, T., Yoshimura, T., and Esaki, N. (1999). Cold-active serine alkaline protease from the psychrotrophic bacterium *Shewanella* strain Ac10: gene cloning and enzyme purification and characterization. *Appl. Environ. Microbiol.* 65, 611–617.

Kurata, A., Uchimura, K., Kobayashi, T., and Horikoshi, K. (2010). Collagenolytic subtilisin-like protease from the deep-sea bacterium *Alkalimonas collagenimarina* AC40T. *Appl. Microbiol. Biotechnol.* 86, 589–598. doi: 10.1007/s00253-009-2324-x

Kurata, A., Uchimura, K., Shimamura, S., Kobayashi, T., and Horikoshi, K. (2007). Nucleotide and deduced amino acid sequences of a subtilisin-like serine protease from a deep-sea bacterium, *Alkalimonas collagenimarina* AC40T. *Appl. Microbiol. Biotechnol.* 77, 311–319. doi: 10.1007/s00253-007-1164-9

Kwon, Y. T., Kim, J. O., Moon, S. Y., Yoo, Y. D., and Rho, H. M. (1995). Cloning and characterization of the gene encoding an extracellular alkaline serine protease from *Vibrio metschnikovii* strain RH530. *Gene* 152, 59–63. doi: 10.1016/0378-1119(94)00648-C

Lane, D. J. (1991). "16S/23S rRNA sequencing," in *Nucleic Acid Techniques in Bacterial Systematics*, eds E. Stackebrandt and M. Goodfellow (Chichester: John Wiley and Sons), 115–175.

Liu, Y. G., and Whittier, R. F. (1995). Thermal asymmetric interlaced PCR: automatable amplification and sequencing of insert end fragments from P1 and YAC clones for chromosome walking. *Genomics* 25, 674–681. doi: 10.1016/0888-7543(95)80010-J

Maciver, B., Mchale, R. H., Saul, D. J., and Bergquist, P. L. (1994). Cloning and sequencing of a serine proteinase gene from a thermophilic *Bacillus* species and its expression in *Escherichia coli*. *Appl. Environ. Microbiol.* 60, 3981–3988.

Marchlerbauer, A., Anderson, J. B., Derbyshire, M. K., Deweesescott, C., Gonzales, N. R., Gwadz, M., et al. (2007). CDD: a conserved domain database for interactive domain family analysis. *Nucleic Acids Res.* 35, 237–240. doi: 10.1093/nar/gkl951

Okamoto, M., Yonejima, Y., Tsujimoto, Y., Suzuki, Y., and Watanabe, K. (2001). A thermostable collagenolytic protease with a very large molecular mass produced by thermophilic *Bacillus* sp. strain MO-1. *Appl. Microbiol. Biotechnol.* 57, 103–108. doi: 10.1007/s002530100731

Olivera, N. L., Sequeiros, C., and Nievas, M. L. (2007). Diversity and enzyme properties of protease-producing bacteria isolated from sub-Antarctic sediments of Isla de Los Estados, Argentina. *Extremophiles* 11, 517–526. doi: 10.1007/s00792-007-0064-3

Ottmann, C., Rose, R., Huttenlocher, F., Cedzich, A., Hauske, P., Kaiser, M., et al. (2009). Structural basis for Ca2+-independence and activation by homodimerization of tomato subtilase 3. *Proc. Natl. Acad. Sci. U.S.A.* 106, 17223–17228. doi: 10.1073/pnas.0907587106

Peek, K., Veitch, D. P., Prescott, M., Daniel, R. M., Maciver, B., and Bergquist, P. L. (1993). Some characteristics of a proteinase from a thermophilic *Bacillus* sp. expressed in *Escherichia coli*: comparison with the native enzyme and its processing in *E. coli* and in vitro. *Appl. Environ. Microbiol.* 59, 1168–1175.

Philominathan, S. T., Koide, T., Hamada, K., Yasui, H., Seifert, S., Matsushita, O., et al. (2009). Undirectional binding of clostridial collagenase to triple helical substrates. *J. Biol. Chem.* 284, 10868–10876. doi: 10.1074/jbc.M807684200

Ran, L. Y., Su, H. N., Zhao, G. Y., Gao, X., Zhou, M. Y., Wang, P., et al. (2013). Structural and mechanistic insights into collagen degradation by a bacterial collagenolytic serine protease in the subtilisin family. *Mol. Microbiol.* 90, 997–1010. doi: 10.1111/mmi.12412

Ran, L. Y., Su, H. N., Zhou, M. Y., Wang, L., Chen, X. L., Xie, B. B., et al. (2014). Characterization of a novel subtilisin-like protease myroicolsin from deep sea bacterium Myroides profundi D25 and molecular insight into its collagenolytic mechanism. *J. Biol. Chem.* 289, 6041–6053. doi: 10.1074/jbc.M113.513861

Rawlings, N. D., Barrett, A. J., and Bateman, A. (2010). MEROPS: the peptidase database. *Nucleic Acids Res.* 38, D227–D233. doi: 10.1093/nar/gkp971

Rawlings, N. D., Morton, F. R., and Barrett, A. J. (2006). MEROPS: the peptidase database. *Nucleic Acids Res.* 34, D320–D325. doi: 10.1093/nar/gkj089

Sadat-Mekmene, L., Genay, M., Atlan, D., Lortal, S., and Gagnaire, V. (2011). Original features of cell-envelope proteinases of *Lactobacillus helveticus*. A review. *Int. J. Food Microbiol.* 146, 1–13. doi: 10.1016/j.ijfoodmicro.2011.01.039

Saitou, N., and Nei, M. (1987). The neighbor-joining method: a new method for reconstructing phylogenetic trees. *Mol. Biol. Evol.* 4, 406–425.

Talbot, V., and Bianchi, M. (1997). Bacterial proteolytic activity in sediments of the Subantarctic Indian Ocean sector. *Deep Sea Res. Part II Top. Stud. Oceanogr.* 44, 1069–1084. doi: 10.1016/S0967-0645(96)00107-5

Tamura, K., Peterson, D., Peterson, N., Stecher, G., Nei, M., and Kumar, S. (2011). MEGA5: molecular evolutionary genetics analysis using maximum parsimony methods. *Mol. Biol. Evol.* 28, 2731–2739. doi: 10.1093/molbev/msr121

Tan-Wilson, A., Bandak, B., and Prabu-Jeyabalan, M. (2012). The PA domain is crucial for determining optimum substrate length for soybean protease C1: structure and kinetics correlate with molecular function. *Plant Physiol. Biochem.* 53, 27–32. doi: 10.1016/j.plaphy.2012.01.005

Thompson, J. D., Higgins, D. G., and Gibson, T. J. (1994). CLUSTAL W: improving the sensitivity of progressive multiple sequence alignment through sequence weighting, position-specific gap penalties and weight matrix choice. *Nucleic Acids Res.* 22, 4673–4680. doi: 10.1093/nar/22.22.4673

Yan, B. Q., Chen, X. L., Hou, X. Y., He, H. L., Zhou, B. C., and Zhang, Y. Z. (2009). Molecular analysis of the gene encoding a cold-adapted halophilic subtilase from deep-sea psychrotolerant bacterium *Pseudoalteromonas* sp. SM9913: cloning, expression, characterization and function analysis of the C-terminal PPC domains. *Extremophiles* 13, 725–733. doi: 10.1007/s00792-009-0263-1

Yang, J., Li, J., Mai, Z. M., and Zhang, S. (2013). Purification, characterization, and gene cloning of a cold-adapted thermolysin-like protease from *Halobacillus* sp. *SCSIO* 20089. *J. Biosci. Bioeng.* 115, 628–632. doi: 10.1016/j.jbiosc.2012.12.013

Zhang, X. Y., Han, X. X., Chen, X. L., Dang, H. Y., Xie, B. B., Qin, Q. L., et al. (2015). Diversity of cultivable protease-producing bacteria in sediments of Jiaozhou Bay, China. *Front. Microbiol.* 6, 1021. doi: 10.3389/fmicb.2015.01021

Zhao, G. Y., Chen, X. L., Zhao, H. L., Xie, B. B., Zhou, B. C., and Zhang, Y. Z. (2008). Hydrolysis of insoluble collagen by deseasin MCP-01 from deep-sea *Pseudoalteromonas* sp. *SM*9913: collagenolytic characters, collagen-binding ability of C-terminal polycystic kidney disease domain, and implication for its novel role in deep-sea sedimentary particulate organic nitrogen degradation. *J. Biol. Chem.* 283, 36100–36107. doi: 10.1074/jbc.M804438200

Zhao, H. L., Chen, X. L., Xie, B. B., Zhou, M. Y., Gao, X., Zhang, X. Y., et al. (2012). Elastolytic mechanism of a novel M23 metalloprotease pseudoalterin from deep-sea *Pseudoalteromonas* sp. *CF*6-2: cleaving not only glycyl bonds in the hydrophobic regions but also peptide bonds in the hydrophilic regions involved in cross-linking. *J. Biol. Chem.* 287, 2717–2725. doi: 10.1074/jbc.M112.405076

Zhou, M. Y., Chen, X. L., Zhao, H. L., Dang, H. Y., Luan, X. W., Zhang, X. Y., et al. (2009). Diversity of both the cultivable protease-producing bacteria and their extracellular proteases in the sediments of the South China Sea. *Microb. Ecol.* 58, 582–590. doi: 10.1007/s00248-009-9506-z

Zhou, M. Y., Wang, G. L., Li, D., Zhao, D. L., Qin, Q. L., Chen, X. L., et al. (2013). Diversity of both the cultivable protease-producing bacteria and bacterial extracellular proteases in the coastal sediments of King George Island, Antarctica. *PLoS ONE* 8, e79668. doi: 10.1371/journal.pone.0079668

Conflict of Interest Statement: The authors declare that the research was conducted in the absence of any commercial or financial relationships that could be construed as a potential conflict of interest.

Advantages of publishing in Frontiers

OPEN ACCESS
Articles are free to read for greatest visibility and readership

FAST PUBLICATION
Around 90 days from submission to decision

HIGH QUALITY PEER-REVIEW
Rigorous, collaborative, and constructive peer-review

TRANSPARENT PEER-REVIEW
Editors and reviewers acknowledged by name on published articles

Frontiers
Avenue du Tribunal-Fédéral 34
1005 Lausanne | Switzerland

Visit us: www.frontiersin.org
Contact us: info@frontiersin.org | +41 21 510 17 00

REPRODUCIBILITY OF RESEARCH
Support open data and methods to enhance research reproducibility

DIGITAL PUBLISHING
Articles designed for optimal readership across devices

FOLLOW US
@frontiersin

IMPACT METRICS
Advanced article metrics track visibility across digital media

EXTENSIVE PROMOTION
Marketing and promotion of impactful research

LOOP RESEARCH NETWORK
Our network increases your article's readership